Sun. Jun 6, 2021

[J] Poster | U (Union)：Union

5:15 PM - 6:30 PM JST | 8:15 AM - 9:30 AM UTC | Ch.01_1

[U-04] Promotion of SDGs in JpGU

convener:Yukihiro Takahashi(Department of Cosmosciences, Graduate School of Science, Hokkaido University), Chiaki T. Oguchi(Institute for Environmental Science and Technology, Graduate School of Science and Engineering, Saitama University), Richard Simon Wallis(The University of Tokyo), Eiichi Tajika(Department of Earth and Planetary Science, Graduate School of Science, The University of Tokyo)

[U04-P01] SDGs and academic researches in the Solid Earth Science Section

*Michihiko Nakamura[1], Yo Fukushima[2] (1.Department of Earth Science, Graduate School of Science, Tohoku University, 2.Disaster Science Division, International Research Institute of Disaster Science, Tohoku University)

[U04-P02] **Ongoing research in Human Geosciences and its possible contributions to SDGs**

*Reiichiro Ishii[1], Makoto Taniguchi[1], Naoki Masuhara[1], Sanghyun Lee[1] (1.Research Institute for Humanity and Nature)

[U04-P03] Contribution of SDGs in Subtropical Islands

*Jun Yasumoto[1] (1.University of the Ryukyus, Faculty of Agriculuture)

[U04-P04] Education for Sustainable Development (ESD) and environmental studies promoted by Seikei Gakuen

*Hitoshi Fujiwara[1], Atsushi MIYASHITA[1], Masumi Zaiki[2], Hironobu Oda[2], Atsuko Ikegami[1] (1.Education and Research Center for Sustainable Development/Faculty of Science and Technology, Seikei University, 2.Education and Research Center for Sustainable Development/Faculty of Economics, Seikei University)

[J] Poster | U (Union)：Union

5:15 PM - 6:30 PM JST | 8:15 AM - 9:30 AM UTC | Ch.01_2

[U-09] Advancing SDGs through inclusive partnerships II: Engaging with communities

convener:Hidenroi Nakamura(Toyama Prefectural University), Vincent Tong(University College London), Mika Shimizu(Kyoto University), Fumiko Noguchi(United Nations University, Institute for the Advanced Study of Sustainability)

[U09-P01] SDGs community and social engagement in education and research: Implication for JpGU

*Hidenroi Nakamura[1] (1.Toyama Prefectural University)

[J] Poster | O (Public) : Public

5:15 PM - 6:30 PM JST | 8:15 AM - 9:30 AM UTC | Ch.02_1

[O-02] Natural disasters and people -Listen to the voice of the Earth on the Japanese Geoparks-

convener:Noritaka Matsubara(Graduate School of Regional Resource Management, University of Hyogo), Kyohei Sano(Graduate School of Regional Resource Management, University of Hyogo), Suzuka Koriyama(Itoigawa city), Hikaru Yokoyama(Hokusho University)

[O02-P01] New coronavirus response in Fossa Magna Museum

*Takahiko Ogawara[1], Ko Takenouchi[1], Yousuke Ibaraki[1], Takeo Kobayashi[2], Takuma Katori[2] (1.Fossa Magna Museum, 2.Itoigawa City Hall Geopark Promotion Office)

[O02-P02] Short-Term Effects of SNS Marketing: a Case Study in Hakusan Tedorigawa Geopark

*Susan May[1] (1.Hakusan Tedorigawa Geopark Promotion Council)

[O02-P03] Activities to promote the local sustainable development - Report at the time of spread of COVID-19 infection from Mt.Kurikoma Area Geopark -

*Yui Hasegawa[1], Rie Nakagawa[1], Seiya Tanaka[1], Jun Nagao[1] (1.Mt.Kurikoma Area Geopark Promotion Committee)

[O02-P04] Geotourism in Corona (COVID-19) related crisis - Advantage of being outdoors : In case of San'in Kaigan UNESCO Global Geoprk -

*Noritaka Matsubara[1], NAGAHAMA SATOSHI[1] (1.Graduate School of Regional Resource Management, University of Hyogo)

[O02-P05] Operation of geo-tours using online delivery tools under COVID-19

*Taku Morimoto[1] (1.Unzen Volcanic Area Geopark Promotion Office)

[O02-P06] Holding of event the Lake Shikaribetsu Igloo Village under COVID-19 measures

*Kanamori Syosaku[1], Hiroki Matsumoto[1], Onishi Jun[1] (1.Tokachi-Shikaoi Geopark Promotion Council)

[O02-P07] Stay-at-home Project with Local Students in Toya-Usu UNESCO Global Geopark

*NIRE KAGAYA[1], Yoshiaki Hata[1], Akihito Kato[2], Kiyono Kuroda[2], Koki Takagi[2], Kazuma Iwamura[2], Kanako Kitada[2], Koki Tomita[2], Mina Shionoya[2] (1.Toya-Usu UNESCO Global Geopark Council, 2.Date-Midorigaoka Highschool)

[O02-P08] Developing the San’in Kaigan Geopark Trail and the promotion of geotourism during COVID-19 Pandemic

*Hiroshi Nakase[1] (1.San'in Kaigan Geopark Promotion Council)

[O02-P09] A comparative study of educational on-site and online geotours in Hamamatsu-Hamanako Aspiring Geopark, Japan

*Hiroki Nagano[1], Masato Koyama[2], Yusuke Suzuki[2], Megumi Fukuyama[2] (1.Hamamatsu Technical High School, 2.Shizuoka University)

[O02-P10] Topographic evolution after the Aso-4 pyrocrastic flow and the meaning for disaster prevention in the Oita Bungoono Geopark, Japan

*Toshikazu Yoshioka[1] (1.Oita Bungoono Geopark Promotion Council)

[O02-P11] Conservation and Utillization of Natural Disaster Monument on Tosashimizu Geopark Plan

*Moriguchi Natsuki[1], Satoru Imai[1], Aika Sakuda[1], Kouichi Saruta[1], Michiru Sakai[1] (1.Tosashimizu Geopark Promotion Council)

[O02-P12] Records and countermeasure of disasters in Shimokita Geopark

*Satoshi Ishikawa[1], Kirika Kitagawa[1] (1.Shimokita geopark promotion council)

[O02-P13] Inform of weather disasters in geoparks

*Hiroshi Sato[1,2], Shinichi Sugimoto[3], Makoto Aoi[4], Shinya Miura[4], Hinako Suzuki[4] (1.Mt.Bandai Museum, 2.Bandaisan Geopark Council, 3.Unzen Volcanic Area Global Geopark, 4.National Research Institute for Earth Science and Disaster Resilience)

[O02-P14] How to Prevent Elderly People from Natural Disasters - An Example in Unzen Volcanic Area UNESCO Global Geopark -

Shunsei OGATA[1], Hiyori KADOHATA[1], Tasuku KONDO[1], Miraku TANAKA[1], Kosei HASHIDA[1], Shinsho FUJIO[1], Mizuho IWANAGA[1], Aiko ENGUCHI[1], Seren OTA[1], Rika TANAKA[1], Toru YAMAUCHI[2], Hiroaki OSAKO[2], *Marekazu OHNO[3] (1.Glocal Course of Nagasaki Prefectural Koka High School, 2.Nagasaki Prefectural Koka High School , 3.Unzen Volcanic Area Geopark Promotion Office)

[O02-P15] Disaster and Disaster Prevention Learning in the Naeba-Sanroku Geopark

*Kouhei Nakano[1] (1.Naeba-sanroku Geopark Promotion Council)

[O02-P16] Lives of the local people on the collapsing land and the flowing land by river water -Think about geohazard program of Miyoshi geopark project-

*Azusa Tonotani[1], Katsunori Ozakai[1], Mizuki Tochitani[1], Hiroyuki Ohnishi[1], Toshiaki Matsumoto[1] (1.Geopark Promotion office in Miyoshi city)

[O02-P17] Toward restoration of Geosites damaged by natural disaster with reaching consensus in local community: a case of Suzaki Coast in Seiyo City, Japan.

*Takumi Sakakiyama[1], Kazunari Kimura[2], Yuya Kato[3], Masahito Ono[1], Tsukasa Takahashi[1] (1.Seiyo City, 2.NAIBA Co. Ltd., 3.Noyama Company)

[O02-P18] Let's investigate the earth activity from Shimonita Geopark

*Hara Hideo[1] (1.Geopark Shimonita council)

[O02-P19] **The foundations of Yuzawa Geopark: a unification and a compilation of six geological maps published by the Geological Survey of Japan and Akita Prefecture**

*Akio Sasaki[1], Kohei Yamawaki[1], Yukio Fujimoto[1], Syoichi Goi[1], Shoei Chiba[1] (1.Network of Earth Science Museum for Akita)

[O02-P20] Conservation concerns in Yuzawa Geopark: Distributions and seasonal variation in blood-sucking flies and an invasive plant species

*Haruki Takayanagi[1] (1.Yuzawa City Geopark Promotion Council)

[O02-P21] The relationship between the former plate boundary and residents, especially the signboard production process

*Kato Satomi[1] (1.Mt. Apoi Geopark Promotion Council)

[O02-P22] Fossil collecting experience to solve summer vacation indipendent study in Itoigawa UNESCO Global Geopark

*Yousuke Ibaraki[1], Yutaka Furumi, Emma Longhorn, Takahiko Ogawara[1], Ko Takenouchi[1], Takuma Katori[2], Takeo Kobayashi[2] (1.Fossa Magna Museum, 2.Itoigawa Geopark Council)

[O02-P23] Geosite Map and Card in a Fun and Interesting Way by Local Elementary School Students: a Case Study of Geosite in Nankikumano Geopark with Takaike Elementary School

*Hiroko Shibasaki[1] (1.Nanki-Kumano GeoPark Guide Club)

[O02-P24] **Examples of joint projects (or joint events) between a museum and Sado Island Geopark**

*Takeyoshi SADAKANE[1], Mituhisa AIDA[1] (1.Sado Geopark Promotion Council)

[O02-P25] A Guide program that promote Proactive learning in School trip
- Practice at Toya-Usu UNESCO Global Geopark -

*Hikaru Yokoyama[1] (1.Hokusho University)

[O02-P26] Educational Program on spring water of Aso UNESCO Global Geopark related with elcetrical conductivity (Part 2)
Cooperated Research on Minamiaso Spring Water

*Tsuneomi Kagiyama[1], Koki Nagata[2], Toshikazu Maeda[3], Yuto Takeuchi[3], Haruki Watanabe[3], Kozue Inoue[3] (1.Aso Geopark Promotion Council, 2.Aso Volcano Museum, 3.Takamori Senior High School)

[O02-P27] Looking back on 11 years of the educational activities of the Dinosaur Valley Fukui Katsuyama Geopark

*Sumiaki Machi[1] (1.Dinosaur Valley Fukui Katsuyama Geopark Promotion Council)

[J] Poster | O (Public)：Public

5:15 PM - 6:30 PM JST | 8:15 AM - 9:30 AM UTC | Ch.02_2

[O-05] How to become a scientist? What can they do?

convener:Natsue Abe(Mantle Drilling Promotion Office, MarE3, Japan Agency for Marine-Earth Science and Technology), Rie Hori, S.(Department of Earth Science, Faculty of Science, Ehime University)

[O05-P01] Only Ph.D. holders can work in the research and science field?

*Natsue Abe[1,2], Rie Hori, S.[3] (1.Mantle Drilling Promotion Office, MarE3, Japan Agency for Marine-Earth Science and Technology , 2.Graduate School of Natural Science & Technology, Kanazawa University, 3.Ehime University)

[O05-P02] Skills required to work at the science museum

★Invited Papers

*Mayumi ARAI[1] (1.National Museum of Emerging Science and Innovation)

[O05-P03] Discussion

[J] Poster | O (Public) : Public

1:45 PM - 3:15 PM JST | 4:45 AM - 6:15 AM UTC | Ch.27

[O-07] Poster presentations by senior high school students

convener:Tatsuhiko Hara(International Institute of Seismology and Earthquake Engineering, Building Research Institute), Katsuyoshi Michibayashi(Department of Earth and Planetary Sciences, Nagoya University), Miwa Kuri(Japan Meteorological Agency), Keiko Konya(Japan Agency for Marine-Earth Science and Technology)

[O07-P01] Weather in Fukuoka Prefecture in the Edo period from the Nakamura Heizaemon diary

*Rui ANDOU[1], *Rio HAYASHIDA[1], *Hikari ARASE[1], *Mira EGUCHI[1], *Touko HAGIHARA[1] (1.Ikeda Senior High School)

[O07-P02] Discussion on Economic Effects of Muroto Deep Sea Water – How Does Deep Sea Water Industry Contribute to Revitalize the Community? –

*Kaede Yauoka[1] (1.Muroto High School)

[O07-P03] Observation of Columnar Joints and Research on its Origin

Atsushi Watanabe[1], *Iroha Kawaguchi[1], *Ryosuke Sugioka[1], *Mizuki Hukumuro[1], *Akihiro Amamiya[1], *Towa Serizawa[1] (1.Nirayama Highschool)

[O07-P04] A study of microplastics that is included in the rivers and coast of the Izu Peninsula

Atsushi Watanabe[1], *Namiki Kawai[1], *Koji Sadakane[1], *Yuichirou Takahashi[1], *Mayuko Toriikouji[1], *Daisuke Yamamoto[1], *Miori Yabuta[2], *Tubasa Ozawa[2], *Takaya Nishida[2], *Haruki Mimura[2], *Nanami Hujii[2], Ryosuke Yoshida[2] (1.Nirayama Highschool, 2.Shimoda Highschool)

[O07-P05] Consideration of method to increase artificial ruby

Atsushi Watanabe[1], *Yuichirou Nagatsu[1], *Moe Hatakeyama[1], *Koutarou Matsumoto[1], *Yudai Komiyama[1] (1.Nirayama Highschool)

[O07-P06] Earthquake prediction by Electric magnetic wave

*Masayuki Masa[1], *Nozomu Sakai[1], Michiya Sasaki[1], Souhei Kato[1], Ousuke Yagasaki[1], Mizuho Fujiwara[1], Maika Yashima[1] (1. Tokyo Metropolitan Tama High School of Science and Technology)

[O07-P07] Comparison of heated products of glucose with citric acid added

*Takumi Ohtsu[1] (1.Tokyo Metropolitan Tama High School of Science and Technology)

[O07-P08] Development of iron (II) phosphate lithium-ion battery using the adsorption power of Aso loess

*Ayumi Hoshi[1], *Sora Nozaki[1] (1.Tokyo Metropolitan Tama High School of Science and Technology)

[O07-P09] Method of Recovering Perfluorinated Compounds by coffee grounds

*Kouki Morimoto[1], *Issei Yamazeki[1], *Renon Shimizu[1] (1.Tokyo Metropolitan Tama High School of Science and Technology)

[O07-P10] Research into Moriya Formation Formed in Northen Fossa Magna

*Yusuke Morozumi[1] (1.Suwa Seiryo high school)

[O07-P11] A Consideration of a Landing Exploration on Europa

*Taichi Ito[1] (1.Seishin Gakuen High School)

[O07-P12] Relationship between five gigantic jets in the past and cloud-to-ground lightning

*Fuga Suzuki[1], *Yuya Takahashi[1], Sorachi Nishibori[1], Yuki Ito[1], Takumi Miyamoto[1] (1.Shizuoka Prefectural Iwata Minami High School)

[O07-P13] Examination of the fall position by the light emission of the Narashino meteorite fireball

*Ryunosuke Kamiya[1], *Haruka Sato[1], Kosuke Arimura[1], Saki Ozawa[1], Hana Miki[1], Yuka Ogawa[1], Honoka Tanabe[1] (1.Shizuoka Prefectural Iwata Minami High School)

[O07-P14] The Change of Microtopography of Samejima Coast Caused by the Storm Surge Brought by Hagibis

*Takeshi Totsuka[1], Yuya Takahashi[1], *Kosuke Arimura[1], Koki Suzuki[1], Shun Ichikawa[1], Rabu Kato[1] (1.Shizuoka Prefectural Iwata Minami High School)

[O07-P15] Putting legs on snake swimming robot going to be useless?Seeking truth of Tetrapodophis

*Ryoya Sato[1], *Kokoro Ikeda[1], *Ryota Ogawa[1], *Riko Tomioka[1], *Akari Hitomi[1], *Kanon Yamaguchi[1] (1.Tokyo Tech High School of Science and Technology)

[O07-P16] Consideration of snowmelt type lahar at Mt. Katta, Zao

*Haruya Shishido[1], *Reiki Syoji[1], *Ryo Hikichi[1] (1.Miyagi Prefectural Tagajo Senior High School)

[O07-P17] Geological structure of Urato Katsurashima Island and Nonoshima Island, Shiogama City

*Asahi Oyama[1], *Hikaru Sasaki[1], *Yuhi Suzuki[1], *Hayato Murakami[1], *Misaki Kuga[1] (1.Miyagi Prefectural Tagajo Senior High School)

[O07-P18] Threats and impacts of urban tsunami
-Simulate a tsunami when a Nankai Trough giant earthquake occurs using a tsunami generator-

*Misaki Suda[1], *Kenshin Okazaki[1], *Zen Sato[1], *Yusei Niinuma[1], *Kousei Matsuura[1], *Ayaka Akisawa[1] (1.Miyagi Prefectural Tagajo Senior High School)

[O07-P19] Countermeasures against Heat Island Phenomenon: Proposal for a New Building System

*Hiroaki HAYASHI[1] (1.Yokohama Science Frontier High School)

[O07-P20] An evaluation of artificial landform in Chiba prefecture called “Kawamawashi”

*Kodai SHIBUYA[1] (1.Yokohama Science Frontier High School)

[O07-P21] The relationship between sunspot number and typhoons

*Takeru TODA[1] (1.Yokohama Science Frontier High School)

[O07-P22] On the study of Fukui Earthquake Fault IX

*Kazuho Kuwajima[1], *Ryouhei Matta[1], *Youhei Morise[1], *Ayano Yashima[1] (1.Fujishima High School of Fukui prefecture)

[O07-P23] **Approach to the current situation and issues of geothermal power generation utilization based on field surveys**

*Kisho Kurosawa[1], *Tatsuki Miyamoto[1], *Nozomi Kawaharata[1], *Shoki Yashima[1], *Yusuke Oba[1] (1.FurukawaReimei High School)

[O07-P24] Study of mechanism of Light Emission by Spectroscopic Observation of Meteor

*Yui Sato[1], *Yuki Kato[1] (1.Miyagi Prefectual Furukawa Reimei Senior High School)

[O07-P25] Relationship between mineral crystallization and impurities.

*Usami Kenta[1], *Ryo Nakane[1], *Hiroyuki Sueno[1], Syotaro Kawana[1], Ryota Naito[1], Kazuhiko Hoshi[1], Mitsuhide Sai[1], Takuma Watanabe[1] (1.Johoku high school)

[O07-P26] Analysis of water quality of irrigation ponds focused on land use, irrigation systems and periodic pond draining

*Ayane INOUE[1], *Haruto TAKEYAMA[1], *Kousuke MANO[1], *Rio YAMANO[1] (1.Hyogo Prefectural Kakogawa Higashi High School)

[O07-P27] The Process of Raised-Bed River Formation and Factors that Affect It

*Natsuki KAMISASA[1], *Yuta KONDO[1], *Haruto TAKEYAMA[1], *Yasuharu TOMITA[1], *Rikushi NAGAO[1], *Naka NOHAMA[1] (1.Hyogo Prefectural Kakogawa Higashi High School)

[O07-P28] Studies of the SDGs on the Sanriku Geopark. The sea urchin spread trench in the Taneichi Formation.

*Kyougo Sakashita[1], *Asahi Sekibata[1], *Rina Nakajo[1], *Yuto Kugoi[1], *Hikaru Sasaki[1] (1.Marient Chikyu-tanken club senier)

[O07-P29] Studies of the SDGs on the Sanriku Geopark. The Aoba Lake and Shimamori Basin.

*Mizuki Kimura[1], * Naho Simodate[1], *Kahono Hinata[1], *Yuma Keicho[1], *Kouki Takahashi[1] (1.Marient Chikyu-tanken club senier)

[O07-P30] Proposal of Hachinohe Canyon to Sanriku Geopark Geosite.

*Sarina Shinohe[1], * Miyu Abe[1], * Akari Nakamura[1], *Yukihito Yasuhara[1], *Kensuke Shimomura[1] (1.Marient Chikyu-tanken club senier)

[O07-P31] Proposal of an index for estimating the distance from the source rock

*Ayaka Mitsui[1], *Reiji Iwamoto[1], *Keishi Okumi[1], *Mayu Naito[1], *Yamato Yasuhara[1], *Natsuki Yamamoto[1], *Naoko Kodama[1], *Akito Sasaki[1], *Akira Tada[1], *Takuto Nakanou[1], *Tomohiko Maeda[1], *Yuya Muromoto[1], *Ryusei Moriyama[1] (1.Hyogo Prefectural Himejihigashi Senior High School)

[O07-P32] Energy calibration of a cosmic-ray detector

*moe kimura[1] (1.Tokyo Metropolitan Hibiya High School)

[O07-P33] Floating waterdrops using a straw commutator

*Aoba Takahara[1], Yuri Yasui[1], Takaya Sato[1] (1.Niigata Prefectural Takada high school)

[O07-P34] The rotating-Water-tank that is replaced hot water tank and ice water tank

*Masamune Minou[1] (1.Niigata Prefectural Takada high School)

[O07-P35] Comparison of the surface of Mars with the previous one in the approach of Mars Spread of dust storm on November 17th

*Sayaka Mizutani[1], *Takumi Uchiyama[1], Riho Kagami[1], Aoi Takemoto[1] (1.Ichinomiya High School)

[O07-P36] Tumulus inspection project by using cosmic-ray muon

*Tomoyo Ishizawa[1], *Satoshi Ono[1], *Asahi Shiozaki[1], *Wakana Yanagimoto[1], *Kenshiro Aoki[1], *Yuna Ishii[1], *Sogo Kimura[1], *Yuki Shimada[1], *Aoi Soga[1], *Yuga Takemori[1], *Rino Tomiku[1], *Kana Hashizume[1], Miki Ohtsuka[1] (1.Waseda University Honjo Senior High School)

[O07-P37] Calculating the nebula density from the size of the emission nebula

*Yuki Shirai[1] (1.Totsuka High School)

[O07-P38] Strength evaluation of structures by making and improving quake-vibration generators

*Runaya Igari[1], *Yuto Meguro[1], *Rin Goto[1], Kenshiro Kamata[1] (1.Miyagi Rifu high school)

[O07-P39] Time dependence of ocean salinity

*Honami Hashimoto[1], Annu Ito[1] (1.Miyagi Rifu highschool)

[O07-P40] Toward "Solid-State Version Chromatography" Second Report

*Yuichiro Okuno[1], *Akihisa Wada[1], *Yudai Kozono[1], *Ryota Iwamoto[2], *Mai Fujitani[2], *Kyoya Okada[3], *Kusunori Sumi[3], *Arata Fujimoto[3] (1.Imamiya Technology Senior High School of Osaka Prefecture:The evening course, 2.Otemae Senior High School of Osaka Prefecture:The evening course, 3.Kasugaoka Senior High School of Osaka Prefecture:The evening course)

[O07-P41] How to extract bioethanol effectively by distillation.

*Ataru Kunihisa[1] (1.Wakasa high school)

[O07-P42] Confusion of the people in the northwestern area of Saitama Prefecture due to rumors after the 1923 Kanto Earthquake

*Miharu Shinoda[1] (1.Sakae Higashi High School)

[O07-P43] A quest for the best condition of a crystal radio's detection

*Motoaki Osone[1] (1.Yashiro High School)

[O07-P44] What cause columner joint changes?

*Yugo Sakurai[1], *Yuki Enomoto[1], *Kanta Hayashibe[1] (1.Yashiro High School)

[O07-P45] Preliminary analysis of HAYABUSA-2's Doppler-Shift

*Azumi Sofue[1], *Naoko Nishino[1], *Riri Iida[1], *Riri Numata[1] (1.Wakayama Shin-ai Senior High School)

[O07-P46] Estimation of a ceiling thickness using the muography technique with a small cosmic-ray detector

*Nana Kobayashi[1] (1.Kaichi High School)

[O07-P47] A proposal of an inverse analysis method for ballistic ejecta flying focusing on crater shape in phreatic eruption

*Kouki Nishino[1], Neo Suzuki[1], Natsumi Waki[1] (1.Kanagawa Prefectural Yokosuka Senior High School)

[O07-P48] The survey of Micro-Plastics included in River sediments.

*Taichi Ichikawa[1], Ryuke Kawai[1], Suzuka Fukunaga[1], Tessho Yamamoto[1], Takumi Sato[1] (1.GIZAN SENIOR HIGH SCHOOL)

[O07-P49] Relationship between sprites and the lightning charge moment

*syunsuke nakao[1], *sora wake[1] (1.Prefectural Kochi Ozu High School)

[O07-P50] Potential Small Hydropower Generation in Kamikawa Basin -Hydro Energy Map Visualizing Power Generation-

*Airi Takei[1], *Akira Tamaki[1], *Naoki Kudo[1], *Asahi Takahashi[1], *Hikaru Kawashima[1] (1.Hokkaido Asahikawa Nishi High School)

[O07-P51] Consideration of brachiopod biota change events in the Kuzu limestone layer

*Omi Kono[1], Tokio Chiba[1] (1.Kaijo senior high school)

[O07-P52] Estimation of the variation in mechanism in the amount of spring water in Otomeyama Park, Shinjuku City

*Kuya Aoyama[1], Taichi Shimokobe[1], Masamune Kanou[1] (1.Kaijo high school)

[O07-P53] Modeling the earthquake damage in adeveloped land

*Shungo Kokubun[1], *Satoru Takahashi[1], *Hiroshi Takeuchi[1], *Haruki Tamakawa[1], *Masafumi Kaneko[1], Takumi Nanbu[1] (1.Miyagi Prefecture Sendai Daisan High School)

[O07-P54] Influence of Calcium chloride on frost columns

*Manaka Oya[1], Shohei Nanri[1] (1.Ichikawa gakuen Ichikawa senior high school)

[O07-P55] Differences in fog generation conditions in the Edogawa estuary -Examples of Edogawa-ku and Ichikawa-shi-

*Kenta Torii[1], Shohei Nanri[1] (1.Ichikawa gakuen Ichikawa senior high school)

[O07-P56] Development of variable slope type underwater embankment

*Kei Omura[1], Shohei Nanri[1] (1.Ichikawa gakuen Ichikawa senior high school)

[O07-P57] Environmental impact assessment of air and soil substances using spring water of Minowa as an index

*Mari Taki[1], Shohei Nanri[1] (1.Ichikawa gakuen Ichikawa senior high school)

[O07-P58] Development of an automatic meteor shower observation and the notification system ~Web broadcast of meteor appearance~

*Koichi Sato[1], *Koshi Ri[1], *Shunsuke Isoda[1], *Honoka Ohno[1] (1.Chuo University Junior and Senior High School)

[O07-P59] Meteorological and geographical conditions of river flooding-Comparison of the past and present of the Miyata River-

*Eri Yoshida[1], *Minami Oikawa[1], *Kotomi Shibata[1], *Chihiro Terazaki[1], *Kurumi Yabe[1] (1.Ibaraki prefectural Hitachi first senior high school)

[O07-P60] Where are solar panels actually used? Research on the present situation of Kashiwa City, Chiba prefecture, Japan.

*Souri Mizukami[1] (1.SHIBYA SENIOR HIGH SCHOOL)

[O07-P61] Decline and Fall of Martian Polar Capse; Whether the Dast Storm Is Warm the Polar Cap

*Kei Inoue[1], Hibiki Aminaka[1], Yuho Takagi[1], Nanami Yasuda[1], Yuki Tanaka[1], Tomoki Ugawa[1], Rio Mogi[1], Kyouka Miyake[1], Momoha Takashima[1], Mako Misumi[1], Kaho Okada[1] (1.Kumamoto Prefectural Daiichi High School)

[O07-P62] Spacial correlation between slow earthquake and mantle- derived hot spring in Southwest Japan

*Yui Kobayashi[1] (1.Shizuoka Higashi High School)

[O07-P63] **Visualize water current using vitamin B_2**

*Mutsuki Kamata[1], *Yuuma Nakagawa[1], *Io Kato[1], *Tokito Hirose[1], *Yuuki Matsui[1], *Kosuke Mafune[1], *Akihito Yamada[1], Kazumi Igawa[1] (1.Zushi-Kaisei Senior High School)

[O07-P64] Designe of lunar crater exploration rover

*Kosuke Kameoka[1] (1.Meikei High School)

[O07-P65] Distribution of Gravel in the Sakawa River and Factors Affecting the Distribution

*Nozomi Uemachi[1], *Misaki Yamamiya[1], Yosuke Saito[1] (1.Tokyo Gakugei University Senior High School)

[O07-P66] Detection of Cherenkov light with acrylic and photodetecto

*Juri Urano[1], *Yuka Kuze[1], *Kaho Kubota[1] (1.Toshimagaoka Joshigakuen senior high school)

[O07-P67] Research the View of Mt.Fuji with a Self-Made Observation Device

*Ryoo Niigawa[1], *Rin Takezoe[1] (1.Tokyo Metropolitan Tachikawa High School)

[O07-P68] Bad visibility in the past at Tachikawa High School

*Tomoya Ushizaka[1] (1.Tokyo Metropolitan Tachikawa High School)

[O07-P69] Analysis of visibility around Tachikawa High School

*Takumi Yasuhara[1] (1.Tokyo Metropolitan Tachikawa High School)

[O07-P70] The relationship between the shape and power generation amount of the simple wind power generators

*Sora Fukui[1] (1.Tokyo Metropolitan Tachikawa High School)

[O07-P71] **Is « evacuate to rise » the Right Action?**
Research and Proposition of Major Evacuation Routes to Shelters in Shibuya

*Sakura Oona Marie Sueoka[1] (1.Tokyo Metropolitan Kokusai High School)

[O07-P72] Mechanism of how the Shirata river looks blue

*Shuhei Sugai[1], *Ryosuke Yoshida[1] (1.Shimoda high school)

[O07-P73] Determining the Properties of Seyfert Galaxies

*Kuya ABE[1], *Kuranosuke IEHATA[1], *Koki TANII[1], *Tamotsu FUJIMOTO[1] (1.Nara Prefectural Seisho High School)

[O07-P74] Observation of Radio Waves from the Moon

*Koya YAMASHITA[1], *Ichika TSUTSUMI[1], *Atsushi HIRANUMA[1], *Ikumi MATSUYOSHI[1] (1.Nara Prefectural Seisho High School)

[O07-P75] Making Snow Meter Using Neutron Cosmic Rays Observation Data Collected By Cosmic Watch

*Kei Ikushima[1], Rikako Kono[2], Kaduo Tanaka[2], Akita Yuji[1] (1.Hiroo Gakuen High School, 2.Touhoku University)

[O07-P76] Water storage capacity of the green dam – Role of forest soil -

*Nanami Aoki[1] (1.Kyoto Prefectural Sagano High School)

[O07-P77] Measurement of Radon Concentration for Earthquake Prediction in the Woods for Field Practice Owned by Sagano H. S.

*Ayaka Kawabata[1], *Takahiro Kawabata[2] (1.Kyoto Prefectural Sagano High School, 2.Graduate School of Science, Osaka University)

[J] Poster | O (Public)：Public

1:45 PM - 3:15 PM JST | 4:45 AM - 6:15 AM UTC | Ch.28

[O-07] Poster presentations by senior high school students

convener:Tatsuhiko Hara(International Institute of Seismology and Earthquake Engineering, Building Research Institute), Katsuyoshi Michibayashi(Department of Earth and Planetary Sciences, Nagoya University), Miwa Kuri(Japan Meteorological Agency), Keiko Konya(Japan Agency for Marine-Earth Science and Technology)

[J] Poster | A (Atmospheric and Hydrospheric Sciences)：A-AS Atmospheric Sciences, Meteorology & Atmospheric Environment

5:15 PM - 6:30 PM JST | 8:15 AM - 9:30 AM UTC | Ch.07_2

[A-AS05] Atmospheric Chemistry

convener:Tomoki Nakayama(Graduate School of Fisheries and Environmental Sciences, Nagasaki University), Naoko Saitoh(Center for Environmental Remote Sensing), Sakae Toyoda(Department of Chemical Science and Engineering, Tokyo Institute of Technology), Risa Uchida(Japan Automobile Research Institute)

[AAS05-P01] The Relation between HONO Emission and the Amount of Carbon and Nitrogen Compounds in the Activated Sludge

*Chika Minejima[1], Yuta Orii[1], Ryosuke Fujinuma[1], Toshikazu Suenaga[2], Shohei Riya[2], Akihiko Terada[2], Masayuki Ohyama[4], Norimichi Takenaka[5], Keiichi Sato[3] (1.International Christian University, 2.Tokyo University of Agriculture and Technology, 3.Asia Center for Air Pollution Research (ACAP), 4.Osaka Institute of Public Health, 5.Osaka Prefecture University)

[AAS05-P02] Constraining the origin of tropospheric nitrous acid using triple oxygen isotopes as tracers

*Fumiko Nakagawa[1], Peng Lai[1], Kazuya Hirano[1], Masanori Ito[1], Urumu Tsunogai[1] (1.Graduate School of Environmental Studies, Nagoya University)

[AAS05-P03] **Changes in tropospheric nitrogen dioxide vertical column densities over Japan and Korea during the COVID-19 using Pandora and MAX-DOAS**

*Yongjoo Choi[1], Yugo Kanaya[1], Hisahiro Takashima[2], Kihong Park[3], Haebum Lee[3], Jihyo Chong[3,4], Jae Hwan Kim[5] (1.Japan Agency for Marine-Earth Science and Technology, 2.Faculty of Science, Fukuoka University, 3.Gwangju Institute of Science and Technology, 4.Environmental Management Division, Yeongsan River Basin Environmental Office, Gwangju 61945, Korea, 5.Pusan National University)

[AAS05-P04] Estimation of emission source of CO from biomass burning observed with ground-based FTIR spectrometers at Tsukuba since 2010

Daisuke Suzuki[2], *Hideaki Nakajima[1,2], Isao Murata[2], Isamu Morino[1] (1.National Institute for Environmental Studies, 2.Graduate School of Environmental Studies, Tohoku University)

[AAS05-P05] Evaluation of NICAM-TM CO data using MOPITT CO data

*Miyajima Hiroshi[1], Naoko Saitoh[1], Yosuke Niwa[2] (1.Center for Environmental Remote Sensing, Chiba University, 2.National Institute for Environmental Studies)

[AAS05-P06] **Evaluation of the global chemistry transport model CHASER utilizing TROPOMI formaldehyde measurements**

*Hossain Mohammed Syedul Hoque[1], Kengo Sudo[1,3], Hitoshi Irie[2], Takashi Sekiya[3] (1.Graduate School of Environmental Studies, Nagoya University, Japan, 2.Center for Environmental Remote Sensing (CEReS), Chiba University, Japan, 3.Japan Agency for Marine-Earth Science and Technology (JAMSTEC), Yokohama, Japan)

[AAS05-P07] Ozone steady-state at the semi-urban region, Shadnagar, in Southern India

*Vijay Kumar Sagar[1] (1.National Remote Sensing Centre, Hyderabad, ISRO)

[AAS05-P08] A relationship between surface oxidant concentration and daily maximum temperature, and its long-term variability

*Atsushi Shimizu[1], Tatsuya Nagashima[1] (1.National Institute for Environmental Studies)

[AAS05-P09] Analysis of tropospheric ozone budgets in CMIP6 experiments

*Paul T Griffiths[1], Lee T Murray[2], Guang Zeng[3], Vaishali Naik[4], Prodromos Zanis[5], Alexander T Archibald[1] (1.National Centre for Atmospheric Science, Cambridge University, 2.University of Rochester, Rochester, NY, USA, 3.National Institute of Water and Atmospheric Research, Wellington, New Zealand, 4.NOAA Geophysical Fluid Dynamics Laboratory, Princeton, NJ, USA, 5.Department of Meteorology and Climatology, Aristotle University of Thessaloniki, Thessaloniki, Greece)

[AAS05-P10] Study of tropospheric CS_2 photooxidation chemistry

*Yuanzhe Li[1], Kazuki Kamezaki[2], Sebastian Danielache[2] (1.Green Science And Engineering Division, Graduate School Of Science And Technology, Sophia University, 2.Department of Materials & Sciences, Faculty of Science & Technology, Sophia University)

[AAS05-P11] **Effects of hydroxyl radical exposure on chemical composition of secondary organic aerosol formed from sabinene ozonolysis**

*Kei Sato[1,2], Yu Morino[1], Takashi Imamura[1], Yoshizumi Kajii[1,2] (1.National Institute for Environmental Studies, 2.Kyoto University)

[AAS05-P12] Impact of nighttime aging on optical properties of toluene secondary organic aerosol

*Tomoki Nakayama[1], Kei Sato[2], Sathiyamurthi Ramasamy[2], Takashi Imamura[2], Yoshizumi Kajii[3,2] (1.Nagasaki University, 2.NIES, 3.Kyoto University)

[AAS05-P13] Volatility of nanoparticles generated from jet engine lubrication oil

*Nobuyuki Takegawa[1], Anna Nagasaki[1] (1.Graduate School of Science, Tokyo Metropolitan University)

[AAS05-P14] Vertical structural measures of atmospheric pollutants using XU-S

*Kazuyo Yamaji[1], Tetsuya Miyakoshi[2], Satoshi Komatsu[2], Isao Kanda[3] (1.Kobe University, 2.ShinMaywa Industries, Ltd. , 3.Japan Meteorological Corporation)

[AAS05-P15] **Continuous and multi-wavelength measurement of aerosol extinction coefficient by long-path propagation of LED light at Chiba, Japan**

*Ikuya Nishiwaki[1], Hitoshi Irie[2], Nofel D. Lagrosas[1], Hiroaki Kuze[2] (1.Chiba University, 2.Center for Environmental Remote Sensing, Chiba University)

[AAS05-P16] Aerosol type classification of ground-based remote sensing data by k-means clustering

*Hiroyasu Kobayashi[1], Hitoshi Irie[2], Masahiro Momoi[1] (1.Chiba University, 2.Center for Environmental Remote Sensing, Chiba University)

[AAS05-P17] Validation of MERRA-2 Reanalysis Aerosol Products Using Ground-based Observations in Phimai, Thailand, and Factors that Affect Aerosol Optical Depth over the Indochina Peninsula

*Takeru Ohno[1], Hitoshi Irie[1], Arlindo M da Silva[2], Ravi C Govindaraju[2] (1.Center for Environmental Remote Sensing, Chiba University, 2.Global Modeling and Assimilation Office, NASA Goddard Space Flight Center, Greenbelt, Maryland)

[AAS05-P18] Exploring ground-based aerosol optical properties to improve satellite estimates of surface particulate matter concentrations

*Alessandro Damiani[1], Hitoshi Irie[1], Kodai Yamaguchi[1], Hossain Mohammed Syedul Hoque[2], Tomoki Nakayama[3], Yutaka Matsumi[2], Yutaka Kondo[4] (1.CEReS, Chiba University, 2.Nagoya University, 3.Nagasaki University, 4.National Institute of Polar Research)

[AAS05-P19] Development of international air quality and sky research remote sensing (A-SKY) network

*Hitoshi Irie[1], Alessandro Damiani[1], Toshihiko Takemura[2], Thanawat Jarupongsakul[3], Manish Naja[4] (1.Center for Environmental Remote Sensing, Chiba University, 2.Research Institute for Applied Mechanics, Kyushu University, 3.Department of Geology, Faculty of Science, Chulalongkorn University, 4.Aryabhatta Research Institute of Observational Sciences (ARIES))

[AAS05-P20] Prediction of changes in DSS emission using the Earth System Model of the Meteorological Research Institute

*Takashi Maki[1], Taichu Y Tanaka[1], Thomas Sekiyama[1], Mizuo Kajino[1], Naga Oshima[1], Tsuyoshi Koshiro[1] (1.Meteorological Research Institute)

[AAS05-P21] Methane emission trends of China in 2009-2018 induced by atmospheric observations

*Fenjuan Wang[1], Shamil S Maksyutov[1], Rajesh Janardanan[1], Akihiko Ito[2], Isamu Morino[1], Yukio Yoshida[1], Yasunori Tohjima[1], Johannes W. Kaiser[3], Greet Janssens-Maenhout[4], xin Lan[5], Ivan Mammarella[6], Jost V. Lavric[7], Tsuneo Matsunaga[1] (1.NIES National Institute of Environmental Studies, 2.Finnish Meteorological Institute, 3.Deutscher Wetterdienst, 4.European Commission Joint Research Centre, 5.Earth System Research Laboratory, 6.University of Helsinki, 7.Max Planck Institute for Biogeochemistry)

[AAS05-P22] **Characteristics of methane vertical distributions over India**

*Dingkun Zhang[1], Naoko Saitoh[1], Dmitry Belikov[1], Prabir Patra[2], Naveen Chandra[3] (1.Center for Environmental Remote Sensing, Chiba University, 2.Japan Agency for Marine-Earth Science and Technology, 3.National Institute for Environmental Studies)

[AAS05-P23] Temporal and spatial variations of the mole fraction, carbon and hydrogen isotope ratios of atmospheric methane in the Western Pacific region

*Yasuda Mahito[1], Shinji Morimoto[1], Shuji Aoki[1], Ryo Fujita[2], Taku Umezawa[3] (1.Center for Atmospheric and Oceanic Studies, Graduate School of Science, Tohoku University, 2.Department of Climate and Geochemistry Research, Meterorological Reserach Research Institute, Tsukuba Japan, 3.National Institute for Environmental Studies, Tsukuba, Japan)

[AAS05-P24] Variations of atmospheric carbon dioxide and its radioisotope in the arctic region

*Hikaru Sekine[1], Shinji Morimoto[1], Chinatsu Yamada[1], Daisuke Goto[2], Masayo Minami[3], Toshio Nakamura[3], Shuji Aoki[1] (1.Center for Atmospheric and Oceanic studies, 2.National Institute of Polar Research, 3.Institute for Space-Earth Environmental Research)

[AAS05-P25] Preparation of O_2/N_2 dataset from the surface to the middle stratosphere around Japan traceable to NMIJ gravimetric scale

*Shigeyuki Ishidoya[1], Shinji Morimoto[2], Kazuhiro Tsuboi[3], Satoshi Sugawara[4], Daisuke Goto[5], Nobuyuki Aoki[1], Shohei Murayama[1], Yosuke Niwa[6], Shuji Aoki[2], Hidekazu Matsueda[3], Kentaro Ishijima[3] (1.Advanced Industrial Science and Technology, 2.Tohoku University, 3.Meteorological Research Institute, 4.Miyagi University of Education, 5.National Institute of Polar Research, 6.National Institute for Environmental Studies)

[AAS05-P26] Temporal variation of the ozone profile observed with FTIR at Tsukuba

*Isao Murata[1], Hideaki Nakajima[2], Isamu Morino[2], Masanori Takeda[1,2] (1.Graduate School of Environmental Studies, Tohoku University, 2.National Institute for Environmental Studies)

[J] Poster | A (Atmospheric and Hydrospheric Sciences)：A-HW Hydrology & Water Environment

5:15 PM - 6:30 PM JST | 8:15 AM - 9:30 AM UTC | Ch.08_2

[A-HW23] Isotope Hydrology 2021

convener:Masaya Yasuhara(Rissho Univ.), Kohei Kazahaya(Geological Survey of Japan, AIST), Shinji Ohsawa(Institute for Geothermal Sciences, Graduate School of Science, Kyoto University), Kazuyoshi Asai(Geo Science Laboratory)

[AHW23-P01] Detection of slab-derived fluid in saline ground water collected from coastal area of Seto Inland Sea, Japan

★Invited Papers

*Yoko Togo[1], Kohei Kazahaya[1], Yuki Tosaki[1], Masaaki Takahashi[1], Noritoshi Morikawa[1], Hiroshi A Takahashi[1], Yuri Nakamura[1], Akihiko Inamura[1], Hinako Shimizu[1], Hiroyuki Matsuzaki[2] (1.National Institute of Advanced Industrial Science and Technology, 2.University of Tokyo)

[AHW23-P02] Geochemical characteristics and origins of saline groundwater in the southern Boso Peninsula, Chiba, Japan

*Masaya Yasuhara[1], Akihiko Inamura[2], Ryotaro Mabuchi[3], Seongwon Lee[1], Noritoshi Morikawa[2] (1.Rissho University, 2.Geological Survey of Japan, AIST, 3.Out-Sourcing Technology Co., Ltd.)

[AHW23-P03] Isotope and water quality compositions of groundwater in the bedrock and sediment deposits in Kofu basin

*Ruri Isobe[1], Takashi Nakamura[2] (1.Interdisciplinary Center for River Basin Environment, University of YAMANASHI, 2.Interdisciplinary Centre for River Basin Environment, University of YAMANASHI)

[AHW23-P04] **The influence of weathering and hydrological cycles on Li isotopic compositions in river water and groundwater of the Ganges–Brahmaputra–Meghna River system in Bangladesh**

*Toshihiro Yoshimura[1], Daisuke Araoka[2], Hodaka Kawahata[3], Zakir Hossain[4], Naohiko Ohkouchi[1] (1.Japan Agency for Marine-Earth Science and Technology, 2.National Institute of Advanced Industrial Science and Technology, 3.Atmosphere and Ocean Research Institute, The University of Tokyo, 4.Jashore University of Science and Technology)

[AHW23-P05] Numerical modeling on the spatial distribution of d-excess values in river water in Japan

*Masaaki Takahashi[1], Hinako Shimizu[1], Akihiko Inamura[1], Noritoshi Morikawa[1] (1.The National Institute of Advanced Industrial Science and Technology)

[AHW23-P06] Temporal variation of stable isotopes in precipitation based on the intermittent sampling for 1998-2018 at Tiksi, northeastern Siberia

*Kimpei Ichiyanagi[1], Hotaek Park[2], Masahiro Tanoue[3] (1.Kumamoto University, 2.JAMSTEC, 3.National Institute for Environmental Studies)

[AHW23-P07] Tritium concentration in recent precipitation in central Japan

*Kazuyoshi Asai[1] (1.Geo Science Laboratory)

[AHW23-P08] An isotopic study on the role of groundwater in streamflow generation in the concrete-lined Nomi-gawa river, Ohta Ward, Tokyo, Japan

*Masaya Yasuhara[1], Seongwon Lee[1], Yuki Itoh[2], Akihiko Inamura[3], Noritoshi Morikawa[3], Takashi Nakamura[4] (1.Rissho University, 2.Saitama Agricultural Cooperatives, 3.Geological Survey of Japan, AIST, 4.University of Yamanashi)

[AHW23-P09] Inorganic nitrogen concentrations and nitrogen and oxygen isotope ratios of nitrate in shallow groundwater in an urban area, Shinagawa, Tokyo, Japan

*Yuki Itoh[1], Masaya Yasuhara[2], Seongwon Lee[2], Takashi Nakamura[3], Akihiko Inamura[4] (1.Saitama Agricultural Cooperatives, 2.Rissho Univ., 3.Yamanashi Univ., 4.Geological Survey of Japan, AIST)

[J] Poster | A (Atmospheric and Hydrospheric Sciences)：A-CG Complex & General

5:15 PM - 6:30 PM JST | 8:15 AM - 9:30 AM UTC | Ch.08_3

[A-CG38] Dynamics of Oceanic and Atmospheric Waves, Vortices, and Circulations

convener:Yuki Tanaka(Faculty of Marine Science and Technology, Fukui Prefectural University), Kunihiro Aoki(Japan Agency for Marine Earth Science and Technology), Yukiharu Hisaki(University of the Ryukyus), Norihiko Sugimoto(Keio University, Department of Physics)

[ACG38-P01] A statistical mechanics of phytoplankton diversity

*Kunihiro Aoki[1], Yoshio Masuda[2] (1.Japan Agency for Marine Earth Science and Technology, 2.Faculty of Environmental Earth Science, Hokkaido University)

[ACG38-P02] Essential spectrum of internal waves arising in rotating stratified fluid

*andrei giniatoulline[1] (1.Department of Mathematics, Los Andes University, Bogota, Colombia, South America)

[ACG38-P03] Statistical analysis of ocean waves in the sea of Japan

*Yukiharu Hisaki[1] (1.University of the Ryukyus)

[ACG38-P04] Observing system simulation experiments for new satellite observation missions on Venus

*Yukiko Fujisawa[1], Norihiko Sugimoto[1], Mirai Abe[1], Asako Hosono[2], Mimo Shirasaka[3], Hiroki Ando[4], Masahiro Takagi[4], Chi Ao[5], Itziar Garate Lopez[6], Sebastien Lebonnois[7], Tomotaka Yamamoto[8], Yosuke Kawabata[8], Satoshi Ikari[8], Takeshi Imamura[8], Masaru Yamamoto[9], Shin-ya Murakami[1], Masataka Imai[10], Toru Kouyama[10] (1.Keio University, 2.Toshimagaoka Women High School, 3.Seisen Senior High School, 4.Kyoto Sangyo University, 5.Jet Propulsion Laboratory, California Institute of Technology, 6.Bilboko Ingeniaritza Eskola (UPV/EHU), 7.Sorbonne Universite, 8.Tokyo University, 9.Research Institute for Applied Mechanics, Kyushu University, 10.National Institute of Advanced Industrial Science and Technology)

[J] Poster | H (Human Geosciences)：H-DS Disaster geosciences

5:15 PM - 6:30 PM JST | 8:15 AM - 9:30 AM UTC | Ch.09_1

[H-DS08] Human environment and disaster risk

convener:Tatsuto Aoki(School of Regional Development Studies, Kanazawa University), Hiroshi, P. Sato(College of Humanities and Sciences, Nihon University)

[HDS08-P01] The role of residents' resilience on the recovery process in a torrential rain

*Shoji Ohtomo[1], Reo Kimura[2] (1.Kanto Gakuin University, 2.University of Hyogo)

[HDS08-P02] Flood damage mapping of 2020 Typhoon Ulysses in the Philippines

*Naoko Nagumo[1], Kentaro Aida[1], Miho Ohara[1], Masakazu Fujikane[1] (1.International Centre for Water Hazard and Risk Management, PWRI)

[HDS08-P03] An example of using Google Earth Engine in providing and sharing information on wide-area typhoon disasters in international joint research projects

*Kentaro Aida[1], Naoko Nagumo[1], Miho Ohara[1] (1.International Centre for Water Hazard and Risk Management, PWRI)

[HDS08-P04] Estimating the amount of waste treatment units in the event of a disaster with self-help and mutual support

*Yoshinobu MIZUI[1,2] (1.University of Tsukuba, 2.NationalResearch Institute for Earth Science and Disaster Resilience)

[HDS08-P05] Possibility of support for disaster victims by accommodation facilities-Advance evacuation and acceptance in the event of a disaster-

Yuka SUZUKI[1], *Tatsuto Aoki[2] (1.Kanazawa University, 2.School of Regional Development Studies, Kanazawa University)

[HDS08-P06] Effect of synchrony bias on excitation of evacuation behavior during tsunami-From the evacuation behavior of residents in Noto Town, Ishikawa Prefecture during the 2019 Yamagata-oki Earthquake-

Mayu KITAMURA[1], *Tatsuto Aoki[2] (1.Kanazawa University, 2.School of Regional Development Studies, Kanazawa Univ.)

[HDS08-P07] Status of provision of disaster prevention information and learning to international students at national and public universities and their issues

*CHENYUE LU[1], Kiyomi HAYASHI[2], Tatsuto AOKI[2] (1. Division of Regional Development Studies,Graduate School of Human and Sociology-Environmental Studies,Kanazawa University, 2.School of Regional Development Studies, Kanazawa University)

[J] Poster | H (Human Geosciences)：H-TT Technology & Techniques

5:15 PM - 6:30 PM JST | 8:15 AM - 9:30 AM UTC | Ch.09_3

[H-TT19] Geographic Information System and Cartography

convener:Mamoru Koarai(Earth Science course, College of Science, Ibaraki University), Kazunari Tanaka(Department of Civil Engineering and Urban Design, Faculty of Engineering, Osaka Institute of Technology), W. Kazuhiko Nakamura(The University of Tokyo)

[HTT19-P01] Susceptibility assessment of post-seismic landslides with an index representative of seismic cracks

*Shui Yamaguchi[1], Mio Kasai[2] (1.Graduate School of Agriculture, Hokkaido University, 2.Research Faculty of Agriculture, Hokkaido University)

[HTT19-P02] Development of information platform for topographical recognition by CS topographic map

*Hiromu Daimaru[1], Kenichiro Toda[2], Wataru Murakami[1], Ryuichi Sekoguchi[3], Yoichi Kayama[3], Keichi Katsube[3], Hiroo Imaki[4], Koji Ijima[4], Ryosuke Wayama[5] (1.Forestry and Forest Products Research Institute, 2.Nagano Prefecture Forestry Research Center, 3.Aero Asahi Corporation, 4.Pacific Spatial Solutions Co., Ltd., 5.Northern System Service Co., Ltd.)

[J] Poster | H (Human Geosciences)：H-CG Complex & General

5:15 PM - 6:30 PM JST | 8:15 AM - 9:30 AM UTC | Ch.09_4

[H-CG26] Adaptation to climate change and its social implementation

convener:Hiroya Yamano(National Institute for Environmental Studies), Yoichi Ishikawa(JAPAN Agency for Marine-Earth Science and Technology), KOJI DAIRAKU(University of Tsukuba), Makoto Tamura(Global and Local Environment Co-creation Institute, Ibaraki University)

[HCG26-P01] ASSESSMENT OF WIND/SOLAR ENERGY POTENTIAL AS A POWER GENERATION SOURCES AT SOME SELECTED LOCATIONS IN PAKISTAN

*Muhammad Abid KHAN[1], KOJI DAIRAKU[1] (1.University of Tsukuba)

[J] Poster | H (Human Geosciences)：H-CG Complex & General

5:15 PM - 6:30 PM JST | 8:15 AM - 9:30 AM UTC | Ch.09_5

[H-CG29] Advanced life support systems with closed bio-ecosystems and thier applications

convener:Masanori Shinohara(Teikyo University of Science), Hiroshi Katoh(Division of Plant Functional Genomics, Advanced Science Research Promotion Center, Organization for the Promotion of Regional Innovation, Mie University), Shunta Kimura(Institute of Space and Astronautical Science / Space Exploration Innovation Hub Center, Japan Aerospace Exploration Agency), Midori Ong(University of Tsukuba)

[HCG29-P01] Growth of cyanobacterium, *Nostoc* sp. HK-01, after exposure to several harsh environments.

*Miku Tokita[1], Midori Ong[1], Hiroshi Katoh[2], Kaori Tomita-Yokotani[1] (1.University of Tsukuba, 2.University of Mie)

[HCG29-P02] Relationship between seed formation during tomato growth and microgravity generated by a hand-made 3D-clinostat.

*Yuan Takase[1], Kaori Totami-Yokotani[1] (1.University of Tsukuba)

[HCG29-P03] Identification of *Nostoc* sp. HK-01 proteins found in dry environment

*Hiroko Tanaka[1], Tomoko Abe[1], Hiroshi Katoh[2], Midori Ong[3], Kaori Tomita-Yokotani[3] (1.Graduate School of Science and Engineering, University of Tokyo Denki, 2.Organization for the Promotion of Regional Innovation, Mie University, 3.Faculty of Life and Environmental Sciences, University of Tsukuba)

[HCG29-P04] History of biological systems in closed-ecological systems

*Hiroshi Katoh[1] (1.Mie University)

[HCG29-P05] Advanced use of potatoes (*Solanum tuberosum* L.) for manned space activities

*Yota Tsukizaki[1], Toshisada Suzuki[2], Kaori Tomita-Yokotani[1] (1.University of Tsukuba, 2.Kagawa University)

[J] Poster | S (Solid Earth Sciences)：S-SS Seismology

5:15 PM - 6:30 PM JST | 8:15 AM - 9:30 AM UTC | Ch.10_1

[S-SS04] Earthquake prediction and forecast

convener:Shingo Watada(Division of Monitoring Science, Earthquake Research Institute, University of Tokyo), Masayuki Obayashi(Japan Agency for Marine-Earth Science and Technology)

[SSS04-P01] **Effects of Earth tides on the mainshock of the 2011 Tohoku Earthquake**

*Yoshiki SUE[1] (1.none)

[SSS04-P02] Statistical Study and Probability of Foreshocks on the Japan Mainland

*Hong Peng[1], James Mori[1] (1. Earthquake Hazards Division, Disaster Prevention Research Institute, Kyoto University)

[SSS04-P03] Comments on the Brownian Passage Time model for recurrent earthquakes with uncertain origin times

*Masajiro Imoto[1], Nobuyuki Morikawa[1], Hiroyuki Fujiwara[1] (1.National Research Institute for Earth Science and Disaster Resilience)

[SSS04-P04] Relationship between the Moderate Repeating Earthquakes and the Larger-scale Earthquakes on the trench side

*Masayuki Tanaka[1] (1.Meteorological Research Institute)

[SSS04-P05] Validation of forecast experiment on the Kamaishi repeating earthquakes based on numerical simulations

*Shingo Yoshida[1], Jun'ichi Fukuda[1], Toshihiro Igarashi[1] (1.Earthquake Research Institute, University of Tokyo)

[J] Poster | S (Solid Earth Sciences)：S-SS Seismology

5:15 PM - 6:30 PM JST | 8:15 AM - 9:30 AM UTC | Ch.10_2

[S-SS11] Strong Ground Motion and Earthquake Disaster

convener:Kazuhiro Somei(Geo-Research Institute), Yasuhiro Matsumoto(Kozo Keikaku Engineering)

[SSS11-P01] Elasto-plastic soil-water coupling seismic response analysis of a sedimentary basin with a three-dimensional geometry

*Toshihiro Noda[1], Tomohiro Toyoda[1], Shuhei Iwai[2], Akira Asaoka[3] (1.Disaster Mitigation Research Center, Nagoya University, 2.Graduate School of Engineering, Nagoya University, 3.Association for the Development of Earthquake Prediction)

[SSS11-P02] Identification of potential problems for disaster mitigation using “the Nankai Trough Earthquake Extra Information”, a new Japanese earthquake forecast information -how to communicate the "uncertainty" of science to society-

*Sayaka Irie[1], Ryu Ohtani[2], Mamoru Hyodo[3], Yoshinari Hayashi[4], Manabu Hashimoto[5], Takane Hori[6], Nobumasa Kawabata[7], Kunihiko Kumamoto[8], Takayoshi Iwata[9], Takashi Yokota[10], Kazunori Tanihara[11], Yo Fukushima[12] (1.NHK Broadcasting Culture Research Institute , 2.National Institute of Advanced Industrial Science and Technology, 3.Osaka Regional Headquarters, Japan Meteorological Agency, 4.Kansai University, 5.Disaster Prevention Research Institute, Kyoto University (DPRI), 6. Japan Agency for Marine-Earth Science and Technology (JAMSTEC) , 7.Crisis and Environment Management Policy Institute(CeMI), 8.Edogawa University, 9.Center for Integrated Research and Education of Natural Hazards,Shizuoka University, 10.Disaster Prevention Research Center,Aichi Institute of Technology, 11.Nippon Television Network, 12.International Research Institute of Disaster Science,Tohoku University, (IRIDeS))

[SSS11-P03] Research Project for Disaster Prevention on the great Earthquakes along the Nankai trough

*Shuichi Kodaira[1], Hiroyuki Fujiwara[2], Narumi Takahashi[1,2] (1. Japan Agency for Marine-Earth Science and Technology, 2.National Research Institute for Earth Science and Disaster Resilience)

[SSS11-P04] Formulas for using simple array to determine Love-wave characteristics based on rotational component of microtremors

*Ikuo Cho[1], Kunikazu Yoshida[2], Hirotoshi Uebayashi[3] (1.National Institute of Advanced Industrial Science and Technology, 2.Geo-Research Institute, 3.Institute for Integrated Radiation and Nuclear Science, Kyoto University)

[SSS11-P05] Assessment of applicability of a proposed method to estimate phase velocity using arbitrary 5-site arrays

*Huan Zhang[1], Kahori Iiyama[2], Hitoshi Morikawa[1] (1.Department of Civil and Environmental Engineering, Tokyo Institute of Technology, 2.KAJIMA Technical Research Institute)

[SSS11-P06] Comprehensive Research Project for the Nara-bonchi-toen Fault Zone

*Tomotaka Iwata[1] (1.Disaster Prevention Research Institute, Kyoto University)

[SSS11-P07] Small-aperture Microtremor Array Surveys in the Nara Basin, Japan

*Kimiyuki Asano[1], Tomotaka Iwata[1], Haruko Sekiguchi[1] (1.Disaster Prevention Research Institute, Kyoto University)

[SSS11-P08] Dense Microtremor Surveys on the Eastern Part of the Nara Basin, Japan

*Masayuki Yoshimi[1], Kimiyuki Asano[2], Tomotaka Iwata[2], Hiro Nimiya[1], Takeshi Sugiyama (1.Geological Survey of Japan, AIST, 2.DPRI, Kyoto Univ.)

[SSS11-P09] Microtremor characteristics and subsurface structure in the vicinity of the Shikano-Yoshioka Fault, Tottori, Japan

*Tatsuya Noguchi[1], Kazuki Kobayashi[2], Ryo Ashida[1], Isamu Nishimura[3], Takao Kagawa[1] (1.Faculty of Engineering, Tottori University, 2.Graduate School of Sustainability Science, Tottori University, 3.Graduate School of Engineering, Tottori University)

[SSS11-P10] Determination of 3-D subsurface structure model in central Tottori, Japan

*Tatsuya Noguchi[1], Masaki Yamamuro[1], Isamu Nishimura[2], Takao Kagawa[1] (1.Faculty of Engineering, Tottori University, 2.Graduate School of Engineering, Tottori University)

[SSS11-P11] Estimation of Subsurface Structure and Ground Motion Characteristics in the Landslide Areas from Microtremor Observations – Case of Nawashiro and Amedaki, Kokufu-cho, Tottori City –

*Isamu Nishimura[1], Atsushi Shimada[2], Tatsuya Noguchi[2], Takao Kagawa[2] (1.Graduate School of Engineering Department of Social Infrastructure Engineering, Tottori University, 2.Social Systems and Civil Engineering, Department of Engineering, Tottori University)

[SSS11-P12] Modeling of subsurface velocity structures from seismic bedrock to ground surface for Yamanashi region

*Shigeki Senna[1], Atsushi Wakai[1], Yatagai Atsushi[2], Tadashi Sato[2], Hisanori Matsuyama[2], Hiroyuki Fujiwara[1] (1.National Research Institute for Earth Science and Disaster Resilience, 2.OYO Corporation)

[SSS11-P13] Modeling of subsurface velocity structures from seismic bedrock to ground surface for Kumamoto region

*Shigeki Senna[1], Atsushi Wakai[1], Yatagai Atsushi[2], Yoshiaki Inagaki[2], Hisanori Matsuyama[2], Hiroyuki Fujiwara[1] (1.National Research Institute for Earth Science and Disaster Resilience, 2.OYO Corporation)

[SSS11-P14] Basic study of a real-time damage estimation system for liquefaction

*Shohei Naito[1], Hiromitsu Nakamura[1], Shigeki Senna[1], Yoshinori Iwanami[2] (1.National Research Institute for Earth Science and Disaster Resilience, 2.MITSUBISHI SPACE SOFTWARE CO.,LTD.)

[SSS11-P15] Estimation of subsurface motion from surface seismic records: investigation on evaluation at deep levels

*Tomotsugu Watanabe[1], Hiroshi Takenaka[1], Masanao Komatsu[1], Mitsutaka Oshima[2] (1.Okayama University , 2.Shimizu Corporation)

[SSS11-P16] Estimation of seismic ground motions on the surface ground at MeSO-net stations

*Atsushi Wakai[1], Shigeki Senna[1] (1.National Research Institute for Earth Science and Disaster Resilience)

[SSS11-P17] Strong motion simulation of an intraslab earthquake beneath Kanto region using MeSO-net observation data

*Wataru Suzuki[1], Takeshi Kimura[1], Hisahiko Kubo[1], Takayuki Miyoshi[1] (1.National Research Institute for Earth Science and Disaster Resilience)

[SSS11-P18] Ground-motion simulation for the 2016 Kumamoto earthquake (Mj7.3) based on the strong-motion prediction recipe

*Asako Iwaki[1], Nobuyuki Morikawa[1], Takahiro Maeda[1], Hiroyuki Fujiwara[1] (1.National Research Institute for Earth Science and Disaster Prevention)

[SSS11-P19] Characterized source model of M7.3 2016 Kumamoto eq. by 3D reciprocity GFs inversion with special reference to velocity pulse at KMMH16

*Anatoly Petukhin[1], Hiroshi Kawase[2], Fumiaki Nagashima[2], Eri Ito[2] (1.Geo-Research Institute, 2.DPRI, Kyoto University)

[SSS11-P20] Evaluation of near-source ground motion during the 2008 Iwate-Miyagi Nairiku earthquake by using stochastic slip models and three-dimensional velocity structures

*Takeshi Nakamura[1], Masataka Sawada[1] (1.Central Research Institute of Electric Power Industry)

[SSS11-P21] **Source rupture process of the 2018 Hokkaido eastern Iburi earthquake estimated from waveform inversion with empirical Green's functions**

*SHUANGLAN WU[1], Atsushi Nozu[1], Yosuke Nagasaka[1] (1.PORT AND AIRPORT RESEARCH INSTITUTE)

[SSS11-P22] Calibrating Thailand's local magnitude scale: a preliminary result

*Mongkolchai Sukmee[1], Sutthipong Noisagool[1,2], Satoru Tanaka[3], Weerachai Siripunvaraporn[1,2], Songkhun Boonchaisuk[4,2], Yasushi Ishihara[5], Taewoon Kim[6], Hitoshi Kawakatsu[7], Nozomu Takeuchi[7], Kenji Kawai[8], Yuki Suzuki[8] (1.Department of Physics, Faculty of Science, Mahidol University , 2.Thailand Center of Excellence in Physics, Ministry of Higher Education, Science, Research and Innovation, 3.Volcanoes and Earth's Interior Research Center (VERC), Research Institute for Marine Geodynamics (IMG), Japan Agency for Marine-Earth Science and Technology (JAMSTEC), 4.Geoscience Program, Mahidol University, Kanchanaburi Campus, 5.Research Institute for Marine Geodynamics (IMG), Japan Agency for Marine-Earth Science and Technology (JAMSTEC), 6.Subduction Dynamics Research Center (SDR), Research Institute for Marine Geodynamics (IMG), Japan Agency for Marine-Earth Science and Technology (JAMSTEC), 7.Earthquake Research Institute, The University of Tokyo, 8.Department of Earth and Planetary Science, School of Science, The University of Tokyo)

[SSS11-P23] Strong ground motion simulation of the Fukushima-ken Oki earthquake of February 13, 2021 (M_J 7.3)

*Yosuke Nagasaka[1] (1.Port and Airport Research Institute)

[SSS11-P24] Strong Motion Generation Area for the 2021 off Fukushima, Japan, Earthquake Estimated based on the Empirical Green's Function Method

*Kazuhiro Somei[1], Ken Miyakoshi[1] (1.Geo-Research Institute)

[J] Poster | S (Solid Earth Sciences)：S-EM Earth's Electromagnetism

5:15 PM - 6:30 PM JST | 8:15 AM - 9:30 AM UTC | Ch.11_1

[S-EM13] Geomagnetism, paleomagnetism and rock magnetism

convener:Chie Kato(Faculty of Social and Cultural Studies, Kyushu University), Tetsuro Sato(Earthquake Research Institute, The University of Tokyo)

[SEM13-P01] Brunhes-Matuyama geomagnetic reversal record from Terasaki, Boso Peninsula

*Hirokuni Oda[1], Hiroomi Nakazato[2], Futoshi Nanayama[1], Yumiko Harigane[1] (1.Institute of Geology and Geoinformation, Geological Survey of Japan, AIST, 2.National Agriculture and Food Research Organization)

[SEM13-P02] Plaeomagnetic study of the Kusatsu-Shirane volcano, Gunma, Japan

*Nagisa Sawada[1], Nobuko Kametani[2], Kazuo Kawasaki[1], Yasuo Ishizaki[1], Akihiko Terada[3] (1.University of Toyama, 2.Mount Fuji Research Institute, Yamanashi Prefectural Government, 3.Tokyo Institute of Technology)

[SEM13-P03] The Laschamp and a new post-Laschamp excursions repeating directional swings from Lake Suigetsu varved sediments

*Masayuki Hyodo[1,2], Takeshi Nakagawa[3], Hayato Matsushita[2], Ikuko Kitaba[3], Keitaro Yamada[3], Shota Tanabe[2], Balazs Bradak[1,4], Danielle McLean[5], Richard A. Staff[6], Victoria C. Smith[5], Paul G. Albert[5], Akiteru Yamasaki[7], Junko Kitagawa[8,7] (1.Research Center for Inland Seas, Kobe University, 2.Department of Planetology, Kobe University, 3.Research Centre for Palaeoclimatology, Ritsumeikan University, 4.Department of Physics, University of Burgos, 5.School of Archaeology, University of Oxford, 6.Scottish Universities Environmental Research Centre (SUERC), University of Glasgow, 7.Fukui Prefectural Satoyama-Satoumi Research Institute, 8.Varve Museum)

[SEM13-P04] Rock-magnetic properties of topmost sediments in Omura Bay, Nagasaki Prefecture

*Naoto Ishikawa[1], Yoriko Yokoo[2], Kazumi Matsuoka[3] (1.Faculty of Sustainable Design, Toyama University, 2.Faculty of Scinece and Engineering, Doshisha University, 3.Institute for East China Sea Research, Nagasaki University)

[SEM13-P05] Paleomagnetic Dating on Tsunami Boulders from the Kingdom of Tonga

*Tetsuro Sato[1], Norihiro Nakamura[2], Hiroyuki Nagahama[3], Masahiko Sato[4], Kazuhisa Goto[4], Masashi Watanabe[5], Akira Ikeda[3], Kenji Satake[1], Taaniela Kula[6] (1.Earthquake Research Institute, The University of Tokyo, 2.Institute for Excellence in Higher Education, Tohoku University, 3.Department of Earth Science, Tohoku University, 4.Department of Earth and Planetary Science, The University of Tokyo, 5.Faculty of Science and Engineering, Chuo University, 6.Ministry of Lands and Natural Resources)

[SEM13-P06] Influence of biogenic magnetite on paleointensity estimations inferred from FORC-PCA of sediments from the western equatorial Pacific

Kosuke Inoue[1], *Toshitsugu Yamazaki[1], Yoichi Usui[2] (1.Atmosphere and Ocean Research Institute, The University of Tokyo, 2.Japan Agency for Marine-Earth Science and Technology)

[SEM13-P07] Solitary magnetostrophic Rossby waves

*Kumiko Hori[1,2], Steve M Tobias[2], Chris A Jones[2] (1.Graduate School of System Informatics, Kobe University, 2.Department of Applied Mathematics, University of Leeds)

[SEM13-P08] Effects of driving mode of convection on a spherical dynamo action with a small inner core

*Futoshi Takahashi[1], Hinami Taniguchi[2] (1.Faculty of Science, Kyushu University, 2.School of Science, Kyushu University)

[SEM13-P09] Rock-magnetic and mineralogical properties of the exsolved magnetite in plagioclase crystal

*Masahiko Sato[1], Masashi Ushioda[2], Ryoichi Nakada[3], Yujiro Tamura[4], Shinji Yamamoto[4] (1.The University of Tokyo, 2.Shikoku Research Institute Inc., 3.Japan Agency for Marine-Earth Science and Technology, 4.Yohohama National University)

[SEM13-P10] Rock-magnetic properties of isocubanite from submarine hydrothermal deposits in the Okinawa Trough

*Chie Kato[1], Masao Ohno[1], Yoshihiro Kuwahara[1], Tadahiro Hatakeyama[2], Yasuhiro Yamada[3], Shuhei Totsuka[4], Kazuhiko Shimada[1], Jun-ichiro Ishibashi[1], Toshiro Nagase[5] (1.Kyushu University, 2.Okayama University of Science, 3.Tokyo University of Science, 4.National Institute of Advanced Industrial Science and Technology, 5.Tohoku University)

[SEM13-P11] Contribution of equatorially antisymmetric buoyancy to polarity reversals in geodynamo models

*Takumi Kera[1], Hiroaki Matsui[3], Masaki Matsushima[2], Yuki Nishida[1], Yuto Katoh[1] (1.Department of Geophysics, Graduate School of Science, Tohoku University, 2.Tokyo Institute of Technology, 3.Dept. of Earth and Planetary Sciences, University of California, Davis)

[SEM13-P12] **Simultaneous observation of the geomagnetic field at different sites using two SQUID magnetometer systems**

*Jun Kawai[1], Miki Kawabata[1], Masakazu Miyamoto[1] (1.Applied Electronics Laboratory, Kanazawa Institute of Technology)

[J] Poster | S (Solid Earth Sciences)：S-MP Mineralogy & Petrology

5:15 PM - 6:30 PM JST | 8:15 AM - 9:30 AM UTC | Ch.12_1

[S-MP25] Deformed rocks, Metamorphic rocks and Tectonics

convener:Yumiko Harigane(Geological Survey of Japan, National Institute of Advanced Industrial Science and Technology (AIST)), Yoshihiro Nakamura(Geological Survey of Japan, National Institute of Advanced Industrial Science and Technology)

[SMP25-P01] Multiple igneous activities recorded in the Nidar ophiolite complex, eastern Ladakh

*Akinori Sato[1], Takeshi Imayama[1], Dripta Dutta[2] (1.Okayama University of Science, 2.Indian Institute of Technology Bombay)

[SMP25-P02] Geology and missing tectonics in the Inashi-Hase area of the eastern part of the Ryoke belt, central Japan

*Akira Ono

[SMP25-P03] Kinematics of North Almora Thrust estimated from mylonite, India

*Hirotoshi Kotama[1], Jun-ichi Ando[1], Kaushik Das[1], Dyuti Prakash Sarkar[1] (1.Hiroshima University)

[SMP25-P04] Illite crystallization and faulting caused by hydrothermal fluid

*Jun-ichi Ando[1], Kota Kojima[1], Kaushik Das[1], Naotaka Tomioka[2], Seiichiro Uehara[3] (1.Department of Earth and Planetary Systems Science, Hiroshima University, 2.Kochi Institute for core sample research, Japan Agency for Marine-Earth Science and Technology, 3.The Kyushu university museum)

[SMP25-P05] Episodic fluid explosion in shallow and middle crust revealed by hydrothermal brecciation

*Geri Agroli[1], Atsushi Okamoto[1], Masaoki Uno[1], Noriyoshi Tsuchiya[1] (1.Tohoku University)

[SMP25-P06] Pseudotachylyte in a marble from the Takine Group (Abukuma Terrane) and its similarity to pseudotachylyte from the Higo Mertamorphic Rocks

*Tadao Nishiyama[1], Ebo Adou Douha[1] (1.Department of Earth and Environmental Sciences, School of Science, Graduate School of Science and Technology, Kumamoto University)

[SMP25-P07] **Frictional melting process during formation of pseudotachylyte, Sarwar-Junia fault zone, India**

*Jun-ya Okazaki[1], Jun-ichi Ando[1], Kaushik Das[1] (1.Earth and Planetary Systems Science Program, Division of Advanced Science and Engineering, Hiroshima University)

[SMP25-P08] Neoarchean magmatism and Paleoproterozoic high-pressure granulite-facies metamorphism from the southern Motloutse Complex, eastern Botswana: Implications for the western extension of the Central Zone of the Limpopo Complex

*Thembiso Otladisang Basupi[1,2], Toshiaki Tsunogae[1,3], Kazuki Takahashi[1], Yukiyasu Tsutsumi[4] (1.Graduate of Life and Environmental Sciences, University of Tsukuba, 2.Department of Earth and Environmental Sciences, Botswana International University of Science and Technology, 3.Department of Geology, University of Johannesburg, 4.Department of Geology and Paleontology, National Museum of Nature and Science)

[SMP25-P09] Petrography of a sulfide-rich garnet-sillimanite-biotite gneiss from Brattnipene, Sør Rondane Mountains, East Antarctica

*Hayato Ikeda[1], Tetsuo Kawakami[1] (1.Kyoto University)

[SMP25-P10] Microstructural characteristics of ultra-high pressure metamorphic rocks from the Dabie-Shan, eastern China

*Katsuyoshi Michibayashi[1], Kouhei Asano[1] (1.Department of Earth and Planetary Sciences, Graduate School of Environmental Studies, Nagoya University)

[SMP25-P11] Metamorphic history of the Suo metamorphic rocks inferred from two-stage garnet in pelitic schist

*Shunsuke Endo[1], Maki Ito[1] (1.Department of Earth Science, Interdisciplinary Faculty of Science and Engineering, Shimane University)

[SMP25-P12] Hidden intact coesite in deeply subducted rocks and its geological implications

*Tomoki Taguchi[1], Yui Kouketsu[2], Yohei Igami[3], Tomoyuki Kobayashi[4], Akira Miyake[3] (1.Department of Earth Sciences, Faculty of Education and Integrated Arts and Sciences, Waseda University, 2.Department of Earth and Planetary Science, Graduate School of Environmental Studies, Nagoya University, 3.Department of Geology and Mineralogy, Graduate School of Science, Kyoto University, 4.Faculty of Health and Sports, Nagoya Gakuin University)

[SMP25-P13] Metamorphic zoning and *P–T* conditions of contact metamorphic rocks in the Unai area, Yamaguchi prefecture, Japan.

*Kakeru Sakamoto[1], Toshiaki Shimura[1] (1.Graduate School of Sciences and Technology for Innovation, Yamaguchi University)

[SMP25-P14] Progressive metamorphism of the Ryoke metamorphic rocks from No-jima Island, South of Yamaguchi Prefecture

*ZEJIN LU[1] (1.Graduate School of Science and Engineering for Innovation, Yamaguchi University)

[SMP25-P15] *P–T–t* path of Ryoke metamorphic rocks in Kitsuki area, Kunisaki Peninsula, Oita prefecture, Japan.

*Kentaro Mutabaru[1], Toshiaki Shimura[1] (1.Yamaguchi University)

[SMP25-P16] *P-T* estimations of Ryoke metamorphic rocks in the Takato-Ohshika area, Nagano, Japan

*Yoshihiro Nakamura[1], Kazuhiro Miyazaki[1], Yutaka Takahashi[1] (1.Geological Survey of Japan, National Institute of Advanced Industrial Science and Technology)

[SMP25-P17] Ultrahigh-temperature HP granulite facies stage of the Early Jurassic pre-Sanbagawa metamorphism

*Kenta Yoshida[1], Sota Niki[3], Hikaru Sawada[1], Ryosuke Oyanagi[1], Takafumi Hirata[3], Kenji Asakura[2], Takao Hirajima[2] (1.Japan Agency for Marine-earth Science and Technology, 2.Kyoto University, 3.The University of Tokyo)

[SMP25-P18] **Meliorating the spatial resolution of SEM-EBSD**

*Thomas Jing Yi Yeo[1], Norio Shigematsu[1] (1.Research Institute of Earthquake and Volcano Geology, Geological Survey of Japan, National Institute of Advanced Industrial Science and Technology)

[SMP25-P19] Strain in quartz inclusion probed by Raman spectroscopy

*Yui Kouketsu[1], Yuki Tomioka[1], Tomoki Taguchi[2] (1.Department of Earth & Planetary Sciences, Graduate School of Environmental Studies, Nagoya University, 2.Department of Earth Sciences, Faculty of Education and Integrated Arts and Sciences, Waseda University)

[J] Poster | S (Solid Earth Sciences)：S-MP Mineralogy & Petrology

5:15 PM - 6:30 PM JST | 8:15 AM - 9:30 AM UTC | Ch.12_2

[S-MP26] Physics and Chemistry of Minerals

convener:Masahiro KAYAMA(Department of General Systems Studies, Graduate School of Arts and Sciences, The University of Tokyo), Itaru Ohira(Department of Chemistry, Faculty of Science, Gakushuin University)

[SMP26-P01] Pressure-induced phase transitions in wülfingite (Zn(OH)2): Raman spectroscopic and First-principles study

*Masami Kanzaki[1], Longli Guan[1], Ran Wang[1] (1.Institute for Planetary Matereials, Okayama University)

[SMP26-P02] Elastic wave velocity of ε-FeOOH across the pressure-induced spin transition of iron

*Osamu Ikeda[1], Tatsuya Sakamaki[1], Hiroshi Fukui[2,3], Hiroshi Uchiyama[4], Alfred Q.E. Baron[3,4], Akio Suzuki[1] (1.Department of Earth Science, Graduate School of Science, Tohoku University, 2.Graduate School of Material Science, University of Hyogo, 3.RIKEN SPring-8 Center, 4.Japan Synchrotron Radiation Research Institute)

[SMP26-P03] Phase transition of M3+OOH-type oxyhydroxides under high pressure

*Akio Suzuki[1] (1.Department of Earth Science, Graduate School of Science, Tohoku University)

[SMP26-P04] Density measurement of silicate melt by the buoyancy test under high pressure

*Akio Suzuki[1] (1.Department of Earth Science, Graduate School of Science, Tohoku University)

[SMP26-P05] Structural study on the $Ca_2MgAl_2Si_4O_{14}$ composition melt under pressure

*Natsumi Adachi[1], Satoru Urakawa[1], Hidenori Terasaki[1] (1.OKAYAMA UNIVERSITY)

[SMP26-P06] Unique luminescence of rhodochrosite at low temperature

*Reina Masuda[1], Ayane Asano[1], Nobuhiro Kusano[1], Hirotsugu Nishido[1] (1.Biosphere-Geosphere Science, Okayama University of Science)

[SMP26-P07] Amesite and Al-serpentine accompanied with the serpentinite in Yakiyama, Iizuka, Fukuoka

*Yuki Isshiki[1], Seiichiro Uehara[2], Yuya Takeda[1] (1.Department of Earth and Planetary Sciences Faculty of Science, Kyushu University, 2.The Kyushu University Museum)

[SMP26-P08] Phase transitions and pressure calibration points

*Shigeaki Ono[1] (1.Japan Agency for Marine-Earth Science and Technology)

[SMP26-P09] The study on stability and properties of N-doped spinel Based on CGCNN and DFT

*SOK I TAM[1], CHI PUI TANG[1], Pak Kin Leong[1], Kin Tak U[1] (1.Macau University of Science and Technology)

[J] Poster | S (Solid Earth Sciences)：S-VC Volcanology

5:15 PM - 6:30 PM JST | 8:15 AM - 9:30 AM UTC | Ch.13_1

[S-VC27] Mitigation of volcanic disasters - basic and applied researches

convener:Shinji Takarada(Geological Survey of Japan, National Institute of Advanced Industrial Science and Technology), Mitsuhiro Yoshimoto(Mount Fuji Research Institute, Yamanashi Prefectural Government), Tatsuro Chiba(Asia Air Survey Co., Ltd.), Yousuke Miyagi(National Research Institute for Earth Science and Disaster Resilience)

[SVC27-P01] Disaster-stricken vehicles dug up for the first time in 30 years and characteristics of pyroclastic surge deposits in 1991 on Unzen Volcano

*Daisuke Nagai[1], Shinichi Sugimoto[2] (1.Mt.Unzen disaster memorial hall, 2.Unzen volcanic area global geopark)

[SVC27-P02] Selective pulverization of pumiceous groundmass in pumice pulverization processes in a laboratory

*Shingo Takeuchi[1] (1.Central Research Institute of Electric Power Industry, Civil Engineering Research Laboratory, Geosphere Sciences)

[SVC27-P03] A case of sediment-related disaster in a volcanic area due to an earthquake off the coast of Fukushima Prefecture on February 13, 2021

*Takayama Toko[1], Tatsuro Chiba[1], Hiromichi Moriike[1], Tatsuya Ochiai[1] (1.Asia Air Survey Co.,Ltd.)

[SVC27-P04] Accelerating Two-Dimensional Lava Flow Simulations with OpenACC

*Yasuhiro Ishimine[1] (1.Mount Fuji Research Institute, Yamanashi Prefectural Government)

[SVC27-P05] Present situation of water pollution problem caused by 2018 Iwo-Yama volcano eruption in Kirishima volcanic complex

*Yoshikazu Kikawada[1], Haruka Yamamoto[2] (1.Faculty of Science and Technology, Sophia University, 2.Graduate School of Science and Technology, Sophia University)

[SVC27-P06] Training program of the human resource development for volcanic disaster management officers in JAPAN -Preliminary report-

*Kenji Niihori[1], Akio Sato[1], Maokoto Konno[1], Mitsuhiro Yoshimoto[2] (1.Organization of Volcanic Disaster Mitigation, NPO., 2.Mount Fuji Research Institute, Yamanashi Prefectural Government)

[SVC27-P07] Experiment for understanding of climber’s movement and tendency in Nasu Volcano

*Yousuke Miyagi[1], Mitsuhiro Yoshimoto[2], Yasuhiro Ishimine[2], Ryo Honda[2], Tomohiro Kubo[2] (1.National Research Institute for Earth Science and Disaster Resilience, 2.Mount Fuji Research Institute, Yamanashi Prefectural Government)

[SVC27-P08] **Eruption Sequences and Precursory Activities of Large-scale Volcanic Eruptions, and Construction of Large-scale Volcanic Eruption Database**

*Shinji Takarada[1], Yasuaki Kaneda[1], Fumihiko Ikegami[1], Yuki Nishino[1], Nobuo Geshi[1] (1.Geological Survey of Japan, National Institute of Advanced Industrial Science and Technology)

[J] Poster | S (Solid Earth Sciences)：S-VC Volcanology

5:15 PM - 6:30 PM JST | 8:15 AM - 9:30 AM UTC | Ch.13_2

[S-VC29] Hydrothermal systems of volcanoes

convener:Yasuhiro Fujimitsu(Department of Earth Resources Engineering, Faculty of Engineering, Kyushu University), Wataru Kanda(Volcanic Fluid Research Center, School of Science, Tokyo Institute of Technology), Takeshi Ohba(Department of chemistry, School of Science, Tokia University)

[SVC29-P01] Groundwater composition around the Aso caldera: multivariate statistical analysis and its implications for independent variables and geographical variations

*Hikaru Iwamori[1], Hitomi Nakamura[2], Noritoshi Morikawa[2], Masaaki Takahashi[2], Akihiko Inamura[2], Satoru Haraguchi[1], Tatsuji Nishizawa[3], Shuhei Sakata[1] (1.Earthquake Research Institute, The University of Tokyo, 2.AIST, 3.TITECH)

[SVC29-P02] Temporal variation of chemical composition of hot spring waters at Ebinokogen Ioyama Volcano in Kirishima Volcanic Group

*Keigo Mori[1], Jun-ichiro Ishibashi[1], Takeshi Matsushima[1], Harue Masuda[2], Syogo Oshima[3], Saki Tsutsumi[3], Yasuhisa Tajima[4] (1.Graduate School of Science, Kyushu University, 2.Graduate school of Science, Osaka City University, 3.West Japan Engineering Consultants, Inc,, 4.Nippon Koei Co., Ltd,)

[SVC29-P03] Temporal variations of helium and carbon isotopic compositions of fumarolic gases from Kusatsu-Shirane volcano

*Tomoya Obase[1], Hirochika Sumino[1], Kotaro Toyama[1], Takeshi Ohba[2], Muga Yaguchi[3], Akihiko Terada[4] (1.Department of General Systems Studies, Graduate School of Arts and Sciences, University of Tokyo, 2.Department of chemistry, School of Science, Tokai University, 3.Meteorological Research Institute, Japan Meteorological Agency, 4.Volcanic Fluid Research Center, Tokyo Institute of Technology)

[SVC29-P04] Change in fluoride ion concentration in Bandaiko hot spring at east flank of Kusatsu-Shirane volcano and its relationship with volcanic activity

*Haruka Yamamoto[1], Yoshikazu Kikawada[2] (1.Graduate School of Sophia University, 2.Faculty of Science and Technology, Sophia University)

[SVC29-P05] Volcanic ash from the June 17, 1962 eruption of Yakedake volcano, and its water-soluble components

*Muga Yaguchi[1], Yasuo Hirayama[2], Takeshi Ohba[3], Nozomi Numanami[3] (1.Meteorological Research Institute, JMA, 2.Nagano Meteorological Office, JMA, 3.School of Science, Tokai University)

[SVC29-P06] Tectonic controlled and hydrothermal alterations of geothermal reservoirs in El Salvador

*JOSE ANIBAL ERAZO[1], Noriyoshi Tsuchiya[1], Masaoki Uno[1], Arturo Quezada[2], Pedro Antonio Santos[2], Ryoichi Yamada[1], Hiroyuki Yamagishi[1], Shinichi Yamasaki[1], Alvaro Josue Amaya[3] (1.Graduate school of environmental studies , 2.LaGeO _ El Salvador, 3.UES _ El Salvador)

[SVC29-P07] **DAS-Seismic and temperature data acquisition using DAS and DTS measurements at the Ohnuma, geothermal field, Tohoku, Japan**

*Junzo Kasahara[1,2], Yoko Hasada[1,3], Kuzume Haruyasu[1], Hitoshi Mikada[4], Yoshihiro Fujise[5] (1.ENAA, 2.Shizuoka University, 3.Daiwa Exploration and Consulting Co. Ltd., 4.Graduate School of Kyoto University, 5.WELMA)

[SVC29-P08] **Ground surface Heat balance measurements at Izu-Oshima volcano**

*Shin'ya Onizawa[1], Nobuo Matsushima[2] (1.Volcanology Research Department, Meteorological Research Institute, JMA, 2.Geological Survey of Japan, National Institute of Advanced Industrial Science and Technology)

[SVC29-P09] Behavior of magmatic hydrothermal system of Kusatsu-Shirane Volcano inferred from numerical simulations

*Yasuo Matsunaga[1], Wataru Kanda[1] (1.School of Science, Tokyo Institute of Technology)

[SVC29-P10] Comprehension of hydrothermal systems in the East African Rift System –Collaborative Research with Kenya by SATREPS–

*Yasuhiro Fujimitsu[1], Jun Nishijima[1], Takeshi Tsuji[1], Kotaro Yonezu[1], Tatsuya Wakeyama[2], Ryuichi Itoi[3] (1.Department of Earth Resources Engineering, Faculty of Engineering, Kyushu University, 2.Platform of Inter-/Transdisciplinary Energy Research, Kyushu University, 3.School of Engineering, Kyushu University)

[J] Poster | S (Solid Earth Sciences)：S-CG Complex & General

5:15 PM - 6:30 PM JST | 8:15 AM - 9:30 AM UTC | Ch.15_3

[S-CG44] Petrology, Mineralogy & Resource Geology

convener:Koichi Momma(National Museum of Nature and Science), Yu Nishihara(Geodynamics Research Center Ehime University), Tatsuo Nozaki(Submarine Resources Research Center, Research Institute for Marine Resources Utilization, Japan Agency for Marine-Earth Science and Technology), Nobutaka Tsuchiya(Department of Geology, Faculty of Education, Iwate University)

[SCG44-P01] Intrusive and emplacement process of the Tono plutonic complex: Constraints from dating and isotopic analysis of zircons

*Yasuhiro Ogita[1], Kazusa Sando[2], Kozue Ishibashi[3], Shuhei Sakata[4], Takeshi Ohno[5], Satoshi Suzuki[3], Tatsunori Yokoyama[1], Saya Kagami[1], Mitsuhiro Nagata[1], Takashi Yuguchi[2] (1.Tono Geoscience Center, Japan Atomic Energy Agency, 2.Faculty of Science, Yamagata University, 3.Graduate school of Science and Engineering, Yamagata University, 4.Earthquake Research Institute, University of Tokyo, 5.Faculty of Science, Gakushuin University)

[SCG44-P02] Whole-rock chemical composition of the Nojima granodiorite in northern part of Awaji Island, southwestern Japan

*Akihiro Ishihara[1], Motohiro Tsuboi[1] (1.Kwansei Gakuin University)

[SCG44-P03] Influence of inclusions on hydrogen generated during low temperature serpentinization

*Asuka Sugawara[1], Ryohei Kawakita[1], Tsubasa Otake[2], Tsutomu Sato[2] (1.Graduate school of Engineering, Hokkaido University, 2.Faculty of Engineering, Hokkaido University)

[SCG44-P04] **Detailed characteristics of Raman spectra of carbonaceous materials in fault rocks nearby the Median Tectonic Line**

*Hiroshi Mori[1], Yuki Nobe[1], Ken Yamaoka[2], Yosuke Tomooka[1], Yui Kouketsu[3], Tetsuya Tokiwa[1] (1.Shinshu University, 2.The University of Tokyo, 3.Nagoya University)

[SCG44-P05] Trace element composition of chromian spinel in the Sanbagawa ultramafic rocks

*Yuki Aoshima[1], Yuji Ichiyama[1], Jung-Woo Park[2] (1.Chiba University, 2.Seoul National University)

[SCG44-P06] The trace element composition of sapphire in the xenolith of garnet-bearing andesitic tuff of the Donzurubo Formation, the Nijo Group, Japan.

*Mayuko Fukuyama[1], Masatsugu Ogasawara[2] (1.Graduate School of Engineering Science, Akita University, 2.Geological Survey of Japan, National Institute of Advanced Industrial Science and Technology)

[SCG44-P07] **Microstructures of spherical pyrite in the Kuroko deposits: possible mechanism of pyrite growth on bubble**

*Atsushi Okamoto[1], Yoeri van de Ridder[2], Oliver Plumper[2], Markus Ohl[2], Ryoichi Yamada[1] (1.Tohoku University, 2.Utrecht University)

[SCG44-P08] **The mineral occurrence of kaolinitic saprolite beneath the sedimentary kaolin deposit at Seto district**

*Haruna Asai[1], Kikuchi Ryosuke[1], Tsubasa Otake[1], Tsutomu Sato[1] (1.Hokkaido University)

[SCG44-P09] Borate concentration processes in modern evaporitic and hydrothermal environments: Constraints on the formation of a boron-rich environment on prebiotic earth

*Sara Rinka Christensen [1], Akizumi Ishida[1], Takeshi Kakegawa[1] (1.Department of Earth Science, Graduate School of Science, Tohoku University)

[SCG44-P10] Experimental study on propagation of elastic wave in supercritical geothermal reservoirs

*Katsuya Mizuno[1], Noriyoshi Tsuchiya[1], Nobuo Hirano[1] (1.Tohoku university)

[J] Poster | S (Solid Earth Sciences)：S-CG Complex & General

5:15 PM - 6:30 PM JST | 8:15 AM - 9:30 AM UTC | Ch.16_1

[S-CG53] Reducing risks from earthquakes, tsunamis & volcanoes: new applications of realtime geophysical data

convener:Masashi Ogiso(Meteorological Research Institute, Japan Meteorological Agency), Masumi Yamada(Disaster Prevention Research Institute, Kyoto University), Yusaku Ohta(Research Center for Prediction of Earthquakes and Volcanic Eruptions, Graduate School of Science, Tohoku University), YAMAMOTO Naotaka CHIKASADA(National Research Institute for Earth Science and Disaster Resilience)

[SCG53-P01] High precision of Realtime tsunami prediction based on the amplification

*Narumi Takahashi[1], Kentaro Imai[2] (1.National Research Institute for Earth Science and Disaster Resilience, 2.Japan Agency for Marine-Earth Science and Technology)

[SCG53-P02] Generation Requirements of PL Waves for Shallow Earthquakes around Japan-Possibility of Immediate Tsunami Prediction

*Keishi Osuga[1], Takashi Furumura[1] (1.Department of Earth and Planetary Science, School of Science, The University of Tokyo)

[SCG53-P03] Evaluation of simple source time function in rapid source parameter determination system (AQUA)

*Hisanori Kimura[1], Youichi Asano[1] (1.National Research Institute for Earth Science and Disaster Resilience (NIED))

[J] Poster | S (Solid Earth Sciences)：S-CG Complex & General

5:15 PM - 6:30 PM JST | 8:15 AM - 9:30 AM UTC | Ch.16_2

[S-CG54] Ten years from the 2011 Tohoku Earthquake: A milestone of Solid Earth Science

convener:Ryota Hino(Graduate School of Science, Tohoku University), Shuichi Kodaira(Research Institute of Marine Geodynamics, Japan Agency for Marine-Earth Science and Technology), Toru Matsuzawa(Research Center for Prediction of Earthquakes and Volcanic Eruptions, Graduate School of Science, Tohoku University), Takeshi Iinuma(National Research and Development Agency Japan Agency for Marine-Earth Science and Technology)

[SCG54-P01] Ground motion waveforms in the epicentral area of the 2011 Tohoku-Oki earthquake with large displacements, retrieved from ocean-bottom dynamic pressure change data

*Tatsuya Kubota[1], Tatsuhiko Saito[1], Hiroaki Tsushima[2], Ryota Hino[3], Yusaku Ohta[3], Syuichi Suzuki[3], Daisuke Inazu[4] (1.National Research Institute for Earth Science and Disaster Resilience, 2.Meteorological Research Institute, Japan Meteorological Agency, 3.Tohoku University, 4.Tokyo University of Marine Science and Technology)

[SCG54-P02] Detectability of short-term seafloor deformation by S-net pressure observation

*Ryota Hino[1], Tatsuya Kubota[2], Naotaka YAMAMOTO CHIKASADA[2], Yusaku Ohta[1], Hideto Otsuka[1] (1.Graduate School of Science, Tohoku University, 2.National Research Institute for Earth Science and Disaster Resilience)

[SCG54-P03] Vertical seafloor movement after the 2011 Tohoku earthquake and remarkable uplift near the trench axis off Sanriku

*Chie Honsho[1], Motoyuki Kido[2], Fumiaki Tomita[3], Ryota Hino[1] (1.Research Center for Prediction of Earthquakes and Volcanic Eruptions, Graduate School of Science, Tohoku University, 2.International Research Institute of Disaster Science, Tohoku University, 3.Japan Agency for Marine-Earth Science and Technology)

[SCG54-P04] Improvement of spatial resolution and evaluation of uncertainty for the coseismic slip distribution of the 2011 Tohoku-oki Earthquake

*Fumiaki Tomita[1], Takeshi Iinuma[1], Motoyuki Kido[2], Ryota Hino[3], Yusaku Ohta[3], Ryoichiro Agata[1], Takane Hori[1], Naoki Uchida[3] (1.Japan Agency for Marine-Earth Science and Technology, 2.International Research Institute of Disaster Science, Tohoku University, 3.Graduate School of Science, Tohoku University)

[SCG54-P05] Resolving 3D rheology of northeastern Japan using postseismic deformation following the 2011 Tohoku-oki earthquake

*Jun Muto[1], Dhar Sambuddha[1], James Daniel Paul Moore[2], Satoshi Miura[3], Yusaku Ohta[3], Takeshi Iinuma[4] (1.Department of Earth Sciences, Tohoku University, 2.Earth Observatory of Singapore, Nanyang Technological University, Singapore, 3.Department of Geophysics, Tohoku University, 4.Japan Agency for Marine-Earth Science and Technology)

[SCG54-P06] Numerical simulation of earthquake generation cycles along the Japan Trench

*Ryoko Nakata[1], Takane Hori[2], Seiichi Miura[2], Ryota Hino[1] (1.Graduate School of Science, Tohoku University, 2.Research Institute for Marine Geodynamics, Japan Agency for Marine-Earth Science and Technology)

[SCG54-P07] Seismicity near the trench axis and in the outer rise region of southern Japan Trench: Results from ocean bottom seismograph observations

*Koichiro Obana[1], Gou Fujie[1], Yojiro Yamamoto[1], Yuka Kaiho[1], Yasuyuki Nakamura[1], Seiichi Miura[1], Shuichi Kodaira[1] (1.Research Institute for Marine Geodynamics, Japan Agency for Marine-Earth Science and Technology)

[SCG54-P08] Microseismicity prior to the 2011 Tohoku-Oki earthquake around the mainshock hypocenter

*Hirofumi Goto[1], Ryota Hino[1] (1.Graduate School of Science, Tohoku University)

[SCG54-P09] Characteristics of tectonic tremor activity along the Japan Trench before the 2011 Tohoku Oki earthquake

*Hidenobu Takahashi[1,2], Ryota Hino[1], Naoki Uchida[1], Ryosuke Azuma[1], Susumu Kawakubo[1], Kazuaki Ohta[3], Masanao Shinohara[4] (1.Graduate school of Science Tohoku University , 2.Central Research Institute of Electric Power Industry, 3.National Research Institute for Earth Science and Disaster Resilience, 4.Earthquake Research Institute, The university of Tokyo)

[SCG54-P10] Application of ensemble learning noise classifier to automatically determined earthquake catalog after the 2011 Tohoku Earthquake

*Koji Tamaribuchi[1] (1.Meteorological Research Institute)

[SCG54-P11] **Core-Mantle boundaries state estimation applying the strain analysis on frequency domain**

seiji matsumura[2], *Makoto OKUBO[1] (1.Natural Science Cluster, Kochi University, 2.Faculty of Science and Technology)

[SCG54-P12] Tomography and megathrust earthquakes in the Tohoku forearc

*Dapeng Zhao[1] (1.Department of Geophysics, Tohoku University)

[SCG54-P13] Trench fill and graben fill sediments on the incoming plate around the Japan trench

*Yasuyuki Nakamura[1], Shuichi Kodaira[1], Gou Fujie[1], Seiichi Miura[1], Koichiro Obana[1], Mikiya Yamashita[2] (1.Japan Agency for Marine Earth Science and Technology, 2.National Institute of Advanced Industrial Science and Technology)

[J] Poster | S (Solid Earth Sciences)：S-CG Complex & General

5:15 PM - 6:30 PM JST | 8:15 AM - 9:30 AM UTC | Ch.16_3

[S-CG55] Oceanic plate as inputs to subduction zone: from oceanic spreading ridge to subduction trench

convener:Gou Fujie(Japan Agency for Marine-Earth Science and Technology), Makoto Yamano(Earthquake Research Institute, the University of Tokyo), Tomoaki Morishita(School of Geoscience and Civil Engineering, College of Science and Technology, Kanazawa University), Takanori Kagoshima(University of Toyama)

[SCG55-P01] Compilation of bathymetry and seismic reflection data to characterize outer rise faults in the Kuril Trench

*Shuichi Kodaira[1], Tetsuo No[1], Yasuyuki Nakamura[1], Gou Fujie[1], Koichiro Obana[1], Seiichi Miura[1] (1.Research Institute for Marine Geodynamics, Japan Agency for Marine-Earth Science and Technology)

[SCG55-P02] Characteristics of the oceanic plate near the Nosappu fracture zone revealed by the extensive seismic structure studies

*Gou Fujie[1], Koichiro Obana[1], Shuichi Kodaira[1], Katsuyoshi Michibayashi[2] (1.Japan Agency for Marine-Earth Science and Technology, 2.Nagoya University)

[SCG55-P03] Hydrothermal experiments in olivine-orthopyroxene-H2O system at 200-400C: implications for hydrogen generation at high temperatures

*Shuhei Tanaka[1], Atsushi Okamoto[2], OTGONBAYAR DANDAR[2], Masaoki Uno[2], Masakazu Fujii[3] (1.Tohoku University, 2.Graduate school of environmental studies, Tohoku University, 3.National institute of Polar research and SOKENDAI)

[SCG55-P04] Hydration processes of a forearc mantle wedge inferred from the Takadomari serpentinite body in the Kamuikotan Belt, central Hokkaido, Japan

*Shun Takamizawa[1], Yuji Ichiyama[1], Shusaku Yamazaki[2], Akihiro Tamura[3], Tomoaki Morishita[3] (1.Chiba University , 2.Civil Engineering Research Institute for Cold Region, 3.School of Geoscience and Civil Engineering, College of Science and Technology, Kanazawa University)

[SCG55-P05] Petrological features and formation processes of lower crustal cumulate xenoliths from Oki-Dogo Island: A possibility of mantle plume origin

*Rio Higuchi[1], Yuji Ichiyama[1], Akihiro Tamura[2], Tomoaki Morishita[2] (1.Chiba University, 2.Faculty of Geosciences and Civil Engineering, Kanazawa University)

[J] Poster | B (Biogeosciences)：B-PT Paleontology

5:15 PM - 6:30 PM JST | 8:15 AM - 9:30 AM UTC | Ch.17_2

[B-PT02] Biotic History

convener:Isao Motoyama(Faculty of Science, Yamagata University), Takao Ubukata(Division of Geology & Mineralogy, Department of Earth & Planetary Sciences, Kyoto University), Kazuyoshi Moriya(Department of Earth Sciences, Faculty of Education and Integrated Arts and Sciences, Waseda University)

[BPT02-P01] Preliminary reports on the ecology of Cretaceous pantrionychian turtles based on the carapace bone histology

*Haruka Fukasawa[1], Kohei Tanaka[1], Yasuhisa Nakajima[2] (1.University of Tsukuba, 2.Tokyo City University)

[BPT02-P02] Asexual reproduction of planktonic foraminifera: Discovery and its significance

*Haruka TAKAGI[1], Atsushi KURASAWA[2], Katsunori KIMOTO[3] (1.Chiba University, 2.Marine Works Japan Ltd., 3.JAMSTEC)

[BPT02-P03] Oceanic anoxic event 2 observed in Southwestern Newfoundland Ridge

*Kazuyoshi Moriya[1], Yasuko Miyakura[2], Takashi Hasegawa[3], Akiko S. Goto[4] (1.Department of Earth Sciences, Faculty of Education and Integrated Arts and Sciences, Waseda University, 2.Major in Earth Sciences, Resources and Environmental Engineering, Graduate School of Creative Science and Engineering, 3.Faculty of Earth Science and Civil Engineering, Institute of Science and Engineering, Kanazawa University, 4.Center for Ecological Research, Kyoto University)

[BPT02-P04] Radiolarians from the upper Neogene Tatsunokuchi Formation, Miyagi Prefecture: An attempt to research depth-related distribution of extinct species.

*Isao Motoyama[1], Mizuho Aizawa[1] (1.Faculty of Science, Yamagata University)

[J] Poster | G (General)：General

5:15 PM - 6:30 PM JST | 8:15 AM - 9:30 AM UTC | Ch.03_1

[G-01] Disaster prevention education

convener:Hitoshi Nakai(Kobuchisawa Research Institute for Nature and Education), Jiro Komori(Teikyo Heisei University), Shintaro Hayashi(Akita University Graduate School of Education), Tetsuhiko Asano(Senshu University Matsudo Junior High School High School)

[G01-P01] Considering limits of hazard map: A case of a debris flow disaster that struck a village at the southern foot of Yatsugatake in September 1898.

*Hitoshi Nakai[1] (1.Kobuchisawa Research Institute for Nature and Education)

[G01-P02] **A Quantitative Analysis of Nationwide Municipalities' Disaster Prevention Portals**

*Haruka Matsuoka[1], Ami Mori[1], Kei Takashima[1], Tsukasa Sano[1], Asako Sano[2], Seiji Hori[1], Minako Noda[1] (1.Department of Business and Informatics, Tsukuba Gakuin University, 2.Faculty of Home Economics, Otsuma Women's University)

[J] Poster | G (General)：General

5:15 PM - 6:30 PM JST | 8:15 AM - 9:30 AM UTC | Ch.03_2

[G-02] Outreach and geoscience education

convener:Jiro Komori(Teikyo Heisei University), Naoko HASEGAWA(Ochanomizu University), Ken Tsukada(Hiratsuka City Museum), Satoko Oki(Faculty of Environment and information Studies)

[G02-P01] Astronomy outreach with multiple perspectives by music, painting, and tourism

★Invited Papers

*Uenoyama Sachiyo[1], Akihiko Tomita[1], Masami Okyuudo[1] (1.Wakayama University)

[G02-P02] Astronomical environment in which outreach targets are interested and outreach methods utilizing it

*Miyuki Tsuchiya, Mie Enomoto

[J] Poster | G (General)：General

5:15 PM - 6:30 PM JST | 8:15 AM - 9:30 AM UTC | Ch.03_3

[G-03] G03Geoscience education from elementary school to university students

[G03-P01] Practice of Inquiry Activities based on the Field of Earth Science in High School

*Kazuya Kawakatsu[1] (1.Hyogo Prefectural Himeji Higashi senior high school)

[J] Poster | M (Multidisciplinary and Interdisciplinary)：M-IS Intersection

5:15 PM - 6:30 PM JST | 8:15 AM - 9:30 AM UTC | Ch.19_2

[M-IS13] Dynamics of eruption cloud and cumulonimbus; modelling and observation

convener:Eiichi Sato(Meteorological Research Institute), Fukashi Maeno(Earthquake Research Institute, University of Tokyo), Takeshi Maesaka(National Research Institute for Earth Science and Disaster Resilience)

[MIS13-P01] Estimation of ash refractive index and improvement of Himawari-8 volcanic ash algorithm

★Invited Papers

*Hiroshi Ishimoto[1], Masahiro Hayashi[1], Yuzo Mano[1], Rei Kudo[1] (1.Meteorological Research Institute)

[MIS13-P02] Multi-sensor observation of cloud evolution from cumulus to cumulonimbus in Tokyo metropolitan area

*Takeshi Maesaka[1], Tadayasu Ohigashi[1], Koyuru Iwanami[1], Shin-ichi Suzuki[1], Namiko Sakurai[1], Yukari Shusse[1], Kaori Kieda[1], Shingo Shimizu[1], Yasushi Uji[1], Nobuhiro Takahashi[2], Hiroshi Hanado[3], Katsuhiro Nakagawa[3], Tomoo Ushio[4] (1.National Research Institute for Earth Science and Disaster Resilience, 2.Nagoya University, 3.National Institute of Information and Communications Technology, 4.Osaka University)

[MIS13-P03] Application to the volcanic ash obserbation of the X-band solid state marine radar

*Takaaki NISHI[1], Masayuki MAKI[1], Takehiko KOBORI[1], Kanji ENDO[2], Kazuhiko KAIGA[2], Masato IGUCHI[3] (1.Kagoshima Univ., 2.Koden Electronics Co., Ltd, 3.Kyoto Univ.)

[MIS13-P04] Modification of probabilistic estimation method for eruption plume height using weather radars

*Eiichi Sato[1] (1.Meteorological Research Institute)

[MIS13-P05] Ash fall observation using 2D-Video Disdrometer (2)

*Eiichi Sato[1], Kosei Takishita[2], Masato Iguchi[3] (1.Meteorological Research Institute, 2.Division of Earth and Planetary Sciences, Graduate School of Science, Kyoto University, 3.Sakurajima Volcano Research Center, Disaster Prevention Research Institute, Kyoto University)

[MIS13-P06] Sedimentary process of ash deposits from long-term activity of repeated vulcanian eruptions at Sakurajima volcano, Japan

*Takahiro Miwa[1], Futoshi Nanayama[2] (1.National research institute for earth science and disaster resilience, 2.Geological Survey of Japan, AIST)

[J] Poster | M (Multidisciplinary and Interdisciplinary)：M-IS Intersection

5:15 PM - 6:30 PM JST | 8:15 AM - 9:30 AM UTC | Ch.19_3

[M-IS15] Tsunami deposit: research progress after the 2011 Tohoku-oki earthquake and prospects

convener:Masaki Yamada(Department of Geology, Faculty of Science, Shinshu University), Takashi Ishizawa(International Research Institute of Disaster Science, Tohoku University), Masashi Watanabe(Chuo University), Koichiro Tanigawa(Geological Survey of Japan, National Institute of Advanced Industrial Science and Technology)

[MIS15-P01] A study for correlation of mega-tsunami in the Kuril Trench based on the tsunami deposits in the Erimo area, Hokkaido

*RYO NAKANISHI[1], Juichiro Ashi[1,2], Yosuke Miyairi[1], Yusuke Yokoyama[1,3] (1.Atmosphere and Ocean Research Institute, The University of Tokyo, 2.Graduate School of Frontier Science, The University of Tokyo, 3.Department of Earth and Planetary Sciences, Graduate School of Science, The University of Tokyo)

[MIS15-P02] Characteristics of event deposits and their distributions based on a drilling survey in Sekine-hama, the northern part of the Shimokita Peninsula, Aomori Prefecture

*Daisuke Ishimura[1], Masaki Yamada[2], Takashi Ishizawa[3], Kaori Aoki[4], Kai Sato[2] (1.Department of Geography, Tokyo Metropolitan University, 2.Department of Geology, Faculty of Science, Shinshu University, 3.International Research Institute of Disaster Science, Tohoku University, 4. Research Center for Volcanic Hazards and Their Mitigation, Tokyo Metropolitan University)

[MIS15-P03] Tsunami source estimation of paleotsunami deposits formed in the 17th century at Sekinehama, northern Shimokita Peninsula, Aomori Prefecture

*Kai Sato[1], Masaki Yamada[1], Daisuke Ishimura[2], Takashi Ishizawa[3], Toshitaka Baba[4] (1.Depatment of Geology, Faculty of Science, Shiushu University, 2.Department of Geography, Tokyo Metropolitan University , 3.International Research Institute of Disaster Science, Tohoku University, 4.Graduate School of Science and Technology, Tokushima University)

[MIS15-P04] Revised paleotsunami history at Kirikiri, Northeast Japan

*Takashi Ishizawa[1], Yusuke Yokoyama[2], Yosuke Miyairi[2] (1.International Research Institute of Disaster Science, Tohoku University, 2.Atmosphere and Ocean Research Institute, the University of Tokyo)

[MIS15-P05] Distribution and characteristics of the 1983 Nihonkai-chubu earthquake tsunami deposit along the Akita coastal area, Japan

*Takashi Chiba[1], Yuichi Nishimura[2] (1.Faculty of Bioresource Sciences, Akita Prefectural University, 2.Institute of Seismology and Volcanology (ISV), Faculty of Science, Hokkaido University)

[MIS15-P06] Event deposits in a coastal lake at Minami-ise Town, Mie Prefecture during the last 3000 years

*Yumi Shimada[1], Yuki Sawai[1], DAN MATSUMOTO[1], Koichiro Tanigawa[1], Yuichi Namegaya[1], Masanobu Shishikura[1], Kazumi Ito[1], Toru Tamura[1], Shigehiro Fujino[2] (1.Geological Survey of Japan, AIST, 2.Faculty of Life and Environmental Sciences, University of Tsukuba)

[MIS15-P07] Distributions and occurrences of sandy tsunami deposits in caves located along the East Coast of Ishigaki Island, Okinawa Prefecture

*Yoshiro Ishihara[1], Miyu Kitahara[1], Yuuka Okita[1], Ayano Shimabukuro[2], Hajime Naruse[3], Chiaki Katagiri[4], Rintaro Ono[5], Kazuhisa Yoshimura[6] (1. Fukuoka Univ., 2.Yaeyama Museum, 3.Kyoto Univ., 4.Okinawa Prefectural Archaeological Center, 5.National Museum of Ethnology, 6.Kyushu Univ.)

[MIS15-P08] Examining grain-size changes in sediment transport modeling of the 2011 Tohoku-oki tsunami in the Sendai Plain

*Wataru Nakamura[1], Daisuke Sugawara[1] (1.Tohoku University)

[MIS15-P09] Comparison of Observations and Numerical Simulations of Sediment Transport Using the 1707 CE Hoei Tsunami Source Model: Application to Kanigaike Pond in Kochi Prefecture, Japan

*Satoshi Kusumoto[1], Kentaro Imai[1], Narumi Takahashi[2,1], Takane Hori[1], Daisuke Sugawara[3] (1.JAMSTEC, 2.NIED, 3.Tohoku University)

[MIS15-P10] Uncertainty of geological information used in identification of tsunami deposit - Preliminary assessment –

*Takumi Yoshii[1], Takaomi Hamada[1], Yuki Ito[1], Shiro Tanaka[1], Masafumi Matsuyama[1] (1.Central Research Institute of Electric Power Industry)

[J] Poster | M (Multidisciplinary and Interdisciplinary)：M-IS Intersection

5:15 PM - 6:30 PM JST | 8:15 AM - 9:30 AM UTC | Ch.22_2

[M-IS22] Geopark

convener:Takayuki Arima(Yokohama City University), Keiichi Tadokoro(Research Center for Seismology, Volcanology and Earthquake and Volcano Research Center, Nagoya University), Marekazu OHNO(Unzen Volcanic Area Geopark Promotion Office), Takayuki Ogata(Graduate School of Engineering and Science, University of the Ryukyus)

[MIS22-P01] Scientific Roles of the JpGU Session "Geopark"

*Takayuki Ogata[1] (1.Graduate School of Engineering and Science, University of the Ryukyus)

[MIS22-P02] Discussion

[J] Poster | M (Multidisciplinary and Interdisciplinary)：M-IS Intersection

5:15 PM - 6:30 PM JST | 8:15 AM - 9:30 AM UTC | Ch.18_2

[M-IS24] Geophysical fluid dynamics-Transfield approach to geoscience

convener:Keita Iga(Atmosphere and Ocean Research Institute, The University of Tokyo), Shigeo Yoshida(Department of Earth and Planetary Sciences, Faculty of Sciences, Kyushu University), Takatoshi Yanagisawa(Research Institute for Marine Geodynamics, Japan Agency for Marine-Earth Science and Technology), Hidenori AIKI(Nagoya University)

[MIS24-P01] Two-dimensional ideal MHD waves and the continuous Alfvén spectrum on a rotating sphere with a background toroidal magnetic field

*Ryosuke Nakashima[1], Shigeo Yoshida[2] (1.Faculty of Science, Kyushu University, 2.Department of Earth and Planetary Sciences, Faculty of Science, Kyushu University)

[MIS24-P02] Development of sea surface wave breaking observation system using industrial millimeter radar and optical particle size counter

*Hidenori AIKI[1], Fumiyoshi Kondo[2], Haruya Minda[1] (1.Nagoya University, 2.Japan Coast Guard Academy)

[MIS24-P03] Axisymmetric flows and non-axisymmetric phenomena in a cylindrical tank with a rotating bottom

*Keita Iga[1] (1.Atmosphere and Ocean Research Institute, The University of Tokyo)

[MIS24-P04] We examined **Origin of Great Red Spot of Jupiter, Deep Ocean Floor, Pacific Rim Arcuate Archipelago, Origin of Gomagnetic Reversal, and Origin of Asteroid Belt.**

*Akira Taneko[1] (1.SEED SCIENCE Lab.)

[J] Poster | M (Multidisciplinary and Interdisciplinary)：M-IS Intersection

5:15 PM - 6:30 PM JST | 8:15 AM - 9:30 AM UTC | Ch.18_3

[M-IS25] Atmospheric electricity: Electrical phenomena associated with extreme weather

convener:Yasuhide Hobara(Graduate School of Information and Engineering Department of Communication Engineering and Informatics, The University of Electro-Communications), Daohong Wang(Gifu University)

[MIS25-P01] X-band radar and disdrometer observations of winter thunderclouds emitting gamma rays

*Yuuki Wada[1], Teruaki Enoto[1], Mamoru Kubo[2], Kazuhiro Nakazawa[3], Taro Shinoda[3], Daisuke Yonetoku[2], Tatsuya Sawano[2], Takayuki Yuasa, Tomoo Ushio[4], Yousuke Sato[5], Gabriel Sousa Diniz[1], Harufumi Tsuchiya[6] (1.RIKEN, 2.Kanazawa University, 3.Nagoya University, 4.Osaka University, 5.Hokkaido University, 6.JAEA)

[MIS25-P02] Observation of thundercloud gamma-rays in FY2020 with the GOOSE detector aiming at altitude measurements

*Yuuna Tsuji[1], Kazuhiro Nakazawa[1], Shohei Hisadomi[1], Yusaku Ikami[1], Daiki Odani[1], Teruaki Enoto[2], Yuuki Wada[2], Takayuki Yuasa, Harufumi Tsuchiya[3], Taro Shinoda[4], Keigo Ookuma[1], Gabriel Diniz[2] (1.Nagoya University, 2.RIKEN, 3.JAEA, 4.ISEE. Nagoya Univ.)

[MIS25-P03] Hydrometeor distribution in a thundercloud related to a gamma-ray emission event

*Takemoto Kiyomichi[1], Taro Shinoda[1], Masaya Kato[1], Shohei Hisadomi[2], Yuuna Tsuji[2], Kazuhiro Nakazawa[2], Yuuki Wada[3], Teruaki Enoto[3] (1.Institute for Space-Earth Environmental Research, Nagoya University, 2.Department of Physics, Nagoya University, 3.Institute of Physical and Chemical Research)

[MIS25-P04] A Study of 3D Precipitation Core Tracking Method Using Multi-Parameter Phased Array Weather Radar

*Keitaro Asai[1], Hiroshi Kikuchi[1], Yasuhide Hobara[1], Tomoo Ushio[2] (1.The University of Electro Communications, 2.Osaka University)

[MIS25-P05] Special negative lightning strokes in winter with extremely short preceding discharges

*Ting Wu[1], Daohong Wang [1], Nobuyuki Takagi[1] (1.Gifu University)

[MIS25-P06] **Simultaneous Observations of a Winter Lightning Flash in Japan**

*Haitao Huang[1], Daohong Wang[1], Ting Wu[1], Nobuyuki Takagi[1] (1.Gifu University)

[MIS25-P07] Spatio-temporal characteristics of lightning energy in Southeast Asia deduced from ELF observations

*Shunsuke Akama[1], Shu Hirai[1], Yasuhide Hobara[1], Hiroshi Kikuchi[1], Amir Izzani Mohamed[2], Chandima Gomes[3], Kazuo Shiokawa[4], Michael Stock[5] (1.The University of Electro-Communications, 2.University of Malaysia, Pahang, 3.University of the Witwatersrand, Johannesburg, 4.Institute for Space–Earth Environmental Research, 5.Earth Networks)

[MIS25-P08] Sprites observed from the summit of Mt. Fuji and their parent thunderstorm

*Suzuki Tomoyuki[1], Masashi Kamogawa[1], Syugo Hayashi[2] (1.University of Shizuoka, 2.Meteorological Research Institute)

[MIS25-P09] Coupling process of large-scale atmospheric disturbances to the ionosphere through typhoon

*Shu Hirai[1], Yasuhide Hobara[1], Hiroshi Kikuchi[1], Michael Stock[2] (1.The University of Electro-Communications, 2.Earth Networks)

[J] Poster | M (Multidisciplinary and Interdisciplinary)：M-IS Intersection

5:15 PM - 6:30 PM JST | 8:15 AM - 9:30 AM UTC | Ch.21_1

[M-IS26] Gas hydrates in environmental-resource sciences

convener:Hitoshi Tomaru(Department of Earth Sciences, Chiba University), Akihiro Hachikubo(Kitami Institute of Technology), Atsushi Tani(Department of Human Environmental Science, Graduate School of Human Development and Environment, Kobe University), Shusaku Goto(Institute for Geo-Resources and Environment National Institute of Advanced Industrial Science and Technology)

[MIS26-P01] **Geochemical characteristics of headspace gas and pore water in shallow sediment from the Tatar Trough**

*Musashi Yokoyama[1], Ryo Murata[1], Hitoshi Tomaru[1], Ryo Matsumoto[2], A.V. Yatsuk[3], D.A. Shvalov[3] (1.Chiba University, 2.Meiji University, 3.V.I.Ilichev Pacific Oceanological Institute)

[MIS26-P02] Gas hydrate survey at the gas seepage area off Abashiri, the Sea of Okhotsk

*Yuki Moriya[1], Hiromi Kimura[1], Akihiro Hachikubo[1], Satoshi Yamashita[1], Hirotoshi Sakagami[1], Masaaki Konishi[1], Hirotsugu Minami[1], Yasuhito Uchida[2], Hiroshi Yamaguchi[3] (1.Kitami Institute of Technology, 2. Research Institute of Energy, Environment and Geology, Hokkaido Research Organization, 3.Kushiro Fisheries Research Institute, Hokkaido Research Organization)

[MIS26-P03] Total organic carbon and its carbon isotope ratio in subsurface sediments off Hokkaido area

*Daisuke Yahagi[1], Akihiro Hachikubo[1], Masaaki Konishi[1], Hirotoshi Sakagami[1], Hirotsugu Minami[1], Satoshi Yamashita[1], Yasuhito Uchida[2], Hiroshi Yamaguchi[3] (1.Kitami Institute of Technology, 2.Research Institute of Energy, Environment and Geology, Hokkaido Research Organization, 3.Kushiro Fisheries Research Institute, Hokkaido Research Organization)

[MIS26-P04] Characteristics of gas hydrate crystals and their hydrate-bound gases retrieved at the seepage field off Tokachi (the Pacific Ocean)

*Hiromi Kimura[1], Ryoya Kamata[1], Daisuke Yahagi[1], Yuki Moriya[1], Akihiro Hachikubo[1], Masaaki Konishi[1], Hirotoshi Sakagami[1], Hirotsugu Minami[1], Satoshi Yamashita[1] (1.Kitami Institute of Technology)

[MIS26-P05] Gas hydrate survey at the gas seepage area off Hidaka, the Pacific Ocean

*Ryoya Kamata[1], Hiromi Kimura[1], Akihiro Hachikubo[1], Hirotoshi Sakagami[1], Satoshi Yamashita[1], Masaaki Konishi[1], Hirotsugu Minami[1] (1.Kitami Institute Of Technology)

[MIS26-P06] Emission of hydrated gas from seafloor to water column in the western Oki Trough

*Hitoshi Tomaru[1], Tianyou Ze[1], Sonoka Ikemoto[1], Minori Chikada[1] (1.Department of Earth Sciences, Chiba University)

[MIS26-P07] Isotope fractionation between hydrate-bound and ambient gases - case study in Lake Baikal gas hydrates -

*Hiromi Kimura[1], Akihiro Hachikubo[1], Oleg Khlystov[2], Gennadiy Kalmychkov[3], Marc De Batist[4], Hirotoshi Sakagami[1], Hirotsugu Minami[1], Satoshi Yamashita[1] (1.Kitami Institute of Technology, 2.Limnological Institute, SB RAS, 3.Vinogradov Institute of Geochemistry, SB RAS, 4.Ghent University)

[MIS26-P08] Carbon isotope fractionation of carbon monoxide hydrate between gas and hydrate phases

*Hiromi Kimura[1], Akihiro Hachikubo[1], Satoshi Takeya[2] (1.Kitami Institute of Technology, 2.National Institute of Advanced Industrial Science and Technology (AIST))

[MIS26-P09] Hydrogen isotopic fractionation of methane at the formation of synthetic structure I and II gas hydrates

*Ryoya Kamata[1], Akihiro Hachikubo[1], Satoshi Takeya[2] (1.Kitami Institute Of Technology, 2.National Institute of Advanced Industrial Science and Technology (AIST))

[MIS26-P10] Experimental study of CO2 hydrate phase equilibrium in sediments

*Tatsuki Iwamoto[1], Hitoshi Tomaru[1] (1.Chiba University)

[MIS26-P11] Effect of temperature and pressure on hydration number of methane hydrate

*Akihiro Hachikubo[1], Ryoya Kamata[1], Hiromi Kimura[1], Yuta Komagata[1], Go Fuseya[1], Satoshi Takeya[2] (1.Kitami Institute of Technology, 2.National Institute of Advanced Industrial Science and Technology (AIST))

[J] Poster | M (Multidisciplinary and Interdisciplinary)：M-IS Intersection

5:15 PM - 6:30 PM JST | 8:15 AM - 9:30 AM UTC | Ch.22_3

[M-IS27] History X Earth and Planetary Science

convener:Yasuyuki Kano(Earthquake Research Institute, The University of Tokyo), Hiroaki Isobe(Faculty of Fine Arts, Kyoto City University of Arts), Kei Yoshimura(Institute of Industrial Science, The University of Tokyo), kiyomi iwahashi(National Institute of Japanese Literature)

[MIS27-P01] An attempt to convert historical seismic data into GIS data and its challenges

*Junzo Ohmura[1,4], Miki Hamano[2], Yuta Hashimoto[3], Yasuyuki Kano[1,4] (1.Earthquake Research Institute,The University of Tokyo, 2.Graduate School of Letters, Ritsumeikan University, 3.National Museum of Japanese History, 4. Collaborative Research Organization for HistoricalMaterials on Earthquakes and Volcanoes, UTokyo)

[MIS27-P02] Historical materials of unlisted destructive earthquakes at Izu-Bonin Islands in the Meiji period: the 1873 Toshima earthquake and so on

*Kentaro Hattori[1] (1.Kyoto Univ.)

[MIS27-P03] Investigation of the stone monuments related to the hail and frost damage in the southern part of Gunma Prefecture

*Masafumi Aoyama[1] (1.Gunma University)

[J] Poster | M (Multidisciplinary and Interdisciplinary)：M-AG Applied Geosciences

5:15 PM - 6:30 PM JST | 8:15 AM - 9:30 AM UTC | Ch.21_3

[M-AG38] Ten years after the Fukushima Dai-ichi NPP Accident : Dynamics of radionuclides in the environment

convener:Daisuke Tsumune(Central Research Institute of Electric Power Industry), Yuichi Onda(Center for Research on Isotopes and Environmental Dynamics, University of Tsukuba), Kazuyuki Kita(Faculty of Science, Ibaraki University), Yoshio Takahashi(Department of Earth and Planetary Science, Graduate School of Science, The University of Tokyo)

[MAG38-P01] Effects of preferential flow on the spatial heterogeneity and chemical form of Cs-137 in a forest soil

*Junko Takahashi[1], Tetsuya Ono[1], Takuya Sasaki[1], Yuichi Onda[1] (1.Center for Research in Isotopes and Environmental Dynamics, University of Tsukuba)

[MAG38-P02] Contribution of fungal hyphal elongation to radiocesium transfer in deciduous broad-leaved litter

*Yoshito Sasaki[1], Tadafumi Niizato[1], Hiroki Amamiya[2], Kaori Yoshida[1] (1.Japan Atomic Energy Agency, 2.QJ science)

[MAG38-P03] The ^{137}Cs dynamics in a pond of urban area after decontamination

*Honoka Kurosawa[1], Misaki Usuki[1], Shota Moritaka[1], Kenji Nanba[2], Toshihiro Wada[2], Yoshifumi Wakiyama[2] (1.Graduate School of Symbiotic Systems Science and Technology, Fukushima University, 2.Institute of Environmental Radioactivity, Fukushima University)

[MAG38-P04] Variations in riverine ^{137}Cs concentration and its exportation to the ocean during high-flow events at three rivers in Hamadori area

Takuya Niida[1], *Yoshifumi Wakiyama[2], Hyoe Takata[2], Kazuki Fujita[3], Keisuke Taniguchi[4], Alexei Konoplev[2] (1.Graduate School of Symbiotic System and Technology, Fukushima Universiy, 2.Institute of Environmental Radioactivity, Fukushima Universiy, 3.Fukushima Prefectural Centre for Environmental Creation, 4.Center for Research in Isotope and Environmental Dynamics, University of Tsukuba)

[MAG38-P05] Comparison of cesium-bearing microparticles from marine and terrestrial sources

*Hikaru Miura[1], Atsushi Kubo[2], Takashi Ishimaru[3], Yukari Ito[3], Jota Kanda[3], Daisuke Tsumune[1], Yoshio Takahashi[4] (1.Central Research Institute of Electric Power Industry, 2.Shizuoka University, 3.Tokyo University of Marine Science and Technology, 4.The University of Tokyo)

[J] Poster | M (Multidisciplinary and Interdisciplinary)：M-TT Technology & Techniques

5:15 PM - 6:30 PM JST | 8:15 AM - 9:30 AM UTC | Ch.20_2

[M-TT43] Brand-new scope of coupling geophysics being established by infrasound and associated waves

convener:Masa-yuki Yamamoto(Department of systems engineering, Kochi University of Technology), Takayuki Otsu(Japan Weather Association), Mie Ichihara(Earthquake Research Institute, University of Tokyo), Nobuo Arai(Disaster Mitigation Research Center, Nagoya University)

[MTT43-P01] Infrasound detection of mining blasts from eastwards and westwards

*Mami Nogami[1], Takayuki Otsu[1], Makiko Iwakuni[1] (1.Japan Weather Association)

[MTT43-P02] The Infrasound signals excited by a bolide on 29th November 2020

*Makiko Iwakuni[1], Masa-yuki Yamamoto[2], Hiroaki Saito[3], Islam HAMAMA[2], Nobuo Arai[4], Takayuki Otsu[1], Mami Nogami[1], Takahiko Murayama[1] (1.Japan Weather Association, 2.Department of systems engineering, Kochi University of Technology, 3.Cosmosciences, Hokkaido University, 4.Disaster Mitigation Research Center, Nagoya University)

[MTT43-P03] Atmospheric wave energy of the 2020 August 4 explosion in Beirut, Lebanon, from ionospheric disturbances

*Ai Matsushita[1], Bhaskar Kundu[2], Batakrushna Senapati[2], Kosuke Heki[1] (1.Hokkaido University Graduate School of Science, 2.National Institute of Technology, Rourkela)

[MTT43-P04] Infrasound and seismic multiple-site observation of shock waves induced by hypersonic reentry of HAYABUSA-2 sample return capsule on Dec. 6, 2020

*Masa-yuki Yamamoto[1], Yoshihiro Hiramatsu[2], Shinsuke Abe[3], Yoshihiro Kakinami[4], Norihisa Segawa[5], Hiroshi Katao[6], Yoshiaki Ishihara[7], Taichi Kawamura[8], Satoshi Nozawa[9], Muneyoshi Furumoto[10], Phil Bland[11], Eleanor Sansom[11], Hadrien Devillepoix[11], Martin Towner[11], Yuichiro Inoue[1], Islam H. Hamama[1], Masato Yazawa[12], Kazuhisa Fujita[7], Makoto Yoshikawa[7] (1.Kochi University of Technology, 2.kanazawa University, 3.Nihon University, 4.Hokkaido Information University, 5.Kyoto Sangyo University, 6.Kyoto University, 7.JAXA, 8.Institut de Physique du Globe de Paris, 9.Ibaraki University, 10.Tono Research Institute of Earthquake Science, 11.Curtin University, 12.Mathematical Assist Design Laboratory)

[J] Poster | M (Multidisciplinary and Interdisciplinary)：M-ZZ Others

5:15 PM - 6:30 PM JST | 8:15 AM - 9:30 AM UTC | Ch.22_4

[M-ZZ44] Studies of Geoscience : historical, philosophical and STS studies

convener:Michiko Yajima(Tokyo Metropolitan University), Shigeyuki Aoki(Faculty of Letters, Chuo University), Toshihiro Yamada(Taisho University), Akira Yamamoto

[MZZ44-P01] The begining of lady earth scientists in Japan

*Michiko Yajima[1] (1.Tokyo Metropolitan University)

[MZZ44-P02] Finding Geoscientific Evidence in Nuclear Disaster Trials 2: Is Not "responsibility of the government" Scientific?

*Mamoru Hayashi[1] (1.University of TOYAMA)

[MZZ44-P03] Wilkins’s lunar world

*Shigeyuki Aoki[1] (1.Faculty of Letters, Chuo University)

[MZZ44-P04] The Popularization of Science and the Geo-power: Cosmic Evolution, China, and Buddhism in 1920s Shinjo Shinzo

*Toshihiro Yamada[1] (1.Taisho University)

[MZZ44-P05] Japan's first female meteorologist

*Akira Yamamoto

[J] Poster | M (Multidisciplinary and Interdisciplinary)：M-ZZ Others

5:15 PM - 6:30 PM JST | 8:15 AM - 9:30 AM UTC | Ch.22_5

[M-ZZ48] Geology and culture

convener:Hisashi Suzuki(Otani University), Tohru Sakiyama(Institute of Geo History, Japan Geochronology Network), Naoki Takahashi(Natural History Museum and Institute, Chiba)

[MZZ48-P01] Rock species of the cornerstone of the earthen wall in the northeastern part of Ninomaru earthworks of Yamagata Castle

*Ohtomo Yukiko[1], Saito Hitoshi[2] (1.Yamagata University, 2.Yamagata City Board of Education)

[J] Poster | U (Union)：Union

Sun. Jun 6, 2021 5:15 PM - 6:30 PM JST | Sun. Jun 6, 2021 8:15 AM - 9:30 AM UTC | Ch.01_1

[U-04] Promotion of SDGs in JpGU

convener:Yukihiro Takahashi(Department of Cosmosciences, Graduate School of Science, Hokkaido University), Chiaki T. Oguchi(Institute for Environmental Science and Technology, Graduate School of Science and Engineering, Saitama University), Richard Simon Wallis(The University of Tokyo), Eiichi Tajika(Department of Earth and Planetary Science, Graduate School of Science, The University of Tokyo)

The United Nations' Sustainable Development Goals (SDGs) have come to be widely recognized as a common goal for humankind, involving the international community. For many of the 17 goals and 169 targets, earth and planetary science has a significant potential role. It is also important for us, as one of the largest academic societies in Japan, to develop activities in line with the spirit of the SDGs. In this session, we will discuss how the research activities of earth and planetary science are related to the SDGs, how to expand our contributions in the future, and how JpGU itself should be in accordance with the SDGs.

[U04-P01] SDGs and academic researches in the Solid Earth Science Section

*Michihiko Nakamura[1], Yo Fukushima[2] (1.Department of Earth Science, Graduate School of Science, Tohoku University, 2.Disaster Science Division, International Research Institute of Disaster Science, Tohoku University)

[U04-P02] Ongoing research in Human Geosciences and its possible contributions to SDGs

*Reiichiro Ishii[1], Makoto Taniguchi[1], Naoki Masuhara[1], Sanghyun Lee[1] (1.Research Institute for Humanity and Nature)

[U04-P03] Contribution of SDGs in Subtropical Islands

*Jun Yasumoto[1] (1.University of the Ryukyus, Faculty of Agriculuture)

[U04-P04] Education for Sustainable Development (ESD) and environmental studies promoted by Seikei Gakuen

*Hitoshi Fujiwara[1], Atsushi MIYASHITA[1], Masumi Zaiki[2], Hironobu Oda[2], Atsuko Ikegami[1] (1.Education and Research Center for Sustainable Development/Faculty of Science and Technology, Seikei University, 2.Education and Research Center for Sustainable Development/Faculty of Economics, Seikei University)

SDGs and academic researches in the Solid Earth Science Section

*Michihiko Nakamura[1], Yo Fukushima[2]

1. Department of Earth Science, Graduate School of Science, Tohoku University, 2. Disaster Science Division, International Research Institute of Disaster Science, Tohoku University

Solid Earth sciences play an important role in achieving the SDGs in securing mineral, energy, and water resources, carbon capture and storage, geological disposal of high-level radioactive waste, disaster mitigation for earthquakes, volcanic eruptions, and landslides. Integrated viewpoints of SDGs are, in turn, suggestive for the development of Earth and planetary science as a system science. The closer connection of academia to economic and social activities such as ESG investment will strengthen international competitiveness. Based on this recognition, we would like to provide topics that match the scope of this session.

Keywords: SDGs, ESG investment, disaster mitigation

©2021. Japan Geoscience Union. All Right Reserved.

Ongoing research in Human Geosciences and its possible contributions to SDGs

*Reiichiro Ishii[1], Makoto Taniguchi[1], Naoki Masuhara[1], Sanghyun Lee[1]

1. Research Institute for Humanity and Nature

We will share some example topics from ongoing research in Human Geosciences field in Japan, partitularly conducted at Reasearch Institute for Humanity and Nature, and discuss its possible future contributions to the related SDGs

Keywords: SDGs, Resource Use, Ecosystem, Hydrological Cycle

©2021. Japan Geoscience Union. All Right Reserved.

Contribution of SDGs in Subtropical Islands

*Jun Yasumoto[1]

1. University of the Ryukyus, Faculty of Agriculuture

In this paper, we will briefly introduce the project "Watershed Governance Based on Participation and Consensus for
Sustainable Water Resource Use in Subtropical Islands" which is being implemented with the support of JST and aims to solve the SDGs.

Keywords: Watershed Governance, Sustainable Water Resource Use, Subtropical Islands

©2021. Japan Geoscience Union. All Right Reserved.

Education for Sustainable Development (ESD) and environmental studies promoted by Seikei Gakuen

*Hitoshi Fujiwara[1], Atsushi MIYASHITA[1], Masumi Zaiki[2], Hironobu Oda[2], Atsuko Ikegami[1]

1. Education and Research Center for Sustainable Development/Faculty of Science and Technology, Seikei University,
2. Education and Research Center for Sustainable Development/Faculty of Economics, Seikei University

Seikei Gakuen is an educational corporation which includes elementary school, junior high school, high school, and university (graduate school). From the beginning of Seikei Gakuen (1912), we have had educations and learning for ESD; e.g., practical training/studies of agricultural works and observations of nature. In particular, the meteorological observatory has continued weather-monitoring at Kichijoji/Tokyo since 1926. In order to increase the ESD activities, Seikei Education and Research Center for Sustainable Development (ERCS) has been established in April 2018. Seikei Gakuen has also joined the UNESCO Associated Schools Project Network in November 2019.
In this presentation, we will introduce our ESD activities, in particular, environmental studies to exchange information about study programs, educational tools, and so on with participants in the session. We hope enhancement of organized activities in the field of the Earth and Planetary Sciences for SDGs.

Keywords: Education for Sustainable Development, environmental studies, UNESCO Associated Schools Project Network, practical training/studies

©2021. Japan Geoscience Union. All Right Reserved.

[J] Poster | U (Union) : Union

Sun. Jun 6, 2021 5:15 PM - 6:30 PM JST | Sun. Jun 6, 2021 8:15 AM - 9:30 AM UTC | Ch.01_2

[U-09] Advancing SDGs through inclusive partnerships II: Engaging with communities

convener:Hidenroi Nakamura(Toyama Prefectural University), Vincent Tong(University College London), Mika Shimizu(Kyoto University), Fumiko Noguchi(United Nations University, Institute for the Advanced Study of Sustainability)



Sustainable Development Goals (SDGs) provide a comprehensive framework underpinning a wide range of interdisciplinary initiatives in Earth Sciences. With interconnected objectives and impact across natural, social and human sciences, inclusive partnerships between academics, students, citizens, industry, businesses and other stakeholders are critical to the success of these initiatives. Such partnerships involving academics and students across all types of higher education institutions and high schools have profound impact on the local communities across Japan. In this session, we examine the significance of inclusive partnerships in SDG-aligned research, outreach and education initiatives in Japan. We will focus on ways to engage with local communities and the wider Japanese society, including marginalised individuals and groups. We welcome contributions based on i) critical reflections on research and education projects from the perspectives of academics, students and non-academic partners, ii) theoretical examination of the nature of inclusive partnerships in the Japanese cultural contexts, and iii) evidencing impact of inclusive practices in SDG initiatives.

[U09-P01] SDGs community and social engagement in education and research: Implication for JpGU

*Hidenroi Nakamura[1] (1.Toyama Prefectural University)

SDGs community and social engagement in education and research: Implication for JpGU

*Hidenroi Nakamura[1]

1. Toyama Prefectural University

Community engagement in education and research activities of higher education institutions is crucial for SDGs promotion. I reflect and introduce own cases of education and research in Chubu region of Japan, including Toyama, to share the idea and implication for JpGU activities toward inclusive partnership. The cases include education under the COVID-19 in collaboration with a citizen organization promoting SDGs, citizen-led backcasting-based scenario making with a student and researchers, clinical volcano disaster management study in collaboration with local governments, and citizen dialogue study in collaboration with scientists. Implications to JpGU include promoting identification of linkage between three aspects of SDGs, i.e., economy, society and environment, and each discipline and field of activity. Moreover, it is desirable to strive strategic partnership development intentionally and experimentally: linking research and community, linking education and community, and linking research, education and community.

Keywords: SDGs, community engagement, partnership, collaboration, linkage

©2021. Japan Geoscience Union. All Right Reserved.

[J] Poster | O (Public)：Public

Sun. Jun 6, 2021 5:15 PM - 6:30 PM JST | Sun. Jun 6, 2021 8:15 AM - 9:30 AM UTC | Ch.02_1

[O-02] Natural disasters and people -Listen to the voice of the Earth on the Japanese Geoparks-

convener:Noritaka Matsubara(Graduate School of Regional Resource Management, University of Hyogo), Kyohei Sano(Graduate School of Regional Resource Management, University of Hyogo), Suzuka Koriyama(Itoigawa city), Hikaru Yokoyama(Hokusho University)

People benefit from the earth, while sometimes geological activities bring disaster to human society. Geoparks aim to reconnect human society at all levels to our home planet and to celebrate how the planet with 4.6 billion years long history has shaped every aspect of our lives and society. Many geoparks in tectonically active areas of the world have a crucial role in helping mitigate geo-hazards through awareness-raising and constructing disaster response strategies. In this session, we discuss how people have lived with geological activities and natural hazards, and how to deal with new threats, including COVID-19, in nature through geoparks.

[O02-P01] New coronavirus response in Fossa Magna Museum

*Takahiko Ogawara[1], Ko Takenouchi[1], Yousuke Ibaraki[1], Takeo Kobayashi[2], Takuma Katori[2] (1.Fossa Magna Museum, 2.Itoigawa City Hall Geopark Promotion Office)

[O02-P02] Short-Term Effects of SNS Marketing: a Case Study in Hakusan Tedorigawa Geopark

*Susan May[1] (1.Hakusan Tedorigawa Geopark Promotion Council)

[O02-P03] Activities to promote the local sustainable development - Report at the time of spread of COVID-19 infection from Mt.Kurikoma Area Geopark -

*Yui Hasegawa[1], Rie Nakagawa[1], Seiya Tanaka[1], Jun Nagao[1] (1.Mt.Kurikoma Area Geopark Promotion Committee)

[O02-P04] Geotourism in Corona (COVID-19) related crisis - Advantage of being outdoors : In case of San'in Kaigan UNESCO Global Geoprk -

*Noritaka Matsubara[1], NAGAHAMA SATOSHI[1] (1.Graduate School of Regional Resource Management, University of Hyogo)

[O02-P05] Operation of geo-tours using online delivery tools under COVID-19

*Taku Morimoto[1] (1.Unzen Volcanic Area Geopark Promotion Office)

[O02-P06] Holding of event the Lake Shikaribetsu Igloo Village under COVID-19 measures

*Kanamori Syosaku[1], Hiroki Matsumoto[1], Onishi Jun[1] (1.Tokachi-Shikaoi Geopark Promotion Council)

[O02-P07] Stay-at-home Project with Local Students in Toya-Usu UNESCO Global Geopark

*NIRE KAGAYA[1], Yoshiaki Hata[1], Akihito Kato[2], Kiyono Kuroda[2], Koki Takagi[2], Kazuma Iwamura[2], Kanako Kitada[2], Koki Tomita[2], Mina Shionoya[2] (1.Toya-Usu UNESCO Global Geopark Council, 2.Date-Midorigaoka Highschool)

[O02-P08] Developing the San’in Kaigan Geopark Trail and the promotion of geotourism during COVID-19 Pandemic

*Hiroshi Nakase[1] (1.San'in Kaigan Geopark Promotion Council)

[O02-P09] A comparative study of educational on-site and online geotours in Hamamatsu-Hamanako Aspiring Geopark, Japan

*Hiroki Nagano[1], Masato Koyama[2], Yusuke Suzuki[2], Megumi Fukuyama[2] (1.Hamamatsu Technical High School, 2.Shizuoka University)

[O02-P10] Topographic evolution after the Aso-4 pyrocrastic flow and the meaning for disaster prevention in the Oita Bungoono Geopark, Japan

*Toshikazu Yoshioka[1] (1.Oita Bungoono Geopark Promotion Council)

[O02-P11] Conservation and Utillization of Natural Disaster Monument on Tosashimizu Geopark Plan

*Moriguchi Natsuki[1], Satoru Imai[1], Aika Sakuda[1], Kouichi Saruta[1], Michiru Sakai[1] (1.Tosashimizu Geopark Promotion Council)

[O02-P12] Records and countermeasure of disasters in Shimokita Geopark

*Satoshi Ishikawa[1], Kirika Kitagawa[1] (1.Shimokita geopark promotion council)

[O02-P13] Inform of weather disasters in geoparks

*Hiroshi Sato[1,2], Shinichi Sugimoto[3], Makoto Aoi[4], Shinya Miura[4], Hinako Suzuki[4] (1.Mt.Bandai Museum, 2.Bandaisan Geopark Council, 3.Unzen Volcanic Area Global Geopark, 4.National Research Institute for Earth Science and Disaster Resilience)

[O02-P14] How to Prevent Elderly People from Natural Disasters - An Example in Unzen Volcanic Area UNESCO Global Geopark -

Shunsei OGATA[1], Hiyori KADOHATA[1], Tasuku KONDO[1], Miraku TANAKA[1], Kosei HASHIDA[1], Shinsho FUJIO[1], Mizuho IWANAGA[1], Aiko ENGUCHI[1], Seren OTA[1], Rika TANAKA[1], Toru YAMAUCHI[2], Hiroaki OSAKO[2], *Marekazu OHNO[3] (1.Glocal Course of Nagasaki Prefectural Koka High School, 2.Nagasaki Prefectural Koka High School , 3.Unzen Volcanic Area Geopark Promotion Office)

[O02-P15] Disaster and Disaster Prevention Learning in the Naeba-Sanroku Geopark

*Kouhei Nakano[1] (1.Naeba-sanroku Geopark Promotion Council)

[O02-P16] Lives of the local people on the collapsing land and the flowing land by river water - Think about geohazard program of Miyoshi geopark project-

*Azusa Tonotani[1], Katsunori Ozakai[1], Mizuki Tochitani[1], Hiroyuki Ohnishi[1], Toshiaki Matsumoto[1] (1.Geopark Promotion office in Miyoshi city)

[O02-P17] Toward restoration of Geosites damaged by natural disaster with reaching consensus in local community: a case of Suzaki Coast in Seiyo City, Japan.

*Takumi Sakakiyama[1], Kazunari Kimura[2], Yuya Kato[3], Masahito Ono[1], Tsukasa Takahashi[1] (1.Seiyo City, 2.NAIBA Co. Ltd., 3.Noyama Company)

[O02-P18] Let's investigate the earth activity from Shimonita Geopark

*Hara Hideo[1] (1.Geopark Shimonita council)

[O02-P19] **The foundations of Yuzawa Geopark: a unification and a compilation of six geological maps published by the Geological Survey of Japan and Akita Prefecture**

*Akio Sasaki[1], Kohei Yamawaki[1], Yukio Fujimoto[1], Syoichi Goi[1], Shoei Chiba[1] (1.Network of Earth Science Museum for Akita)

[O02-P20] Conservation concerns in Yuzawa Geopark: Distributions and seasonal variation in blood-sucking flies and an invasive plant species

*Haruki Takayanagi[1] (1.Yuzawa City Geopark Promotion Council)

[O02-P21] The relationship between the former plate boundary and residents, especially the signboard production process

*Kato Satomi[1] (1.Mt. Apoi Geopark Promotion Council)

[O02-P22] Fossil collecting experience to solve summer vacation indipendent study in Itoigawa UNESCO Global Geopark

*Yousuke Ibaraki[1], Yutaka Furumi, Emma Longhorn, Takahiko Ogawara[1], Ko Takenouchi[1], Takuma Katori[2], Takeo Kobayashi[2] (1.Fossa Magna Museum, 2.Itoigawa Geopark Council)

[O02-P23] Geosite Map and Card in a Fun and Interesting Way by Local Elementary School Students: a Case Study of Geosite in Nankikumano Geopark with Takaike Elementary School

*Hiroko Shibasaki[1] (1.Nanki-Kumano GeoPark Guide Club)

[O02-P24] **Examples of joint projects (or joint events) between a museum and Sado Island Geopark**

*Takeyoshi SADAKANE[1], Mituhisa AIDA[1] (1.Sado Geopark Promotion Council)

[O02-P25] A Guide program that promote Proactive learning in School trip
- Practice at Toya-Usu UNESCO Global Geopark -

*Hikaru Yokoyama[1] (1.Hokusho University)

[O02-P26] Educational Program on spring water of Aso UNESCO Global Geopark related with elcetrical conductivity (Part 2)
Cooperated Research on Minamiaso Spring Water

*Tsuneomi Kagiyama[1], Koki Nagata[2], Toshikazu Maeda[3], Yuto Takeuchi[3], Haruki Watanabe[3], Kozue Inoue[3] (1.Aso Geopark Promotion Council, 2.Aso Volcano Museum, 3.Takamori Senior High School)

[O02-P27] Looking back on 11 years of the educational activities of the Dinosaur Valley Fukui Katsuyama Geopark

*Sumiaki Machi[1] (1.Dinosaur Valley Fukui Katsuyama Geopark Promotion Council)

New coronavirus response in Fossa Magna Museum

*Takahiko Ogawara[1], Ko Takenouchi[1], Yousuke Ibaraki[1], Takeo Kobayashi[2], Takuma Katori[2]

1. Fossa Magna Museum, 2. Itoigawa City Hall Geopark Promotion Office

Itoigawa Fossa Magna Museum is a core facility of the Itoigawa UNESCO Global Geopark. The museum opened in 1994 and was renovated in 2015. The museum's main exhibits are jade, limestone fossils, Itoigawa-Shizuoka Tectonic Line and formation of the Japanese archipelago. 90,270 people visited the museum in 2019.
The number of visitors in 2020 is 49.4% of the previous year's level (April to November), and the Fossa Magna Museum has implemented the following measures. (1) Corona prevention and three densification measures that allow visitors to visit the museum with peace of mind. (2) Development of a website that provides virtual tours of the museum and introduces the highlights of outdoor exhibits. (3) Introducing the museum remotely using Zoom and other tools.

Corona prevention and three densification measures at the Fossa Magna Museum

The following measures have been implemented at the Fossa Magna Museum: Prohibition of visitors from seven prefectures (April 8 to April 24, 2020). Temperature check and entry into the museum (April 8 to June 18, 2020; temperature check is ongoing). Temporary closure of the museum in response to the spread of infection (April 25 to May 30, 2020). Entry restricted to residents of non-Niigata Prefecture (June 1 to June 18, 2020). Stone appraisal service will be suspended (from March 9, 2020 to March 2021). The use of the Fossil Valley will be suspended (April 1, 2020 to June 30, 2020).
The temperature of each visitor was taken by a staff member using a non-contact thermometer when entering the museum. In order to solve this problem, the museum introduced an automatic temperature-taking device equipped with AI. This device automatically measures the body temperature of each visitor and calls for attention if the visitor is not wearing a mask.
Stone appraisal service is the museum's own promotion activity, in which visitors can bring in up to five stones and have their names appraised free of charge. As a countermeasure against the three densities of the corona disaster, the museum considered distributing numbered tickets and making advance reservations via the Internet or telephone. However, it has been decided to suspend these measures until the end of March 2021.
Therefore, the Fossa Magna Museum held an outdoor appraisal class (1,000 yen per class) during the summer vacation as an alternative to stone appraisal. For this event, we used the stone specimen kit "Hirokko" created by the Itoigawa City Tourism Association. Total of 16 workshops were held, with 122 participants from inside and outside the city.

Development of a website to introduce virtual tours of the museum and highlights of the outdoor exhibits

The Fossa Magna Museum was faced with the challenge of how to enjoy the museum when it is closed. In the fall of 2019, the Itoigawa Geopark Council conducted photography and virtual tours of the exhibition rooms using Matterport, a 3D model camera developed by Hokkaido Map Co. And a local cable TV station filmed a video of a curator giving a tour of the museum and posted it on the website.

Museum Introduction Using Zoom

Since the Corona disaster, the use of web conferencing systems such as Zoom has been developing rapidly. The Fossa Magna Museum conducted an online virtual tour of the museum using Zoom at the University Festival of the Faculty of Science of Niigata University (October 18) and the Chubu Block

©2021. Japan Geoscience Union. All Right Reserved.

Conference of the Japanese Geoparks Network (November 21). This was achieved by using a smartphone and a gimbal to connect to the Zoom conference room via a cell phone line. At the Chubu Block Conference, we not only provided a tour of the museum, but also broadcasted real-time indoor experiments and videos that we had taken in advance.
Virtual tours have the potential to make it possible to visit places that have been difficult to visit in large groups, such as conventional tours.

Keywords: Itoigawa UNESCO Global Geopark, Fossa Magna Museum, Countermeasures against new coronavirus infectious

©2021. Japan Geoscience Union. All Right Reserved.

Short-Term Effects of SNS Marketing: a Case Study in Hakusan Tedorigawa Geopark

*Susan May[1]

1. Hakusan Tedorigawa Geopark Promotion Council

Hakusan Tedorigawa Geopark, located in Hakusan City, Ishikawa Prefecture, is located near Kanazawa City –a famous and popular tourist destination. With the aim of increasing the number of tourists to the Geopark, from August 2020 we began a Social Network marketing campaign using the paid advertisement functions of Facebook and Instagram.

Online ads can be made to target certain areas, and we targeted Ishikawa Prefecture and the surrounding prefectures. From August to November we excluded the two prefectures directly neighboring Ishikawa Prefecture. As a result, views from Ishikawa Prefecture were the highest, with views becoming less frequent further from Ishikawa. This was also evident in views to the website, with the majority being from Ishikawa, with an increase in views from nearby prefectures.

As a result of the campaign we saw an immediate, but short-lived increase in views to our website as a result of advertisement clicks, which gradually decreased over time. Our Instagram account went from 302 followers in July, to 827 in February –a 174% increase. We noticed that advertisements containing pictures of scenery had high click rates, and advertisements were most popular with middle-aged people. As expected, advertisements concerning education and activities for children were most popular with middle aged women.

In addition to the effects to our website views, we also saw a small effect in the field. During September we conducted a survey at several key sights in the Geopark, and 2 people of the 168 people surveyed said that they came as a result of the advertisement, proving that although small, the advertisements had an effect. However, after running a campaign for approximately one month, where visitors were encouraged to visit a museum in exchange for a discount coupon, no visitors came to receive the coupon. Therefore it is believed that an instant response from viewers requires a greater reward and/or a longer run time.

As we continue this campaign we will continue to measure the effects both through online analysis and in-field surveys. Not only do we hope to see an increase in tourists, but also an increase in awareness of the Geopark.

Keywords: SNS, Marketing, Facebook, Instagram, Geopark, Tourism

©2021. Japan Geoscience Union. All Right Reserved.

Activities to promote the local sustainable development - Report at the time of spread of COVID-19 infection from Mt.Kurikoma Area Geopark -

*Yui Hasegawa[1], Rie Nakagawa[1], Seiya Tanaka[1], Jun Nagao[1]

1. Mt.Kurikoma Area Geopark Promotion Committee

Due to the effects of the spread of COVID-19, it became difficult to hold events where people could gather and various projects that had been previously planned. However, we worked to find projects that we could carry out only because our normal activities were restricted.
In conservation activities, we made use of the grant system and cooperated with researchers from universities and research institutes to promote research on disaster prevention education, social services, ecology, etc., and actively engaged in research activities that are at the root of Mt.Kurikoma Area Geopark.
In educational activities, we received requests from teachers to conduct learning activities as usual, mainly at elementary schools in the city, and implemented Geopark learning programs 50 times after taking sufficient measures to spread the disease. We also provided online information on Mt.Kurikoma Area Geopark Visitor Center and guidebooks were distributed free of charge to support learning.
In economic activities, we prepared guidelines for guiding activities to prevent the spread of COVID-19 infection, and studied and implemented safety management measures such as setting a limit on the number of guides and guiding with masks.
With regard to the "Kurikoma Sanroku no Megumi," an initiative to certify products that take advantage of the location and regional characteristics of Mt.Kurikoma Area Geopark, an e-commerce site was set up in the summer as part of support for certified businesses whose sales have declined due to the spread of COVID-19. For about three months, the EC site was set up to sell an assortment of partially certified products in the confectionery category. After that, the site was revised based on the sales results, and at the end of the year, sales for year-end gifts were conducted and 62 applications were received. At present, a stamp rally is being held until June 30, 2021, in which 17 stores, including stores in the food (restaurant) sector, are participating.
From these, we will consider sustainable regional development using Geoparks in COVID-19.

Keywords: Mt.Kurikoma Area Geopark, Geopark, Sustainable Development, Local Participation, Empowerment

©2021. Japan Geoscience Union. All Right Reserved.

Geotourism in Corona (COVID-19) related crisis - Advantage of being outdoors : In case of San'in Kaigan UNESCO Global Geoprk -

*Noritaka Matsubara[1], NAGAHAMA SATOSHI[1]

1. Graduate School of Regional Resource Management, University of Hyogo

The Corona (COVID-19) has a great impact on tourism in the world. UNWTO reports international tourist numbers could fall 60-80% in 2020. The other hand, number of tourists increased on some geosite and activity group in the San'in Kaigan UNESCO Global Geopark. We discuss why the number of tourists has increased or not changed in some sites and activities.

Keywords: geopark, tourism, COVID-19

©2021. Japan Geoscience Union. All Right Reserved.

Operation of geo-tours using online delivery tools under COVID-19

*Taku Morimoto[1]

1. Unzen Volcanic Area Geopark Promotion Office

1. Introduction

The COVID-19 has greatly affected social activities around the world. In the geopark programs, many activities and events had to be postponed or cancelled. While it has become difficult to conduct activities in the “face-to-face” style, the “online” forms of activities have gained the attention.

In 2020-2021, the Council of Unzen Volcanic Area Geopark (hereinafter called Unzen Geopark) conducted learning activities for secondary schools and took part in the exchange program for primary schools with the Oita Bungoono Geopark, using a web-meeting system “Zoom”. As these activities were held indoors, it was found that they could be easily conducted as long as the Internet environment (e.g., wired LAN) was stable.

As for the online geo-tours delivered from outdoors, they required a great deal of effort, compared to the indoor activities, including the selection of delivery tools, checking the Internet environment at each site of the tour, and acquiring camera techniques. This presentation will share the experience of online geo-tours conducted by the Unzen Geopark in 2020, and report on the types of delivery tools, and advantages, points of concern and issues in different methods.

2. Tools used for the online geo-tours

The online geo-tours were conducted in 2 ways: both ways used a mobile Wi-Fi router, but one in combination with Zoom (smartphone ver.) only, and the other with GoPro video camera and Zoom (PC ver.) together. The former method is to use a smartphone with Zoom app and an image stabilizer with anti-shake function. This method has an advantage of enabling interaction via smartphone screen and having a Q&A session during the tour. Its disadvantage is that the camera and sound-collection functions depend on the performance of smartphone. The latter method is to use the live-streaming function of GoPro and a platform for online streaming such as YouTube and Twitch. For the platform, Twitch is recommended as its transmission delay is short. An advantage of this method is that it can deliver sharp images of the sites to viewers, while it requires an initial cost for purchasing equipment. Since GoPro allows only one-way communication from the host to viewers, it is necessary to connect the Zoom from other devices if a Q&A session is conducted during the tour.

3. Issues and points of concern in conducting online geo-tours

The Unzen Geopark conducted online geo-tours guided by official Geopark Guides during the evaluation for revalidation of geopark status by the Japan Geopark Committee and in the event hosted by Oita Prefecture. One of the issues faced in the tours was that even if the Wi-Fi router was within the coverage area of the carrier used, there was a problem with Internet connectivity at some sites. Even in open fields with no geographical distance or obstacles, there were cases that Wi-Fi connection did not work. Therefore, when conducting online tours, it is important to carefully check the Wi-Fi connection at each site in advance and set the tour route including where to place the Wi-Fi router.

It is also necessary to have the camerawork that prevents viewers from getting screen sickness, and to put “pauses” for viewers to enjoy the scenery. During the tours, staff of the Unzen Geopark operated the

©2021. Japan Geoscience Union. All Right Reserved.

camera while the Guides explained about the site, but due to the fast pace of Guides switching the explaining subjects and walking, there were times when a “gap” occurred between the scenery shown and the contents of explanation. If the camera moves fast, it will elicit screen sickness from viewers and will not fully covey the appeal of the tour. It is important to always remember to guide the tour from the standpoint of the viewers watching through the screen.

In the event hosted by Oita Prefecture, it was planned to live-stream “a walk” in hot-spring town of Obama. However, due to an error caused by updating the GoPro app just before the event, it became impossible to live-stream a walking tour. We had to give up the walking tour, and changed to conduct the tour using the built-in camera of a PC connected to Zoom and showing the scenery that could be delivered without moving the PC. This kind of sudden trouble happens anytime, so it is important to always make an alternative plan when conducting an online tour.

4. Future prospects

It was found that anyone can easily start online tours if they become familiar with equipment and delivery tools. If more geoparks start conducting online geo-tours, it will be possible to deliver geo-tours jointly with other geoparks under common themes in the future.

Keywords: Live streaming, online geo-tours, Zoom, GoPro, mobile Wi-Fi router

©2021. Japan Geoscience Union. All Right Reserved.

Holding of event the Lake Shikaribetsu Igloo Village under COVID-19 measures

*Kanamori Syosaku[1], Hiroki Matsumoto[1], Onishi Jun[1]

1. Tokachi-Shikaoi Geopark Promotion Council

Tokachi Shikaoi Geopark is a geopark that covers the entire area of Shikaoi Town in the Tokachi region of Hokkaido. Theme of the geopark is “The story of life developed by volcanoes and freezing.” There are several geopark sites related to the cold climate. Lake Shikaribetsu in the northern part of Shikaoi Town is a representative site of Tokachi Shikaoi Geopark, and it freezes completely in winter. Since 1980, an event entitled "Shikaribetsuko-Kotan",which means “Lake Shikaribetsu Igloo Village”, has been held at Lake Shikaribetsu in winter. Kotan means village in Ainu language. At this event, many buildings called igloos are built using snow and ice on the frozen lake. There are many interesting activities such as ice bars, open-air bath, concerts in the igloos. This "Shikaribetsuko-Kotan" is also an important “site” of Tokachi Shikaoi Geopark.
"Shikaribetsuko-Kotan" in 2021 is held for about two months from January 30, 2021 under measures against COVID-19, while many domestic events have been canceled due to the influence of the corona disaster. In this presentation, we will report how the event was and discuss the ideal way of events under the influence of COVID-19.

Keywords: COVID-19, geopark

©2021. Japan Geoscience Union. All Right Reserved.

Stay-at-home Project with Local Students in Toya-Usu UNESCO Global Geopark

*NIRE KAGAYA[1], Yoshiaki Hata[1], Akihito Kato[2], Kiyono Kuroda[2], Koki Takagi[2], Kazuma Iwamura[2], Kanako Kitada[2], Koki Tomita[2], Mina Shionoya[2]

1. Toya-Usu UNESCO Global Geopark Council, 2. Date-Midorigaoka Highschool

In 2020, it was almost impossible to hold group events and outdoor activities as COVID-19 raged in Japan, and brown bears were spotted in our community more often than ever.
Under such a challenging circumstance, we sought to organize activities in different ways. In this presentation, we would like to give you one of the activities we did while observing the social distancing policy. We will present an educational project, “Let’s make together Lake Toya’s underwater model!”, which was carried out in collaboration with local elementary school pupils and junior and senior high school students.
This project was designed to make a 1/1,000 scale (1.3 m x 1.3 m) model of Lake Toya that reproduces the lake’s topography with local children. The model has been exhibited at the Lake Toya Tourist Information Center.
The nine-month project was developed as follows.
-Stage 1 (‘Stay-at-home event’): Participants made 148 layered model parts (37 layers x 4 divisions);
-Stage 2: Students of Date Midorigaoka High School Geography Course assembled the parts and painted the model; and
-Stage 3: The students made a presentation, and the model exhibition began.
If you ask a professional to make this kind of model, no one can be involved in the process. We designed this project as a participatory event for the people in the area. A total of 150 people (and their families) participated in making the model, and the completed work will be a symbolic exhibit of the Geopark in the future. We plan to use the model for teaching the history of regional topography formation and the risk reduction of geological disasters.
The COVID-19 pandemic will trigger significant changes to the communication and values that we appreciate. Each Geopark must think of what role the world expects from Geoparks and what contributions we can make to the world. To this end, Geoparks in Japan and the world have done various practices while being aware of the world after COVID-19, which have given us many thoughtful insights and new ideas.
Geoparks in Japan have domestic and international networks such as JGN, APGN, and GGN. These networks’ significance is represented in the diversity that encourages us to simultaneously address multiple challenges based on each region’s unique characteristics, and the oneness that unites us to promote such diverse activities by sharing “failures” and “know-how on success”. In our presentation, we will share with you one of our various practices by talking about our trials, errors, and the resulting success.

Keywords: Geopark, Geomorphology, Disaster Risk Reduction Education, Education for Sustainable Development

©2021. Japan Geoscience Union. All Right Reserved.

Developing the San’in Kaigan Geopark Trail and the promotion of geotourism during COVID-19 Pandemic

*Hiroshi Nakase[1]

1. San'in Kaigan Geopark Promotion Council

The establishing a long trail route, 230km long east-west route connecting Tottori City, Tottori Prefecture and Kyotango City, Kyoto Prefecture was completed in February 2020.

Even during the time of sharp drop down of number of tourist and a severe decline of tourism industry because of COVID-19 pandemic, the trail walk activity was safely conducted in 2020 using the newly completed trail, under the title of "Now is the time to return to nature! To the San'in Kaigan Geopark Trail!", with regional campaigns to revitalize the local economy, maintain and secure employment and consumption, maintain the health of local residents, promote the use of national parks, and foster awareness of environmental protection.

In implementing the activity, a system was established so that visitor centers, geoguides, outdoor activity businesses, retailers, and restaurants can cooperate to conserve geosites and provide services in order to strengthen geotourism after COVID-19 pandemic.

Through poster session, we will introduce the contents of this campaign, its results of 2020, and future developments of it.

Keywords: San’in Kaigan Geopark, tourism, protection and conservation

©2021. Japan Geoscience Union. All Right Reserved.

A comparative study of educational on-site and online geotours in Hamamatsu-Hamanako Aspiring Geopark, Japan

*Hiroki Nagano[1], Masato Koyama[2], Yusuke Suzuki[2], Megumi Fukuyama[2]

1. Hamamatsu Technical High School, 2. Shizuoka University

We made a practical study of on-site and online geotours in Hamamatsu-Hamanako Aspiring Geopark, central Japan, to clarify and compare educational effects of each type of tours. In August and October of 2019, we made two on-site bus tours (tours 1a and 1b), both of which were based on the same scenario focusing on the geological formation of Lake Hamanako and its deformation by the AD1498 tsunami disaster. In September and November of 2020, we made two online tours (tours 2 and 3) using the internet meeting application Zoom because of restriction under the COVID-19 pandemic. While tour 2 focused on the same scenario as tours 1a and 1b, tour 3 was based on the different scenario, which focused on the geological formation, historical floods, and relating agricultural/industrial products in the alluvial plain of the Tenryugawa River. All of the on-site and online tour participants were children and their parents, which were recruited by advertisement in elementary schools in the City of Hamamatsu. Main results of pre- and post-tour questionnaire surveys are as follows: (1) Understanding level of geological process (L1), pride level for regional geosites (L2), motivation level for further learning (L3), and total satisfaction level (L4) all show significant increases after tour 3, comparing with those before the tour. (2) L1 and L4 after tour 3 show significant increases comparing with those after tour 2. This is probably resulted from the decrease of connection troubles during tour 3 by improvement of networking instruments, (3) L1 and L4 after tour 3 are similar with those after tour 1a/1b. This may mean that educational effects of good online tours are equivalent as those of on-site tours.

Keywords: Geopark education, Online tour, Educational effect

表１　オンラインツアー第２回事後アンケート結果と，同オンライン第１回及び対面ツアーとの比較

質問項目		全体 (n=37)	第１回比	対面比	児童等 (n=27)	第１回比	対面比	大人 (n=10)	第１回比	対面比
1	浜名湖（天竜川）の地形の成り立ちを説明できるようになった	3.3	**+0.6	-0.3	3.2	**+0.8	-0.2	3.5	+0.4	-0.3
2	地域に浜名湖（天竜川）があることを誇りに思うようになった	3.7	+0.2	+0.0	3.6	+0.1	-0.0	3.9	+0.5	+0.2
3	自分の住んでいる地域にについて自分から勉強したくなった	3.3	+0.0	-0.0	3.1	-0.0	-0.1	3.7	+0.0	+0.2
4	ツアー全体の満足度	3.7	**+0.4	-0.1	3.5	*+0.5	-0.2	3.9	**+0.5	-0.0

（表中の＊は$p<0.1$，＊＊は$p<0.05$であり，前者は有意傾向，後者は有意差があることを示している。）

©2021. Japan Geoscience Union. All Right Reserved.

Topographic evolution after the Aso-4 pyrocrastic flow and the meaning for disaster prevention in the Oita Bungoono Geopark, Japan

*Toshikazu Yoshioka[1]

1. Oita Bungoono Geopark Promotion Council

The southwestern part of Oita Prefecture, where the Oita Bungoono Geopark is located east of the Aso v olcano, and the plateau formed by the Aso-4 pyroclastic flow that erupted about 90,000 years ago is spreading. The plateau was dissected by the Ono River and other rivers, and the remaining part of the plateau is called "Haru" and is used as a vast agricultural land. Of the dissected valleys, the valley bottom of the basin formed by relatively small rivers has been used as a residential area because it is easy to obtain water for living. On the other hand, the Ono River, which is one of the longest rivers in Kyushu, forms a deep valley while meandering, and although several river terraces can be seen along the river, the alluvial plain is hardly distributed.
The central city area of Mie Town, where the Bungo Ono City Hall is located, is located near the confluence of the Mie River and Tamada River, which are tributaries of the Ono River. After merging with the Tamada River, the Mie River does not head toward the main stream, the Ono River, but flows southeast toward the mountains, and after merging with the Matsuo River, flows north and joins the Ono River. The area near the confluence with the Matsuo River is a constriction, and upstream of it is accompanied by a wide alluvial lowland, but after the confluence it forms a deep valley.
These topographic features are greatly related to the characteristics of disasters in this area. First of all, along the Ono River, there is a disaster caused by the rise in water level during rainfall. The Ono River has a large basin area, and the upstream area includes areas with high rainfall such as the Aso, Kuju, and Sobo-Katamuki mountains. In addition, dencely welded tuff of the Aso-4 pyroclastic flow is distributed along the main stream, and the valley bottom plain is narrow because lateral erosion is hindered, and the water level rises at once when the water level rises. On the other hand, the lowlands along the tributary Mie River have their exits blocked, so once flooding occurs and the surrounding lowlands are flooded, drainage may become difficult. In addition, the small tributaries that flow into the Mie River are relatively steep and the valley width is narrow, so it can be pointed out that a disaster may occur due to debris flow. Furthermore, on the slope of the plateau edge, the base may be eroded by the gushing of groundwater, and the upper part of the slope may easily collapse.
The content of this presentation was given at the Association of Disaster Prevention Expert of Miemachi in October 2020, and efforts are being made to help with disaster prevention activities in the region.

Keywords: Oita Bungoono Geopark, Aso-4 pyroclastic flow, Ono River, topographic evolution, disaster prevention

©2021. Japan Geoscience Union. All Right Reserved.

Conservation and Utillization of Natural Disaster Monument on Tosashimizu Geopark Plan

*Moriguchi Natsuki[1], Satoru Imai[1], Aika Sakuda[1], Kouichi Saruta[1], Michiru Sakai[1]

1. Tosashimizu Geopark Promotion Council

Tosashimizu City in Kochi Prefecture, which corresponds to the area of the Tosashimizu Geopark plan, is facing the Pacific Ocean, and there are concerns about damage caused by the Nankai Trough earthquake and the resulting massive tsunami. In the past Earthquakes, such as the Hakuho, Hōei, Ansei Nankai, and Showa Nankai earthquakes, the city was severely damaged by earthquakes and tsunamis, which have been recorded in documents and monuments. In the Tosashimizu Geopark plan, seven stone monuments with records of Nankai Trough earthquakes and tsunamis existing in the area were designated as "Earthquake and Tsunami Related Monuments" as a cultural site. However, it was pointed out in the 2017 review for membership in the Japanese Geoparks Network that there was no legal basis for conservation. In addition, the use of the site for disaster prevention education was not sufficiently advanced.
In order to solve these problems, the Tosashimizu Geopark Promotion Council, in cooperation with citizens' groups and Tosashimizu City, conducted an exhaustive survey of the existing monuments recording past natural disasters in the area in 2019. As a result, 13 monuments related to other natural disasters, such as floods, were found, in addition to the earthquake and tsunami monuments that had already been designated as sites. These monuments were registered as "Natural Disaster Monuments" by the Geospatial Information Authority of Japan, and those with particularly high historical value were registered as tangible cultural properties designated by the city.
The Tosashimizu Geopark Promotion Council has reorganized these monuments as "Monuments to Natural Disasters," which include not only about earthquake and tsunami disasters, but also flood and typhoon disasters, and is promoting their use for disaster prevention education and awareness-raising about disaster prevention and mitigation. We conducted disaster prevention studies using the natural disaster monument at local elementary schools last year, and the monument will be included in a supplementary reader for social studies issued by the Board of Education. In addition, in cooperation with the Crisis Management Division, the division in charge of disaster prevention in Tosashimizu City, we are working to realize integrated disaster prevention and mitigation activities.
We will report on our action to preserve and utilize the stone monuments that record natural disasters in the Tosashimizu Geopark Plan. We will also discuss the prospects for disaster prevention and mitigation activities based on the use of natural disaster monuments in cooperation with citizens and local governments.

Keywords: Natural Disaster Monument, earthquakes, tsunamis, floods

©2021. Japan Geoscience Union. All Right Reserved.

Records and countermeasure of disasters in Shimokita Geopark

*Satoshi Ishikawa[1], Kirika Kitagawa[1]

1. Shimokita geopark promotion council

In Shimokita Geopark, local resident did not have enough disaster prevention awareness because of relatively much countermeasure for assumed disasters. So Shimokita Geopark Promotion Council strives to maintain and improve local resident's disaster prevention awareness by explanation of the example of hazards and countermeasures in other area and the disaster occurrence mechanism.

Keywords: Shimokita Geopark, Disaster, disaster prevention awareness

©2021. Japan Geoscience Union. All Right Reserved.

Inform of weather disasters in geoparks

*Hiroshi Sato[1,2], Shinichi Sugimoto[3], Makoto Aoi[4], Shinya Miura[4], Hinako Suzuki[4]

1. Mt.Bandai Museum, 2. Bandaisan Geopark Council, 3. Unzen Volcanic Area Global Geopark, 4. National Research Institute for Earth Science and Disaster Resilience

The land of Japan is prone to earthquakes and volcanic disasters, but the most frequent disasters are meteorological disasters. Typhoon-Vera class disasters are rare, but in recent years, rainfall caused by line-shaped precipitation system and river bank failures due to flooding. Especially in 2018 and 2019, meteorological disasters occurred in many parts of Japan. These disasters are not unique to others, but can also occur in geopark areas.

Therefore, the disaster prevention working group of the Japan Geopark Network (hereinafter referred to as JGN) thought that these disasters should be communicated in all geopark areas, and consulted with the National Research Institute for Earth Science and Disaster Resilience (hereinafter referred to as NIED). JGN and NIED signed an agreement on comprehensive cooperation in 2018, and have been working on a system called the "Earthquake!" to communicate the real-time occurrence of earthquakes in each region.

We have also decided to collaborate on weather-related disasters that have occurred frequently in recent years. The content of the collaboration is to create explanatory display panels on recent weather disasters and to display these panels in the Geopark area.The purpose of this project is to improve disaster literacy by viewing disasters as a personal challenge.

As the JGN, which has proposed putting more efforts into disaster prevention at UNESCO Geopark, we would like to continue to strengthen activities to inform of various disasters in geopark regions throughout Japan.

Keywords: weather disaster, disaster prevention, Geopark

©2021. Japan Geoscience Union. All Right Reserved.

How to Prevent Elderly People from Natural Disasters - An Example in Unzen Volcanic Area UNESCO Global Geopark -

Shunsei OGATA[1], Hiyori KADOHATA[1], Tasuku KONDO[1], Miraku TANAKA[1], Kosei HASHIDA[1], Shinsho FUJIO[1], Mizuho IWANAGA[1], Aiko ENGUCHI[1], Seren OTA[1], Rika TANAKA[1], Toru YAMAUCHI[2], Hiroaki OSAKO[2], *Marekazu OHNO[3]

1. Glocal Course of Nagasaki Prefectural Koka High School, 2. Nagasaki Prefectural Koka High School , 3. Unzen Volcanic Area Geopark Promotion Office

There are a lot of active faults in the areas recognized as Unzen Volcanic Area Geopark. These group of active faults are estimated to cause earthquakes with the possibilities of 0.5 - 1 % in 30 years and 0.8 - 2 % in 50 years (The Headquarters for Earthquake Research Promotion, 2006), and these numbers are relatively high in Japan, where earthquakes often happen. In addition, in the great Shimabara earthquake in 1992, 26 people were killed and 39 people are injured (Ota, 1984), and Tachibana bay area, which is located to the west of Shimabara peninsula, sometimes has series of volcanic earthquakes including ones with a seismic intensity of 5. These facts show that in Shimabara Peninsula, not only volcanic eruptions but also earthquakes which cause extensive damage can happen.

In this area, aging problem is also serious. The percentage of people who are over 65 years old is as much as 36.2 %, which is clearly high compared with the national average (28.1 %). Therefore, it is highly possible that a large number of elderly people will need to evacuate when a large earthquake occurs. Thus, we set our goal to establish a disaster prevention plan to protect the elderly.

In order to find out the difference of the awareness of disaster prevention among different generations, we conducted a research by sending out a questioner on their awareness of disaster prevention in daily lives to our school’ s students and their elderly family members: 409 people in total. We also examined the route from their residential areas to the evacuation center and compared it with the information put on the existing hazard map.

The result of the questioner showed that the elderly family members are more likely to be aware of disaster prevention than the students. This is equivalent to the result of a research conducted on university students and their family (Cabinet Office, 2016; Shimizu, 2011). Also, by examining the route to evacuate from their houses to the nearest evacuation center, we found out that the following three points are not put in the existing hazard map: (1) It has a long gentle slope, which is tough for the elderly to walk. (2) It has deep gutters at the side, which require extra caution if it is dark. (3) It has walls which can break down if an earthquake with a seismic intensity of 5 occurs.

These two results indicate that it is possible that the elderly people, who have greater awareness of disaster prevention, have difficulty in their evacuation. Therefore, we concluded that one way to prevent many elderly people from natural disasters is to make a detailed hazard map for each region, and raise young people’ s awareness of disaster prevention to make them “leading evacuees” when needed.

Keywords: Unzen Volcanic Area UNESCO Global Geopark, Nagasaki Prefectural Koka High School, Earthquake Hazards, Disaster Prevention

©2021. Japan Geoscience Union. All Right Reserved.

Disaster and Disaster Prevention Learning in the Naeba-Sanroku Geopark

*Kouhei Nakano[1]

1. Naeba-sanroku Geopark Promotion Council

Under the theme of "Natural Disasters and People", we will introduce two practices that we have already done in 2020. (Practice1 and Practice 2) One is for the general public, the other is for certified geo-guide members.

Practice 1:
We conducted a field tour called "Treasure Tour" for the general public by visiting some scars of disaster in the Naeba-Sanroku Geopark area. The followings are places we visited during this tour.
1) The Chikuma River Outcrops
・Located in front of the Sakae Village Office.
・It emerged after the 2019 East Japan Typhoon(Hagibis);
2) Aokura Avalanche Site
・It occurred in 1961 and killed 11 people.
・We visited the cenotaph during the tour.
3) The Nakajo River Collapse
・ It is scar of the 2011 Nagano North Earthquake.
4) The North Nagano Prefecture Earthquake Memorial Museum "Kizuna".
・We conducted this tour for not be forgotten of the fact that happened in March.12.2011.

Practice 2:
As a part of the guide training, a workshop was held by the disaster prevention section of Tsunan Town Office to understand the utility of hazard maps and create an evacuation plan called "Time Line" for just in case.

In order to raise awareness of disaster prevention among residents, we will continue to strengthen collaborative relations between the Geopark and the disaster prevention section of the local government.

©2021. Japan Geoscience Union. All Right Reserved.

Lives of the local people on the collapsing land and the flowing land by river water -Think about geohazard program of Miyoshi geopark project-

*Azusa Tonotani[1], Katsunori Ozakai[1], Mizuki Tochitani[1], Hiroyuki Ohnishi[1], Toshiaki Matsumoto[1]

1. Geopark Promotion office in Miyoshi city

Japan is known as one of the tectonic belt in the world. Therefore, various geohazards are caused such as the earthquake (subduction-zone and inland), volcanic eruption, the collapse of land (ex. land slide) and a heavy rain in Japan.

Miyoshi geopark project area is located in Tokushima prefecture and consists of all over the Miyoshi city area. As a feature of mainly geosciences are ;
1. Japanese median tectonic line (MTL) runs to east- west detection in this area. The south area of MTL is Shikoku Moutains and the north area is located Sanuki Mountain Range.
2. The south area mostly consists of Sambagawa metamorphic rock, and high mountains rise around 1500 m.
3. The average annual rainfall of Shikoku Mountains area in Miyoshi is about 2500 mm (heavy rain condition).
4. The Sanuki Mountain Range mainly consists of layers of sand stones and mud stones. Those layers often show the dip slope structure.
5. Yoshino river flows in Miyoshi area, sometimes cause floods at the middle and lower Yoshino-river area.

Those features triggered to cause the various geohazard such as the collapse of land (ex. land slide) and flood in past. Local people in this area lives together with distinctive geohazard for a long time, and we can see various those life style in local area even today. By way of example, Yokai stories (the oral tradition) in Miyoshi area are deeply associated with life style in a steeply and dangerous mountains area. Other example, local area name such as “Shima” area. Shima area is located in Ikeda town, and is often flooded because is located in the lowest river terrace.

Thus, a lot of original life style together with distinctive geohazard have been handed down in Miyoshi geopark project area. However, local area people don’t understand about each geohazard mechanism enough.

In this poster, we will introduce about the life style together with distinctive geohazard for a long time, and approach to various geohazards in Miyoshi geopark project area.

Keywords: Miyoshi geopark project, Geohazard, Land slide, Flood, MTL

©2021. Japan Geoscience Union. All Right Reserved.

Toward restoration of Geosites damaged by natural disaster with reaching consensus in local community: a case of Suzaki Coast in Seiyo City, Japan.

*Takumi Sakakiyama[1], Kazunari Kimura[2], Yuya Kato[3], Masahito Ono[1], Tsukasa Takahashi[1]

1. Seiyo City, 2. NAIBA Co. Ltd., 3. Noyama Company

In Japanese archipelago located in the deformation zone, we are always in the risk of catastrophic natural disasters that cause serious and widespread damage to society. The measures for these disasters will be carried out based on risk assessments and disaster prevention plans led by the government and institutes. The National Research Institute for Earth Science and Disaster Resilience (NIED) and the Volcanological Society of Japan cooperated to compile Database on Volcanic Hazard Maps and Reference Material.(1) The risk of huge earthquake occurrence is evaluated at Nankai Trough Earthquake Evaluation Study Group(2) sponsored by the Japan Meteorological Agency. On the other hand, it should be promoted the disaster prevention and reduction for Landslide Disaster in local communities by creating the Community Disaster Management Plan. However, the collapsed slopes are quickly covered because of ensuring lifeline and safety are taken the priorities during emergency. Therefore, it is difficult to educate inhabitants through field observations for slope failures. In this case, the slope failures occurred at a distance from the living area, such as natural heritage and geological heritage may be a good opportunity to understand the mechanism and talk about the restoration and utilization.

There is acidic tuff layer with vertical stripes in the Kurosegawa Tectnic Zone on the outcrops of the Suzaki Coast in Mikame, Seiyo City, Ehime Prefecture, Southwest Japan. The Suzaki Coast is one of the Geosites conservated by the Shikoku Seiyo Geopark. There are a cliff-shaped outcrops along the coast, and the path is maintained at this foot. Due to the rain from July 6th to the morning of 7th, 2020, The slope collapse occurred on a part of the slope on the mountain side of the path on the Suzaki Coast. The width of the slope failure is about 10 m, and the height from the coast to the collapse head is about 55 m. In addition, according to the results of a simple survey conducted in August, the amount of sediment deposited was estimated to be about 800 m^3. Although the collapsed sediment contains some acidic tuff gravel, it is considered to be a surface collapse of the sediment part existing at the upper part of the cliff because the weathered soil originating from the acidic tuff is the main component. The path is still restricted. It is difficult to remove the collapsed soil by heavy machinery or human power because the location of the path is not suitable to berth ships. Here, we have taken aerial photographs about once a month using a small drone, and simply monitored change in the amount of collapsed soil. As a result, after the passage of Typhoon Haishen in September, the collapsed soil deposited under the path moved due to the waves, and the collapsed soil deposited on the path also decreased slightly. In contrast, the amount of change was insignificant from October to February. Consequently, it is supposed that the movement of colluvium is more affected by waves than rainfall. If we experience waves caused by typhoons that reach the upper part of the path several times in the future, it is expected that the amount of soil will be reduced to a scale where restoration of the original can be started.

Furthermore, our group is going to present the educational program named "Seiyo Nature and Culture College" at March 13th, 2021 and the reactions of the participants and staffs. This program is going to plan the excursion to watch the collapsed soil mass in the Suzaki Coast and take the meeting about this.

Referred websites

(1) NIED "Database on Volcanic Hazard Maps and Reference Material":

©2021. Japan Geoscience Union. All Right Reserved.

http://vivaweb2.bosai.go.jp/v-hazard/ (last access on 2021.02.08)
(2) Japan Meteorological Agency "Nankai Trough Earthquake Evaluation Study Group":
https://www.data.jma.go.jp/svd/eqev/data/nteq/assessment.html (last access on 2021.02.08)

Keywords: Shikoku Seiyo Geopark, Suzaki Coast, Slope Failure, Drone, Disaster Prevention and Reduction

©2021. Japan Geoscience Union. All Right Reserved.

Let's investigate the earth activity from Shimonita Geopark

*Hara Hideo[1]

1. Geopark Shimonita council

Intro

The Shimonita town of Southwest Gunma is the town which is full of located nature. Shimonita basin is a plateau of Shinshu and a basin in during Kanto plains.It is two major special products such as "Shimonita-negi" and the konjac.
Shimonita-machi is the place that ever prospered as a course linking Edo to Shinshu.It is dotted with industrial inheritances using nature, the topography in a town.For examle,world helitage Arfune colad strage.It is one of the Japanese Geoparks that are 43 places in Japan.Typhoon Hagibis in 2019, It brought the damage such as floods in our area.The guide of the Shimonita Geopark tells the lesson of the flood in a guided tour.I discuss it about the story of the Shimonita Geopark and guide who introduce the lesson of the disaster by the main subject.

Three stories of Shimonita Geopark

Story.1 Great upheavals from the bottom of the sea to the land
Story.2 The ancient volcanic activity that separated plateau and Kanto plains
Story.3 The town of the course along the median tectonic line

Geopark Promoting activity and Disaster Resilience Education

We work on guide tourism, school education, disaster prevention education, activation of the local industry. The guide conveys an activity of the dynamic earth from nature of Shimonita. The typhoon Hagibis in caused a flood and changed the scenery. The guide tells a photograph and the damage situation at the time of the flooding in the case of the typhoon. And they convey about nature's wrath behind the scenery of beautiful nature to a tour visitor.
A tour visitor understands nature through this activity definitely, and we hope that it comes to be prepared for a disaster.

Keywords: Geodiversity, Geotourism, Education of Geology, Geopark, education for disaster prevention

©2021. Japan Geoscience Union. All Right Reserved.

The foundations of Yuzawa Geopark: a unification and a compilation of six geological maps published by the Geological Survey of Japan and Akita Prefecture

*Akio Sasaki[1], Kohei Yamawaki[1], Yukio Fujimoto[1], Syoichi Goi[1], Shoei Chiba[1]

1. Network of Earth Science Museum for Akita

The Yuzawa Geopark consists of approximately 300 geosites in the Yuzawa city, which are covered by six geological maps published by the Geological Survey of Japan and the Akita Prefecture.

It is difficult to understand geological events in this region using these maps alone, because of the different formation names at the same period, no-radiometric dates of volcanic rocks, and various coloration in these maps.

We began to work the project of the unification and compilation of six geological maps in 2017. During this project, we gathered the published papers including radiometric dates, preformed the geological field survey, collected fossils and rocks, and reconstructed the standard stratigraphic column for the study region. Based on these data, we compiled the distributions of formations from the same age in the study region.

The seamless geological map (B0 size) and a corresponding 226 page report were completed in 2020. These works provide valuable information including eruption ages of volcanic rocks from the Oligocene to the Pleistocene, and also newly discovered locations of molluscan and plant fossils. The seamless geological map and the report are useful for making the geo-story of geosites in the Yuzawa Geopark in near future.

References

Ozawa A. et.al. (1961)Uzenkanayama, (1979) Yuzawa, (1979) Asamai published by Geological Survey of Japan.
Usuta M. et.al. (1979)Yokote, (1981) Inaniwa, (1982) Akinomiya-Kurikomasan published by Akita Prefecture.
Takashima K. et.al. (1999) J. Min. Petr. Econ. Geol. Vol.94, p.1-10,
Kondo H.et.al. (2004) Island Are.vol.13, p.18-46.

Keywords: Geopark, Formation names, Fossil, Pyroclastic rock, Radiometric dating, Seamless geological map

©2021. Japan Geoscience Union. All Right Reserved.

Conservation concerns in Yuzawa Geopark: Distributions and seasonal variation in blood-sucking flies and an invasive plant species

*Haruki Takayanagi[1]

1. Yuzawa City Geopark Promotion Council

Yuzawa Geopark, located in Yuzawa City, Akita, Japan, is subject to two conservation issues that are common to many urban greenspaces: pest species are of concern for sustainable tourism, and invasive species threaten the integrity of the satoyama landscape. The first step in the management of both of these species groups is to clarify their distribution and seasonal variation. Here, we focused on blood-sucking flies (*Hirosia* spp.) in tourism hotspots, and on the invasive *Rudbeckia laciniata* in areas where it has colonized the satoyama landscape. Using dry ice traps, we found that blood-sucking flies were most abundant in early August, and that *Hirosia iyoensis* and *Hirosia sapporoensis* may have mutually exclusive spatial distributions. Visual surveys for *R. laciniata* confirmed that these plants occupy orchards, mined areas, and areas around silos at high densities, and have a patchy distribution in downstream areas. Appropriate mitigative measures are presented and discussed based on these results.

Keywords: blood-sucking flies, conservation, invasive species

©2021. Japan Geoscience Union. All Right Reserved.

The relationship between the former plate boundary and residents, especially the signboard production process

*Kato Satomi[1]

1. Mt. Apoi Geopark Promotion Council

Themes of Mt. Apoi Geopark is A Story of gifts from deep inside the earth connecting land and people together. Mt. Apoi is made up of peridotite that was thrust up from the depths of the earth by global-scale dynamic ground movement. Mt. Apoi Geopark is a stage featuring narratives that connect the planet’ s constitution, nature and people.

Sub- theme A: Peridotites- the interior and dynamic movement of the earth

The Hidaka Mountains formed as a result of a collision between two continental plates 13 million years ago. At that time, part of the mantle under the crust was thrust up onto the earth's surface to form the Horoman peridotite complex, which includes Mt. Apoi. The relatively fresh peridotites on and around the mountain contain valuable information from deep inside the earth's mantle, making them the subject of global attention. Mt. Apoi Geopark provides a variety of opportunities to learn about and enjoy phenomena relating to the earth's transformation. These include its status as the site of a plate collision, oddly shaped masses made of cooled and solidified magma, and rocks from far-off southern seas.

Sub- theme B: Alpine Plants- scarcity and the natural environment

Despite its low altitude, Mt. Apoi provides habitats for alpine vegetation due to its unique soil, weather and geographical conditions. Hidakaso (Callianthemum miyabeanum) and a host of other endemic species grow here, and the area's alpine plant communities have been collectively designated as a Special Natural Monument of Japan. In addition to alpine plants, the area is also home to the endemic Apoimaimai snail (Paraegista apoiensis) and Himechamadaraseseri (Pyrgus malvae; a butterfly not found anywhere else in Japan), as well as the Japanese pika (a relict species from the Ice Age). Mt. Apoi Geopark's valuable and diverse ecosystem provides opportunities to learn about and enjoy the natural environment.

Sub- theme C: Human History- the community of the nature and human life

The beautiful scenery of oddly shaped rocks (including masses called Oyako-iwa, Sobira-iwa and Cape Enrumu) along the Samani coast is a highlight of Hidaka's coastal road. Legends handed down by indigenous Ainu people in Samani, where Mt. Apoi Geopark is located, often feature these rocks. Cape Enrumu has long been known as a favorable natural harbor thanks to an ideal landform that shelters ships from strong winds, helping Samani to prosper as an important trading hub for Kitamaebune merchant vessels from the Edo period (1603 - 1868) onward. The rich history of people living with Mt. Apoi and the

©2021. Japan Geoscience Union. All Right Reserved.

sea continues to the present day in Mt. Apoi Geopark, making it an ideal place to learn about and enjoy the symbiosis between humans and nature.

Keywords: Former plate boundary, signboard

©2021. Japan Geoscience Union. All Right Reserved.

Fossil collecting experience to solve summer vacation indipendent study in Itoigawa UNESCO Global Geopark

*Yousuke Ibaraki[1], Yutaka Furumi, Emma Longhorn, Takahiko Ogawara[1], Ko Takenouchi[1], Takuma Katori[2], Takeo Kobayashi[2]

1. Fossa Magna Museum, 2. Itoigawa Geopark Council

Itoigawa UNESCO Global Geopark had held many education and outreach activities before 2009, when the Itoigawa Geopark was authorized as a member of the Global Geoparks Network. In 2020, many activities had to be cancelled because of the COVID-19 pandemic, but we held an education and outreach event with fossils using the grant for science museum activities from the Japanese Council of Science Museums.

The activity contains four events, using variable geology of Itoigawa Geopark, to search for fossils of Paleozoic, Mesozoic and Cenozoic in Itoigawa City, and fossil collecting experience and museum tour in Fukui Prefecture Dinosaur Museum.

This activity catered to elementary and junior high school students and their parents. To prevent new coronavirus infection, we limited the numbers of participants of each event to under 10.

The notice of the activity are, to distribute a flyer for all elementary and junior high school students, to publish the article of the participation offer of the activity in the public information paper of Itoigawa City, and to announce the participation offer in Itoigawa Geopark official Facebook. Applications were made to the Fossa Magna Museum, with applications only accepted by telephone to secure equitableness.

In the Itoigawa Geopark, Jade, Fossa Magna and many kinds of rocks on the beach are treated as main themes and used for promotion. But the fossils are treated as one of many themes.

Fossils are an interesting theme for not only children but adults, and useful for familiarization with geology. In the sign-up period for this activity, we received many calls from the morning of the first day. The number of applications exceeded our expectation. However, even with many events cancelled because of the pandemic, it is evidence of the high popularity of fossils.

Through the activity, participants look for and find fossils themselves, and received an explanation, and they may thought about ancient times when the creatures which became fossils lived. Perhaps there are children who would like to be a paleontologist. Fossil collecting of the dinosaur age was done in Ichiburi, Itoigawa City and in Fukui Prefecture, but no dinosaur fossils were found. However all of the participants found fossils of the dinosaur age, so the participants were satisfied to join the activity.

In 2020 fiscal year, we are planning an activity to make fossil replicas in March using the remainder of the grant for science museum activities from the Japanese Council of Science Museums. We would like to further promote the fossils of Itoigawa Geopark for education and outreach activities.

Keywords: Itoigawa UNESCO Global Geopark, Fossa Magna Museum, fossil collecting, education and outreach activity, geo-diversity

©2021. Japan Geoscience Union. All Right Reserved.

©2021. Japan Geoscience Union. All Right Reserved.

Geosite Map and Card in a Fun and Interesting Way by Local Elementary School Students: a Case Study of Geosite in Nankikumano Geopark with Takaike Elementary School

*Hiroko Shibasaki[1]

1. Nanki-Kumano GeoPark Guide Club

Cooperation with local schools is important for Geopark activities.

A good way to do this is to implement them in community studies and integrated learning.

(Takenouchi et al. 2014, Teramoto et al. 2017, Ueki 2019, etc.).

Ideally, children should choose Geopark activities as a means of learning because they want to learn independently. This is what leads to "fostering the qualities and abilities to find issues on their own, learn on their own, think on their own, make independent decisions, and solve problems better," which leads to the development of human resources to support sustainable regions.

The governing body of the Nanki-Kumano Geopark has a program to dispatch certified Geopark guides and specialists to schools. The presenter, a certified Geopark guide, has a relationship with local elementary and junior high schools and the Board of Education, and was able to collaborate on this project.

In this presentation, we will introduce an example of one of the activities conducted from July to December 2020 with 5th graders of Takaike Elementary School in Kozagawa Town, Wakayama Prefecture. The town is dotted with major villages along the Kozagawa River system, a second-class river running through the southern part of Wakayama Prefecture. In the middle to lower reaches of the mainstream, there are geosites such as the " Ichimai-iwa(monoliths) of Kozagawa River " and the " The Mushikui-iwa(insect-eating) Rock in Takaike " along the river, and the " Taki-no-hai (waterfall) " in a tributary stream. These are composed of the " Kozagawa arc-shaped dike", which is considered to be a part of the ring dike of the Kumano caldera (Miura, 1999) that was active during the Miocene of the Neogene period, and rocks related to siliciclastic igneous activity during the same period. The students in the same grade have been learning about these rock formations and landscapes that are characteristic of Kozagawa Town in their comprehensive studies every year.

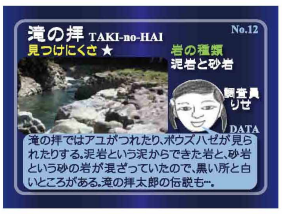
In order to deepen their study, they requested the cooperation and guidance of a Geopark guide, and took advantage of the aforementioned system.

In this way, this activity started with the school and the children as the main actors, both in setting the theme of the integrated study and in the way of interacting with the Geopark guide. Therefore, the presenter respected the independence and will of the children as much as possible during the activity. The results are reported here.

Keywords: Geo-education, integrated learning, community studies, geosite card, geosite pamphlet

©2021. Japan Geoscience Union. All Right Reserved.







上：パンフレット

右：カード一例

©2021. Japan Geoscience Union. All Right Reserved.

Examples of joint projects (or joint events) between a museum and Sado Island Geopark

*Takeyoshi SADAKANE[1], Mituhisa AIDA[1]

1. Sado Geopark Promotion Council

Sado Museum is one of the main facilities of Sado Island Geopark.
Active collaboration between this museum and Sado Island Geopark has been a challenge for many years, and during the revalidation process in 2019, it was suggested that the museum could be used as a place of "learning-based exhibits that would interest children about Geopark".

Two events for children jointly held at Sado Museum in 2020 were the first step towards this goal.
First of all, the exhibition was collaborated with a stamp rally. The stamp rally is organized every year under the initiative of Niigata University. A stamp rally means going to different locations to collect stamps on a card. In many rallies you can win prizes according to the number of stamps you collect. The stamp rally is a themed event designed to encourage people to visit Geoparks in Niigata Prefecture. The theme for 2020 was "Microfossils in Geoparks," and Sado Museum held a mini exhibition in line with this theme. Also, we participated in the "Sado Museum Festival" organized by this museum as an event for children. In our program, entitled "Rock Garden Treasure Hunt", visitors were asked to solve quizzes about rocks on display while walking around the museum's courtyard.

Through these activities, we believe that we were able to increase the number of children who visit the museum and introduce Sado Island Geopark to younger children. Sado Island Geopark has been steadily promoting cooperation by holding special exhibitions at Sado Museum and by having Geopark guides show visitors around the museum.
In this presentation, I will describe the details, effects, and challenges of the various events held at Sado Museum.

Keywords: geopark, Sado-Island, Museum

©2021. Japan Geoscience Union. All Right Reserved.

A Guide program that promote Proactive learning in School trip - Practice at Toya-Usu UNESCO Global Geopark -

*Hikaru Yokoyama[1]

1. Hokusho University

The area around Lake Toya in the southwestern part of Hokkaido was certified as a "Global Geopark" in 2009. This area is known as a place where you can not only enjoy the scenery and hot springs, but also learn about valuable geology and volcanic disaster prevention. Many schools visit the area as a place to visit for school trip, and in recent years, they have been seen learning outdoors as part of disaster prevention learning.

Now, the practice of "Proactive, Interactive and Deep learning" has been required in the field of education. Therefore, I wondered if it would be possible to provide a program that encourages students to learn independently even on school trips to Geoparks. So I assumed that the student would take the initiative in learning by changing from a learning style in which the guide "tells" to a style in which the student's "awareness of natural things / events" is valued.

Last year, I was able to practice this guide program in an elementary school's school trip. As a result of the practice, many children enjoyed "thinking" through quizzes and Interact based on the discovered events. In addition, a questionnaire one week later revealed that most of the tours left an impression on students. In this presentation, I will report on the programs that I practiced and how the students participated learned.

Part of this work was supported by JSPS KAKENHI Grant Number JP17K01041.

Keywords: Proactive, Interactive and Deep learning, School trip, Disaster prevention learning, Guide program

©2021. Japan Geoscience Union. All Right Reserved.

Educational Program on spring water of Aso UNESCO Global Geopark related with elcetrical conductivity (Part 2) Cooperated Research on Minamiaso Spring Water

*Tsuneomi Kagiyama[1], Koki Nagata[2], Toshikazu Maeda[3], Yuto Takeuchi[3], Haruki Watanabe[3], Kozue Inoue[3]

1. Aso Geopark Promotion Council, 2. Aso Volcano Museum, 3. Takamori Senior High School

Spring water is one of the important components of Aso UNESCO Global Geopark. We made an education program for local community to have more understandings on spring water of Aso Geopark. This poster presents a reslt on cooperated research with Takamori Senior High School.
We carried out water survey around Minamiaso Spring Waters. We found three types of waters; spring water around the caldera wall about 10 mS/m, spring water around the southern caldera floor about 23 mS/m (
just near from the foot of the central cones about 30 mS/m), and hotspring water more than 100 mS/m. This means waters have different relation with Aso volcanic system. Citizens use this low conductivity water for sake-making, and high conductivity water for bread making, etc.
We made educational programs how to understand the difference of electrical conductivity of spring waters; at first for high school students, and for kids and citizens later. We introduce our program briefly.
We have to express thanks to Kumamoto Prefecture for supporting us.

Keywords: Aso UNESCO Global Geopark, Spring water, Electrical conductivity

©2021. Japan Geoscience Union. All Right Reserved.

Looking back on 11 years of the educational activities of the Dinosaur Valley Fukui Katsuyama Geopark

*Sumiaki Machi[1]

1. Dinosaur Valley Fukui Katsuyama Geopark Promotion Council

The Dinosaur Valley Fukui Katsuyama Geopark became a member of the Japanese Geopark Network 11 years ago. We will look back on the 11 years of our educational activities.
Educational activities at geoparks have many meanings: encouraging understanding of the area and geoparks, fostering the people who leads the next generation of the area and also the world, giving a chance to study geology and so on. There are 12 schools (9 elementary schools + 3 junior high schools) in the geopark area. These schools are the member of UNESCO Asocciated Schools, base for ESD (Education for Sustainable Development) promotion.
We will analize the changes of the educational activities in this 11 years and discuss about the prospects and challenges.

Keywords: Geopark, Education, Dinosaur Valley Fukui Katsuyama Geopark, Katsuyama city

©2021. Japan Geoscience Union. All Right Reserved.

[J] Poster | O (Public)：Public

Sun. Jun 6, 2021 5:15 PM - 6:30 PM JST | Sun. Jun 6, 2021 8:15 AM - 9:30 AM UTC | Ch.02_2

[O-05] How to become a scientist? What can they do?

convener:Natsue Abe(Mantle Drilling Promotion Office, MarE3, Japan Agency for Marine-Earth Science and Technology), Rie Hori, S.(Department of Earth Science, Faculty of Science, Ehime University)

The earth and planetary sciences deal with many issues that are very close to our daily lives. Such researchers in this area are active in many parts of Japan. In this session, we introduce such researchers and people involved in this field and their activities, how they landed their current position. Many people may not know how to become a scientist. Either many of students may wonder how they apply their learned in university and their skills to society? We will have presentations on what they have learned and how they can use the skills they have acquired during their studies at universities and graduate schools in society.
Junior and senior high school students who want to go into the field of earth and planetary sciences are welcome to participate in this session and ask questions. We also welcome submissions from people who develop human resources and expand their colleagues.

[O05-P01] Only Ph.D. holders can work in the research and science field?

*Natsue Abe[1,2], Rie Hori, S.[3] (1.Mantle Drilling Promotion Office, MarE3, Japan Agency for Marine-Earth Science and Technology , 2.Graduate School of Natural Science & Technology, Kanazawa University, 3.Ehime University)

[O05-P02] Skills required to work at the science museum

★Invited Papers

*Mayumi ARAI[1] (1.National Museum of Emerging Science and Innovation)

[O05-P03] Discussion

Only Ph.D. holders can work in the research and science field?

*Natsue Abe[1,2], Rie Hori, S.[3]

1. Mantle Drilling Promotion Office, MarE3, Japan Agency for Marine-Earth Science and Technology , 2. Graduate School of Natural Science & Technology, Kanazawa University, 3. Ehime University

The earth and planetary sciences deal with many issues that are very close to our daily lives. Such researchers in this area are active in many parts of Japan. We introduce such researchers and people involved in this field and their activities, how they landed their current position. Many people may not know how to become a scientist. Either many students may wonder how they apply their learned in university and their skills to society? We are going to explain their career pass, how to receive a Ph.D., how to get the position, and what they have learned, and how they can use the skills they have acquired during their studies at universities and graduate schools in society. Junior and senior high school students who want to go into the field of earth and planetary sciences are welcome to participate in this session and ask questions.

Keywords: Ph.D. holders, career pass, Earth and Planetary Sciences

©2021. Japan Geoscience Union. All Right Reserved.

Skills required to work at the science museum

*Mayumi ARAI[1]

1. National Museum of Emerging Science and Innovation

A variety of human resources work at the Science Museum. There are not only people who plan permanent exhibitions, special exhibitions, events, programs for schools, but also people who perform demonstrations and explanations, technical staff, receptionists, public relations, general affairs, accounting, and information system personnel. Shops, restaurants, cafes, security, cleaning, etc. may be outsourced to external organizations / institutions, but such tenant staff are also important to support the science museum. And unlike employees, human resources such as volunteers are also indispensable to science museums. In this way, the science museum is consist of human resources with various roles. Therefore, staffs working at the science museum are not only the person have a doctor's degree or a master's degree, but also those who have bachelor's degree from liberal arts or those who have professional skills.
In this presentation, we will consider the skills required to work at the science museum and propose the skills that will be needed more in the future.

©2021. Japan Geoscience Union. All Right Reserved.

[J] Poster | O (Public) | Public

[O-05] How to become a scientist? What can they do?

convener:Natsue Abe(Mantle Drilling Promotion Office, MarE3, Japan Agency for Marine-Earth Science and Technology), Rie Hori, S.(Department of Earth Science, Faculty of Science, Ehime University)

Sun. Jun 6, 2021 5:15 PM - 6:30 PM Ch.02

The earth and planetary sciences deal with many issues that are very close to our daily lives. Such researchers in this area are active in many parts of Japan. In this session, we introduce such researchers and people involved in this field and their activities, how they landed their current position. Many people may not know how to become a scientist. Either many of students may wonder how they apply their learned in university and their skills to society? We will have presentations on what they have learned and how they can use the skills they have acquired during their studies at universities and graduate schools in society.

Junior and senior high school students who want to go into the field of earth and planetary sciences are welcome to participate in this session and ask questions. We also welcome submissions from people who develop human resources and expand their colleagues.

5:15 PM - 6:30 PM

[O05-P03]Discussion

©Japan Geoscience Union

[J] Poster | O (Public)：Public

Sun. Jun 6, 2021 1:45 PM - 3:15 PM JST | Sun. Jun 6, 2021 4:45 AM - 6:15 AM UTC | Ch.27

[O-07] Poster presentations by senior high school students

convener:Tatsuhiko Hara(International Institute of Seismology and Earthquake Engineering, Building Research Institute), Katsuyoshi Michibayashi(Department of Earth and Planetary Sciences, Nagoya University), Miwa Kuri(Japan Meteorological Agency), Keiko Konya(Japan Agency for Marine-Earth Science and Technology)

Senior high school students provide poster presentations on subjects in fields of earth and planetary sciences. This session provides an opportunity for senior high school students to give their presentations in the JpGU meeting and to have discussions with researchers. This session has been conducted as a public outreach session since 2006.

[O07-P01] Weather in Fukuoka Prefecture in the Edo period from the Nakamura Heizaemon diary

*Rui ANDOU[1], *Rio HAYASHIDA[1], *Hikari ARASE[1], *Mira EGUCHI[1], *Touko HAGIHARA[1] (1.Ikeda Senior High School)

[O07-P02] Discussion on Economic Effects of Muroto Deep Sea Water – How Does Deep Sea Water Industry Contribute to Revitalize the Community? –

*Kaede Yauoka[1] (1.Muroto High School)

[O07-P03] Observation of Columnar Joints and Research on its Origin

Atsushi Watanabe[1], *Iroha Kawaguchi[1], *Ryosuke Sugioka[1], *Mizuki Hukumuro[1], *Akihiro Amamiya[1], *Towa Serizawa[1] (1.Nirayama Highschool)

[O07-P04] A study of microplastics that is included in the rivers and coast of the Izu Peninsula

Atsushi Watanabe[1], *Namiki Kawai[1], *Koji Sadakane[1], *Yuichirou Takahashi[1], *Mayuko Toriikouji[1], *Daisuke Yamamoto[1], *Miori Yabuta[2], *Tubasa Ozawa[2], *Takaya Nishida[2], *Haruki Mimura[2], *Nanami Hujii[2], Ryosuke Yoshida[2] (1.Nirayama Highschool, 2.Shimoda Highschool)

[O07-P05] Consideration of method to increase artificial ruby

Atsushi Watanabe[1], *Yuichirou Nagatsu[1], *Moe Hatakeyama[1], *Koutarou Matsumoto[1], *Yudai Komiyama[1] (1.Nirayama Highschool)

[O07-P06] Earthquake prediction by Electric magnetic wave

*Masayuki Masa[1], *Nozomu Sakai[1], Michiya Sasaki[1], Souhei Kato[1], Ousuke Yagasaki[1], Mizuho Fujiwara[1], Maika Yashima[1] (1. Tokyo Metropolitan Tama High School of Science and Technology)

[O07-P07] Comparison of heated products of glucose with citric acid added

*Takumi Ohtsu[1] (1.Tokyo Metropolitan Tama High School of Science and Technology)

[O07-P08] Development of iron (II) phosphate lithium-ion battery using the adsorption power of Aso loess

*Ayumi Hoshi[1], *Sora Nozaki[1] (1.Tokyo Metropolitan Tama High School of Science and Technology)

[O07-P09] Method of Recovering Perfluorinated Compounds by coffee grounds

*Kouki Morimoto[1], *Issei Yamazeki[1], *Renon Shimizu[1] (1.Tokyo Metropolitan Tama High School of Science and Technology)

[O07-P10] Research into Moriya Formation Formed in Northen Fossa Magna

*Yusuke Morozumi[1] (1.Suwa Seiryo high school)

[O07-P11] A Consideration of a Landing Exploration on Europa

*Taichi Ito[1] (1.Seishin Gakuen High School)

[O07-P12] Relationship between five gigantic jets in the past and cloud-to-ground lightning

*Fuga Suzuki[1], *Yuya Takahashi[1], Sorachi Nishibori[1], Yuki Ito[1], Takumi Miyamoto[1] (1.Shizuoka Prefectural Iwata Minami High School)

[O07-P13] Examination of the fall position by the light emission of the Narashino meteorite fireball

*Ryunosuke Kamiya[1], *Haruka Sato[1], Kosuke Arimura[1], Saki Ozawa[1], Hana Miki[1], Yuka Ogawa[1], Honoka Tanabe[1] (1.Shizuoka Prefectural Iwata Minami High School)

[O07-P14] The Change of Microtopography of Samejima Coast Caused by the Storm Surge Brought by Hagibis

*Takeshi Totsuka[1], Yuya Takahashi[1], *Kosuke Arimura[1], Koki Suzuki[1], Shun Ichikawa[1], Rabu Kato[1] (1.Shizuoka Prefectural Iwata Minami High School)

[O07-P15] Putting legs on snake swimming robot going to be useless?Seeking truth of Tetrapodophis

*Ryoya Sato[1], *Kokoro Ikeda[1], *Ryota Ogawa[1], *Riko Tomioka[1], *Akari Hitomi[1], *Kanon Yamaguchi[1] (1.Tokyo Tech High School of Science and Technology)

[O07-P16] Consideration of snowmelt type lahar at Mt. Katta, Zao

*Haruya Shishido[1], *Reiki Syoji[1], *Ryo Hikichi[1] (1.Miyagi Prefectural Tagajo Senior High School)

[O07-P17] Geological structure of Urato Katsurashima Island and Nonoshima Island, Shiogama City

*Asahi Oyama[1], *Hikaru Sasaki[1], *Yuhi Suzuki[1], *Hayato Murakami[1], *Misaki Kuga[1] (1.Miyagi Prefectural Tagajo Senior High School)

[O07-P18] Threats and impacts of urban tsunami
-Simulate a tsunami when a Nankai Trough giant earthquake occurs using a tsunami generator-

*Misaki Suda[1], *Kenshin Okazaki[1], *Zen Sato[1], *Yusei Niinuma[1], *Kousei Matsuura[1], *Ayaka Akisawa[1] (1.Miyagi Prefectural Tagajo Senior High School)

[O07-P19] Countermeasures against Heat Island Phenomenon: Proposal for a New Building System

*Hiroaki HAYASHI[1] (1.Yokohama Science Frontier High School)

[O07-P20] An evaluation of artificial landform in Chiba prefecture called “Kawamawashi”

*Kodai SHIBUYA[1] (1.Yokohama Science Frontier High School)

[O07-P21] The relationship between sunspot number and typhoons

*Takeru TODA[1] (1.Yokohama Science Frontier High School)

[O07-P22] On the study of Fukui Earthquake Fault IX

*Kazuho Kuwajima[1], *Ryouhei Matta[1], *Youhei Morise[1], *Ayano Yashima[1] (1.Fujishima High School of Fukui prefecture)

[O07-P23] **Approach to the current situation and issues of geothermal power generation utilization based on field surveys**

*Kisho Kurosawa[1], *Tatsuki Miyamoto[1], *Nozomi Kawaharata[1], *Shoki Yashima[1], *Yusuke Oba[1] (1.FurukawaReimei High School)

[O07-P24] Study of mechanism of Light Emission by Spectroscopic Observation of Meteor

*Yui Sato[1], *Yuki Kato[1] (1.Miyagi Prefectual Furukawa Reimei Senior High School)

[O07-P25] Relationship between mineral crystallization and impurities.

*Usami Kenta[1], *Ryo Nakane[1], *Hiroyuki Sueno[1], Syotaro Kawana[1], Ryota Naito[1], Kazuhiko Hoshi[1], Mitsuhide Sai[1], Takuma Watanabe[1] (1.Johoku high school)

[O07-P26] Analysis of water quality of irrigation ponds focused on land use, irrigation systems and periodic pond draining

*Ayane INOUE[1], *Haruto TAKEYAMA[1], *Kousuke MANO[1], *Rio YAMANO[1] (1.Hyogo Prefectural Kakogawa Higashi High School)

[O07-P27] The Process of Raised-Bed River Formation and Factors that Affect It

*Natsuki KAMISASA[1], *Yuta KONDO[1], *Haruto TAKEYAMA[1], *Yasuharu TOMITA[1], *Rikushi NAGAO[1], *Naka NOHAMA[1] (1.Hyogo Prefectural Kakogawa Higashi High School)

[O07-P28] Studies of the SDGs on the Sanriku Geopark. The sea urchin spread trench in the Taneichi Formation.

*Kyougo Sakashita[1], *Asahi Sekibata[1], *Rina Nakajo[1], *Yuto Kugoi[1], *Hikaru Sasaki[1] (1.Marient Chikyu-tanken club senier)

[O07-P29] Studies of the SDGs on the Sanriku Geopark. The Aoba Lake and Shimamori Basin.

*Mizuki Kimura[1], * Naho Simodate[1], *Kahono Hinata[1], *Yuma Keicho[1], *Kouki Takahashi[1] (1.Marient Chikyu-tanken club senier)

[O07-P30] Proposal of Hachinohe Canyon to Sanriku Geopark Geosite.

*Sarina Shinohe[1], * Miyu Abe[1], * Akari Nakamura[1], *Yukihito Yasuhara[1], *Kensuke Shimomura[1] (1.Marient Chikyu-tanken club senier)

[O07-P31] Proposal of an index for estimating the distance from the source rock

*Ayaka Mitsui[1], *Reiji Iwamoto[1], *Keishi Okumi[1], *Mayu Naito[1], *Yamato Yasuhara[1], *Natsuki Yamamoto[1], *Naoko Kodama[1], *Akito Sasaki[1], *Akira Tada[1], *Takuto Nakanou[1], *Tomohiko Maeda[1], *Yuya Muromoto[1], *Ryusei Moriyama[1] (1.Hyogo Prefectural Himejihigashi Senior High School)

[O07-P32] Energy calibration of a cosmic-ray detector

*moe kimura[1] (1.Tokyo Metropolitan Hibiya High School)

[O07-P33] Floating waterdrops using a straw commutator

*Aoba Takahara[1], Yuri Yasui[1], Takaya Sato[1] (1.Niigata Prefectural Takada high school)

[O07-P34] The rotating-Water-tank that is replaced hot water tank and ice water tank

*Masamune Minou[1] (1.Niigata Prefectural Takada high School)

[O07-P35] Comparison of the surface of Mars with the previous one in the approach of Mars Spread of dust storm on November 17th

*Sayaka Mizutani[1], *Takumi Uchiyama[1], Riho Kagami[1], Aoi Takemoto[1] (1.Ichinomiya High School)

[O07-P36] Tumulus inspection project by using cosmic-ray muon

*Tomoyo Ishizawa[1], *Satoshi Ono[1], *Asahi Shiozaki[1], *Wakana Yanagimoto[1], *Kenshiro Aoki[1], *Yuna Ishii[1], *Sogo Kimura[1], *Yuki Shimada[1], *Aoi Soga[1], *Yuga Takemori[1], *Rino Tomiku[1], *Kana Hashizume[1], Miki Ohtsuka[1] (1.Waseda University Honjo Senior High School)

[O07-P37] Calculating the nebula density from the size of the emission nebula

*Yuki Shirai[1] (1.Totsuka High School)

[O07-P38] Strength evaluation of structures by making and improving quake-vibration generators

*Runaya Igari[1], *Yuto Meguro[1], *Rin Goto[1], Kenshiro Kamata[1] (1.Miyagi Rifu high school)

[O07-P39] Time dependence of ocean salinity

*Honami Hashimoto[1], Annu Ito[1] (1.Miyagi Rifu highschool)

[O07-P40] Toward "Solid-State Version Chromatography" Second Report

*Yuichiro Okuno[1], *Akihisa Wada[1], *Yudai Kozono[1], *Ryota Iwamoto[2], *Mai Fujitani[2], *Kyoya Okada[3], *Kusunori Sumi[3], *Arata Fujimoto[3] (1.Imamiya Technology Senior High School of Osaka Prefecture:The evening course, 2.Otemae Senior High School of Osaka Prefecture:The evening course, 3.Kasugaoka Senior High School of Osaka Prefecture:The evening course)

[O07-P41] How to extract bioethanol effectively by distillation.

*Ataru Kunihisa[1] (1.Wakasa high school)

[O07-P42] Confusion of the people in the northwestern area of Saitama Prefecture due to rumors after the 1923 Kanto Earthquake

*Miharu Shinoda[1] (1.Sakae Higashi High School)

[O07-P43] A quest for the best condition of a crystal radio's detection

*Motoaki Osone[1] (1.Yashiro High School)

[O07-P44] What cause columner joint changes?

*Yugo Sakurai[1], *Yuki Enomoto[1], *Kanta Hayashibe[1] (1.Yashiro High School)

[O07-P45] Preliminary analysis of HAYABUSA-2’s Doppler-Shift

*Azumi Sofue[1], *Naoko Nishino[1], *Riri Iida[1], *Riri Numata[1] (1.Wakayama Shin-ai Senior High School)

[O07-P46] Estimation of a ceiling thickness using the muography technique with a small cosmic-ray detector

*Nana Kobayashi[1] (1.Kaichi High School)

[O07-P47] A proposal of an inverse analysis method for ballistic ejecta flying focusing on crater shape in phreatic eruption

*Kouki Nishino[1], Neo Suzuki[1], Natsumi Waki[1] (1.Kanagawa Prefectural Yokosuka Senior High School)

[O07-P48] The survey of Micro-Plastics included in River sediments.

*Taichi Ichikawa[1], Ryuke Kawai[1], Suzuka Fukunaga[1], Tessho Yamamoto[1], Takumi Sato[1] (1.GIZAN SENIOR HIGH SCHOOL)

[O07-P49] Relationship between sprites and the lightning charge moment

*syunsuke nakao[1], *sora wake[1] (1.Prefectural Kochi Ozu High School)

[O07-P50] Potential Small Hydropower Generation in Kamikawa Basin -Hydro Energy Map Visualizing Power Generation-

*Airi Takei[1], *Akira Tamaki[1], *Naoki Kudo[1], *Asahi Takahashi[1], *Hikaru Kawashima[1] (1.Hokkaido Asahikawa Nishi High School)

[O07-P51] Consideration of brachiopod biota change events in the Kuzu limestone layer

*Omi Kono[1], Tokio Chiba[1] (1.Kaijo senior high school)

[O07-P52] Estimation of the variation in mechanism in the amount of spring water in Otomeyama Park, Shinjuku City

*Kuya Aoyama[1], Taichi Shimokobe[1], Masamune Kanou[1] (1.Kaijo high school)

[O07-P53] Modeling the earthquake damage in adeveloped land

*Shungo Kokubun[1], *Satoru Takahashi[1], *Hiroshi Takeuchi[1], *Haruki Tamakawa[1], *Masafumi Kaneko[1], Takumi Nanbu[1] (1.Miyagi Prefecture Sendai Daisan High School)

[O07-P54] Influence of Calcium chloride on frost columns

*Manaka Oya[1], Shohei Nanri[1] (1.Ichikawa gakuen Ichikawa senior high school)

[O07-P55] Differences in fog generation conditions in the Edogawa estuary -Examples of Edogawa-ku and Ichikawa-shi-

*Kenta Torii[1], Shohei Nanri[1] (1.Ichikawa gakuen Ichikawa senior high school)

[O07-P56] Development of variable slope type underwater embankment

*Kei Omura[1], Shohei Nanri[1] (1.Ichikawa gakuen Ichikawa senior high school)

[O07-P57] Environmental impact assessment of air and soil substances using spring water of Minowa as an index

*Mari Taki[1], Shohei Nanri[1] (1.Ichikawa gakuen Ichikawa senior high school)

[O07-P58] Development of an automatic meteor shower observation and the notification system
~Web broadcast of meteor appearance~

*Koichi Sato[1], *Koshi Ri[1], *Shunsuke Isoda[1], *Honoka Ohno[1] (1.Chuo University Junior and Senior High School)

[O07-P59] Meteorological and geographical conditions of river flooding-Comparison of the past and present of the Miyata River-

*Eri Yoshida[1], *Minami Oikawa[1], *Kotomi Shibata[1], *Chihiro Terazaki[1], *Kurumi Yabe[1] (1.Ibaraki prefectural Hitachi first senior high school)

[O07-P60] Where are solar panels actually used? Research on the present situation of Kashiwa City, Chiba prefecture, Japan.

*Souri Mizukami[1] (1.SHIBYA SENIOR HIGH SCHOOL)

[O07-P61] Decline and Fall of Martian Polar Capse; Whether the Dast Storm Is Warm the Polar Cap

*Kei Inoue[1], Hibiki Aminaka[1], Yuho Takagi[1], Nanami Yasuda[1], Yuki Tanaka[1], Tomoki Ugawa[1], Rio Mogi[1], Kyouka Miyake[1], Momoha Takashima[1], Mako Misumi[1], Kaho Okada[1] (1.Kumamoto Prefectural Daiichi High School)

[O07-P62] Spacial correlation between slow earthquake and mantle- derived hot spring in Southwest Japan

*Yui Kobayashi[1] (1.Shizuoka Higashi High School)

[O07-P63] **Visualize water current using vitamin B_2**

*Mutsuki Kamata[1], *Yuuma Nakagawa[1], *Io Kato[1], *Tokito Hirose[1], *Yuuki Matsui[1], *Kosuke Mafune[1], *Akihito Yamada[1], Kazumi Igawa[1] (1.Zushi-Kaisei Senior High School)

[O07-P64] Designe of lunar crater exploration rover

*Kosuke Kameoka[1] (1.Meikei High School)

[O07-P65] Distribution of Gravel in the Sakawa River and Factors Affecting the Distribution

*Nozomi Uemachi[1], *Misaki Yamamiya[1], Yosuke Saito[1] (1.Tokyo Gakugei University Senior High School)

[O07-P66] Detection of Cherenkov light with acrylic and photodetecto

*Juri Urano[1], *Yuka Kuze[1], *Kaho Kubota[1] (1.Toshimagaoka Joshigakuen senior high school)

[O07-P67] Research the View of Mt.Fuji with a Self-Made Observation Device

*Ryoo Niigawa[1], *Rin Takezoe[1] (1.Tokyo Metropolitan Tachikawa High School)

[O07-P68] Bad visibility in the past at Tachikawa High School

*Tomoya Ushizaka[1] (1.Tokyo Metropolitan Tachikawa High School)

[O07-P69] Analysis of visibility around Tachikawa High School

*Takumi Yasuhara[1] (1.Tokyo Metropolitan Tachikawa High School)

[O07-P70] The relationship between the shape and power generation amount of the simple wind power generators

*Sora Fukui[1] (1.Tokyo Metropolitan Tachikawa High School)

[O07-P71] **Is « evacuate to rise » the Right Action?**
Research and Proposition of Major Evacuation Routes to Shelters in Shibuya

*Sakura Oona Marie Sueoka[1] (1.Tokyo Metropolitan Kokusai High School)

[O07-P72] Mechanism of how the Shirata river looks blue

*Shuhei Sugai[1], *Ryosuke Yoshida[1] (1.Shimoda high school)

[O07-P73] Determining the Properties of Seyfert Galaxies

*Kuya ABE[1], *Kuranosuke IEHATA[1], *Koki TANII[1], *Tamotsu FUJIMOTO[1] (1.Nara Prefectural Seisho High School)

[O07-P74] Observation of Radio Waves from the Moon

*Koya YAMASHITA[1], *Ichika TSUTSUMI[1], *Atsushi HIRANUMA[1], *Ikumi MATSUYOSHI[1] (1.Nara Prefectural Seisho High School)

[O07-P75] Making Snow Meter Using Neutron Cosmic Rays Observation Data Collected By Cosmic Watch

*Kei Ikushima[1], Rikako Kono[2], Kaduo Tanaka[2], Akita Yuji[1] (1.Hiroo Gakuen High School, 2.Touhoku University)

[O07-P76] Water storage capacity of the green dam – Role of forest soil -

*Nanami Aoki[1] (1.Kyoto Prefectural Sagano High School)

[O07-P77] Measurement of Radon Concentration for Earthquake Prediction in the Woods for Field Practice Owned by Sagano H. S.

*Ayaka Kawabata[1], *Takahiro Kawabata[2] (1.Kyoto Prefectural Sagano High School, 2.Graduate School of Science, Osaka University)

Weather in Fukuoka Prefecture in the Edo period from the Nakamura Heizaemon diary

*Rui ANDOU[1], *Rio HAYASHIDA[1], *Hikari ARASE[1], *Mira EGUCHI[1], *Touko HAGIHARA[1]

1. Ikeda Senior High School

Motivation for research

We have been restoring the climate data for the Edo period in Japan from historical documents which were written before the official weather observation records were started in the 16th year of the Meiji period. This year, we analyzed the historical document called the "Nakamura Heizaemon diary" from Kitakyushu.The diary contains information about the actual conditions of people's lives and daily events and was written in the 55 years from 1812 to 1866.

The purpose of the research

1.To create a database in conjunction with the historical documents that we examined in the last few years.

2.Therefore, based on the previous research,we examined the relationship between the “weather appearance rate” and the “detail rate" which measures the accuracy of the records.

The research method

We classified the weather in the historical documents to make the classifications closer to the definitions currently used by Japan Meteorological Agency and the weather was classified as snowy, rainy, cloudy, or sunny.

Data#1 Weather appearance rate(graph1)

The annual trend of the weather appearance rate is as shown in the graph. The sunny appearance rate was the highest at 64.1% in 1828, and the lowest was 39.3% in 1860.The rainy appearance rate was highest at 41.2% in 1860 and lowest at 20.9% in 1813.

Data#2 The weather appearance rate according to the season(graph2)

Looking at the seasonal weather appearance rate , in 1836, when severe damage to crops caused the Tenpo famine, the rainy appearance rate in the summer was 45.7% and the sunny appearance rate was 32.6%. In fact, the usual sunny and rainy appearance rate was reversed.In 1860, the sunny appearance rate fell in the period from spring to autumn, and the sunny and rainy appearance rate in spring and summer were reversed.

Data#3 Annual composition ratio of descriptions of rain(graph3)

The Nakamura Heizaemon diary was written by one person who focused on recording rain .In the all of descriptions, weather described as only “rain” was 79.9%, and other records described the weather as “rainy weather”, “white rain”, “light rain”, “sprinkles of rain”, “light showers”, “drizzle”. The description of “heavy rain” or “strong rain” in 1836 was 10.2%.

Data#4 Summer rain by description / annual composition ratio(graph4)

Looking at the ratio of summer rain, 1836,which is considered to have been a year when heavy rain fell all through the summer, 20.9% of the rain was recorded as “heavy rain” combined with “strong rain”.In the summer of 1831, the record of “strong rain” was remarkable at 23.5%.

detail rate(reference)

Here, we decided to examine the accuracy of recording using the “detail rate” we found in a paper by Professor Sho Kenjiro of Nagoya Institute of Technology.

Data#5 The “detail rate” 1811 to 1866(graph5)

The average for the entire period was 29.9%, the highest rate was 46.2% in 1865 and the lowest rate was 3.6% in 1814.From 1812 to 1866 at the end of the Tokugawa shogunate, the weather records became

©2021. Japan Geoscience Union. All Right Reserved.

more detailed and correlated with the rainy appearance rate .The line of dashes shows the trend of the graph.

Data#6 The “detail rate” for four seasons(graph6)

The “detail rate” for all the four seasons increased towards the end of the Edo period.The “detail rate” of the Nakamura Heizaemon diary for the entire period was 29.9%, which was the same as the Joubu diary, which we had researched previously. The trend of the rainy appearance rate and the trend of the “detail rate” for 55 years are in agreement.

Data#6 Comparison of weather appearance rate every 30 years between the historical documents(graph7)

Comparing the historical documents, "Nijoke diary" and "Myohoin diary" are records of the same place, Kyoto. The "Nijōke diary" is uncomplicated and the rainy appearance rate during the same period is low.

Discussion1

(1)The “detail rate” of the Nakamura Heizaemon diary for the entire period was 29.9%, which was the same as the Joubu diary, which we had researched previously. The trend of the rain appearance rate and the trend of the “detail rate” for 55 years are in agreement.

It is suggested that "rain appearance rate" can be corrected by "detail rate".

Discussion2

In 1836, when the annual composition ratio of heavy rain was 10.2%, it was described as “heavy rain” only in the summer, and the composition ratio of heavy rain was 20.9%.

Summary of the study

1.The composition ratio of “heavy rain” in 1836 was 10.2%, and it is considered that it was the summer when heavy rain fell.

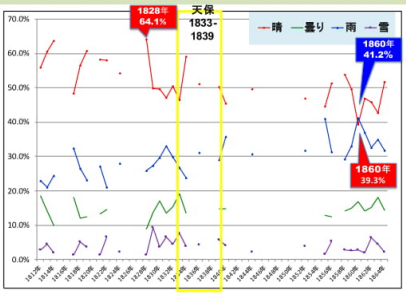
2.The “detail rate” for the entire period is 29.9%, which is higher than the previous research.It is said that the higher the detail rate, the higher than the rainy appearance rate ,and the Nakamura Heizaemon diary also shows a correlation as in previous studies.

Keywords: Nakamura Heizaemon diary, detail rate

©2021. Japan Geoscience Union. All Right Reserved.

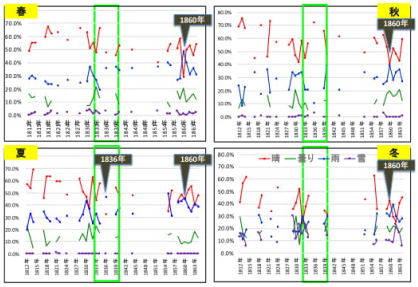
天気の出現率　1812年～1864年(全期間)

Graph1



四季の天気の出現率　1812～1866年

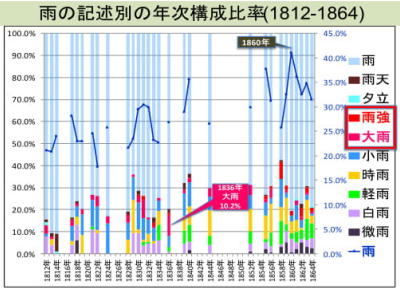
Graph2



天気の出現率の年次推移は左上の graph1 のとおりで、1828 年の晴れの出現率が 64.1%で最高で、最低は 1860 年の 39.3%であった。右上の graph2 のように四季の天気の出現率は「天保の飢饉」で一番被害が苛烈であった 1836 年は雨の出現率が晴れの出現率を逆転している。

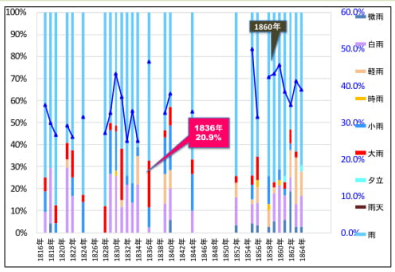
雨の記述別の年次構成比率(1812-1864)

Graph3



夏(6月～8月)の雨の記述別・年次構成比率(1812-1864)

Graph4

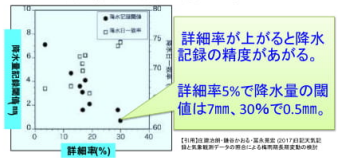


雨の記述別の年次構成比率をみると、1836 年は大雨の比率が高く、さらに、季節ごとの構成比率をみると 1831 年と 1836 年は夏季に大雨の降った年だったとわかった。

詳細率

reference

【定義】天気記録で「晴れ」や「雨」と1語の記録されているのではなく、複数種類の天気が併記されたり、時間変化に関する記述や「大雨」などの降水規模の記述がある日数の比率

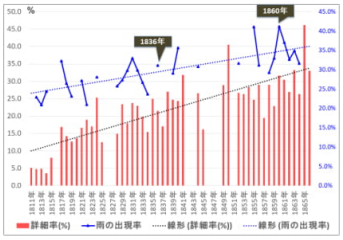


詳細率が上がると降水記録の精度があがる。

詳細率5%で降水量の閾値は7mm、30%で0.5mm。

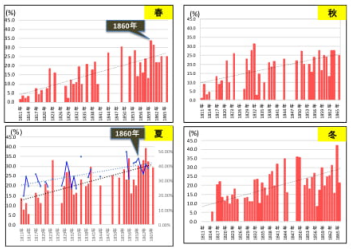
詳細率　1811年~1866年

Graph5



四季の詳細率

Graph6



古文書の30年ごとの天気の出現率の比較

Graph7



中村平左衛門日記の全期間の「詳細率」の平均は 29.9%で、最高は 1865 年の 46.2%で、最低は 1814 年で 3.6%であった。1812 年から幕末の 1866 年に行くに従い天気記録が詳細になり、雨の出現率の傾向と一致する。

graph7 のように、過年度に調べた古文書間で比較すると、「二條家内々御番所日次記」「妙法院日次記」は同じ京都の記録であるが、「二條家内々御番所日次記」は記述が単純で、同一期間の雨の出現率は低くなっている。一方「妙法院日次記」は記録が詳細で雨の出現率が高い結果となっている。詳細率と雨の出現率が関係することを示唆している。

このことから、詳細率で雨の出現率が補正できると考える。

©2021. Japan Geoscience Union. All Right Reserved.

Discussion on Economic Effects of Muroto Deep Sea Water –How Does Deep Sea Water Industry Contribute to Revitalize the Community? –

*Kaede Yauoka[1]

1. Muroto High School

This research will reveal how much deep sea water industry contributes to economic development in Muroto City, Kochi Prefecture.
Muroto City has a very unique underwater topography especially in the west coast of the City. Approximately 2 to 3 km off the land, a steep cliff is formed and the ocean depth suddenly falls into about 1,000m. Due to the cliff underwater, deep sea water upwells and approaches to the land. It allows Muroto to intake deep sea water easily with low coast, compared with other area in the world. In 1989, Kochi Prefectural Deep Sea Water Laboratory was established in Muroto City. That was the very first research facility on deep sea water in Japan then. Since the establishment of the facility, the number of deep sea water-related companies and facilities has been increased in the City. The biggest number of such companies and facilities is 14 in 2010, 2012, and 2014. The latest survey shows that those numbers are 11 as of 2019.
Those deep sea water industry development has been recognized as a new local industry in the area. Deep sea water products, such as bottled water and cosmetics, has been publicized and commercialized all over Japan. It is predicted that the industry brought a big economic effect to Muroto City. This research utilizes 1) the number of companies and facilities, 2) creation of new employment, 3) the number of visitors to deep sea water-related facilities as data to analyze a scale of economic effect and a level of contribution to Muroto City’ s economic development. In order to obtain precise data, this research is implemented with a collaboration with Muroto City Industrial Promotion Section, Deep sea water-related companies, and Muroto Geopark Promotion Committee.
This research will also compare the scale of economic effect of deep sea water industry with other local industry, fishery and agriculture. If a result can be determined that deep sea water industry plays a more significant role in terms of local economic development than other industry, this research will also analyze main cause of it. According to surveys and interviews implemented so far, any specific studies or analysis has not been done to find why deep sea water industry has been success in Muroto. It is expected that a reason will be a key for local revitalization in this City.

©2021. Japan Geoscience Union. All Right Reserved.

Observation of Columnar Joints and Research on its Origin

Atsushi Watanabe[1], *Iroha Kawaguchi[1], *Ryosuke Sugioka[1], *Mizuki Hukumuro[1], *Akihiro Amamiya[1], *Towa Serizawa[1]

1. Nirayama Highschool

It is widely known that hexagonal columnar joints is more than others. From our previous studies which use data from the Izu Peninsula and overseas columnar joints, it is known that ‘The complicated shapes of columnar joints mean the magma solidified quickly, and the more simple the shapes are, the slower the magma sets’. There is a positive correlation between the rapidity of magma’s solidification and the complexity of columnar joints’ shapes.

We conducted an analysis which investigated discovers this relationship in terms of circularity. Using the standard deviation of circularity and the kurtosis of heptagonal number distribution, we made one graph of columnar joints and distinguished it into three areas: upper left, lower left, and lower right. In this graph, the vertical axis is ‘deviation of circularity’ and the horizontal axis is ‘kurtosis of heptagonal number distribution’.The upper left’s rock was made in a thin dyke and the cooling was heterogeneous. As for the lower right, the magma was solidified underground, and the other’s magma was so thick that it set slowly. This magma’s cooling was homogeneneous under natural conditions. This history and the feature of this graph are similar, so according to this graph and circumstances, the kurtosis of circularity decreases, as the homogeneity of cooling magma increases and vice versa.

We pictured the procedure of forming starch columnar joints every three minutes. We finally found that cracks occur from one point and continuously, and columnar joints which stick to the container were larger than those which lie in the center. From this observation, we established a hypothesis that natural columnar joints which were made of magma adjacent to rock are relatively larger.

We once tried to make rock columnar joints, using an electric furnace(AS ONE HTR-1010). This purpose was to make the model of occuring columnar joints. As a result, there were quenching edges on the surface and irregular joints inside, however we weren’t able to make ‘columnar’ joints. We believe this was because the time of cooling was very short and that the experiment was small, compared to natural formations.

Keywords: Columnar Joints, Izu Peninsula

©2021. Japan Geoscience Union. All Right Reserved.

A study of microplastics that is included in the rivers and coast of the Izu Peninsula

Atsushi Watanabe[1], *Namiki Kawai[1], *Koji Sadakane[1], *Yuichirou Takahashi[1], *Mayuko Toriikouji[1], *Daisuke Yamamoto[1], *Miori Yabuta[2], *Tubasa Ozawa[2], *Takaya Nishida[2], *Haruki Mimura[2], *Nanami Hujii[2], Ryosuke Yoshida[2]

1. Nirayama Highschool, 2. Shimoda Highschool

The reseach of microplastics of Nirayama Highschool

Taking over the research of our seniors, we aimed to establish a method for collecting microplastics that could be used by high school students, and to investigate the extent of microplastics in the seas and rivers around the Izu Peninsula.

The experimental procedure is as follows. First, 500 L of water is collected, filtered, dried, and added to a potassium hydroxide solution. After 2 days, sodium iodide solution is added and the overflow method is performed, and the supernatant is collected. The collected supernatant is filtered, dried, and observed using a microscope and blue light.

Experimental results and discussion. Many small microplastics were discovered in Kano River, Ganyudo and Numazu Port. The percentage of small microplastics was higher in Ganyudo than in Kano River. It is thought that the microplastics are being scraped off while flowing through the river. In addition, the number of microplastics was higher in Ganyudo and Numazu Port, which are located at the mouth of the Kano River. The main reason for this is thought to be that microplastics contained in the three rivers that flow into the Kano River, the Daiba, Raikou, and Kise Rivers, flowed into the Kano River.

Next, the Kakita River. Since the Kakita River is fed by a spring, we thought that there would be no microplastics collected in the middle reaches.

However, the collection results showed that there were more microplastics in the middle reaches, but small amounts were also collected in the lower reaches.

The reason why microplastics were discovered in the Kakita River is that there are culvert channels as well as clear channels around the Kakita River, which causes domestic wastewater to flow into the Kakita River. There is a water purification facility upstream of the water sampling point in the middle of the river, and we thought that a small amount of microplastics remaining there were discovered this time. In order to improve the detection accuracy of microplastics, we tried fluorescence observation with blue light and observation with a polarizing microscope. The sample was stained with Nile-Red and fluorescence was observed. As a result, fluorescence was observed in polypropylene and polyethylene. In addition, when the shrimp shells and bark were dyed with Nile Red, it was found that they were not stained with Nile Red. A polarizing microscope showed a difference in polarization between plastic and shrimp shells and bark. From this, it is considered that the detection accuracy of microplastics can be improved by observation with a fluorescence and polarizing microscope.

The reseach of microplastics of Shimoda Highschool

We have studied a method for analyzing microplastics in a short time without using expensive potassium iodide. Sampling was performed mainly on microplastics on the Izu Peninsula.

Sampling was performed at two locations on the Shirahama coast, and comparisons were made before and after the typhoon at the same location. Specific gravity separation using sodium chloride was performed, and the type of plastic was detected using a self-made hydrometer.

When sand was collected on the Shirahama coast and the composition of the plastic pieces was confirmed, the sand on the Shirahama coast had a very high polypropylene content, followed by polystyrene contained in Styrofoam. We compared the differences between the two sampling points, but

©2021. Japan Geoscience Union. All Right Reserved.

no significant difference was detected in the composition or number of plastics. When the number of microplastics was compared between before the typhoon approached and on the day when the typhoon approached, there was a 14-fold difference in the number. The sand was collected from the high tide line so that it would not be affected by anything other than weather conditions. As the approaching typhoon increased the amount of microplastic detected, it was found that strong winds increased the amount of microplastic carried to the coast. Due to the color and shape of the MP, there were many relatively large pieces of green and blue plastic pieces, some of which were thought to be related to marine leisure. We thought that our research would lead to environmental protection on the Izu Peninsula because of the lack of MP data on the Izu Peninsula. In this study, we succeeded in discriminating the type of plastic by a new method. In the future, we will explore ways to reduce polypropylene, which was the most common on the Shirahama coast. We also want to compare the proportion of plastic contained in seawater and the proportion of plastic contained in sand.

Keywords: Izu Peninsula, Micro Plastics, Shirahama coast, Kano river

©2021. Japan Geoscience Union. All Right Reserved.

Consideration of method to increase artificial ruby

Atsushi Watanabe[1], *Yuichirou Nagatsu[1], *Moe Hatakeyama[1], *Koutarou Matsumoto[1], *Yudai Komiyama[1]

1. Nirayama Highschool

Gemstones have always fascinated many people. There are only a small number of gemstones produced by the movement of the earth's interior, compared to the large demand. For this reason, the technology to produce gems by hand has developed.

Rubies are one of the gems for which there is an artificial process. Today, they are used not only as gemstones but also as abrasives.

There have been many previous studies on the generation of artificial rubies by the flux method, but most of them were done using platinum crucibles. The platinum crucible is expensive, so there are many obstacles to using it for research by high school students.

So, in this study, we focused on the generation and enlargement of artificial rubies without using a platinum crucible by the flux method. Instead of platinum crucibles, we used alumina crucibles

This research is a continuation of the research done at our school last year. In contrast to last year's research, which focused on the relationship between crystal size and temperature changes during crystal formation (heating, holding, and cooling temperatures, etc.), this research focused on two new aspects to increase crystal size: enlargement by condensation nuclei and enlargement by changes in evaporation inhibitors.

The flow of the experiment is as described below. Aluminum oxide, molybdenum oxide, sodium carbonate, lithium carbonate, and chromium oxide were weighed, placed in an alumina crucible, stirred so that each material was evenly distributed, and heated in an electric furnace. After heating, we scraped out the crystals that had formed in a way that they adhered to the inner wall of the crucible, and measured their size using a microscope and a micrometer. The color of the crystals was also recorded in photographs.

We experimented with varying the aforementioned materials. Specifically, we varied the evaporation inhibitor by 0 and 2 times, and added gypsum, calcium oxide, calcium hydroxide, and lithium sulfate, respectively.

As a result of repeated experiments, it was found that gypsum was involved in the enlargement of crystals, that sulfate may be involved in the enlargement of crystals because it was the only substance other than gypsum that produced crystals when mixed with potassium sulfate, and that there is a correlation between the evaporation inhibitor and the enlargement of crystals, and that the optimal amount of evaporation inhibitor is between 0 and 2 times.

Keywords: ruby, flux method

©2021. Japan Geoscience Union. All Right Reserved.

Earthquake prediction by Electric magnetic wave

*Masayuki Masa[1], *Nozomu Sakai[1], Michiya Sasaki[1], Souhei Kato[1], Ousuke Yagasaki[1], Mizuho Fujiwara[1], Maika Yashima[1]

1. Tokyo Metropolitan Tama High School of Science and Technology

This research detects a presage phenomenon by earthquake and done Electric magnetic wave radiation, and to assume that earthquake prediction is possible, Electric magnetic wave radiation observation by an earthquake presage is performed and seismic magnitude and an area in the epicenter are predicted the signal strength from a relation of duration and data in the radiation direction. A presage phenomenon with earthquake is caught.

The Electric magnetic wave radiation measurement generates at space, I'm doing every second record of the signal strength by 2 receivers. An antenna is used for judgment of area specification using omni-directional and a directivity antenna. I judge as signal intensity data including thunderbolt data, the ionosphere data and solar activity data, etc. and decide as a presage of an earthquake. It's confirmed whether the phenomenon which occurred to the time of an eastern Japan great earthquake is detected.

It was possible to catch a presage of the big earthquake which occurred at Miyagi, Fukushima and Ibaraki during March 20 from February 13, 2021. I resembled a signal fluctuation of an eastern Japan great earthquake of 2011/3 closely, and time signal-less reference signal level was also fluctuating. There was also little fluctuation range by a short time for reduced level. When shaking isn't felt big by an observation point, this phenomenon is also the phenomenon which doesn't show.

This research would like to increase an observation point and elucidate a mechanism of occurrence.

Keywords: earthquake, prediction, Electric magnetic wave radiation

©2021. Japan Geoscience Union. All Right Reserved.

Comparison of heated products of glucose with citric acid added

*Takumi Ohtsu[1]

1. Tokyo Metropolitan Tama High School of Science and Technology

Currently,there are problems with the method of disposing of plastic and the depletion of petroleum, which is the raw material of plastic, so we use lemon juice (citric acid) and sugar (sucrose) to make plastic into polyester.
I wondered if I could do it. However, since there are many factors to consider such as sucrose having glycosidic bonds, first, while changing the mixing ratio of cirtic acid and glucose, observe what each heating product will be regular.
I wondered if there was.

Keywords: cirtic acid, glucose

©2021. Japan Geoscience Union. All Right Reserved.

Development of iron (II) phosphate lithium-ion battery using the adsorption power of Aso loess

*Ayumi Hoshi[1], *Sora Nozaki[1]

1. Tokyo Metropolitan Tama High School of Science and Technology

Now, the depletion of phosphorus is regarded as a problem worldwide. In order to solve this problem, we wondered if phosphorus could be adsorbed from surplus fertilizer in fields and reused. Adsorption is performed using Aso loess. Aso ocher is the ocher-colored soil that can be found in the mountains of Aso, and is also known as "limonite." About 70% of its constituents are made of iron. In addition, it has high binding properties with various gases and harmful substances, and is demonstrating its adsorptive power in a lot of fields. When phosphoric acid is adsorbed on Aso loess, the phosphoric acid and iron contained in Aso loess combine to form iron phosphate. The ultimate goal is to utilize the iron phosphate as a positive electrode material for iron (II) phosphate lithium-ion batteries. As a first step, this time we conducted an experiment to confirm the adsorption power of Aso loess.

Keywords: Aso loess, Iron (II) Phosphate Lithium Ion Battery

©2021. Japan Geoscience Union. All Right Reserved.

首都圏オープン2021（TSEF2021）2021314

肥料から流出したリン酸の阿蘇黄土による回収

東京都立都立多摩科学技術高等学校
1年　星歩実・野崎昊

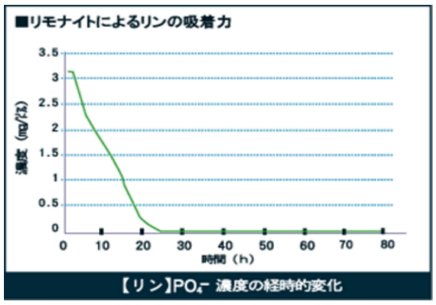
1．背景

今、リンの枯渇が世界的に問題視されている。その問題を解決するため、畑等の余剰肥料からリンを吸着し、再利用できないかと考えた。吸着は阿蘇黄土を使って行う。
阿蘇黄土とは、阿蘇の山の中でとれる黄土色の土のことで、別名を「リモナイト」という。その成分の約7割は鉄分でできている。また、様々なガスや有害物質との結合性が高く、その吸着力をあらゆる分野で発揮している。



2．先行研究

先行研究により、阿蘇黄土が水溶液中のリンの吸着が可能であるということがわかっている。



株式会社日本リモナイトホームページより

3．仮説

阿蘇黄土でリン酸を吸着すると、リン酸と阿蘇黄土内に含まれる鉄が結合しリン酸鉄という形になる。そのリン酸鉄をリン酸鉄（Ⅱ）リチウムイオンバッテリーの正極材料として活用することができるのではないか。

4．研究計画

私達は、肥料から吸着したリン酸を使ってリン酸鉄リチウムイオンバッテリーを作ることを目標にしている。

Step1
阿蘇黄土を使用して、肥料からリン酸の吸着を行う。

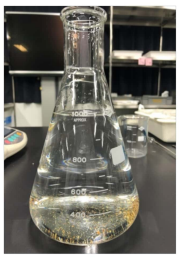
Step 2
吸着したリン酸を何らかの方法でリン酸鉄のまま取り出す。

Step 3
取り出したリン酸鉄を利用してリン酸鉄リチウムイオンバッテリーの正極材料を作る。

6．実験法方

今回は阿蘇黄土の吸着力を確かめることを目的に、以下の実験を行った。
（1）肥料と純水の混濁液を作る
（2）混濁液の上澄みに阿蘇黄土を混ぜ、リンを回収する
（3）黄土を混ぜる前と後のリン酸の濃度でどれほど回収したかを調べる
※リン酸の濃度を調べる方法として、パックテスト使用する。

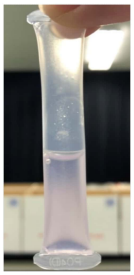
（1）　（2）　（3）



肥料と純水の混濁液

上澄み液と阿蘇黄土

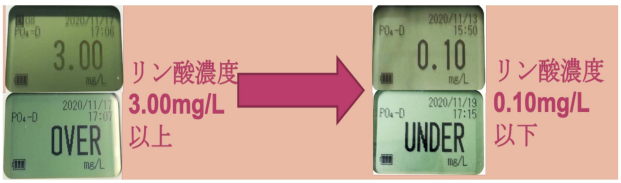




パックテスト

5．結果

阿蘇黄土を混ぜる前と後では、混ぜた後のほうがリン酸の濃度は小さくなった。



（上：デジタルリン酸パックテスト数値）

5．結果

結果から、阿蘇黄土によりリン酸は吸着されたことがわかった。今回の実験で、先行研究にもある通り、阿蘇黄土にはリンを吸着する作用があることを確認することができた。

5．今後の展望

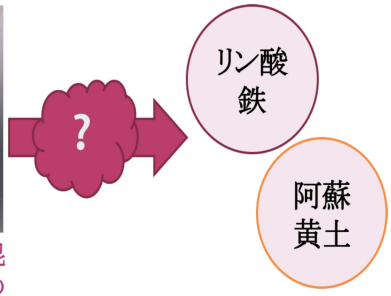
今回の実験で、阿蘇黄土による肥料中のリンの吸着力を確認できた。今後の課題として

1．リンを吸着した阿蘇黄土からどのようにリン酸鉄を取り出すか
2．取り出したものがリン酸鉄であることの証明はどのように行うのか

の２つが挙げられる。



阿蘇黄土を混ぜた混濁液をろ過したもの



©2021. Japan Geoscience Union. All Right Reserved.

Method of Recovering Perfluorinated Compounds by coffee grounds

*Kouki Morimoto[1], *Issei Yamazeki[1], *Renon Shimizu[1]

1. Tokyo Metropolitan Tama High School of Science and Technology

There are organofluorine compounds that are potentially carcinogenic, bioaccumulative, and persistent. Among them,perfluorooctane sulfonic acid (PFOS) and perfluorooctanoic acid (PFOA) were widely used in the life related products. Until recently, organofluorine compounds have been widely used mainly in products related to daily life due to their chemical stability, and are used especially for water-repellent coating processing, but many of them have flowed into the environment. Due to this, in recent years, there have been many reports on the environmental pollution of organic fluorine compounds. Coffee, on the other hand, is a beverage consumed around the world and its consumption is increasing year by year. However, most of coffee bean residue, which is the extraction residue, is incinerated as food waste. Therefore, as one of the effective uses of coffee grounds, the use of coffee grounds as an adsorbent for harmful substances is being sought. In this study, coffee grounds are known to have adsorption capacity for toxic substances, but their effectiveness against organofluorine compounds is not known. Therefore, an adsorbent using coffee bean residue is prepared, and the presence or absence of an adsorbing ability for PFOS and PFOA, in particular, is clarified this time. As a result, we believe it would be better if we could find new reuse values for coffee grounds and reduce environmental pollution and food waste. In this experiment, we conducted a water passing experiment using coffee bean dregs that had been subjected to untreated, boiling, bleaching and carbonization (240 ˚C, 400 ˚C), and environmental water (well water) that contained a large amount of activated carbon and PFOA. For each treatment, it was considered that the adsorption capacity would change by adding the treatment to the coffee grounds, and the bean grounds samples were prepared under the above four treatment conditions. In the water passing experiment, the column tube equipment for the water passing experiment was made by collecting and preparing materials suitable for the experiment conducted this time, and fine adjustment was carried out. The results obtained showed that coffee grounds had adsorption ability for PFOA. It was also found that addition of each treatment could improve the adsorption ability of most coffee grounds. In the carbonization treatment, it was found that the adsorption capacity was improved by the treatment at a higher temperature.

Keywords: Coffee grounds, Perfluorinated Compounds , Adsorption

©2021. Japan Geoscience Union. All Right Reserved.

Research into Moriya Formation Formed in Northen Fossa Magna

*Yusuke Morozumi[1]

1. Suwa Seiryo high school

1.Research motive
There is Moriya Formation around Mt.Moriya in Suwa. It didn’t investigate its details such as geological age or connection with other areas. So I thought I wanted to investigate them.
2.Research wayI did research in 13 places across Moriya Formation and I recorded fossil, lithofacies, and strike and dip. Based on the results of my research, I drew a geological map or make a conjecture about Moriya Formation’s geological age. And I compared with Shimonita Formation.
3.Research results
Research results and Geological map

Based on the results of my research, I drew a geological map. However, Shell fossils were produced from two outcrops, and these were called outcrops A and B. Outcrop A deposits volcanic ash gravel layer, gravel layer, and silt layer from the bottom, and outcrop B deposits volcanic ash gravel layer, coarse-grained sand layer, fine-grained sand layer, coarse-grained sand layer, and silt layer from the bottom.
Fossils of Moriya Formation

The fossils produced from outcrops A and B and the age of development of the major fossil species produced are shown in the figure. The fossils produced are divided into four types: those that inhabited the gradual Miocene, those that inhabited the Early Miocene and Middle Miocene, and those that inhabited after the Miocene.

Shimonita Formation’s Research

Since the Shimonita Formation is certified as a Japanese Geopark, I compared mainly the materials and literature surveys of previous studies. From Kurihara(2005), the Shimonita Formation has developed early Miocene species as a whole. And Sr isotope analysis using Mytilus tichanovitchi showed 20.4 ±0.2 Ma, and the upper limit was around 16.8 Ma from the production of planktonic foraminifera.

4.Considration
Based on the research results, I drew columnar maps of the Moriya outcrops A and B and the Shimonita Formation. Comparing them, it is considered that there is no big difference in the geological ages of the two layers because they have something in common, such as the production of Macoma and Mytilus tichanovitchi, which were developed from the Oligocene. In addition, the Moriya Formation has many mid-Miocene development species, but it is not found in the Shimonita Formation, and the Shimonita Town Formation shows 16.8 Ma, so the geological age of the Moriya Formation is 16 Ma, which is a little newer than the Shimonita Formation. Presumed. Matsumaru (1962) reported the production of large higher foraminifera in warm waters from the Moriya Formation, and it is believed that the Moriya Formation was formed in warm waters. We collected Kimura scallops and Anadara genus, which are characteristic of the Miocene Kadonosawa fauna, which developed from the Moriya Formation in the warm sea. However, Mytilus tichanovitchi from the Moriya class is considered to be evidence of the early Miocene cooling event. In that case, the Moriya Formation is considered to have been deposited in the

©2021. Japan Geoscience Union. All Right Reserved.

cold sea, which is inconsistent with the results of previous studies. However, Anadara and others are not effective phase-indicating fossils, and it is possible that they could adapt to the cold sea. However, no other strata, such as the Moriya Formation, where fossils of the Early Miocene cooling event period and the Middle Miocene Kadonosawa Animal Group coexist have been confirmed at this time. From the above, it is considered that the Moriya Formation was deposited during the transition period from the cold Miocene to the warm Miocene around the Early Miocene and the Middle Miocene.

Keywords: Moriya Formation, Fossa Magna

©2021. Japan Geoscience Union. All Right Reserved.



図1：①守屋層と②下仁田層の位置



図2：産出したMytilus tichanovitchi
上：守屋層産　下：下仁田層産

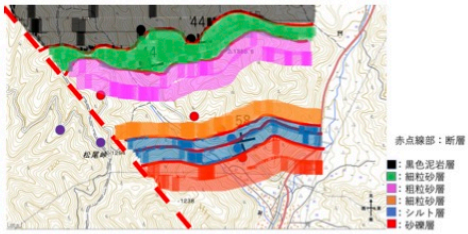


図3：作成した守屋層下部の地質図



図4：守屋層から産出した主な化石種の生息した年代

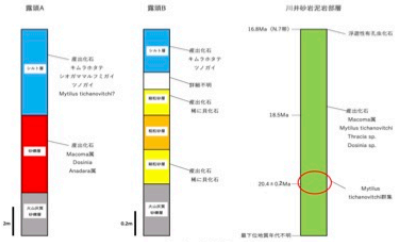


図5：作成した柱状図

©2021. Japan Geoscience Union. All Right Reserved.

A Consideration of a Landing Exploration on Europa

*Taichi Ito[1]

1. Seishin Gakuen High School

Europa, a Jovian moon, is said to have a huge ocean under its ice-surface, drawing attention as a major target of astrobiological research. Although NASA plans to send a probe and to do many flybys of Europa in 2020s, no landing project exists. So, I concentrated my research on a landing exploration.

Because a landing exploration on Europa can give us crucial information about the essence of lives, I regard this research extraordinarily significant.

Europa’ s atmosphere is rarefied. Therefore, I thought that parachutes would not be effectual. Hence, the purpose of this research is to consider the way to land softly with reverse thrust for an astrobiological exploration. The hypotheses I made are as follows:

[the Hypotheses]
The lander will be loaded onto a mother machine and undock at a height of 20km above Europa. The landing engine: hydrazine thruster (specific impulse: approx. 220 to 235s) The undocked lander whose initial velocity is 0m/s starts free fall, starts reverse thrust at an altitude, and comes to halt on the surface. The lander moves only vertically. The thrust, the effective exhaust velocity, and the propellant mass flow rate are constant.

In launching, they accelerate an object from 0 to a velocity, while, in reverse thrust, they decelerate an object from 0 to a velocity. In other words, you can think of soft landing as playing launching backwards. Grounded on this similarity, I thought if I could apply the derivation of the Tsiolkovsky rocket equation related to launching of rockets.

$\Delta V = c \ln(1/\mu)$

Provided that, ΔV: velocity change due to jetting, c: effective exhaust velocity, μ: mass ratio. In addition, based on relational expressions I created, I input a concrete condition,

Let

g as the gravitational acceleration of the target of landing
m_Max as the maximum mass of the lander
μ as the mass ratio of the lander
c as the effective exhaust velocity of the thruster
F as the thrust of the thruster
Then,

the Total Fall Altitude: $x_{total}=c^2/F*m_{Max}(\mu \ln(1/\mu)-(1-\mu))+c^2/2g*(\ln(1/\mu))^2$
the Altitude to Start Reverse Thrust: $x_{jet}=c^2/F*m_{Max} (\ln(1/\mu)-(1-\mu)-m_{Max}/2F*g(1-\mu)^2)$
the Altitude of Free Fall: $x_{free}=1/2g*(c \ln(1/\mu)-(c\ m_{Max} (1-\mu))/F*\ g)^2$
the Total Fall Time: $t_{total}=c/g*\ln(1/\mu)$

©2021. Japan Geoscience Union. All Right Reserved.

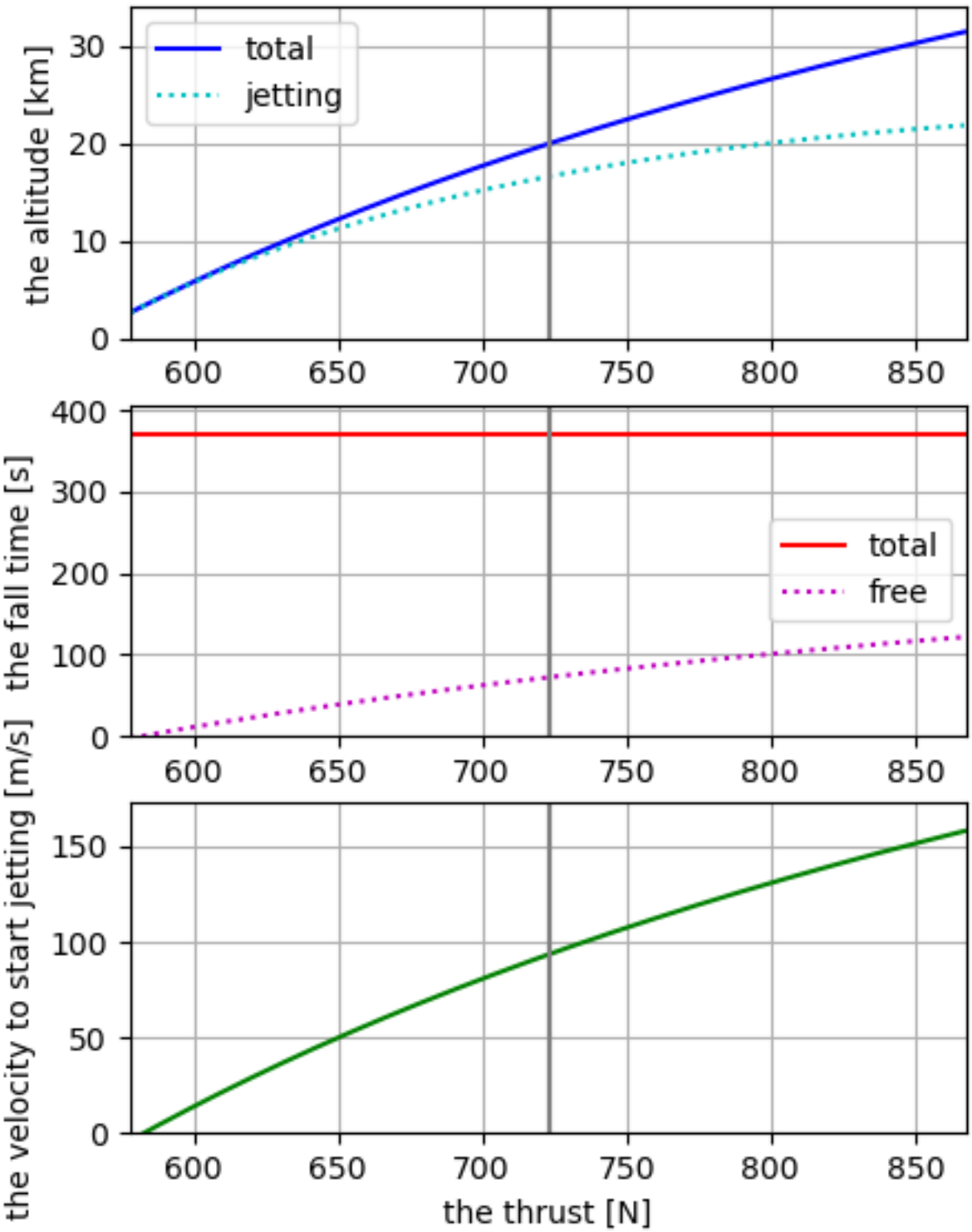
the Time of Reverse Thrust: t_jet=(c m_Max (1-μ))/F
the Time of Free Fall: t_free=c/g ln(1/μ)-(c m_Max (1-μ))/F
the Velocity to Start Reverse Thrust: v_Max=c ln(1/μ)-(c m_Max (1-μ))/F*g

Here, I made a Python program which outputs an approximate value of the thrust by using the bisection method with any accuracy, calculates each altitudes and times of reverse thrust, free fall and total, and draws graphs. If I run the program by taking 9.8m/s^2 for the gravitational acceleration of the Earth, 1.3m/s^2 for the gravitational acceleration of Europa, 500kg for the maximum mass, 220s for the specific impulse, 0.8 for the mass ratio, and 20km for the altitude to start falling, it outputs these approximate values:
F = 723.46875 ±0.03125 [N] x_total = 19.9992723959987 ±0.002981374671238882 [km] x_jet = 16.623466418409254 ±0.0017754098712466657 [km] x_free = 3.3758059775894473 ± 0.0012059647999922163 [km] t_total = 370.0749974103356 [s] t_jet = 298.0087258810587 ± 0.012872391079497447 [s] t_free = 72.06627152927692 ±0.012872391079469025 [s] v_Max = 93.68615298805997 ±0.016734108403312575 [m/s]
and following graphs.

As a result, I could set when and where to start falling, start reverse thrust and reach the surface by deciding the performance of the lander.

Keywords: Europa, Landing Exploration, Lives, Probe, Space Exploration, Reverse Thrust

©2021. Japan Geoscience Union. All Right Reserved.



©2021. Japan Geoscience Union. All Right Reserved.

Relationship between five gigantic jets in the past and cloud-to-ground lightning

*Fuga Suzuki[1], *Yuya Takahashi[1], Sorachi Nishibori[1], Yuki Ito[1], Takumi Miyamoto[1]

1. Shizuoka Prefectural Iwata Minami High School

Four gigantic jets have been observed from our school. According to previous studies, before and after the gigantic jet in 2017 occurred, the number of cloud-to-ground lightnings and the amount of their energy had been prone to decrease (Yamashita, 2017). This study aims to examine whether the other gigantic jets have a similar tendency. We investigated the positional relationship between the gigantic jets and cumulonimbus with infrared images, and the numeral one between cloud-to-ground lightnings with observational data. Based on the results, the tendency mentioned in the previous study was confirmed. Gigantic jets also tend to occur at the edge of huge cumulonimbus and the area cloud-to-ground lightnings were observed remarkably in. This indicates that gigantic jets occur if numerous charges are stored there.

Keywords: Transient Luminous Events, Gigantic Jet, Cloud-to-Ground Lightning

©2021. Japan Geoscience Union. All Right Reserved.

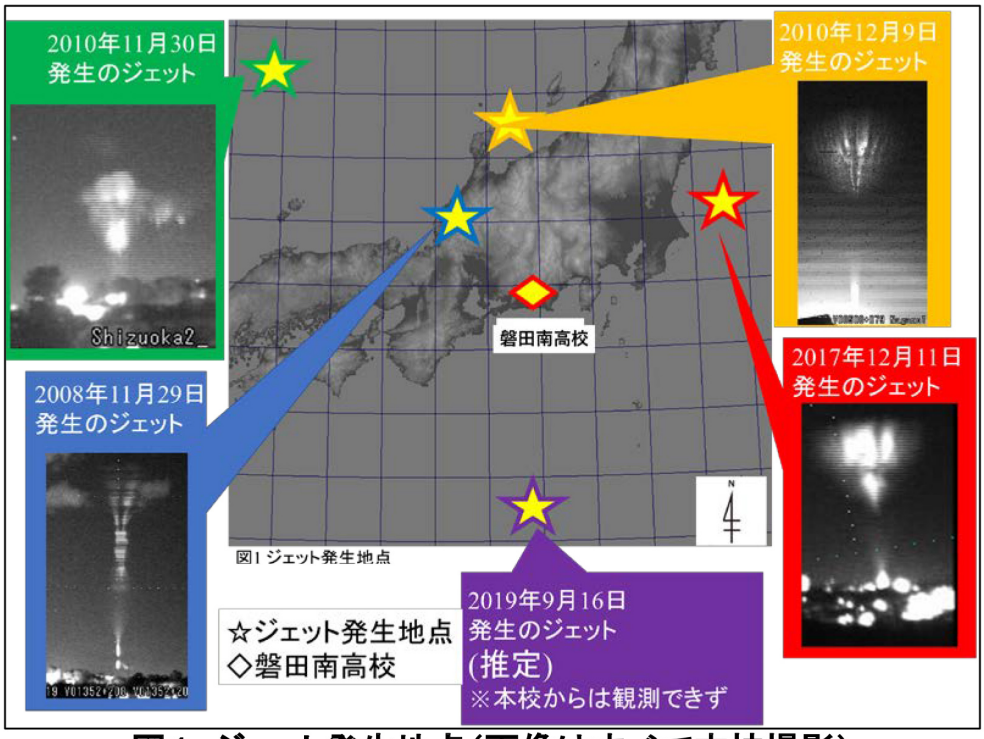


図1　ジェット発生地点（画像はすべて本校撮影）

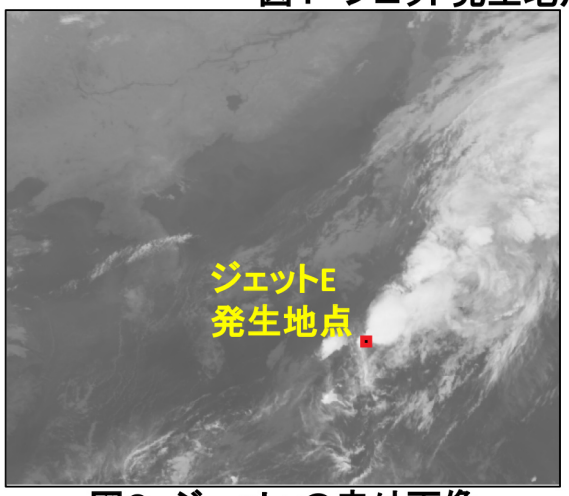


図2　ジェットEの赤外画像

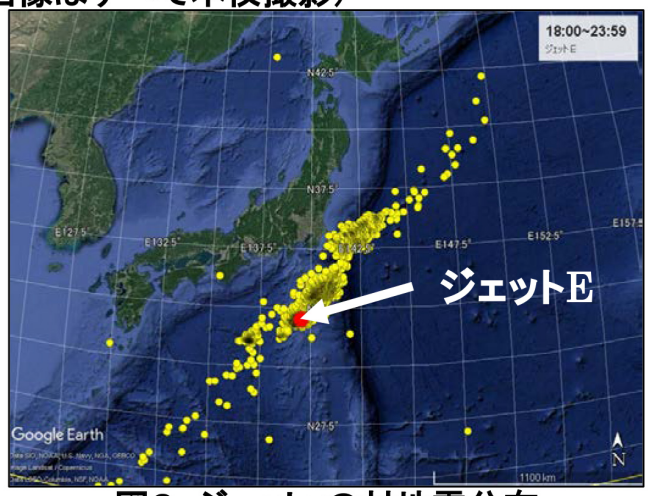


図3　ジェットEの対地雷分布

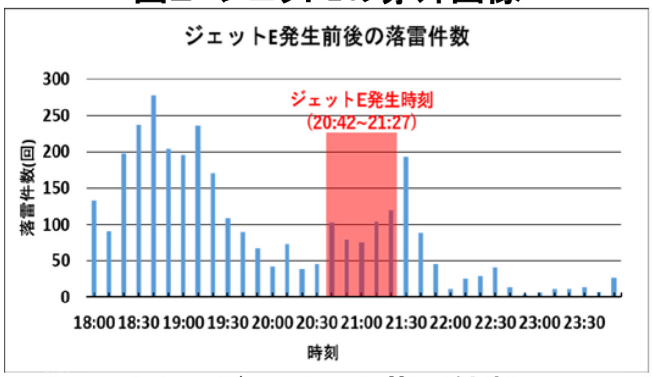


図4　ジェットEの落雷件数

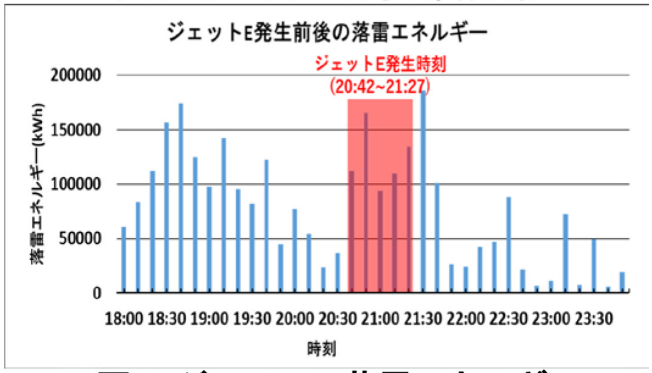


図5　ジェットEの落雷エネルギー

表1　5つのジェットの赤外雲画像と対地雷の比較

	A	B	C	D	E
赤外雲画像	積乱雲南西端	積乱雲南端	積乱雲南寄り	積乱雲南端	積乱雲南西端
空間分布	対地雷群南端	対地雷群南端	対地雷群北東端	対地雷群南西端	対地雷群南西端
対地雷時間変化	10分前から対地雷なし	不明	20分前から対地雷なし	1時間前から対地雷減少傾向	2時間前から対地雷減少傾向

©2021. Japan Geoscience Union. All Right Reserved.

Examination of the fall position by the light emission of the Narashino meteorite fireball

*Ryunosuke Kamiya[1], *Haruka Sato[1], Kosuke Arimura[1], Saki Ozawa[1], Hana Miki[1], Yuka Ogawa[1], Honoka Tanabe[1]

1. Shizuoka Prefectural Iwata Minami High School

At 2:32 a.m. on July 2, 2020, a fireball was observed flowing from west to east over the Kanto region. The fireball turned out to be a meteorite that had fallen in Narashino City, Chiba Prefecture.We conducted this research based on the video taken at our school.
We identified the trajectory of the fireball and the latitude, longitude, and altitude of the start and end points of its emission from it, and then examined the location of the fall.
As a result, we found that the fireball continued to fall while being subjected to physical factors, and fell in a parabolic motion after the emission ended.The total horizontal distance traveled by the fireball was close to the linear distance between the start of the emission and Narashino City. In other words, we found that the the location of the fall of the fireball can be estimated from the video taken.

Keywords: Narashino meteorite fireball, The location of the fall

©2021. Japan Geoscience Union. All Right Reserved.



図1.本校観測の習志野隕石火球の連続写真
（2020年7月2日2時32分）

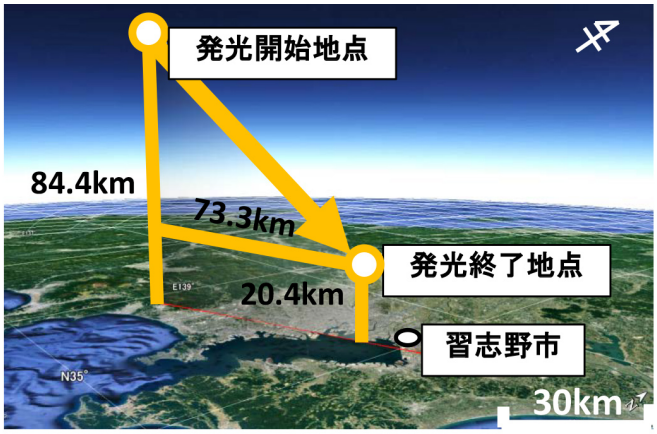


図2.立体的な習志野隕石火球の軌道

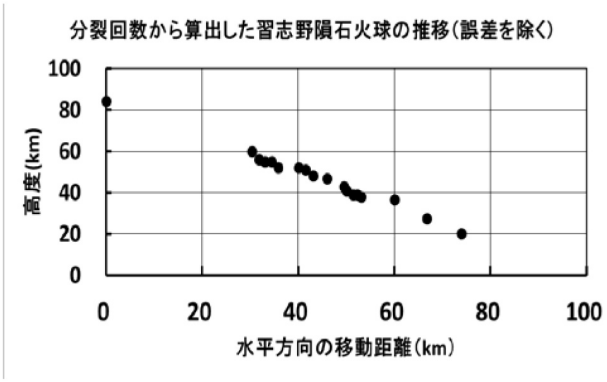


図3.誤差を除いた習志野隕石火球の推移

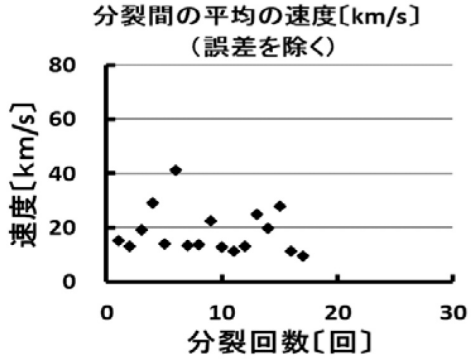


図4.誤差を除いた分裂間の平均の速度

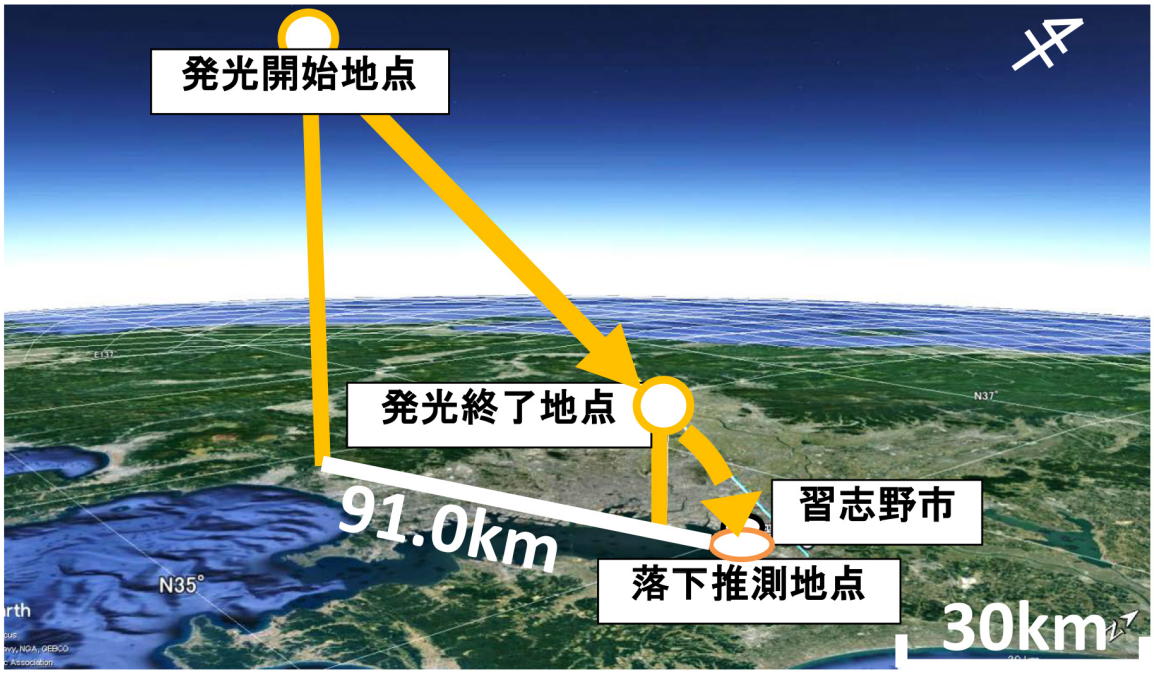


図5.物理的要因を受けた場合の落下推測地点

©2021. Japan Geoscience Union. All Right Reserved.

The Change of Microtopography of Samejima Coast Caused by the Storm Surge Brought by Hagibis

*Takeshi Totsuka[1], Yuya Takahashi[1], *Kosuke Arimura[1], Koki Suzuki[1], Shun Ichikawa[1], Rabu Kato[1]

1. Shizuoka Prefectural Iwata Minami High School

The Enshu Sea Samejima coast, where our school conducts regular surveying, showed significant coastal erosion on October 17, 2019, with the shoreline receding and the boardwalk destroyed. A study was conducted to elucidate the extent and cause of this damage.

We conducted meteorological observations, aerial photography, level surveying, mineral analysis, grain size analysis, and trench surveys to determine the cause of coastal erosion.

As a result, it was found that the topographic cross-sectional area decreased significantly after the passage of Hagibis, the average grain size of the sand became finer as it moved away from the coast, and the sediments showed a tendency toward upward finer grainedness and a structure that appeared to be a hummocky diagonal stratification. This indicates that the seaward side of Samejima Beach was eroded by the storm surge of Hagibis, and that storm surge sediments were deposited behind the landward side of the beach.

Keywords: Samejima coast, Hagibis, level surveying, grain size analysis, trench surveys

©2021. Japan Geoscience Union. All Right Reserved.

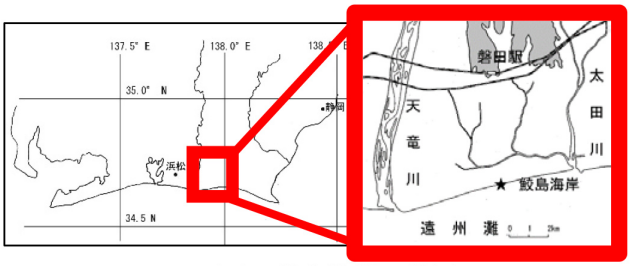


図1. 鮫島海岸の位置



図2. 台風通過前の海岸入口西側の空撮



図3. 台風通過後の海岸入口西側の空撮

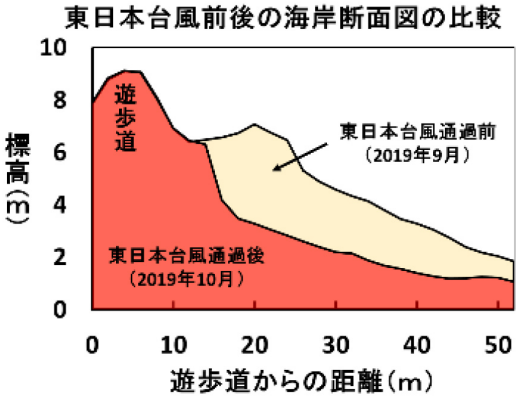


図4. 東日本台風前後の海岸断面図の比較

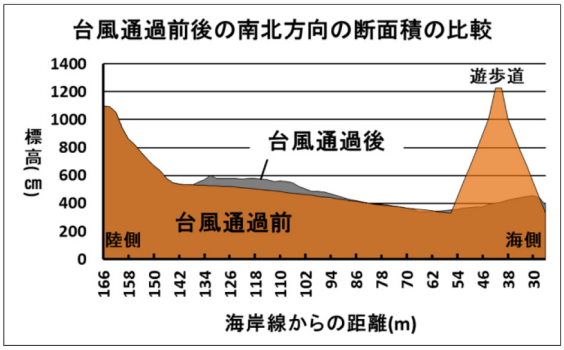


図5. 台風通過前後の地形断面図の重ね合わせ

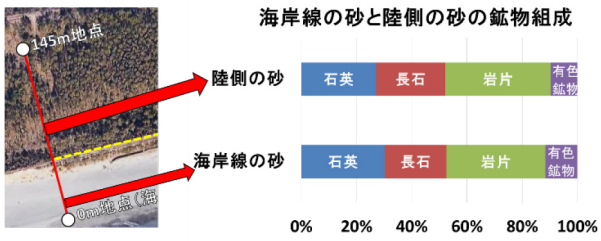


図6. 陸側(100m地点)と海側(0m地点)の鉱物組成

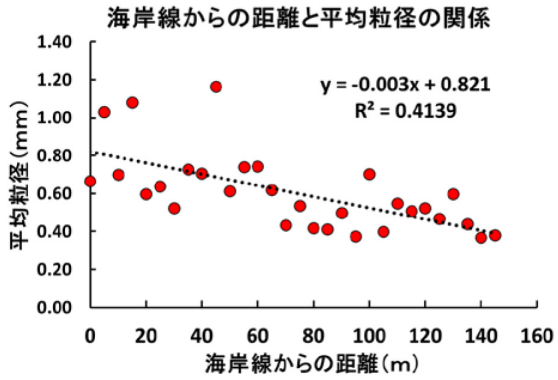


図7. 南北方向の平均粒径の変化

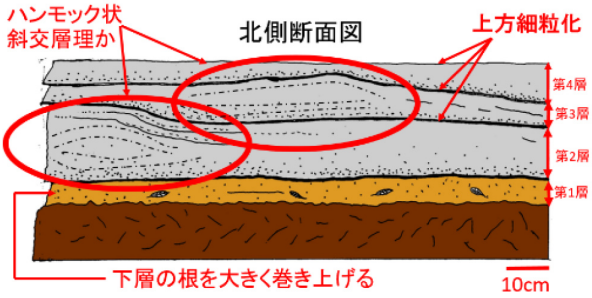


図8. 堆積物のスケッチ

©2021. Japan Geoscience Union. All Right Reserved.

Putting legs on snake swimming robot going to be useless? Seeking truth of Tetrapodophis

*Ryoya Sato[1], *Kokoro Ikeda[1], *Ryota Ogawa[1], *Riko Tomioka[1], *Akari Hitomi[1], *Kanon Yamaguchi[1]

1. Tokyo Tech High School of Science and Technology

Our team heard a new way to research ancient creatures called Robokaseki. Our research target is Tetorpodophis. Tetoraodophis is a snake-shaped creature, which lived 110 to 120 millions years ago. We are building a robot that moves like Tetoraodophis as robot and studying about how legs has been used. Ancient creatures are in the course of evolution, so their movement is considered to be simple and efficient. In the study of Tetrapodophis, we think we can elucidate the movement and ecology.
One of the most important studies in palaeontology is creatures evolution. Fossil is the only evidence that shows a real evolution pattern. On the other hand, fossil has only small information. Then, imitating movement of the robot can help predict the soft tissue and their movement and speed. Collecting data of robots speed and movement can be useful.Therefore, it is possible to predict their abilities and this will help to study creatures evolution.
There are several hypotheses of the roles of Tetrapodophis’ s legs. To catch prey or copulation partner, to swim and paddle. However there is no conclusion of theirs legs.
There are several theories about the role of legs that have been found in the literature on Tetrapodophis. The first theory is that the legs were used to hunt prey or mate with partners during life on land. The second theory is that they were used for swimming in the form of paddles during life in the water. Therefore, no conclusions have been drawn as to how the legs of Tetrapodophis were used.
Tetorapodophis which has found is 20cm long and their limbs are 1.5cm long. Fossil shows that hind legs are supported by strong bones than forefoot, so it is considered that hind legs are more used than forefoot. Limbs have something like finger, and that can be considered as they had same size or bigger than palm wedding.
To study more about Tetorapodophis’ s legs, in experiment we made a snake-shaped under water robot by reference to Tetorapodophis fossil. As a result, it is easy to change direction with forefeet and a way of swimming can be stabilized by using hind legs. Forefeet are too small to produce propulsive effect, but it can make instantaneous power, so it can be said that they have great effect on hind legs.
Also, moving hind legs and tail can stabilize robot and more propulsive. For those reasons putting legs on a snake-shaped underwater robot is making sense.
There are three issues that we would like to solve in the future. The first is to make the snake- shaped robot behave more like a real living thing. Our robot cannot dive or surface. If our robot become able to dive and surface, we would find more ways to use their legs and investigate its usefulness.
The second is to identify the habitat. The stratum where the fossil was found is thought to have been a shallow inland sea. Therefore, we expect that it was an aquatic organism. In order to prove this, we are going to investigate whether the robot can walk on land or not. And that will reveal whether it could have been active on land or not.
The third is to prove the reconstructions. If a robot cannot swim or moves in a way that does not fit the expected living environment, it is not a correct reproduction. Therefore, we believe that the shape of the robot with reasonable movements will prove the reconstructions.
We hope that this study will solve these three issues and that the use of robots in the study of palaeontology will become widespread.
There are several theories about the role of legs that have been found in the literature on Tetrapodophis.

©2021. Japan Geoscience Union. All Right Reserved.

The first theory is that the legs were used to hunt prey or mate with partners during life on land. The second theory is that they were used for swimming in the form of paddles during life in the water. Therefore, no conclusions have been drawn as to how the legs of Tetrapodophis were used.

Keywords: Tetrapodophis, Imagine a creature from a fossil and reproduce as robot, Restore

©2021. Japan Geoscience Union. All Right Reserved.

水中蛇型ロボットに脚をつけたら蛇足か
古代の化石から生物を再現して実証する

東京工業大学附属科学技術高等学校

佐藤諒弥　池田こころ　雄川綾太　人見あかり　富岡りこ　山口海音

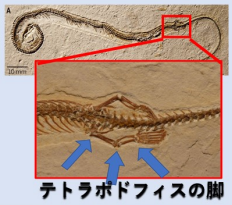
指導教諭　岩城純

10 mm

1. 研究目的







海に囲まれた日本では、海洋研究は重要であり未知の事柄が多い。水中探査ロボットは、海中調査を行う上で不可欠である。私達は、脚を持った蛇の**化石テトラポドフィスの形状を参考にした水中蛇型ロボット**を作成し、その動きを検証して、新たな水中蛇型ロボットの形を提案することが目的である

ロボットによる化石復元の意義

化石の復元は間違った形や生態にされてしまうこともある。そこでロボットを用いて形や生態を再現する。

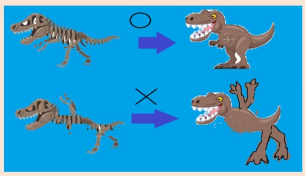
正確に復元しないとロボットは不自然な動作をして動かない

↓

自然に動くとき、その動きは実物に近いと類推

↓

新たな動作方法の発見



2　研究方法

テトラポドフィス（図1）は、脚を持った蛇型生物である。この生物は、陸上で生活していると考えられていたが、近年は水中で四肢をパドルのように使って生活していたと考えられている。そこで本研究では、テトラポドフィスの脚の使い方を推測し実験をすることで、従来の蛇型ロボットに脚をつけると機能性が上がる可能性があるのではないかという仮説を立てた。ここでは、図2に示すテトラポドフィスと似た生物のホライモリを参考に、テトラポドフィスの骨格を基にした脚付き蛇型ロボットを作成し、脚の役割について検証した。

・1億1000万年前に生息
・生息環境不明
・全長約20cm,
手足は約1.5cm
⇒手足の用途は不明



図1

・現在生息
・真洞穴性
・全長約20～30cm,
手足約2cm
⇒手足では地を這う
ことなどに使用

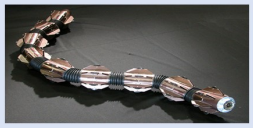


図2

化石からだけではテトラポドフィスの動きがわからないため、類似している生物のホライモリの動きを参考にロボットを製作した

先行研究例　蛇型水中ロボット

○ ACM-R5
ー東京工業大学 広瀬茂男名誉教授ら



体をくねらせるヘビのほふく推進を取り入れた水陸両用の口ボット

瓦礫が散乱する福島第一原子力発電所内部の探査において、高い適正を発揮した

先行研究例　ロボ化石

日本地質学会 **「ジオルジュ」**2019後期号
「水中で動く化石」 P7～9

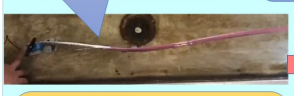
NPO日本水中ロボネット　水中ビークル・フリーミーティングの技術報告
9.7 ロボ化石工作マニュアル
「生体模倣(Biomimetic)水中ロボットの検討　ウミサソリ ロボ化石を作る」（2018）
文と写真 AFK研究所(同) 近藤敏康 イラスト よ志
http://uwr.sakura.ne.jp/oppama/tech-info/UmisasoriRobot_r2.pdf



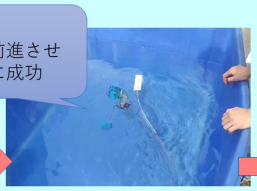
近藤氏のマニュアルを元に作成したロボ化石
＜シンダーハーネスを再現＞

3. ロボットの製作過程

1号機
蛇型ロボットを試作
バタつくだけで進まなかった。



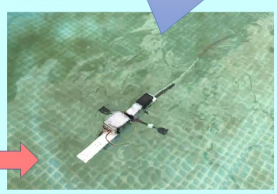
2号機
蛇型を前進させることに成功



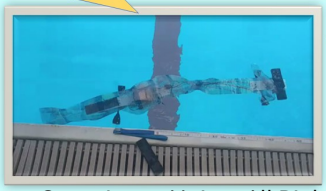
3号機
浮力調整を行い蛇型ロボットしてはスムーズに動くようになった



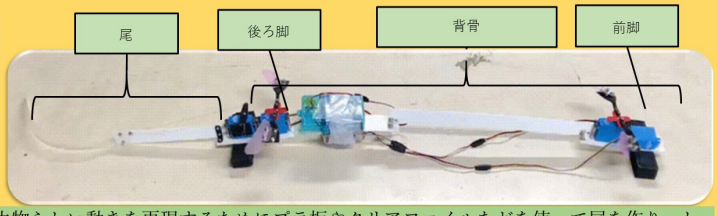
4号機
前脚付き蛇型ロボットを試作　計測実験を開始。



最終完成機
化石の骨格を基に四肢をつけ、外装をつけて泳がせることに成功！



ロボットの仕組み



生物らしい動きを再現するためにプラ板やクリアファイルなどを使って尾を作り、しなやかな動きを実現した。脚ヒレは水を掻くときにヒレが立ち、脚が前に戻るときは倒れこんで水の抵抗が小さくなるようにした。

©2021. Japan Geoscience Union. All Right Reserved.

©2021. Japan Geoscience Union. All Right Reserved.

Consideration of snowmelt type lahar at Mt. Katta, Zao

*Haruya Shishido[1], *Reiki Syoji[1], *Ryo Hikichi[1]

1. Miyagi Prefectural Tagajo Senior High School

Miyagi Prefecture is blessed with fine weather in the summer and snows in the winter. And it is a land that has developed with many benefits from active volcanoes such as Mt. Zao and Mt. Kurikoma. Therefore, we investigated and examined the damage caused by the snowmelt type lahar, targeting Mt. Zao, which has been active in recent years.
It was found that the pyroclastic surge calculated from the amount of eruption has the ability to prepare a large amount of snowmelt water. Even if all the 2m of snow in the pot is melted, there is still room. Damage is expected to increase in years with heavy snowfall, such as the year of the La Nina phenomenon.

Keywords: Lahar, Zao

©2021. Japan Geoscience Union. All Right Reserved.

Geological structure of Urato Katsurashima Island and Nonoshima Island, Shiogama City

*Asahi Oyama[1], *Hikaru Sasaki[1], *Yuhi Suzuki[1], *Hayato Murakami[1], *Misaki Kuga[1]

1. Miyagi Prefectural Tagajo Senior High School

We were interested in the fact that the two strata, the Matsushima Formation and the Otsuka Formation, were clearly exposed during the Urato Geological training in 2019, and considered the geological structure of Nonoshima Island.
In this study, as a continuation of the study, we decided to expand the scope of the study to Katsurashima Island on the west side and interpret the geological structure of the Urato Islands in a wider range.
[Results] It was found that a syncline structure exists in the eastern part of Katsura Island. The syncline axis was south-southeast and the plunge angle was 2 ˚. As a result of drawing, it was found that there are anticline structures and syncline structures with gentle slopes from Nonoshima to Katsurashima. It was also confirmed that the stratum was lying on its side.
[Discussion] In the history of the formation of the Japanese archipelago, the Matsushima Formation was brought about by volcanic activity and crustal movements caused by the expansion of the Sea of Japan. The location of the slump structure was confirmed in the Matsushima Formation due to the earthquake during deposition. In addition, a normal fault was confirmed as the condition of the pulling field continued. In addition, it is probable that at the point where the overturned stratum was confirmed, the earthquake motion at the stage where this tension field was generated caused a collapse or a submarine landslide in the water.

Keywords: Formation

©2021. Japan Geoscience Union. All Right Reserved.

Threats and impacts of urban tsunami -Simulate a tsunami when a Nankai Trough giant earthquake occurs using a tsunami generator-

*Misaki Suda[1], *Kenshin Okazaki[1], *Zen Sato[1], *Yusei Niinuma[1], *Kousei Matsuura[1], *Ayaka Akisawa[1]

1. Miyagi Prefectural Tagajo Senior High School

The Great East Japan Earthquake that occurred on March 11, 2011 caused a tsunami of up to 4.6 m in the city of Tagajo, killing 188 people. One of the factors that caused many casualties in Tagajo City is the characteristic of the urban tsunami, "the tsunami rushed in from unexpected directions." Based on this feature, we are conducting research on what kind of measures can be taken to suppress wave height, wave speed, and wave power.
The urban tsunami observed in Tagajo City is thought to be observed in the "Nankai Trough Giant Earthquake". In order to prevent such damage, we thought that it would be possible to minimize the damage caused by the tsunami by simulating the urban area at the time of the tsunami using tsunami generators, water source devices, building models, etc. ..

Keywords: Tsunami, Urban Tsunami, The Great East Japan Earthquake

©2021. Japan Geoscience Union. All Right Reserved.

Countermeasures against Heat Island Phenomenon: Proposal for a New Building System

*Hiroaki HAYASHI[1]

1. Yokohama Science Frontier High School

Introduction

Recently, the heat island phenomenon has become more serious and environmental problem peculiar to cities. The main causes are artificialization due to ground surface cover and high density of urban forms. Therefore, the heat island effect appears mainly in urban areas and needs to be considered separately from global warming. As a countermeasure, the reduction of artificial exhaust heat and the use of wind from the sea to create Wind Path have been mentioned. This time, I focused on the Wind Path and devised an environmentally friendly building structure and system to efficiently cool and utilize the harmful building wind, even in places where no wind reaches from the sea.

Methods and Results

1. Design of a cooling system using endothermic reaction of chemicals: (a) ammonium sulfate, (b) citric acid, (c) baking soda, and (d) urea were selected as relatively safe chemicals that undergo endothermic reaction when dissolved in water, and dissolved in water (100 cc, 35˚C) at different concentrations. The time course of temperature decrease was compared. When 5 mol of (a) was dissolved, the water temperature dropped to 24.5˚C. When 4 mol of (b) was dissolved, the water temperature dropped rapidly to 19˚C. (c) the water temperature dropped only to a maximum of 28˚C. The cooling effect of (a), (b), and (d) among the four types was high, and among them, the cooling effect of (d) was the highest. Therefore, two mixtures of (a) + (d) and (b) + (d) were dissolved in water, expecting a synergistic effect. However, all of them dropped to around 13˚C and there was no difference, and the expected synergistic effect compared to urea alone could not be obtained.

2. Relationship between walls and wind speed: A model of a cylindrical building was built with side and front walls, and the change in wind speed under the building was measured. The results showed that the buildings with side walls had stable wind speeds overall. In particular, the wind speeds at the 5-25 cm point were all above the average wind speed of 2.0 m/s. In addition, buildings with side and front walls had average wind speeds above 3.0 m/s at the 5 cm point, which were above the average wind speed values for buildings with only side walls at all points.

3. Building Wind-Based Cooling System: A building model with side and front walls was constructed, and wind was applied to the building to measure the ground surface temperature under the following three conditions; (a) building only, (b) radiator filled with water at 23˚C, and (c) radiator filled with cooled urea water. The average wind speed through the radiator was 1.2 m/s. The ground surface temperatures at 10, 15, and 20 cm distances from the radiator were (a) 39.7, 37.8, and 35.7˚C, (b) 38.0, 37.2, and 36.2˚C, and (c) 34.6, 35.1, and 35.2˚C, respectively, a decrease of about 5˚C at 10 cm and about 3˚C at 15 cm. There was not much difference in the surface temperature at 20 cm. When radiators filled with urea water were used, the temperature increase over time was suppressed and the surface temperature under the building was cooled down to the 15 cm point.

©2021. Japan Geoscience Union. All Right Reserved.

Summary and Discussion

As for the structure of the building, it was found that the wind was more concentrated when the side and front walls were attached to the surface of the building. As the cooling water for the wind, several chemicals that cause endothermic reactions when dissolved in water were investigated, and urea, used alone, provides an efficient and strong cooling effect. Urea is safe for the human body and is widely used in skin creams and fertilizers, etc. After cooling the building air, urea can be dissolved and diluted after filtered from the waste water, which is environmentally friendly and can be used as a fertilizer for plants. In devising a building system, it would be even better for the environment if urea could be extracted directly from the urine in the building effluent and sewage. It is said that humans discharge about 30 g of urea per day. There are reports of recovering urea through direct filtration by osmotic urea separation using a dialyzer used for artificial kidneys, and there are proposals to recover urine directly from underground septic tanks in cities. In future, specific methods to extract urea from urine discharged from buildings should be studied. In order to consolidate the complex building wind, the direction and the building structure need to be studied in more detail. In this experiment, a cylindrical building with only one side wall and one front wall in a small area was tested. For realization, experiments should be conducted to expand the area of walls to be attached to the building, or to have multiple buildings densely packed like a city, in order to construct a new Wind Path.

Keywords: heat island phenomenon, Wind Path, urea

©2021. Japan Geoscience Union. All Right Reserved.

An evaluation of artificial landform in Chiba prefecture called “Kawamawashi”

*Kodai SHIBUYA[1]

1. Yokohama Science Frontier High School

Kawamawashi landform is an artificial landform constructed in the Kazusa region of central Chiba Prefecture, where the curved part of a river is cut off and the detached old river channel is used as a paddy field. As the man-made landforms peculiar to the Kazusa region, including the Kawamawashi landforms, are gradually being lost, we attempted to evaluate them in order to utilize the Kawamawashi landforms. The geological features and locations in the Kazusa area were summarized by literature survey, and a field survey was conducted to one of the Kawamawashi landforms, and a comparison of the Kawamawashi landforms was made using a rapid survey map and past aerial photographs. As a result, it became clear that it is difficult to evaluate the geological features of the river-forming landforms more than "mainly mudstone".

Keywords: Kawamawashi, artificial landform, Kazusa region, mudstone

©2021. Japan Geoscience Union. All Right Reserved.

千葉県上総地方における川廻し地形の評価

横浜市立横浜サイエンスフロンティア高等学校
2-6 17 澁谷耕大

川廻しとは

千葉県中部の房総丘陵からの河川沿いに見られる人工地形であり、曲流を短絡し旧河道を田地として用いるために江戸時代から行われた、治水工事と新田開発を兼ねた工事及びそれによって形成された地形。

目的

田地の減少？ → 利活用のための評価

- 希少地形の荒廃
- 旧河道→活用しづらい可能性？
- そもそも評価が少ない

方法

- 地形図により川廻し地形の特徴を調査
  - ➢ 場所や規模
  - ➢ 航空写真による確認
- フィールドワークにおいて実際の使用状況を確認

結果①

1. 規模は多様
2. 面積は70000㎡程度が多い
3. 水田もしくは荒れ地
4. 養老川と夷隅川沿い双方に

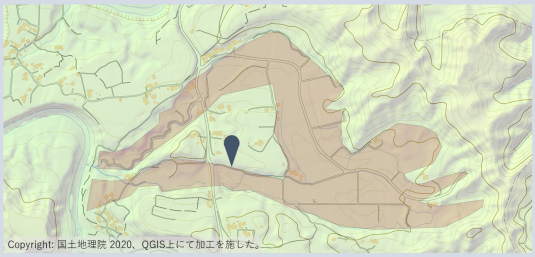


結果②



年月日: 2020/09/22
場所: 千葉県市原市

水田 / 一部休耕地
滑走斜面に泥岩



結論

川廻し地域は、基本的に泥岩を主とした田地であることが明らかとなった。フィールドワークにおいては基本的に水田が見られたものの、耕作が行われていない土地も見られた。また、地図上では荒れ地も見られた。

よって以下の結論が得られた。

- 泥岩を主体としており、軟弱地盤といえる
- 大規模な建設を行うには向かない
- 様々な規模を持つため評価は一定に出来ない

主な参考文献

- 八木 令子, 吉村 光敏, 小田島 高之, 房総丘陵を水源とする河川の地域特性と地形誌, 2017, 千葉県立中央博物館自然誌研究報告, 特別号第10号, p. 21-44
- 白井 哲之, 半固結地層地域の地形形成-1-小櫃川沿岸の段丘地形形成に関する予察的研究, 2017,千葉大学教育学部研究紀要 25(第1部), p. 159-169

今後

地誌学的な検討が不足しており、施工背景についての調査が行われていなかったことがある。

また評価基準の客観性が不足しているため、評価基準の明確化が必要であると考える。

©2021. Japan Geoscience Union. All Right Reserved.

The relationship between sunspot number and typhoons

*Takeru TODA[1]

1. Yokohama Science Frontier High School

Introduction

I wanted to connect meteorological phenomena and astronomy. Then I focused on the sun. The sun has been giving a huge amount of energy to the earth. And it should have effect on meteorological phenomena. On the other hand, typhoon is disaster that cause great damage to Japan every year. If it can be predicted, the damage can be reduced. For that reason, this study’ s goal is to show that solar activity has effect on the number and power of typhoons.

Method

Sunspot number was used to see the solar activity. Sunspot number is index that shows how active the sun with sunspots that appear on it. Assuming that the relative number of sunspots is R, the observation method, observation device, and the coefficient for correcting individual differences between observers is k, the number of sunspot groups is g, and the total number of sunspots is s, it is defined this.

R=k10g+s (1)

The definition of typhoon is tropical cyclone with maximum wind speed of over 34 knots in western pacific. On this report it means that in the global. ACE (Accumulated Cyclone Energy) is index shows lifespan and power of tropical cyclone. In order to see the transition over a long period of time, the relative number of black spots, the number of typhoons, and the ACE from 1951 to 2020 are summarized with using the data published on the Internet.

Conclusion

Figure 1 shows the relationship between the sunspot number and the number of typhoons in the western pacific from 1951 to 2020, and Figure 2 shows the two-year time lag correlation since 1990. From these figures, it can be seen that the number of typhoons has changed two years later than sunspot number since 1990. The correlation coefficient was 0.47 at this time. Figure 3 shows the relationship between the sunspot number and the number of typhoons in the globe from 1951 to 2020, but the two-year time lag correlation seen in the western pacific was not found. Also relationship between sunspot number and ACE was not found. From these, It cannot be concluded that solar activity directly affects the typhoon, but at least it seems to be related. The two-year time lag correlation seen since 1990 was very weak, but clearly stronger than the others. However, it is limited in western pacific. Possible causes are factors that affect typhoons other than solar activity. For example, the El Nino phenomenon is known to be related to ACE. By examining the differences between the western pacific since 1990 that has two-year time lag correlation and other regions and times, we can investigate the effects of the sun in detail. The problem for the future is to consider other factors as well. Therefore, we will first investigate the meteorological difference between the time when there is a time lag correlation and the time when there is not it.

Acknowledgments

I would like to thank Ms. Sato for giving us appropriate advice from the beginning to the end and for her polite guidance.

©2021. Japan Geoscience Union. All Right Reserved.

References
National Astronomical Observatory of Japan https://www.nao.ac.jp/

Japan Meteorological Agency https://www.jma.go.jp/jma/index.html

Sunspot Index and Long-term Solar Observations www.sidc.be/silso/

International Best Track Archive for Climate Stewardship https://www.ncdc.noaa.gov/ibtracs/

National Hurricane Center
https://www.ncdc.noaa.gov/ibtracs/

Hiroko Miyahara 2009-12 Solar activity, cosmic rays, and climate change

Keywords: typhoon, sun, sunspot

図1　黒点相対数と西太平洋の台風数

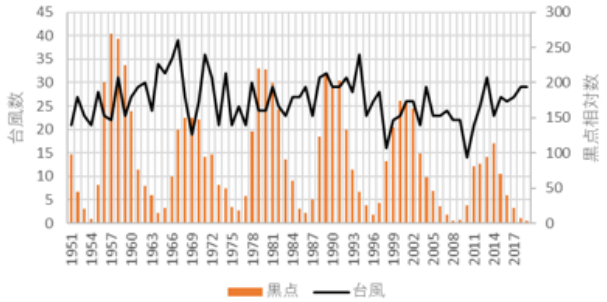


図2　黒点相対数と1990年以降のタイムラグ相関

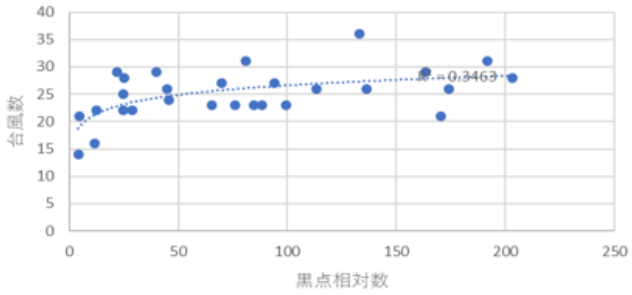
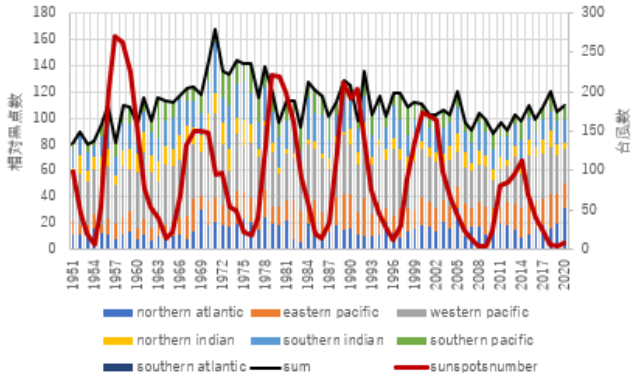


図3　全球の台風数と相対黒点数



©2021. Japan Geoscience Union. All Right Reserved.

On the study of Fukui Earthquake Fault IX

*Kazuho Kuwajima[1], *Ryouhei Matta[1], *Youhei Morise[1], *Ayano Yashima[1]

1. Fujishima High School of Fukui prefecture

The purpose of our research is identifying the main shock fault surface, which caused the M5.0 event on september 4 in 2020. The important point to understand this research is that there are a lot of reverse faults in
Japan. In addition, a character of the land-form by the fault is a straight structure. According to previous studies,a varied fault expected in the west side of Fukui plain. In this study we thought that the main shock might occured on the expected faults. We desided hypocenter of event by the Win-system. Win-system is a software to identify the hypocenters. With this system, we detected 44 hypocenters of the main shocks and aftershocks. We found that the decided epicenters concentrated on the west side of Fukui plain.Hypocenters of the first 13 aftershocks that occurred just after the main shock distributed like a plane. Therefore, these aftershocks occurred on the fault plane which had caused the main shock. We define this plane as a main shock fault surface. On the other hand, the other aftershocks were scattered outside from the main shock fault surface. We define these as extended type aftershocks.From the initial 13 aftershocks distribution,it was found that the main shock surface runs from West-southwest to East-northeast and incline North-northwest. After 30 aftershock epicenters show the distribution from east to west more widely than aftershocks of mainshock fault surface.

Keywords: Fukui Earthquake, fault, intensity of lower 5

©2021. Japan Geoscience Union. All Right Reserved.

Approach to the current situation and issues of geothermal power generation utilization based on field surveys

*Kisho Kurosawa[1], *Tatsuki Miyamoto[1], *Nozomi Kawaharata[1], *Shoki Yashima[1], *Yusuke Oba[1]

1. FurukawaReimei High School

Our electricity energy consumption is steadily increasing. Currently, most of the energy continues to depend on thermal power generation, but the fact that most fossil fuels depend on imports and the emission of large amounts of greenhouse gases such as CO2 have been regarded as problems. While investigating and learning about the "effective utilization of geothermal resources," which is a characteristic of the region, geothermal power generation has major advantages such as low power generation costs and low environmental impact, while resources in Japan. I learned the fact that the penetration rate is low for the amount. Regarding geothermal power generation, which is an energy resource peculiar to the region, we will clarify the current situation and issues regarding geothermal energy and its utilization based on site tours and references, and the ideal scientific approach to the utilization of geothermal energy. Practical training and surveys were conducted with the aim of finding out. Based on the results, I worked on this research to approach scientifically.

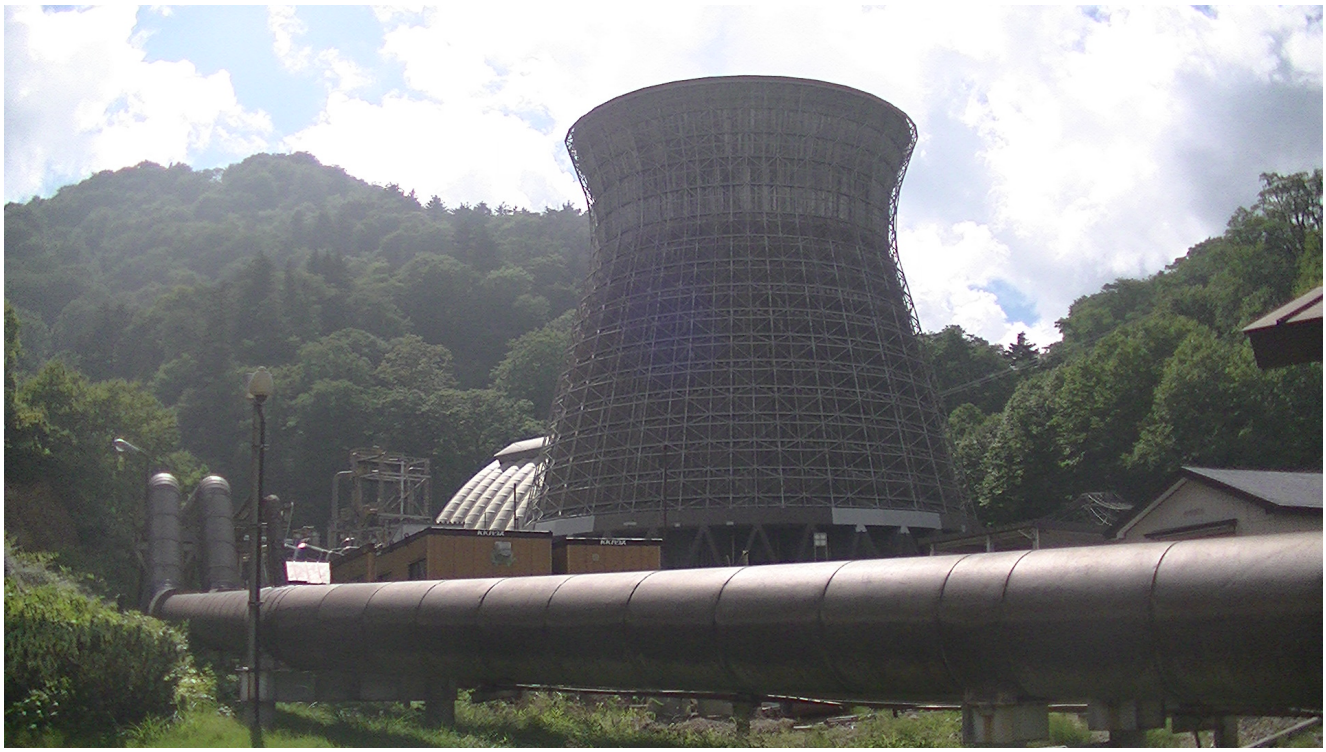
On August 23, 2020, we visited two contrasting and distinctive power plants in the neighboring Iwate prefecture. Japan's first commercial power plant, Matsukawa Geothermal Power Plant, and Matsuo Hachimantai Geothermal Power Plant, a new style run by the private sector, which started full-scale operation in 2019. After completing the on-site training, we thought that each power plant was almost unmanned and the labor cost for operation was overwhelmingly lower than that of thermal power and nuclear power. For that reason, I felt that geothermal power generation, which has a large amount of power generation, does not impose a burden on the environment, and has a low power generation cost itself, is a power generation method that matches the coming era. Despite this, the introduction of geothermal power plants seems to be stagnant, as the Matsuo Hachimantai geothermal power plant went into full-scale operation in Japan for the first time in 22 years. Considering the reason, I was interested in the balance between the size of the construction cost and the sales revenue for it, such as the excavation of additional production wells seen at the Matsukawa Geothermal Power Plant, and the cost of geothermal power generation using the Matsukawa Geothermal Power Plant as an example. I made a trial calculation.

It cannot be said that the construction of geothermal power plants in Japan is saturated. It is mainly concentrated in Hokkaido, Tohoku, and Kyushu, and it is essential that there is a stable hydrothermal system underground, which is thought to be due to the limited location, but it is also necessary to consider other reasons.

A hot spring binary power generation is being carried out at a hot spring inn in Naruko, Osaki City, and we are considering a future site visit. In addition, we are making a geothermal power generation model to solve the problems that became clear from this survey. The geothermal power generation model uses corrugated cardboard to create the image of a volcano, and a pressure cooker is installed inside to reproduce the production well. A turbine is attached to the outside to reproduce the power plant. Using this, I would like to conduct experiments on the current power generation efficiency due to the shape of the turbine and the loss of thermal energy associated with power generation. It also aims to disseminate energy education to local junior high school students using these models.

©2021. Japan Geoscience Union. All Right Reserved.

Keywords: Geothermal power generation, energy



©2021. Japan Geoscience Union. All Right Reserved.

Study of mechanism of Light Emission by Spectroscopic Observation of Meteor

*Yui Sato[1], *Yuki Kato[1]

1. Miyagi Prefectual Furukawa Reimei Senior High School

1. Purposes
The purpose of this study is to infer the type of elements related to the emission from the spacing of emission lines on the spectroscopic image of meteors, and to clarify the relationship between the altitude and the intensity of the emission lines by observing a meteor simultaneously at multiple points.

2. Hypothesis
・By determining the type and percentage of elements that make up the meteor material from the type and intensity of emission lines, we can clarify the characteristics and tendencies of each meteor shower
・Since the parent bodies of meteor showers are different, the elements detected by observation tend to be different in each meteor shower
・The relationship between the intensity of emission lines and the altitude of the meteor's emission can be derived by simultaneous observations at multiple points, and the mechanism and conditions of meteor emission can be clarified

3. Method
The process of identifying the elements is in the following order.
(1)Take a picture of a meteor with an SLR camera equipped with a diffraction grating and determine the scale of the diffraction grating and the number of pix to each emission line.
(2) Identify the wavelength of each emission line and determine the element from which the emission originates by referring to the literature.

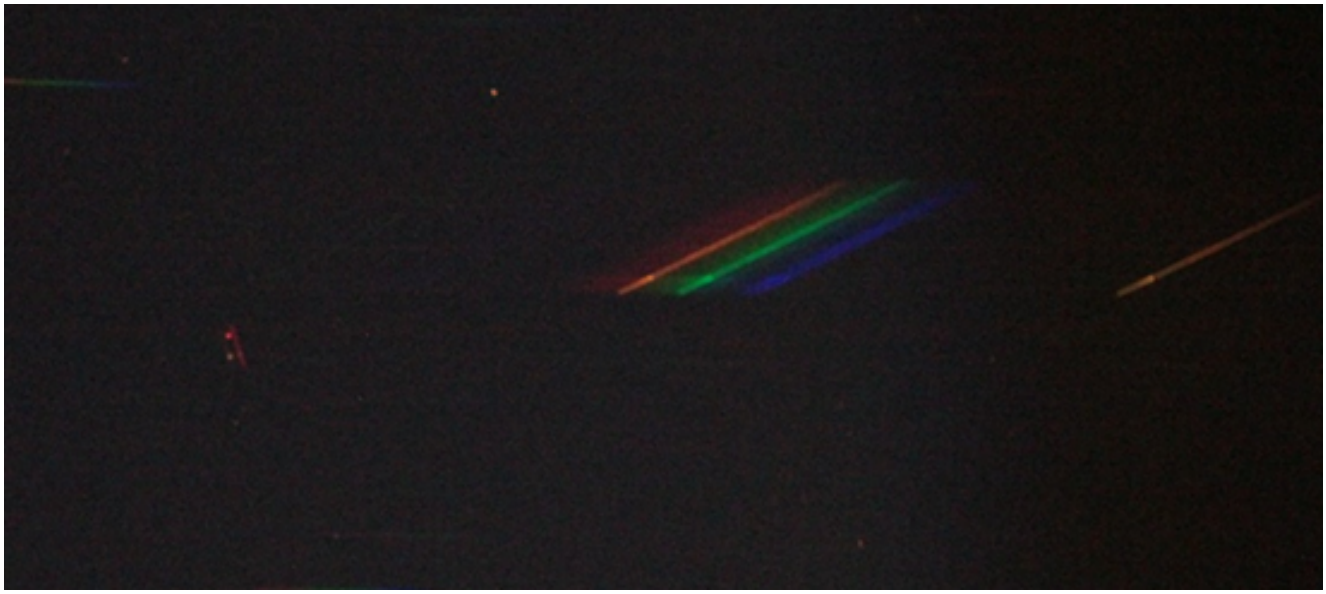
4. Results・Consideration
From the start of the study in 2014 until now, about 570,000 images have been taken and 58 spectral images have been obtained.
One spectroscopic image was obtained for the 2020 Orion meteor shower. Although we estimated three elements from the image, Mg, Na, and Fe, they showed an error of about 10 nm in the measured values. In addition, the emission line estimated to be Fe (529 nm) appeared to be emitted at a slightly earlier than the other two emission lines, suggesting that it may be an oxygen forbidden line (558 nm). These errors may have been caused by incomplete focusing, which obscured the image.
In order to improve the accuracy, we will reconsider the observation method, such as focus adjustment before starting observation and measures against condensation on the lens, especially in winter. Thus, the incident angle of the meteor was tilted to the diffraction grating, which may be the reason for the large error. Therefore, it is necessary to keep the angle of the diffraction grating perpendicular to the radiant point of the meteor shower by rotating the camera by 15 degrees every hour to improve the spectral accuracy.

5. Prospects
We would like to clarify the tendencies of elements in each meteor shower by continuous observation, because there are few meteor showers observed in the same year. We will continue to estimate the altitude and pursue the relationship between the oxygen forbidden line emission and the altitude,

©2021. Japan Geoscience Union. All Right Reserved.

because it is difficult to collect the data by simultaneous observation at multiple points at the same time.

Keywords: Meteors, Diffraction grating, Spectroscopic observation



©2021. Japan Geoscience Union. All Right Reserved.

Relationship between mineral crystallization and impurities.

*Usami Kenta[1], *Ryo Nakane[1], *Hiroyuki Sueno[1], Syotaro Kawana[1], Ryota Naito[1], Kazuhiko Hoshi[1], Mitsuhide Sai[1], Takuma Watanabe[1]

1. Johoku high school

Crystals produced by crystallizing from hot water or magma come in various sizes, lengths, and thicknesses. As a factor that changes these, the presence of impurities that are not related to the components of the product can be considered. However, it is not known how impurities affect the crystallized minerals. In this study, $NH_4H_2PO_4$ is crystallized with NaCl as an impurity.

Keywords: mineral , impurities, crystal



©2021. Japan Geoscience Union. All Right Reserved.

Analysis of water quality of irrigation ponds focused on land use, irrigation systems and periodic pond draining

*Ayane INOUE[1], *Haruto TAKEYAMA[1], *Kousuke MANO[1], *Rio YAMANO[1]

1. Hyogo Prefectural Kakogawa Higashi High School

Recently, irrigation ponds have had poor water quality. Therefore, we focused on land use around the ponds and “Ikeboshi” or regularly draining pond water, and researched the water quality of ponds in the Higashi Harima region. We measured COD, NH4-N, NO2-N, and PO4-P in August and December. It was found that fertilizing rice fields plays a large factor in increasing nitrogen concentration. Nitrogen and phosphorus levels in the ponds in residential areas weren’ t high because runoff of household effluents has decreased due to improvements in running drainpipes. Also, Ikeboshi may restrain the increase in concentration of nitrogen and phosphorus.

Keywords: irrigational ponds, analysis of water quality, land use , irrigation systems, periodic pond draining

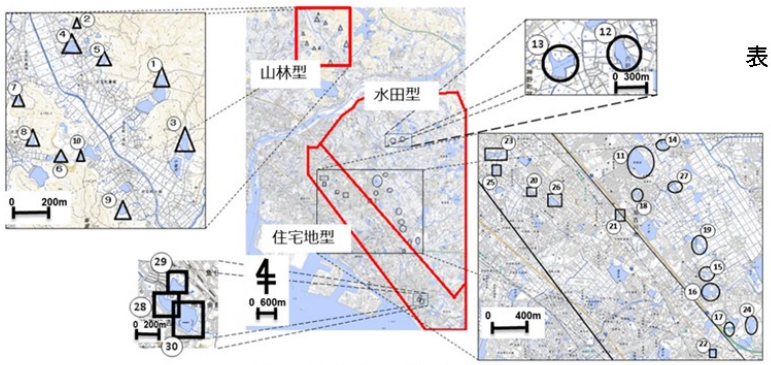


図1 対象ため池の分布

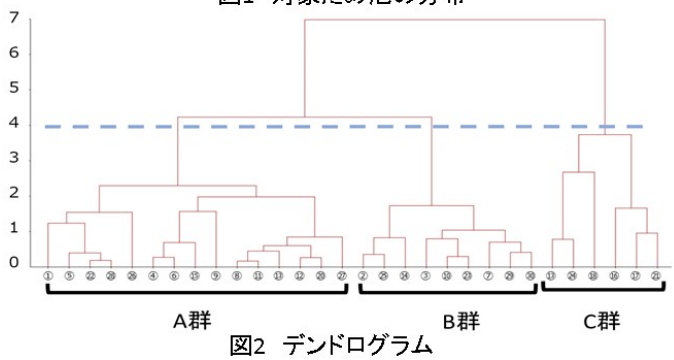


図2 デンドログラム

表1 クラスターごとの平均濃度 （単位はmg/l）

	リン酸態リン	COD	亜硝酸態窒素	アンモニウム態窒素
A	0.054	23	0.052	0.51
B	0.047	43	0.029	0.25
C	0.44	23	0.13	1.8

表2 クラスターごとのため池の内訳

A群	池干し有	池干し無
山林型	3	3
水田型	2	3
住宅地型	4	0

B	池干し有	池干し無
山林型	2	2
水田型	0	1
住宅地型	4	0

C群	池干し有	池干し無
山林型	0	0
水田型	1	4
住宅地型	0	1

©2021. Japan Geoscience Union. All Right Reserved.

The Process of Raised-Bed River Formation and Factors that Affect It

*Natsuki KAMISASA[1], *Yuta KONDO[1], *Haruto TAKEYAMA[1], *Yasuharu TOMITA[1], *Rikushi NAGAO[1], *Naka NOHAMA[1]

1. Hyogo Prefectural Kakogawa Higashi High School

In this study, features of raised-bed rivers in Japan were measured using GSI Maps and some other kinds of maps in order to clarify ‘in what kinds of areas’ and ‘how’ raised-bed rivers are formed. As a result, two things were found; 1.The bed of a raised-bed river rises as sediment accumulates near the point at which the slope greatly changes so that the slope becomes more gentle, and that point moves downstream as the riverbed rises over time. 2.Some raised-bed rivers are wide in the upstream alluvial fan sections and get narrower in the downstream floodplain sections. It became clear that the formation of raised-bed rivers is related not only to human influence but also to landforms.

Keywords: raised-bed river, alluvial fan, cross-sectional view, longitudinal view, overhead view

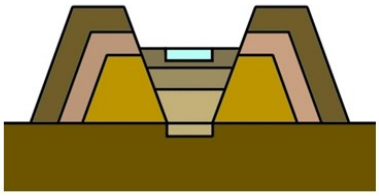


図1

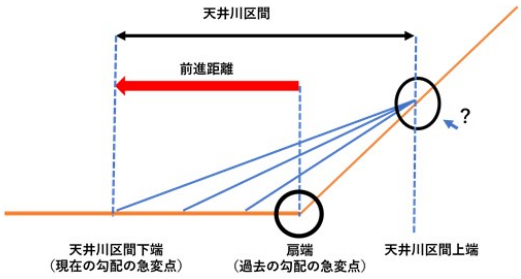


図2

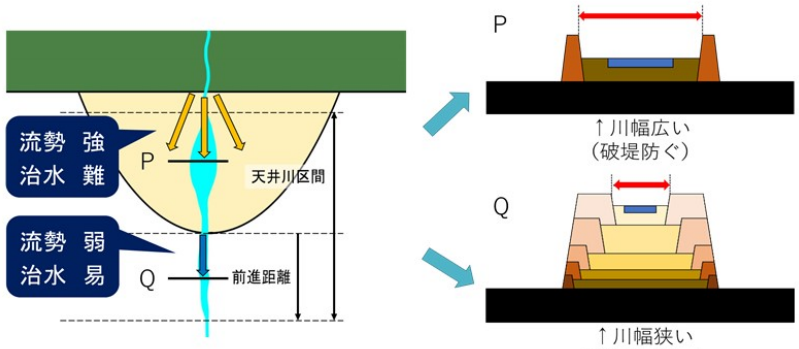


図3

©2021. Japan Geoscience Union. All Right Reserved.

Studies of the SDGs on the Sanriku Geopark. The sea urchin spread trench in the Taneichi Formation.

*Kyougo Sakashita[1], *Asahi Sekibata[1], *Rina Nakajo[1], *Yuto Kugoi[1], *Hikaru Sasaki[1]

1. Marient Chikyu-tanken club senier

The Sanriku Geopark covers the area from Aomori Prefecture through the coast of Iwate Prefecture and down to Miyagi Prefecture. Hachinohe City Marine Science Museum is located on the northern edge of that and to that belongs to the Mariento Chikyu Tanken club. We learned about Sanriku Geopark from 2019. And we announced this activity at the jpGU2019 and the Japanese Geoparks Network Meeting at Ohoita and jpGU2020.

SDO (Sustainable Development Objectives), a set of targets adopted by the United Nations in September 2015. Now, we must strive to achieve SDGs with society as a whole for the future of humanity. Geopark activity is very compatible with the SDGs. We felt that Sanriku Geoparks efforts toward SDGs were few. And so we examined the relationship between each geosite and the SDGs with GEO-KAMISHIBAI. GEO-KAMISHIBAI helps us understand the history of the land and people's lives.

The Geosite of Taneichi seaside park contains the sea urchin spread trench. The sea urchins grown in the trenches of the Hirono town are the best in Honshu in terms of quality and production.

We investigated the reason and found the following: Nanbu-Moguri is diving to a depth of 20 meters, taking the sea urchin and moving it to the trenches. Fresh seawater is constantly circulating in the trenches that that extend off the coast. The trenches are full of tides, so it is rich in seaweed. Working in shallow grooves is safer than diving off the coast.

The secret to the success was the co-operation between Nanbu-Moguri, the Taneichi Formation, and its trenches.

We made 3GEO-KAMISHIBAI. The titles are as follows: What does a sea urchin eating? The secret of the algae growing in the trench. The Taneichi Formation and sea urchin spread trench.

These are all related to 3Goal of SDGs; Goal 2: Zero hunger. Goal 12: Responsible consumption and production. Goal 14: Life below water.
Unfortunately, we can't exhibit GEO-KAMISHIBAI because of an Corona-Virus (COVID-19) problem. We understood the relationship between sea urchin, geocite and SDGs in Hirono town by conducting a survey and the making of GEO-KAMISHIBAI. We would like to publicize what we have learned using GEO-KAMISHIBAI.

Keywords: Sanriku、Geopark, Geosites, Taneichi Formation, Regional activity, Club activities

©2021. Japan Geoscience Union. All Right Reserved.



図１　種市層ウニ増殖溝の位置



図２　ジオ紙芝居　種市層ウニ増殖溝

©2021. Japan Geoscience Union. All Right Reserved.

Studies of the SDGs on the Sanriku Geopark. The Aoba Lake and Shimamori Basin.

*Mizuki Kimura[1], * Naho Simodate[1], *Kahono Hinata[1], *Yuma Keicho[1], *Kouki Takahashi[1]

1. Marient Chikyu-tanken club senier

The Sanriku Geopark covers the area from Aomori Prefecture through the coast of Iwate Prefecture and down to Miyagi Prefecture. Hachinohe City Marine Science Museum is located on the northern edge of that and to that belongs to the Mariento Chikyu Tanken club. We learned about Sanriku Geopark from 2019. And we announced this activity at the jpGU2019 and the Japanese Geoparks Network Meeting at Ohoita and jpGU2020.

The Aoba Lake and Shimamori Basin are located south of Hachinohe City (Figuer1). These were newly registered on the Sanriku Geopark in 2020. The history of geology and water control can be seen at the Aoba Lake and Shimamori Basin has beautiful countryside and history of agricultural cultivation.

SDO (Sustainable Development Objectives), a set of targets adopted by the United Nations in September 2015. Now, we must strive to achieve SDGs with society as a whole for the future of humanity. Geopark activity is very compatible with the SDGs. We felt that Sanriku Geoparks efforts toward SDGs were few. And so we examined the relationship between each geosite and the SDGs with GEO-KAMISHIBAI. GEO-KAMISHIBAI helps us understand the history of the land and people's lives.

We made 3GEO-KAMISHIBAI. The titles are as follows: Rice from Yomari-Dam? Meander in Niidagawa. Water springs of Shimamori Basin (Pictur1). The relationship between each title and SDGs is shown below.

Rice from Yomasari-Dam ? : Goal 6: Clean water and sanitation. Goal 2: Zero hunger.

Meander in Niidagawa : Goal 6: Clean water and sanitation. Goal 15: Life on land.

Water springs of Shimamori Basin: Goal 6: Clean water and sanitation. Goal 11: Sustainable cities and communities.
Unfortunately, we can't exhibit GEO-KAMISHIBAI because of a Corona-Virus (COVID-19) problem. We understood the relationship between people's lives and their history, geocite and SDGs in here by conducting a survey and the making of GEO-KAMISHIBAI. We would like to publicize what we have learned using GEO-KAMISHIBAI.

Keywords: Geosites, Shimamori Basin, Aoba Lake, Yomasari-Dam, Regional activity, Club activities

©2021. Japan Geoscience Union. All Right Reserved.



図１ 島守盆地と青葉湖の位置



写真１ ジオ紙芝居 島守湧水群

©2021. Japan Geoscience Union. All Right Reserved.

Proposal of Hachinohe Canyon to Sanriku Geopark Geosite.

*Sarina Shinohe[1], * Miyu Abe[1], * Akari Nakamura[1], *Yukihito Yasuhara[1], *Kensuke Shimomura[1]

1. Marient Chikyu-tanken club senier

The Sanriku Geopark covers the area from Aomori Prefecture through the coast of Iwate Prefecture and down to Miyagi Prefecture. Hachinohe City Marine Science Museum is located on the northern edge of that and to that belongs to the Mariento Chikyu Tanken club. We learned about Sanriku Geopark from 2019. And we announced this activity at the jpGU2019 and the Japanese Geoparks Network Meeting at Ohoita and jpGU2020.

Hachinohe Canyon is an open-pit limestone mine. (Fig.1) Its official name is The Hachinohe Limestone Mine. The quarry is 1,000 meters from east to west and 1800 meters from north to south. The mine’s lowest point is currently 170 meters below sea level. It is said to be the furthest place from the sky in Japan. They are shown in Figures 1 and Picture 1. This mine contributed to a Hachinohe city's becoming an industrial city. And its wonderful view is also a tourist attraction. But this isn't authorized by Geosite category in Sanriku Geopark.

SDO (Sustainable Development Objectives), a set of targets adopted by the United Nations in September 2015. Now, we must strive to achieve SDGs with society as a whole for the future of humanity. Geopark activity is very compatible with the SDGs. We felt that Sanriku Geoparks efforts toward SDGs were few. And so we examined the relationship between each geosite and the SDGs with GEO-KAMISHIBAI. GEO-KAMISHIBAI helps us understand the history of the land and people's lives.

We made 3GEO-KAMISHIBAI. The titles are as follows: Where did the Megalodon come from? Long belt conveyer. How to use the huge hole?

These are all related to Goal of SDGs; Goal 12: Responsible consumption and production. Goal 11: Sustainable cities and communities. Goal 13: Climate action.

In particular, there was a lively discussion of the title of How to use the huge hole?. There were many opinions, including tourist attractions, theme parks, garbage disposal facilities and disaster prevention facilities. We chose the idea of building a huge facility that combines those opinions.

Unfortunately, we can't exhibit GEO-KAMISHIBAI because of a Corona-Virus (COVID-19) problem. We understood the relationship between people's lives and their history, geocite and SDGs in Hachinohe Canyon by conducting a survey and the making of GEO-KAMISHIBAI.
It is strongly recommended that the Hachinohe Canyon be a geo-site for Sanriku Geopark. And we would like to publicize what we have learned using GEO-KAMISHIBAI.

Keywords: Sanriku Geopark, Geosites, Limestone, Megalodon, Regional activity, Club activities

©2021. Japan Geoscience Union. All Right Reserved.

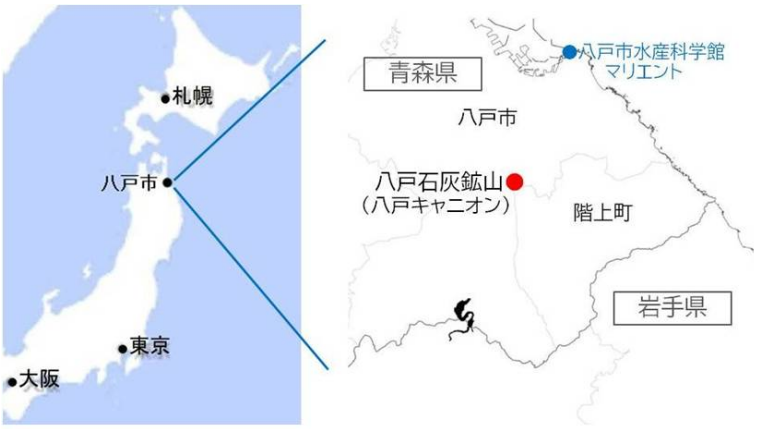


図１　八戸石灰鉱山の位置

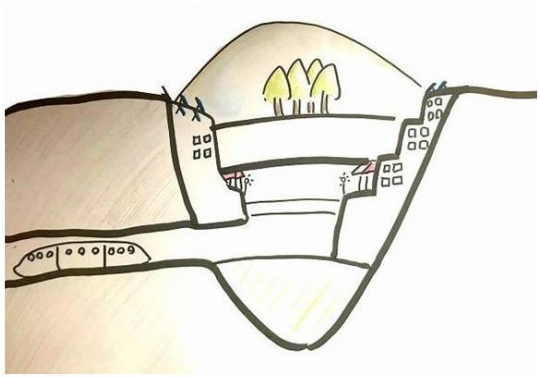


図２　八戸キャニオンの再利用案

©2021. Japan Geoscience Union. All Right Reserved.

Proposal of an index for estimating the distance from the source rock

*Ayaka Mitsui[1], *Reiji Iwamoto[1], *Keishi Okumi[1], *Mayu Naito[1], *Yamato Yasuhara[1], *Natsuki Yamamoto[1], *Naoko Kodama[1], *Akito Sasaki[1], *Akira Tada[1], *Takuto Nakanou[1], *Tomohiko Maeda[1], *Yuya Muromoto[1], *Ryusei Moriyama[1]

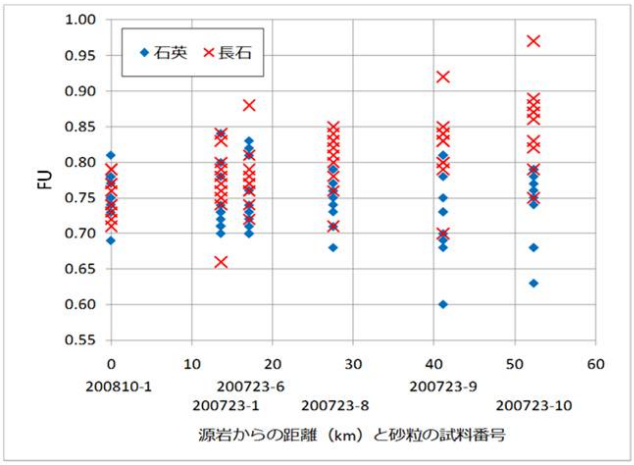
1. Hyogo Prefectural Himejihigashi Senior High School

The volume ratio of quartz / feldspar was calculated from the quartz and feldspar of the Ibo River flowing in the southwestern part of Hyogo prefecture.

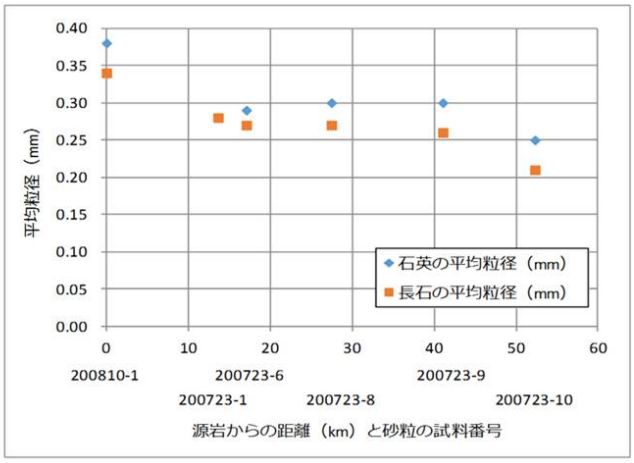
In the Ibo River basin, the average grain sizes of quartz and feldspar are almost the same. The FU value of quartz does not change much, but the FU value of feldspar increases downstream because feldspar melts very quickly. The volume ratio y of quartz / feldspar to the distance x from the source rock is indicated by an approximate straight line of y = 0.024x + 0.58. These show that the distance from the source rock can be estimated mathematically. Everyone intuitively knows that the particles are rounder and the quartz / feldspar is larger toward the downstream, but this study showed that it can be expressed by an equation for the first time.

Keywords: Ibo River , FU value, volume ratio of quartz / feldspar, source rock

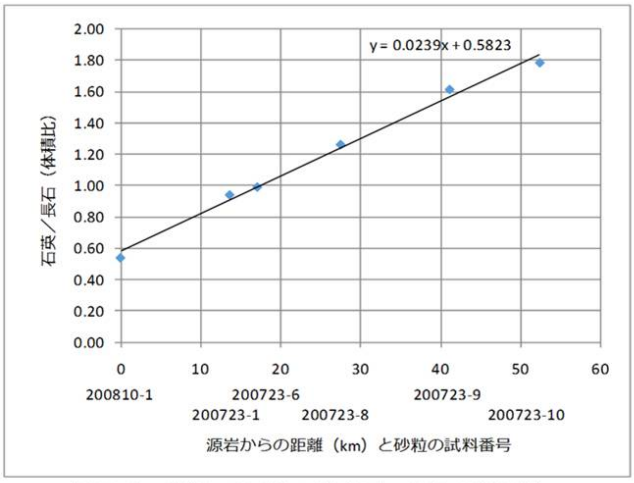
©2021. Japan Geoscience Union. All Right Reserved.



源岩からの距離と石英と長石のFU（各試料10粒ずつ）



源岩からの距離と砂粒の粒径



源岩からの距離と石英／長石（体積比）（直線は近似直線）

©2021. Japan Geoscience Union. All Right Reserved.

Energy calibration of a cosmic-ray detector

*Moe Kimura[1]

1. Tokyo Metropolitan Hibiya High School

CosmicWatch, a cosmic ray detector used in our research group, converts cosmic ray-derived fluorescence in a plastic scintillator into electrical signals using a semiconductor detector.

Cosmic rays are high-energy radiation from space, and CosmicWatch mainly detects muons.

CosmicWatch detects mainly muons. However, the correspondence between the signal value obtained by CosmicWatch and the energy value has not been investigated.

Therefore, we used Co60 and Cs137 radiation sources to investigate the correspondence between the signal values of the obtained peaks and the energy values.

The energy of the γ-rays emitted by the decay of radiation sources Co60 and Cs137 are known and are 318 keV and 662 keV, respectively.

Usually, plastic scintillators are used, but in this study, we also investigated using CsI scintillators, which are more specialized for detecting γ-rays.

CsI scintillators were chosen because they have higher energy sensitivity than plastic scintillators and are relatively inexpensive and easy to handle among inorganic scintillators.

In addition, the CsI scintillator had a larger fluorescence than the plastic scintillator, and the obtained signal value exceeded the upper limit of the analog-to-digital conversion in the circuit.

Therefore, we intentionally attenuated the signal value by delaying the acquisition time of the signal value while measuring.

This method was used to calibrate the energy of CosmicWatch.

In addition to the above, we measured and compared the frequency of radiation exposure when the detector was placed directly on the ground and when it was indoors, and considered the radiation exposure of the ground near our house.

Keywords: Radiation, CsI scintilator, Cosmic rays

©2021. Japan Geoscience Union. All Right Reserved.

Floating waterdrops using a straw commutator

*Aoba Takahara[1], Yuri Yasui[1], Takaya Sato[1]

1. Niigata Prefectural Takada high school

At the previous research,the experiment of floating a seed of Acer Rubrum was done. We thought of floating waterdrops in the same way.We replaced a sirocco fan with a blower in order to increase the wind speed,and we did the experiment. After controlling the wind speed by changing the length of straws,we found that the wind speed which could float waterdrops was about from 6.5m/s to 8.2m/s. However the wind speed distribution was far from our expectation because we made a lot of error. From now on, we need to devise the wind speed and the distribution so that we can float waterdrops for a long time.

Keywords: Meteorology

©2021. Japan Geoscience Union. All Right Reserved.

The rotating-Water-tank that is replaced hot water tank and ice water tank

*Masamune Minou[1]

1. Niigata Prefectural Takada high School

The rotating-water-tank experiment is the one to cause the meandered flow of water that is similar to westerlies by rotating tanks and difference of temperature. But in an intricate movement of a fluid, it is difficult to know phenomena that was caused by a specific factor. I studied effects that are caused by the difference of temperature through observation of the whole difference and thew common point between two kinds of rotating-water-tanks. As a result, I knew that difference of temperature affects the shape of waveform and the direction of the level flow and causes the rise and the fall of water. In the future, I want to give thorough cosideration by using substantial figure.

©2021. Japan Geoscience Union. All Right Reserved.

Comparison of the surface of Mars with the previous one in the approach of Mars Spread of dust storm on November 17th

*Sayaka Mizutani[1], *Takumi Uchiyama[1], Riho Kagami[1], Aoi Takemoto[1]

1. Ichinomiya High School

Observations of Mars were carried out from June 26 in conjunction with the 2020 Mars semi-major approach, and with the information that a dust storm had occurred since November 11, a comparison was made between the global dust storm that occurred during the 2018 major approach and the 2020 dust storm. For the comparison, we devised an image processing method and used the difference of the development maps.
The equipment used was a CMOS camera (made by ZWO),3x Barlow lens, 20cm Schmidt-Cassegrain telescope, ADC (Atmospheric Dispersion Compensation System) and IRVB filter.

Keywords: Mars, dust storm

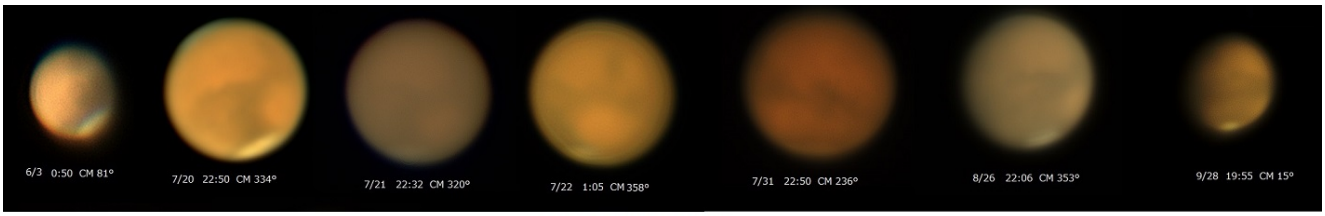


図1　2018年大接近観測画像

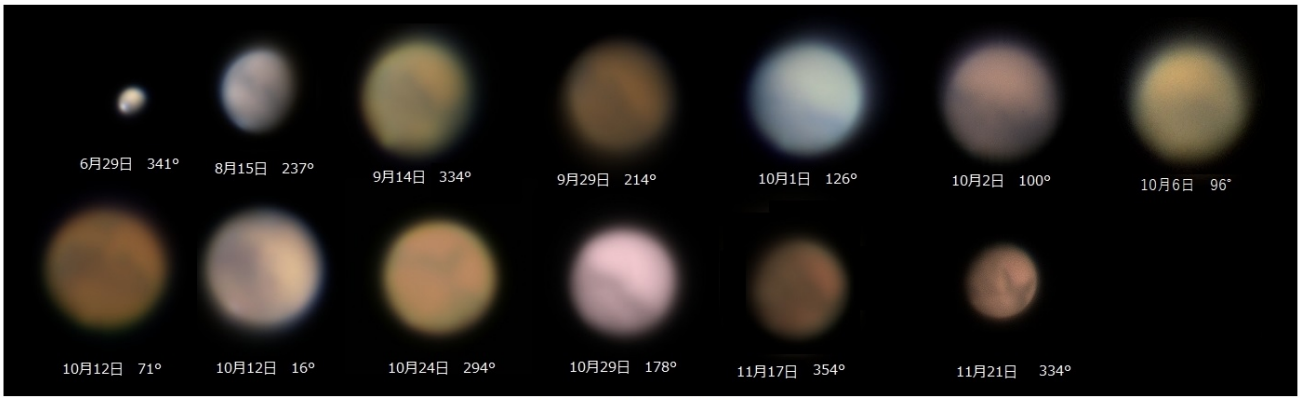


図2　2020年準大接近観測画像

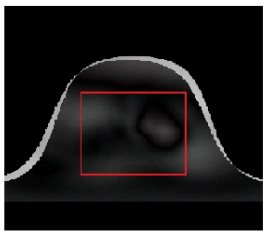


図3　10.12と11.17の展開図の差の絶対値

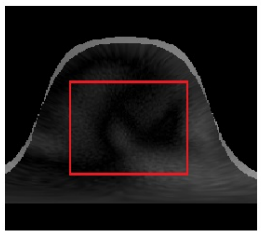


図4　9.14と11.21の展開図の差の絶対値

©2021. Japan Geoscience Union. All Right Reserved.

Tumulus inspection project by using cosmic-ray muon

*Tomoyo Ishizawa[1], *Satoshi Ono[1], *Asahi Shiozaki[1], *Wakana Yanagimoto[1], *Kenshiro Aoki[1], *Yuna Ishii[1], *Sogo Kimura[1], *Yuki Shimada[1], *Aoi Soga[1], *Yuga Takemori[1], *Rino Tomiku[1], *Kana Hashizume[1], Miki Ohtsuka[1]

1. Waseda University Honjo Senior High School

Higashiyatsu tumulus is a round barrow that has a horizontal stone chamber,which is located in our school. We are interested in the tumulus and want to know the details of the inside structure. Since it has great historical value, we decided to use a new method of imaging internal objects without destructing called muography. We have developed a new detector that detects cosmic-ray muons, and the prototype has been constructed. We first set it inside the school building and took data on the time when muons were thought to have passed through the detector.We evaluated the detector performance analyzing the data, and then measured the zenith angle distribution of cosmic-ray muons. In addition to those studies, we have proceeded the investigation of the tumulus itself by searching the historical records. We would like to improve the detector and install it in the tumulus to reconstruct the internal structure in three dimensions in the future.

Keywords: muography, integration of arts and sciences, cosmic ray, muon, archeology, interdisciplinary

©2021. Japan Geoscience Union. All Right Reserved.

Calculating the nebula density from the size of the emission nebula

*Yuki Shirai[1]

1. Totsuka High School

This study is a survey of the nebula density of the Emission Nebula-especially the M42 Orion Nebula, the M43, the M8 Lagoon Nebula, the M20 Trifid Nebula. I will compare and examine the nebula densities of the above four objects from the size of the emission nebula by analysis and calculation.
Visible light images were taken using a 400mm telephoto lens. The radius of the nebula was calculated by analyzing the visible light images using the graph function of Subaru image analysis software Makali`i. The density was calculated from the radius, temperature, and spectral type of the ionized star.
As one of the results, the density of the Orion Nebula , with the density obtained by calculation being 411cm^{-3}, compared to the density of 410cm^{-3}(nebula cluster series-emission nebula) obtained by observing the 21cm radio emission line. As described above, I got the result which has a very small error.

Keywords: emission nebula, density of emission nebula, evolution of HII region



©2021. Japan Geoscience Union. All Right Reserved.

Strength evaluation of structures by making and improving quake-vibration generators

*Runaya Igari[1], *Yuto Meguro[1], *Rin Goto[1], Kenshiro Kamata[1]

1. Miyagi Rifu high school

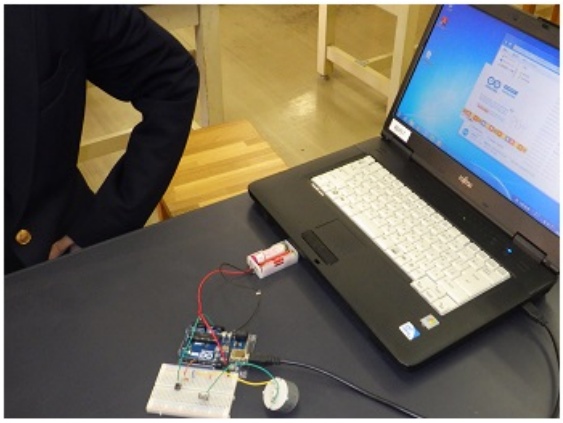
We made a simple seismic motion generator using empty cans and motors around us, and made a model of how the structures on the stratum due to the multi-layer structure are affected. In order to bring this vibration closer to the actual one, we are attempted reproduce it while electronically controlling it using Arduino. In order to construct layer, biscuits powder was used to reduce the weight and we conducted an experiment to observe how the structures such as houses would be affected and damaged in addition to the results of the earthquake by constructing the wooden framework on the stratum model.

In addition, we also observed how the shaking of earthquakes caused by heavy objects is involved by conducting experiments on the structures on the stratum with the weight of metal bodies such as iron, copper, and brass. Among them, we are trying to reproduce the shaking caused by the occurrence of a motor-controlled earthquake using Arduino programming.

There are still issues with the motor output and vibration frequency, but we plan to discuss how to make the quaking model closer to reality.

Keywords: Quaking model, Electric controlle, Geotechnical Engineering





©2021. Japan Geoscience Union. All Right Reserved.

Time dependence of ocean salinity

*Honami Hashimoto[1], Annu Ito[1]

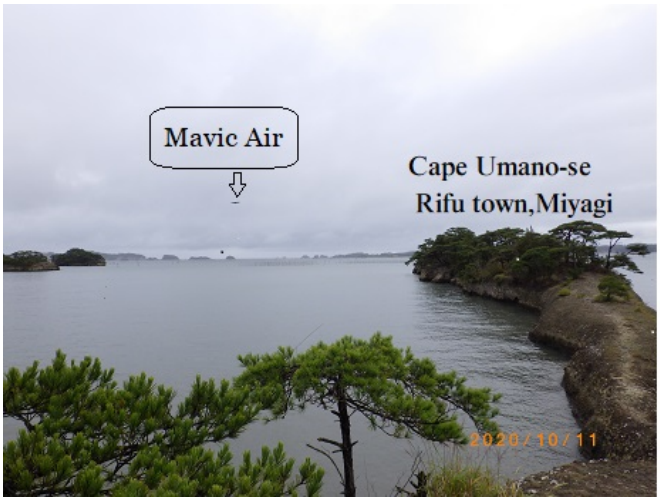
1. Miyagi Rifu highschool

Since 2018, the Natural Science club of Rifu High School has been conducting a monitoring activities on seasonal changes in the salt content of seawater in various shoe of Matsushima Bay. The survey are concentrated to the total salt content (%) and the amount of each cation of Na + / K + / Ca2 + (mg / L = ppm).

The seawater sampling locations are set in Shichigahama town Miyagi Prefecture, which is close to the outer ocean, Higashi-Shiogama at the bay front, cape Umanose in Matsushima Town, and Oshima in the back of the bay. We have found that the closer to the open sea, the larger the changes in cation content and saline content, while the closer to the inner bay, the more affected by land water and fine topography.
As a major tendency, the total saline components increases as expected in the summer when the amount of evaporation rate is higher. But according to the survey up to last year, when we observed each cation, only Na + cation increases in January in the winter.

This year, we will consider how small changes in topography and coastal distances bring about differences in seawater salt content, which taking into account the effects of topography and organisms based on the water sampling activity by highschool students drone operation up to about 200m.

Keywords: Ocean Saline components, Drone techniques, Year-term changing of ocean saline





©2021. Japan Geoscience Union. All Right Reserved.

Toward "Solid-State Version Chromatography" Second Report

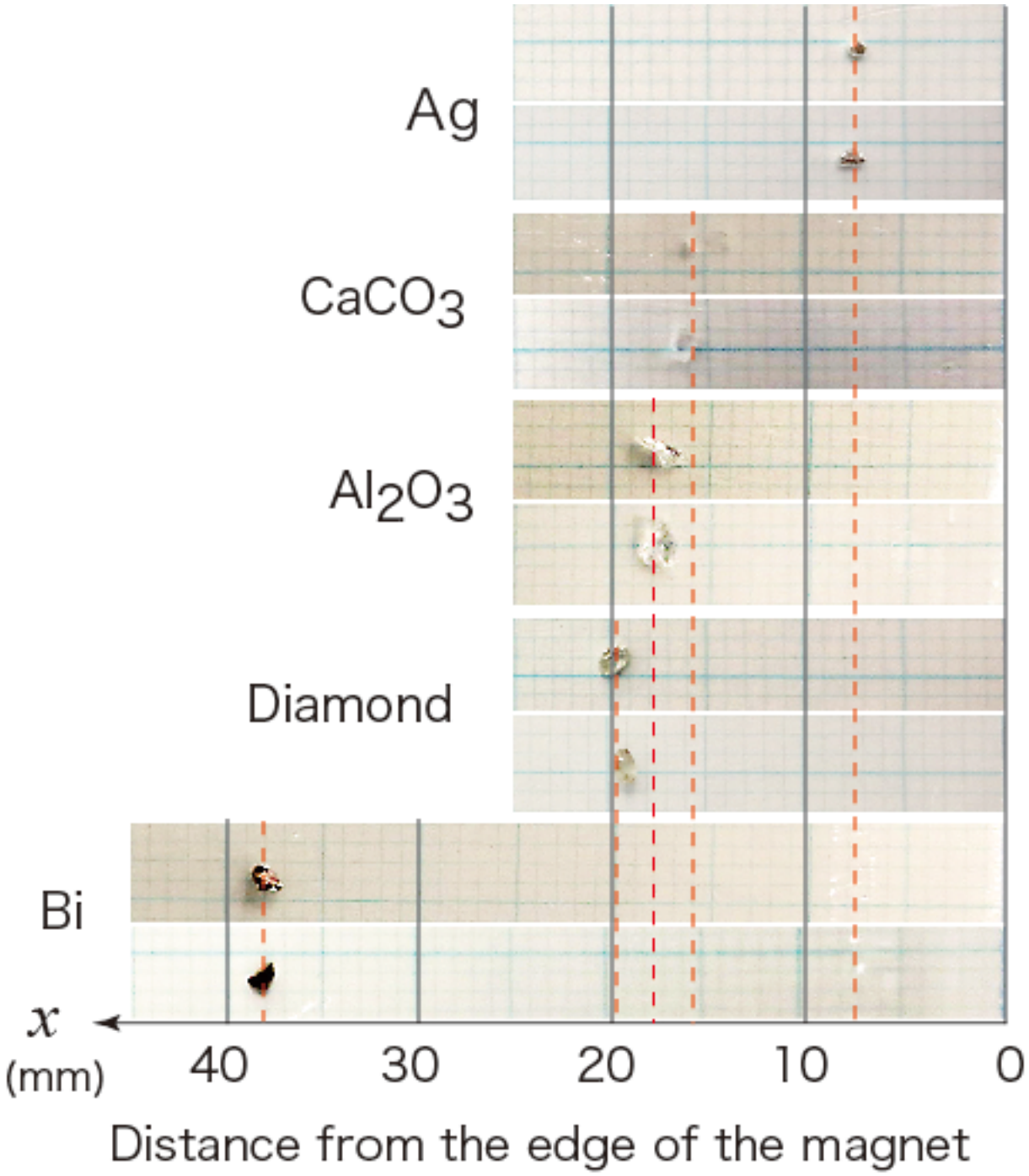
*Yuichiro Okuno[1], *Akihisa Wada[1], *Yudai Kozono[1], *Ryota Iwamoto[2], *Mai Fujitani[2], *Kyoya Okada[3], *Kusunori Sumi[3], *Arata Fujimoto[3]

1. Imamiya Technology Senior High School of Osaka Prefecture:The evening course, 2. Otemae Senior High School of Osaka Prefecture:The evening course, 3. Kasugaoka Senior High School of Osaka Prefecture:The evening course

Last year, we proposed the principle of separating and collecting a mixture of diamagnetic solid particles by material. In order to demonstrate this principle, we constructed an apparatus and conducted experiments. As a result, particles of six inorganic materials and six organic materials were collected on the collection plate as a group of particles that differed by material. We were able to verify the effectiveness of the apparatus based on this principle. This time, in order to further improve the separation accuracy of the apparus, we designed three types of magnetic circuits and conducted comparison experiments. As a result, we were able to separate corundum and calcite, which could not be separated by last year's apparatus. The resolution of the magnetic susceptibility was 0.4×10^{-7} emu/g. This technique has potential as a solid-state version of chromatography for separating solid mixtures by material.

Keywords: microgravity, magnetic separation, diamagnetic material, solid chromatography, translational motion

©2021. Japan Geoscience Union. All Right Reserved.



©2021. Japan Geoscience Union. All Right Reserved.

How to extract bioethanol effectively by distillation.

*Ataru Kunihisa[1]

1. Wakasa high school

In Japan, the number of Solidago altissima is increasing, and it is rampant.Therefore, we have been researching whether bioethanol can be used as a new energy resource by producing bioethanol from Solidago altissima.Mix crushed Solidago altissima and sulfuric acid and sterilize with autograve.Then, it was centrifuged, activated carbon was added, and the mixture was filtered, and then cultured for 3 days to try to produce ethanol.At present, ethanol has not been recovered yet.In the future, we will carry out experiments by changing the amount of sulfuric acid added. Ultimately, we would like to discover the possibility that Solidago altissima will become a new energy resource with the goal of efficiently extracting ethanol.

Keywords: Solidago altissima, bioethanol, a new energy resource

©2021. Japan Geoscience Union. All Right Reserved.

Confusion of the people in the northwestern area of Saitama Prefecture due to rumors after the 1923 Kanto Earthquake

*Miharu Shinoda[1]

1. Sakae Higashi High School

In the northwestern area of Saitama Prefecture, no damage was caused by the 1923 Kanto Earthquake. But a massacre of Koreans occurred due to false rumors in these areas. In this study, we surveyed stone monuments and other literature. In the Ohara grave of Yukokuji Temple located in Kumagaya City, Saitama Prefecture, there is a stone monument for the 1923 Kanto Earthquake. It says that a false rumor occurred and people were confused. According to Matsubara (2013), on September first after the main shock, the trains and telegraphs stopped between Tokyo and Urawa. On September third, an extra newspaper had false information about Koreans and it spread to many areas. The newspaper said that Koreans set on fire. As a result, about 150 Koreans were killed in Kumagaya and Honjo Cities in Saitama Prefecture. Later it was found that the rumor was false. Today still with the development of technology, life has become very convenient. But the false rumors are likely to occur. That is why, more than ever, we need to think about the credibility of the various information we get in our daily lives, and we should deal with emergencies calmly so that we will not be misled by false rumors.

Keywords: The 1923 kanto Earthquake, False rumor , The northwestern area of Saitama Prefecture

©2021. Japan Geoscience Union. All Right Reserved.



【「供養塔」の裏面に記されている碑文】　／は改行部分を示す

噫大正十二年九月一日午前十一時五十八分突如帝都ヲ中心トシテ勃發シタル大惨禍関東大震災ハ／瞬時ニシテ幾万ノ生霊ト幾百億ノ財貨トヲ奪ヒ去リシ振古未曽有ノ大惨害ナリキ當時我國ハ歐州／大戦ノ影響ヲ受ケ國内景気ハ非常ナル好調時代ニ在リ一般的ニ放縦ト贅澤ノ弊ヲ露呈シ吾世ノ春／ヲ謳歌シツヽアリシ時ナリシカハ恐怖モ一入大ニ狼狽又甚シカリシナリ一時全ク交通機関ハ素ヨ／リ通信機関ノ杜絶流言蜚語ノ百出其真相ヲ知ルニ由ナク或ハ此儘暗黒世界ヲ現出スルニアラサル／ナキヤヲ思ハシムルノ状態ナリキ此事實ヨリ災後ノ國民ハ俄然強キ反省ニ目覚メ此惨害ハ天ノ下／シ給ヘル戒ナリ天譴ナリトシテ異常ナル緊張ニ立戻リ専ラ復興ノ気魂ニ燃ヘ懸命ノ努力ヲ奮ヒ極／メテ迅速ニ其實ヲ擧クルヲ得タリシモ此災禍ノ為ニ犠牲トナリシ多クノ生霊ニ對シテハ誠ニ痛恨／哀惜ノ情ニ禁ヘサル所ナリ本市ニ於テ遭難セル生霊ハ熊谷寺及圓光寺ノ両墓地ニ埋葬シ季節ノ放養ヲ怠ラサリシモ将来其荒廢センコトヲ虞レ且ツ分葬シアルコトノ不便ヲ除カンカ爲メ今回ノ市内／有志胥謀リ両墓地ノ遺骨ヲ一ニシ茲ニ熊谷寺墓地内ニ地ヲ相シテ本供養塔ヲ建立シ以テ生霊ノ瞑／福ヲ祈ラントス　犠牲ノ霊不慮ノ遭難慰ムルニ由ナシト雖モ此尊キ犠牲カ同胞國民ノ自覺反省ヲ／促シ緊張堅實ナル風氣作興ニ寄興セル済世ノ供徳ハ盖シ大ナルモノアリト謂フヘク豈誰カ徒死ナ／リトセンヤ聊當時ノ概況ヲ録シテ誌トス／

昭和十三年七月　埼玉縣熊谷市長　勲六寺　新井良作書／坂群熊　水友勝　刻

図 1. 熊谷市熊谷寺の大原墓地に建つ供養塔(写真)とその裏面に記されている碑文

Fig.1 The photo of surface of the stone monument built in the Ohara Grave of Yukokuji Temple, Kumagaya City and inscription on the back.

表 1. 関東地震の発生から埼玉県北西部での事件が起こるまでの経緯

Table.1 Background to the incident in the northwestern area of Saitama Prefecture after occurrence of the Kanto Earthquake.

<table>
<tr><th></th><th>9月1日</th><th>9月2日</th><th>9月3日</th><th>9月4日</th><th>9月5日</th><th>9月6日</th><th>9月7日</th></tr>
<tr><td>地震と震災</td><td>本震発生（11時58分）
東京で大火災</td><td colspan="5">大小の余震の継続</td></tr>
<tr><td>東京から熊谷方面への交通機関</td><td>浦和以北の（現在の）高崎線が運転再開</td><td colspan="2"></td><td>東京と埼玉の都県境の荒川鉄橋が開通</td><td colspan="2"></td></tr>
<tr><td>東京方面から埼玉県北西部への避難</td><td colspan="3">浦和まで徒歩でたどり着いた避難民が熊谷方面へ列車で移動</td><td colspan="3">東京方面より鉄道を利用した避難が可能</td></tr>
<tr><td>新聞社の動向</td><td colspan="2">東京の新聞社は全て発行が不可能</td><td>東京の1社が流言を掲載した号外を発行</td><td colspan="2"></td><td>各新聞社が発行を再開</td></tr>
<tr><td>埼玉県北西部に広がった流言</td><td></td><td>東京にて、「放火」等の流言が発生</td><td colspan="4">埼玉県内にも流言が波及</td></tr>
<tr><td rowspan="2">埼玉県北西部での事件</td><td rowspan="2"></td><td colspan="2" rowspan="2">埼玉県内に在住していたあるいは東京方面から避難してきた朝鮮人の拘束</td><td colspan="3">朝鮮人の虐殺</td><td rowspan="2">事件の終息</td></tr>
<tr><td>深谷市（3日の夜より）
本庄市・熊谷市・上里町</td><td>上里町</td><td>寄居町</td></tr>
</table>

©2021. Japan Geoscience Union. All Right Reserved.

A quest for the best condition of a crystal radio's detection

*Motoaki Osone[1]

1. Yashiro High School

This research was designed to see both electric and chemical features of minerals. It was found that the differences of sounds among various types of materials were caused by their direct and alternative I-V curve character. Moreover, it was also revealed that the increase in oxygen on minerals' surfaces is one of the main causes of their rectifying effect. For the future study, since there can be other causes of rectifying effect, this research should be deepened by further experiments such as examining more species and changing the direction of voltage toward crystal orientation.

©2021. Japan Geoscience Union. All Right Reserved.

What cause columner joint changes?

*Yugo Sakurai[1], *Yuki Enomoto[1], *Kanta Hayashibe[1]

1. Yashiro High School

“Columnar joint” mean a hexagonal prism made from lava. When lava touch ground and is rapidly cooled causing volume contraction, they change into columnar joint. Even though scientists are making progress, there is no exact answer why there are difference in size and length between each columnar joint. We thought we may prove the environment of old period by discovering the answer, so we conducted experiments to clarify the causes.

It’s hard to do experiment using lava, so we used cornstarch as a model of columnar joint. It’s said most of their features are common with columnar joint because both them relate to volume contraction.

We named each container A~H and put cornstarch mixed with water, and dried.

A water:70g starch:30g container’s depth : shallow way : Incubator 40°

B water:70g starch:50g container’s depth : shallow way : Incubator 40°

C water:100g starch:140g container’s depth : deep way : Incubator 70°

D water:50g starch:70g container’s depth : shallow way : Incubator 70°

E water:50g starch:70g container’s depth : deep way : Incubator 70°

F water:50g starch:70g container’s depth : shallow way : Incubator 70°

G water:50g starch:70g container’s depth : deep way : light bulb

H water:50g starch:70g container’s depth : shallow way : light bulb

Comparing C with E, we found that the form of crack don’t depend on the depth of container.

Comparing D and E and F, there are few differences between drying incubator and light bulb. However, comparing F and H, there are obvious differences between them.

Comparing A with B, we found that the more it contains cornstarch, the more crock become complex.

Therefore, we supposed the gap of ease of warming caused these differences. the more it’s hard to warm, the more crocks become complex.

In conclusion, we made a hypothesis that “whether lave become columnar jointing is depend on the gap of ease of warming between inside and outside”. It’s still debatable, but it will contribute the development of geoscience.

©2021. Japan Geoscience Union. All Right Reserved.

©2021. Japan Geoscience Union. All Right Reserved.

Preliminary analysis of HAYABUSA-2’s Doppler-Shift

*Azumi Sofue[1], *Naoko Nishino[1], *Riri Iida[1], *Riri Numata[1]

1. Wakayama Shin-ai Senior High School

The school previously analyzed the data received for one day during Hayabusa2’s first Earth swing-by and found that the received frequency was Doppler-shifted. We concluded that this was caused by the change in relative motion between Hayabusa2 and the Earth due to the Earth’s rotation. On the occasion of Hayabusa2’s return, we were able to obtain much longer reception data than that mentioned above, including three days the re-approach and nine days after it started to move away from the Earth. Not only the large effect of the Earth’s rotation, but we also challenged the quantitative analysis of the relatively small effect on the Doppler shift caused by the change in the relative motion between the orbital motion of the Earth and that of Hayabusa2.

©2021. Japan Geoscience Union. All Right Reserved.

Estimation of a ceiling thickness using the muography technique with a small cosmic-ray detector

*Nana Kobayashi[1]

1. Kaichi High School

Since cosmic-ray muons are shielded by the ceiling inside a building, the detection rate of penetrated cosmic-ray muons is decreased on a lower level. It has been applied as muography e.g. observation of the interior of pyramids. I estimated the thickness of the ceiling of the school building by using this technique with the handmade cosmic-ray detector and I also confirmed the consistency between the measured result and value from the drawing of the building.
First, we measured the arrival rate of cosmic-ray muons on the 1st to 5th floors of the school and in the schoolyard (0 floors) using a cosmic-ray detector so-called Cosmic Watch. Two Cosmic Watch detectors were stacked on top of each other, and only the cosmic rays that passed through both upper and lower detectors were counted to limit the solid angle to the direction perpendicular to the ground. I confirmed that the frequency of arrival of cosmic rays decreased as the floor was lowered.
Then, we simulated the correlation between the thickness of concrete, which is the main component of the ceiling, and the arrival rate of cosmic-ray muons, and compared the simulation results with the arrival rates at each floor. I obtained the path length of the cosmic-ray muons with the averaged energy of muons and the stopping power of the concrete.
The total thickness of the ceiling from the measurement was 253 cm and from the drawing was 290 cm.

Keywords: cosmic-ray

©2021. Japan Geoscience Union. All Right Reserved.

A proposal of an inverse analysis method for ballistic ejecta flying focusing on crater shape in phreatic eruption

*Kouki Nishino[1], Neo Suzuki[1], Natsumi Waki[1]

1. Kanagawa Prefectural Yokosuka Senior High School

In recent years, many of the casualties has increased in sudden phreatic eruption. As its countermeasure, the experimental research on the safty of shelters for volcanic disaster prevention is being conducted. However, experimental conditions such as impact velocity of lapilli and block ejecta (ballistic ejecta), which are important in shelter design, largely depend on the experience of expert for volcanology. This is because the actual scattering behavior of the ballistic ejecta is not well understood. Therefore, in this study, we focus on the shape of the crater caused by the impact of the ballistic ejecta. We understand the characteristics of the crater shape that change depending on the impact conditions by the free fall test and the indentation test, and propose an inverse analysis method of the ballistic ejecta scattering behavior.

©2021. Japan Geoscience Union. All Right Reserved.

The survey of Micro-Plastics included in River sediments.

*Taichi Ichikawa[1], Ryuke Kawai[1], Suzuka Fukunaga[1], Tessho Yamamoto[1], Takumi Sato[1]

1. GIZAN SENIOR HIGH SCHOOL

"Micro-Plastics(MP)",recently taken up as a problem,inflow from also rivers.Most of the research on MP in the river are that for analyzing river water.Therefore,we think that if we can make clear the amount of MP in river sediments on the basis of this research,we can estimate the amount of MP that flowed from upstream or flow out to downstream or to the ocean.

Keywords: Micro-Plastics, River sediments, River environment

©2021. Japan Geoscience Union. All Right Reserved.

Relationship between sprites and the lightning charge moment

*syunsuke nakao[1], *sora wake[1]

1. Prefectural Kochi Ozu High School

We are studying the phenomenon of sprites. Sprites are a kind of Transient Luminous Events, and Transient Luminous Events are luminescence phenomena that occur with lighting in the mesosphere at an altitude of about 50 to 100 kilometers. The mechanism of sprites is as follows. A positive polarity lightning strike neutralizes the positive charge in the upper layers of the cloud, and a downward electric field is generated from the ionosphere toward the upper cloud layer. The electric field causes electrons at an altitude of around 60 kilometers to rise and collide with nitrogen atoms, putting them in an excited state. Sprites occur as a result of the release of energy when these nitrogen atoms return to their ground state. However, not all positive polarity lightning strikes produce sprites. We investigated relationship between the charge moment of the lightning and sprites to clarify the conditions for its occurrence. The charge moment is a value defined as the product of the amount of charge discharged by lightning and the altitude, and there is a paper that says this value is large for lightning that generates sprites. We tested whether this was also true for our own data. We have data on the images and locations of sprites when they occurred. By acquiring the data, the time and location of the lightning, and the magnetic field data from the electromagnetic waves generated by the lightning, we analyzed the charge moments of the lightning that generated sprites and the lightning that did not, and compared them to see if there was any difference.

As a method of verification, we first identified the location of the sprite's occurrence using data taken from multiple observation points. The next step was to identify the lightning, the thunderbolt that generated the sprite. Finally, we compared the size of the lightning charge moment at the time of sprite generation. It is not possible to directly determine the value of the lightning charge moment but the strength of the magnetic field of electromagnetic waves generated by lightning is proportional to the lightning charge moment. Therefore, we analyzed the relationship between the magnitude of the magnetic field strength and the magnitude of the lightning charge moment.

This section describes how to analyze the location of sprite generation. We are observing the high-altitude luminescence phenomenon together with 32 high schools in Japan. And in the observed data, there are successful events observed simultaneously from two or more locations. The position and direction of these sprites were identified by referring to the stars in the same location.

Next, we found the lightning at the time when the sprite occurred and timed the two data sets to identify the lightning. We obtained information on lightning from several companies and research institutes, and identified lightning from lightning that occurred at the same time when the sprites occurred.

Then, Chubu University provided us with data on the strength of the magnetic field of the electromagnetic waves generated by lightning. Thanks to the data, we compared the integrated magnetic field values for lightning with sprites and without them.

Keywords: TLEs, Lightning

©2021. Japan Geoscience Union. All Right Reserved.

Potential Small Hydropower Generation in Kamikawa Basin -Hydro Energy Map Visualizing Power Generation-

*Airi Takei[1], *Akira Tamaki[1], *Naoki Kudo[1], *Asahi Takahashi[1], *Hikaru Kawashima[1]

1. Hokkaido Asahikawa Nishi High School

In recent years, greenhouse gas has been generated by fossil fuel consumption. Power generation using renewable energy is become popular in order to reduce greenhouse gas. Renewable energy's merits are that it is undepletable and help eliminate CO_2 generation. On the other hand, renewable energy's demerits are its unstable generation. Small hydropower generation has those merits, and moreover, stable generation. Asahikawa has many rivers and aqueducts. Also, Asahikawa has a place where small hydropower is already generated, so we think that Asahikawa can be developed as a small hydropower town if we use the data. However, Asahikawa is a few case and a few suitable locations. In order to overcome this, we found a small hydro energy map. It is a map that the installable area of small hydropower generation and the estimated power generation is shown on the order of one-fifty thousand scale about the particular river. Originally, the small hydro energy map used the river, however, we will use the aqueducts developed for agriculture. We can find suitable places if we can create a small hydro energy map using aqueducts located in Kamikawa basin and expected power generation.
In order to make a small hydro energy map, we need the correct calculation method of power generation. So we compared actual planned power generation of Toei power plant with our estimated theoretical power generation. And these values matches within an error of 3 percent. We calculated the estimated power generation of the three aqueducts at a total of 23 points. By creating this map, we could see the energy distribution latent in the aqueduct. We think that it is possible to more exactness locate and choose a site the best point for power generation.

Keywords: Small Hydropower Generation

©2021. Japan Geoscience Union. All Right Reserved.

Consideration of brachiopod biota change events in the Kuzu limestone layer

*Omi Kono[1], Tokio Chiba[1]

1. Kaijo senior high school

In Kuzuu, Sano City, Tochigi Prefecture, which is the area covered in this study, the restoration of the sedimentary environment of upper limestone and lower limestone has been elucidated using rock flakes. However, the cause and timing of dolomite formation in the central layer has remained unclear for a long time, and conditions directly indicating deposition environment have not been confirmed. Therefore, we investigated the species of limestone limbs of the upper and lower layers, which had been suggested to have been of different species, using formic acid treatment, and examined the presence or absence of differences in the upper and lower layers. We will clarify the change events of species during deposition and ultimately identify the factors of dolomite formation in the middle layer.

Keywords: Geology, Fossil, Paleoenvironmental estimation

図 1

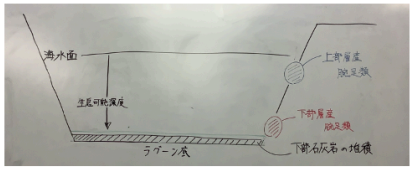


図 2

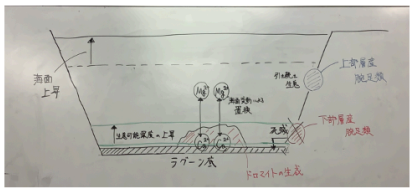
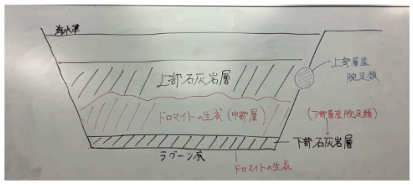
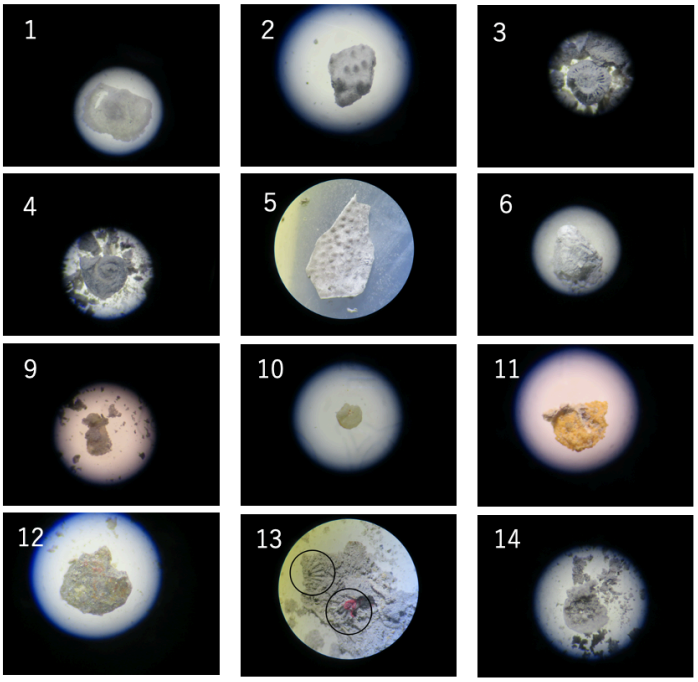


図 3



腕足類一覧（番号は予稿の番号と同一）
7、8に関しては同定後破壊されてしまったため写真は無い



©2021. Japan Geoscience Union. All Right Reserved.

Estimation of the variation in mechanism in the amount of spring water in Otomeyama Park, Shinjuku City

*Kuya Aoyama[1], Taichi Shimokobe[1], Masamune Kanou[1]

1. Kaijo high school

In this study, we estimated the fluctuation mechanism in the amount of spring water at Otomeyama Park in Shinjuku by comparing it with the groundwater level and water temperature in wells.

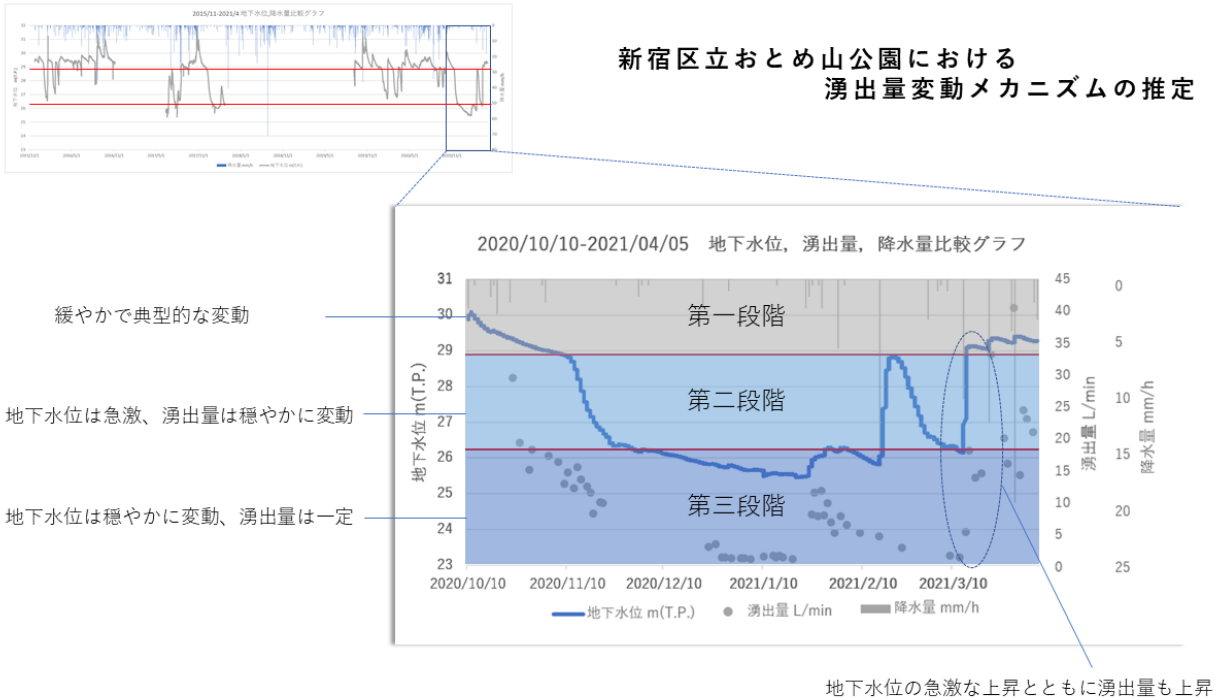
From October 2020 to January 2021, there was a period when there was only 16 mm of total rainfall in 90 days. At this time, the amount of spring water decreased by 87% compared to a normal year, and according to the groundwater level that decreased at the same time, it was classified into the following three stages with different water levels.

The first stage is when the groundwater level declines slowly but the amount of spring water reaches 1L/min, which is considered to be the base flow rate; the second stage is when the groundwater level fluctuates but the amount of spring water does not change; and the third stage is when the amount of spring water increases rapidly.

It can be said that the amount of spring water inflow, groundwater level, and water temperature in the well are controlled in these three stages.

This is thought to be due to the difference in strata.

Keywords: meteorology, hydrology, geology



©2021. Japan Geoscience Union. All Right Reserved.

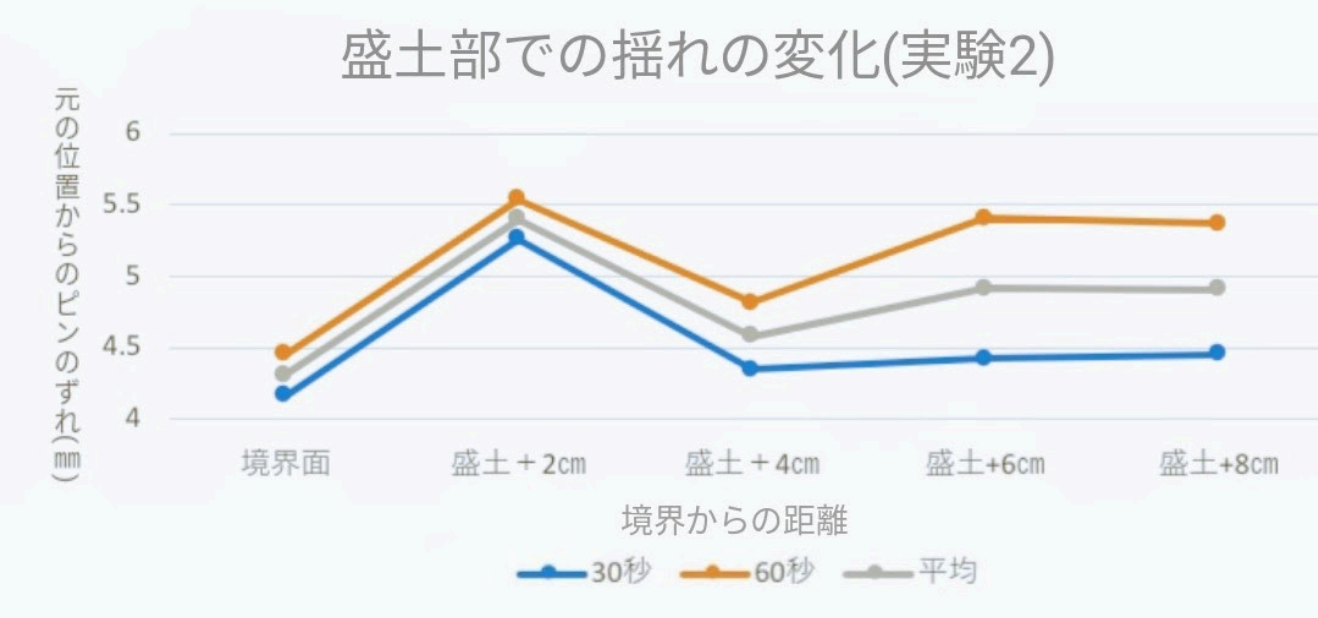
Modeling the earthquake damage in adeveloped land

*Shungo Kokubun[1], *Satoru Takahashi[1], *Hiroshi Takeuchi[1], *Haruki Tamakawa[1], *Masafumi Kaneko[1], Takumi Nanbu[1]

1. Miyagi Prefecture Sendai Daisan High School

We search about the relationship between banking and the effect of earthquake is close thing to our lives.And there are many secondly disaster.We focus on collapse of buildings.From previous research,on the embankment,earthquake damage is heavy.Purpose of research,we make model which reproduce closer to actual movement.We used shaking machine and took a video.In the result only on the border represent actual movement.

Keywords: earthquake, Analog experiment, Embankment



©2021. Japan Geoscience Union. All Right Reserved.

Influence of Calcium chloride on frost columns

*Manaka Oya[1], Shohei Nanri[1]

1. Ichikawa gakuen Ichikawa senior high school

The purpose of this research is to investigate the effect of calcium chloride on frost columns. In order to begin the investigation, an environment which allows the growth of frost columns was made. Frost columns grow when the air temperature is below 0℃, the temperature inside the dirt is above 0℃, and the dirt must be moist. To meet these conditions, the cool incubator was set below 0℃, and an instrument to incubate the dirt(Kanuma pumice) was made. After adjusting the temperature inside the cool incubator, soil particle size, and the temperature of the water used for incubation, the conditions for the growth of frost columns were observed. Next, the effect of calcium chloride on frost columns based on its molar concentration was researched. As a result, frost columns were observed when the cool incubator was set at -10℃, and took 4 hours for it to be detected. After applying calcium chloride upon the frost columns, the lowest molar concentration of calcium chloride in the dirt to prevent the growth of frost columns was 12.9×10-3mol/L.

Keywords: Frost columns, Calcium chloride

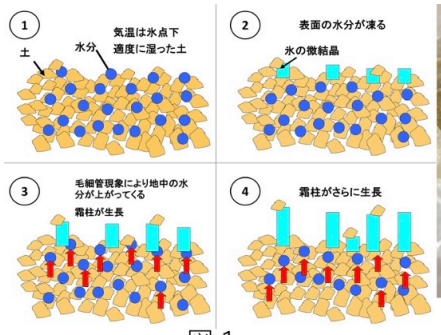


図 1



図 3

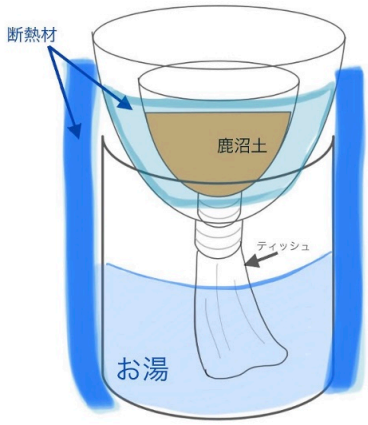


図 2 霜柱作成装置

出典: (NGKサイエンスサイト)

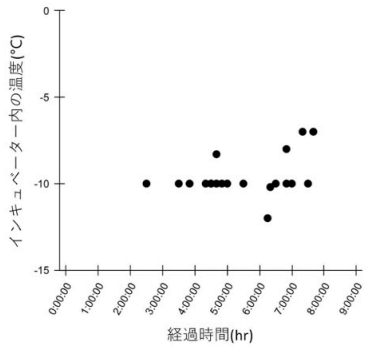


図 4 室温と経過時間の関係

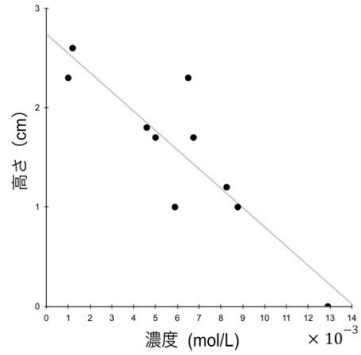


図 5 塩化カルシウムの濃度と霜柱の高さの関係

©2021. Japan Geoscience Union. All Right Reserved.

Differences in fog generation conditions in the Edogawa estuary -Examples of Edogawa-ku and Ichikawa-shi-

*Kenta Torii[1], Shohei Nanri[1]

1. Ichikawa gakuen Ichikawa senior high school

The aim of this research is clarifying the reason why fog of Ichikawa City, Chiba is a little thicker than that of Edogawa City, Tokyo.

Firstly, I checked the conditions for fog to occur, and they turned out to be as follows:
(1)The air contains a lot of water vapor.
(2)The temperature is high.
(3)The altitude is high. (Limited to areas of plains)

Ichikawa City and Edogawa City has geographical continuity that is why I selected Condition 1 as one relevant to this research.

Secondly, I focused on wind as the factor which makes a difference to the amount of water vapor. Examining directions of the winds at various points in southern Kanto on the morning of November 26th, 2020, I found a certain regular pattern of wind, that means, the larger current of wind proved to be. These currents turned out to meet around the area of Ichikawa City and Funabashi City, which Ichikawa City is bordered on the east by, and differ in volumetric humidity and temperature. These differences make fog occur in Ichikawa City firstly.

In conclusion, it is a natural consequence that the fog of Ichikawa City is thicker than that of the other areas including Edogawa City because Ichikawa City is the source of the fog.

Keywords: Fog, Edogawa river

©2021. Japan Geoscience Union. All Right Reserved.

Development of variable slope type underwater embankment

*Kei Omura[1], Shohei Nanri[1]

1. Ichikawa gakuen Ichikawa senior high school

We conducted research on variable slope type underwater embankment with the aim of developing underwater embankment that have a higher energy-reducing effect on tsunamis than conventional types. The research was conducted by combining a demonstration experiment in a laboratory using a small model and a computer simulation. In the demonstration experiment, waveforms were collected using an ultrasonic sensor, and the effect of the variable slope type underwater embankment was verified as compared with the case where a normal fixed underwater embankment was installed and where there was no underwater embankment. In addition, in the demonstration experiment, by using BB bullets as a tracer, the distance traveled by the waves of water molecules was estimated, and the changes in the amount of energy possessed by the waves were also compared. In the simulation, two-dimensional physics software, Algodoo, was used, and the accuracy of the demonstration experiment was verified using the discrete element method by reproducing the environment of the demonstration experiment. As a result of the experiment, it was found that the energy of the waves passing through the variable slope type underwater embankment tended to be dispersed over a wide area. In addition, the total amount of energy possessed by waves decreased the most when the conventional fixed underwater breakwater was installed. From these facts, the variable slope type underwater embankment reduces the load on the embankment compared to the conventional breakwater and disperses the wave energy over a wide area to reduce the amount of energy that rushes to the ground in a certain period of time, and the breakwater on the ground collapses. Ultimately, we would like to connect not only the variable slope type but also the curved underwater embankment whose shape itself changes.

Keywords: tsunami, Underwater embankment

©2021. Japan Geoscience Union. All Right Reserved.

Environmental impact assessment of air and soil substances using spring water of Minowa as an index

*Mari Taki[1], Shohei Nanri[1]

1. Ichikawa gakuen Ichikawa senior high school

In this study, air temperature, water temperature, pH, RpH, electrical conductivity, and COD were measured in the spring water of Minowa, Ichikawa City, Chiba Prefecture.
The pH value was lower than the RpH value, and it was found that the electrical conductivity depends on the amount of precipitation. COD was measured from September 18, 2020 to December 11, 2020. As a result, although there are some fluctuations, it was clarified that the water quality is generally good according to the graph of the environmental standard (lakes) regarding the conservation of the living environment of the Ministry of the Environment.

Keywords: Spring water, Ichikawa, Chiba

©2021. Japan Geoscience Union. All Right Reserved.

Development of an automatic meteor shower observation and the notification system
~Web broadcast of meteor appearance~

*Koichi Sato[1], *Koshi Ri[1], *Shunsuke Isoda[1], *Honoka Ohno[1]

1. Chuo University Junior and Senior High School

Introduction

Radio meteor observation is a worldwide method using a receiver and antenna for receiving a specific radio wave frequency (*i.e.,* HRO or FRO method). Meteors traversing the ionosphere create ionizing trails. The HRO or FRO method is based on the characteristic that ionized meteor trail reflects radio waves in a certain frequency band transmitted from the ground. The audio data obtained by this method is output as image files by HROFFT or MROFFT software. The conventional method of radio meteor observation requires expensive devices such as receivers, and it is needed to construct the observation system. Therefore, we have developed an automatic observation system and a quick notification system of meteor appearance so that anyone can easily observe meteor showers. In our previous study, we have succeeded in constructing an automatic meteor observation system with HRO, completely automating the process from detection of meteor appearance signals to data output, and stably collecting quantitative data and meteor appearance information. The system we have developed was equipped with a function to broadcast only the analyzed values of audio data, which is recorded during meteor observation. Furthermore, it could be more user-friendly and practical when the system automatically detects the meteor appearance signals from the audio data and broadcasts the signals. In this study, we aimed to upgrade our system with a new function of “quick notification of meteor appearances.”

Method

Our system consists of three sections: 1) the radio meteor observation section using a 2-element antenna and radio wave receiver, 2) the analysis section using a computer with Arduino, and 3) the bot-transmitting section made by Python running on a computer. We carried on three experiments in this study: 1) transmitting the audio (recorded) data of meteor observation to the devices, 2) transmitting the audio (in real-time) data of meteor observation to the devices, and 3) analyzing the audio (recorded) data and notifying the meteor appearance to the devices when a meteor appearance signal was detected.

Results and Discussion

The meteor audio data was analyzed by the Fast Fourier Transform (FFT) library in Arduino in order to extract the specific data observed at the time of meteor appearance (data with a frequency of approximately 495 Hz where the volume increases significantly). And then, we converted the meteor appearance data into the text data. The text data was shared and broadcasted to the bots created on Discord and LINE platforms.

In Experiment 1, the data transmitted by the bot running on Python was consistent with the received data

©2021. Japan Geoscience Union. All Right Reserved.

on the devices. It means that a “quick notification of meteor appearance system” was available. In Experiment 2, we succeeded in transmitting the data in real-time without any significant difference. In Experiment 3, we demonstrated a function to analyze the audio data and notify the meteor appearance to the devices when the meteor appearance signal was detected. Therefore, we succeeded in completely automating the procedure from the radio meteor observation section to the bot-transmitting section with a low-cost and simple method.

This system automatically distinguishes the meteor appearance signal from noises by analyzing the audio data collected during the radio meteor observation. When a meteor appearance signal is detected, the signal is broadcasted simultaneously to the devices as meteor appearance information. Our new system is expected to obtain the meteor appearance information easier with personal devices (*e.g.,* smartphones).

Conclusion

Our system with new functions allows us to broadcast the meteor appearance information to the individual devices in real-time at low-cost, instead of the conventional high-cost method. Our next goal is to provide “meteor shower forecasting” using our detecting system of the meteor appearance signals and the data storage system.

Keywords: Radio meteor observation, Automatic web broadcasting, Arduino, Python

©2021. Japan Geoscience Union. All Right Reserved.

Meteorological and geographical conditions of river flooding-Comparison of the past and present of the Miyata River-

*Eri Yoshida[1], *Minami Oikawa[1], *Kotomi Shibata[1], *Chihiro Terazaki[1], *Kurumi Yabe[1]

1. Ibaraki prefectural Hitachi first senior high school

In recent years, heavy rain disasters have occurred frequently all over the country. During the 2019 typhoon in East Japan, the Naka River (Mito City, Ibaraki) and Kuji River (Hitachiomiya City, Ibaraki) were flooded, but the Miyata River (Hitachi City, Ibaraki) did not flood. We investigated if the Miyata River was resistant to flooding, and as a result, we found that if flooded when Typhoon Kathleen approached the Kanto region in 1946.

Therefore, we wanted to consider the cause of river flooding geologically, categorize the conditions under which flood damage occurs, grasp the causes of disasters in advance, and utilize this knowledge for disaster mitigation.

Currently, we are investigating flood damage during the period from 2010 to July 2020, and investigating the relationship between the average slope of flooded rivers and precipitation per unit time, but no typified relationship was found. In the future, we plan to further analyze flooded rivers nationwide and conduct a field survey of the flooded areas of the Miyata River.

©2021. Japan Geoscience Union. All Right Reserved.

Where are solar panels actually used? Research on the present situation of Kashiwa City, Chiba prefecture, Japan.

*Souri Mizukami[1]

1. SHIBYA SENIOR HIGH SCHOOL

The purpose of this study is to find out where the solar panels are widely used. I comparedthe land-cover map created by JAXA with Google Earth to see the distribution of solar panels. I analyzed the data with QGIS to find where the solar panels are actually used.

Keywords: Land use, Agricultural land, solar panels



©2021. Japan Geoscience Union. All Right Reserved.

Decline and Fall of Martian Polar Capse; Whether the Dast Storm Is Warm the Polar Cap

*Kei Inoue[1], Hibiki Aminaka[1], Yuho Takagi[1], Nanami Yasuda[1], Yuki Tanaka[1], Tomoki Ugawa[1], Rio Mogi[1], Kyouka Miyake[1], Momoha Takashima[1], Mako Misumi[1], Kaho Okada[1]

1. Kumamoto Prefectural Daiichi High School

Mars in 2020 approached the earth for the first in two years. According to our previous research, Mars in 2018 had a global dust storm which cover Mars. It turned out that the dust storm promoted increasing in temperature and it decreased Martian polar ice cup’s surface area earlier than usual. Therefore, we set up a hypothesis that a dust storm warms up Mars’s atmosphere. The purposes of this study are researching Martian south polar ice cup’s surface area change in 2020 and we reveal the effect of the dust storm on Mars’s atmosphere through the experiment.

We collected 169 photos of Mars taken in all over the world from Internet, and we calculated Martian polar ice cup’s surface area. As a result, we found the area change is the same as Mars without a dust storm. We can say that the dust heats up Mars’s atmosphere. Moreover, we found Mars in 2020 had a dust storm from November 12 but it had nothing to the area change because the polar cap had been very small.

In the second place, we tried the experiment to consider atmospheric effects by using pyranometers and incandescent light bulb. We prepared the following four models. “Dust floating in the high altitude”, “Dust floating in the low altitude”, “There is no dust”, “Volcanic ash covering the earth”. We substituted the rock wool for the dust and volcanic ash. We observed temperature change through warming each model with incandescent light bulb.

The following are result of the experiment. Model with the largest temperature rise was “Dust floating in the low altitude”. In addition, this kept holding heat even after turning off the light. Model with the second largest temperature rise was “There is no dust”. However there was sudden temperature drop. “Dust floating in high altitude” hardly increased in temperature compared to the above two. “Volcanic ash covering the earth” had very little change. This is most unaffected by solar radiation.

According to results of the experiment, dust storm in 2018 corresponds to “Dust floating in low altitude”. Volcanic ash reduces temperature then there are dusts in the sky. (Parasol effect) On the other hand, the global dust storm has the ability to increase temperature.(Greenhouse effect) In this way, there is the exact opposite temperature change. We consider the cause is dusts rise from the surface of Mars.

We want to keep continuing this study. Future prospects are elucidation of the dust storm mechanism and occurrence condition. In addition, we will use the experimental methods. For example, not only Mars, but also phenomena on earth.

©2021. Japan Geoscience Union. All Right Reserved.

Spacial correlation between slow earthquake and mantle- derived hot spring in Southwest Japan

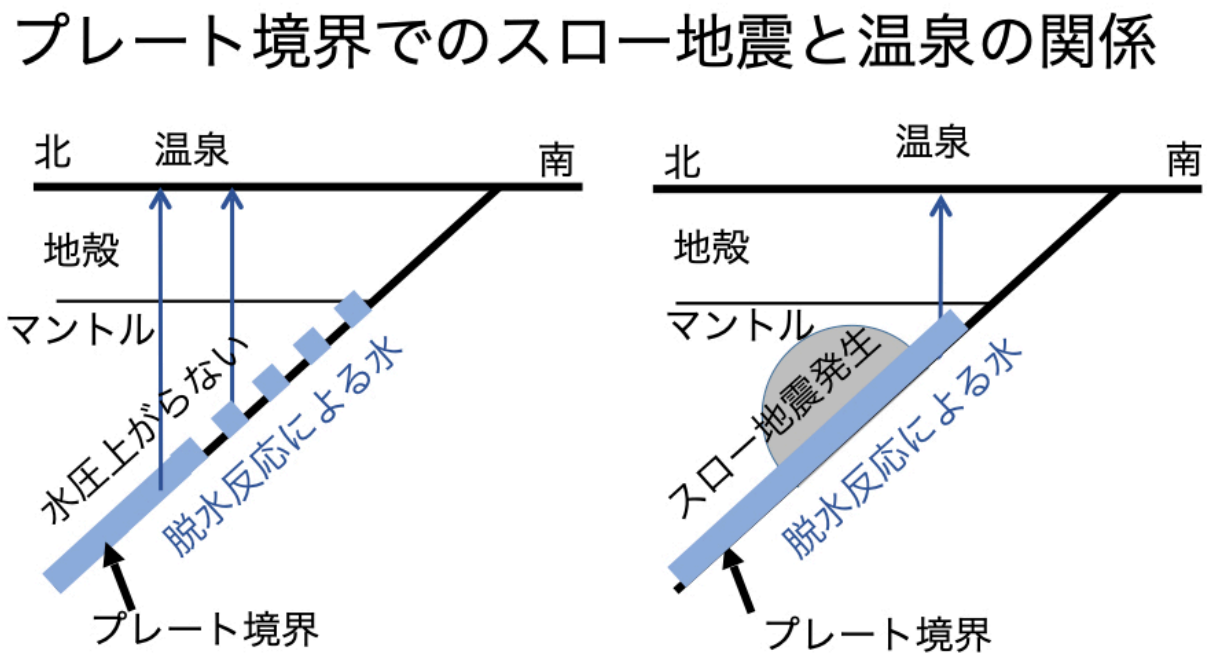
*Yui Kobayashi[1]

1. Shizuoka Higashi High School

Slab-derived fluids cause slow earthquakes and mantle-derived hot springs in Southwest Japan arc. In this study, the relationship between the locations of slow earthquakes and the mantle-derived hot springs in Southwest Japan is studied. Spacial correlation is evaluated between the number of slow earthquakes (National Research Institute for Earth Science and Disaster Prevention database) and Li/Cl values ratios of mantle-derived hot springs (AIST Deep Groundwater database). When the locations of slow earthquake are shifted 7 km to the south, the correlation is the largest. This indicates that the mantle-derived hot springs are located to the south of the region where the slow earthquakes are occurring (Figure).

Explanation of figure.
Schematic diagram showing the slow-earthquake occurring in the fluid-filled region in the slab-mantle boundary and the mantle-derived hot springs coming from the margins of the slow-earthquake region.

Keywords: slow earthquakes, Slab-derived fluid, mantle-derived hot springs



©2021. Japan Geoscience Union. All Right Reserved.

Visualize water current using vitamin B_2

*Mutsuki Kamata[1], *Yuuma Nakagawa[1], *Io Kato[1], *Tokito Hirose[1], *Yuuki Matsui[1], *Kosuke Mafune[1], *Akihito Yamada[1], Kazumi Igawa[1]

1. Zushi-Kaisei Senior High School

The deep ocean current mainly sinks in the polar regions such as off the coast of Greenland and in the Weddell Sea in the south pole. Then, it comes up to the surface in the Pacific and the Indian Ocean after making a circuit of Earth. Therefore, this current plays one of the important roles in long-term heat transportation in the polar regions, low latitudes and middle latitudes and has a great influence on Earth climate. However, there are many things that haven't been solved yet. The mechanism of upwelling is a prime example. The reasons for its sinking in the polar regions are low temperature and the high salinity of water. Nevertheless, the mechanism of its upwelling in the Pacific and the Indian ocean hasn’t been solved yet and people have been still studying.

These days global warming clearly begins to have an influence on our lives, so it is necessary to take measures against it. However, it is important to understand Earth’s potential climate control function more deeply to make global warming slower and realize the best living environment for all living things, including human beings.

For this reason, we have experimented by reproducing submarine topographies in an aquarium on the basis of a hypothesis that they have an influence on upwelling, and we have searched into what causes upwelling to discover the mechanism of its upwelling. Concretely, we set ices on the left end of the aquarium to reproduce low seawater temperature at polar regions and set mimicked seamounts made of plaster to reproduce submarine topography such as ridge, hotspots in Indian ocean. Also, we visualized water current using aqueous solution dissolved blue ink and try watching turbulence caused by current’s hitting seamounts and upwelling water. In addition to those, not only visualization but also measurement did we make by setting High speed Response Temperature Progs (given by Shimazu-Rika) one by one and changing their height to measure water temperature by 0.01℃ every 0.1 second, and try quantifying water current too detail for us to watch.

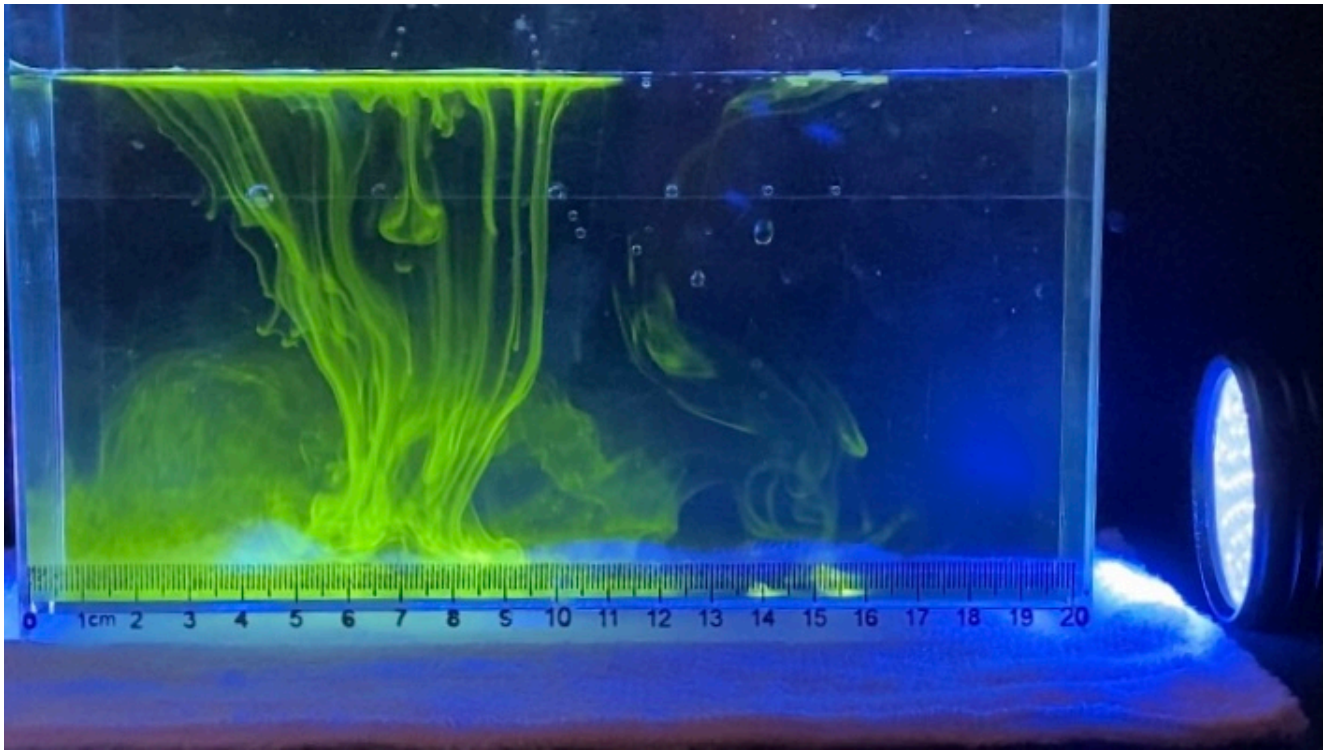
However, visualizing with ink has various problems. For example, because of aqueous solution’s uniformity, ink will spread all over the aquarium and the ink’s concentration is getting lower, so it gets more difficult to perceive ink. Besides, from the beginning, ink is difficult to perceive. Therefore, we focused on vitamin B_2’s fluorescent action and thought that we can improve such ink’s defect if we use powdered vitamin B_2 instead of ink. For this reason, we tried to visualize water current using vitamin B_2. Also, we groped for a method to use powdered vitamin B_2 for almost indefinite time without consuming powder by putting ingenuity into powder as it has advantages.

The new visualization method found through this study will be very useful in making a consideration about the deep ocean current from now on, this will make it easier to visualize sea turbulence and will be possible to observe accurately. Also, the way we present this time is considered that it can be applied to various fields on visualizing the current, at this conference, nothing is more pleasing if the way we use vitamin B_2 becomes popular from now on. We will announce visualization of sea turbulence we

©2021. Japan Geoscience Union. All Right Reserved.

experiment using vitamin B_2 we mentioned above and the ability of vitamin B_2.

Keywords: Sea



©2021. Japan Geoscience Union. All Right Reserved.

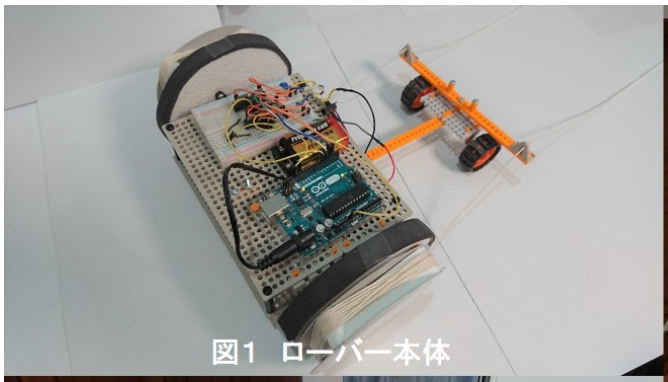
Designe of lunar crater exploration rover

*Kosuke Kameoka[1]

1. Meikei High School

The purpose of this study is to design a lunar rover that runs stably and securely on the sloping surface of lunar craters. First, I produced a rover of specification to keep the balance of the body with a rope. Second, I sent the rover in three courses that imitated the slope of the lunar craters. It ran under the three conditions; slope angle, surface relief and gravity, and evaluated the performance with two standards. Results of three type of driving experiments showed that the rover could run safely on the course. It is concluded that the rover have the potential to drive stably on the slopes of lunar craters.

Keywords: driving test, Arduino, simulated track


図1　ローバー本体

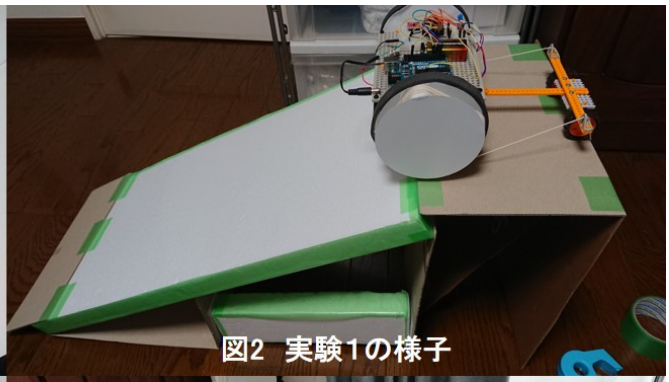

図2　実験1の様子


図3　実験2の様子


図4　実験4の様子

©2021. Japan Geoscience Union. All Right Reserved.

Distribution of Gravel in the Sakawa River and Factors Affecting the Distribution

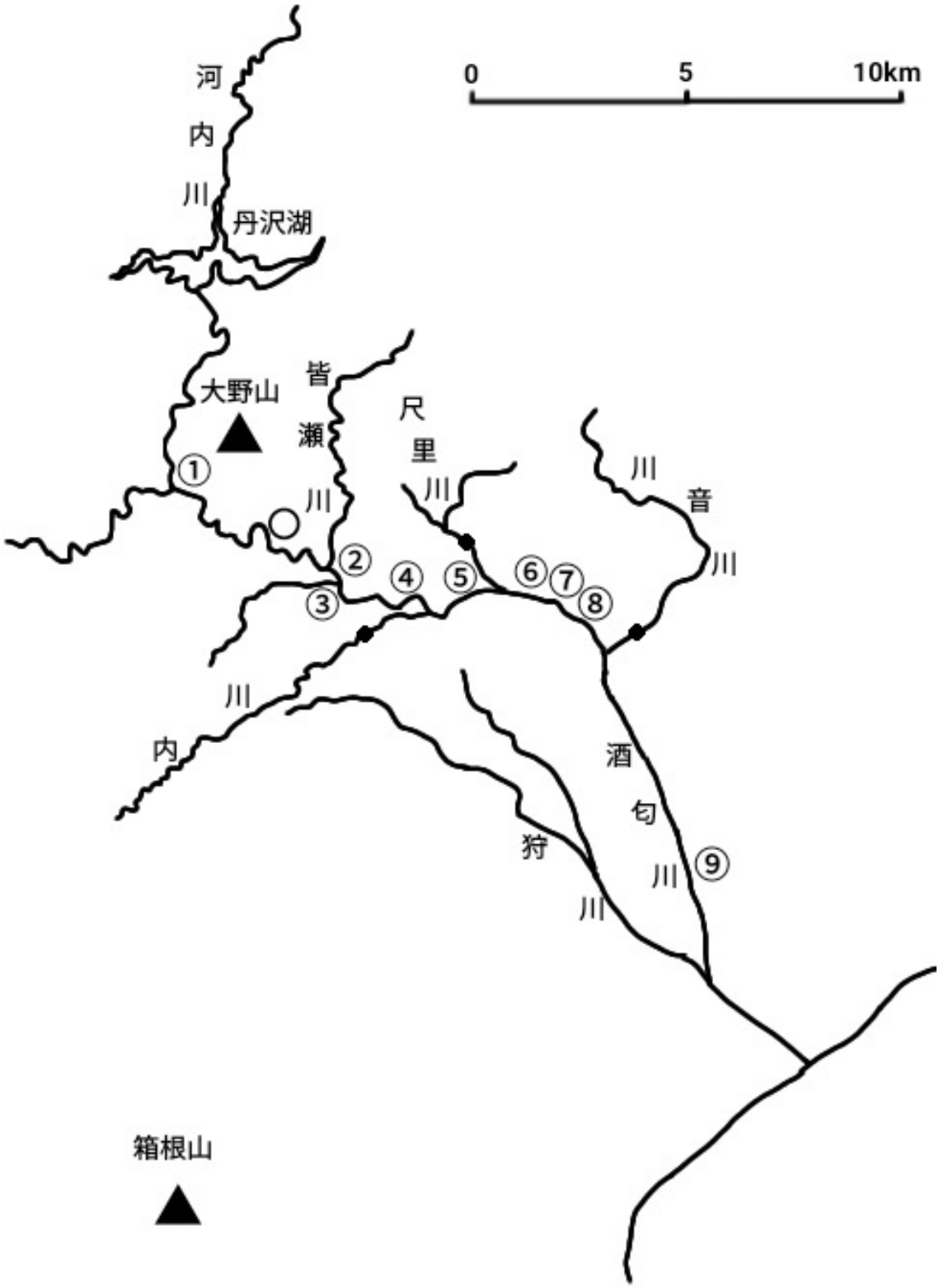
*Nozomi Uemachi[1], *Misaki Yamamiya[1], Yosuke Saito[1]

1. Tokyo Gakugei University Senior High School

The distribution of rock in the midstream and downstream of the Sakawa River was studied.
In this study, two types of samples were taken at nine points: the first was 200 rocks collected in order of size from the surface of a 1m x 1m frame; the second was the 10 largest rocks within 10m from the frame. The investigation has been done three times. In the first stage, the rock distribution in the midstream and downstream of the river was surveyed at points 1, 6 and 9 in the attached map. The result was that several kinds of gravel decreased We hypothesized that this was due to the topographical characteristics of the fan and the valley bottom plain, and conducted the second stage of the survey at points 3, 4, and 5 shown in the attached figure, sandwiched between the valley bottom plain and the fan edge, respectively. In the third stage, to confirm these hypotheses, the surveys were conducted at point 2 in the attached map, which is upstream of the weir at point 3, and at points 7 and 8, which are the middle and lower parts of the same sandbar as point 6.
In conclusion, in addition to the armoring and the feature of the grain size distribution of the sandbar, the following four things were found from the first and second stages of the survey. First, large rocks were deposited due to selective transport in the two sections where the river gradient and depositional topography changed. The average grain size and weight percentage of tonalite and green schist decreased rapidly between points 3 and 4. These types of rocks were deposited by selective transport because of their large average grain size at point 3. Andesite, basalt, and fine-grained tuff were deposited by the same principle between points 4 and 5. Secondly, sandstone and conglomerate were rarely found in the area after point 6, suggesting that clastic rocks were susceptible to abrasion. Third,as there was almost no increase in the number of rocks that could be supplied by the tributaries at the points after the tributary confluence, it can be said that the tributaries in the middle and lower reaches did not affect the gravel distribution in the mainstream. Finally, the weight percentage of andesite and basalt and the grain size of the largest rock increased at point 4. The possibility that the andesite and basalt are supplied by the Sekimoto Hills and Asama Mountain in the vicinity of this point is under investigation. The results of the third stage of the survey are currently being analyzed. We would like to make a presentation including these results.

Keywords: The Sakawa River, river bed stones, sorting, abrasion, sandbars, armoring

©2021. Japan Geoscience Union. All Right Reserved.



©2021. Japan Geoscience Union. All Right Reserved.

Detection of Cherenkov light with acrylic and photodetecto

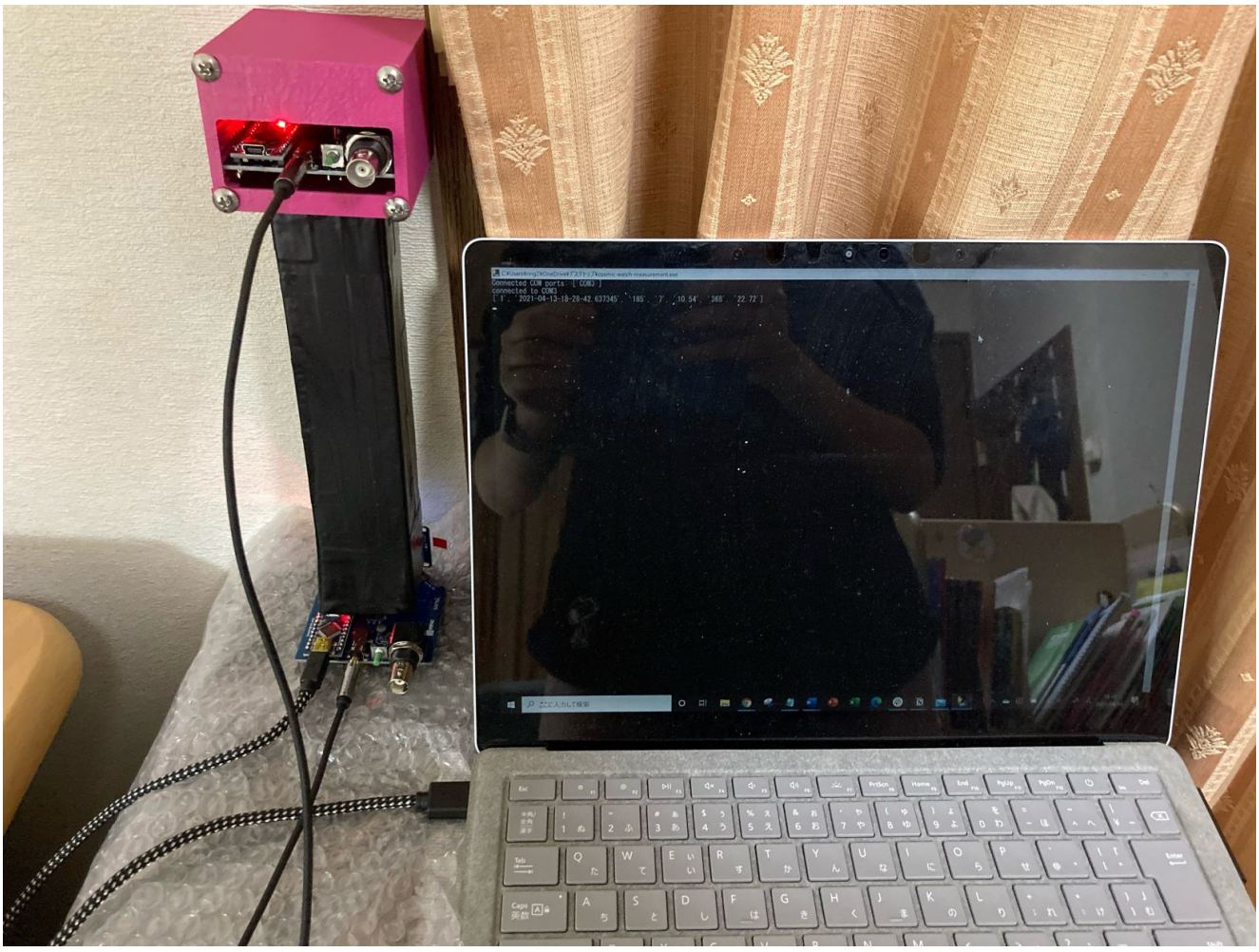
*Juri Urano[1], *Yuka Kuze[1], *Kaho Kubota[1]

1. Toshimagaoka Joshigakuen senior high school

We detected Cherenkov light with a handmade cosmic-ray detector so-called "Cosmic Watch". Cherenkov light is observed when cosmic ray goes through the substances which have a large refractive index. In this research, we used acrylic (4 cm * 4 cm * 20 cm). We flattened the surface of the acrylic with some pieces of sandpaper and abrasive to improve the transmission of the Cherenkov light to the photodetector sensor. We covered the acrylic with aluminum foil and black plastic tape to shading and shielding from electrical noise and light leakage. We put another Cosmic Watch with a plastic scintillator on the Cosmic Watch with acrylic and measured signal coincidences to prevent noise detection.

In this research, we succeeded in detecting a Cherenkov light in a certain condition. We would like to optimize for detection of Cherenkov light by changing conditions like material or its size.

Keywords: Cosmic Rays



©2021. Japan Geoscience Union. All Right Reserved.

Research the View of Mt.Fuji with a Self-Made Observation Device

*Ryoo Niigawa[1], *Rin Takezoe[1]

1. Tokyo Metropolitan Tachikawa High School

The astronomy meteorology club at our school has been making meteorological observations including visibility for more than 70 years. Visibility is the maximum distance at which objects can be clearly seen with the naked eye, and has been used as an indicator of air pollution. 4 years ago, a senior started a study to analyze visibility observation data for the past 50 years. Last year, a senior developed a new visibility observation device that uses a camera controlled by a small computer to take pictures regularly. In this study, we made a similar device to photograph around Mt. Fuji, and investigated the relationship between the view of Mt. Fuji and surrounding clouds and meteorological phenomena.
Analysis of past visual visibility observation data showed that the ratio of the number of days Mt. Fuji was visible per month was more than 50% in winter and less than 10% in summer.
The cloud characteristic of Mt. Fuji was noticed and analyzed from the photographing data for 6 months. As a result, most apron clouds occurred in midwinter, and they were associated with low temperatures at the top of Mt. Fuji. Cap clouds occurred three or four times a month, and they were associated with high humidity at the top of Mt. Fuji.

Keywords: Mt.Fuji, Visibility, Cap clouds, Apron clouds

©2021. Japan Geoscience Union. All Right Reserved.

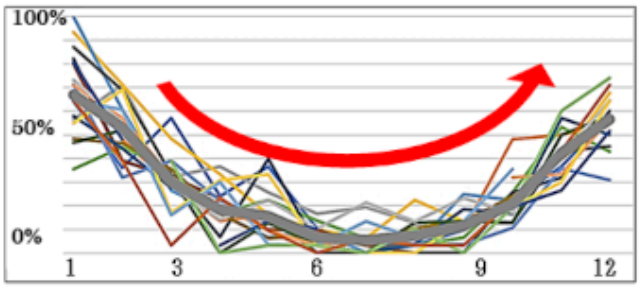


図1　過去の富士山が見えた日数の
1年間の変化(1959～1985年)



図2　観測装置が撮影した前掛け雲(上)と笠雲(下)

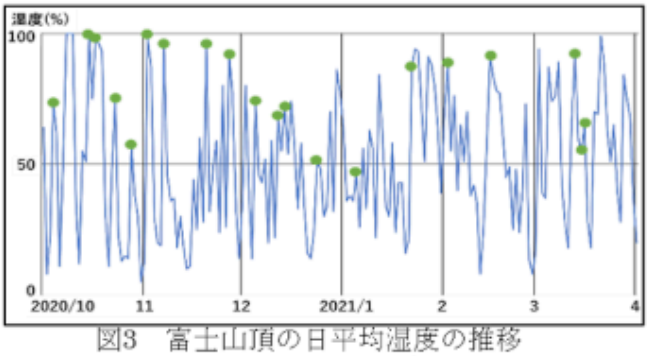


図3　富士山頂の日平均湿度の推移
（笠雲発生日に丸）

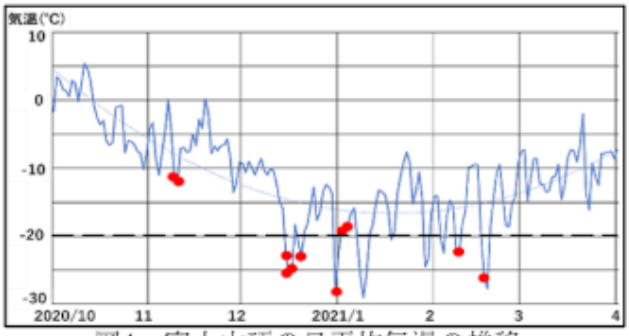
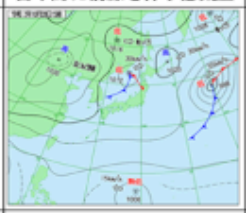
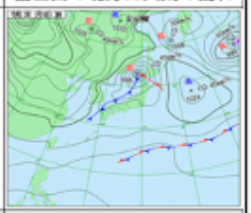


図4　富士山頂の日平均気温の推移
（前掛け雲発生時に丸）

表1　それぞれの気圧配置の例と
当てはまる事例の割合

	日本海に前線を伴う低気圧	富士山の北方に大気の乱れ
天気図の例		
日本大学の研究 2002/9/28～ 2003/3/31	9回/31回 ＝ 29%	18回/31回 ＝ 58%
我々の観測 2020/9/25～ 2021/3/31	5回/ 21回＝ 24%	13回/21回 ＝ 62%

©2021. Japan Geoscience Union. All Right Reserved.

Bad visibility in the past at Tachikawa High School

*Tomoya Ushizaka[1]

1. Tokyo Metropolitan Tachikawa High School

Transitions of visibility in the past for 10years in TachikawaVisibility is a meteorological term indicating the distance with which an object can be identified from the observation site and is information to measure how far we can see.
It is used as an indicator of air pollution.
Tachikawa high school astronomy meteorological club have been observing visibility for about 70 years since the 1950s.
A senior of the club conducted a survey focused on visibility and analyzed data.
The results show the condition of visibility was very bad in Tachikawa in the past.
In this study, the cause of visibility was investigated by comparing the data of visual range data for about 10 years from 1957 when visibility was the worst with recorded meteorological phenomena (smoke, haze, fog, inversion layer, and wind dust).
For the survey, we used monthly reports written in the past and interviewed our alumni.
The data of visibility showed that visibility tended to be poor in winter especially in the morning and phenomena such as soot, haze and inversion layer were more frequent during the same period than the present.
After 1965, the number of soot and haze decreased and the visibility tended to improve accordingly.
Also, unlike the soot and haze generated by the soaring dust and dirt, the inversion layer and fog caused by changes in temperature did not increase nor decrease throughout the 10 years.
The author discovered that the poor visibility and the occurrence of meteorological phenomena related to visibility are associated with each other.

Keywords: visibility , meteorological, air pollution

©2021. Japan Geoscience Union. All Right Reserved.

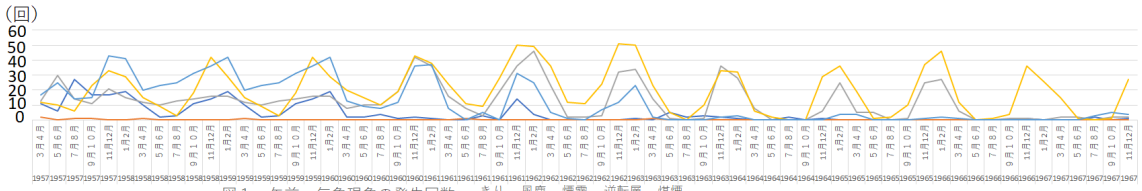


図１　午前　気象現象の発生回数

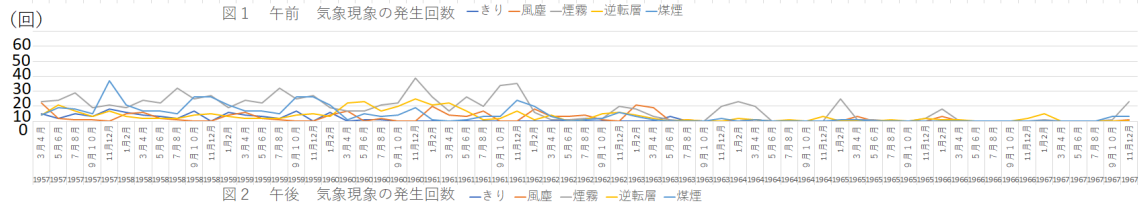


図２　午後　気象現象の発生回数

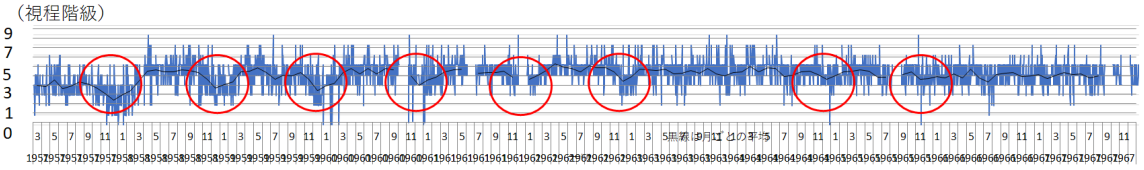


図３　午前の視程階級

赤丸で囲った部分は視程が悪化していた部分

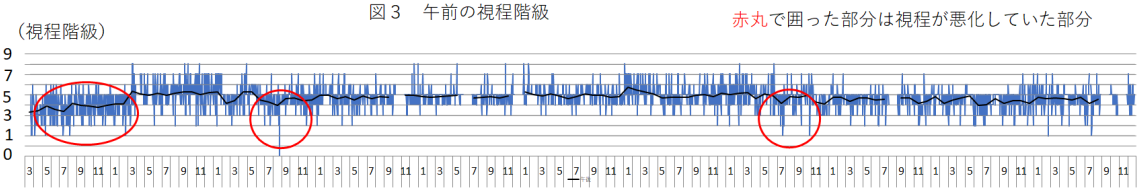


図４　午後の視程階級

視程階級	目標物を認めることができる最大距離
0	50m未満
1	50m以上　200m未満
2	200m以上 500m未満
3	500m以上　1km未満
4	1km以上　2km未満
5	2km以上　4km未満
6	4km以上　10km未満
7	10km以上　20km未満
8	20km以上　50km未満
9	50km以上

図５　先行研究にて作成された本校オリジナルの視程階級表

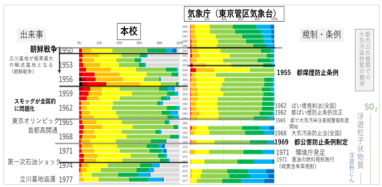


図６　先行研究にて作成した本校の視程のデータと気象庁のデータ



図７　当時の記録が残っている月報



図８　立川基地新聞

©2021. Japan Geoscience Union. All Right Reserved.

Analysis of visibility around Tachikawa High School

*Takumi Yasuhara[1]

1. Tokyo Metropolitan Tachikawa High School

In Tachikawa high school, we have continued weather observations including visibility for about 70years, but the number of missing data has been increasing since 1985. The visibility observation was resumed several years ago. However, because it was difficult to continue the observation on time, a senior person made an observation device for visibility by himself. In this study, the relationship between weather phenomena or air pollution and visibility was investigated by analyzing the tendency of visibility. As a result, it was found that changes in visibility were affected by weather and seasons. It was also found that the visibility in the morning is worse than in the afternoon due to the influence of forward scattering. In the future, we aim to automate visibility judgement by deep learning.

Keywords: Meteorology, Visibility, Visibility Observations

©2021. Japan Geoscience Union. All Right Reserved.

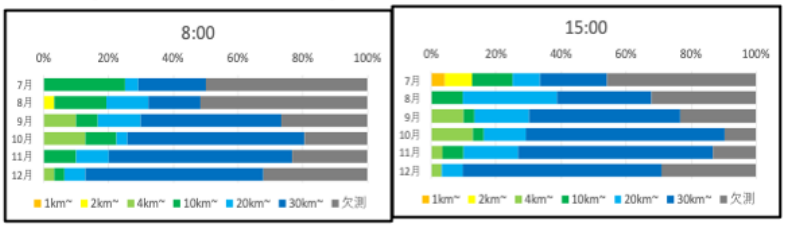
視程階級表

視程階級	視程距離	番号	目標物
1	0.1km	①	目の前のマンション
2	0.45km	②	YAZAWA Deux Bldg.
3	0.75km	③	立川病院
4	1.0km	④	ラポール西国立
5	3.0km	⑤	一橋大学法人本部棟
6	4.3km	⑥	多摩総合医療センター(府中病院)
6	4.9km	⑦	ライオンズガーデン西国分寺
7	13km	⑧	グレーシアタワー三鷹
8	25km	⑨	新宿ビル群
8	36km	⑩	東京スカイツリー

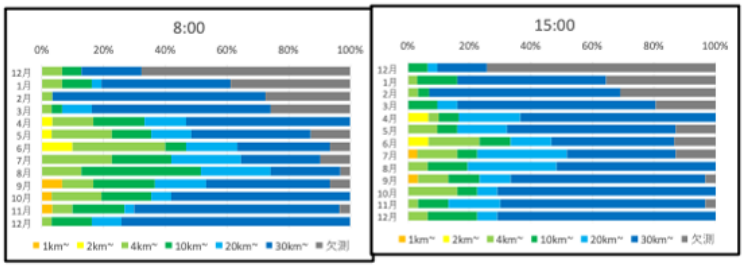


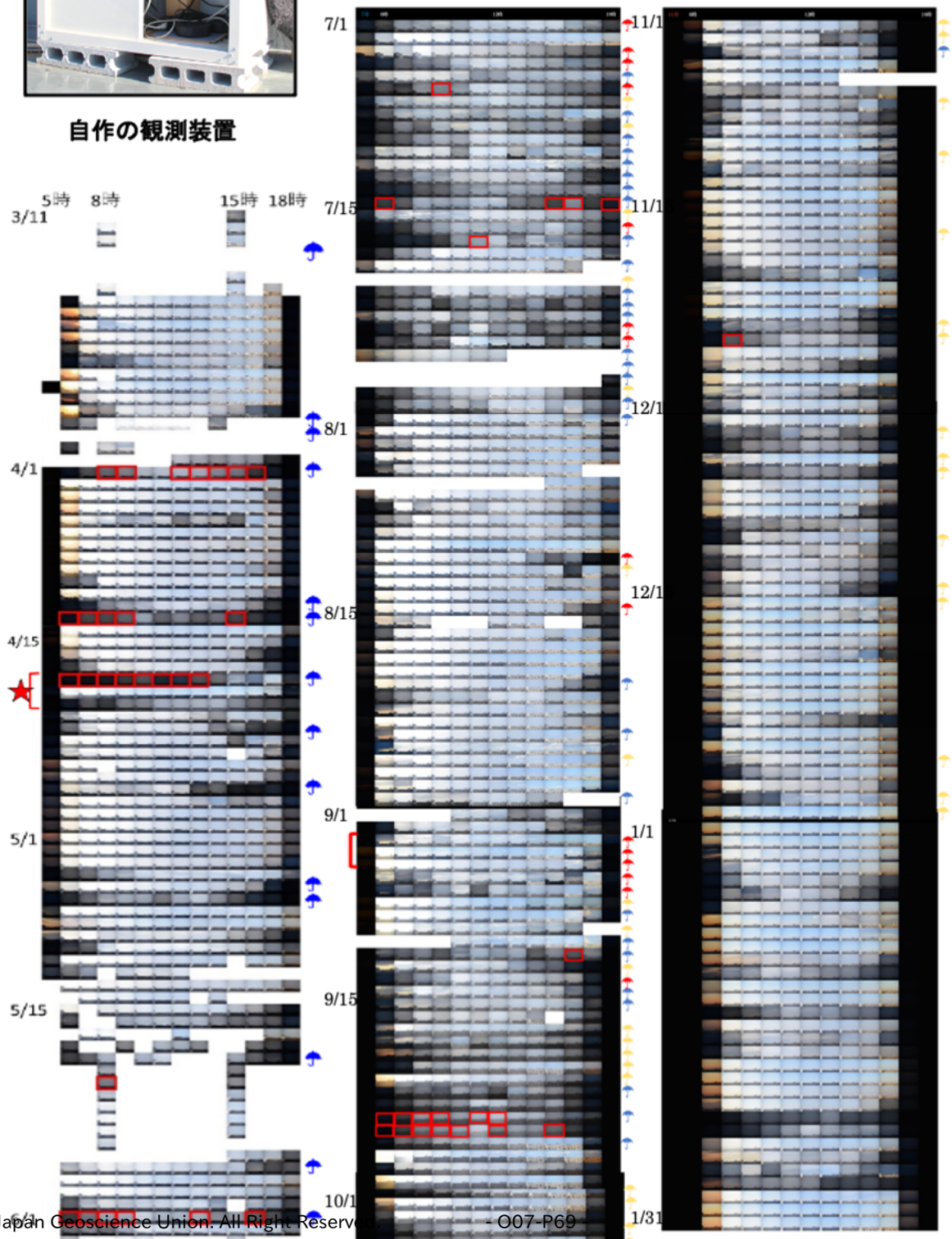
自作の観測装置

目視による月ごとの視程(8時・15時)



画像による月ごとの視程(8時・15時)





©2021. Japan Geoscience Union. All Right Reserv

©2021. Japan Geoscience Union. All Right Reserved.

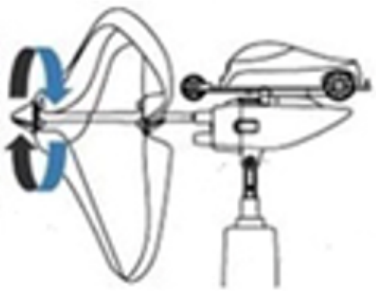
The relationship between the shape and power generation amount of the simple wind power generators

*Sora Fukui[1]

1. Tokyo Metropolitan Tachikawa High School

Since I was interested in the relationship between the shape of the wind power generator and the generated power, I conducted three experiments using a simple wind power generator of my own making and examined the relationship between the shape of the generator and the generated power. In the first experiment, the amount of power generated at each constant wind speed was measured using the loopwing type, and the value was smaller than the ideal value as the wind speed increased. This calls for more efficient use of power. In the second experiment, a multi-wing type generator and a savonius type generator were made. The savonius type was made by reusing discarded bicycles and unused buckets. Using these data, the wind velocity at the time of maximum power generation and minimum power generation was measured, and the power generation per unit wind-receiving area was calculated. On the other hand, the multi-winged wind generator had the advantage of starting to spin in a weak wind than the savonius type generator. In the third experiment, the generated power and the wind velocity were measured on the roof of the school using the wind power generator. As a result, the problem of stable electricity supply became clear.

Keywords: wind power generator, hub dynamo, stable supply



図ループウィング型



図 多翼型



図 サボニウス型

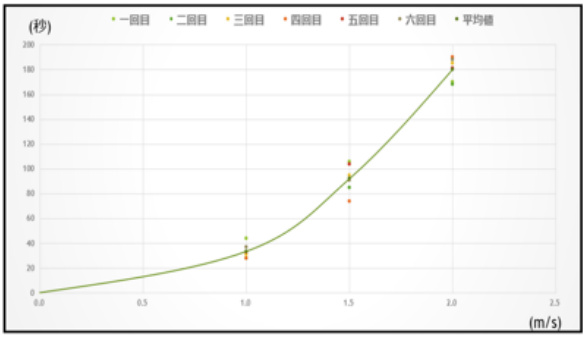


図 ループリング型を用いた実験結果

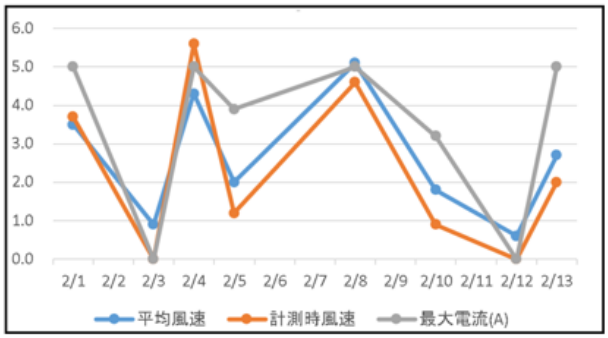


図 屋上での多翼型を用いた実験結果

©2021. Japan Geoscience Union. All Right Reserved.

Is «evacuate to rise »the Right Action?

Research and Proposition of Major Evacuation Routes to Shelters in Shibuya

*Sakura Oona Marie Sueoka[1]

1. Tokyo Metropolitan Kokusai High School

Is «evacuate to rise »always the right action?
In this research, I have verified the famous phrase "evacuate to rise". Furthermore, I have evaluated 15 shelters certified by the Shibuya City, and proposed major routes to these shelter from different points.

Keywords: Earthquake, Evacuate, Natural Disaster

©2021. Japan Geoscience Union. All Right Reserved.

Mechanism of how the Shirata river looks blue

*Shuhei Sugai[1], *Ryosuke Yoshida[1]

1. Shimoda high school

The Izu Peninsula, which faces Suruga Bay on the east side and Sagami Bay on the west side, is located at the eastern end of Shizuoka Prefecture. The Shirata River flows through the Izu Peninsula, and there was a sulfur mining trace upstream. We began our research with an interest in the pale-blue-looking points downstream, and eventually verified the sulfur production and also conducted a water quality survey of the surrounding area. At the site, pH was measured at each point of the mainstream and tributaries of Shirata River. We brought back the clay from the sulfur mining trace, and our analysis showed that the sulfer was contained 30% of the mass of the clay. The Shirata River, which supports the water supply in Higashiizu Town, was also the place that caused the oldest pollution in Japan from the Edo period to the Meiji period. We need to know more the Sirata River in order to coexist with peace of mind.

Keywords: Shirata River, Izu Peninsula, sulfur, colloid, water

©2021. Japan Geoscience Union. All Right Reserved.



©2021. Japan Geoscience Union. All Right Reserved.

Determining the Properties of Seyfert Galaxies

*Kuya ABE[1], *Kuranosuke IEHATA[1], *Koki TANII[1], *Tamotsu FUJIMOTO[1]

1. Nara Prefectural Seisho High School

Spectroscopic observations of ten Seyfert galaxies were performed at the Bisei Observatory in Okayama Prefecture and the data was analyzed using “BeSpec” software. The width and intensity of Hα, Hβ, He II, [N II], [O III] and [S II] emission lines were calculated. The result was the, type 1 galaxies products the so wide emission lines of hydrogen and helium. In contrast, it was found that type 2 galaxies produced emission lines for helium, sulfur and nitrogen which were slightly longer than the overall sample mean. In conclusion, it was determined that hydrogen and helium are found in the cores of Seyfert galaxies whereas there oxygen, nitrogen and sulfur are distributed throughout the fringe areas of Seyfert galaxies. Furthermore, we categorized the type of 6 galaxies again.

Keywords: Spectroscopic observation, Emission line, Active galactic nucleus

表　観測データから求めた各銀河の輝線幅（FWZI）

銀河名	型		観測日	輝線幅				
				He II	Hβ	[O III]	Hα	[S II]
NGC2782	–	1	2020.04.10	—	—	—	70.6	36.4
NGC3516	1.5	1	2020.04.10	—	50.0	28.1	139.2	24.0
NGC4151	1.5	1.5	2016.12.09	114.4	122.6	48.2	279.8	32.2
			2020.04.10	96.5	130.5	44.1	272.8	32.2
NGC5548	1.5	1	2020.04.10	16.5	107.6	36.3	258.0	43.0
NGC7469	1.2	1	2019.11.16	115.1	109.4	36.3	220.0	18.5
			2020.09.05	—	—	—	197.0	23.2
			2020.09.05	118.4	98.7	44.2	212.6	27.8
			2020.09.05	123.7	86.5	56.2	239.6	23.1
			2020.09.05	124.4	107.6	40.2	221.4	18.5
			2020.09.05	127.7	82.9	40.2	219.2	18.5
NGC3227	1.5	1.5	2020.04.10	84.4	96.1	44.1	159.3	27.6
NGC4051	1.5	1.5	2020.04.10	84.0	72.3	40.1	155.4	32.2
NGC1275	2	1.9	2016.10.21	45.6	69.7	44.5	148.6	25.0
			2019.11.16	58.2	57.3	60.2	131.5	23.9
NGC4258 （M106）	1.9	1.9	2020.04.10	—	—	26.5	36.4	28.7
NGC1068 （M77）	2	2	2016.10.21	78.4	54.7	72.3	136.7	44.4
			2019.11.16	71.4	44.1	67.8	116.0	32.2
			2020.09.05	—	49.4	—	—	—
			2020.09.05	68.1	53.8	68.2	138.9	41.4
			2020.09.05	72.8	51.2	64.1	132.0	36.8
			2020.09.05	78.1	55.6	72.4	143.0	31.0

©2021. Japan Geoscience Union. All Right Reserved.

Observation of Radio Waves from the Moon

*Koya YAMASHITA[1], *Ichika TSUTSUMI[1], *Atsushi HIRANUMA[1], *Ikumi MATSUYOSHI[1]

1. Nara Prefectural Seisho High School

There are radio waves from familiar things such as smartphone. These from the sun has already observed few years ago. However, these from the moon hasn’ t done yet. So, our research project is to survey relationship between intensity of the radio waves and moon age. On the other hand, we researched the apparent temperature too. First, we turned the antenna directly to the moon, sky and radio wave absorber. Second, we recorded these data which displayed by tester randomly, and analyzed them. As a result, Value of the moon radio waves were 0.109 0.272 0.270 0.245, and the moon age which is at that time were 13.4 4.9 7.9 11.9. In conclusion, the value of the full moon radio waves bear no relation to moon age, and surface temperature too. The cause of the result is difference of the moon`s altitude and the amount of cloud.

Keywords: Radio telescope, Moon age, Surface temperature

表　月齢と電波強度・月の表面温度の関係

	2020/12/28 18:36	2021/1/18 18:28	2021/1/21 18:23	2021/1/25 18:14
月の形（月齢）	小望月（13.4） 	三日月（4.9） 	半月（7.9） 	十日夜の月（11.9） 
気温Ta（℃）	8.0	2.0	7.0	9.0
高度（° ）	37.1	38.4	65.3	53.5
電波強度 $\frac{Vmoon-Vsky}{Va-Vsky}$	0.109	0.272	0.270	0.245
Tmoon（℃）	30.6	75.1	75.7	69.1

©2021. Japan Geoscience Union. All Right Reserved.

Making Snow Meter Using Neutron Cosmic Rays Observation Data Collected By Cosmic Watch

*Kei Ikushima[1], Rikako Kono[2], Kaduo Tanaka[2], Akita Yuji[1]

1. Hiroo Gakuen High School, 2. Touhoku University

One of the methods to observe volcanic activity is to measure the change in gravity, but in winter, snow falls on the gravity measuring instruments and affects the measurement due to the gravity of the snow. In order to correct for this, it is necessary to measure the amount of snowfall and modify the data. The use of cosmic rays has been attracting attention as a method to measure the amount of snow cover. In this method, a cosmic ray detector is placed under the snow, and the amount of snow cover is calculated from the decay of the cosmic ray energy. In this study, we aimed to reduce the cost of this method by using Cosmic Watch, an inexpensive and compact cosmic ray detector. The cosmic ray detector consists of two main components: a scintillator and a photomultiplier. The scintillator emits a small amount of light when a cosmic ray penetrates it, and this light is measured and recorded as an electrical signal using a photomultiplier. The voltage value of the electrical signal obtained is proportional to the energy of the cosmic ray. In this study, two cosmic ray detectors are stacked on top of each other and only the data detected simultaneously by the two detectors are recorded. By using the coincidence measurement, the noise data other than cosmic rays can be reduced drastically.
When neutron cosmic rays pass through snow, the energy of the cosmic rays decays in proportion to the amount of snow cover, so the amount of snow cover can be calculated by measuring the energy of the cosmic rays. However, Cosmic Watch can observe many other cosmic rays in addition to neutrons, so it is necessary to collect only the neutron data needed for the snow meter. To do this, we need to perform Pulse Shape Discrimination (PSD), which is a cosmic ray analysis method to determine the type of cosmic ray by integrating the voltage decay of the waveform data of the electrical signal obtained from the photomultiplier. This method is based on the fact that the attenuation of the electric signal is different for each type of cosmic ray depending on the characteristics of the scintillator. I installed a scintillator called EJ276, which can easily perform PSD of neutrons, in Cosmic Watch to collect data of neutron cosmic rays. In order to obtain a waveform outline, the voltages were acquired continuously over a number of times. Now that we are able to obtain neutron data through PSD, we would like to conduct experiments using actual snow and water tanks to see if we can correctly calculate the amount of snow and water from neutron cosmic rays.

Keywords: Cosmic rays, Neutron, Arduino, Snow meter

©2021. Japan Geoscience Union. All Right Reserved.

Water storage capacity of the green dam –Role of forest soil -

*Nanami Aoki[1]

1. Kyoto Prefectural Sagano High School

In the Sagano High School Woods for Field Studies (SWFS), we have been conducting research about the water source recharge function and flood mitigation function of the forest (Matsuki, 2019). The purpose of this study was to find out the water retention capacity of forest soil by conducting a soil profile investigation and a soil physical properties investigation at SWFS and three other locations with different pedogenic factors. As a result of the surveys, the soil of SWFS was classified as brown forest soil (wet) and those of Umihoshi Park, in northern Kyoto Prefecture, were classified into brown forest soil (slightly dry), reddish brown forest soil, and grey soil. It was discovered that the water retention capacity of the soils was greatly influenced by topographical factors. The survey of the soil in the valley of Umihoshi Park showed the gas phase rate was low and water permeability was poor, suggesting that rainfall could easily lead to Horton overland flow.

Keywords: Soil Profile, Hydraulic conductivity, Three phases of distribution, Soil penetration strength, Soil classification

©2021. Japan Geoscience Union. All Right Reserved.

Measurement of Radon Concentration for Earthquake Prediction in the Woods for Field Practice Owned by Sagano H. S.

*Ayaka Kawabata[1], *Takahiro Kawabata[2]

1. Kyoto Prefectural Sagano High School, 2. Graduate School of Science, Osaka University

Radon is a gaseous, radioactive isotope formed in the decay chains of elements such as thorium and uranium. It has been identified that the atmospheric concentration of radon increases before earthquakes because it is released from the ground through cracks caused by the seismic stress.
In the present study, we measured the atmospheric radon concentration in the Woods for Field Studies owned by Sagano High School in order to examine the relationship between earthquakes and the atmospheric radon concentration. We acquired a "Radon Scout Professional" radon detector and tested its performance using two samples containing thorium and uranium. After the test, we placed it in a well-ventilated, water-proof container and installed it in the school forest. The measurements are still on-going. In this presentation, we will report the details of the measurements and our results.

Keywords: Experiment forest, Forest, Earthquake, Radon

©2021. Japan Geoscience Union. All Right Reserved.

[J] Poster | O (Public)：Public

Sun. Jun 6, 2021 1:45 PM - 3:15 PM JST | Sun. Jun 6, 2021 4:45 AM - 6:15 AM UTC | Ch.28

[O-07] Poster presentations by senior high school students

convener:Tatsuhiko Hara(International Institute of Seismology and Earthquake Engineering, Building Research Institute), Katsuyoshi Michibayashi(Department of Earth and Planetary Sciences, Nagoya University), Miwa Kuri(Japan Meteorological Agency), Keiko Konya(Japan Agency for Marine-Earth Science and Technology)

Senior high school students provide poster presentations on subjects in fields of earth and planetary sciences. This session provides an opportunity for senior high school students to give their presentations in the JpGU meeting and to have discussions with researchers. This session has been conducted as a public outreach session since 2006.

[J] Poster | A (Atmospheric and Hydrospheric Sciences)：A-AS Atmospheric Sciences, Meteorology & Atmospheric Environment

Sun. Jun 6, 2021 5:15 PM - 6:30 PM JST | Sun. Jun 6, 2021 8:15 AM - 9:30 AM UTC | Ch.07_2

[A-AS05] Atmospheric Chemistry

convener:Tomoki Nakayama(Graduate School of Fisheries and Environmental Sciences, Nagasaki University), Naoko Saitoh(Center for Environmental Remote Sensing), Sakae Toyoda(Department of Chemical Science and Engineering, Tokyo Institute of Technology), Risa Uchida(Japan Automobile Research Institute)

This session provides a forum for the presentation of the broad spectrum of tropospheric and stratospheric chemistry, including various research topics (e.g., dynamical processes, air quality and climate), approaches (modeling, field measurements, remote sensing, and laboratory studies), and species (gas and aerosol). This session also provides an opportunity for discussing possible future collaboration with other research fields relevant to atmospheric chemistry. We strongly encourage authors to prepare presentation slides and a poster in English.

[AAS05-P01] The Relation between HONO Emission and the Amount of Carbon and Nitrogen Compounds in the Activated Sludge

*Chika Minejima[1], Yuta Orii[1], Ryosuke Fujinuma[1], Toshikazu Suenaga[2], Shohei Riya[2], Akihiko Terada[2], Masayuki Ohyama[4], Norimichi Takenaka[5], Keiichi Sato[3] (1.International Christian University, 2.Tokyo University of Agriculture and Technology, 3.Asia Center for Air Pollution Research (ACAP), 4.Osaka Institute of Public Health, 5.Osaka Prefecture University)

[AAS05-P02] Constraining the origin of tropospheric nitrous acid using triple oxygen isotopes as tracers

*Fumiko Nakagawa[1], Peng Lai[1], Kazuya Hirano[1], Masanori Ito[1], Urumu Tsunogai[1] (1.Graduate School of Environmental Studies, Nagoya University)

[AAS05-P03] Changes in tropospheric nitrogen dioxide vertical column densities over Japan and Korea during the COVID-19 using Pandora and MAX-DOAS

*Yongjoo Choi[1], Yugo Kanaya[1], Hisahiro Takashima[2], Kihong Park[3], Haebum Lee[3], Jihyo Chong[3,4], Jae Hwan Kim[5] (1.Japan Agency for Marine-Earth Science and Technology, 2.Faculty of Science, Fukuoka University, 3.Gwangju Institute of Science and Technology, 4.Environmental Management Division, Yeongsan River Basin Environmental Office, Gwangju 61945, Korea, 5.Pusan National University)

[AAS05-P04] Estimation of emission source of CO from biomass burning observed with ground-based FTIR spectrometers at Tsukuba since 2010

Daisuke Suzuki[2], *Hideaki Nakajima[1,2], Isao Murata[2], Isamu Morino[1] (1.National Institute for Environmental Studies, 2.Graduate School of Environmental Studies, Tohoku University)

[AAS05-P05] Evaluation of NICAM-TM CO data using MOPITT CO data

*Miyajima Hiroshi[1], Naoko Saitoh[1], Yosuke Niwa[2] (1.Center for Environmental Remote Sensing, Chiba University, 2.National Institute for Environmental Studies)

[AAS05-P06] Evaluation of the global chemistry transport model CHASER utilizing TROPOMI formaldehyde measurements

*Hossain Mohammed Syedul Hoque[1], Kengo Sudo[1,3], Hitoshi Irie[2], Takashi Sekiya[3] (1.Graduate School of Environmental Studies, Nagoya University, Japan, 2.Center for Environmental Remote Sensing (CEReS), Chiba University, Japan, 3.Japan Agency for Marine-Earth Science and Technology (JAMSTEC), Yokohama, Japan)

[AAS05-P07] Ozone steady-state at the semi-urban region, Shadnagar, in Southern India

*Vijay Kumar Sagar[1] (1.National Remote Sensing Centre, Hyderabad, ISRO)

[AAS05-P08] A relationship between surface oxidant concentration and daily maximum temperature, and its long-term variability

*Atsushi Shimizu[1], Tatsuya Nagashima[1] (1.National Institute for Environmental Studies)

[AAS05-P09] Analysis of tropospheric ozone budgets in CMIP6 experiments

*Paul T Griffiths[1], Lee T Murray[2], Guang Zeng[3], Vaishali Naik[4], Prodromos Zanis[5], Alexander T Archibald[1] (1.National Centre for Atmospheric Science, Cambridge University, 2.University of Rochester, Rochester, NY, USA, 3.National Institute of Water and Atmospheric Research, Wellington, New Zealand, 4.NOAA Geophysical Fluid Dynamics Laboratory, Princeton, NJ, USA, 5.Department of Meteorology and Climatology, Aristotle University of Thessaloniki, Thessaloniki, Greece)

[AAS05-P10] Study of tropospheric CS_2 photooxidation chemistry

*Yuanzhe Li[1], Kazuki Kamezaki[2], Sebastian Danielache[2] (1.Green Science And Engineering Division, Graduate School Of Science And Technology, Sophia University, 2.Department of Materials & Sciences, Faculty of Science & Technology, Sophia University)

[AAS05-P11] **Effects of hydroxyl radical exposure on chemical composition of secondary organic aerosol formed from sabinene ozonolysis**

*Kei Sato[1,2], Yu Morino[1], Takashi Imamura[1], Yoshizumi Kajii[1,2] (1.National Institute for Environmental Studies, 2.Kyoto University)

[AAS05-P12] Impact of nighttime aging on optical properties of toluene secondary organic aerosol

*Tomoki Nakayama[1], Kei Sato[2], Sathiyamurthi Ramasamy[2], Takashi Imamura[2], Yoshizumi Kajii[3,2] (1.Nagasaki University, 2.NIES, 3.Kyoto University)

[AAS05-P13] Volatility of nanoparticles generated from jet engine lubrication oil

*Nobuyuki Takegawa[1], Anna Nagasaki[1] (1.Graduate School of Science, Tokyo Metropolitan University)

[AAS05-P14] Vertical structural measures of atmospheric pollutants using XU-S

*Kazuyo Yamaji[1], Tetsuya Miyakoshi[2], Satoshi Komatsu[2], Isao Kanda[3] (1.Kobe University, 2.ShinMaywa Industries, Ltd. , 3.Japan Meteorological Corporation)

[AAS05-P15] **Continuous and multi-wavelength measurement of aerosol extinction coefficient by long-path propagation of LED light at Chiba, Japan**

*Ikuya Nishiwaki[1], Hitoshi Irie[2], Nofel D. Lagrosas[1], Hiroaki Kuze[2] (1.Chiba University, 2.Center for Environmental Remote Sensing, Chiba University)

[AAS05-P16] Aerosol type classification of ground-based remote sensing data by k-means clustering

*Hiroyasu Kobayashi[1], Hitoshi Irie[2], Masahiro Momoi[1] (1.Chiba University, 2.Center for Environmental Remote Sensing, Chiba University)

[AAS05-P17] Validation of MERRA-2 Reanalysis Aerosol Products Using Ground-based Observations in Phimai, Thailand, and Factors that Affect Aerosol Optical Depth over the Indochina Peninsula

*Takeru Ohno[1], Hitoshi Irie[1], Arlindo M da Silva[2], Ravi C Govindaraju[2] (1.Center for Environmental Remote Sensing, Chiba University, 2.Global Modeling and Assimilation Office, NASA Goddard Space Flight Center, Greenbelt, Maryland)

[AAS05-P18] Exploring ground-based aerosol optical properties to improve satellite estimates of surface particulate matter concentrations

*Alessandro Damiani[1], Hitoshi Irie[1], Kodai Yamaguchi[1], Hossain Mohammed Syedul Hoque[2], Tomoki Nakayama[3], Yutaka Matsumi[2], Yutaka Kondo[4] (1.CEReS, Chiba University, 2.Nagoya University, 3.Nagasaki University, 4.National Institute of Polar Research)

[AAS05-P19] Development of international air quality and sky research remote sensing (A-SKY) network

*Hitoshi Irie[1], Alessandro Damiani[1], Toshihiko Takemura[2], Thanawat Jarupongsakul[3], Manish Naja[4] (1.Center for Environmental Remote Sensing, Chiba University, 2.Research Institute for Applied Mechanics, Kyushu University, 3.Department of Geology, Faculty of Science, Chulalongkorn University, 4.Aryabhatta Research Institute of Observational Sciences (ARIES))

[AAS05-P20] Prediction of changes in DSS emission using the Earth System Model of the Meteorological Research Institute

*Takashi Maki[1], Taichu Y Tanaka[1], Thomas Sekiyama[1], Mizuo Kajino[1], Naga Oshima[1], Tsuyoshi Koshiro[1] (1.Meteorological Research Institute)

[AAS05-P21] Methane emission trends of China in 2009-2018 induced by atmospheric observations

*Fenjuan Wang[1], Shamil S Maksyutov[1], Rajesh Janardanan[1], Akihiko Ito[2], Isamu Morino[1], Yukio Yoshida[1], Yasunori Tohjima[1], Johannes W. Kaiser[3], Greet Janssens-Maenhout[4], xin Lan[5], Ivan Mammarella[6], Jost V. Lavric[7], Tsuneo Matsunaga[1] (1.NIES National Institute of Environmental Studies, 2.Finnish Meteorological Institute, 3.Deutscher Wetterdienst, 4.European Commission Joint Research Centre, 5.Earth System Research Laboratory, 6.University of Helsinki, 7.Max Planck Institute for Biogeochemistry)

[AAS05-P22] **Characteristics of methane vertical distributions over India**

*Dingkun Zhang[1], Naoko Saitoh[1], Dmitry Belikov[1], Prabir Patra[2], Naveen Chandra[3] (1.Center for Environmental Remote Sensing, Chiba University, 2.Japan Agency for Marine-Earth Science and Technology, 3.National Institute for Environmental Studies)

[AAS05-P23] Temporal and spatial variations of the mole fraction, carbon and hydrogen isotope ratios of atmospheric methane in the Western Pacific region

*Yasuda Mahito[1], Shinji Morimoto[1], Shuji Aoki[1], Ryo Fujita[2], Taku Umezawa[3] (1.Center for Atmospheric and Oceanic Studies, Graduate School of Science, Tohoku University, 2.Department of Climate and Geochemistry Research, Meterorological Reserach Research Institute, Tsukuba Japan, 3.National Institute for Environmental Studies, Tsukuba, Japan)

[AAS05-P24] Variations of atmospheric carbon dioxide and its radioisotope in the arctic region

*Hikaru Sekine[1], Shinji Morimoto[1], Chinatsu Yamada[1], Daisuke Goto[2], Masayo Minami[3], Toshio Nakamura[3], Shuji Aoki[1] (1.Center for Atmospheric and Oceanic studies, 2.National Institute of Polar Research, 3.Institute for Space-Earth Environmental Research)

[AAS05-P25] Preparation of O_2/N_2 dataset from the surface to the middle stratosphere around Japan traceable to NMIJ gravimetric scale

*Shigeyuki Ishidoya[1], Shinji Morimoto[2], Kazuhiro Tsuboi[3], Satoshi Sugawara[4], Daisuke Goto[5], Nobuyuki Aoki[1], Shohei Murayama[1], Yosuke Niwa[6], Shuji Aoki[2], Hidekazu Matsueda[3], Kentaro Ishijima[3] (1.Advanced Industrial Science and Technology, 2.Tohoku University, 3.Meteorological Research Institute, 4.Miyagi University of Education, 5.National Institute of Polar Research, 6.National Institute for Environmental Studies)

[AAS05-P26] Temporal variation of the ozone profile observed with FTIR at Tsukuba

*Isao Murata[1], Hideaki Nakajima[2], Isamu Morino[2], Masanori Takeda[1,2] (1.Graduate School of Environmental Studies, Tohoku University, 2.National Institute for Environmental Studies)

The Relation between HONO Emission and the Amount of Carbon and Nitrogen Compounds in the Activated Sludge

*Chika Minejima[1], Yuta Orii[1], Ryosuke Fujinuma[1], Toshikazu Suenaga[2], Shohei Riya[2], Akihiko Terada[2], Masayuki Ohyama[4], Norimichi Takenaka[5], Keiichi Sato[3]

1. International Christian University, 2. Tokyo University of Agriculture and Technology, 3. Asia Center for Air Pollution Research (ACAP), 4. Osaka Institute of Public Health, 5. Osaka Prefecture University

Introduction & Research Purpose

OH radical is a strong oxidant and an essential component in the earth’ s atmosphere. However, quantification is very difficult because of its extremely high reactivity and low concentrations (Akimoto et al., 2002). Therefore, measuring precursor concentrations of OH radical is used to estimate its concentration. Gaseous nitrous acid, HONO, is one of the major OH precursors (Kleffmann, 2007).

$HONO + h\nu\ (\lambda < 400nm) \rightarrow NO + OH$

Despite the importance of HONO, its source is still not well understood. Soil was suggested as one of the missing sources (Su et al., 2011); thus, we use activated sludge to surrogate soil as it contains various organisms the same as any soil. Activated sludge is used in most of wastewater treatment plants. This study aims to elucidate the relation between HONO emission under aerobic conditions with carbon content, nitrogen content, and concentrations of inorganic nitrogen species such as NH_4^+, NO_2^-, and NO_3^-.

Experiments and Results

HONO fluxes from activated sludge were measured every 3 hours during daytime (AM9:00~PM6:00), October 6th, 2020 to 9:00, October 8th, 2020 using the filter pack method and ion chromatography. The measurement was started from the point of feeding the activated sludge. The filter pack was replaced every 3 hours. At night, samples were taken continuously for 15 hours from PM6:00 to AM9:00. Non-Purgeable Organic Carbon (NPOC) as carbon content and Total Nitrogen (TN) were also measured at the same time using TOC instrument (SHIMADZU TOC-V CSH). Secondly, NH_4^+, NO_2^-, NO_3^-, NPOC and TN concentration measurement was tried from the time of feeding on a separate day in order to find the change in chemical forms of nitrogen.

The result suggests that the HONO flux has strong relation with the carbon content under aerobic conditions. Further details will be discussed at the presentation.

Keywords: nitrous acid, activated sludge, soil

©2021. Japan Geoscience Union. All Right Reserved.

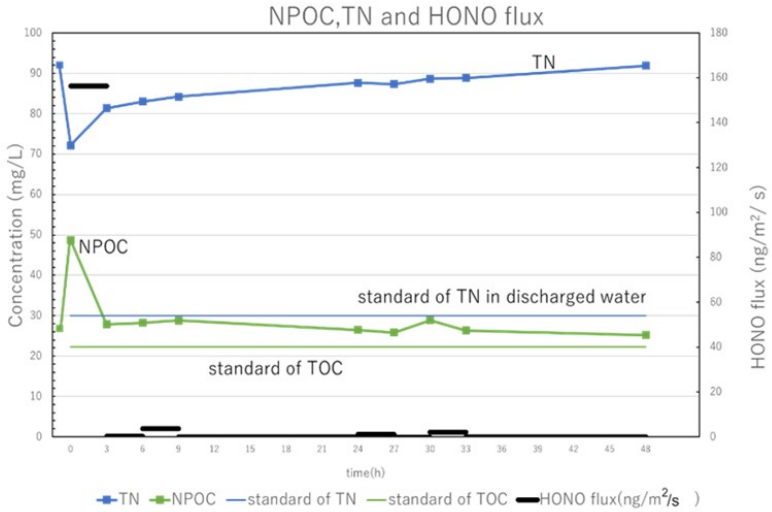


Figure 1. Time series of HONO fluxes, Carbon content (Non-Purgeable Organic Carbon (NPOC)) and Total Nitrogen (TN). Standards of Total Organic Carbon (TOC) and TN indicate the concentrations of TOC and TN in the released water from a wastewater treatment plant in Tokyo (TOC 22.2 mg/L, TN 30 mg/L). Feeding time was at the hour 0.

©2021. Japan Geoscience Union. All Right Reserved.

Constraining the origin of tropospheric nitrous acid using triple oxygen isotopes as tracers

*Fumiko Nakagawa[1], Peng Lai[1], Kazuya Hirano[1], Masanori Ito[1], Urumu Tsunogai[1]

1. Graduate School of Environmental Studies, Nagoya University

The photolysis of nitrous acid (HONO) has been recognized as a potentially important source of OH radicals, which is known as a major oxidant in the atmosphere removing reductive trace gases such as methane and NMHCs. Atmospheric HONO originates from both primary sources (direct emissions) and secondary sources (chemical formation in the atmosphere), however, their contributions to the atmospheric HONO production have not been well understood. Here, we determined a $\Delta^{17}O$ value of HONO together with $\Delta^{17}O$ value of $NO_2$and NO, because $\Delta^{17}O$ value of HONO produced via “secondary formation” is expected to have highly positive values as those of NO_2, while no $\Delta^{17}O$ anomaly should be observed for HONO which is emitted directly from various sources on the ground, making it possible to quantify their contribution to the atmospheric HONO production with $\Delta^{17}O$ measurement.

$\Delta^{17}O$ values of HONO, $NO_2$and NO was determined by combining sensitive determination method on isotope compositions of NO_2^-(Komatsu *et al.*, 2008; Tsunogai *et al.*, 2010) with a slightly modified filter-pack method (Noguchi *et al.*, 2007), in which HONO, $NO_2$and NOxwere collected as NO_2^-on alkaline (K_2CO_3) impregnated filter, triethanolamine (TEA)-coated filter, and mixture of 2-Phenyl-4,4,5,5-tetramethylimidazoline-3-oxide-1-oxyl (PTIO) and TEA-coated filter, respectively. Atmospheric HONO, $NO_2$and NO were collected at Nagoya University, which is located in a suburban area of Nagoya City. The sample collection period was fixed to three days with a flow rate of 10 L/min for HONO or $NO_2$and 1 L/min for NO, respectively.The $\Delta^{17}O$ values of $NO_2$and HONO showed similar diurnal variations; higher value on the day time than the night time. The result suggests that the atmospheric HONO is formed mainly by both direct emission and chemical reaction of NO_2 in the urban atmosphere.

Keywords: nitrous acid, triple oxygen isotopes, urban air, nitrogen dioxide, nitrogen monoxide

©2021. Japan Geoscience Union. All Right Reserved.

Changes in tropospheric nitrogen dioxide vertical column densities over Japan and Korea during the COVID-19 using Pandora and MAX-DOAS

*Yongjoo Choi[1], Yugo Kanaya[1], Hisahiro Takashima[2], Kihong Park[3], Haebum Lee[3], Jihyo Chong[3,4], Jae Hwan Kim[5]

1. Japan Agency for Marine-Earth Science and Technology, 2. Faculty of Science, Fukuoka University, 3. Gwangju Institute of Science and Technology, 4. Environmental Management Division, Yeongsan River Basin Environmental Office, Gwangju 61945, Korea, 5. Pusan National University

Using the measurements from ground-based remote sensing instruments, we investigated the changes in tropospheric nitrogen dioxide vertical column densities (NO_2 TropVCD) over Japan and Korea before and after the COVID-19 pandemic. Three sites for MAX-DOAS (Yokosuka, Cape Hedo, and Gwangju) and one site for Pandora (Busan) were selected for this study because these sites have been in operation for more than five years, allowing the results caused by COVID-19 in 2020 to be compared with previous reference years, 2015–2018 (2016–2018 for Busan) and 2019. To elucidate the relationship of NO_2 TropVCD with human activity during 2020, Google mobility data was also used as a proxy of transportation and industry activity. Because the behavior of NO_2 also depends on the meteorological variables, we also investigated the difference in meteorological fields from ERA5 along with spatial distribution of NO_2 TropVCD from Ozone Monitoring Instrument (OMI) satellite. During the Chinese New Year holidays, the NO_2 TropVCDs at three urban sites showed a rapid decrease due to less business and industry activities, then the level of NO_2 VCD slowly recovered but was consistently lower than the level of before the Chinese New Year holidays due to shorten NO_2 lifetime or low emission rate. During the periods of spontaneous social distancing in Korea (March–May) and Japan (April–May), decreasing activities of transportation and industry, especially in Japan, was obvious. NO_2 TropVCD in Busan and Gwangju showed a moderate correlation with the industrial sector, whereas that in Yokosuka showed moderate correlation with both the transportation and industrial sector. The monthly difference between reference years and 2020 showed that the average reduction in three urban sites was pronounced in May to September with high mean normalized bias (MNB; −48% to −32%) compared to the cold season (−27% to −11%). The difference in monthly variation of NO_2 TropVCD with reference years will be discussed in terms of meteorological variables, such as wind speed, temperature, and downward UV radiation.

Keywords: Tropospheric nitrogen dioxide vertical column densities , MAX-DOAS, Pandora, COVID-19

©2021. Japan Geoscience Union. All Right Reserved.

Estimation of emission source of CO from biomass burning observed with ground-based FTIR spectrometers at Tsukuba since 2010

Daisuke Suzuki[2], *Hideaki Nakajima[1,2], Isao Murata[2], Isamu Morino[1]

1. National Institute for Environmental Studies, 2. Graduate School of Environmental Studies, Tohoku University

Carbon monoxide (CO) is mainly produced by fossil fuels burning, biomass burning, and oxidization of hydrocarbons. CO is a precursor of tropospheric ozone generation and is an extremely important substance in atmospheric chemistry because it affects the abundance of various atmospheric trace components by reacting with OH radicals. It has a lifespan of several weeks to two months in the atmosphere, and there is a large regional ununiformity in its abundance and source. In recent years, it has been found that the emission of CO from the Asian region has a great influence on the global concentration, and it is desired to improve the estimation of its source. In Tsukuba (36.1N, 140.1E), since December 1998, we have been observing atmospheric trace components using solar infrared spectra with Bruker's high-resolution Fourier transform infrared spectrometer (FTIR). In this study, in order for clarifying the source of CO measured above Tsukuba, the altitude distribution of CO and hydrogen cyanide (HCN) was derived from the infrared spectra obtained by this FTIR. In this analysis, the source of CO was estimated using CO-HCN correlation. HCN has a lifetime of several years in the atmosphere and is mainly produced by biomass combustion. In this analysis, HCN was used as a proxy for biomass combustion.

For the period from April 2010 to May 2019, the altitude distribution of CO and HCN was analyzed from the observed spectra of FTIR in Tsukuba using the inversion analysis program of SFIT4. For the obtained altitude distribution, the partial column amounts of CO and HCN in the two layers 0-5 km and 5-18 km were obtained, and the correlations between them were analyzed. As a result, a significant positive correlation was confirmed between CO and HCN column amount at 5-18 km in spring. From the CO/HCN ratio obtained from the correlation analysis, the ratio of biomass combustion-derived CO in the atmospheric CO partial column was calculated, and the average value from March to May was about 70%. In addition, the air mass observed by FTIR in this season was subjected to backward trajectory analysis using METEX. We extracted cases where those air mass trajectories passed within 100 km from the forest fire observed by the MODIS sensor onboard the satellites Terra/Aqua. At an altitude of 5-18 km in the spring, the extracted trajectories mainly originated from northeastern China to the Eurasian continent. The results suggest that the observed enhanced CO over Tsukuba may have originated from forest fires in the area of latitude 50-60 N.

Keywords: carbon monoxide, Fourier transform infrared spectrometer , hydrogen cyanide, biomass burning, trajectory analysis, FTIR

©2021. Japan Geoscience Union. All Right Reserved.

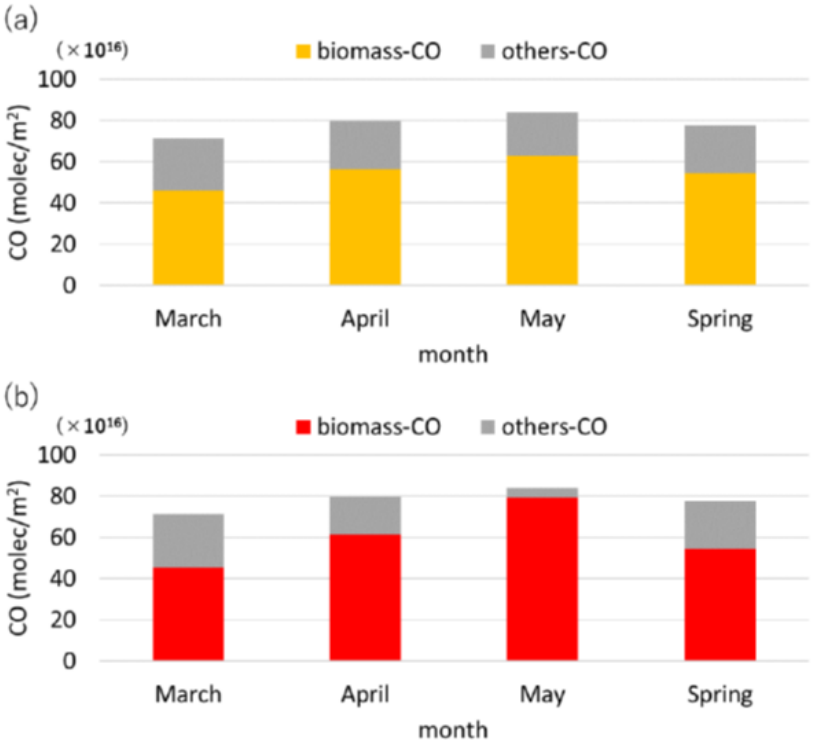


図１．高度5-18 km、バイオマス燃焼起源COのパーシャルカラム量。(a) すべての月のCO/HCN Biomass比に、春季の回帰直線の傾きの値を使用。(b) 各月のCO/HCN Biomass比に、各月の回帰直線の傾きの値を使用

Figure 1. Biomass burning-origin CO partial column for 5-18 km. (a) Calculated by annual averaged CO/HCN ratio and spring residual line's slope. (b) Calculated by monthly CO/HCN ratio and monthly residual line's slope.

©2021. Japan Geoscience Union. All Right Reserved.

Evaluation of NICAM-TM CO data using MOPITT CO data

*Miyajima Hiroshi[1], Naoko Saitoh[1], Yosuke Niwa[2]

1. Center for Environmental Remote Sensing, Chiba University, 2. National Institute for Environmental Studies

Carbon monoxide (CO) in the atmosphere is produced by incomplete combustion of carbonaceous materials and oxidation of hydrocarbons; biomass burning is one of the major sources of CO in the atmosphere. The main sink of atmospheric CO is a reaction with hydroxyl radical (OH). The lifetime of tropospheric CO is around two months, which results in its longer transport in hemispheric scale.

This study has compared CO concentrations simulated by Nonhydrostatic Icosahedral Atmospheric Model-based Transport Model (NICAM-TM) with CO concentrations observed by Measurement of Pollution In the Troposphere (MOPITT) on board the Terra satellite. Here, we have compared MOPITT CO data with NICAM-TM CO data with and without applying MOPITT CO averaging kernel functions (AK).

In the lower troposphere (850 hPa), NICAM-TM CO was lower than MOPITT CO in most regions except active biomass burning areas. NICAM-TM CO was significantly lower in the middle latitudes (30º–60ºN) where there are large anthropogenic CO emissions; the negative bias of NICAM-TM CO data against MOPITT CO data was about 30%. This implies the possibility of the underestimation of anthropogenic emissions in the NICAM-TM CO simulations. In the upper troposphere (250 hPa), NICAM-TM CO was lower than MOPITT CO in almost all regions; the negative bias of upper tropospheric NICAM-TM CO data was about 30% in low and mid-latitudes in both hemispheres in spring season.

In addition, seasonal variations in NICAM-TM CO data were much lower than those in MOPITT CO data in the upper troposphere. MOPITT CO there was largest in mid-latitude in spring and the differences between MOPITT and NICAM-TM CO was also largest in spring of all the season; these differences were also evident after applying MOPITT CO AK to NICAM-TM CO data. Comparisons with MOPITT CO data suggest that the negative bias in NICAM-TM CO data in the upper troposphere can be partly attributed to the underestimation of anthropogenic emissions and transport process from the surface to the upper troposphere in the NICAM-TM CO simulations.

Keywords: CO, satellite remote sensing, transport model

©2021. Japan Geoscience Union. All Right Reserved.

Evaluation of the global chemistry transport model CHASER utilizing TROPOMI formaldehyde measurements

*Hossain Mohammed Syedul Hoque[1], Kengo Sudo[1,3], Hitoshi Irie[2], Takashi Sekiya[3]

1. Graduate School of Environmental Studies, Nagoya University, Japan, 2. Center for Environmental Remote Sensing (CEReS), Chiba University, Japan, 3. Japan Agency for Marine-Earth Science and Technology (JAMSTEC), Yokohama, Japan

Tropospheric Monitoring Instrument (TROPOMI) has been providing observations of important atmospheric pollutants with an unprecedented horizontal resolution (~7×3.5 km^2) since August 2017. Such high-resolution global observations offer a unique opportunity to evaluate regional and global models at higher precision. In this study, TROPOMI formaldehyde (HCHO) measurements from June to December 2019 are used to evaluate the HCHO simulations from the global chemistry transport model CHASER-V4 (based on MIROC 5). In the evaluation's initial steps, the averaging kernel information from the TROPOMI HCHO measurements is applied to the CHASER HCHO. Overall, the CHASER simulations captured the observed global spatial variation of HCHO well, with a correlation coefficient (R) ~0.70. On a global scale, the mean bias error (CHASER –TROPOMI) and the root mean square error is -0.23 $\times 10^{16}$ and 0.31 $\times 10^{16}$ molecules cm^{-2}, respectively. The R values over eastern China, eastern and western US, and South America were ~ 0.9, indicating excellent agreement between the datasets. A negative correlation was observed over India and Southeast Asia during the monsoon season (June –August). One of the potential reasons for such disagreement could be the intense wet deposition of HCHO during the monsoon months, which the model might not capture well. However, previous studies reported that CHASER reproduced the OMI (Ozone Monitoring Instrument) nitrogen dioxide columns over India very well, including the monsoon season. Moreover, the lower TROPOMI HCHO columns over India and Southeast Asia during the monsoon are consistent with the ground-based MAX-DOAS (multi-axis differential optical absorption spectroscopy) HCHO observations in India and Thailand. Thus, the reason for the disagreement between CHASER and TROPOMI HCHO columns over India and Southeast Asia during the monsoon is not apparent yet. Other potential causes such as sources of HCHO other than biogenic emissions, high and low NOx conditions, etc., are required to be investigated.

Keywords: CHASER , TROPOMI , Formaldehyde (HCHO)

©2021. Japan Geoscience Union. All Right Reserved.

Ozone steady-state at the semi-urban region, Shadnagar, in Southern India

*Vijay Kumar Sagar[1]

1. National Remote Sensing Centre, Hyderabad, ISRO

The photo steady-state (PSS, $\phi=1$) of ozone (O_3) is considered when the production of O_3 (PO3) and sink of O_3 (S_{O3}) are in equilibrium. In the PSS, O_3 forms when NO_2 is destroyed and reform fast after reaction with O_3 in the sunlight. A hypothetical photo-stationary state (HPPS) can be assumed when the rate change of ozone balances with its net production (P_{netO3}) and net transport (T_{netO3}) in and out of small volume around the monitoring. The transport process is difficult to address without the set of spatial concentrations measurement, emissions inventories, and meteorological data for chemistry-transport modeling. Therefore the HPPS can be considered. However, detailed chemical observation and chemical transport models are used to study ozone production and its transport. In the real atmosphere, $\phi<1$ represents the involvement of transport and $\phi>1$ represents the involvement of peroxy radicals which converts NO to NO_2.
The Ozone concentration in PSS and HPPS framework were studied. The continuous observation of NO, NO_2, O_3 concentrations with a temporal resolution of 1 minute was hourly averaged during the August 2014 to April 2017 period. The hourly values of J_{NO2} were calculated using the radiative transfer model Tropospheric Ultraviolet and Visible (TUV) model. The average difference between the O_3 and O_{3HPPS} was observed 4.08 ppb while the difference between O_3 and O_{3pss} was observed -0.16 ppb in the daytime between 06:00 to 18:00 hours local through the study period. The net local transport was found at 52.78 ppb/h at the same time. The ozone that was transported was supported due to its long lifetime at the site. The study suggests that the site was ozone sink prominent and the ozone was transported at the site to balance the observed ozone throughout the study period.

©2021. Japan Geoscience Union. All Right Reserved.

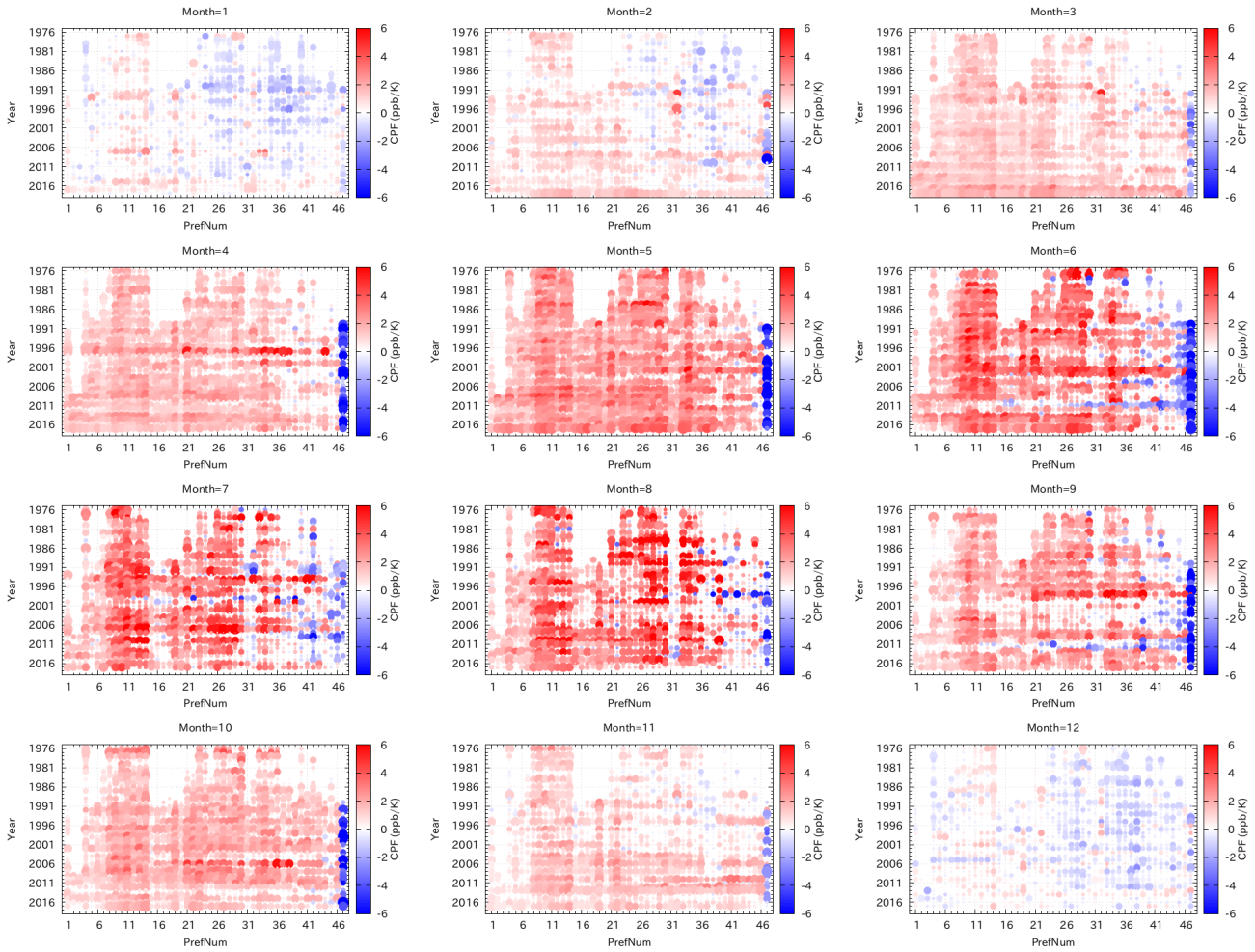
A relationship between surface oxidant concentration and daily maximum temperature, and its long-term variability

*Atsushi Shimizu[1], Tatsuya Nagashima[1]

1. National Institute for Environmental Studies

The climate penalty factor (CPF) for each prefecture and each month in last 42 years in Japan were estimated from mean 8 hours maximum surface oxidant and daily maximum temperature observations, and compared with CPF calculated by chemical transport model CMAQ. Opposite to general tendency of positive CPF all over Japan, negative CPF was confirmed in western part of Japan during winter. Large positive CPF was found during June and August around urbanized areas (Kanto and Kinki). Sporadic perturbations were dominant in several years/months. Horizontal variations of CPF calculated by CMAQ were dependent on the horizontal grid scale.

Keywords: oxidant, maximum temerature, climate penalty factor



©2021. Japan Geoscience Union. All Right Reserved.

Analysis of tropospheric ozone budgets in CMIP6 experiments

*Paul T Griffiths[1], Lee T Murray[2], Guang Zeng[3], Vaishali Naik[4], Prodromos Zanis[5], Alexander T Archibald[1]

1. National Centre for Atmospheric Science, Cambridge University, 2. University of Rochester, Rochester, NY, USA, 3. National Institute of Water and Atmospheric Research, Wellington, New Zealand, 4. NOAA Geophysical Fluid Dynamics Laboratory, Princeton, NJ, USA, 5. Department of Meteorology and Climatology, Aristotle University of Thessaloniki, Thessaloniki, Greece

A grand challenge in the field of chemistry-climate modelling is to understand the connection between anthropogenic emissions, atmospheric composition and the radiative forcing of trace gases and aerosols. The AerChemMIP model intercomparison project, part of CMIP6, focuses on calculating the radiative forcing of gases and aerosol particles over the period 1850 to 2100.

We present an analysis of the trends in tropospheric ozone budget in UKESM1 and other models from CMIP6 experiments. We discuss these trends in terms of chemical production and loss of ozone as well as physical processes such as transport and deposition. Where possible, AerChemMIP attribution experiments such as histSST-piCH4, will be used to quantify the effect of individual emissions and forcing changes on the historical ozone burden and budget. For future experiments, we focus on analogous experiments from the SSP3-70 scenario, a ‘regional rivalry’ shared socioeconomic pathway involving significant emissions changes.

Keywords: ozone, tropospheric, ozone budget

©2021. Japan Geoscience Union. All Right Reserved.

Study of tropospheric CS_2 photooxidation chemistry

*Yuanzhe Li[1], Kazuki Kamezaki[2], Sebastian Danielache[2]

1. Green Science And Engineering Division, Graduate School Of Science And Technology, Sophia University, 2. Department of Materials & Sciences, Faculty of Science & Technology, Sophia University

Abstract

Carbon disulfide (CS_2) is an atmospheric trace gas whose main sources in the atmosphere are from oceans and soils (Khalil et al., 1984). Anthropogenic emissions have increased in recent years, producing a strong regional distribution. CS_2 is a reactive atmospheric sulfur gas, and as such it has a relatively short lifetime, ranging from a few days to half a month (Khan et al., 2017). Its oxidation end products in the atmosphere are carbonyl sulfide (COS) and sulfur dioxide (SO_2). Therefore, CS_2 indirectly contributes to the production of sulfate aerosols, which influence atmospheric radiative properties and stratospheric ozone depletion.

The OH-initiated oxidation of CS_2 in the presence of O_2 is considered to be the main CS_2 sink pathway. By forming an intermediate SCSOH at first, followed by a series of oxidation reactions with O_2 to produce COS and SO_2, this process removes 75~88% of atmospheric CS_2 (Khan et al., 2017). The current literature suggests that the conversion ratio of CS_2 to COS is 0.83 (Stickel et al., 1993), but this result may be underestimated because only reaction with OH radicals considered and CS_2 photochemistry is neglected.

The mechanism of CS_2 photooxidation was first proposed by Wine et al. (1981). According to the CS_2 UV-Vis absorption spectrum, there is a strong absorption band at 280~360 nm, which would first photo excite CS_2 from ground state to $CS_2(^3A_2)$ state (usually presented as CS_2^* state). Then the majority of CS_2^* particles will be de-excited into CS_2 ground state molecules after collision with air molecules (N_2, O_2 and H_2O). Because of the rapid photochemical reaction rate of CS_2, a small portion of CS_2^* is oxidized with O_2 to produce COS and SO_2 during the pseudo-steady state process of continuous CS_2 photo excitation reaction and CS_2^* quenching reaction. In addition, the solar flux spectrum in the troposphere is strong enough to trigger the above CS_2 photochemistry.

In this study, an updated CS_2 photochemical network is studied by a 1-D atmospheric photochemical model (PATMO). Reaction path analysis is carried out using an open-source reaction network viewer (ReNView). From the simulated result, major reduced sulfur species (CS_2, COS and SO_2) reproduce field measurements. When the zenith angle of sunlight is 0°, our result shows that the conversion ratio of CS_2 to COS is 0.87. The reaction rate *r* for the net CS_2 photo-induced oxidation and CS_2 + OH reactions at 1 km are about 18 and 144 molecule cm^{-3} s^{-1} respectively. These results indicate that, under favorable light conditions photochemistry is a relevant tropospheric sink of CS_2.

References

Khalil, M. and Rasmussen, R. (1984). Global sources, lifetimes and mass balances of carbonyl 761 sulfide (OCS) and carbon disulfide (CS_2) in the earth’ s atmosphere. *Atmospheric Environment 762 (1967)*, 18(9):1805–1813.

©2021. Japan Geoscience Union. All Right Reserved.

Khan, A., Razis, B., Gillespie, S., Percival, C., Shallcross, D., Global analysis of carbon disulfide (CS2) using the 3-D chemistry transport model STOCHEM, *Aims Environ. Sci. (2017)*, *4*, 484–501.

Stickel, R. E. *et al.* (1993), *Journal of Physical Chemistry*, 97(51), pp. 13653–13661.

Wine, P. H., Chameides, W. L., Ravishankara, A. R., Potential role of CS2 photooxidation in tropospheric sulfur chemistry, *Geophys. Res. Lett. (1981)*, *8*, 543-546.

Keywords: CS2, Photochemistry, Modeling, PATMO, Sulfur chemistry

©2021. Japan Geoscience Union. All Right Reserved.

Effects of hydroxyl radical exposure on chemical composition of secondary organic aerosol formed from sabinene ozonolysis

*Kei Sato[1,2], Yu Morino[1], Takashi Imamura[1], Yoshizumi Kajii[1,2]

1. National Institute for Environmental Studies, 2. Kyoto University

Sabinene, a bicyclic monoterpene with an exocyclic double bond, is a major monoterpene emitted from Japanese cedar. We investigated OH initiated aging of secondary organic aerosol (SOA) formed from sabinene ozonolysis using a laboratory environmental chamber. SOA mass concentration and f43 and f44 ratios of SOA were monitored by an Aerodyne high-resolution time-of-flight aerosol mass spectrometer, where f43 and f44 are the ratios of *m/z* 43 and *m/z* 44 to total SOA mass, respectively. SOA mass concentration increased immediately after SOA was exposed to OH radicals due to photochemical aging. The f43 ratio, attributed to alcohols, carbonyls, and peroxides, increased only immediately after the start of exposure, whereas the f44 ratio, attributed to carboxylic acids, continuously increased during the exposure. Offline SOA samples collected before and after the exposure to OH radicals were analyzed by a liquid chromatograph negative-mode electrospray ionization mass spectrometer. Major products present in the particle phase were monomeric products, $C_{8\text{-}10}H_{12\text{-}18}O_{3\text{-}6}$, and dimeric products, $C_{17\text{-}19}H_{26\text{-}32}O_{7\text{-}9}$. Monomeric products include sabinic acid, norsabinic acid, and sabinalic acid as reported in previous studies. As a result of exposure to OH radicals highly functionalized eight to nine carbon products increased, whereas dimeric products decreased. Formation of highly functionalized products will be explained by gas phase OH initiated reaction of sabinaketone and nine carbon lactones, major gaseous products formed from sabinene ozonolysis. Decrease in dimeric products will be explained by decomposition of dimeric products due to OH initiated oxidation in the particle phase.

Keywords: Air pollution, Fine particulate matter, Biogenic volatile organic compound, Highly oxygenated molecule, Volatility basis-set model, Intramolecular hydrogen shift

©2021. Japan Geoscience Union. All Right Reserved.

Impact of nighttime aging on optical properties of toluene secondary organic aerosol

*Tomoki Nakayama[1], Kei Sato[2], Sathiyamurthi Ramasamy[2], Takashi Imamura[2], Yoshizumi Kajii[3,2]

1. Nagasaki University, 2. NIES, 3. Kyoto University

Toluene is known as an important precursor of anthropogenic secondary organic aerosol (SOA) in the troposphere. In the atmosphere, toluene is mainly oxidized by OH radical to generate gaseous oxidation products in addition to SOA. Whereas OH aging of the toluene-SOA will be negligible under dark conditions after sunset, a part of these oxidation products in gas-phase and/or SOA can be further oxidized with NO_3 or O_3 even in the nighttime. The SOA generated during OH oxidation of toluene in the presence of NO_x is known to have significant light absorption at the ultraviolet and shorter visible wavelengths (*i.e.*, known as brown carbon) [*e.g.*, Nakayama et al. 2013] and possibly contributes to the radiation balance and photochemical reactions in the atmosphere. In this work, the impact of NO_3 and O_3 aging on wavelength-dependent optical properties of the toluene SOA has been studied.

The SOA was generated during OH oxidation of toluene in the absence of NO_x in a 6 m^3 stainless steel photochemical chamber with Teflon coating. As sources of OH, either of photolysis of H_2O_2 or ozonolysis of tetramethylethylene was used. After enough amounts of SOA were generated, N_2O_5 (precursor of NO_3), O_3, or NO_2 was injected to the chamber under dark conditions. The NO_2 injection experiment was conducted to confirm the possible effects of NO_2 reactions, because both of NO_3 and NO_2 were generated during thermal decomposition of N_2O_5. Temporal variations of the optical properties of the SOA were measured by two photoacoustic spectrometers (absorption and scattering at 375, 405, 532, 781 nm) and a cavity ring-down spectrometer (extinction at 532 nm). Chemical properties and size distributions of SOA were measured by an Aerodyne aerosol mass spectrometer and a scanning mobility particle sizer, respectively. Gaseous reactants and products were monitored by a Fourier transform-infrared spectrometer and a proton transfer reaction time-of-flight mass spectrometer.

Mass concentrations of toluene-SOA were significantly enhanced and nitrocresols and nitrosalicylic alcohols were generated after NO_3 aging, but no clear enhancement was observed after O_3 aging [Ramasamy et al. 2019]. The toluene-SOA did not show light absorption properties at all wavelengths studied before NO_3 or O_3 aging. Significant light absorption was observed after NO_3 aging at 375 and 405 nm, but neither O_3 nor NO_2 additions. Nitro-aromatic compounds such as nitrocresols and nitrosalicylic alcohols generated from cresols during NO_3 aging are considered to be responsible for the observed light absorption. In the presentation, the atmospheric implications of the results will also be discussed.

References

Nakayama, T. et al., Wavelength and NO_x dependent complex refractive index of SOAs generated from the photooxidation of toluene, *Atmos. Chem. Phys.*, 13, 531-545, doi:10.5194/acp-13-531-2013 (2013).
Ramasamy, S. et al., Investigation of dark condition nitrate radical- and ozone-initiated aging of toluene secondary organic aerosol: Importance of nitrate radical reactions with phenolic products, *Atmos. Environ*., 219, 117049, doi:10.1016/j.atmosenv.2019.117049 (2019).

Keywords: Toluene, Secondary organic aerosol, Optical properties, Brown carbon

©2021. Japan Geoscience Union. All Right Reserved.

Volatility of nanoparticles generated from jet engine lubrication oil

*Nobuyuki Takegawa[1], Anna Nagasaki[1]

1. Graduate School of Science, Tokyo Metropolitan University

The characterization of particle emissions from jet aircraft equipped with turbofan engines is an important issue in the assessment of the impacts of aviation on climate and human health. The primary importance of aviation-produced aerosol particles in assessing the climate impacts is the formation of contrail cirrus clouds from black carbon (BC) emitted at aircraft cruising altitudes. In the method for measuring non-volatile particles (assumed to be equivalent with BC) from turbofan engines, a volatile particle remover (VPR) heated to 623 K is generally used to vaporize volatile compounds such as sulfate and organics. Tetracontane (n-$C_{40}H_{82}$) is used as a test compound for evaluating the removal efficiency of volatile particles in VPRs. Recent studies showed that the formation of nanoparticles from jet engine lubrication oil could be an important source of aerosol particles in aircraft emissions under real-world operating conditions (e.g., Fushimi et al. Atmos. Chem. Phys., 19, 6389-6399, 2019). The volatility of nanoparticles composed of jet engine lubrication oil has not been well characterized. The purpose of this study is to investigate the volatility of nanoparticles generated from unburned jet engine lubrication oil (Mobil Jet Oil II) and compare it with those from triacontane (n-$C_{30}H_{62}$) and tetracontane. The particle number fraction remaining downstream of a custom-made evaporation tube was measured for particle diameters of 30 and 50 nm. The temperature of the evaporation tube was varied from room temperature to 673 K, and the temperature dependency of the particle number fraction for jet engine lubrication oil, triacontane, and tetracontane particles was investigated. The results from the laboratory experiments were used for the interpretation of the volatility of aircraft exhaust particles under real-world operating conditions observed at Narita International Airport.

Keywords: Aerosol, Aircraft emission, Jet engine lubrication oil

©2021. Japan Geoscience Union. All Right Reserved.

Vertical structural measures of atmospheric pollutants using XU-S

*Kazuyo Yamaji[1], Tetsuya Miyakoshi[2], Satoshi Komatsu[2], Isao Kanda[3]

1. Kobe University, 2. ShinMaywa Industries, Ltd. , 3. Japan Meteorological Corporation

Vertical profiles of meteorological properties and atmospheric pollutant concentrations and these diurnal patterns were collected by using XU-S (Experimental Unmanned / Utility aircraft by ShinMaywa) over the northeast side of Awaji Island faced to the Osaka bey on early December, 2020, under a drone utilization promotion project by Hyogo prefecture and the New Industry Research Organization.In the early morning of 2nd December, monitoring data of the ground site indicated more chill and ground surface NO and NO_2 concentrations were increased, on the other hand, Oxidant (Ox) concentration became lower in comparison with the other days. Diurnal vertical profiles of O_3 and $PM_{2.5}$ concentrations and meteorological parameters were measured by POM (Personal Ozone Monitor), p-sensor, iMet-XQ2 mounted on XU-S, respectively. In the monitoring launched at 7:00 on 2nd December, atmospheric temperature profile suggested that the ground inversion layer was developed until around 50-100m alt. Meanwhile, O_3 concentrations were very low, less than 10 ppbv up to 50 m alt., but 20-40 ppbv in 50-500 m layers. $PM_{2.5}$ concentrations were around 13 mg/m^3 on the surface and were decreased to around 5 mg/m^3 in the upper layers from 50 m alt. Primary pollutants were trapped in the developed ground inversion layer within 50 m alt., where O_3 concentrations were depressed through the process of the NO titration until the early morning. During the second monitoring launched at 11:00, constructed atmospheric vertical gradient started to be disappearing and the vertical O_3 and $PM_{2.5}$ concentrations were close to constant values up to 500 m alt., respectively. In the afternoon, the atmospheric vertical gradient was mostly disappeared. Comparisons between observed and simulated vertical and diurnal profiles will be conducted to understand the uncertainties of simulated O_3.

Keywords: vertical profiles of atmospheric pollutants, vertical observations by using the fixed-wing unmanned aircraft, ozone, PM2.5

©2021. Japan Geoscience Union. All Right Reserved.

Continuous and multi-wavelength measurement of aerosol extinction coefficient by long-path propagation of LED light at Chiba, Japan

*Ikuya Nishiwaki[1], Hitoshi Irie[2], Nofel D. Lagrosas[1], Hiroaki Kuze[2]

1. Chiba University, 2. Center for Environmental Remote Sensing, Chiba University

It is well recognized that aerosols play a critical role in determining the Earth's radiation budget. Nevertheless, the accurate estimate of their direct and indirect radiative forcing is still challenging due to the complexity of their behavior in the ambient atmosphere. Ground-based remote sensing and optical observations have been conducted to characterize aerosol properties. A sunphotometer has widely been used for measuring the optical thickness of aerosols, but their data availability can be affected by clouds and time (usually daytime only). On the other hand, a visibility meter can provide visibility data and, consequently, aerosol extinction data even under cloudy conditions, whereas its operation is limited to a single wavelength (e.g., 875 nm). A nephelometer can provide aerosol scattering coefficients at multiple wavelengths, though the data often need corrections due to the relative humidity difference between the ambient and instrumental conditions. Under this circumstance, this study proposes a long-path measurement of aerosol extinction coefficients using a three-color, light-emitting diode (LED) light source emitting at 405, 455, and 505 nm. This approach realizes continuous and multi-wavelength observation (both day and night) of aerosol extinction coefficients near the ground surface level. A near-horizontal light path with a round-trip distance of around 600 m has been established inside the campus of Chiba University. A Newtonian telescope with a diameter of 130 mm collimates the LED light and directs it to a retro-reflector set up about 300 m away from the LED. The reflected light is condensed by a 130 mm diameter Newtonian telescope, and the light emitted from the eyepiece is introduced to the center of the optical fiber and detected by a UV-visible spectrometer. To remove background signals especially during the daytime, a square wave modulation to the LED light source is applied. Using this method, background signals are collected when the LED is off. These background signals are subtracted from the signals when the LED is on. With this instrument, test observations were performed from November 27 to December 5, 2020, together with a visibility meter (Vaisala, PWD52), a nephelometer (TSI3563), and a weather monitor. As expected, the raw signal was found to be directly proportional to the visibility but inversely proportional to the scattering coefficient and relative humidity. The extinction coefficient calculated from the visibility using the Koschmeider equation was compared with that derived from our instrument (at 505 nm). While the data from the visibility meter ranged up to 0.0006 km-1[LND1], our instrument indicated significant underestimation. However, their temporal variations were highly correlated (R = 0.88). This also implies that by using the long-path LED light, extinction coefficients for higher visibility (> 35 km) can be estimated.

Keywords: aerosol extinction coefficient, spectrometer, LED

©2021. Japan Geoscience Union. All Right Reserved.

Aerosol type classification of ground-based remote sensing data by k-means clustering

*Hiroyasu Kobayashi[1], Hitoshi Irie[2], Masahiro Momoi[1]

1. Chiba University, 2. Center for Environmental Remote Sensing, Chiba University

Aerosols, microscopic particles suspended in the air, are known to affect climate through their direct effects of scattering and absorbing solar radiation and indirect effects of altering the radiation budget via the role of cloud condensation nuclei. Since the effects on climate are different depending on the type of aerosols, it is important to classify the observation data into aerosol types. SKYNET is an international ground-based remote sensing observation network focusing mainly on aerosol observations by the skyradiometer. Data from more than 100 observation sites are available. This study attempts to develop a k-means clustering algorithm in order to classify normalized aerosol parameters retrieved from skyradiometer observations at SKYNET sites (e.g., complex refractive index, single scattering albedo, and asymmetry parameters) into different aerosol types for characterizing each observation site. To check our developed clustering algorithm and parameters used, we first applied our method to more than 120,000 AERONET data obtained for the past 10 years and compared the results of classification with those from previous studies. Especially for the biomass burning and urban clusters indicated by our method, the sites were classified into almost the same clusters as expected from previous studies, and their mean parameters were also found to be similar. This suggests that our method is reasonable particularly for biomass burning and urban clusters. In addition, our classification results for SKYNET sites will be presented in this presentation.

Keywords: Aerosol classification, SKYNET, Clustering algorithm

©2021. Japan Geoscience Union. All Right Reserved.

Validation of MERRA-2 Reanalysis Aerosol Products Using Ground-based Observations in Phimai, Thailand, and Factors that Affect Aerosol Optical Depth over the Indochina Peninsula

*Takeru Ohno[1], Hitoshi Irie[1], Arlindo M da Silva[2], Ravi C Govindaraju[2]

1. Center for Environmental Remote Sensing, Chiba University, 2. Global Modeling and Assimilation Office, NASA Goddard Space Flight Center, Greenbelt, Maryland

Biomass burning (BB) occurs during the dry season (December–April) over the Indochina Peninsula (ICP), resulting in poor air quality. We validated the Modern-Era Retrospective analysis for Research and Applications, Version 2 (MERRA-2) aerosol optical depth (AOD) and absorption aerosol optical depth (AAOD) data using a sky radiometer, and aerosol extinction coefficient (AEC) data using Multi-Axis Differential Optical Absorption Spectroscopy (MAX-DOAS) at the SKYNET Phimai site (15.18˚N, 102.56˚E) from 2009 to 2019. The validation analysis showed high correlation coefficients for the three MERRA-2 aerosol products. Compared with ground-based observations, the AOD, AAOD, and AEC were underestimated by 17%, 38%, and 62%, respectively. During the dry season, the height of the maximum AEC value near the ground from MERRA-2 was higher than that from MAX-DOAS. This was likely caused by uncertainty in the MERRA-2 model, such as its vertical profile simulation. Therefore, we expect that the validation analysis could contribute to the accuracy of MERRA-2 simulations conducted in regions affected by BB and anthropogenic emissions. We also analyzed factors that influence AOD over northwest ICP (NWIC), northeast ICP (NEIC), and south ICP (SIC) based on the validated MERRA-2 AOD data. Seasonal variation analysis showed that the major drivers of seasonal variation over the three regions were the organic carbon (OC) AOD and sulfate AOD. The OC AOD was dominant during the dry season, accounting for up to 50% of total AOD in March. The sulfate AOD was high throughout the year, accounting for more than 25% of the total AOD. In particular, the sulfate AOD over the NEIC was ~75% of the total AOD from September to November, indicating the strong impact of sulfate transport from China. Negative trends in AOD were found at Phimai and over the NEIC (1.0% and 1.2% $year^{-1}$, respectively).

Keywords: MERRA-2, Biomass Burning, AOD, Indochina Peninsula, Validation , SKYNET

©2021. Japan Geoscience Union. All Right Reserved.

Exploring ground-based aerosol optical properties to improve satellite estimates of surface particulate matter concentrations

*Alessandro Damiani[1], Hitoshi Irie[1], Kodai Yamaguchi[1], Hossain Mohammed Syedul Hoque[2], Tomoki Nakayama[3], Yutaka Matsumi[2], Yutaka Kondo[4]

1. CEReS, Chiba University, 2. Nagoya University, 3. Nagasaki University, 4. National Institute of Polar Research

Estimates of surface-level particulate matter (PM) concentrations from satellites, essential to complement surface network observations over extra-urban regions, mainly rely on the observed aerosol optical depth (AOD). Therefore, it is crucial exploring how column and profile optical properties are related to aerosol concentrations. Since this can be best achieved by using ground-based observations, we analyzed collocated observations of fine particulate matter (PM2.5), ambient black carbon (BC) as well as columnar aerosol optical properties from a skyradiometer and aerosol extinction profiles from multi-axis differential optical absorption spectroscopy (MAX-DOAS), with an emphasis on the ultraviolet (UV) spectral region. After accounting for the influence of the humidity and the different aerosol extinction profiles, we found that the partial column (i.e., the lowest 1 km layer) of the fine fraction aerosol optical depth ($fAOD_{pc}$), obtained by combing skyradiometer and MAX-DOAS retrievals, reproduced the variability of the PM2.5 better than the columnar fAOD. In the same way, although BC dominates the total absorption in the near-infrared (NIR) spectral range, we showed that the partial column aerosol absorption optical depth ($fAAOD_{pc}$) at UV wavelengths was related to the BC variability better than the corresponding column-based estimates. The observed relationship between the $fAAOD_{pc}$ and an estimated BC partial column was reproduced from Modern-Era Retrospective analysis for Research and Applications, Version 2 (MERRA-2) and resulted in an estimate close to a reasonable BC mass absorption cross-section. Overall, our results point to a right consistency among the used datasets and between them and MERRA-2, stress the well-known sensitivity to the aerosol absorption in the UV spectral region, and highlight the efficacy of combined MAX-DOAS & skyradiometer observations. We expect that these findings will allow a more in-depth evaluation of satellite estimates of surface particulate matter concentrations.

Keywords: aerosol, remote sensing, skyradiometer

©2021. Japan Geoscience Union. All Right Reserved.

Development of international air quality and sky research remote sensing (A-SKY) network

*Hitoshi Irie[1], Alessandro Damiani[1], Toshihiko Takemura[2], Thanawat Jarupongsakul[3], Manish Naja[4]

1. Center for Environmental Remote Sensing, Chiba University, 2. Research Institute for Applied Mechanics, Kyushu University, 3. Department of Geology, Faculty of Science, Chulalongkorn University, 4. Aryabhatta Research Institute of Observational Sciences (ARIES)

The international air quality and sky research remote sensing (A-SKY) network has been developed. The idea for this new network comes from simultaneous observations by the multi-axis differential optical absorption spectroscopy (MAX-DOAS) and the skyradiometer. Such unique simultaneous observations are currently in operation at 5 sites, namely, Chiba (Japan), Fukue (Japan), Kasuga (Japan), Phimai (Thailand), and Haldwani (India). The primary objectives of A-SKY are 1) to quantitatively evaluate long-term variations of important trace gases and aerosols and 2) to understand their interaction with climate. Furthermore, the validation of satellite observations, climate model simulations, and data assimilations are also within the scope of the A-SKY activity. Recent findings from each of our improved MAX-DOAS and skyradiometer technologies and their simultaneous observations are highlighted in this talk. For example, the long-term MAX-DOAS observation at Chiba revealed the presence of almost-constant annual variations in the planetary boundary layer ozone concentration from 2013 to 2019, whereas reductions in nitrogen dioxide (NO_2) and formaldehyde (HCHO) concentrations occurred at rates of approximately 6-10%/year. Under such dominant volatile-organic-compounds-limited conditions, the MAX-DOAS-derived concentration ratio of HCHO/NO_2 was found to be below unity for all months. Beside, the partial column (column below an altitude of 1 km) absorption aerosol optical depth at ultraviolet wavelengths derived from the simultaneous MAX-DOAS and skyradiometer observations was found to be correlated well with the surface black carbon mass concentration data. With such new findings, the potential contribution to atmospheric chemistry is discussed.

Keywords: network, MAX-DOAS, skyradiometer, trace gases, aerosols

©2021. Japan Geoscience Union. All Right Reserved.

Prediction of changes in DSS emission using the Earth System Model of the Meteorological Research Institute

*Takashi Maki[1], Taichu Y Tanaka[1], Thomas Sekiyama[1], Mizuo Kajino[1], Naga Oshima[1], Tsuyoshi Koshiro[1]

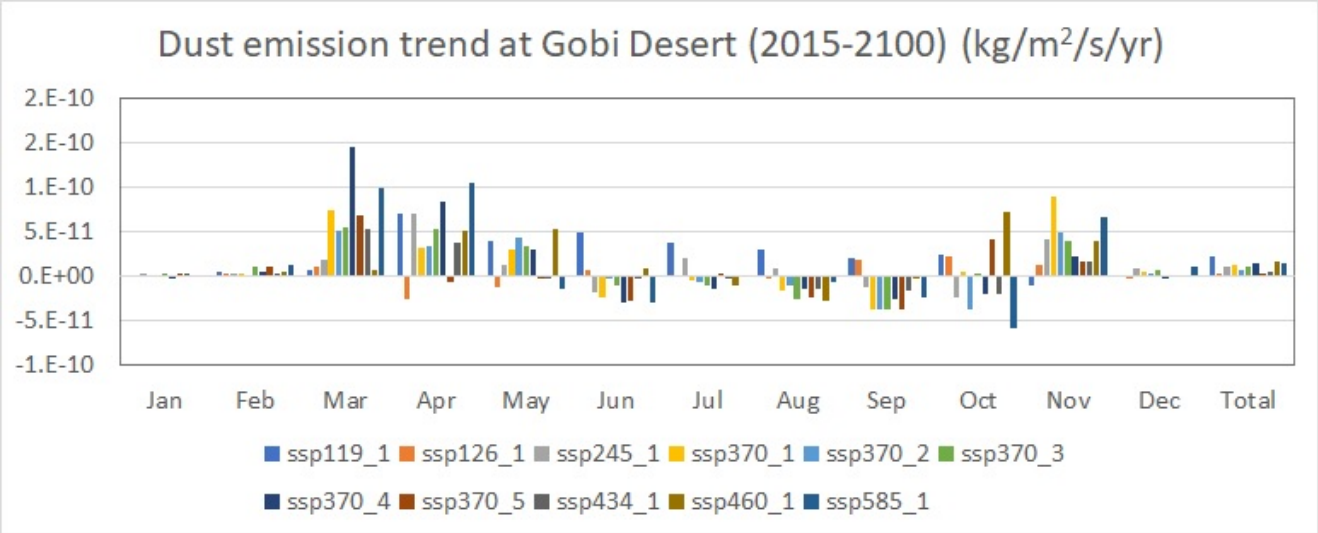
1. Meteorological Research Institute

1. Background
Yellow sand (DSS) is emitted in the arid regions of East Asia and arrives near Japan mainly in the springtime. The impact around Japan is limited to traffic disruptions and impact to people's lives, but near the source of the dust, it can have a significant social and economic impact, including human deaths. DSS is said to affect not only human activities but also climate and weather, and advanced numerical prediction centers are actively conducting tests to introduce aerosols including DSS into numerical models. Although DSS has such important social, economic, and scientific impacts, we do not yet have sufficient knowledge of how the amount of DSS emitted and transported to downstream areas will change with future climate change. This is because the generation of DSS is very sensitive to wind speed near the ground surface and ground surface conditions (snow cover, soil moisture, sand quality, vegetation, etc.), making accurate prediction of these factors extremely difficult. In this study, we attempted to analyze the results of future predictions of DSS emissions and various parameters related to it using the predictions of the Coupled Model Intercomparison Project (CMIP6) of the Earth System Model (MRI-ESM2) developed by the Meteorological Research Institute.
2. Method
MRI-ESM2 (Yukimoto et al., 2019) is an Earth system model that combines various modules such as atmosphere, ocean, land, aerosol, and atmospheric chemistry via couplers. The resolution of MRI-ESM2 in the CMIP6 experiment is TL159 (120 km horizontal grid spacing) for atmosphere, TL95 (180 km horizontal grid spacing) for aerosols, and T42 (280 km horizontal grid spacing) for atmospheric chemistry. The number of ensemble members is 5, and the past reproduction experiments were conducted from January 1850 to December 2014, and after that, 7 different SSP scenario experiments were conducted until December 2100 (of which only SSP370 has 5 ensemble members). The aerosol model is MASINGAR mk-2 (Tanaka et al., 2005), which has been developed by the Meteorological Research Institute. This model treats dust (DSS), sea salt, sulfate, black carbon, and organic aerosols assuming external mixing. For the natural aerosols, dust and sea salt, the model calculates the amount of dust and sea salt emitted based on the various surface conditions calculated by MRI-ESM2. For dust, which is the theme of this study, we adopt a scheme to calculate the amount of dust emission based on parameters such as friction velocity, soil moisture, vegetation, and snow cover.
3.Results and Discussion
The trend of DSS emission amount in the Gobi Desert is shown in Figure 1. Although there was a slight increase in many scenarios and ensembles throughout the entire period, an increasing trend was observed in many experiments during the spring season, which is the main period of DSS emission. In terms of correlations with factors closely related to DSS emission, the correlation with friction velocity was the largest throughout the entire period, and correlations with soil moisture and snow equivalent water were also observed in the spring season (Table omitted). Further analysis of these factors will be conducted and a presentation will be made on the presentation.
4. Acknowledgements
This work was supported by the Environment Research and Technology Development Fund of the Environmental Restoration and Conservation Agency of Japan (5-2001) and JSPS KAKENHI Grant Number

©2021. Japan Geoscience Union. All Right Reserved.

19H04316.

Keywords: Yellow sand (Dust and Sand Storm), Earth system model, Future prediction



©2021. Japan Geoscience Union. All Right Reserved.

Methane emission trends of China in 2009-2018 induced by atmospheric observations

*Fenjuan Wang[1], Shamil S Maksyutov[1], Rajesh Janardanan[1], Akihiko Ito[2], Isamu Morino[1], Yukio Yoshida[1], Yasunori Tohjima[1], Johannes W. Kaiser[3], Greet Janssens-Maenhout[4], xin Lan[5], Ivan Mammarella[6], Jost V. Lavric[7], Tsuneo Matsunaga[1]

1. NIES National Institute of Environmental Studies, 2. Finnish Meteorological Institute, 3. Deutscher Wetterdienst, 4. European Commission Joint Research Centre, 5. Earth System Research Laboratory, 6. University of Helsinki, 7. Max Planck Institute for Biogeochemistry

The reduction of methane emissions of China causes great interest as its significant increase in the last decade. Accuracy quantification of methane budgets of China plays a critical role in implementing national mitigation strategies. In this study, we present top-down estimates of methane emissions of China from 2009-2018 deduced from atmospheric inversions using the high-resolution (0.1° ×0.1°) global inverse model NIES-TM-FLEXPART-VAR. Surface observations, GOSAT retrieval, and a combination of surface observations and GOSAT are used to constrain inversions and the results are compared. Prior fluxes contained the latest Emission Database for Global Atmospheric Research (EDGAR v5) emissions, augmented by biomass burning emissions from the Global Fire Assimilation System (GFASv1.2) and wetland emissions from the Vegetation Integrative Simulator for Trace Gases (VISIT) model. The estimated results are further analyzed for a ten-year period and two five-year periods, which can serve as an independent evaluation of the coming global stock under the Paris Agreement.

Keywords: GOSAT, methane emissions, China, high-resolution inverse model

©2021. Japan Geoscience Union. All Right Reserved.

Characteristics of methane vertical distributions over India

*Dingkun Zhang[1], Naoko Saitoh[1], Dmitry Belikov[1], Prabir Patra[2], Naveen Chandra[3]

1. Center for Environmental Remote Sensing, Chiba University, 2. Japan Agency for Marine-Earth Science and Technology, 3. National Institute for Environmental Studies

Methane, the second most important greenhouse gas after carbon dioxide, accounts for 27% of India's greenhouse gas emissions [Garg et al., 2011]. Methane emissions from South Asia including India have a great contribution to global methane emissions [e.g., Patra et al., 2013]. Chandra et al. [2017] discussed the seasonal variations of methane columns over India by using methane column amounts data from the short-wave infrared (SWIR) band of Thermal and Near-infrared Sensor for Carbon Observation (TANSO)-Fourier Transform Spectrometer (FTS) on board Greenhouse gases Observing SATellite (GOSAT) and simulations by an Atmospheric General Circulation Model-based Atmospheric Chemistry-Transport Model (AGCM-ACTM). In this study, we have analyzed seasonal variations of methane vertical profiles over India by using MIROC4.0-based ACTM (MIROC4-ACTM) [Patra et al., 2018] and GOSAT/TANSO-FTS thermal infrared (TIR) band (hereafter referred as “GOSAT-TIR”).

Following the method proposed by Chandra et al. [2017], we calculated total column methane (XCH_4) and partial column methane ($XpCH_4$) from MIROC4-ACTM σ-pressure coordinates; here, $\sigma = 1.0–0.8$ is defined as Lower Troposphere (LT), $\sigma = 0.8–0.6$ as Mid-Troposphere 1 (MT1), $\sigma = 0.6–0.4$ as Mid-Troposphere 2 (MT2), $\sigma = 0.4–0.2$ as Upper Troposphere (UT), and $\sigma = 0.2–0.0$ as Upper Atmosphere (UA). In the MIROC4-ACTM simulations, two schemes of for emissions from wetlands and rice paddies are adapted [Cao et al., 1996 and Walter et al., 2001].

First, comparisons of XCH_4 and $XpCH_4$ between the Cao and WH schemes showed large differences over India in summer and autumn. Overall, seasonal variations of $XpCH_4$ derived from the Cao schemes of MIROC4-ACTM showed better agreements to the seasonal variations based on GOSAT-TIR than those based on the previous work (AGCM-ACTM) in the three regions over India: Arid India (AI), Eastern Indo-Gangetic Plain (EIGP), and Southern Peninsula (SP). In the UA layer, MIROC4-ACTM $XpCH_4$ values were closer to GOSAT-TIR $XpCH_4$ values in the all three regions. In the LT layer, MIROC4-ACTM $XpCH_4$ values were much higher than $XpCH_4$ values from the other two data in the all three regions. In the MT1 layer, MIROC4-ACTM $XpCH_4$ were closer to $XpCH_4$ in contrast to AGCM-ACTM presented in the previous work in the AI and SP regions. As for the EIGP region, variations in XCH_4 and $XpCH_4$ were relatively large due to variations in elevations, which makes it difficult to draw meaningful conclusions.

Keywords: methane, India, MIROC4-ACTM

©2021. Japan Geoscience Union. All Right Reserved.

Temporal and spatial variations of the mole fraction, carbon and hydrogen isotope ratios of atmospheric methane in the Western Pacific region

*Yasuda Mahito[1], Shinji Morimoto[1], Shuji Aoki[1], Ryo Fujita[2], Taku Umezawa[3]

1. Center for Atmospheric and Oceanic Studies, Graduate School of Science, Tohoku University, 2. Department of Climate and Geochemistry Research, Meterorological Reserach Research Institute, Tsukuba Japan, 3. National Institute for Environmental Studies, Tsukuba, Japan

To understand atmospheric CH_4 variations in the Western Pacific region, we have conducted systematic observations of the CH_4 mole fractions and its carbon and hydrogen isotope ratios ($d^{13}C$ and dD) using air samples collected on board container ships that regularly sail between Japan and Australia/New Zealand. In this study, we analyzed the observation data from 2006 to 2019.
In the temperate zones of both hemispheres, clear seasonal cycles in the CH_4 mole fractions, $d^{13}C$ and dD were observed. Using an atmospheric four-box model with prescribed CH_4 sink, we estimated the contribution of CH_4 sources to the seasonal CH_4 change. The results suggest that the seasonal change in the northern hemisphere is caused by the balance between CH_4 release from biogenic CH_4 sources such as wetlands in summer and CH_4 destruction by the reaction with OH radicals that become maximum also in summer. On the other hand, the seasonal CH_4 change in the southern hemisphere is almost determined by the seasonal changes in the amount of the CH_4 destruction by OH radicals.
In the Western Pacific, the CH_4 mole fractions, $d^{13}C$ and dD showed clear latitudinal gradients, with CH_4 mole fraction increasing and $d^{13}C$ and dD decreasing from south to north throughout a year. These observational facts suggest that there are isotopically lighter CH_4 sources (microbial origin) in the northern hemisphere. The latitudinal distributions of the CH_4 mole fractions and $d^{13}C$ obtained in this study were compared with those observed by the National Oceanic and Atmospheric Administration (NOAA/GMD) at background sites far from CH_4 source region (hereafter called as NOAA sites). During the boreal summer, the CH_4 and $d^{13}C$ in the Western Pacific showed lower and higher values, respectively, compared to those at the NOAA sites, suggesting that the Western Pacific region could be more strongly affected by the destruction by OH radicals. On the other hand, in the boreal winter, the CH_4 mole fractions were higher in the Western Pacific than the background NOAA sites. This would be due to the prevailing westerly winds in the winter season, which transported the air-mass strongly influenced by land CH_4 sources into the Western Pacific region.
The CH_4 mole fractions observed in the Western Pacific, at Syowa Station(69.0˚ S, 39.4˚ E) and Ny-Alesund(78.6˚ N, 11.6˚ E) showed increasing trends after 2006. In contrast, $d^{13}C$ and dD decreased after 2006.We employed the four-box model to investigate the cause of the long-term CH_4 variability. When the CH_4 destruction rate by reaction with OH radical is fixed after 2006, an increase in CH_4 emission after 2006 and decreases in $d^{13}C$ and dD of aggregated CH_4 sources in all latitudinal bands after 2007 are required to reproduce the observed CH_4, $d^{13}C$ and dD values. This suggests that biogenic CH_4 emission has increased since 2006.

Keywords: Methane, Isotopic ratio, Western Pacific

©2021. Japan Geoscience Union. All Right Reserved.

Variations of atmospheric carbon dioxide and its radioisotope in the arctic region

*Hikaru Sekine[1], Shinji Morimoto[1], Chinatsu Yamada[1], Daisuke Goto[2], Masayo Minami[3], Toshio Nakamura[3], Shuji Aoki[1]

1. Center for Atmospheric and Oceanic studies, 2. National Institute of Polar Research, 3. Institute for Space-Earth Environmental Research

To elucidate fossil fuel CO_2 input into the atmosphere, we analyzed temporal variations of CO_2, O_2 and CO concentration and $^{14}CO_2$ at Ny Alesund, Svalbard (79˚N, 13˚E) since 2012. Short-term variations of the atmospheric CO_2 concentration on the scale of hours to days were extracted from the Ny Aleusnd data at first and the durations of higher CO_2 with higher CO and lower O_2 were defined as CO_2 event in this study. Then, using a Lagrangian particle dispersion model and fossil fuel CO_2 emission database, we estimated the amount of CO_2 increase during the CO_2 events and compared it with the observation. As a result, the modeled values well reproduced the observations for the CO_2 events with air mass inflow from European regions, but the modeled values were lower than the observed values for CO_2 events from northern Russia. Using the flask observations of atmospheric $^{14}CO_2$ in the case of the CO_2 event from northern Russia, we estimated that the fossil fuel CO_2 was responsible to the CO_2 event. In order to evaluate the amount and distribution of the CO_2 emission by fossil fuel combustion, continuous observations of CO_2, O_2 and CO and systematic $^{14}CO_2$ observation are valuable.

Keywords: carbon dioxide, global warming, atmospheric observations

©2021. Japan Geoscience Union. All Right Reserved.

Preparation of O_2/N_2 dataset from the surface to the middle stratosphere around Japan traceable to NMIJ gravimetric scale

*Shigeyuki Ishidoya[1], Shinji Morimoto[2], Kazuhiro Tsuboi[3], Satoshi Sugawara[4], Daisuke Goto[5], Nobuyuki Aoki[1], Shohei Murayama[1], Yosuke Niwa[6], Shuji Aoki[2], Hidekazu Matsueda[3], Kentaro Ishijima[3]

1. Advanced Industrial Science and Technology, 2. Tohoku University, 3. Meteorological Research Institute, 4. Miyagi University of Education, 5. National Institute of Polar Research, 6. National Institute for Environmental Studies

Atmospheric delta(O_2/N_2), defined by $[(O_2/N_2)_{sample}/(O_2/N_2)_{ref} -1]x10^6$, has been widely used to evaluate the global CO_2 budget and air-sea O_2 flux (e.g. Manning and Keeling, 2006; Tohjima et al., 2015). However, an absolute value of $(O_2/N_2)_{ref}$ has not been determined by each laboratory with required high-precision, which prevent a direct comparison of the observed delta(O_2/N_2) among the laboratories. To resolve the problem, Aoki et al. (2019) developed O_2, N_2, Ar and CO_2 standard mixtures with sufficient precision (less than 5 per meg in delta(O_2/N_2)) to determine the absolute value of $(O_2/N_2)_{ref}$ traceable to gravimetric scale of National Metrology Institute of Japan (NMIJ/AIST scale). For the direct comparison of delta(O_2/N_2), it is also known that natural and artificial molecular-diffusive fractionations must be considered especially for the aircraft and scientific balloon observations (e.g. Ishidoya et al., 2013, 2014; Stephens et al., 2021). In the present study, we prepare the tropospheric and stratospheric O_2/N_2 dataset around Japan traceable to NMIJ/AIST scale. For this purpose, we corrected an effect of the diffusive fractionations on delta(O_2/N_2) by using the simultaneously measured delta(Ar/N_2) and stable isotopic ratios of N_2, O_2 and Ar. The correction is applied to the air samples collected onboard MD90, B737, CRJ, ERJ and C130 aircrafts (updated from Ishidoya et al., 2012, 2014) and a stratospheric scientific balloon (updated from Ishidoya et al., 2013) over Japan; some air samples were measured by Environmental Management Research Institute of AIST (EMRI/AIST) and the others were by Tohoku University (TU) on their own scales. Then, we converted the corrected delta(O_2/N_2) to the NMIJ/AIST scale based on the inter-comparison experiments using our gravimetric standard mixtures (Aoki et al., 2021). We also applied the scale conversion to the delta(O_2/N_2) observed at some surface stations; Takayama, Minamitorishima and Ryori, Japan (updated from Ishidoya et al., 2017 and our unpublished data). From the prepared delta(O_2/N_2) dataset, we found secular decreasing trends of delta(O_2/N_2) for the period 1999-2020 both for the tropospheric and the stratospheric data, of which change rates were consistent with those reported by Scripps O_2 program (Keeling and Manning, 2014). We also confirmed that the spatial variations in the tropospheric and the stratospheric delta(O_2/N_2) were generally consistent with those expected from the surface O_2 flux and the atmospheric transport. These results suggest that we can compare each laboratory’ s delta(O_2/N_2) values, obtained by analyzing the air samples collected at various observational platforms, with a traceability to NMIJ/AIST.

Acknowledgements

We thank crews and staffs of Japan Airlines and J-Air for their kind cooperation to the air sampling on board MD90, CRJ, B737 and ERJ and staffs of Tohoku University for their works to analyze the air samples. We also thank staffs of Japan Meteorological Agency for their works to collect the air samples on board C130 and maintain the continuous measurements at Minamitorishima and Ryori. We would like to acknowledge many staffs of Japan Ministry of Defense for supporting the C-130H aircraft observation.

©2021. Japan Geoscience Union. All Right Reserved.

This study was partly supported by the JSPS KAKENHI Grant Number 15H02814, 18H03365, 19H01975, 19K03963 and 19K05554, and the Global Environment Research Coordination System from the Ministry of the Environment, Japan (grant nos. METI1454 and METI1953).

Keywords: atmospheric O2/N2 ratio, aircraft observation, scientific balloon, diffusive fractionation of O2 and N2, gravimetric standard gas

©2021. Japan Geoscience Union. All Right Reserved.

Temporal variation of the ozone profile observed with FTIR at Tsukuba

*Isao Murata[1], Hideaki Nakajima[2], Isamu Morino[2], Masanori Takeda[1,2]

1. Graduate School of Environmental Studies, Tohoku University, 2. National Institute for Environmental Studies

Vertical profile of ozone was observed with solar infrared spectroscopy using a Fourier transform spectrometer (FTIR) at Tskuba from 2014 to 2020. SFIT4 spectral fitting program was used to derive the profile. We use the microwindow of 1000.0 - 1005.0 cm^{-1} and parameters recommended by the Network for the Detection of Atmospheric Composition
Change/InfraRed Working Group (NDACC/IRWG). The degrees of freedom for signal (DOFS) is around 5 for this analysis, which means that we can get 5 independent vertical information of the retrieved target gas profile.
Brewer and ozonesonde observations at Tateno were used to validate the retrieved total column and profile for the observation on same days in 2019. Tsukuba site has an advantage, in that the Tateno (JMA’s aerological observatory) is located close to our site. The total columns by FTIR show 4.9 % higher in average than Brewer and the standard deviation is 2.4 %, which agree with Vigouroux, et al.[2008]. This 5 % of bias may due to the uncertainty of the line intensity. After the height resolution matching, the profiles from FTIR and ozonesonde agree within 10% between 18 and 35 km. Comparison for the 15-day (58 spectra) observations shows the FTIR/sonde partial column ratio of 1.02 ±0.05, 1.11 ±0.19, and 1.03 ±0.05 for 0 - 9.8 km, 9.8 - 18.3 km, and 18.3 - 27.7 km, respectively, indicating good agreement within ~10%.
Linear trends were fitted to the temporal variations of total column, partial columns for 0 - 9.8 km, 9.8 - 18.3 km, 18.3 - 27.7 km, and 27.7 - 120 km and all shows negative values between -0.4 and -2.8 % for the period of 2014 - 2020. We don't know why but the total ozone in Japan (Sapporo, Tsukuba, and Naha) observed by Japan Meteorological Agency also shows decrease after 2014. We will investigate the mechanism.

Keywords: FTIR, ozone, height profile

©2021. Japan Geoscience Union. All Right Reserved.

[J] Poster | A (Atmospheric and Hydrospheric Sciences)：A-HW Hydrology & Water Environment

Sun. Jun 6, 2021 5:15 PM - 6:30 PM JST | Sun. Jun 6, 2021 8:15 AM - 9:30 AM UTC | Ch.08_2

[A-HW23] Isotope Hydrology 2021

convener:Masaya Yasuhara(Rissho Univ.), Kohei Kazahaya(Geological Survey of Japan, AIST), Shinji Ohsawa(Institute for Geothermal Sciences, Graduate School of Science, Kyoto University), Kazuyoshi Asai(Geo Science Laboratory)

The purpose of the session is to review the present state of knowledge of isotope hydrology, by bringing together hydrologists, geologists, volcanologists, geochemists, agronomists, ecologists, engineers and so on.

[AHW23-P01] Detection of slab-derived fluid in saline ground water collected from coastal area of Seto Inland Sea, Japan

★Invited Papers

*Yoko Togo[1], Kohei Kazahaya[1], Yuki Tosaki[1], Masaaki Takahashi[1], Noritoshi Morikawa[1], Hiroshi A Takahashi[1], Yuri Nakamura[1], Akihiko Inamura[1], Hinako Shimizu[1], Hiroyuki Matsuzaki[2] (1.National Institute of Advanced Industrial Science and Technology, 2.University of Tokyo)

[AHW23-P02] Geochemical characteristics and origins of saline groundwater in the southern Boso Peninsula, Chiba, Japan

*Masaya Yasuhara[1], Akihiko Inamura[2], Ryotaro Mabuchi[3], Seongwon Lee[1], Noritoshi Morikawa[2] (1.Rissho University, 2.Geological Survey of Japan, AIST, 3.Out-Sourcing Technology Co., Ltd.)

[AHW23-P03] Isotope and water quality compositions of groundwater in the bedrock and sediment deposits in Kofu basin

*Ruri Isobe[1], Takashi Nakamura[2] (1.Interdisciplinary Center for River Basin Environment, University of YAMANASHI, 2.Interdisciplinary Centre for River Basin Environment, University of YAMANASHI)

[AHW23-P04] The influence of weathering and hydrological cycles on Li isotopic compositions in river water and groundwater of the Ganges–Brahmaputra–Meghna River system in Bangladesh

*Toshihiro Yoshimura[1], Daisuke Araoka[2], Hodaka Kawahata[3], Zakir Hossain[4], Naohiko Ohkouchi[1] (1.Japan Agency for Marine-Earth Science and Technology, 2.National Institute of Advanced Industrial Science and Technology, 3.Atmosphere and Ocean Research Institute, The University of Tokyo, 4.Jashore University of Science and Technology)

[AHW23-P05] Numerical modeling on the spatial distribution of d-excess values in river water in Japan

*Masaaki Takahashi[1], Hinako Shimizu[1], Akihiko Inamura[1], Noritoshi Morikawa[1] (1.The National Institute of Advanced Industrial Science and Technology)

[AHW23-P06] Temporal variation of stable isotopes in precipitation based on the intermittent sampling for 1998-2018 at Tiksi, northeastern Siberia

*Kimpei Ichiyanagi[1], Hotaek Park[2], Masahiro Tanoue[3] (1.Kumamoto University, 2.JAMSTEC, 3.National Institute for Environmental Studies)

[AHW23-P07] Tritium concentration in recent precipitation in central Japan

*Kazuyoshi Asai[1] (1.Geo Science Laboratory)

[AHW23-P08] An isotopic study on the role of groundwater in streamflow generation in the concrete-lined Nomi-gawa river, Ohta Ward, Tokyo, Japan

*Masaya Yasuhara[1], Seongwon Lee[1], Yuki Itoh[2], Akihiko Inamura[3], Noritoshi Morikawa[3], Takashi Nakamura[4] (1.Rissho University, 2.Saitama Agricultural Cooperatives, 3.Geological Survey of Japan, AIST,

4.University of Yamanashi)

[AHW23-P09] Inorganic nitrogen concentrations and nitrogen and oxygen isotope ratios of nitrate in shallow groundwater in an urban area, Shinagawa, Tokyo, Japan

*Yuki Itoh[1], Masaya Yasuhara[2], Seongwon Lee[2], Takashi Nakamura[3], Akihiko Inamura[4] (1.Saitama Agricultural Cooperatives, 2.Rissho Univ., 3.Yamanashi Univ., 4.Geological Survey of Japan, AIST)

Detection of slab-derived fluid in saline ground water collected from coastal area of Seto Inland Sea, Japan

*Yoko Togo[1], Kohei Kazahaya[1], Yuki Tosaki[1], Masaaki Takahashi[1], Noritoshi Morikawa[1], Hiroshi A Takahashi[1], Yuri Nakamura[1], Akihiko Inamura[1], Hinako Shimizu[1], Hiroyuki Matsuzaki[2]

1. National Institute of Advanced Industrial Science and Technology, 2. University of Tokyo

Southwest Japan is a place where slab-derived fluid supplies as hydrothermal fluids in the forearc region, as typified by the Arima hot springs (Kazahaya et al., 2014). In this study, oxygen and hydrogen isotope ratios, Li/Cl, Br/Cl, I/Cl ratios, and iodine isotope ratios of saline groundwater and spring water collected in Hiroshima, Hyogo, and Kagawa prefectures (Shodo-shima) were analyzed to investigate halogen characteristics of slab-derived fluid.

The chlorine concentrations in the groundwater samples ranged from 1760 to 16600 mg/L. Oxygen and hydrogen isotope ratios indicated that the samples from the western area with high chlorine concentrations were mainly seawater, while the samples from the eastern area with low chlorine concentrations were mainly meteoric water. According to Kazahaya et al. (2014), high Li/Cl ratios of groundwater are characteristic of slab-derived fluids. The Li/Cl ratio of groundwater was higher in the eastern area, suggesting the presence of slab-derived fluid. The samples with high Li/Cl ratios were characterized by low Br/Cl ratios and high I/Cl ratios compared to seawater. In addition, iodine isotope ratios ($^{129}I/^{127}I$) showed relatively lower in the eastern region (i.e., older iodine age), suggesting that low iodine isotope ratios are characteristic of slab-derived fluids in this region. The characteristics of halogen ratios and iodine isotope ratios of slab-derived fluids should be investigated and compared in various regions for further investigation.

Keywords: Slab-derived fluid, Halogen, Groundwater

©2021. Japan Geoscience Union. All Right Reserved.

Geochemical characteristics and origins of saline groundwater in the southern Boso Peninsula, Chiba, Japan

*Masaya Yasuhara[1], Akihiko Inamura[2], Ryotaro Mabuchi[3], Seongwon Lee[1], Noritoshi Morikawa[2]

1. Rissho University, 2. Geological Survey of Japan, AIST, 3. Out-Sourcing Technology Co., Ltd.

Ascent of deep-seated saline water toward the ground surface and its mixing with local shallow groundwater and river water has long been recognized to take place in and around the shallow well, *Kanamari Kobo Ido* (Tateyama City) and *Yunotani* (Futtsu City), both in the southern Boso Peninsula, Chiba, Japan. The saline water in this region is characterized by its high chloride ion (Cl^-) concentration of about 5,100-5,800 mg/L and 1,000-1300 mg/L for the *Kanamari Kobo Ido* and *Yunotani*, respectively. The oxygen and hydrogen isotopes, Li/Cl ratio, and $^3He/^4He$ ratio support an assumption that saline water is of see water origin which was subjected to sediment-water solute exchange to a large extent. On the other hand, we attempted to quantify the amount of Cl^- brought to the ground surface from the depth by the ascent of deep-seated saline water. As the result, its Cl^- amount was estimated at about 120 kg/day in November 2019 for the *Kanamari Kobo Ido* and its vicinity. Taking into account the Cl^- concentration of *Kanamari Kobo Ido* groundwater, the volume of deep-seated saline water mixed with river water and shallow groundwater in the area was estimated to be 24 m^3/day.

Keywords: deep-seated saline water, saline water ascent, river water, mixing, chloride ion, isotope

©2021. Japan Geoscience Union. All Right Reserved.

Isotope and water quality compositions of groundwater in the bedrock and sediment deposits in Kofu basin

*Ruri Isobe[1], Takashi Nakamura[2]

1. Interdisciplinary Center for River Basin Environment, University of YAMANASHI, 2. Interdisciplinary Centre for River Basin Environment, University of YAMANASHI

Nationwide, Kofu basin in Japan is well renowned for the presence of natural hot water springs. The extraction depth of the hot water in this basin varies while it is also found that the water is being extracted both from the bedrock and sedimentary deposits. However, the exact mechanism of the groundwater recharge process in this basin is yet unknown. Thus, this study is primarily focused in identifying the isotope and water quality compositions of groundwater in the bedrock and sediment deposits and understand the deep groundwater recharge processes in this basin.

For the purpose of the study, 485 borehole data and 307 hot spring water samples were collected from Kofu basin. The lithological analysis using the boreholes estimated bedrock distribution (granite) from surface to 1000+m deep, extending from the north to the central part of Kofu. The distribution of the deep groundwater isotope showed inverse relationship with topography i.e. altitude effect is found prevalent for isotopic variations. Those results suggest the possibility of mountains as the main area for the groundwater recharge to the basin floor. Thus, the presentation will show the isotope and water quality compositions of groundwater in the bedrock and sediment deposits and find the inter-relation between them.

©2021. Japan Geoscience Union. All Right Reserved.

The influence of weathering and hydrological cycles on Li isotopic compositions in river water and groundwater of the Ganges–Brahmaputra–Meghna River system in Bangladesh

*Toshihiro Yoshimura[1], Daisuke Araoka[2], Hodaka Kawahata[3], Zakir Hossain[4], Naohiko Ohkouchi[1]

1. Japan Agency for Marine-Earth Science and Technology, 2. National Institute of Advanced Industrial Science and Technology, 3. Atmosphere and Ocean Research Institute, The University of Tokyo, 4. Jashore University of Science and Technology

The silicate weathering of continental rocks plays a vital role in determining ocean chemistry and global climate. Spatiotemporal variations in Li isotope ratio (δ^7Li) in terrestrial waters identify regimes of current and past weathering processes. Here we examine (1) monthly dissolved δ^7Li variation in the Ganges River' s lower reaches, and (2) spatiotemporal variation of river water of the Brahmaputra, Meghna rivers, and groundwater in Bangladesh. From the beginning to maximum flood discharges of the rainy season (i.e., from June to September), Li concentrations and δ^7Li in the Ganges River show remarkable changes, with a large influence from the Himalayan sources. However, most Li discharge across the rainy season is a steady-state condition and strongly influenced by the secondary mineral formation in the low-altitude floodplain. For groundwater samples shallower than ~60 m depth, both δ^7Li and Li/Na are highly scattered regardless of the sampling region, suggesting the variable extent of fractionation. For deep groundwater (70–310 m) with a long residence time of about 3,000 to 20,000 years, the lower δ^7Li values indicate more congruent weathering. These results suggest that Li isotope fractionation in rivers and groundwater depends on the timescale of water-mineral interaction, which plays an essential role in determining the isotopic signature of terrestrial Li inputs to the ocean.

Keywords: Weathering, Bangladesh, Lithium isotope ratios, Groundwater, Ganges River

©2021. Japan Geoscience Union. All Right Reserved.

Numerical modeling on the spatial distribution of d-excess values in river water in Japan

*Masaaki Takahashi[1], Hinako Shimizu[1], Akihiko Inamura[1], Noritoshi Morikawa[1]

1. The National Institute of Advanced Industrial Science and Technology

There are many studies on the spatial distribution of δD and δ^{18}O values in river water in Japan, and numerical modeling are also shown. Latitude, altitude, annual mean temperature, distance from the coastline, precipitation amount, etc. are used as topographical and geographical parameters. On the other hand, there are many studies on the spatial distribution of d-excess values (δD−8xδ^{18}O) in river water, such as Katsuyama et al. (2015), but no numerical modeling has been shown, yet. From previous studies on the spatial distribution of d-excess values in river water, it is clarified that it does not depend on latitude, altitude, distance from the coastline, etc., and is also recognized that d-excess values change extremely at the (central) watershed.

This study presents the effect of "summer" and "winter" precipitation amounts on the spatial distribution of d-excess values in river water.

Keywords: river water, d-excess value, spatial distribution, numerical modeling

©2021. Japan Geoscience Union. All Right Reserved.

Temporal variation of stable isotopes in precipitation based on the intermittent sampling for 1998-2018 at Tiksi, northeastern Siberia

*Kimpei Ichiyanagi[1], Hotaek Park[2], Masahiro Tanoue[3]

1. Kumamoto University, 2. JAMSTEC, 3. National Institute for Environmental Studies

Recent global warming affects significant impacts on air temperature and sea ice extent through the atmospheric hydrological cycle in the Arctic region. Stable water isotopes are useful tracer for estimating the moisture source and transportation pathway in the atmospheric hydrological cycle. From 1998 to 2018, daily precipitation samples were intermittently collected at Tiksi, northern Siberia, Russia. Totally 1,519 samples for $\delta^{18}O$ and 1,024 samples for $\delta^{2}H$ were analyzed by the Isotope Ratio Mass Spectrometry (IRMS) by the 10th September 2007 and by the Cavity Ring-Down Spectroscopy (CRDS) after 11th September 2007. At the last JpGU meeting (abstract ID; AHW34-P10), we reported the depleting trend of deuterium excess (d-excess) in precipitation. Comparing with another isotopic data from July 2015 to June 2017 observed at Samoylov Island near Tiksi (Bonne et al., 2020), annual mean values of surface air temperature, $\delta^{2}H$, and $\delta^{18}O$ were matching well. However, annual mean d-excess at Samoylov Island was more than 10‰ higher than the observation at Tiksi. This fact indicates the depleting trend of d-excess at Tiksi might be caused by the insufficient quality check of observation data. Therefore, new quality control method by using relationships between $\delta^{18}O$ or $\delta^{2}H$ in precipitation samples analyzed by the IRMS and surface air temperature at Tiksi were adapted to the samples analyzed by the CRDS. The temperature effects for $\delta^{18}O$ and $\delta^{2}H$ by the IRMS were 0.47‰ and 3.15‰, respectively. Finally, 1,257 samples for $\delta^{18}O$ and 820 samples for $\delta^{2}H$ were selected to calculate monthly mean values. From the monthly mean surface air temperature at Tiksi from 1998 to 2018, long-term increasing trends in March, April, October, and November were significant (0.24-0.42℃/month within 5% statistically significance). Furthermore, the difference in air temperature, evaporation, and 850hPa winds fields between first 5 years (1998-2002) and last 5 years (2014-2018) of the observation period were investigated by using the NCEP reanalysis. The positive anomalies in air temperature, evaporation, and southwesterly (northerly) wind anomalies were found in the northern Siberian continent (along the coast of the Arctic Ocean) in March and April (October and November). On the other hand, the relationships between surface air temperature and $\delta^{18}O$ in precipitation were found only in April (0.50‰/℃) and October (0.73‰/℃) within 5% statistically significance. The difference in temperature effect between April and October might be caused by the difference in moisture source evaporated from land and open water in the Arctic Ocean.

Keywords: isotopic composition, precipitation, northeastern Siberia

©2021. Japan Geoscience Union. All Right Reserved.

Tritium concentration in recent precipitation in central Japan

*Kazuyoshi Asai[1]

1. Geo Science Laboratory

Tritium is a effective age-dating tracer in classifying groundwater into old (>70 y) and young (<70 y) water. Sustainable use of this age tracer requires a long-term record of precipitation tritium concentrations. In this presentation, we will introduce the tritium concentration of monthly precipitation measured in Nagoya City from 2010 to the present.

Keywords: precipitation, tritium, Nagoya city

©2021. Japan Geoscience Union. All Right Reserved.

An isotopic study on the role of groundwater in streamflow generation in the concrete-lined Nomi-gawa river, Ohta Ward, Tokyo, Japan

*Masaya Yasuhara[1], Seongwon Lee[1], Yuki Itoh[2], Akihiko Inamura[3], Noritoshi Morikawa[3], Takashi Nakamura[4]

1. Rissho University, 2. Saitama Agricultural Cooperatives, 3. Geological Survey of Japan, AIST, 4. University of Yamanashi

A role of groundwater in streamflow generation in a concrete-lined urban river was studied for the days of no rainfall from July 2015 to September 2019 in the Nomi-gawa river, Ohta Ward, Tokyo, Japan. Although the entire surface of side walls and riverbed is covered with concrete, groundwater seeps out through discharge pipes on the concrete walls and gaps in the riverbed concrete plates, making a considerable contribution in the river runoff formation. A two-component mixing analysis on the basis of oxygen isotope ratio of water made it clear that this kind of groundwater seepage accounts for in the range between 20% and 30% for the wet season and about 10% for the dry season, of the discharge in the Nomi-gawa river. These estimates are in accordance with those in our previous report (Fujioka et al., 2018) based on electric conductivity of water. The difference of groundwater contribution in the formation of river runoff can be attributed to the different groundwater levels in the vicinity of the river for the wet summer and dry winter seasons.

Keywords: urban river, concrete-lined channel, groundwater seepage, streamflow generation, oxygen isotope of water

©2021. Japan Geoscience Union. All Right Reserved.

Inorganic nitrogen concentrations and nitrogen and oxygen isotope ratios of nitrate in shallow groundwater in an urban area, Shinagawa, Tokyo, Japan

*Yuki Itoh[1], Masaya Yasuhara[2], Seongwon Lee[2], Takashi Nakamura[3], Akihiko Inamura[4]

1. Saitama Agricultural Cooperatives, 2. Rissho Univ., 3. Yamanashi Univ., 4. Geological Survey of Japan, AIST

A geochemical study on shallow groundwater of the densely-populated Kitashinagawa district in Shinagawa City, in the heart of Tokyo was carried out from January 2019 through February 2020, when water samples were collected from 7 shallow wells once every two months. In Kitashinagawa district, despite quite a small area of about 60 m (N-S) by 100 m (E-W), its shallow groundwater represents a wide range of nitrate (NO_3^-) concentration: for example1.6-34.1 mg/L NO_3^- in February 2019 (dry season) and 0.0-34.8 mg/L NO_3^- in July 2019 (wet season). Nitrogen ($d^{15}N$) and oxygen ($d^{18}O$) isotope ratios of nitrate also show a large range of values, about 10-25‰ and 2-20‰ for $d^{15}N$ and $d^{18}O$, respectively. For many wells, the ratio of enrichment of oxygen to nitrogen is found close to 1:2 for $d^{18}O$ and $d^{15}N$ plots, and on $d^{15}N$ vs. ln [NO_3-N] plots they yield a straight line, which can be explained using the Rayleigh equation and is indicative of the occurrence and progress of denitrification. In contrast, some wells fall on a straight line for $d^{15}N$ vs. 1/[NO_3-N] plots, indicating mixtures of two or three sources (water bodies). An overall conclusion is then that nitrate in shallow groundwater in the study area is primarily of sewage leakage origin (Itoh et al., 2020), but its concentration is subject to alternation to a large extent by the denitrification and/or by the mixing with other water bodies such as rainfall infiltration (natural recharge) and water supply leakage with different nitrogen characteristics.

Keywords: densely-populated urban area, shallow groundwater, inorganic nitrogen concentration, nitrogen and oxygen isotopes, mixing, denitrification

©2021. Japan Geoscience Union. All Right Reserved.

[J] Poster | A (Atmospheric and Hydrospheric Sciences)：A-CG Complex & General

Sun. Jun 6, 2021 5:15 PM - 6:30 PM JST | Sun. Jun 6, 2021 8:15 AM - 9:30 AM UTC | Ch.08_3

[A-CG38] Dynamics of Oceanic and Atmospheric Waves, Vortices, and Circulations

convener:Yuki Tanaka(Faculty of Marine Science and Technology, Fukui Prefectural University), Kunihiro Aoki(Japan Agency for Marine Earth Science and Technology), Yukiharu Hisaki(University of the Ryukyus), Norihiko Sugimoto(Keio University, Department of Physics)

Oceanic and atmospheric dynamics aims at abstracting general principles from observed phenomena and constructing a system of mathematical models, thereby leading to the understanding, prediction, and parameterization of those phenomena. It provides perspectives for the advancement of sciences in various areas such as turbulence, wind waves, internal waves, Rossby waves, tides, coastal and equatorial boundary processes, mesoscale and submesoscale eddies, meandering of jets and fronts, general circulation, and ocean-atmosphere coupled modes. It has also been and will continue to be benefited by new uses of ideas and methods from such theories as resonance, nonlinear interaction, stability analysis, spectral analysis, probability, statistics, and dynamical systems. In this session, we solicit presentations on observational, experimental, numerical, and theoretical studies of oceanic and atmospheric dynamics and on exploratory use of new ideas and methods. We also welcome presentations on interdisciplinary studies in fields such as ecosystems, climate, and environment.

[ACG38-P01] A statistical mechanics of phytoplankton diversity

*Kunihiro Aoki[1], Yoshio Masuda[2] (1.Japan Agency for Marine Earth Science and Technology, 2.Faculty of Environmental Earth Science, Hokkaido University)

[ACG38-P02] Essential spectrum of internal waves arising in rotating stratified fluid

*andrei giniatoulline[1] (1.Department of Mathematics, Los Andes University, Bogota, Colombia, South America)

[ACG38-P03] Statistical analysis of ocean waves in the sea of Japan

*Yukiharu Hisaki[1] (1.University of the Ryukyus)

[ACG38-P04] Observing system simulation experiments for new satellite observation missions on Venus

*Yukiko Fujisawa[1], Norihiko Sugimoto[1], Mirai Abe[1], Asako Hosono[2], Mimo Shirasaka[3], Hiroki Ando[4], Masahiro Takagi[4], Chi Ao[5], Itziar Garate Lopez[6], Sebastien Lebonnois[7], Tomotaka Yamamoto[8], Yosuke Kawabata[8], Satoshi Ikari[8], Takeshi Imamura[8], Masaru Yamamoto[9], Shin-ya Murakami[1], Masataka Imai[10], Toru Kouyama[10] (1.Keio University, 2.Toshimagaoka Women High School, 3.Seisen Senior High School, 4.Kyoto Sangyo University, 5.Jet Propulsion Laboratory, California Institute of Technology, 6.Bilboko Ingeniaritza Eskola (UPV/EHU), 7.Sorbonne Universite, 8.Tokyo University, 9.Research Institute for Applied Mechanics, Kyushu University, 10.National Institute of Advanced Industrial Science and Technology)

A statistical mechanics of phytoplankton diversity

*Kunihiro Aoki[1], Yoshio Masuda[2]

1. Japan Agency for Marine Earth Science and Technology, 2. Faculty of Environmental Earth Science, Hokkaido University

.

Keywords: Biodiversity, Statistical mechanics, Ocean ecosystem, Ocean circulation, Maximum entropy method

©2021. Japan Geoscience Union. All Right Reserved.

Essential spectrum of internal waves arising in rotating stratified fluid

*andrei giniatoulline[1]

1. Department of Mathematics, Los Andes University, Bogota, Colombia, South America

For viscous and inviscid compressible fluid, we consider the three-dimensional models which involve simultaneously the stratification and rotation of the fluid. The rotation corresponds to the rotation of the Earth over the vertical axis, and the stratification corresponds to the non-homogeneous distribution of density due to the gravitational force. We find the structure and the localization of spectrum of normal vibrations of the inner waves for various boundary conditions. We prove that, when the spectral parameter belongs to the essential spectrum, there arises the resonance effect of non-uniqueness of the limit amplitude of internal waves. The results may find application in the study of the Ocean and Atmosphere.

Keywords: Dynamical systems, Internal waves, Resonance effect, Rotational fluid, Stratified fluid, Essential spectrum

©2021. Japan Geoscience Union. All Right Reserved.

Statistical analysis of ocean waves in the sea of Japan

*Yukiharu Hisaki[1]

1. University of the Ryukyus

Wave climate is important for marine disaster prevention. The Sea of Japan is a semi-enclosed sea that connects the Tsushima Strait and the Mamiya Strait to other sea areas. Therefore, waves in the Japan Sea are more influenced by local winds than by distant swells. In this study, we investigated the interannual variability of the wave height distribution using the ERA5 reanalysis data. First, we compared the wave heights by ERA5 with those by GPS buoys around Japan. The agreement between them is good. Next, the difference in the accuracy of the ERA5 wave height was compared between the short and long fetch cases. In the short fetch case, the accuracy of the ERA5 wave heights is significantly lower than that of the long fetch case.
Wave heights by ERA5 and those by JMA (Japan Meteorological Agency) moored buoys (1990 to 2000) were compared. The agreement between them was good. In addition, the accuracy of ERA5 wave height after incorporating altimeter data into ERA5 wave data from 1992 was compared with those of wave height before that. The difference in the accuracy between them was small.
Next, the spatial distribution of ERA5 monthly mean wave height anomalies from climatological values from 1979 to 2019 was examined by empirical orthogonal function (EOF) analysis. The first mode is a pattern of variability in the central region of the sea of Japan (around 40N, 135E). The second mode is a pattern that fluctuates alternately in the north and south of the Sea of Japan (around 35N, 131E and 45N, 140E). The correlation between the EOF time series of monthly mean wind anomalies and the EOF time series of wave height anomalies was investigated. The first mode of wave height anomalies is correlated with the second mode of EOF wind anomalies over almost the entire Japan Sea area. The second EOF mode of wave height anomaly is correlated with the first EOF mode of wind anomaly in the northern part of the sea of Japan.
The monthly wave height anomaly maps were classified by self-organizing map analysis. Some frequent wave height anomaly maps corresponded to the distributions of EOF first and second modes of wave height anomaly. The frequency of the distribution patterns with high wave height anomaly in the central area of the sea of Japan has been increasing in recent years. This is consistent with the trend of the EOF first mode time series of wave height anomalies. In addition, wave height anomalies in the northern and southern areas of the sea of Japan corresponded most closely to the distribution patterns of wind anomalies in the northern area of the sea of Japan. This is consistent with the result that the second EOF mode of wave height anomalies is correlated with the first EOF mode of wind anomalies in the northern part of the sea of Japan.

Keywords: wave height, Sea of Japan

©2021. Japan Geoscience Union. All Right Reserved.

Observing system simulation experiments for new satellite observation missions on Venus

*Yukiko Fujisawa[1], Norihiko Sugimoto[1], Mirai Abe[1], Asako Hosono[2], Mimo Shirasaka[3], Hiroki Ando[4], Masahiro Takagi[4], Chi Ao[5], Itziar Garate Lopez[6], Sebastien Lebonnois[7], Tomotaka Yamamoto[8], Yosuke Kawabata[8], Satoshi Ikari[8], Takeshi Imamura[8], Masaru Yamamoto[9], Shin-ya Murakami[1], Masataka Imai[10], Toru Kouyama[10]

1. Keio University, 2. Toshimagaoka Women High School, 3. Seisen Senior High School, 4. Kyoto Sangyo University, 5. Jet Propulsion Laboratory, California Institute of Technology, 6. Bilboko Ingeniaritza Eskola (UPV/EHU), 7. Sorbonne Universite, 8. Tokyo University, 9. Research Institute for Applied Mechanics, Kyushu University, 10. National Institute of Advanced Industrial Science and Technology

Observation system simulation experiment (OSSE) is a method for testing a virtual observation system using a data assimilation method, which enables us to evaluate planned observation by reproducibility of a target phenomenon. On Earth, it is actively used for objective evaluation of meteorological forecasting skill when new observations, such as satellite observations, are introduced (e.g., Masutani et al., 2010) [1]. However, there are few examples of OSSE for planetary satellite observation missions. Since a planetary satellite mission is limited in time and resources, it would be quite useful to investigate its effectiveness by using OSSE in advance to optimize its instruments and observation plans.

To implement OSSE, we need both a data assimilation system and a reliable meteorological model which can reproduce the atmospheric phenomena realistically. We have developed “AFES-Venus” (Sugimoto et al., 2014a) [2] which is based on AFES (Atmospheric GCM For the Earth Simulator) optimized for the Earth simulator, and “ALEDAS-V” (AFES LETKF Data Assimilation System for Venus) (Sugimoto et al., 2017) [3] which is the first data assimilation system for the Venus atmosphere using AFES-Venus and Local Ensemble Transform Kalman Filter (LETKF). In this presentation, we show an overview of four OSSEs conducted by this assimilation system (Table).

The radio occultation measurements mission between multiple small satellites is expected as a method to observe the vertical temperature distribution at altitudes in about 40-90km penetrating a thick cloud cover at altitudes in about 48–70 km. In addition, the observation frequency and coverage would be significantly improved compared to the radio occultation between the Earth and satellites. In this study, OSSE was performed for the observation points by actual orbit calculation[4], and the effectiveness of the orbit was investigated from (1) the reproducibility of “cold collar” [5,6] and (2) the improvement of the speed of “super rotation”, which are notable atmospheric phenomena on Venus.

Observations of the Venus Orbiter "Akatsuki" provide us horizontal distributions of the horizontal wind derived from cloud tracking of the UVI camera and of temperature observed by the LIR camera. In this study, the observational limits of Akatsuki were reduced, and OSSE was performed for various observation coverages (day and night side, or latitude area) and observation frequencies, and the effectiveness of the observations was investigated from (3) the reproducibility of “planetary-scale equatorial Kelvin waves with 4-day period” [7] and (4) the improvement of phases of “thermal tides”.

[1] Masutani, M., J. S. Woollen, S. J. Lord, G. D. Emmitt, T. J. Kleespies, S. A. Wood, S. Greco, H. Sun, J. Terry, V. Kapoor, R. Treadon, and K. A. Campana (2010), J. Geophys. Res., 115.
[2] Sugimoto, N., M. Takagi, and Y. Matsuda (2014a), J. Geophys. Res. Planets, 119, 1950–1968.

©2021. Japan Geoscience Union. All Right Reserved.

[3] Sugimoto, N., A. Yamazaki, T. Kouyama, H. Kashimura, T. Enomoto, and M. Takagi (2017), Scientific Reports, 7(1), 9321.
[4] Yamamoto, T., S. Ikari, H. Ando, T. Imamura, A. Hosono, M. Abe, Y. Fujisawa, N. Sugimoto, Y. Kawabata, R. Funase, and S. Nakasuka, (2021), Journal of the Japan Society for Aeronautical and Space Sciences, submitted.
[5] Sugimoto, N., M. Abe, Y. Kikuchi, A. Hosono, H. Ando, M. Takagi, I. Garate-Lopez, S. Lebonnois, and C. Ao (2019b), Journal of Japan Society of Civil Engineers A2: Applied Mechanics, 75(2), 477–486.
[6] Fujisawa, Y., N. Sugimoto, C. Ao, A. Hosono, H. Ando, M. Takagi, I. Garate-Lopez and S. Lebonnois, in preparation.
[7] Sugimoto, N., Y. Fujisawa, M. Shirasaka, A. Hosono, M. Abe, H. Ando, M. Takagi, M. Yamamoto, (2021), Atmosphere, Vol.12, No.1, 14, 16pp.

Keywords: Venus atmosphere, Data assimilation, Observing system simulation experiment

©2021. Japan Geoscience Union. All Right Reserved.

Experimental Case	Virtual observation data	Orbit
I. Radio Occultation Measurement Among Small Satellites		
① Reproduction of cold collar	temperature (IPSL Venus GCM)	Orbit with many observations near the poles
② Improvement of super-rotation	temperature (AFES-Venus)	Orbit with many observations in low latitudes
II. Camera images (assuming Akatsuki UVI or LIR)		
③ Reproduction of 4-day equatorial Kelvin wave	horizontal wind (CCSR/GCM)	Varying observation latitude and frequency
④ Improvement of phases of thermal tides	temperature (AFES-Venus)	Varying observation longitude and frequency

Table: Cases of observing system simulation experiments, virtual observation data and orbit used in the experiments

実験	仮想の観測データ	軌道
Ⅰ小型衛星を用いた衛星間電波掩蔽観測		
① コールドカラー再現	温度 (IPSL Venus GCM)	極付近にも多く観測が存在する軌道
② スーパーローテション速度改善	温度(AFES-Venus)	低緯度に多く観測が存在する軌道
Ⅱカメラ観測（e.g.あかつき UVI LIR 観測）		
③ 4 日周期ケルビン波再現	水平風速(CCSR/GCM)	複数の観測緯度や観測頻度
④ 熱潮汐波の位相改善	温度(AFES-Venus)	複数の観測経度や観測頻度

表: 観測システムシミュレーション実験の種類、及び実験に用いた仮想観測データと軌道

©2021. Japan Geoscience Union. All Right Reserved.

[J] Poster | H (Human Geosciences)：H-DS Disaster geosciences

Sun. Jun 6, 2021 5:15 PM - 6:30 PM JST | Sun. Jun 6, 2021 8:15 AM - 9:30 AM UTC | Ch.09_1

[H-DS08] Human environment and disaster risk

convener:Tatsuto Aoki(School of Regional Development Studies, Kanazawa University), Hiroshi, P. Sato(College of Humanities and Sciences, Nihon University)

This session discusses disaster risks being inherent in the natural and human environment, which sometimes happen to appear at a disaster, from the viewpoint of not only natural sciences but also social and human sciences. Examples of discussion subjects are as follows: uncertainty of forecasting disaster and problems of huge disaster with low frequency that raised from the 2011 Tohoku earthquake, the methodology for improving hazard maps, national recovery plans considering probable changes or sustainability of the society, international cooperation for disaster mitigation, problems of active faults or liquefaction, adjusting disaster mitigation plan to the regional characteristics, technical development for supporting disaster prevention, education for the disaster mitigation.

[HDS08-P01] The role of residents' resilience on the recovery process in a torrential rain

*Shoji Ohtomo[1], Reo Kimura[2] (1.Kanto Gakuin University, 2.University of Hyogo)

[HDS08-P02] Flood damage mapping of 2020 Typhoon Ulysses in the Philippines

*Naoko Nagumo[1], Kentaro Aida[1], Miho Ohara[1], Masakazu Fujikane[1] (1.International Centre for Water Hazard and Risk Management, PWRI)

[HDS08-P03] An example of using Google Earth Engine in providing and sharing information on wide-area typhoon disasters in international joint research projects

*Kentaro Aida[1], Naoko Nagumo[1], Miho Ohara[1] (1.International Centre for Water Hazard and Risk Management, PWRI)

[HDS08-P04] Estimating the amount of waste treatment units in the event of a disaster with self-help and mutual support

*Yoshinobu MIZUI[1,2] (1.University of Tsukuba, 2.NationalResearch Institute for Earth Science and Disaster Resilience)

[HDS08-P05] Possibility of support for disaster victims by accommodation facilities-Advance evacuation and acceptance in the event of a disaster-

Yuka SUZUKI[1], *Tatsuto Aoki[2] (1.Kanazawa University, 2.School of Regional Development Studies, Kanazawa University)

[HDS08-P06] Effect of synchrony bias on excitation of evacuation behavior during tsunami-From the evacuation behavior of residents in Noto Town, Ishikawa Prefecture during the 2019 Yamagata-oki Earthquake-

Mayu KITAMURA[1], *Tatsuto Aoki[2] (1.Kanazawa University, 2.School of Regional Development Studies, Kanazawa Univ.)

[HDS08-P07] Status of provision of disaster prevention information and learning to international students at national and public universities and their issues

*CHENYUE LU[1], Kiyomi HAYASHI[2], Tatsuto AOKI[2] (1. Division of Regional Development Studies,Graduate School of Human and Sociology-Environmental Studies,Kanazawa University, 2.School of Regional Development Studies, Kanazawa University)

The role of residents' resilience on the recovery process in a torrential rain

*Shoji Ohtomo[1], Reo Kimura[2]

1. Kanto Gakuin University, 2. University of Hyogo

Disasters linked to natural hazards have increased sharply in the last 20 years (UNDR, 2020). Despite the massive disasters that have occurred, there are limitations to the national disaster prevention and mitigation frameworks that aim to reduce the impact of disasters. In recent times, the strategy of promoting resilient communities that have the ability to recover from disasters has become of interest. The study examined the relationships between the recovery process and residents' resilience in the torrential rain in western Japan in 2018.

High infrastructural damages and fatalities were recorded in Okayama and Hiroshima prefecture in the torrential rain. The study conducted a web-based questionnaire from January 31 to February 12 2019, about 6 months after the torrential rain hit western Japan in 2018. Target areas were in 13 districts in Hiroshima prefecture and 6 districts in Okayama prefecture that suffered damage caused by the torrential rain. The result of the analysis of the recovery calendar (Kimura, 2005) indicated that recovery was progressed in the "disaster utopia" (up to 1.5 ~ 2 months after) and "reentry to everyday life" (up to 6 ~ 12 months after) phases (Figure 1). Next, to examine the difference in residents' life-recovery progress up to the "disaster utopia" and "reentry to everyday life" phase, GLM analysis was implemented using count data of recovery calendar for each period. Firstly, a Bayesian GLM with Poisson distribution was conducted to predict the count data for life recovery up to the "disaster utopia" phase, with gender, age, the level of flooding damage, and human suffering as interactive terms with psychological resilience, and psychological resilience and other variables were taken as the independent variables. As a result, the main effects of gender, dummy variable of flooding damage (vs. flooded above the floor), human suffering, and the interaction effect of age ×psychological resilience were found. Concerning these effects, male residents' life-recovery scores were higher than female residents' (Figure 2_a). Moreover, the life recovery of residents with flooding above the floor level was lower than other residents (Figure 2_b). The more human suffering the poorer the life-recovery scores (Figure 2_c). Moreover, although older residents' life recovery was lowest when their psychological resilience was low, older residents' life recovery was the highest when their psychological resilience was high (Figure 2_d). Secondly, when examining changes up to the "reentry to everyday life" phase, the difference in life-recovery count data from the "disaster utopia" phase to the "reentry to everyday life" phase was calculated. In addition, a similar Bayesian GLM with Poisson distribution was conducted to predict the difference in life-recovery count data. We found the main effects of gender and the dummy variable of flooding damage (vs. flooded above the floor), and the interaction effect of psychological resilience ×the dummy variable of flooding damage (vs. flooded above the floor). Concerning these effects, female residents' life-recovery scores were higher than male residents (Figure 4_a). Moreover, the life-recovery scores of residents with flooding above the floor level were higher than other residents (Figure 4_b). Contrary to our expectation, the weaker the psychological resilience of residents with flooding above the floor level, the greater their tendency to perceive life recovery.

Thus, residents' recovery from disasters differed depending on the level of damage and the time phase. The "disaster utopia" phase up to 2 months after the disaster is the stage where residents who have experienced less damage begin recovering. Even older residents or residents who have suffered serious

©2021. Japan Geoscience Union. All Right Reserved.

damage are more able to overcome the adverse situation and recover soon, if they have strong psychological resilience. The “reentry to everyday life” phase up to 6 months after the disaster is the stage when residents who have experienced serious damage begin recovering. Residents with weaker resilience are more likely to engage in recovery activities during this stage. Although psychological resilience does not have a direct impact on life recovery, it may increase the pace of life recovery. The study suggests the importance of resource of the community for disaster risk management, such as residents’ resilience, in addition to the level of damage and the time phase after the disaster, to fully understand recovery.

Keywords: Disaster risk management, Recovery calendar, Resilience, Torrential rain

©2021. Japan Geoscience Union. All Right Reserved.

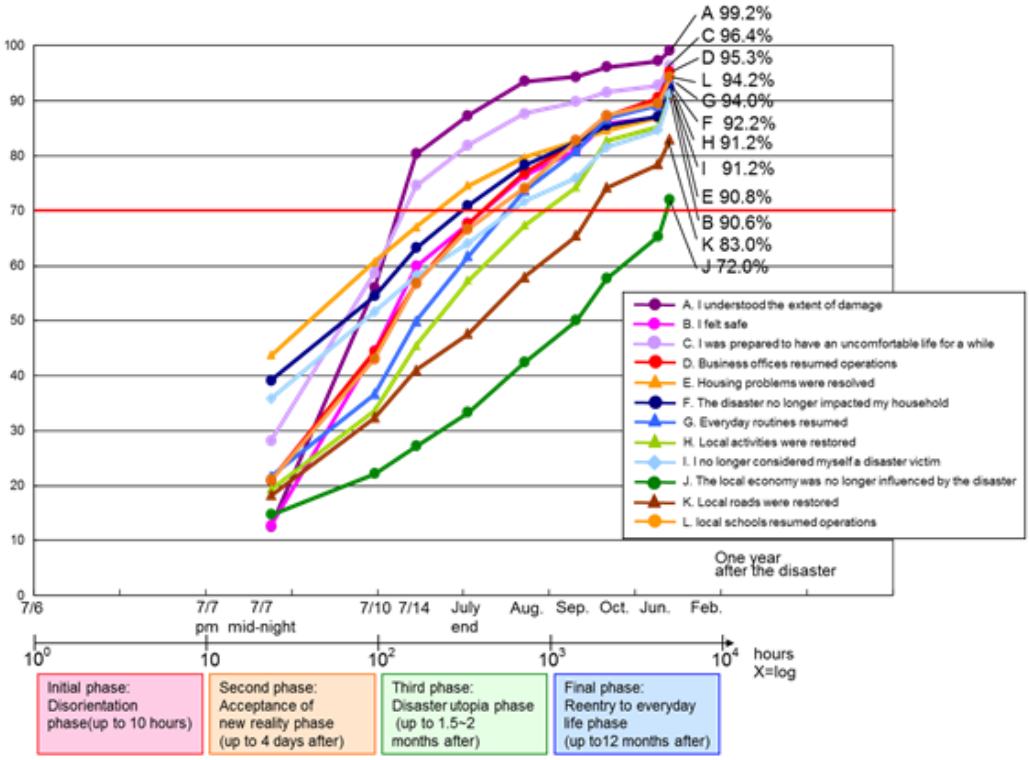


Figure 1 Life-recovery calendar of the torrential rain in western Japan in 2018

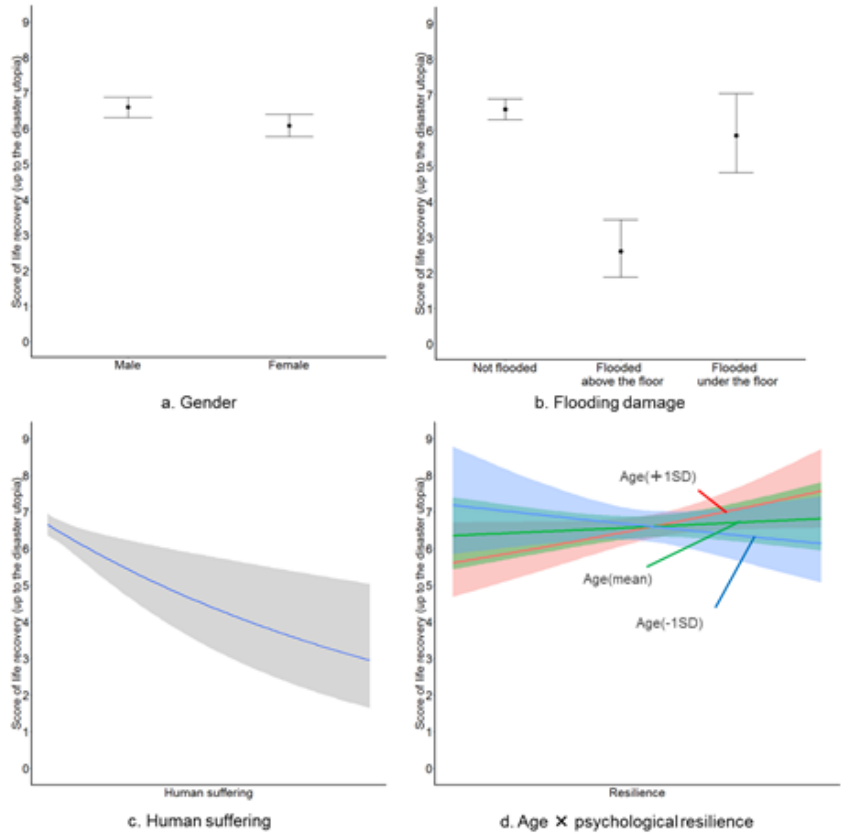
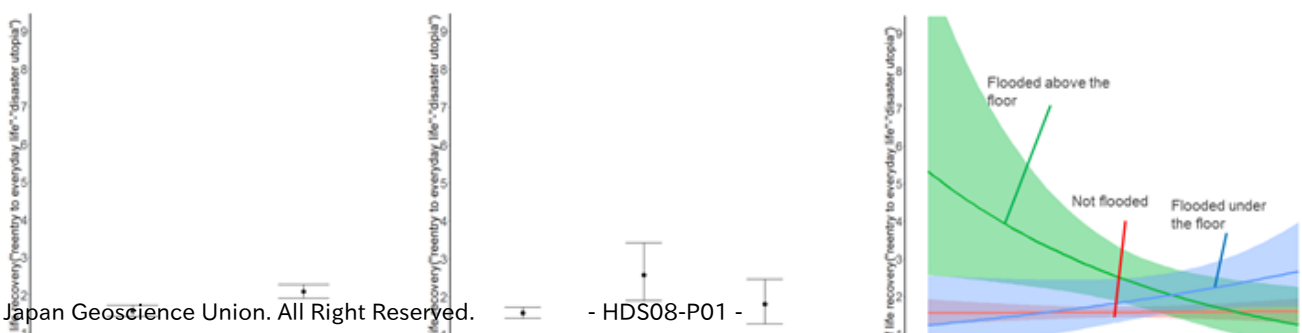


Figure 2 The plots of the posterior distribution of parameters of gender, flooding damage, human suffering, age × psychological resilience (changes in life recovery up to the "disaster utopia" phase).



©2021. Japan Geoscience Union. All Right Reserved.

©2021. Japan Geoscience Union. All Right Reserved.

Flood damage mapping of 2020 Typhoon Ulysses in the Philippines

*Naoko Nagumo[1], Kentaro Aida[1], Miho Ohara[1], Masakazu Fujikane[1]

1. International Centre for Water Hazard and Risk Management, PWRI

Typhoon Ulysses (international name: Vamco) crossed the Central Luzon Region of the Philippines in November 2020, bringing strong winds and torrential rainfall and causing 101 casualties throughout the country. The numbers of flooding and landslide/soil collapse were 264, while affected municipalities/cities reached 541 and affected persons were 5,184,824 in total (as of 13 January 2021). Also, the maximum numbers of evacuees reached to 556,318 (as of 15 November 2020). In flood-prone countries such as the Philippines, hazards and damage should be carefully investigated, and the collected data should be systematically sorted out for future disaster response, recovery and flood risk assessment. However, it is often difficult to get a whole picture of a disaster, especially when it is a widespread event. In addition, the recent worldwide pandemic of COVID-19 has made it difficult for experts to conduct sufficient field surveys. Therefore, this study conducted flood-related data mapping using satellite observation rainfall, satellite images and reports released on the web by the National Disaster Risk Reduction Management Council (NDRRMC) of the Philippines to understand the floods and damage caused by Typhoon Ulysses. Rainfall due to Typhoon Ulysses was particularly intense in the eastern part of Luzon Island; the 3-day-rainfall reached over 300 mm between 11 and 14 November. As a result, several rivers flooded at different locations of the island. The flood events of the Pasig-Marikina River in Metro Manila and the Cagayan River in Cagayan Valley Region, Northern Luzon, have been considered the most serious since the 2009 flood by Typhoon Ondoy and the 1980 flood by Typhoon Aring, respectively. Large numbers of people were reported to be affected in the regions of Central Luzon, Cagayan Valley, Bicol and Metro Manila as they lived along the typhoon course, while the house damage was concentrated in the regions of Central Luzon and Bicol. Also, 2991 evacuation centers were opened three days after the typhoon landed and 324,617 persons were evacuated inside the evacuation centers along with the other 231,701 persons evacuated outside the centers across the country, and more than 30-40 % of the population was evacuated in some municipalities. Mapping both hazard and damage data can be instrumental in understanding the characteristics of a disaster spatiotemporally, and such analytic understanding will be useful not only for recording disasters but also for sharing a common view of a disaster and identifying the needs for further support.

Keywords: typhoon, satellite image, flood, damage, Philippines

©2021. Japan Geoscience Union. All Right Reserved.

An example of using Google Earth Engine in providing and sharing information on wide-area typhoon disasters in international joint research projects

*Kentaro Aida[1], Naoko Nagumo[1], Miho Ohara[1]

1. International Centre for Water Hazard and Risk Management, PWRI

ICHARM has been conducting the SATREPS project with Philippine research members since 2020. The project's objective is to research disaster assessment to contribute to hydrology, agriculture, and water management under climate change. However, field surveys and local activities have been restricted even by local researchers due to the pandemic of COVID-19. In these circumstances, Typhoon Ulysses hit Luzon Island in early November 2020, and heavy rainfall caused large-scale floods in various parts of the country. According to the National Disaster Risk Reduction and Management Council (NDRRMC) of the Philippines, a large number of people were forced to evacuate because so many houses were severely damaged as a result of flooding. However, the overall picture of the damage caused or to be caused by the typhoon remained unknown during the disaster.

In such a case, earth observations (EO) by satellites have been proven extremely useful. Among various current operational EO-satellites, the Sentinel series by the European Space Agency (ESA) and the Landsat series by the National Aeronautics and Space Administration (NASA) provide satellite images of different areas on the planet free of charge. Sentinel-1 synthetic aperture radar (SAR) images and Sentinel-2 optical images are frequently acquired at intervals of 5 or 6 days, respectively. Such operations are beneficial for ground monitoring.

Similar to these satellite data, the information provided by government agencies is also essential for understanding the whole picture of a disaster. Information such as the number of victims, shelters, and evacuees of each municipality is regularly released by NDRRMC through the Internet. Though such information itself is very useful, it can be even more useful to understand the entire situation if visualized on a map.

Therefore, this project used the Google Earth Engine (GEE) to share the overall picture of the disaster situation due to Typhoon Ulysses. GEE is a cloud-type mapping application provided by Google. Using global satellite data and geographic information stored on Google's server, a special computer program is applied to process such data and information to help users understand them visually while looking at the screen. In other words, the most significant merit of GEE is that it can quickly launch a system that can collect and share information anywhere in the world without depending on the area of residence or human and economic resources. And, the application can visualize information for mapping, making it ready to be shared easily by many people with user-friendly functions such as enlarging and reducing images, as long as they have an Internet environment.

The information shared among the members in this project is disaster information released by NDRRMC, inundation area estimated based on Sentinel-1 SAR images, visible images and the estimated inundation area from the Sentinel-2 optical sensor, and precipitation products from satellites. The precipitation products are hourly and cumulative precipitation distributions using the satellite global precipitation map (GSMaP) provided by the Japan Aerospace Exploration Agency (JAXA) and the Integrated Multi-satellitE

©2021. Japan Geoscience Union. All Right Reserved.

Retrievals for GPM (IMERG) provided by NASA. These products were applied to the Pampanga River basin, Pasig River, Laguna Lake, Marikina River basin, and Cagayan River in the three main watersheds in northern Luzon Island.

Visualization with these GEE systems is considered to have the following significance from the viewpoint of disaster response: 1) Although the whole picture of the disaster could not be understood due to a widespread disaster, visualization of information was useful to capture a rough image of the damage distribution. To have an idea of the disaster makes it possible to predict how it may further develop or which areas need support more urgently than other areas; 2) Although, due to COVID-19, researchers from both countries could not go to the target site and meet each other, information shared among the members created a foundation for discussions on disaster response and recovery; 3) Although satellite-based visible images only offer inundation area, adding a land-use map to the inundation area map produced a useful tool for disaster response and restoration efforts; and 4) By increasing the number of information layers, the resultant map can be used not only immediately after a disaster but also at various subsequent stages, for example, to show the progress of restoration and reconstruction.

Keywords: Flood, Satellite data , Information sharing, Google Earth Engine, Philippines, Typhoon

©2021. Japan Geoscience Union. All Right Reserved.

Estimating the amount of waste treatment units in the event of a disaster with self-help and mutual support

*Yoshinobu MIZUI[1,2]

1. University of Tsukuba, 2. NationalResearch Institute for Earth Science and Disaster Resilience

1. Introduction

In recent years, regional disasters that cause enormous damage have occurred almost every year in various parts of Japan. As a self-help activity, there is a labor shortage due to the work of cleaning up the victim's house, but there are also disaster volunteers who voluntarily participate from inside and outside the area to make up for the shortage.
Since the Great East Japan Earthquake on March 11, 2011, I have been involved in the operation of disaster volunteer centers in various places, but I found it difficult to adjust the actual amount of work and the number of victims in the disaster area. To solve this problem, it is important to understand the amount of work required for self-help and mutual support and the total number of activists, and to clarify the breakdown of the total number of mutual support.
T In this study, we will grasp the total amount of self-help and mutual support. We first examined the total number of activities including self-help and mutual support in past disasters. We also calculated the amount of disaster waste treated in units of 100 people, which is the unit of the amount of treatment required to make a rough estimate.

2. Survey method

It is necessary to grasp the total amount of disaster waste caused by a disaster and clarify the breakdown amount for which self-help and mutual support are in charge of processing work. The target disaster waste is waste that can be manually cleaned on the premises of private land. The Ministry of the Environment investigates and reports on the breakdown of waste for each disaster.
Self-help / mutual support targets cleanup waste in disaster waste (waste discharged when citizens clean up damaged items at home), and cleanup waste includes combustibles and wood chips, Tatami, incombustibles, household waste, etc.
By dividing the amount of cleanup waste by the amount of self-help and mutual support activities, the unit amount of cleanup waste disposal work by self-help and mutual support can be obtained.

3. result

In 2015, the flood damage in Joso City, Kinugawa basin, was used as a model. The Joso City Disaster Volunteer Center was active for 58 days.
Assuming that one-quarter of the residents in the area where the evacuation order was issued were self-help volunteers, the total number of volunteers was 504,842 in 58 days. The total amount of disaster waste from floods in 2015 was 52,400 tons.
It was assumed that the waste to be cleaned up was combustibles, incombustibles, and earth and sand, and as condition (1), it was assumed that combustibles were almost 100% as household waste and incombustibles and earth and sand were 50%. In addition, as condition (2), a trial calculation was made assuming that combustibles are 100% and incombustibles and earth and sand are 25%. The weight ratio of combustibles and incombustibles / earth and sand will be ignored this time.
In the case of condition (1), combustibles account for 6.4% of the total amount of waste. Incombustibles account for 35.25%. Sediment is 6.0%. The ratio and weight of the target cleanup waste are
6.4 + 35.25 + 6.0 = 47.65%

©2021. Japan Geoscience Union. All Right Reserved.

52,400t ×47.65 = 24,968.6t
Assuming that this cleanup waste was processed by 504,842 people, 4.946 tons can be processed per 100 people.
In the case of condition (2), combustibles account for 6.4% of the total amount of waste. Incombustibles account for 17.625%. Sediment is 3.0%. The ratio and weight of the target cleanup waste are
6.4 + 17.625 + 3.0 = 30.025%
52,400t ×30.025 = 15,733.1t
Assuming that this cleanup waste was processed by 504,842 people, 3.116 tons can be processed per 100 people.
Also, using the estimation formula of the Ministry of the Environment, the total amount is estimated to be about 9541.933 tons. Assuming that this cleanup waste was processed by 504,842 people, 1.890 tons can be processed per 100 people.
As a result, it was found that the disaster waste treatment unit that can be treated in one day is 3t (2-5t) / 100 people.

Keywords: Self-help, mutual support, disaster volunteers, disaster waste, waste disposal

©2021. Japan Geoscience Union. All Right Reserved.

Possibility of support for disaster victims by accommodation facilities-Advance evacuation and acceptance in the event of a disaster-

Yuka SUZUKI[1], *Tatsuto Aoki[2]

1. Kanazawa University, 2. School of Regional Development Studies, Kanazawa University

Background

In order for Japan, where many natural disasters occur, to become a tourism-oriented country, it is essential to have a disaster prevention plan that keeps in mind that tourists who do not know the land will be affected.

The purpose of this study is the following two. One is to clarify the disaster prevention situation of tourists in Kanazawa City, and the other is to examine the possibility of supporting evacuees in the event of a large-scale disaster by accommodation facilities. To discuss this, we conducted interviews with the Crisis Management Division of Kanazawa City Hall, interviews and conducted a questionnaire survey with hotels (24 facilities) in Kanazawa City.

Kanazawa is one of the major tourist destinations in Japan. In addition, the Morimoto-Togashi fault zone, which is said to have a high probability of earthquake occurrence, exists in the center of the city, and it is assumed that a wide area of the city center will be flooded even with a planned-scale flood.

As an evacuation site in the event of a disaster

The regional disaster prevention plan of Kanazawa City does not specify how to deal with tourists and people who have difficulty returning home in the event of a disaster. Kanazawa City has signed an agreement with a cooperative of accommodation facilities for the purpose of utilizing accommodation facilities as a temporary evacuation site for tourists and those who have difficulty returning home. However, in the interviewed to the Crisis Management Division of the city hall, regular meetings were not held after the conclusion of the agreement, and the disaster management plan of the accommodation facility was not grasped. At present, it is hard to say that the agreement is effective.

On the other hand, there is also a problem on the accommodation facility side that accepts tourists. None of the facilities answered that they have a good understanding of earthquakes originating from the Morimoto-Togashi fault zone. It became clear that the awareness of the disaster assumption was low. Reflecting this, 42% (10/24 facilities) have not formulated a disaster prevention manual. Only 13% (3/24 facilities) have prepared manuals for both earthquakes and floods. 33% (8/24 facilities) do not expect to open the facilities as evacuation shelters in the event of a disaster. Even among facilities that are expected to accept evacuees, only 25% (6/24 facilities) are expected to accept tourists other than the guests of their own facilities.

In addition, 42% (10/24 facilities) of facilities that can accept evacuees for about 3 days, and 21% (5/24

©2021. Japan Geoscience Union. All Right Reserved.

facilities) that can accept evacuees for 1 week or more. It was. This indicates that the Kanazawa city government needs to evacuate tourists out of the city in a short period of time.

As an evacuation site for preventive evacuation

In the case of floods, preventive evacuation is important. 54% (13/24 facilities) answered that they could accept evacuees for preventive evacuation in some way. In the hearing for the facility, "if there is a request of the city government, acceptance of the citizens is also taken into account," there was some hotels that answered. On the other hand, another hotel said that it is difficult to distinguish evacuees from general guests before a disaster occurs, and they will be provided for a fee based on the reservations made by the guests. It was shown that there are certain difficulties in accepting preventive evacuation by accommodation facilities.

One hotel considering accepting preventive evacuees said, "Proactively providing evacuation shelters, will lead to the improvement of the hotel brand and disaster prevention can be monetized as our main business." The provision of shelters for accommodation facilities was a disaster response as CSR in response to government requests. This result shows that this could be developed into a model of responding to disasters as a social business and connecting it to the original business.

Conclusion

It was confirmed that the effectiveness of the disaster prevention agreement between Kanazawa City and accommodation facilities is currently questionable. In order to make it more effective, various types of support from the government will be required.

Accommodation facilities are also required to actively understand the disaster risks of their own facilities and the surrounding area. In preventive evacuation, it will be possible to take disaster prevention measures as an opportunity for social business and actively take measures. We would like to point out that introducing such a perspective into the BCP can be beneficial to companies, governments, and citizens.

Keywords: Accommodations, Evacuee, Preventive evacuation, Shelter, Social business

©2021. Japan Geoscience Union. All Right Reserved.

Effect of synchrony bias on excitation of evacuation behavior during tsunami-From the evacuation behavior of residents in Noto Town, Ishikawa Prefecture during the 2019 Yamagata-oki Earthquake-

Mayu KITAMURA[1], *Tatsuto Aoki[2]

1. Kanazawa University, 2. School of Regional Development Studies, Kanazawa Univ.

Research objectives

Japan is one of the world's highest affected countries by disaster. Within those disaster, the tsunami disaster is one of the most damaging. As a characteristic of disaster prevention actions against tsunami disasters, it may be possible to reduce human damage by evacuating using seismic motion and/or tsunami information prior to the arrival of the tsunami. and there are many studies and activities have been done to encourage evacuation.

In previous studies, psychological studies have also been conducted on the relationship between evacuation behavior and disaster experience / disaster prevention awareness. According to them, it has been clarified that human cognitive bias has a great influence as one of the factors that cause "evacuation delay" and "people who do not evacuate".

Therefore, in this study, we conducted a questionnaire survey of residents living in the tsunami inundation area of Noto Town, located in the northern part of the Noto Peninsula, Ishikawa Prefecture. And we investigated and analyzed how cognitive bias affected the evacuation behavior. At the time of the Yamagata-oki earthquake (M_{JMA}6.7), Noto Town are shaken of seismic scale 3 by JMA and only a tsunami advisory was issued. However, more than 500 residents moved to evacuation site. The area around the study area is the area where one-sixth of the seismic intensity was observed in the Noto Hanto earthquake in 2007. And the tsunami hazard map revised after the Great East Japan Earthquake in 2011.

Result

The questionnaire was distributed and collected by mail to 999 households in the district. The number of collections was 255 (25.5%), 55% for men (N = 141), 40% for women (N = 103), and 4% for others (N = 11). By age, the elderly aged 60 and over account for 65% (N = 165). The fact that household representatives are respondents to the questionnaire and that the aging rate in the target area is close to 50% influences the high proportion of elderly respondents in the questionnaire.

As a result, it was found that 25% of the respondents were evacuated from the tsunami. Respondents were classified into the following four patterns. (1) Evacuated during both of the Noto Hanto and the Yamagata-Oki earthquakes, (2) Evacuated only during the Noto Hanto earthquake, (3) Evacuated during the Yamagata-oki earthquake even though did not evacuated during Noto Hanto earthquake, ④ Did not evacuated during both the earthquakes. The composition of the respondents was (1) 4% (N = 9), (2) 3% (N = 6), (3) 19% (N = 43), and (4) 75% (N = 174). The important point is there were some cases where people who did not evacuate during the Noto Hanto earthquake evacuated this time.

Focusing on the residents who responded as (3), we asked for them multiple answers about the reasons for evacuation. As a result, the answers were obtained that "due to earthquake motion (20 people)", "due to tsunami information (19 people)", and "because they live in the inundation area (16 people)". In addition, the following answers followed. "Because I was instructed to evacuate (8 people)" "Because my neighbors were evacuating (8 people)" "Because someone told me to evacuate (7 people)". These results mean that in addition to the sense of crisis and information, "synchronization bias" such as "evacuation behavior of surrounding people and voices from others" acted positively. Furthermore, among the

©2021. Japan Geoscience Union. All Right Reserved.

categories (1) to (4), the highest percentage of those with synchronization bias affected was in (3), and the percentage was 30%.

Discussion

In the context of disaster prevention, synchronization bias is often cited along with normalcy bias as a reason for residents not to evacuate. However, the results of this study showed that by intentionally biasing the population in synchronization, people who did not evacuate voluntarily may be able to evacuate. It is also able to pointed out the importance of social capital to enhance disaster prevention capabilities, such as community disaster prevention leaders who calling for evacuation in emergencies and communities where residents can communicate on a daily basis.

In disaster prevention and mitigation, not only physical measures such as stockpiling but also psychological measures are important. As part of education for disaster prevention, we need to learn about cognitive bias.

Keywords: Tsunami, Evacuation, Synchronous bias, 2019 Yamagata-oki Earthquake

©2021. Japan Geoscience Union. All Right Reserved.

Status of provision of disaster prevention information and learning to international students at national and public universities and their issues

*CHENYUE LU[1], Kiyomi HAYASHI[2], Tatsuto AOKI[2]

1. Division of Regional Development Studies,Graduate School of Human and Sociology-Environmental Studies,Kanazawa University, 2. School of Regional Development Studies, Kanazawa University

In this study, we will clarify the status of dissemination of disaster prevention information and the implementation and support of disaster prevention to international students learning at national and public universities. Questionnaires were distributed by mail to departments that support international students at 179 universities nationwide (collection number 78, collection rate 43.6%).

Results

1) Status of provision of disaster prevention information at orientation

52.6% of univ. provide disaster information at orientation, and 55.1% of univ. distribute and post disaster information issued by local governments. 44.9% of univ. provide disaster information in languages other than Japanese. The languages used was English (100%), Simplified Chinese (54.3%), Korean (37.1%), Traditional Chinese (14.3%), and other languages (11.4%).

2) Status of learning opportunities related to disaster prevention

When it comes to safety confirmation systems and training for their use between univ. and international students, only 30 univ. "have system, and are training". Regarding "evacuation drills at univ.", 34 univ. "conducted and many international students participated" and 16 univ. "conducted but the participation rate of international students was low". At 66 univ., there were no disaster prevention events in collaboration with the local community. Only 15 univ. provided guidance on disaster drills of local community and encouraged international students to participate.

18 univ. have "established" classes for international students studying disasters and disaster prevention of Japan, and 4 of them "take many international students". There were 58 universities that did not provide Japanese language education including vocabulary and expressions of a disaster.

3) Issues felt by the university

The following issues were raised as problems in disaster prevention support and guidance for international students.

Insufficient communication and Japanese proficiency (43 univ.)
Unrecognized possibility of disaster (30 univ.)
Influence of culture and lifestyle of country of origin (28 univ.)
Incomprehensible jargon (28 univ.)
Insufficient understanding and image of disasters and disaster prevention caused by the lack of disaster experience and learning opportunities in the home country (26 univ.)

The following issues were also raised.

International students do not fully understand the characteristics of the natural environment and the

©2021. Japan Geoscience Union. All Right Reserved.

structure of the town in their area (22 univ.)
Undeveloped information provision routes and venues (22 s univ.)
Difficulty in collaboration between international students and the community at the time of the disaster (21 univ.)
Weak connection between international students and the community (21 univ.)

In addition, we asked each university's views on the need for learning support, guidance and information provision for community-related disasters for international students. 45 universities replied, "We should not only disseminate and train information on disaster prevention on campus, but also support and provide information on disasters related to the region, but we have not fully implemented it."

Issues and improvement measures considered from the results of the questionnaire
When international students begin their college life in Japan where the high-risk area in disaster, information provision, training, events, orientation and classes at univ. can be an important opportunity to recognize and prepare for disaster risks.

The departments in charge of international students at many univ. are aware of the following. Problems with Japanese language proficiency, low knowledge and awareness of disaster due to lack of experience and learning, differences in lifestyle, inadequate understanding of the region and inadequate cooperation with the region. In addition, they feel that it is necessary to devise environmental improvement and disaster prevention learning in order to improve these problems. However, they are struggling to be unable to fulfill. There are various things that need to be dealt with in support of international students, and it is difficult to devote a lot of time, labor, cost, and human resources to the enhancement of disaster prevention learning and activities. However, there are some aspects in which the situation can be improved and improved with a little ingenuity and consideration, and it is desirable to start from there.

Keywords: international students, study for disaster prevention, information of disaster prevention, university, questionnaire survey

©2021. Japan Geoscience Union. All Right Reserved.

[J] Poster | H (Human Geosciences)：H-TT Technology & Techniques

Sun. Jun 6, 2021 5:15 PM - 6:30 PM JST | Sun. Jun 6, 2021 8:15 AM - 9:30 AM UTC | Ch.09_3

[H-TT19] Geographic Information System and Cartography

convener:Mamoru Koarai(Earth Science course, College of Science, Ibaraki University), Kazunari Tanaka(Department of Civil Engineering and Urban Design, Faculty of Engineering, Osaka Institute of Technology), W. Kazuhiko Nakamura(The University of Tokyo)

This session discusses various methods which acquire, store, analyze and visualize geospatial data, and presents the outcomes of empirical studies using GIS or mapping methods. The session also deals with applications of digital data, GIS, and mapping to various fields of earth and planetary science and human society. All presentations and discussion of this session are made in Japanese.

[HTT19-P01] Susceptibility assessment of post-seismic landslides with an index representative of seismic cracks

*Shui Yamaguchi[1], Mio Kasai[2] (1.Graduate School of Agriculture, Hokkaido University, 2.Research Faculty of Agriculture, Hokkaido University)

[HTT19-P02] Development of information platform for topographical recognition by CS topographic map

*Hiromu Daimaru[1], Kenichiro Toda[2], Wataru Murakami[1], Ryuichi Sekoguchi[3], Yoichi Kayama[3], Keichi Katsube[3], Hiroo Imaki[4], Koji Ijima[4], Ryosuke Wayama[5] (1.Forestry and Forest Products Research Institute, 2.Nagano Prefecture Forestry Research Center, 3.Aero Asahi Corporation, 4.Pacific Spatial Solutions Co., Ltd., 5.Northern System Service Co., Ltd.)

Susceptibility assessment of post-seismic landslides with an index representative of seismic cracks

*Shui Yamaguchi[1], Mio Kasai[2]

1. Graduate School of Agriculture, Hokkaido University, 2. Research Faculty of Agriculture, Hokkaido University

An intense earthquake can cause numerous landslides over a broad area, causing damage to human lives, property, and infrastructure. The strong tremors weaken the ground strength and induce cracks on the ground surface. Thus, following the earthquake, identification of the ground cracks is rapidly carried out via field survey and/or examining aerial photographs or topographic maps to find slopes in danger of sliding and prevent from further disaster. However, this operation requires more time and effort as the magnitude of the earthquake is more extensive. Hence, we proposed an index (DCI: Dense Crack Index) representative of the density of co-seismic cracks, which can be quickly and easily calculated using airborne LiDAR data before and after the earthquake. This study applied the index to an area (6 km^2) located in the southwestern Aso Caldera, Kumamoto Prefecture, where the 2016 Kumamoto earthquake (Mw 7.0) struck, and the 198 co-seismic and 125 post-seismic slides were recognized in the following four months. They were categorized as shallow landslides. Then, we statistically estimated the susceptibility of post-seismic landslides and examined the improvement of the evaluation accuracy when DCI is incorporated in predictor variables.

First, we calculated the slope angle for each 1-m cell derived from LiDAR survey data acquired before and after the earthquake (Fig. 1-a), and then its standard deviation for 3 ×3 cells. We found that the standard deviation increased by more than 2 degrees after the earthquake in 75% of the locations where co-seismic cracks were identified (Fig. 1-b). The DCI was given as the spatial density of those cells, calculated by the kernel density with a nearby distance of 10 meters (Fig. 1-c).

Weight of Evidence (WoE) and Logistic Regression (LR) methods were applied to estimate the susceptibility for post-seismic slides. The response variable used in these two statistical models was the presence or absence of post-earthquake landslides on the cell, which was identified from aerial photographs and topographic maps obtained four months after the earthquake. Also, the slope angle, profile curvature, slope aspect, distance to edge of co-seismic landslides, distance to epicenter fault, and peak ground acceleration (PGA) were adopted as predictor variables in addition to DCI. This study considered the geology, vegetation, and rainfall conditions as the same due to the small size of the study area.

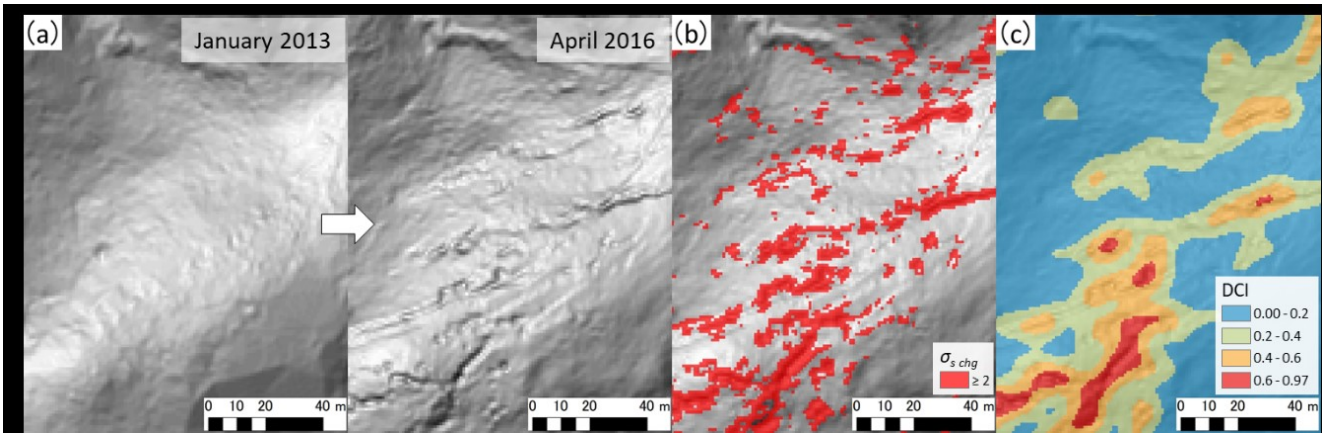
The analysis by the WoE method showed that steep slopes (slope: 40 - 55 degrees) near knick lines (profile curvature: -6 - -4 m^{-1}) affected by strong tremors (PGA: 1050 - 1150 gal) with dense crack appearance (DCI: 0.2 - 1.0) were more likely to slide after the earthquake. This result is in agreement with the report of the field survey conducted in the study area (Kumamoto Prefecture, 2019). The accuracy of the susceptibility assessment by the WoE and LR methods was slightly higher when DCI was included as a predictor variable, with an Area Under the Curve (AUC) value of 0.80 - 0.90 for the ROC curves, compared to the models without DCI (0.70 - 0.85).

As such, the inclusion of DCI in statistical susceptibility assessment improved the accuracy of the models and allowed the identification of slopes in danger of sliding that were consistent with those reported from the field. These results suggest that DCI is an important index for estimating slopes destabilized by seismic motion.

Fig.1:Step of DCI calculation (a: Slope maps of pre- and post- earthquake, b: red indicates the locations where the standard deviation of the slope increased by more than 2 after the earthquake , c: DCI map)

©2021. Japan Geoscience Union. All Right Reserved.

Keywords: post-seismic landslides, seismic cracks, landslide susceptibility assessment, WoE, Logistic regression



©2021. Japan Geoscience Union. All Right Reserved.

Development of information platform for topographical recognition by CS topographic map

*Hiromu Daimaru[1], Kenichiro Toda[2], Wataru Murakami[1], Ryuichi Sekoguchi[3], Yoichi Kayama[3], Keichi Katsube[3], Hiroo Imaki[4], Koji Ijima[4], Ryosuke Wayama[5]

1. Forestry and Forest Products Research Institute, 2. Nagano Prefecture Forestry Research Center, 3. Aero Asahi Corporation, 4. Pacific Spatial Solutions Co., Ltd., 5. Northern System Service Co., Ltd.

Topographical recognition is a fundamental process when considering land use plans for mountain areas. Airborne laser scanning, which has been widely used in recent years, has provided valuable data for landform recognition. We have developed an information system to support landform recognition in the mountain areas by distributing raster tile of CS topographic map, including a converting tool from Geotiff formatted DEM to CS topographic map image by using FME (Safe Software Inc.). This system includes the tool for LEM formatted data that is commonly used in Japan for LiDAR DEM.
The CS map images created by our system are displayed in seamless style and uniform tones. The metadata catalog of the CS map was provided to GKAN that was developed by adding spatial functions to the data catalog server CKAN. The platform enables GIS users to search for stored CS map database and distribute the raster tiles. Furthermore, we also developed a technology that automatically extract shallow landslide scarps and small forest roads from CS topographic maps by using AI.

Keywords: Landform, CS topographic map, Web GIS, GKAN, AI

©2021. Japan Geoscience Union. All Right Reserved.

[J] Poster | H (Human Geosciences)：H-CG Complex & General

Sun. Jun 6, 2021 5:15 PM - 6:30 PM JST | Sun. Jun 6, 2021 8:15 AM - 9:30 AM UTC | Ch.09_4

[H-CG26] Adaptation to climate change and its social implementation

convener:Hiroya Yamano(National Institute for Environmental Studies), Yoichi Ishikawa(JAPAN Agency for Marine-Earth Science and Technology), KOJI DAIRAKU(University of Tsukuba), Makoto Tamura(Global and Local Environment Co-creation Institute, Ibaraki University)

The impacts of climate change will increase in the risks to societies through increased intensities of typhoons and torrential rains, changes in the distribution of organisms, deterioration in quality and yield in the agriculture, forestry and fisheries, etc. In response to this, Japan enforced "Climate Change Adaptation Act" in 2018, aiming to minimize or avoid the damage caused by climate change, and to build a sustainable society.
In this session, toward planning adaptation to climate change and enhancing its social implementation based on scientific knowledge, we will discuss about generation of climate change projection data, assessment of the impacts and risks of climate change in various fields, as well as social implementation of adaptation plans by co-creation with stakeholders and/or by local climate change adaptation acts.

[HCG26-P01] ASSESSMENT OF WIND/SOLAR ENERGY POTENTIAL AS A POWER GENERATION SOURCES AT SOME SELECTED LOCATIONS IN PAKISTAN

*Muhammad Abid KHAN[1], KOJI DAIRAKU[1] (1.University of Tsukuba)

ASSESSMENT OF WIND/SOLAR ENERGY POTENTIAL AS A POWER GENERATION SOURCES AT SOME SELECTED LOCATIONS IN PAKISTAN

*Muhammad Abid KHAN[1], KOJI DAIRAKU[1]

1. University of Tsukuba

The main objective of this research was to investigate the wind power potential and the feasibility of developing a solar PV plant at seven selected locations in Pakistan. In this study, wind speeds were collected over a period of 2005-16 and measured at 10m height. Ten dissemination functions were connected to analyze the wind speed characteristics of these chosen areas and assess the wind power density. In additions, the technical viability study of the proposed crystalline technology-based PV plants with different tracking systems in terms of Fixed, 1-axis, Inclined-axis, and Two-axis were analyzed using Photovoltaic Geographical Information Systems (PVGIS) and PV Watts' s software. The results showed that Kati Bandar has the highest annual wind speed of 4.04 m/s in comparison to other locations, while the lowest value of 1.33m/s was obtained in Islamabad Capital Territory. The maximum power density of 258.75W/m2 is occurred in July at Kati Bandar, while the lowest minimum wind power density of 1.68 W/m2 occurred in September at Islamabad at 10m height. Moreover, the simulation results showed that Two-axis performance is higher than as compared to another track system. Performance results, the performances of four small-scale wind turbines were evaluated. Based on the results, the Pitch wind/30kW Grid wind turbine had the highest annual capacity factor of 56.366%, whereas, WS-12/8kW wind turbine had the minimum at 15.416%. Consequently, the Minimum and the Maximum annual electricity cost in the studied locations are 0.005$/kWh and 0.032 $/kWh using Pitch wind/30kW Grid and WS-12/8kW, respectively. Moreover, the Levelized cost of electricity (LCOE) for PV Plants was estimated. It is found that, LCOE for fixed tilt, 1-axis, Inclined axis and 2-axis tracking modes PV plants for all locations were obtained in the range of 0.178 - 0.239 $/kWh, 0.14 –0.202 $/kWh, 0.145 –0.203 $/kWh and, 0.133 –0.191 $/kWh.

Keywords: Energy potential, probability distribution function, techno-economic, renewable energy, electricity cost

©2021. Japan Geoscience Union. All Right Reserved.

[J] Poster | H (Human Geosciences)：H-CG Complex & General

Sun. Jun 6, 2021 5:15 PM - 6:30 PM JST | Sun. Jun 6, 2021 8:15 AM - 9:30 AM UTC | Ch.09_5

[H-CG29] Advanced life support systems with closed bio-ecosystems and thier applications

convener:Masanori Shinohara(Teikyo University of Science), Hiroshi Katoh(Division of Plant Functional Genomics, Advanced Science Research Promotion Center, Organization for the Promotion of Regional Innovation, Mie University), Shunta Kimura(Institute of Space and Astronautical Science / Space Exploration Innovation Hub Center, Japan Aerospace Exploration Agency), Midori Ong(University of Tsukuba)

In this session, since 2011, we and invited researchers have been introducing and discussing about practical and useful life-support systems in closed bio-ecosystems for inhabitation on extraterrestrial environments. Not only biological studies but also engineering ones
including broad research fields are our target. And also, we assume that it is indispensable to discuss about these interdisciplinary fields beyond the generation for inheriting to our next generation and for developing our field. Theme from old and basic to current and applicative from senior to youth including undergraduate are welcomed.

[HCG29-P01] Growth of cyanobacterium, *Nostoc* sp. HK-01, after exposure to several harsh environments.

*Miku Tokita[1], Midori Ong[1], Hiroshi Katoh[2], Kaori Tomita-Yokotani[1] (1.University of Tsukuba, 2.University of Mie)

[HCG29-P02] Relationship between seed formation during tomato growth and microgravity generated by a hand-made 3D-clinostat.

*Yuan Takase[1], Kaori Totami-Yokotani[1] (1.University of Tsukuba)

[HCG29-P03] Identification of *Nostoc* sp. HK-01 proteins found in dry environment

*Hiroko Tanaka[1], Tomoko Abe[1], Hiroshi Katoh[2], Midori Ong[3], Kaori Tomita-Yokotani[3] (1.Graduate School of Science and Engineering, University of Tokyo Denki, 2.Organization for the Promotion of Regional Innovation, Mie University, 3.Faculty of Life and Environmental Sciences, University of Tsukuba)

[HCG29-P04] History of biological systems in closed-ecological systems

*Hiroshi Katoh[1] (1.Mie University)

[HCG29-P05] Advanced use of potatoes (*Solanum tuberosum* L.) for manned space activities

*Yota Tsukizaki[1], Toshisada Suzuki[2], Kaori Tomita-Yokotani[1] (1.University of Tsukuba, 2.Kagawa University)

Growth of cyanobacterium, *Nostoc* sp. HK-01, after exposure to several harsh environments.

*Miku Tokita[1], Midori Ong[1], Hiroshi Katoh[2], Kaori Tomita-Yokotani[1]

1. University of Tsukuba, 2. University of Mie

We previously reported that dried cells of the terrestrial cyanobacterium, *Nostoc* sp. HK-01, have a high tolerance to several cosmic environmental conditions. The dried cells of the species were used as materials in space exposure experiments. After exposure to harsh environments, there is a possibility that some cells may have suffered severe damage even if it is not evident in their appearance. Detailed observations of individual cells and their related chemical analyses are required by examining cells after exposure to harsh environments. In this study, we focused on the cell germination and continuous proliferation of *Nostoc* sp. HK-01 to confirm the damage.

Keywords: serious environments, terrestrial cyanobacteria, germination of akinetes, Nostoc sp. HK-01

©2021. Japan Geoscience Union. All Right Reserved.

Relationship between seed formation during tomato growth and microgravity generated by a hand-made 3D-clinostat.

*Yuan Takase[1], Kaori Totami-Yokotani[1]

1. University of Tsukuba

The circulationCirculation of foods is be an important matter for long–term manned space activity in extraterrestrial environments, such as on Mars. We have already confirmed that seed formation in tomato plants requires gravity. In this study, we will consider the gravity-required period and its mechanisms during seed formation under microgravity generated by a hand-made 3D-clinostat.

Keywords: Tomato growth, hand-made clinostat

©2021. Japan Geoscience Union. All Right Reserved.

Identification of *Nostoc* sp. HK-01 proteins found in dry environment

*Hiroko Tanaka[1], Tomoko Abe[1], Hiroshi Katoh[2], Midori Ong[3], Kaori Tomita-Yokotani[3]

1. Graduate School of Science and Engineering, University of Tokyo Denki, 2. Organization for the Promotion of Regional Innovation, Mie University, 3. Faculty of Life and Environmental Sciences, University of Tsukuba

Nostoc sp. HK-01, one of terrestrial cyanobacterium, could be used for bio-chemical circulation in a closed ecosystem including space. Furthermore, its high tolerance to desiccation stress has ability of usefulness as a food.
In this study, genes of *Nostoc* sp. HK-01 induced by desiccation stress were investigated.
Nostoc sp. HK-01 cells were dehydrated slowly. Proteins extracted from dehydrated HK-01 cells and wet HK-01 cells applied to SDS-polyacrylamide gel electrophoresis. In comparison with the wet cell proteins, significant abundance changes of some proteins in the dehydrated cells were detected. Further, expression analyses of genes encoding these proteins were performed by real-time PCR. The research will be expected to contribute to an effective utilization of food resources.

Keywords: cyanobacteria, desiccation tolerance, stress protein

©2021. Japan Geoscience Union. All Right Reserved.

History of biological systems in closed-ecological systems

*Hiroshi Katoh[1]

1. Mie University

It will be shown history of this session.

Keywords: closed, ecological systems, biological systems

©2021. Japan Geoscience Union. All Right Reserved.

Advanced use of potatoes (*Solanum tuberosum* L.) for manned space activities

*Yota Tsukizaki[1], Toshisada Suzuki[2], Kaori Tomita-Yokotani[1]

1. University of Tsukuba, 2. Kagawa University

Potato plants are very popular cultivated crops worldwide. Many studies related to the cultivation of potato plants under extraterrestrial environments exist, and here, we focus on the problems infor the cultivation of potato plants for manned space activities. In this study, we will propose the advanced use of potato plants in sever environments such as on Mars.

Keywords: Potato plants, cultivation, manned space activities

©2021. Japan Geoscience Union. All Right Reserved.

[J] Poster | S (Solid Earth Sciences)：S-SS Seismology

Sun. Jun 6, 2021 5:15 PM - 6:30 PM JST | Sun. Jun 6, 2021 8:15 AM - 9:30 AM UTC | Ch.10_1

[S-SS04] Earthquake prediction and forecast

convener:Shingo Watada(Division of Monitoring Science, Earthquake Research Institute, University of Tokyo), Masayuki Obayashi(Japan Agency for Marine-Earth Science and Technology)

This session provides the opportunity for presenting researches on prediction or forecasting of earthquake occurrences in wide sense, including times, places, sizes, or source mechanisms. Also, this session welcomes scientific discussions on possible causal relations to some other observation data, forecasting simulations based on theoretical models, developments and applications on statistical evaluation method for the verification of retrospective experiments, etc.

[SSS04-P01] **Effects of Earth tides on the mainshock of the 2011 Tohoku Earthquake**

*Yoshiki SUE[1] (1.none)

[SSS04-P02] Statistical Study and Probability of Foreshocks on the Japan Mainland

*Hong Peng[1], James Mori[1] (1. Earthquake Hazards Division, Disaster Prevention Research Institute, Kyoto University)

[SSS04-P03] Comments on the Brownian Passage Time model for recurrent earthquakes with uncertain origin times

*Masajiro Imoto[1], Nobuyuki Morikawa[1], Hiroyuki Fujiwara[1] (1.National Research Institute for Earth Science and Disaster Resilience)

[SSS04-P04] Relationship between the Moderate Repeating Earthquakes and the Larger-scale Earthquakes on the trench side

*Masayuki Tanaka[1] (1.Meteorological Research Institute)

[SSS04-P05] Validation of forecast experiment on the Kamaishi repeating earthquakes based on numerical simulations

*Shingo Yoshida[1], Jun'ichi Fukuda[1], Toshihiro Igarashi[1] (1.Earthquake Research Institute, University of Tokyo)

Effects of Earth tides on the mainshock of the 2011 Tohoku Earthquake

*Yoshiki SUE[1]

1. none

1. Introduction
In the 2011 Tohoku earthquake, a clear correlation between the earth tide and the earthquake occurrence was observed for about 10 years just before the main shock occurred near the rupture initiation zone of the main shock (Tanaka, 2012). So, the author reports effects of the earth tides possibly related to occurrence of the mainshock.

2. Effects of earth tides to foreshock-mainshock type earthquake
The largest foreshock occurred at 11:45 on March 9 and the main shock at 14:46 on March 11, with an interval of 51 hours 1 minute. The moon has the largest influence on the earth tides with an orbital period of 24 hours and 50 minutes, or roughly 25 hours. Therefore, the mainshock occurred just after the moon orbited twice. The equation with approximate number is as follows.

Time of mainshock = Time of foreshock + 2 orbits x 25 hours + approx. 1 hour (1)

The 2016 Kumamoto earthquake was also of the foreshock-mainshock type, with an interval of 27 hours and 59 minutes, i.e., one orbit x 25 hours + approx. 3 hours. With 2 data, we have the following equation.

Time of mainshock = time of largest foreshock + number of orbits x 25 hours ±several hours (2)

It is assumed that for the mainshock, the moon was in the same position as in the foreshock, and the moon caused similar deformation to the topography and triggered the earthquake.

In the case of the 2011 Tohoku earthquake, the time for the moon in the middle was 16:12, so the mainshock occurred 1 hour ad 30miutes before it. In the case of the 2016 Kumamoto earthquake, the time for the moon in the middle was 0:33, so the mainshock occurred about one hour after the moon in the middle. In both cases, the moon was almost directly above the epicenter.

3 Effects of the earth tides on the date of occurrence
3-1. 2011 Tohoku Earthquake (Fig. 1)
The lunar phases of the major earthquakes that occurred in the central off-Sanriku area are explained below. The phase of the moon is shown by the difference in ecliptic longitude between the moon and the sun, are 0 degrees at new moon, 90 degrees at first quarter moon and so on. In this area, there is an apparent dependency on 20 to 80 degrees, and the major damaging earthquakes have occurred during this period. Or, large earthquakes occurred around 3rd to 8th day of the lunar calendar (Sue, 2008).

The 2011 earthquake occurred on the 7th day of the lunar calendar, Or 70 degrees from the ecliptic longitude difference between the moon and the sun, which means that the earthquake occurred at the same lunar phase as before (Sue, 2011).

The 2008 survey was conducted in a rectangular area across the trench axis in the central part of Sanriku,

©2021. Japan Geoscience Union. All Right Reserved.

where the southern boarder is 39 degree north. The 2011 M9 earthquake, however, occurred at 38 degrees 6 minutes north, which is roughly 1 degree out of the boarder of the research area. Since the trench axis is running southward almost straight, I assume that the mechanical orientation is generally maintained. I have also conducted research to the southern area of this region, that is called land and offshore of Miyagi Prefecture. And I have confirmed that a cluster of occurrences at a lunar-solar ecliptic longitude difference of 70-95 degrees, and the 1793 earthquake (M8, 7th lunar day) occurred (Sue 2007) .

The case study of the central off-Sanriku area suggests that a area-by-area survey of past earthquakes is effective in estimating the date of occurrence of a new major earthquake that will occur in the same area later.

3-2. The 869 Jogan Earthquake
The 869 Jogan Earthquake is regarded as the similar earthquake of the 2011M9 earthquake. While this earthquake occurred on 26th of the lunar calendar, so the research shall be done carefully.

References
Sue, Y., 2007, Proc. of the Seismological Society of Japan, P2-056.
Sue, Y., 2008, JpGU, Preprints, S145-P004.
Sue, Y., 2011, JpGU, Preprints, MIS036-P87.
Tanaka, S., 2012, Geophys. Res. Lett., 39(7).

Keywords: Earthquake, Earth tides, 2011 Tohoku earthquake

©2021. Japan Geoscience Union. All Right Reserved.

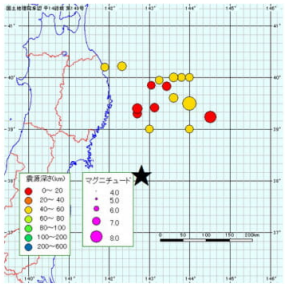
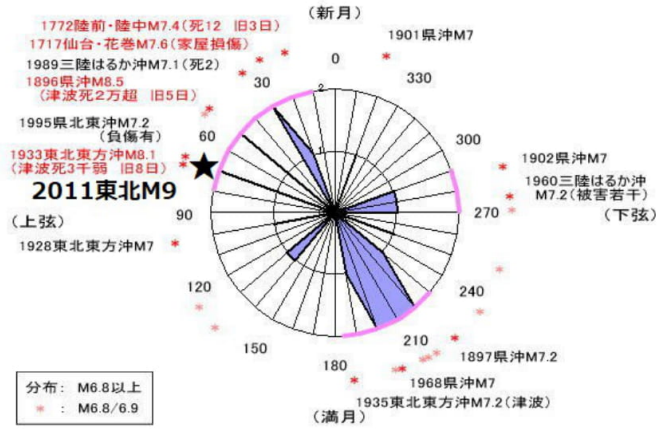
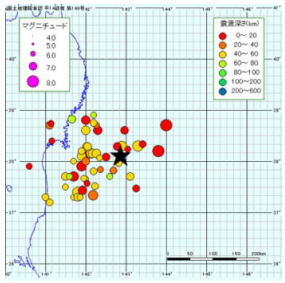
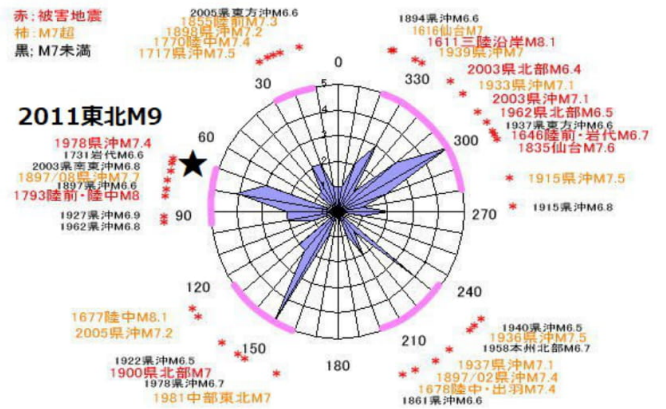
調査領域 Area	解析結果 Result
三陸沖中部 **Central off-Sanriku**  （図: KenMap）	
宮城県陸部及び沖合 （含三陸沖南部海溝寄り） **Land and offshore of Miyagi pref.** 	

図 1 地震発生時の月の位相の分布: データセット（左）と分布（右、中央は発生数、周囲は地震名、赤字は被害地震、2007-8 年作成）。分布は一様で無い。これに 2011 年東北 M9 地震（★）を追加した。大地震が発生した期間で今回も発生している。

Fig.1 The distribution of moon phases at earthquakes: Data set (left) and distribution (right, center is the number of occurrence, surrounding is the name of the earthquakes, and in red are the damaged earthquakes. Produced in 2007-8). The distribution is not uniform. The 2011 Tohoku M9 earthquake (*) is added. The earthquake occurred during the period when major earthquakes occurred so far.

©2021. Japan Geoscience Union. All Right Reserved.

Statistical Study and Probability of Foreshocks on the Japan Mainland

*Hong Peng[1], James Mori[1]

1. Earthquake Hazards Division, Disaster Prevention Research Institute, Kyoto University

Previous studies of foreshocks estimated the rate of foreshock occurrence before moderate and large earthquakes in high seismicity areas, such as California. The studies proposed that it is possible to calculate the probability that a larger earthquake follows a specific event. Here, we use the Japan Meteorological Agency (JMA) earthquake catalogue from 2001 to 2020 to check the temporal and spatial distributions of pairs of earthquakes where a smaller earthquake is followed by a larger earthquake. There is a clear peak for pairs of events which are located within 5 days and 2 km. . This time-space window is what we define as foreshocks. According to our results, it is possible to forecast the probability of a following larger event , but it is difficult to predict its magnitude . In order study the relation between the foreshock-mainshock distance, , we select about 200 mainshocks which have obvious foreshocks and use filtered P waveforms to relocate the foreshocks. This provides us with more accurate locations of foreshocks than the JMA catalog.

Keywords: Statistics, Foreshocks, Japan mainland

©2021. Japan Geoscience Union. All Right Reserved.

Comments on the Brownian Passage Time model for recurrent earthquakes with uncertain origin times

*Masajiro Imoto[1], Nobuyuki Morikawa[1], Hiroyuki Fujiwara[1]

1. National Research Institute for Earth Science and Disaster Resilience

Five recurrent great earthquakes along the Japan Trench off Tohoku (Tohoku-oki–type earthquakes) are reported through studies of tsunami deposits (Earthquake Research Committee; ERC report, 2019). For recurrent earthquakes with uncertain origin times, Ogata (JGR, 1999) formulated the likelihood function in a multiproduct form of a probability density function integrated with respect to origin times over uncertain intervals (ERC report, 2001). The ERC report (2019) estimates the long-term probability of a Tohoku-oki–type earthquake by using a method different from Ogata's. For the sake of comparison, we applied Ogata's formula with the Brownian Passage Time distribution to this earthquake sequence. This revealed that Ogata's formula leads to an extraordinarily small value, at most 0.03, for the shape parameter. A detailed calculation showed that sequences of lower likelihood, relatively larger shape parameters, are less weighted (even by orders of magnitude), and that sequences including the Keicho-Sanriku of the 1611 historical earthquake, one of two candidates for the fourth event, play no crucial role in the maximum likelihood estimation. This must be contrary to the idea that both historical earthquakes, Kyotoku of 1454 and Keichou-Sanriku, are listed with equal possibilities. Accordingly, Ogata's formula could not give a representative model parameter over all possible sequences.

Keywords: Great earthquake, Japan Trench, Probability, Inverse Gaussian distribution, Uncertain origin times

©2021. Japan Geoscience Union. All Right Reserved.

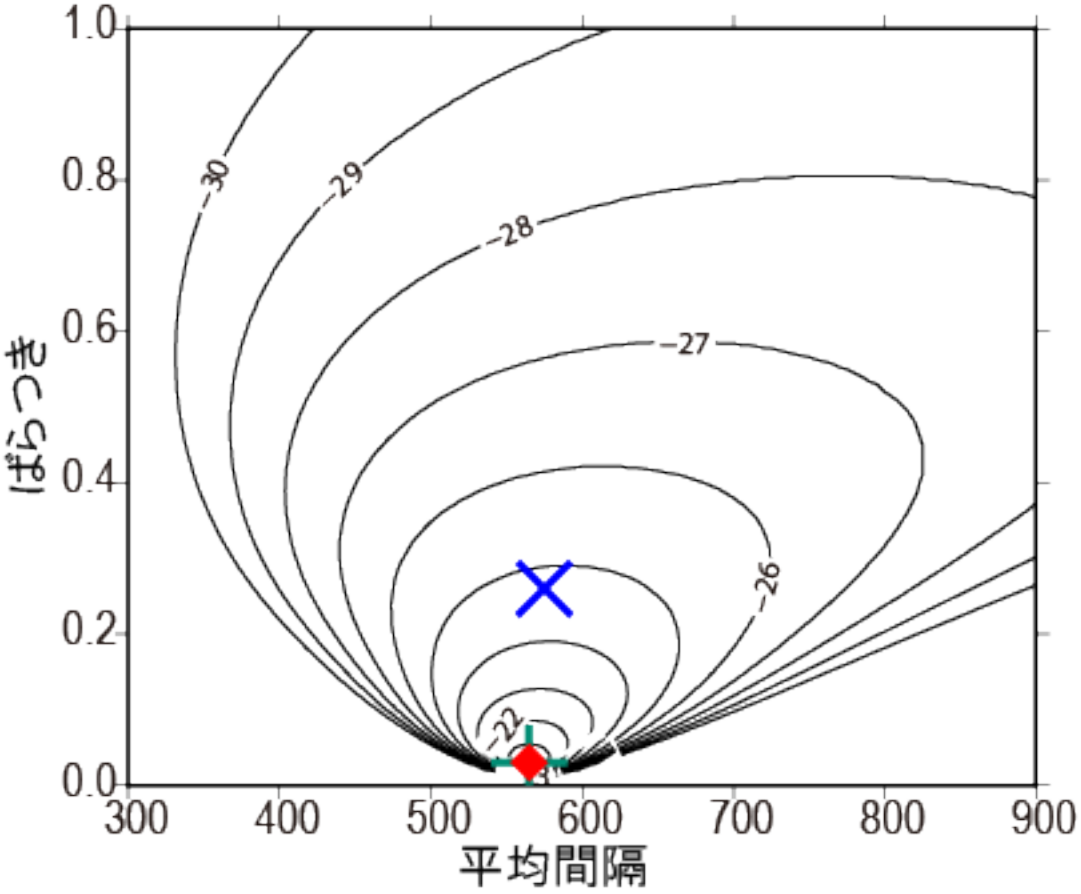


図　対数尤度の等値線
全地震(5回)を用いて，Ogataの方法により算出した対数尤度の等値線．
◆は最尤推定値．第4番が享徳地震あるいは慶長三陸地震で確定の場合には，
最尤推定値は ✚ あるいは ✖ となる．

©2021. Japan Geoscience Union. All Right Reserved.

Relationship between the Moderate Repeating Earthquakes and the Larger-scale Earthquakes on the trench side

*Masayuki Tanaka[1]

1. Meteorological Research Institute

Earthquakes with very similar waveforms (The Moderate Repeating Earthquakes) have been confirmed in various Japanese regions. Most occur at the plate boundaries and are considered to be closely related to regular slippage between plates. Comparing earthquakes of the same magnitude, it is considered that the slip speed between plates is fast when the interval between occurrences is short, and slow when the interval is long. We are tracking the moderate repeating earthquakes that occur repeatedly at almost the same location and have very similar waveforms, using seismic records observed by the Japan Meteorological Agency's velocity-type seismographs and accelerometers. On the other hand, tsunamis and large earthquakes with damage have occurred near the plate boundary. This time, we focused on the timing of occurrence of large-scale earthquakes in areas closer to the trench than where the moderate repeating earthquakes occurred, and investigated the relationship between the moderate repeating earthquakes and large-scale earthquakes.

Keywords: Moderate repeating earthquakes, Large-scale earthquakes, timing

©2021. Japan Geoscience Union. All Right Reserved.

Validation of forecast experiment on the Kamaishi repeating earthquakes based on numerical simulations

*Shingo Yoshida[1], Jun'ichi Fukuda[1], Toshihiro Igarashi[1]

1. Earthquake Research Institute, University of Tokyo

Repeating *M*5-class earthquakes occurred with a regular recurrence interval on the plate boundary offshore Kamaishi before the 2011 *M*9 Tohoku-oki earthquake. Since this event, repeating events of *M*5 to *M*6 occurred with shorter recurrence intervals than before the *M*9 event. We performed a forecast experiment on the Kamaishi repeaters after the Tohoku-oki earthquake based on numerical simulations assuming a large patch containing a small patch on a fault model that undergoes continuous afterslip.Simulations were conducted for various parameter values to produce time history of repeated ruptures.To forecast the *I*th event, we selected several modeled sequences that are able to accurately reproduce the observed event sequence up to the (*I*-1)th event. The averages of the occurrence times and magnitudes over the selected sequenceswere used as ensemble forecasts. Yoshida, Kato, and Fukuda (2016) attempted to predict the 7th event to the 11th event. In addition, the occurrence time of the 12th event, which did not occur before the publication of this paper, was forecasted. In this study, we discuss the forecast result.

Keywords: Kamaishi repeating earthquakes, forecast experiment

©2021. Japan Geoscience Union. All Right Reserved.

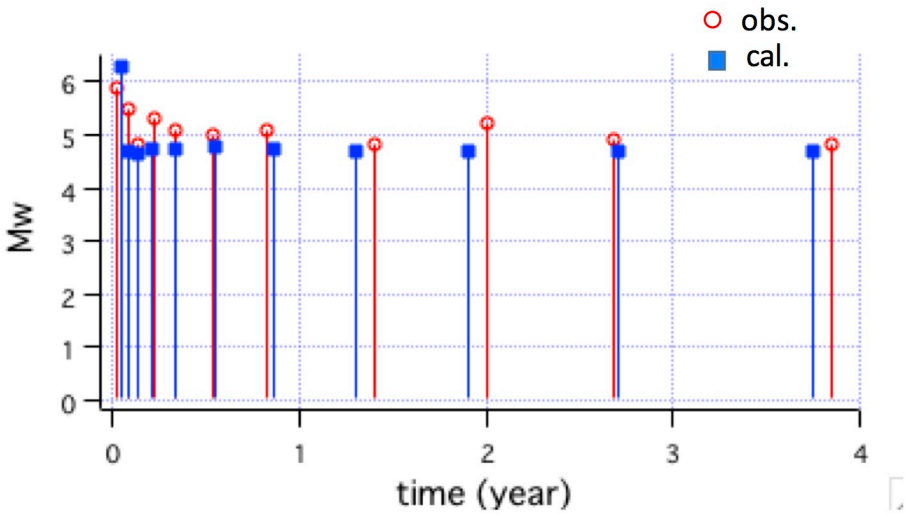


図1 釜石沖繰り返し地震のM-t図．t=0は東北沖地震発生時，赤丸は観測，青の四角はシミュレーション結果の1例．

©2021. Japan Geoscience Union. All Right Reserved.

[J] Poster | S (Solid Earth Sciences)：S-SS Seismology

Sun. Jun 6, 2021 5:15 PM - 6:30 PM JST | Sun. Jun 6, 2021 8:15 AM - 9:30 AM UTC | Ch.10_2

[S-SS11] Strong Ground Motion and Earthquake Disaster

convener:Kazuhiro Somei(Geo-Research Institute), Yasuhiro Matsumoto(Kozo Keikaku Engineering)

Strong ground motion has social impacts as it induces earthquake disasters. We solicit contribution on any seismological topics related to strong ground motion that includes, but are not limited to, source processes, wave propagation, and site effects. We also welcome contribution on earthquake related disaster mitigation.

[SSS11-P01] Elasto-plastic soil-water coupling seismic response analysis of a sedimentary basin with a three-dimensional geometry

*Toshihiro Noda[1], Tomohiro Toyoda[1], Shuhei Iwai[2], Akira Asaoka[3] (1.Disaster Mitigation Research Center, Nagoya University, 2.Graduate School of Engineering, Nagoya University, 3.Association for the Development of Earthquake Prediction)

[SSS11-P02] Identification of potential problems for disaster mitigation using “the Nankai Trough Earthquake Extra Information”, a new Japanese earthquake forecast information -how to communicate the "uncertainty" of science to society-

*Sayaka Irie[1], Ryu Ohtani[2], Mamoru Hyodo[3], Yoshinari Hayashi[4], Manabu Hashimoto[5], Takane Hori[6], Nobumasa Kawabata[7], Kunihiko Kumamoto[8], Takayoshi Iwata[9], Takashi Yokota[10], Kazunori Tanihara[11], Yo Fukushima[12] (1.NHK Broadcasting Culture Research Institute , 2.National Institute of Advanced Industrial Science and Technology, 3.Osaka Regional Headquarters, Japan Meteorological Agency, 4.Kansai University, 5.Disaster Prevention Research Institute, Kyoto University (DPRI), 6. Japan Agency for Marine-Earth Science and Technology (JAMSTEC) , 7.Crisis and Environment Management Policy Institute(CeMI), 8.Edogawa University, 9.Center for Integrated Research and Education of Natural Hazards,Shizuoka University, 10.Disaster Prevention Research Center,Aichi Institute of Technology, 11.Nippon Television Network, 12.International Research Institute of Disaster Science,Tohoku University, (IRIDeS))

[SSS11-P03] Research Project for Disaster Prevention on the great Earthquakes along the Nankai trough

*Shuichi Kodaira[1], Hiroyuki Fujiwara[2], Narumi Takahashi[1,2] (1. Japan Agency for Marine-Earth Science and Technology, 2.National Research Institute for Earth Science and Disaster Resilience)

[SSS11-P04] Formulas for using simple array to determine Love-wave characteristics based on rotational component of microtremors

*Ikuo Cho[1], Kunikazu Yoshida[2], Hirotoshi Uebayashi[3] (1.National Institute of Advanced Industrial Science and Technology, 2.Geo-Research Institute, 3.Institute for Integrated Radiation and Nuclear Science, Kyoto University)

[SSS11-P05] Assessment of applicability of a proposed method to estimate phase velocity using arbitrary 5-site arrays

*Huan Zhang[1], Kahori Iiyama[2], Hitoshi Morikawa[1] (1.Department of Civil and Environmental Engineering, Tokyo Institute of Technology, 2.KAJIMA Technical Research Institute)

[SSS11-P06] Comprehensive Research Project for the Nara-bonchi-toen Fault Zone

*Tomotaka Iwata[1] (1.Disaster Prevention Research Institute, Kyoto University)

[SSS11-P07] Small-aperture Microtremor Array Surveys in the Nara Basin, Japan

*Kimiyuki Asano[1], Tomotaka Iwata[1], Haruko Sekiguchi[1] (1.Disaster Prevention Research Institute, Kyoto University)

[SSS11-P08] Dense Microtremor Surveys on the Eastern Part of the Nara Basin, Japan

*Masayuki Yoshimi[1], Kimiyuki Asano[2], Tomotaka Iwata[2], Hiro Nimiya[1], Takeshi Sugiyama (1.Geological Survey of Japan, AIST, 2.DPRI, Kyoto Univ.)

[SSS11-P09] Microtremor characteristics and subsurface structure in the vicinity of the Shikano-Yoshioka Fault, Tottori, Japan

*Tatsuya Noguchi[1], Kazuki Kobayashi[2], Ryo Ashida[1], Isamu Nishimura[3], Takao Kagawa[1] (1.Faculty of Engineering, Tottori University, 2.Graduate School of Sustainability Science, Tottori University, 3.Graduate School of Engineering, Tottori University)

[SSS11-P10] Determination of 3-D subsurface structure model in central Tottori, Japan

*Tatsuya Noguchi[1], Masaki Yamamuro[1], Isamu Nishimura[2], Takao Kagawa[1] (1.Faculty of Engineering, Tottori University, 2.Graduate School of Engineering, Tottori University)

[SSS11-P11] Estimation of Subsurface Structure and Ground Motion Characteristics in the Landslide Areas from Microtremor Observations – Case of Nawashiro and Amedaki, Kokufu-cho, Tottori City –

*Isamu Nishimura[1], Atsushi Shimada[2], Tatsuya Noguchi[2], Takao Kagawa[2] (1.Graduate School of Engineering Department of Social Infrastructure Engineering, Tottori University, 2.Social Systems and Civil Engineering, Department of Engineering, Tottori University)

[SSS11-P12] Modeling of subsurface velocity structures from seismic bedrock to ground surface for Yamanashi region

*Shigeki Senna[1], Atsushi Wakai[1], Yatagai Atsushi[2], Tadashi Sato[2], Hisanori Matsuyama[2], Hiroyuki Fujiwara[1] (1.National Research Institute for Earth Science and Disaster Resilience, 2.OYO Corporation)

[SSS11-P13] Modeling of subsurface velocity structures from seismic bedrock to ground surface for Kumamoto region

*Shigeki Senna[1], Atsushi Wakai[1], Yatagai Atsushi[2], Yoshiaki Inagaki[2], Hisanori Matsuyama[2], Hiroyuki Fujiwara[1] (1.National Research Institute for Earth Science and Disaster Resilience, 2.OYO Corporation)

[SSS11-P14] Basic study of a real-time damage estimation system for liquefaction

*Shohei Naito[1], Hiromitsu Nakamura[1], Shigeki Senna[1], Yoshinori Iwanami[2] (1.National Research Institute for Earth Science and Disaster Resilience, 2.MITSUBISHI SPACE SOFTWARE CO.,LTD.)

[SSS11-P15] Estimation of subsurface motion from surface seismic records: investigation on evaluation at deep levels

*Tomotsugu Watanabe[1], Hiroshi Takenaka[1], Masanao Komatsu[1], Mitsutaka Oshima[2] (1.Okayama University , 2.Shimizu Corporation)

[SSS11-P16] Estimation of seismic ground motions on the surface ground at MeSO-net stations

*Atsushi Wakai[1], Shigeki Senna[1] (1.National Research Institute for Earth Science and Disaster Resilience)

[SSS11-P17] Strong motion simulation of an intraslab earthquake beneath Kanto region using MeSO-net observation data

*Wataru Suzuki[1], Takeshi Kimura[1], Hisahiko Kubo[1], Takayuki Miyoshi[1] (1.National Research Institute for Earth Science and Disaster Resilience)

[SSS11-P18] Ground-motion simulation for the 2016 Kumamoto earthquake (Mj7.3) based on the strong-motion prediction recipe

*Asako Iwaki[1], Nobuyuki Morikawa[1], Takahiro Maeda[1], Hiroyuki Fujiwara[1] (1.National Research Institute for Earth Science and Disaster Prevention)

[SSS11-P19] Characterized source model of M7.3 2016 Kumamoto eq. by 3D reciprocity GFs inversion with special reference to velocity pulse at KMMH16

*Anatoly Petukhin[1], Hiroshi Kawase[2], Fumiaki Nagashima[2], Eri Ito[2] (1.Geo-Research Institute, 2.DPRI, Kyoto University)

[SSS11-P20] Evaluation of near-source ground motion during the 2008 Iwate-Miyagi Nairiku earthquake by using stochastic slip models and three-dimensional velocity structures

*Takeshi Nakamura[1], Masataka Sawada[1] (1.Central Research Institute of Electric Power Industry)

[SSS11-P21] **Source rupture process of the 2018 Hokkaido eastern Iburi earthquake estimated from waveform inversion with empirical Green's functions**

*SHUANGLAN WU[1], Atsushi Nozu[1], Yosuke Nagasaka[1] (1.PORT AND AIRPORT RESEARCH INSTITUTE)

[SSS11-P22] Calibrating Thailand's local magnitude scale: a preliminary result

*Mongkolchai Sukmee[1], Sutthipong Noisagool[1,2], Satoru Tanaka[3], Weerachai Siripunvaraporn[1,2], Songkhun Boonchaisuk[4,2], Yasushi Ishihara[5], Taewoon Kim[6], Hitoshi Kawakatsu[7], Nozomu Takeuchi[7], Kenji Kawai[8], Yuki Suzuki[8] (1.Department of Physics, Faculty of Science, Mahidol University , 2.Thailand Center of Excellence in Physics, Ministry of Higher Education, Science, Research and Innovation, 3.Volcanoes and Earth's Interior Research Center (VERC), Research Institute for Marine Geodynamics (IMG), Japan Agency for Marine-Earth Science and Technology (JAMSTEC), 4.Geoscience Program, Mahidol University, Kanchanaburi Campus, 5.Research Institute for Marine Geodynamics (IMG), Japan Agency for Marine-Earth Science and Technology (JAMSTEC), 6.Subduction Dynamics Research Center (SDR), Research Institute for Marine Geodynamics (IMG), Japan Agency for Marine-Earth Science and Technology (JAMSTEC), 7.Earthquake Research Institute, The University of Tokyo, 8.Department of Earth and Planetary Science, School of Science, The University of Tokyo)

[SSS11-P23] Strong ground motion simulation of the Fukushima-ken Oki earthquake of February 13, 2021 (M_J 7.3)

*Yosuke Nagasaka[1] (1.Port and Airport Research Institute)

[SSS11-P24] Strong Motion Generation Area for the 2021 off Fukushima, Japan, Earthquake Estimated based on the Empirical Green's Function Method

*Kazuhiro Somei[1], Ken Miyakoshi[1] (1.Geo-Research Institute)

Elasto-plastic soil-water coupling seismic response analysis of a sedimentary basin with a three-dimensional geometry

*Toshihiro Noda[1], Tomohiro Toyoda[1], Shuhei Iwai[2], Akira Asaoka[3]

1. Disaster Mitigation Research Center, Nagoya University, 2. Graduate School of Engineering, Nagoya University, 3. Association for the Development of Earthquake Prediction

The seismic wave propagation is strongly affected by the ground non-uniformity. Especially in the sedimentary basin, the amplification in the sedimentary layer, the lens effect, and the edge effect due to the interference of the surface wave generated at the edge of the basin cause the strong ground motion. In this abstract, we conducted a single-phase elastic/two-phase (i.e., soil-water coupled) elasto-plastic seismic response analysis for the three-dimensional spherical basin shown in Table 1(d) and investigated the effects of three-dimensional structures, elasto-plasticity, and the presence of pore water.
First, a single-phase elastic analysis was performed on the three-dimensional mesh (conformed to Miyamoto et al.[1]) shown in Fig. 1. The analysis was conducted with the analysis code ***GEOASIA***[2] developed by the authors. Assuming a plane strain shear box test, the displacement of the front and back surfaces in *y*-direction was fixed and the periodic boundary was imposed on the left and right surfaces. At the bottom of the model, the vertical displacement was fixed and the viscous boundary condition was imposed in the horizontal direction. The EW component of the Kobe wave shown in Fig. 2 was applied in the *x*-direction as an input wave. As for the elastic material constants, we considered a clear rigidity contrast (11.4 times in the impedance ratio) between the sedimentary layer and the bedrock. As an analysis result, we confirmed the initial emergence of the ring-shaped strain concentration (Fig. 3), the occurrence of the three-dimensional waves and its long-term retention (Fig. 4).
Next, we compared the three-dimensional result with the reduced-dimensional model shown in Table 1(a)-(c) for evaluating the effect of the three-dimensionality of the sedimentary basin. Figure 5 shows the horizontal response on the ground surface at the center of the basin. As indicated in the figure, all reduced models underestimated the maximum acceleration and the residence time of seismic motion. The result suggests the limitation of the evaluation by the reduced-dimensional model. As for the spectral characteristics, the transfer function of the sedimentary layer at the center of the basin in the three-dimensional case in Fig. 6(d) indicated the amplification in the various frequency range, whereas the one-dimensional calculation in (a) just exhibited the theoretical solution.
Moreover, we conducted the two-phase elasto-plastic analysis. The SYS Cam-clay model [3] was used as the elasto-plastic constitutive equation. The typical parameters for consolidated rock and loose sand were assumed for the bedrock and the sedimentary layer, respectively. The analysis results for 1/10 amplitude of the Kobe wave indicated the decrease of the effective stress (liquefaction) in Fig. 7 and the sloshing behavior of the entire sedimentary layer in Fig. 8. The occurrence of liquefaction could also be confirmed in Fig. 9. Furthermore, the running transfer function in Fig. 10 indicated that the liquefaction reduced the transfer of the shear wave in the sedimentary layer.
(Acknowledgement) Numerical simulations were conducted by utilizing a supercomputer system in Kyoto University, Japan. And we received Grant-in-Aid for Scientific Research (Grant-in-Aid for Scientific Research (A): No. 17H01289).
[1] Miyamoto, T., Irihara, W., Suzuki, T., Fujita, K. and Ichimura, T. (2016): Analysis of strain concentration in alluvium using three dimensional nonlinear seismic ground response analysis (in Japanese), Proc. of JSCE, Vol.72, No.4, I_768-I_776.
[2] Asaoka, A., Noda, T., Yamada, E., Kaneda, K. and Nakano, M. (2002): An elasto-plastic description of two distinct volume change mechanisms of soils, Soils and Foundations, Vol.42, No.5, pp.47-57.

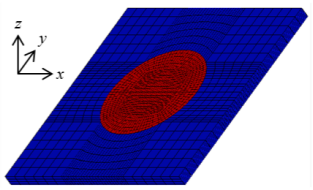
©2021. Japan Geoscience Union. All Right Reserved.

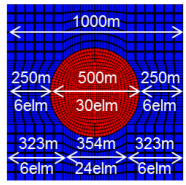
[3] Noda, T., Asaoka, A. and Nakano, M. (2008): Soil-water coupled finite deformation analysis based on a rate-type equation of motion incorporating the SYS Cam-clay model, Soils and Foundations, Vol.48, No.6, pp.771-790.

Keywords: Sedimentary basin, Seismic response analysis, Elasto-plasticity, Soil-water coupling, Three-dimensional

Table 1. Cases of the numerical simulation

Case	(a)	(b)	(c)	(d)
Model	1D	2D	2D	3D
Shear wave	Considered	Considered	Considered	Considered
Amplification	Considered	Considered	Considered	Considered
Reflection	Considered	Considered	Considered	Considered
Refraction	–	Considered	Considered	Considered
Rayleigh wave	–	Considered	–	Considered
Love wave	–	–	Considered	Considered





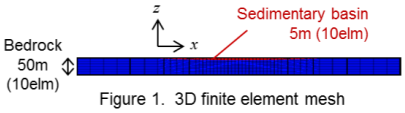


Figure 1. 3D finite element mesh

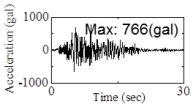


Figure 2. Input wave

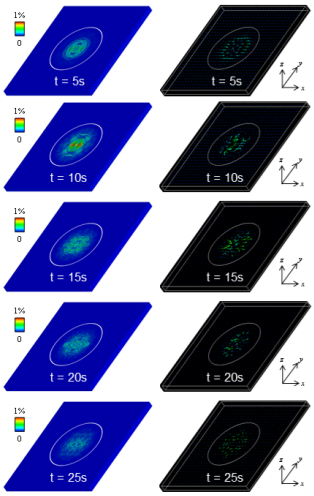


Figure 3. Shear strain (elastic)

Figure 4. Velocity (elastic)

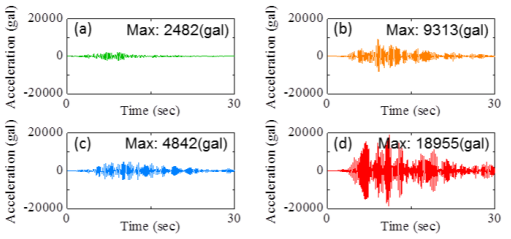


Figure 5 Surface acceleration in x-direction (elastic)

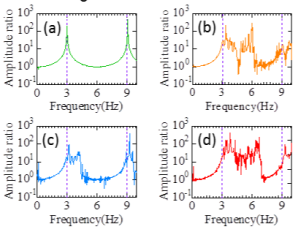


Figure 6 Transfer function of sedimentary basin in x-direction (elastic)

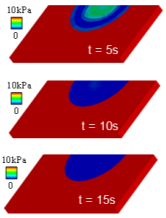


Figure 7. Mean effective stress (elasto-plastic)

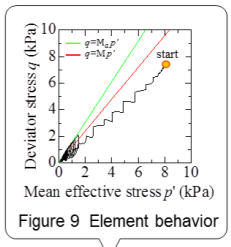


Figure 9 Element behavior

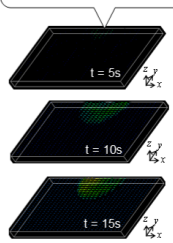


Figure 8. Veloity (elasto-plastic)

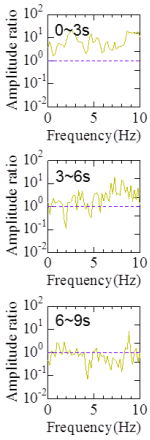


Figure 10. Transfer function (elasto-plastic)

©2021. Japan Geoscience Union. All Right Reserved.

Identification of potential problems for disaster mitigation using “the Nankai Trough Earthquake Extra Information”, a new Japanese earthquake forecast information -how to communicate the "uncertainty" of science to society-

*Sayaka Irie[1], Ryu Ohtani[2], Mamoru Hyodo[3], Yoshinari Hayashi[4], Manabu Hashimoto[5], Takane Hori[6], Nobumasa Kawabata[7], Kunihiko Kumamoto[8], Takayoshi Iwata[9], Takashi Yokota[10], Kazunori Tanihara[11], Yo Fukushima[12]

1. NHK Broadcasting Culture Research Institute , 2. National Institute of Advanced Industrial Science and Technology, 3. Osaka Regional Headquarters, Japan Meteorological Agency, 4. Kansai University, 5. Disaster Prevention Research Institute, Kyoto University (DPRI), 6. Japan Agency for Marine-Earth Science and Technology (JAMSTEC) , 7. Crisis and Environment Management Policy Institute(CeMI), 8. Edogawa University, 9. Center for Integrated Research and Education of Natural Hazards,Shizuoka University, 10. Disaster Prevention Research Center,Aichi Institute of Technology, 11. Nippon Television Network, 12. International Research Institute of Disaster Science,Tohoku University, (IRIDeS)

In 2017, the Japanese government introduced a new earthquake forecast information. When unusual seismic activity or crustal movements are observed around the Nankai trough extending from off the coast of central to the southwest Japanese Islands, the government will issue “the Nankai Trough Earthquake Extra Information” to let people prepare for the massive earthquake. However, with current seismological knowledge, it is difficult to accurately predict the time and magnitude of earthquakes. Therefore, while the information is expected to contribute to disaster mitigation, the information could also cause social disruption. The purpose of this research project is to identify the potential problems (or side effects) the information could bring to society through interdisciplinary collaboration among seismologists, disaster information studies researchers, and journalists. To this end, we apply a scenario method to construct a hypothetical scenario that describes how and when anomalous crustal deformation signals are observed, the information is issued by the government, and disseminated by TV media. Then, the scenario is displayed at scenario workshops where local stakeholders such as municipal officers and local residents discuss how they respond to the information to explore what kind of potential problems could arise. In this presentation, several findings will be introduced.

Keywords: Nankai Trough Earthquake, Nankai Trough Earthquake Extra Information, uncertainty, disaster information

©2021. Japan Geoscience Union. All Right Reserved.

Research Project for Disaster Prevention on the great Earthquakes along the Nankai trough

*Shuichi Kodaira[1], Hiroyuki Fujiwara[2], Narumi Takahashi[1,2]

1. Japan Agency for Marine-Earth Science and Technology, 2. National Research Institute for Earth Science and Disaster Resilience

In the Nankai Trough, where a future great earthquake would cause a national-scale crisis, recent research results revealed diversity and complexity of earthquake occurrence and slip behavior of the earthquake fault. To prepare for such a great earthquake in the Nankai Trough, this project aims to develop a system to rapidly and accurately evaluate crustal activities and distribute information on the current status of the Nankai Trough, including unusual slip behavior which has never observed previously, based on the latest scientific knowledge and data. Also, to maximize the use of the information, this project will investigate how local governments, communities, industries, etc., should take actions for hazard mitigation, particularly when unusual slip behavior is observed. Furthermore, in cooperation with local governments and other organizations, this project conducts a quantitative evaluation of how this project's research results have contributed to the improvement of hazard mitigation and identify practical research and development items for hazard mitigation plans. To achieve these goals, this project has the following three sub-themes. Generation and distribution of information on crustal activity: In this sub-theme, we construct an integrated 3D model of the Nankai Trough seismogenic zone and develop a system to rapidly process observed earthquake data to for evaluating crustal activities in the Nankai Trough by using the 3D model. We will also reanalyze the past observed data to understand the various seismic activities of the Nankai Trough earthquakes. Generation and distribution of information for hazard mitigation: In this sub-theme, we create an information infrastructure for disaster mitigation of earthquake and tsunami hazards and risks by incorporating a time evolution after a large earthquake or unusual slip behavior is observed. In addition, this sub-theme conducts a comprehensive research for "protecting lives," "protecting regional industrial activities," and "protecting metropolitan functions" by maximizing the use of disaster mitigation information. Hazard mitigation and risk communication: To improve knowledge and skill to use earthquake hazard information, we explore how to effectively use the latest information and knowledge about the earthquake hazard at each stage of pre-, during, and post-disaster response. For this purpose, we examine how to disseminate information to utilize the research results for disaster prevention and mitigation in communities and businesses.

Keywords: Nankai Trough, Earthquake Tsunami, Disaster resilience

©2021. Japan Geoscience Union. All Right Reserved.

Formulas for using simple array to determine Love-wave characteristics based on rotational component of microtremors

*Ikuo Cho[1], Kunikazu Yoshida[2], Hirotoshi Uebayashi[3]

1. National Institute of Advanced Industrial Science and Technology, 2. Geo-Research Institute, 3. Institute for Integrated Radiation and Nuclear Science, Kyoto University

Yoshida & Uebayashi (2018, 2020) demonstrated the effectiveness of using a rotational component (i.e., using spatial derivatives) in determining phase velocities of Love waves. Their method is based on a double triangular microtremor array. In this study, we present formulas to determine Love-wave characteristics using a rotational component based on a three-point array.

Cho et al. (2006) developed a general theory to analyze circular-array data of three-component microtremors. The titled formulation begins with equations (16) and (17) of their paper. These are equations representing the radial- and tangential-component waveforms recorded with a three-component seismometer located at (r, θ), where r is the distance from the origin and θ is the azimuthal angle from the x-axis to the y-axis. Taking the divergence and rotation of these waveforms, we can obtain

$D(t, r, \theta) = -\int\int\int ik \exp[-i\omega t - ikr\cos(\phi - \theta)] \zeta^{R}(d\omega, dk, d\phi)$, (divergent component) (1)

$C(t, r, \theta) = -\int\int\int ik \exp[-i\omega t - ikr\cos(\phi - \theta)] \zeta^{L}(d\omega, dk, d\phi)$, (rotational component) (2)

where t is time, i is the imaginary unit, k is the wavenumber, ω is the angular frequency, and ϕ is a wave arriving direction. We set r and θ to 0 in the above divergent- and rotational-component waveforms (D and C, respectively). Taking autocorrelation functions and then taking Fourier transforms yields

$PSD^{R}(\omega) = [c^{R}(\omega)]^{2} PSD^{D}(\omega)/\omega^{2}$, (3), $PSD^{L}(\omega) = [c^{L}(\omega)]^{2} PSD^{C}(\omega)/\omega^{2}$, (4)

where $PSD^{R}(\omega)$ and $PSD^{L}(\omega)$ is the power spectral densities (PSDs) for integrated spectra $\zeta^{R}(d\omega, dk, d\phi)$ and $\zeta^{L}(d\omega, dk, d\phi)$, respectively. $c^{R}(\omega)$ and $c^{L}(\omega)$ are the phase velocities of Rayleigh and Love waves, respectively.Taking the sum of equations (3) and (4), we obtain

$PSD^{R}(\omega) + PSD^{L}(\omega) = [c^{R}(\omega)]^{2} PSD^{D}(\omega)/\omega^{2} + [c^{L}(\omega)]^{2} PSD^{C}(\omega)/\omega^{2}$. (5)

We define the total powers of the horizontal components, $PSD^{H}(\omega)$, as the sum of the PSDs for Rayleigh and Love waves. i.e.,

$PSD^{H}(\omega) = PSD^{R}(\omega) + PSD^{L}(\omega)$. (6)

By the use of equations (5) and (6), we have

$c^{L}(\omega) = [(PSD^{H}(\omega)\omega^{2} - PSD^{D}(\omega)[c^{R}(\omega)]^{2})/PSD^{C}(\omega)]^{1/2}$. (7)

The use of equation (7) assumes that the observation of three-component microtremors was conducted using a triangular (three-point) array. On the right-hand side of equation (7), the phase velocity of

©2021. Japan Geoscience Union. All Right Reserved.

Rayleigh waves, $c^R(\omega)$, is obtained by applying the SPAC method to the vertical-component data from a three-point array, and $PSD^C(\omega)$ and $PSD^D(\omega)$ are obtained by processing two horizontal components of the three-point array (YU2020). $PSD^H(\omega)$ can be obtained from the two horizontal components at a single point (i.e., the sum of the PSDs for either the radial and tangential components or the east-west and north-south components). Therefore, the Love-wave phase velocity is obtained from a three-component three-point array. Once $c^L(\omega)$ is obtained, R/L (Amplitude ratio of Rayleigh to Love waves) of Arai and Tokimatsu (2004) can be obtained using equations (3) and (4). Alternatively, since $c^R(\omega)$ is already obtained, we can obtain the H/V ratio of Rayleigh waves via equation (3). It may be more convenient to use this quantity to model a velocity structure than to use R/L, as the calculation of theoretical values for a fitting becomes simple.

This research was supported by the Japan Society for the Promotion of Science (JSPS) KAKENHI Grant Numbers 19H02287.

Arai & Tokimatsu, 2004. *Bull. Seismol. Soc. Am.*, **94**, 53–63.
Cho, Tada, & Shinozaki, 2006. *Geophys. J. Int.,* **165**, 236–258.
Yoshida & Uebayashi, 2020. *Bull. Seismol. Soc. Am.,* doi://10.1785/0120200139.
Yoshida & Uebayashi, 2018. BUTSURI-TANSA, **71**, 15-23. (in Japanese)

Keywords: microtremor, Love wave , array, rotational component, spatial differentiation, phase velocity

©2021. Japan Geoscience Union. All Right Reserved.

Assessment of applicability of a proposed method to estimate phase velocity using arbitrary 5-site arrays

*Huan Zhang[1], Kahori Iiyama[2], Hitoshi Morikawa[1]

1. Department of Civil and Environmental Engineering, Tokyo Institute of Technology, 2. KAJIMA Technical Research Institute

To estimate earthquake ground motion, it’s necessary to model the ground structure. Then the use of array method was proposed by using microtremors because it’s an inexpensive and mobile means of estimating the phase velocity of surface waves. Based on the analytical solution of Lamb's problem for vertical components of Rayleigh wave, the relationship between two observation points, p and q for example, is given in a discrete representation with the Bessel function of the first kind and higher-order Bessel functions, which is called Complex Coherence Function (CCF) [4]. Zhang and Morikawa [5] extended the CCF to apply it to linear array situation. By adding an extra observation point s, the relationship between p and s can be expressed [6]. At last, the CCF equations have only 5 unknowns left, including the phase velocity. Therefore, we proposed a method [7] to estimate the phase velocity using Artificial Bee Colony (ABC) algorithm [8] under a constraint of kr belongs to [0, 5]. The selection of the constraint condition will affect the results and will be discussed.

The numerical simulations and the site observations’ results confirmed the availability of the proposed algorithm for array shapes with more free arrangement of sensors. When it comes to selecting the constraint condition, constraint condition is a better choice for most 3-site arrays if we expect a wider effective range. For 4-site arrays, we think acceptable results can be obtained with no constraint condition. After comparing with 4-site arrays without constraint condition and related 3-site arrays under r_{ave} constraint condition, we can see that the 4-site arrays' results are influenced by all of the 3-site arrays it contains, meaning that it might not be better than all of the 3-site arrays' results, especially the small regular 3-site array. However, they are better than most of other 3-site arrays which have irregular shapes.

Based on this method, we think the application to more-sites arrays, 5-site arrays for example, can further improve the results. If 5-site arrays were chosen, the 5 unknowns will remain the same but there will be 10 CCFs. On the other hand, since there will be 10 CCFs, we can extend the CCF’s application range and thus there will be 2 more unknowns, for example. In that case, the unknowns are still less than the CCFs and the constraint range, kr belongs to [0, 5], can be wider, too. However, similarly as 4-site arrays, adding more sites will inevitably extend the optimization time. And optimizing one phase velocity result to satisfy all of the CCF equations together will leave the result influenced by all of the CCFs. Still, numerical simulations and the application to ZRS field data using more-sites arrays, 5-site arrays for example, will be conducted to testify the validity of the proposed assumption. And comparisons with conventional methods will be conducted at the same time.

[1] Capon, J. (1969). *Proceedings of the IEEE*, 57(8), 1408-1418.
[2] Aki, K. (1957). *Bull. Earthq. Res. Inst.*, 35, 415-456.
[3] Cho, I., Tada, T., & Shinozaki, Y. (2006). *Journal of Geophysical Research: Solid Earth*, 111(B9).
[4] Shiraishi, H. & Matsuoka, T. (2005). *BUTSURI-TANSA,* 58(2), 137-146.
[5] Zhang, X. & Morikawa, H. (2014). *British Journal of Applied Science & Technology*, 6(4), 350–363.
[6] Morikawa, H. & Iiyama, K. (2015). *Program and Abstracts, The Seismological Society of Japan, Fall Meeting.*

©2021. Japan Geoscience Union. All Right Reserved.

[7] Zhang, H., Iiyama, K. & Morikawa, H. (2020). *17th World Conference on Earthquake Engineering.*
[8] Karaboga, D. & Basturk, B. (2007). *Journal of global optimization*, 39(3), 459-471.

Keywords: Arbitrary-shape array, phase velocity, Complex Coherence Function (CCF), Centerless Circular Array (CCA) method, Spatial Auto-correlation (SPAC) method, Artificial Bee Colony (ABC) algorithm

©2021. Japan Geoscience Union. All Right Reserved.

Comprehensive Research Project for the Nara-bonchi-toen Fault Zone

*Tomotaka Iwata[1]

1. Disaster Prevention Research Institute, Kyoto University

The Nara-bonchi-toen fault zone is south part of Kyoto and Nara basin faults, eastern margin of the Kyoto and Nara basins. Our research group has started to study this active fault zone in detail to get the information for developing the long-term earthquake evaluation and the strong ground motion prediction in 2019-2021FY.
This research group conducts an integrated research on long-term evaluation of earthquake occurrence of the active faults (Sub-theme 1), seismic activity and crustal structure (Sub-theme 2), strong ground motion prediction (Sub-theme 3) and outreach (Sub-theme 4). In 2019FY, Sub-theme 1 conducted to prepare the DEMs in this fault area, field surveys for trench site and height distribution of the basement of the Osaka group in the target area. Sub-theme 2 started the temporal seismic observations for obtaining the stress field in this area, and field surveys to obtain the characteristics of the micro faults. They also conducted the microtremor array observations with the member of Sub-theme 3. Sub-theme 3 conducted the seismic reflection surveys in the south Kyoto and the north Nara basins so as to image the basin and basin-basement structures. They also collected the geological boring well-logs and conducted microtremor array observations. Sub-theme 4 hosted a study group meeting on earthquake hazards in this area, that consists of the researchers, risk management members of local governments and companies in this area. We also show new findings in 2020FY and a research plan in 2021FY.

Keywords: Nara-bonchi-toen Fault Zone, long-term earthquake evaluation of active faults, strong ground motion prediction

©2021. Japan Geoscience Union. All Right Reserved.

Small-aperture Microtremor Array Surveys in the Nara Basin, Japan

*Kimiyuki Asano[1], Tomotaka Iwata[1], Haruko Sekiguchi[1]

1. Disaster Prevention Research Institute, Kyoto University

The Nara-Bonchi-Toen Fault Zone forms the eastern margin of the Kyoto and Nara basins, Japan. The Nara basin is mostly filled by the lower and lowermost parts of the Plio-Pleistocene Osaka Group. Alluvial and terrace deposits distributed over the Osaka Group inside the basin. Improvement on the velocity structure model from the superficial alluvial deposits to the seismic bedrock is quite important for advancing strong motion prediction for future earthquakes from nearby source faults. As a part of Comprehensive Research Project for the Nara-Bonchi-Toen Fault Zone funded by the Ministry of Education, Culture, Sports, Science and Technology (MEXT), Japan, we have carried out various kind of geophysical surveys to investigate the velocity structure in the Kyoto and Nara basins. Miniature to small aperture microtremor array surveys were carried out at 60 sites in the southern part of the Kyoto prefecture from Aug. 2019 to Mar. 2020 to obtain information on S-wave velocity of shallow subsurface sedimentary layers (Asano *et al.*, 2020). The surveyed area is extended to the whole part of the Nara basin in 2020. The total number of surveyed sites is 140 as of Jan. 29, 2021 (Fig. 1), and the field work is still undergoing to cover the whole area of the Nara basin. We will report our results in the Nara basin in this presentation.

We carried out miniature and small equilateral triangle array observations at each measurement. The circumradius is 0.6 m for a miniature array, and the circumradius for a small array depends on site in a range from 5 to 8 m. A portable integrated microtremor observation system HAKUSAN JU410 was installed at each apex of the equilateral triangle and the center of circumscribed circle. The microtremor was recorded continuously more than 15 minutes at a sampling rate of 200 Hz after amplified by 100 times (200V/G).

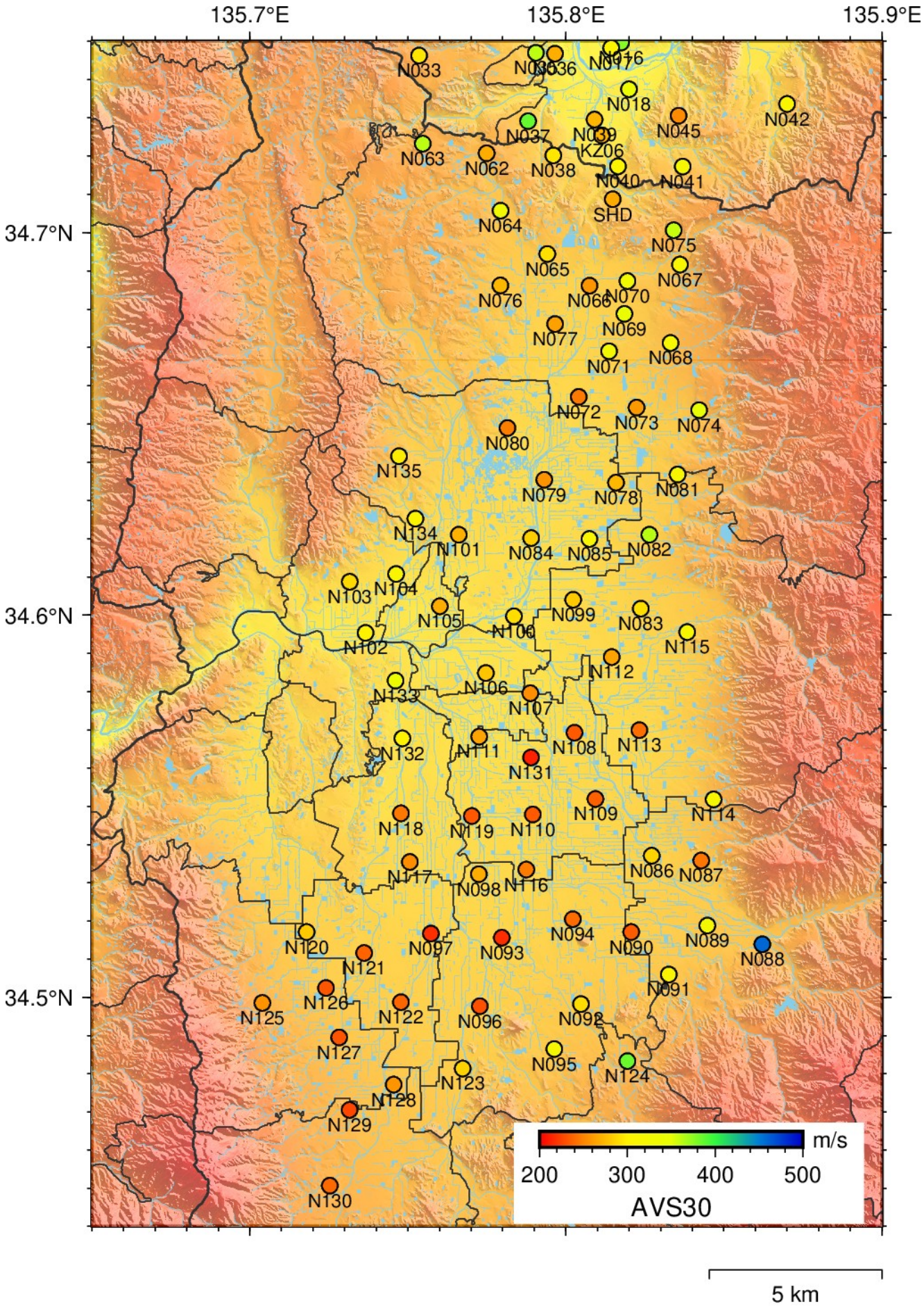
The vertical component of the observed microtremors were analyzed to obtain the spatial autocorrelation (SPAC) coefficients (Aki, 1957). The spatial autocorrelation function was calculated in the frequency domain, and the Fourier spectrum was smoothed by the technique of Konno and Ohmachi (1998). Finally, the phase velocity dispersion curve was estimated by the extended SPAC method (Ling and Okada, 1993; Okada, 2003).

The one-dimensional S-wave velocity structure model for each measurement site was estimated assuming the observed phase velocity dispersion curve as the fundamental mode of the Rayleigh wave using the Markov chain Monte Carlo method. The velocity structure model of deep sedimentary layers and the upper crust was given referring to the existing three-dimensional velocity structure models J-SHISV2 (Fujiwara *et al.*, 2012), and the velocity structure model from the lower crust to upper mantle was given referring to JIVSM (Koketsu *et al.*, 2012). The obtained S-wave velocity structure model will be discussed in terms of the spatial distribution of low-velocity layers with referring to surface geology and boring data information.

Acknowledgement: This work was conducted as a part of Comprehensive Research Project for the Nara-Bonchi-Toen Fault Zone of the Ministry of Education, Culture, Sports, Science and Technology, Japan. We appreciate many residents for cooperation of our survey.

Keywords: Nara Basin, microtremor array survey, velocity structure model

©2021. Japan Geoscience Union. All Right Reserved.



©2021. Japan Geoscience Union. All Right Reserved.

Dense Microtremor Surveys on the Eastern Part of the Nara Basin, Japan

*Masayuki Yoshimi[1], Kimiyuki Asano[2], Tomotaka Iwata[2], Hiro Nimiya[1], Takeshi Sugiyama

1. Geological Survey of Japan, AIST, 2. DPRI, Kyoto Univ.

We are conducting research on the Nara-bonchi-toen Fault Zone (Eastern Marginal Nara Basin Fault Zone). Since the location of these faults have been mainly determined by the topography, it is very important to clarify the depth distribution of the basement rocks to see if there is any depth difference at the fault locations. In this study, we conducted microtremor array surveys and single-point microtremor observations in the Nara Basin to estimate the location of the fault by clarifying depth of the basement. In the Nara Basin, the H/V spectra shows distinct peaks and the peak period changes in accordance with the depth of the basement (e.g., Morikawa et al., 1998). The peak period of the H/V spectrum has been used to develop a 3D velocity structure model of the Nara Basin (Sekiguchi et al., 2019).
Microtremor arrays with a maximum radius of 400 m were observed at five locations on the Narayama hill, two locations in the northern part of Nara City, three locations in the southern part of Nara City, and three locations in the central part of Tenri City. In addition, single-point microtremor observations were conducted at about 300 locations, mainly in the eastern Nara Basin. Six to eight seismometers were used for the single-point microtremor observations, with a spacing of about 100 m to 1 km, and simultaneous observation data of more than 30 minutes were obtained for the application of the two-point SPAC method. The instruments used are all the same, consisting of a three-component velocty-type seismometer (Tokyo Sokushin SE-321, 5V/kine, natural-period 10 seconds) and a data logger (Hakusan LS-8800, GPS time calibration, 24-bit AD conversion). The X direction of the microtremor was set to magnetic north. In addition to the 105 microtremor array stations reported in Yoshimi et al. (2020), we have accumulated more than 600 microtremor data points in total.
In this presentation, we explain the basement depth distribution estimated from the peak period of H/V spectra, along with the basement depth and velocity structure model estimated from the microtremor array. We also show the distribution of the eastern margin fault zone of the Nara Basin illustrated by the basement depth distribution.

Acknowledgments
This research was conducted as part of the "Comprehensive Research Project for the Nara-bonchi-toen Fault Zone" funded by the Ministry of Education, Culture, Sports, Science and Technology (MEXT). We would like to express our gratitude to Nara City, Tenri City, Yamato Koriyama City and local residents for their cooperation in the microtremor array observation.

References
Morikawa, H., Toki, K., Onoe, K., Akamatsu, J., and Takeuchi, T., Estimation of Deep Ground Structure in Northern Nara Basin using Microseism Array Record, 3rd Symposium on Urban Earthquake Hazards, a-26, 143-144, 1998.
Okumura, A., A. Samukawa, T. Sugai, M. Takada, and H. Soma, Comprehensive survey of the fault system at the eastern margin of the Nara Basin, 1996 Summary Report of the Research on Active Faults, Geological Survey of Japan, 51-62, 1997.
Haruko Sekiguchi, K. Asano, and T. Iwata, Three-dimensional velocity structure model of Nara Basin, Jour. Geol. Soc. Japan 125, 715-730, 2019.
M. Yoshimi, K. Asano, T. Iwata, K. Ninomiya, and L. Sugiyama, Microtremor array survey at the eastern

©2021. Japan Geoscience Union. All Right Reserved.

margin of the Nara Basin, JpGU, 2020.

Keywords: H/V spectra, active fault

©2021. Japan Geoscience Union. All Right Reserved.

Microtremor characteristics and subsurface structure in the vicinity of the Shikano-Yoshioka Fault, Tottori, Japan

*Tatsuya Noguchi[1], Kazuki Kobayashi[2], Ryo Ashida[1], Isamu Nishimura[3], Takao Kagawa[1]

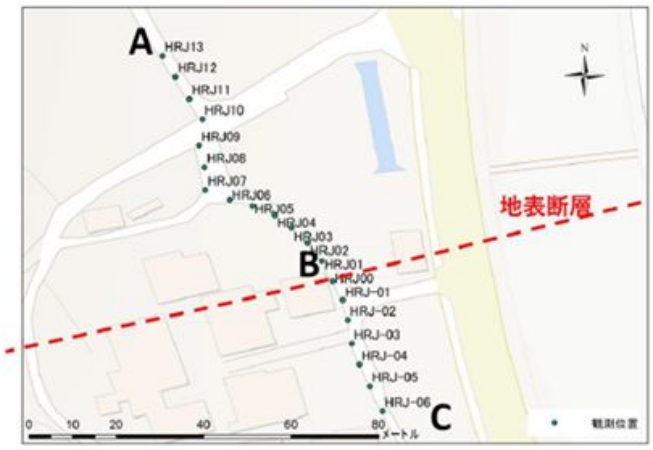
1. Faculty of Engineering, Tottori University, 2. Graduate School of Sustainability Science, Tottori University, 3. Graduate School of Engineering, Tottori University

The Shikano-Yoshioka fault is an earthquake fault that appeared due to the 1943 Tottori earthquake. At both faults, trench surveys, reconnaissance surveys, and interview surveys with residents are conduct-ed as fault displacement surveys. For the ground structure, microtremor exploration and gravity exploration were carried out. In addition, dense microtremor observations were also carried out at and near the fault displacement. However, the difference in ground motion characteristics due to irregularities such as crush zones and step structures due to faults has not been sufficiently investigated.

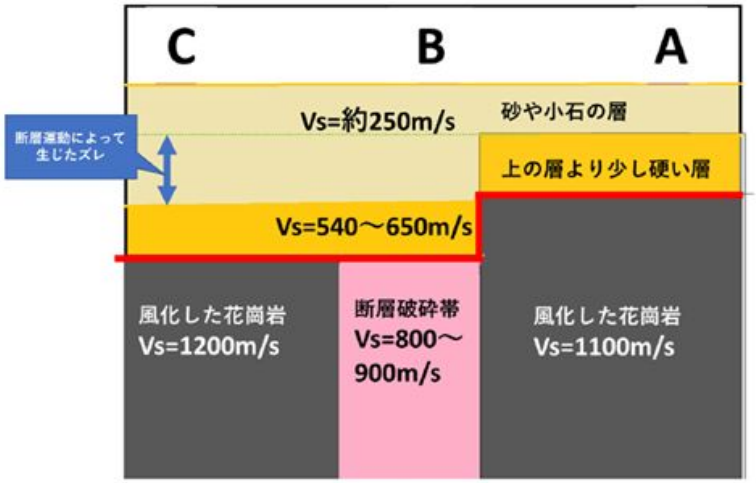
In this study, we grasped the ground motion characteristics in the vicinity of the fault by using the results of dense microtremor observations at the fault displacement location and in the vicinity. As a result, there was a difference in the shape of the microtremor H/V, predominate periods and particle motion of records between the front and the back of the fault displacement point. As the cause of this phenomenon, the correspondence between the results of microtremor observation and underground structure exploration suggests that the crush zone and step structure of the fault are in-volved in the characteristics of microtremor.

Keywords: Shikano-Yoshioka Fault, Microtremor characteristics, subsurface structure

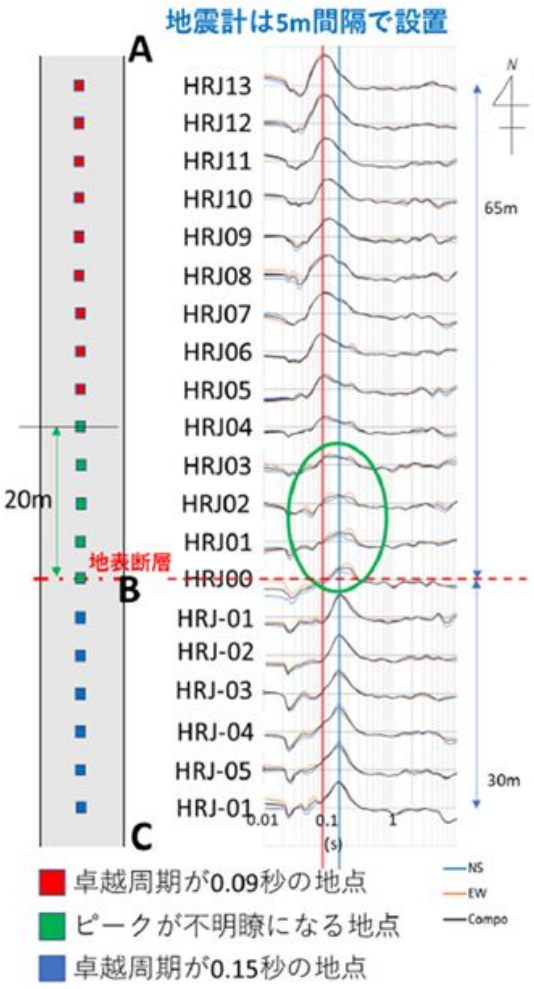
©2021. Japan Geoscience Union. All Right Reserved.



鹿野断層近傍（鹿野町末用地区）の微動観測点



S波反射法による地下構造モデルのイメージ図



微動のH/V

©2021. Japan Geoscience Union. All Right Reserved.

Determination of 3-D subsurface structure model in central Tottori, Japan

*Tatsuya Noguchi[1], Masaki Yamamuro[1], Isamu Nishimura[2], Takao Kagawa[1]

1. Faculty of Engineering, Tottori University, 2. Graduate School of Engineering, Tottori University

In central Tottori prefecture, there was the 2016 earthquake in central Tottori prefecture. This earthquake caused strong ground motion over a wide area and caused damage to buildings. Information on the underground structure is required to examine the causes of damage caused by this earthquake and evaluate the ground motion. In this area, microtremor, gravity observations, and temporary aftershock (strong ground motion) observations were carried out in central Tottori prefecture. Based on these data, an underground structure model has been obtained. In this study, new gravity observations were made mainly in the Hojo area in central Tottori, where many damages occurred. The underground structure was estimated by extending the underground structure model based on microtremor and aftershock observations to a two-dimensional or three-dimensional model using the new and the existing gravity data.

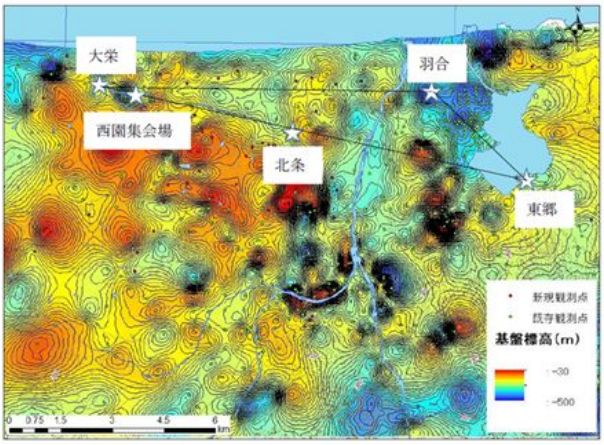
The analysis is as follows. First, a three-dimensional analysis was performed using a two-layer density structure model. The densities of the surface layer and the base layer of the two-layer model were set to 2.2g/cm^3 and 2.5g/cm^3, respectively. 8-seismic observation points with underground velocity structure models and 2-outcrop points of the basement were set as points to determine the depth to the basement. The depth to the basement controlled at the seismic station was the depth to the upper surface of the layer corresponding to Vs = 1700 m/s to 2200 m/s. As a result, it was possible to grasp the distribution of the basement surface in the target area, and it was found that the depth of the basement was 640 m at the deepest part.

Next, we assumed a three-layer density structure model and performed a two-dimensional analysis using gravity anomalies. The density of each layer was set to 2.0 g/cm^3 for the first layer, 2.3g/cm^3 for the second layer, and 2.5g/cm^3 for the third layer. In the velocity structure model, the first layer corresponds to Vs = 100 to 500 m / s layer, the second layer corresponds to Vs = 550 to 150m/s layer, and the third layer corresponds to Vs = 1700 to 3000m/s. The depth of the boundary between the first and second layers is based on the results of microtremor observation, and the depth of the boundary between the second and third layers is based on the results of three-dimensional analysis of the two-layer model. Under these conditions, the density structure model was estimated by trial and error to explain the gravity anomaly. As a result, the undulations of the layer boundaries of each layer could be grasped, and there were areas where the base shapes of the first and second layers were significantly different.

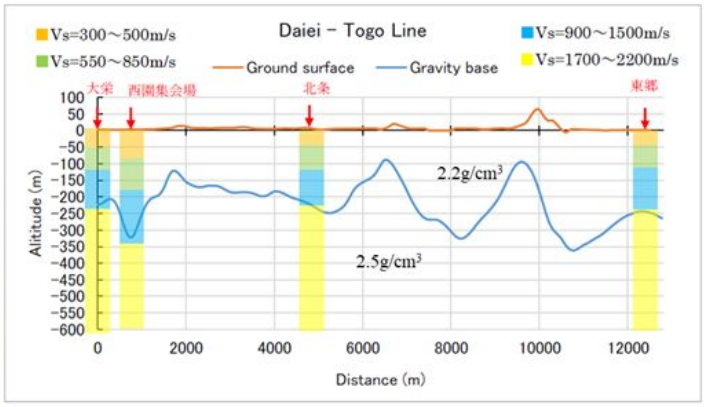
In the future, we plan to try a method of integrating the model of tremor and seismic motion and the model of gravity anomaly and expanding it to a three-dimensional structure. Furthermore, we will investigate the relationship between the undulations of the base surface of the obtained base structure and the damage distribution caused by the earthquake.

Keywords: central Tottori prefecture, 3-D subsurface structure model, gravity survey, microtremor survey, seismic observation

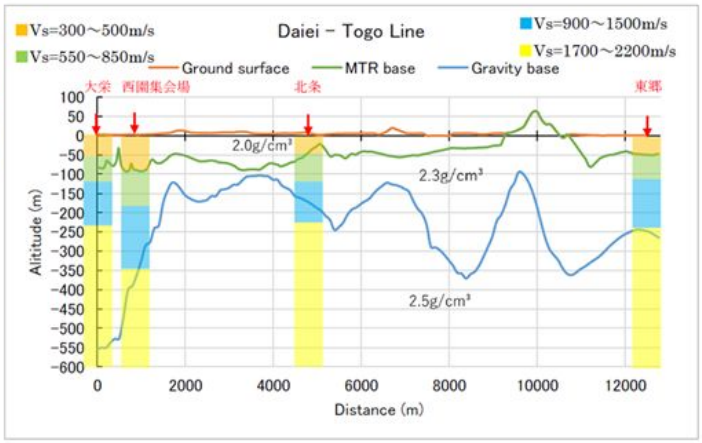
©2021. Japan Geoscience Union. All Right Reserved.



3次元解析結果



2次元解析結果(2層均質モデル)



2次元解析結果(3層均質モデル)

©2021. Japan Geoscience Union. All Right Reserved.

Estimation of Subsurface Structure and Ground Motion Characteristics in the Landslide Areas from Microtremor Observations –Case of Nawashiro and Amedaki, Kokufu-cho, Tottori City –

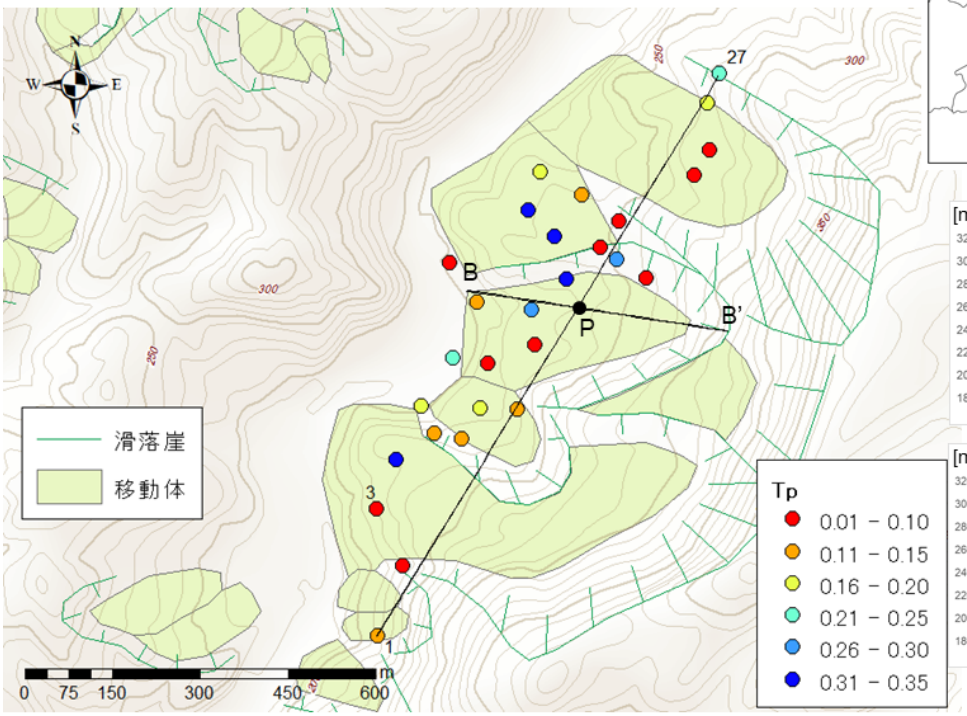
*Isamu Nishimura[1], Atsushi Shimada[2], Tatsuya Noguchi[2], Takao Kagawa[2]

1. Graduate School of Engineering Department of Social Infrastructure Engineering, Tottori University, 2. Social Systems and Civil Engineering, Department of Engineering, Tottori University

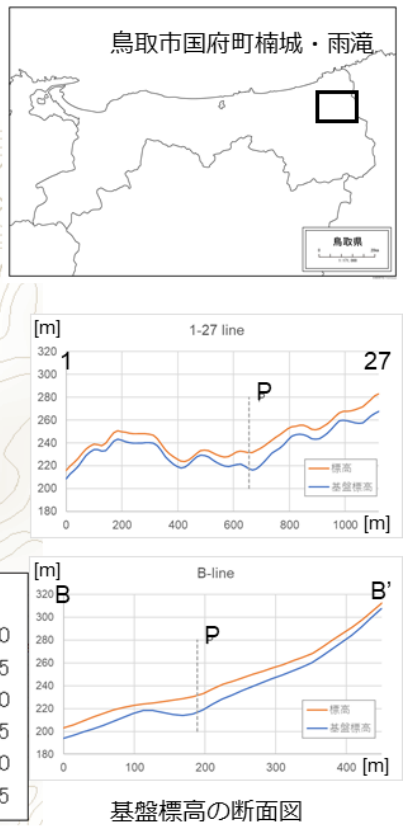
In recent years, landslides caused by earthquakes have resulted in large-scale damage. It is important to understand the ground motion characteristics of landslide areas because landslides often occur repeatedly in the same area based on past activity history. Microtremor surveys have been used to evaluate the ground motions in landslide areas because the sediments above the slip surface are very soft and the velocity contrast is likely to be distinct (e.g., Shima, 1981). In this study, we conducted microtremor observations in Nawashiro and Amedaki, Kokufu-cho, Tottori City, that are classified as landslide areas in the landslide topography map published by the National Research Institute for Earth Science and Disaster Resilience (NIED), and examined the extent to which landslide deposits can be evaluated.
From the landslide topography distribution map, the Nawashiro landslide is classified into three blocks, and the Amedaki landslide is one large body. As a result of the analysis, the predominant periods of microtremor H/V were 0.06-0.35 seconds in both regions. At Nawashiro, each block has its own characteristics of predominant periods. In some blocks, predominant periods of 0.1 seconds or less were widely distributed, while in other blocks, periods of 0.3 seconds were concentrated. At Amedaki, the predominant period tended to be longer at the sites identified as landslide bodies. From the array observation, it was estimated that the layer of Vs = 200 m/s is 6m at Nawashiro and the layer of Vs = 130 m/s is 5m at Amedaki. The S-wave velocities and the predominant periods were used to estimate the layer thicknesses. The layer thicknesses tend to be thicker at the center of the landslide bodies, that may reflect the landslide deposits.

Keywords: Microtremor observation, H/V spectra, Landslide, Subsurface structure

©2021. Japan Geoscience Union. All Right Reserved.



楠城の卓越周期分布



基盤標高の断面図

©2021. Japan Geoscience Union. All Right Reserved.

Modeling of subsurface velocity structures from seismic bedrock to ground surface for Yamanashi region

*Shigeki Senna[1], Atsushi Wakai[1], Yatagai Atsushi[2], Tadashi Sato[2], Hisanori Matsuyama[2], Hiroyuki Fujiwara[1]

1. National Research Institute for Earth Science and Disaster Resilience, 2. OYO Corporation

1. Introduction

The NIED has constructed a shallow and deep integrated underground structure model in the Kanto, Tokai, and Kumamoto regions in order to improve the accuracy of strong motion prediction. In this study, we will focus on the construction of a shallow and deep integrated underground structure model for the Yamanashi region, which is adjacent to the Kanto and Tokai regions. The model construction procedure basically follows the method of the Kanto region (for example, Senna et al., 2017) in which modeling is carried out in advance. Specifically, first, an initial underground structure model was created based on the existing underground model, borehole data and geological information collected so far. Then, the initial underground model was adjusted using the ground vibration characteristics obtained by conducting a dense microtremor array exploration. In this paper, we report the above contents and the features of the modified underground structure model.

2. Initial ground model

Of the initial underground models, the J-SHIS_V2 model of the NIED was basically used as the initial model for the deep underground structure model (deeper than Vs350 (m/s) defined as the engineering bedrock). For shallow underground, a underground model was connected to make it an initial model. After that, the upper surface of the engineering bedrock of the shallow underground was used as the upper surface of the first layer of the deep underground, and the two were integrated to form the initial integrated underground model. For the shallow underground structure model (shallower than Vs350 (m/s)), the geomorphologic classification of J-SHIS was reviewed and revised based on the hydraulic topography classification map, and then the borehole data in Yamanashi prefecture (about 3,000). This was organized and a 250m mesh model was created based on the modified geomorphologic classification.

3. Microtremor array observations and seismic records used

Microtremor array observations are large array observations (three points with array radii of 100, 200, 400m and L-shape with sides 25 to 75 m) at intervals of about 5 km in the lowlands and plateaus indicated by the geomorphologic divisions throughout Yamanashi prefecture. Microtremor observations (4 points with an array diameter of 60 cm and triangles with a side of 5 m to more than 10 m) were carried out at about 500 points at intervals of about 1 km (as of February 2021). The phase velocity and H/V spectrum ratio for each observation point were calculated. Seismic records are recorded using the K-NET and KiK-net seismic stations of the NIED and the JMA recorded in the Metropolitan Area Strong Motion

©2021. Japan Geoscience Union. All Right Reserved.

Network (SK-net) of the Earthquake Research Institute, the University of Tokyo. The R/V spectrum ratio for each observation point was calculated. Based on these ground vibration characteristic data and the initial ground model, joint inversion was performed to obtain a one-dimensional S wave velocity structure at each observation point.

4. Modification of initial ground model based on microtremor array observations and seismic observation results

Chapter 3. using the one-dimensional S-wave velocity structure obtained in the above, the initial deep ground model at each observation point was modified, and a three-dimensional S-wave velocity structure model was created by spatially interpolating each velocity layer in the horizontal direction. Based on the estimated S-wave velocity structure, the deep ground velocity structure (J-SHIS_V2) was modified. Since J-SHIS _V2 is uniformly shallow up to the S wave velocity of 1,000 m/s, the result is deep after correction (Figure 1). After the S-wave velocity of 1,200 m/s, it became shallower on the northwest side of Yamanashi prefecture after the model modification and deeper on the east side. How to modify the shallow underground model. It was created to match the AVS30 (C40 and S-wave velocity structure by inversion) obtained from the microtremor exploration at the point where the microtremor exploration is being carried out.

5. Summary

In this sutudy, we show an example of the construction and results of a shallow and deep integrated underground structure model for the Yamanashi region. In the future, we plan to verify the underground model using seismic records, such as the period and amplification characteristics at seismic stations.

Keywords: Underground structure model, Microtremors, Strong Ground Motion Prediction

©2021. Japan Geoscience Union. All Right Reserved.

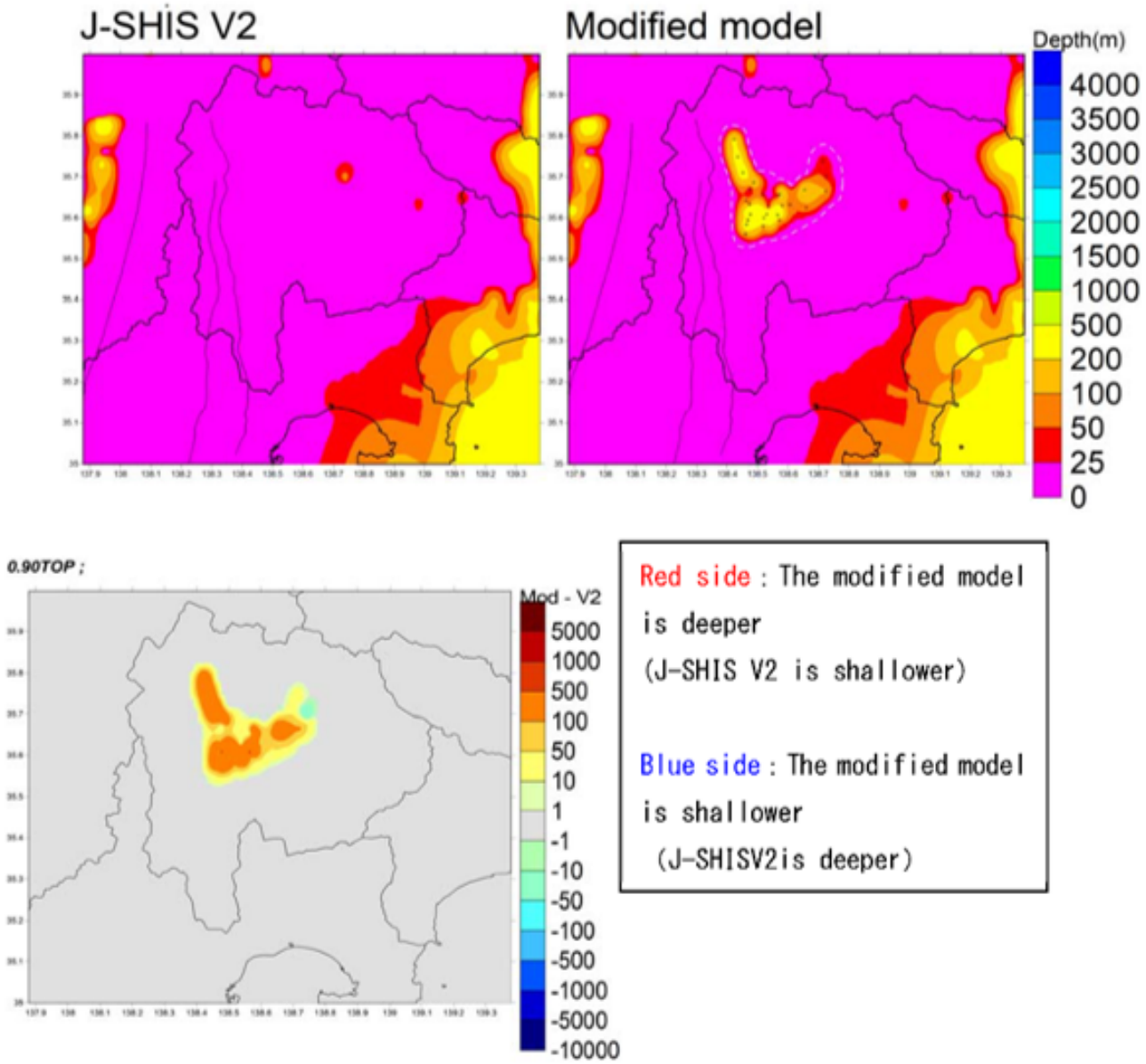


Figure 1. Top depth distribution of modified understructure model (Vs900 (m/s) top depth)

©2021. Japan Geoscience Union. All Right Reserved.

Modeling of subsurface velocity structures from seismic bedrock to ground surface for Kumamoto region

*Shigeki Senna[1], Atsushi Wakai[1], Yatagai Atsushi[2], Yoshiaki Inagaki[2], Hisanori Matsuyama[2], Hiroyuki Fujiwara[1]

1. National Research Institute for Earth Science and Disaster Resilience, 2. OYO Corporation

1. Introduction
The NIED has created a shallow and deep integrated ground structure model using the microtremor array exploration observed in the Kumamoto Plain (Senna et al., 2018). In this study, the range of the shallow and deep integrated underground structure model was expanded by significantly adding microtremor array exploration to the northern part of the Kumamoto Plain and the Aso area. In this study, we report the results of expanding the scope using the method proposed in the above paper.

2. Creation of initial ground model
Regarding the expansion range, of the initial ground models, the J-SHIS_V2 model of the NIED was basically used as the initial model for the deep underground model (deeper than Vs350 (m/s) defined as the engineering bedroock). For shallow underground, a ground model was connected to make it an initial model. After that, the upper surface of the engineering bedrock of the shallow underground was used as the upper surface of the first layer of the deep underground, and the two were integrated to form the initial integrated underground model. For the shallow underground model (shallow than Vs350 (m/s)), the geomorphologic classification of J-SHIS was reviewed and revised based on the flood control topography classification map, and Borehole data (about 12,000) were organized and a 250m mesh model was created based on the modified geomorphologic classification.

3. Microtremor array observations and seismic records used
Microtremor array observations are about 5 km of large array observations (three points with array radii of 100, 200, 400 m and L-shape with sides 25 to 75 m) in the lowlands and plateaus indicated by the geomorphologic in the northern part of Kumamoto Prefecture and the Aso area. 16 points were added at intervals. Including the 26 large array points in the past, there are a total of 42 points. On the other hand, extremely small and irregular array observations (4 points with an array diameter of 60 cm and triangles with a side of 5m to more than 10 m) were carried out at approximately 1 km intervals and in the Aso area at approximately 500 m intervals (2021. As of March). Including the 473 points of the existing microtremor array, the total number is 1327 points. The phase velocity and H/V spectrum ratio for each microtremor observation point were calculated. For the seismic records, the R/V spectrum ratio for each station was calculated using the K-NET and KiK-net seismic stations of the NIED, and the seismic records of local governments and the JMA. Based on these ground vibration characteristic data and the initial underground model, joint inversion was performed to obtain a one-dimensional S wave velocity structure at each observation point.

4. Modification of ground model based on microtremor array observations and seismic observation results
Using the one-dimensional S-wave velocity structure obtained in Chapter 3, the initial deep underground model at each observation point was modified, and a three-dimensional S-wave velocity structure model was created by spatially interpolating each velocity layer in the horizontal direction. Based on the estimated S-wave velocity structure, the deep underground velocity structure (J-SHIS_V2) was modified for the extension. Compared with the J-SHIS_V2 model created in this study, the top depth of the Vs900

©2021. Japan Geoscience Union. All Right Reserved.

layers (Figure1) more reflects the shape of the Aso caldera. There is. The top depth of the Vs2700 layers (Figure2) is deeper near the central crater hills of Aso volcano. This is in harmony with the results of the distribution map of the upward connection residuals of gravity. In the vicinity of Shimabara Bay, the model is based on the results of sound wave exploration and gravity. As a result of the above, we believe that we were able to construct a model that more clearly reflects the structure of the "Beppu-Shimabara Graben" from Oita to Aso, Kumamoto, and the Shimabara Peninsula. The modification of the shallow ground model was made to match the AVS30 (C40 and S-wave velocity structure by inversion) obtained from the microtremor exploration at the point where the microtremor exploration was carried out.

5. Summary

In this paper, we have extended the shallow and deep integrated ground structure model around the Kumamoto Plain that we have created so far, and showed the results. In the future, we plan to acquire past data such as active fault priority surveys, add microtremor array observations, build a underground model for the entire Kumamoto prefecture, and verify it with seismic records.

Keywords: Underground structure model, Microtremors, Strong Ground Motion Prediction

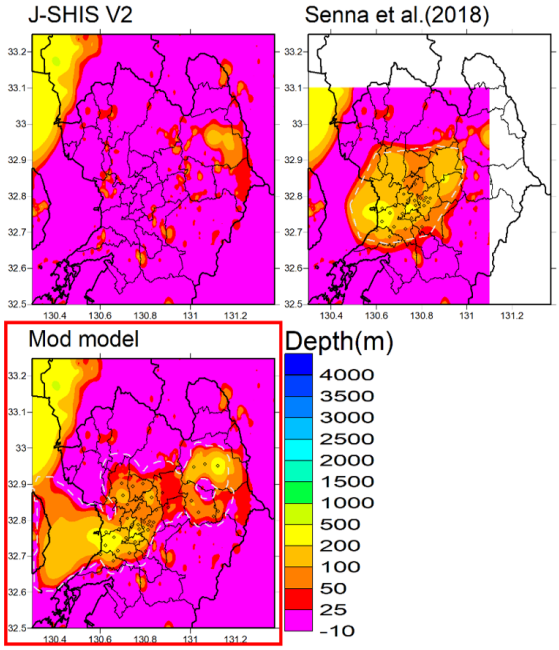


Figure 1. Top depth distribution of underground structure model (Vs900 m/s)
Upper left: J-SHIS V2
Upper right: Senna et al. (2018)
Lower left: Modified model

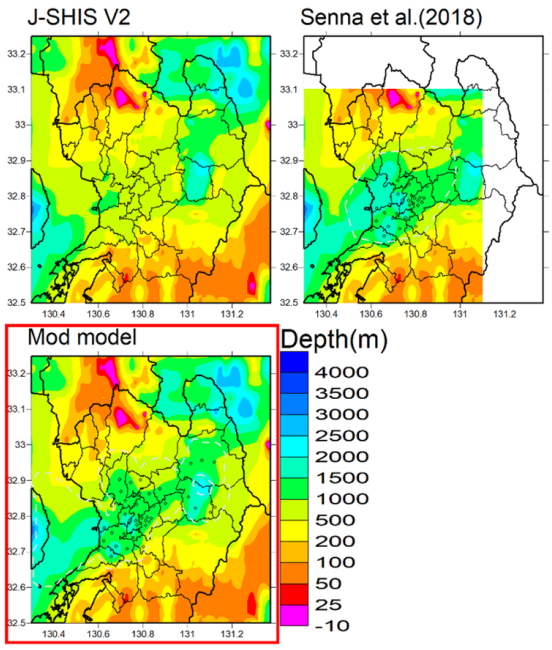


Figure 2. Top depth distribution of underground structure model (Vs2700 m/s)
Upper left: J-SHIS V2
Upper right: Senna et al. (2018)
Lower left: Modified model

©2021. Japan Geoscience Union. All Right Reserved.

Basic study of a real-time damage estimation system for liquefaction

*Shohei Naito[1], Hiromitsu Nakamura[1], Shigeki Senna[1], Yoshinori Iwanami[2]

1. National Research Institute for Earth Science and Disaster Resilience, 2. MITSUBISHI SPACE SOFTWARE CO.,LTD.

The real-time earthquake damage estimation system (Nakamura et al., 2013) makes it possible to immediately estimate damage to buildings, etc. due to earthquake motion in units of towns. It is being used for decision-making during disaster response. However, regarding the liquefaction that occurs due to earthquakes, it is not possible to provide damage estimation information of buildings for now, although there are development examples of liquefaction prediction systems such as Kamiya et al. (2013). Since the damage caused by liquefaction has many effects on various structures and lifelines, it is an urgent task to establish a damage estimation method for early recovery.

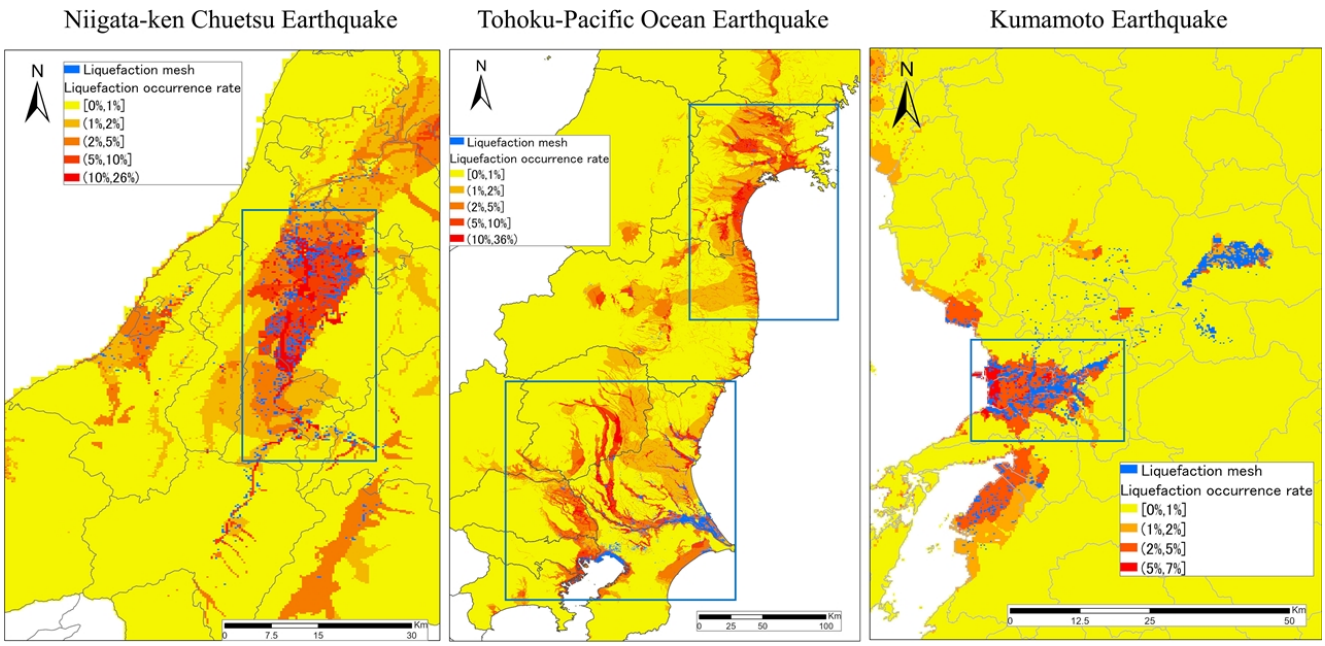
Therefore, we targeted three earthquakes, the Niigata-ken Chuetsu Earthquake, the Tohoku-Pacific Ocean Earthquake, and the Kumamoto Earthquake, and we developed the liquefaction estimation system mainly based on the liquefaction estimation method of Senna et al. (2018). After acquiring strong motion observation records on K-NET and KiK-net, an index deltals obtained from a 10-second integrated value of the real-time seismic intensity (Kunugi et al., 2008) exceeding a threshold (4.5) is calculated and interpolated by the IDW method. After that, a liquefaction occurrence probability in 250m mesh units is calculated by multiplying the regression coefficient α, which differs depending on a region and a microtopography classification group (Matsuoka et al., 2011). In addition, we developed the risk estimation system calculating the total destruction rate of the building due to liquefaction based on the method of Shimizu et al. (2016), by multiplying the liquefaction occurrence probability, the liquefaction area ratio (Yamamoto et al., 2009) and the total collapse rate of the building when liquefaction occurs (Cabinet Office, 2003). These estimation results are stored as a data file in netCDF format, and it is possible to visualize the spatial distribution on a Web browser or a GIS software (Fig. 1).

Next, as a result of comparing the distribution of the liquefaction occurrence rate of the 250 m mesh calculated by the system with the 250 m liquefaction mesh based on aerial photograph interpretation (Wakamatsu et al., 2017), it was confirmed that concerning each of the tree earthquakes, the mesh estimated to have a liquefaction occurrence rate of 2% or more contains about 80 to 90% of the liquefaction mesh within the blue frame area of Fig.1, and this method is effective in grasping the distribution of liquefaction damage. In addition, the 250m mesh was aggregated for each 10km mesh, and the average value of the estimation results by the system was compared with the ratio of the liquefied mesh to the 10km mesh. As a result, a certain correlation was confirmed between the two. On the other hand, in the Kumamoto earthquake, problems such as underestimation of the estimated value were confirmed, and it was found that more appropriate parameter setting is necessary in consideration of geomorphological factors.

In the future, in addition to developing a more precise prediction model of liquefaction occurrence rate based on recent earthquake damages, we are going to construct a real-time liquefaction damage estimation system that can be used for quick understanding of damage status and early restoration of social infrastructure. In addition, regarding building damage caused by liquefaction, sufficient observation data could not be obtained to verify the estimated value, but verification of the possibility of using it as data that contributes to risk evaluation will be an issue.

©2021. Japan Geoscience Union. All Right Reserved.

Keywords: liquefaction, damage estimation, real-time



©2021. Japan Geoscience Union. All Right Reserved.

Estimation of subsurface motion from surface seismic records: investigation on evaluation at deep levels

*Tomotsugu Watanabe[1], Hiroshi Takenaka[1], Masanao Komatsu[1], Mitsutaka Oshima[2]

1. Okayama University , 2. Shimizu Corporation

We need subsurface seismic motions or incident wavefields on a given subsurface level to evaluate the seismic stability of the shallow subsurface structure and the response of buildings through simulating the strong motion. It is conventional that the subsurface motion is estimated from the ground motion record at a free surface position by assuming a vertical plane-wave incidence. However, this approach requires that the vertical and horizontal components of the seismic wave independently propagate as P wave and S wave, respectively, which is theoretically incorrect, and could not represent the correct deformation in the subsurface structure. We have proposed a new method to evaluate the subsurface wavefields from a surface record without the assumption of the plane-wave incidence (Takenaka et al., 2019, SSJ Fall meeting) and applied the method to compare the evaluated motion with the subsurface records at shallow levels of around 100 –200 m (Watanabe et al., 2020, JpGU). The evaluation level is deeper, the actual wavefields could be more different from the conventionally estimated ones based on the assumption of the vertical incident plane wave, due to the oblique incident effect and so on. In this study, we check the effectiveness of our method and the conventional one by reproducing subsurface records in depth of more than 2 km.

Our method needs a horizontally-layered model including the earthquake source. We calculate the synthetic seismograms at the surface station and the subsurface evaluation point assuming the focal mechanism and impulsive source. We then deconvolve the surface record with the surface synthetic seismogram to derive the *effective source time function*. We apply the water level method for the stable deconvolution. The effective source time function has the substantial source time function and the unsimulated effects by the structural model, which are included in the surface record. Then, we convolve the effective source time function with the subsurface synthetic seismogram to derive the target motion at the evaluation point.

We apply our method and conventional one to the surface records observed at the KiK-net (NIED) TKYH02 station for a source of *Mj* 4.8, focal depth 83 km, and epicentral distance 53.73 km. Figure 1 shows the subsurface motion observed and evaluated by three methods, our method and methods based on vertical and oblique plane-wave incidence, respectively. We select the horizontal slowness of S-wave for the oblique plane-wave incidence so as to fit the estimated subsurface waveform of the transverse component to the observed one. We could successfully recover the subsurface motion by our method. In Fig. 1(a), it is found that there are differences in the amplitude of the P-wave coda and later phases on the radial component. The subsurface waveform estimated by our method is similar to one by the method based on the oblique plane-wave incidence. We confirmed that the subsurface acceleration spectra evaluated by three methods recovered the observed one around a few Hz, while our method underestimated the spectra in lower than 1 Hz because of the effect of the water level method. We will also report about the estimation of the subsurface motion using other events and records, the evaluation of incident wavefields, and the estimation at the subsurface evaluation points with horizontal offsets from the surface station and so on.

©2021. Japan Geoscience Union. All Right Reserved.

Keywords: seismic motion, plane wave, strong motion, subsurface wavefield

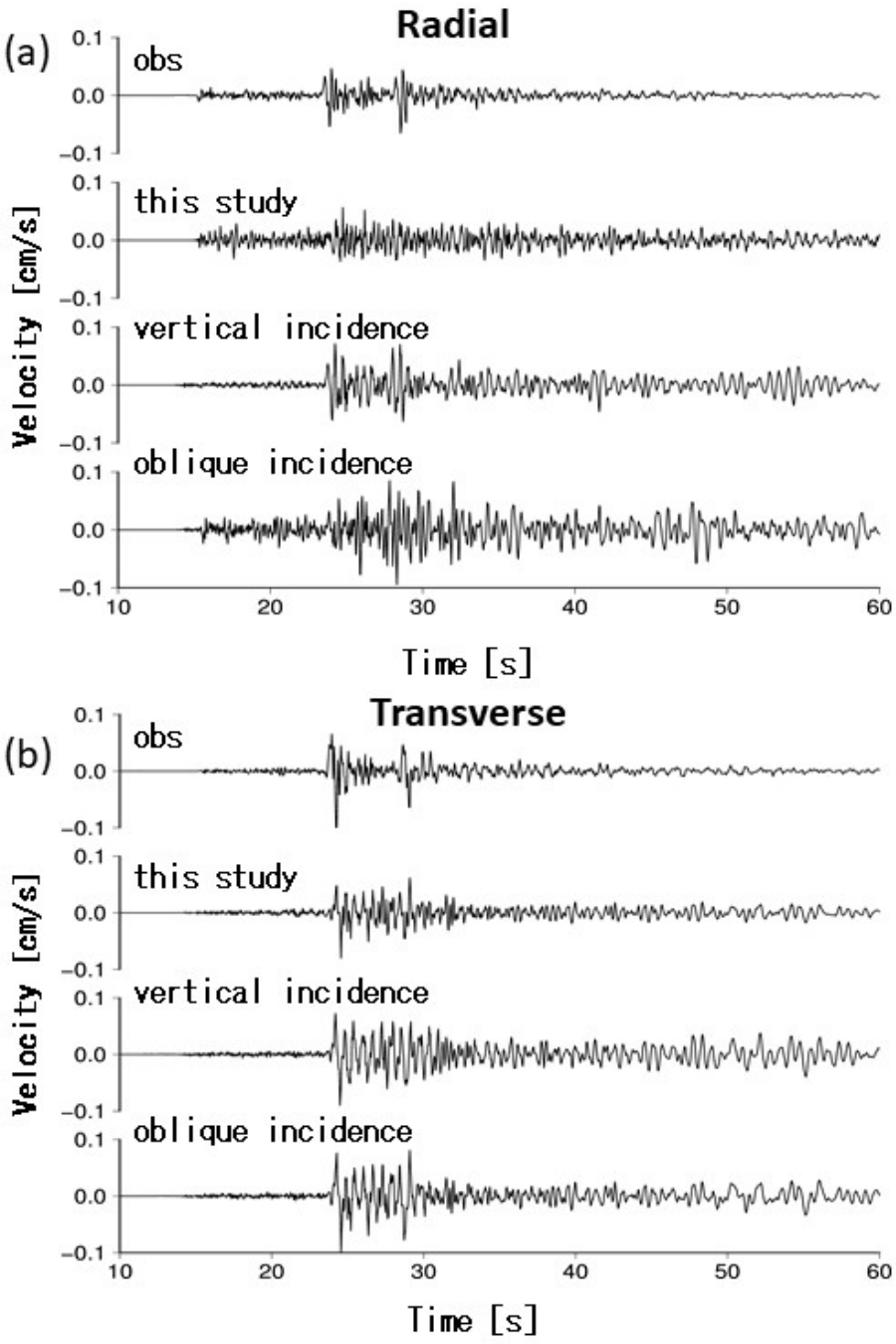


Fig1. Subsurface waveforms observed or estimated from surface records using three methods: (a) the radial and (b) transverse component.

©2021. Japan Geoscience Union. All Right Reserved.

Estimation of seismic ground motions on the surface ground at MeSO-net stations

*Atsushi Wakai[1], Shigeki Senna[1]

1. National Research Institute for Earth Science and Disaster Resilience

In the near future, it is concerned that a large earthquake will occur beneath the Tokyo metropolitan area and there will be severe damage for a lot of houses, buildings and infrastructures. Meanwhile, there are some earthquake observation networks in the area nowadays. Some of the networks provide us with the indexes of earthquake ground motions in a short time. Therefore, the information enables us to understand situation of earthquake ground motions in the area.

In the past national project of Japan, “Metropolitan Seismic Observation network” (hereinafter, referred to as “MeSO-net”) was constructed for the investigation of tectonic plate structures and the estimation of seismic source fault models in the Tokyo metropolitan area around ten years ago [1]. The MeSO-net has about 300 stations with sensors installed at around 20 meters underground in the area. Also, they are spatially distributed at intervals of 2 to 5 kilometers in the area. This network can provide us with the picture of earthquake ground motions with higher spatial resolution, provided that seismic records are acquired on the ground surface.

In recent years, we have worked a subproject of “acquisition of spatially very-high-resolution earthquake observation data and development of the database by private-public partnerships” as a member in a national project or “Tokyo Metropolitan Resilience Project [2].” As one of the issues, we have tackled estimation of seismic ground motions on the ground surface based on bore-hole seismic records observed at each MeSO-net station. This issue needs soil amplification factors between the ground surface and 20 meters below ground.

The procedure is as follows. First, a seismometer has installed on the ground surface at each MeSO-net station during two to three months and some earthquake observation records have been obtained in addition to the bore-hole records at each MeSO-net station. And then, an observed spectral ratio has been obtained by calculating Fourier spectra of seismic records on the ground surface and those in the bore-hole. Also, calculating JMA seismic intensity scale based on records on the ground surface and those in the borehole, increment of seismic intensity has been obtained by subtraction of them. Secondly, a miniature and centerless array microtremor exploration [3] was performed at each MeSO-net station. This method can be adopted principally for estimation of an S-wave velocity structure in the surface ground. It consists of 4-point miniature array with a radius of 60 centi-meters and 3-point centerless array with around 10 meters on a side. An S-wave velocity structure was estimated based on a disperse curve of phase velocity and an H/V spectral ratio calculated from microtremor data at each MeSO-net station. Then a transfer function was obtained using 1-dimensional multiple reflection theory based on the S-wave velocity structure at each MeSO-net station. Finally, an S-wave velocity structure can be enhanced by modifying a transfer function based on an observed spectral ratio at each MeSO-net station. Also, the existing S-wave velocity structures and other geotechnical information can be enhanced based on S-wave velocity structures at MeSO-net stations.

In this study, we will develop the scheme for estimation of earthquake ground motions at each MeSO-net station based on bore-hole seismic records by means of some soil amplification factors mentioned above.

©2021. Japan Geoscience Union. All Right Reserved.

In this presentation, we will report on the results in the analyses of seismic data and microtremor ones at this moment.

References
[1] MEXT (2011): https://www.mext.go.jp/a_menu/kaihatu/jishin/1319360.htm (in Japanese)
[2] NIED (2021): https://forr.bosai.go.jp/e/sub_b.html
[3] I. Cho, S. Senna, and H. Fujiwara (2013), “Miniature array analysis of microtremors,” Geophysics, Vol.78, No.1, pp. KS13-KS23, doi:10.1190/geo2012-0248.1.

Keywords: MeSO-net, soil amplification factor, seismic ground motion, microtremor exploration, S-wave velocity structure

©2021. Japan Geoscience Union. All Right Reserved.

Strong motion simulation of an intraslab earthquake beneath Kanto region using MeSO-net observation data

*Wataru Suzuki[1], Takeshi Kimura[1], Hisahiko Kubo[1], Takayuki Miyoshi[1]

1. National Research Institute for Earth Science and Disaster Resilience

MeSO-net (Metropolitan Seismic Observation network) conducted dense and real-time observation of seismic motion at approximately 300 stations in the metropolitan area. The network has contributed to researches of underground structure and seismic activity, and advancement of strong motion evaluation for the Kanto region. However, to authors' knowledge, the observed waveform itself has not been used for the strong motion simulation as empirical Green's function. We have noticed advantage of the observed MeSO-net data which contains the effects of the small heterogeneities of underground structure we cannot fully model. We, therefore, have performed strong motion simulation for an intraslab earthquake within the Philippine Sea plate beneath Tokyo by applying the empirical Green's function method to the MeSO-net observed waveforms.

We used waveforms recorded during an M_W5.0 intraslab earthquake that occurred at a depth of 57km on September 12, 2015 as empirical Green's functions. This event has a normal-fault-type mechanism of N-S and E-W striking nodal planes with high-dipping angle. We extended these two nodal planes to M7-class fault models for the strong motion simulation. The fault models have one strong motion generation area whose parameters were assumed considering the strong motion evaluation of Cabinet Office. Empirical Green's function simulation was conducted following the method proposed by Irikura (1986) and Irikura et al. (1997).

Simulated acceleration waveforms at MeSO-net E.TYPM station (Shinjuku, Tokyo) show the peak values of approximately 500gal and 250gal for horizontal and vertical components, respectively. The simulation results for N-S and E-W striking fault models are similar. Acceleration response spectra have the peak value at a period around 0.2 seconds and the spectral amplitude decreases as the period approaches to 1 second. It seems that the empirical Green's function used here lacks enough power for long-period components to simulate M7-class earthquake. Further examination to model the long-period components using the theoretical approach is necessary to simulate the strong motions that can be used to promote the disaster resilience in the metropolitan area.

Keywords: MeSO-net, Strong motion simulation, Empirical Green's function method, Strong motion generation area, Intraslab earthquake

©2021. Japan Geoscience Union. All Right Reserved.

Ground-motion simulation for the 2016 Kumamoto earthquake (Mj7.3) based on the strong-motion prediction recipe

*Asako Iwaki[1], Nobuyuki Morikawa[1], Takahiro Maeda[1], Hiroyuki Fujiwara[1]

1. National Research Institute for Earth Science and Disaster Prevention

The 2016 Kumamoto earthquake occurred on April 16, 01:46 JST (M_{JMA}7.3) revealed several issues on the strong-motion prediction in terms of fault size, seismic moment, etc. In this study, we attempt to “predict” the ground motion for the Kumamoto earthquake based on different fault models, aiming to clarify the key parameters and uncertainties to be considered for improving strong-motion prediction for active faults.

First, we set a reference fault model by following the procedure by the “recipe” (Headquarters for Earthquake Research Promotion of Japan, 2017) assuming the fault length was set to be a realistic number, 34 km a priori. The seismic moment calculated from the reference model via the S - M_0 (fault area –seismic moment) relation of the recipe is less than 50 % of the observation. We set two types of alternative models: (1) fault models with the same fault size as the reference model but with doubled seismic moment and (2) fault models with larger fault length but with the same S - M_0 relation.

Using the various fault models and a detailed 3-D velocity structure model (Senna et al. 2017), broadband ground motion was computed by a hybrid technique combining 3-D finite-difference method at long periods (> 1 s) and the stochastic Green’s function method at short periods (< 1 s). We show the effect of considering the uncertainties in S - M_0 relation, fault length, and the depth of fault top on the performance of the ground motion prediction.

Keywords: 2016 Kumamoto earthquake, strong motion, ground-motion simulation, active faults

©2021. Japan Geoscience Union. All Right Reserved.

Characterized source model of M7.3 2016 Kumamoto eq. by 3D reciprocity GFs inversion with special reference to velocity pulse at KMMH16

*Anatoly Petukhin[1], Hiroshi Kawase[2], Fumiaki Nagashima[2], Eri Ito[2]

1. Geo-Research Institute, 2. DPRI, Kyoto University

2016 Kumamoto earthquakes caused severe damage centering on Mashiki residential area. The velocity waveforms at KMMH16 station in Mashiki during the *M*7.3 event show a large velocity pulse observed both by the surface and downhole sensors. Kawase et al., 2017, found that severe damage in Mashiki may be result of strong westward velocity pulse. Question raised by the 2016 Kumamoto earthquakes is how the near-source ground motions with strong velocity pulses at KMMH16 were generated during *M*7.3 event.

In this study, we focus on the characterized SMGA source model. EGF method is widely used for source modelling in this case. However, in case of target site is located just near the fault in the nodal plane of the source mechanism (like KMMH16), the mechanism of the EGF event should perfectly fit the mechanism of the mainshock, which is a rare case. Otherwise, large variations of amplitudes in the vicinity of the nodal plane will produce large errors of ground motion synthetics. Instead, we will use theoretical 3D GFs.

Our approach is non-linear source inversion. This method requires calculation of waveforms and comparison with observations for many source models. To accelerate these calculations, we use precalculated Green’ s functions (GF) by the reciprocity method and the JIVSM velocity structure model. By comparison with aftershock record, we validated this structure for as short as 2 s in periods. For mainshock inversion we expand the target period to 1.5 sec. Target sites are limited to sites close to the fault: KMM005, KMM006, KMMH06, KMMH14, and KMMH16.

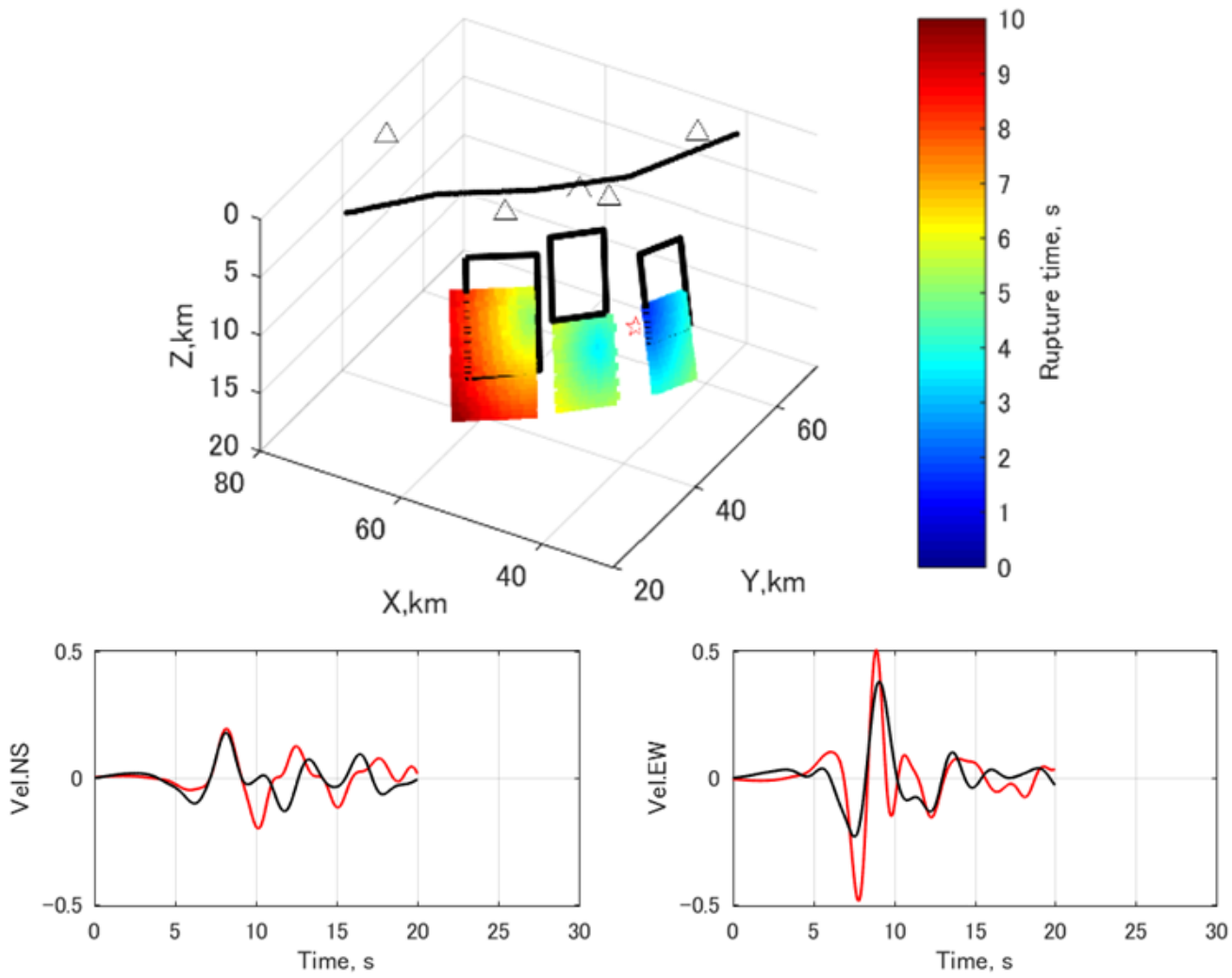
First, we explore the parameter space with the simplex search method with the initial SMGA model of Somei et al. (2019). In this process we were able to reduce a number of search parameters by limiting to effective parameters only. Also, necessary physical constraints for rupture velocity, rupture starting point, etc., as well as their strength, were estimated here. Then, we try to look for an alternative initial SMGA source model by the grid search method, and finally, estimate source model with the simplex search method again.

Resulting model and waveforms for KMMH16 are shown in figure below. Location of SMGAs is deeper than in initial model of Somei et al. (2019). For SMGA2 the deep location agrees well with other source inversions (e.g., Yoshida et al., 2017). SMGA rupture initiation points have physically reasonable location allowing outward propagation from the mainshock hypocenter, without any reverse ruptures. Waveform reproduces short period westward pulse at KMMH16.

Acknowledgements. We use strong motion data from K-NET, KiK-net, and CMT solutions from F-net, provided by the NIED.

©2021. Japan Geoscience Union. All Right Reserved.

Keywords: 2016 Kumamoto earthquake, source inversion, seismic reciprocity, characterised source model, strong motion generation area, Mashiki



Top - SMGA location and rupture time distribution; black rectangular – initial model SMGAs from left to right: SMGA1, SMGA2, SMGA3 for the Hinagu, Futagawa3 and Futagawa2 segments, respectively. Bottom - waveform fit at KMMH16 (black-observed, red-simulated).

©2021. Japan Geoscience Union. All Right Reserved.

Evaluation of near-source ground motion during the 2008 Iwate-Miyagi Nairiku earthquake by using stochastic slip models and three-dimensional velocity structures

*Takeshi Nakamura[1], Masataka Sawada[1]

1. Central Research Institute of Electric Power Industry

The detailed rupture process and heterogeneous subsurface structures should be considered in ground motion evaluations near the source fault at a large earthquake. Numerical simulation methods such as the finite difference method (FDM) and the finite element method (FEM) can incorporate the heterogenous fault slip and three-dimensional structure models into calculations and are useful for grasping seismic motion not only at individual points but also on whole ground surface and seafloor. However, these methods are computationally expensive because they treat a large number of grids and meshes in the computational domain when numerically solving the governing equation, which causes practical limitations on the number of models that can be used as inputs for simulations. However, in the case of a few number of receivers or stations to be evaluated, such as ground motion simulations at important facilities such as power plants, the Green's functions for many point sources can be efficiently calculated by interchanging the source and receiver locations based on the reciprocity theorem and the total number of numerical simulations for many source models can be significantly reduced compared with that by the straightforward approach (e.g., Eisner and Clayton). In this study, we evaluate the displacements including the static component and their deviations near the source fault of the 2008 Iwate-Miyagi Nairiku, Japan, earthquake by calculating waveforms with the reciprocal approach for various slip distribution models that are stochastically generated. We focus on KiK-net IWTH25 station that recorded the peak acceleration amplitude of 3866 gal and the static displacement of 140 cm in the vertical component at the earthquake (Aoi, et al., 2008; Aoi and Morikawa, 2009).
We calculated the Green's functions by using the 3D FDM developed by Nakamura et al. (2012). The finite-fault inversion result for the 2008 earthquake by Asano and Iwata (2011) was employed as a reference model to stochastically generate slip distributions on the fault plane. From their model, we generated 100 cases for the heterogeneous slip distribution based on the slip probability density function (SPDF) by Murphy et al. (2016). We used a point source on a subfault and set a total of 315,216 subfaults with a dense interval of 50 m on the fault plane. We assessed a smoothly spatial distribution of displacements near the fault by employing such dense interval in our simulations, whereas the distribution showed a periodic deformation pattern that is not observed by satellite geodetic surveys if the large subfault interval or size is employed. We used the same initial break point, rake angle, and rupture velocity as those presented in Asano and Iwata (2011). The rise time in subfault was set according to its subfault size. For subsurface velocity structures, we used the Japan Seismic Hazard Information Station (J-SHIS) model (Fujiwara et al., 2009). After confirming an excellent fitting of synthetic waveforms at the IWTH25 surface station for several cases between the straightforward simulation and the reciprocal approach, we generated synthetic waveforms for all slip distribution cases by postprocessing the reciprocal Green's functions.
Our calculation results show that the peak amplitude of the displacement waveform for the fault parallel and orthogonal components and the vertical one is 46±12 cm, 32±11 cm, and 88±26 cm, respectively. The static displacement, which is the mean value in a time window of 40-45 s in which the waveform amplitude converges to a constant value, for the three components is 32±13 cm, 4±10 cm, and 69±20 cm, respectively. Because the source mechanism of the reference model is a reverse fault with the rake

©2021. Japan Geoscience Union. All Right Reserved.

and dip angle of 108 and 51 degrees, respectively, and IWTH25 is located just above the fault plane, both of the static displacement and the peak displacement in the vertical component are larger than those in the horizontal ones in all cases except 5 ones. The static and peak displacement in the vertical component is 6.9 and 6.4 times difference among the cases, respectively, and the maximum value of these displacements is 112 cm and 144 cm, respectively. The peak displacement amplitude in the component is 1.3 times larger on average than the static displacement. Our results also show an attenuation feature of the displacement amplitudes according to the hypocentral distance from the maximum slip position in the source fault. Because IWTH25 is several kilometers away from the surface fault areas, this attenuation relation is significantly associated with the distance to the station location projected on the fault plane compared with the depth of the slip position.

Keywords: Iwate-Miyagi Nairiku earthquake, fault displacement, stochastic slip distribution, reciprocity theorem, finite-difference method

©2021. Japan Geoscience Union. All Right Reserved.

Source rupture process of the 2018 Hokkaido eastern Iburi earthquake estimated from waveform inversion with empirical Green’ s functions

*SHUANGLAN WU[1], Atsushi Nozu[1], Yosuke Nagasaka[1]

1. PORT AND AIRPORT RESEARCH INSTITUTE

The Hokkaido Eastern Iburi earthquake (M_{JMA}6.7) on September 6:03:08 (JST), 2018, occurred in the eastern Iburi region of Hokkaido, Japan, which is reported by the JMA (Japan Meteorological Agency). More than 6000 landslides occurred in the early hours after the earthquake (Yamagishi and Yamazaki, 2018). Tragically, more than 40 people lost their lives, along with 689 people injured (Fire and Disaster Management Agency, Japan, as of 5 October 2018). During this earthquake, large ground motions have been observed, e.g., ground motions at Kik-net Atsuma- (IBUH03) and K-net Mugawa (HKD126), the peak velocity is approximately 150cm/s, and ground motions in the frequency components 1~3Hz are predominant, which are very important to the engineering facilities. In general, the strong crustal earthquakes are with 5-20km depth, e.g., the mainshock of the 2016 Kumamoto earthquake (M_w7.1, depth 12km), the 1995 Kobe (M_w6.9 depth 16km); the 1989 Loma Prieta (M_w6.9, depth 19 km), the 1994 Northridge (M_w6.7, depth 18.2 km) earthquake. However, the 2018 Hokkaido eastern Iburi earthquake was in contrast to the usual situations; it is with Mj6.7 but with hypocentral depth of 37 km but caused large ground motions.

Such special characteristics, the large strong ground motions it generated, its impact on lifeline facilities and buildings, and the serious geological hazards it caused have motivated us to study its rupture features, especially focusing on the generation mechanism of the strong ground motions (e.g., the large pulse velocity). This event was well recorded by permanent strong-motion networks K-net and KiK-net, forming a rich waveform database, which enables us to investigate the rupture process of the earthquake in detail. Therefore, in this analysis, the source rupture process of this event was estimated from the waveform inversion of strong-motion data, and with the adoption of empirical Green’ s functions, which could avoid the possible uncertainties caused by the assumption of subsurface velocity structures, as well as to consider relatively higher frequency ranges of strong ground motions typically up to 2.0 Hz.

Our preferred slip model is illustrated in Figure 1, and the comparisons of observed and synthesized velocity waveforms (0.2 - 2.0 Hz) are illustrated in Figure 2. Figure 1(a) indicates that one large slip region with a maximum slip of approximately 3.4 m was centered ~ 2 km SE of the hypocenter; and in Figure 1(b), two regions with large peak slip velocity were identified, the first one with a peak value of 2.0 m/s was located ~ 6 km SE of the hypocenter, which was mainly contributed to the large pulse velocity of the K-net station HKD126, and the region with serious landslides; and the second one was centered ~ 5 km NW of the hypocenter. The large slip region (with 23~28km in depth) and both the regions with peak slip velocity (with 21~26 km in depth) are located shallower than the hypocenter. The rupture velocity of 2.0 km/s was identified, and the preferred source model corresponds to Mw 7.0 for this event.

The robustness of our preferred slip model was verified through different combinations of EGF events and near-fault stations, which resulted that the locations of the large slip regions are not significantly affected by the selection of the EGF events and the near-fault station. Additionally, based on the preferred source model, the ground motions are synthesized for strong-motion stations that were not used in the inversion

©2021. Japan Geoscience Union. All Right Reserved.

analyses, the synthesized ground motions are consistent with the observed ones. Furthermore, our preferred slip model is consistent very well with the broadband source model proposed by Satoh (2020).

Keywords: the 2018 Hokkaido eastern Iburi earthquake, rupture process, waveforms inversion, empirical Green’ s functions, strong ground motions, large pulse velocity

©2021. Japan Geoscience Union. All Right Reserved.

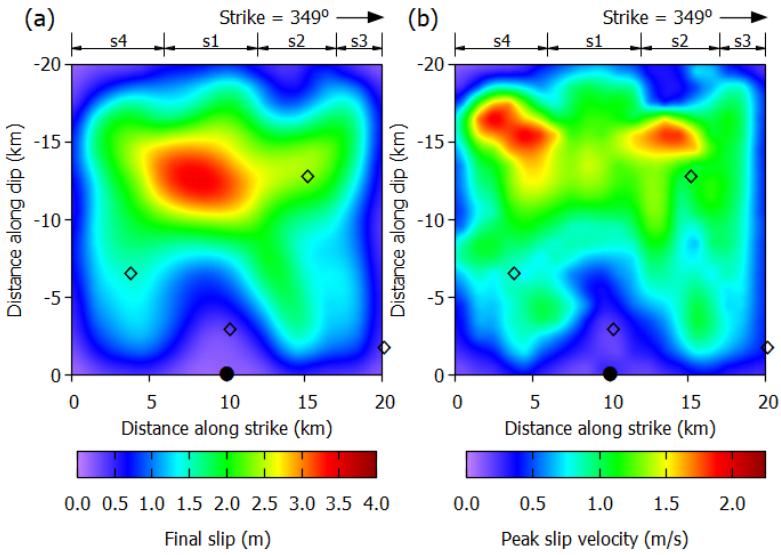


Figure 1. (a) The final slip distribution, and (b) the peak slip velocity of our preferred source model. In each panel, the black dot indicates the JMA hypocenter, which is the rupture starting point assumed for the waveform inversion. The allocation of the adopted 4 EGF events on the fault is also illustrated. The absolute values of the slip were obtained by using the moments of the EGF events.

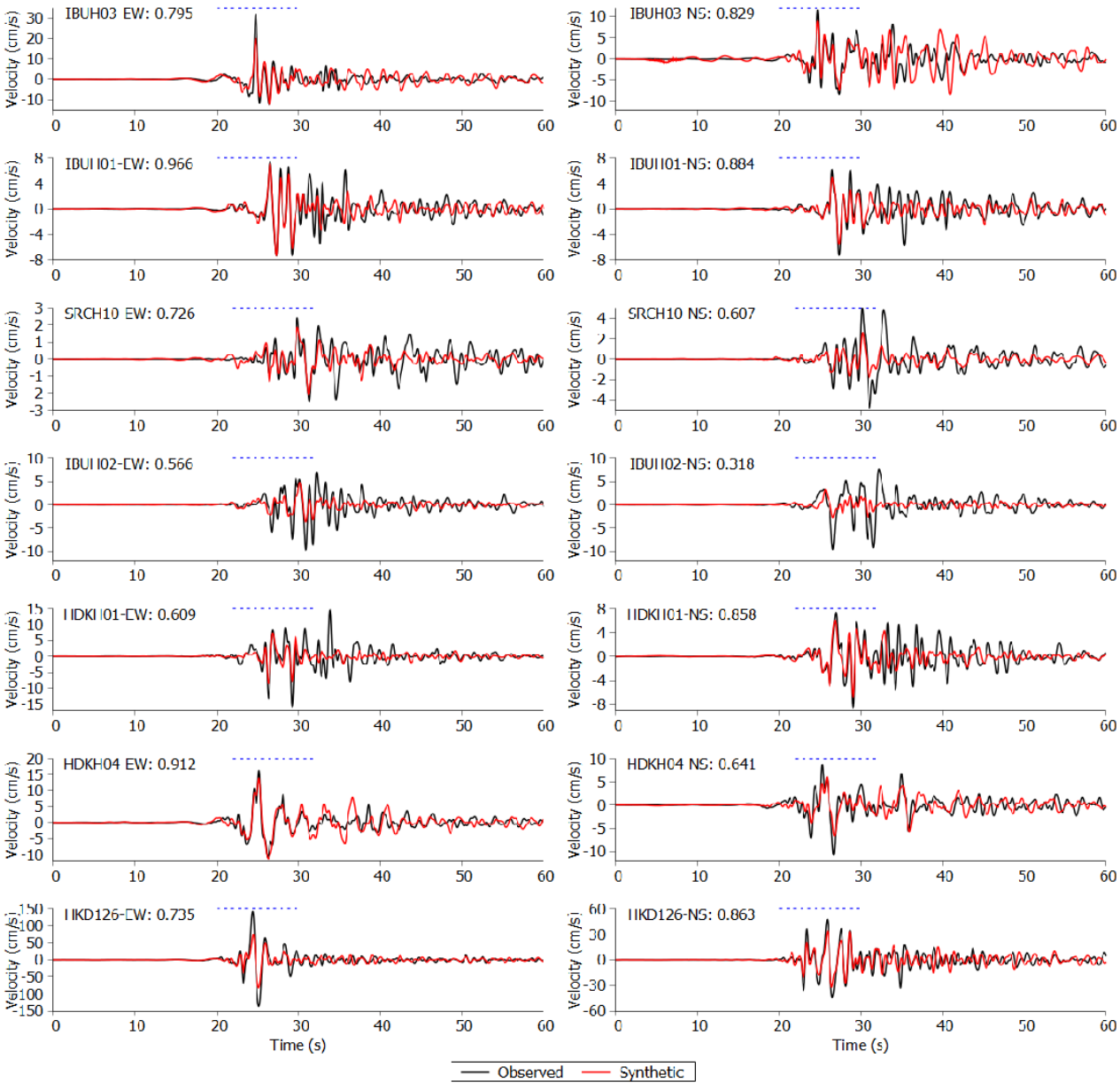


Figure 2. Comparisons of observed and synthesized velocity waveforms (0.2 - 2.0 Hz) based on our preferred source model, and the 10s waveform section under the blue dashed lines are the waveform data used in the inversion analysis. the numbers at the top left of each component are variance reduction (VR) values.

©2021. Japan Geoscience Union. All Right Reserved.

©2021. Japan Geoscience Union. All Right Reserved.

Calibrating Thailand’s local magnitude scale: a preliminary result

*Mongkolchai Sukmee[1], Sutthipong Noisagool[1,2], Satoru Tanaka[3], Weerachai Siripunvaraporn[1,2], Songkhun Boonchaisuk[4,2], Yasushi Ishihara[5], Taewoon Kim[6], Hitoshi Kawakatsu[7], Nozomu Takeuchi[7], Kenji Kawai[8], Yuki Suzuki[8]

1. Department of Physics, Faculty of Science, Mahidol University , 2. Thailand Center of Excellence in Physics, Ministry of Higher Education, Science, Research and Innovation, 3. Volcanoes and Earth's Interior Research Center (VERC), Research Institute for Marine Geodynamics (IMG), Japan Agency for Marine-Earth Science and Technology (JAMSTEC), 4. Geoscience Program, Mahidol University, Kanchanaburi Campus, 5. Research Institute for Marine Geodynamics (IMG), Japan Agency for Marine-Earth Science and Technology (JAMSTEC), 6. Subduction Dynamics Research Center (SDR), Research Institute for Marine Geodynamics (IMG), Japan Agency for Marine-Earth Science and Technology (JAMSTEC), 7. Earthquake Research Institute, The University of Tokyo, 8. Department of Earth and Planetary Science, School of Science, The University of Tokyo

The local magnitude scale (ML) or Richter scale is a fundamental measurement for the regional earthquake study. The backbone digital seismic record in Thailand started in 2007, although there is no study in the local magnitude scale and its calibration. Using the ML without its calibration may lead to large uncertainty in the statistical seismology and geodetic study. In this study, we use the new seismic data from Japanese-Thai joint observation project, Thai Seismic Array (TSAR), and Mahidol University private stations to measure the attenuation characteristic of regional seismic waves. The total number of data is 79 earthquakes with 364 records. The Thai Meteorological Department (TMD) local magnitude is used as an initial value for the iterative grid search optimization. The station correction factor of each station also statistically calculate. The synthetic test on the implemented algorithm and data distribution are satisfied with an error of about 1% from the true attenuation models. For the real data, the geometrical factor, α, is 0.043 and the anelastic attenuation, k, is 0.0017. A best-fit solution of the distance (R in km) correction function from this data set is

$-\log A0 = 1.043 \log R + 0.00171 R - 0.722.$

The calibrated local magnitude is slightly different from Southern California and nearby regions such as Northern Vietnam. This magnitude scaling will be improved and further calibrate with more regional data.

Keywords: Local magnitude, Thailand, Richter scale

©2021. Japan Geoscience Union. All Right Reserved.

Strong ground motion simulation of the Fukushima-ken Oki earthquake of February 13, 2021 (M_J 7.3)

*Yosuke Nagasaka[1]

1. Port and Airport Research Institute

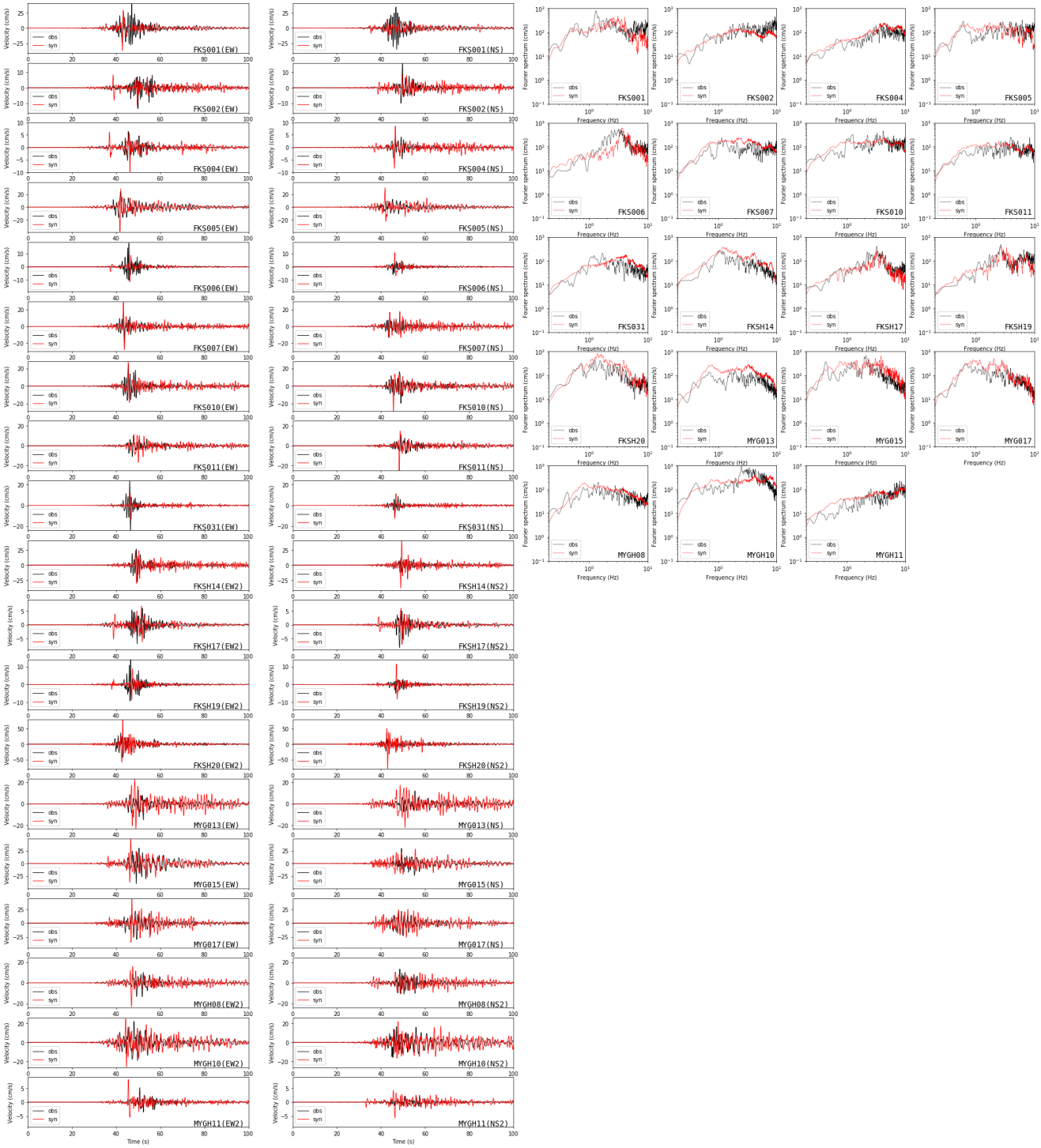
We conducted strong ground motion simulations of the Fukushima-ken Oki earthquake of February 13, 23:07 (JST) with M_J 7.3. As a preliminary model, we used a point source and corrected empirical Green's function method (Kowada et al., 1998; Nozu and Sugano, 2008; Nozu et al., 2009) for the simulation. This model uses the omega-square model as the source spectrum and considers path effect, empirical site amplifications, and empirical phase characteristics to synthesize strong motions. Nineteen K-NET and KiK-net stations are selected as the target. We used empirical site amplification factors by Nozu and Nagao (2005), and empirical site phase characteristics from the observed records of an aftershock occurred on February 15 at 21:26 JST (M_J 5.3).

We fixed the location of the subevent at the hypocenter and determined the seismic moment (=0.8e+19 Nm) and the corner frequency (0.9 Hz) by trial and error. Parameters to consider multiple nonlinear effects (Nozu and Sugano, 2008) are introduced to explain observed strong motions at some stations. Comparisons of observations and synthetics in terms of velocity time histories (0.2 to 2 Hz) and spectral accelerations are shown in the figure.

Good agreements are shown at most of the target stations. On the other hand, at FKS001 (K-NET Soma) where one of the biggest motions were recorded, the peak at 1-2 Hz and the duration of the strong motions are underestimated. We will work on improving the model, for example, by considering the directivity effect to Soma area, multiple asperities, and so on.

Keywords: Strong ground motion simulation, Fukushima-ken Oki earthquake of February 13, 2021, Source model

©2021. Japan Geoscience Union. All Right Reserved.



©2021. Japan Geoscience Union. All Right Reserved.

Strong Motion Generation Area for the 2021 off Fukushima, Japan, Earthquake Estimated based on the Empirical Green's Function Method

*Kazuhiro Somei[1], Ken Miyakoshi[1]

1. Geo-Research Institute

At 23:07 on 13 February 2021 (JST: UTC+9), an M_w 7.1 intra-slab earthquake with reverse faulting occurred off-shore Fukushima prefecture, northeastern Japan. The seismic intensity of 6+ and 6- in JMA scale were widely observed in the Fukushima and Miyagi prefectures. Within the nation-wide strong motion networks (K-NET and KiK-net) operated by NIED, strong ground motions with a peak acceleration 1426 cm/s^2 were recorded at MYGH10 (surface record of KiK-net Yamamoto). For understanding the mechanisms of strong motion generation processes during this event, we estimate the source model composed of strong motion generation area (SMGA) to explain the observed strong motion records in broadband frequency range between 0.3 and 10 Hz.

In this study, we use the empirical Green's function method to simulate the strong motion records at downhole sensors of 18 KiK-net stations located at Miyagi, Fukushima, and Ibaraki prefectures. The observed ground motion records of M_{JMA} 4.7 event (element event) occurring at 23:36 on 13 February 2021, are used as the empirical Green's functions. For an objective estimation of corner frequencies for the target and element events, we apply the source spectral ratio fitting method (Miyake et al., 1999). From the obtained corner frequencies, scaling parameters *N* and *C*, which required for the empirical Green's function method of Irikura (1986), are determined. Then, the parameters of each SMGA (e.g., the size, relative rupture starting point in SMGA, rise time, and rupture velocity) are estimated by trial and error method. Here we assume a squared SMGA on the fault plane with strike angle of N45°E and dip angle of 45°, according to the distribution of aftershocks occurring within 24 h after the mainshock.

As a provisional result, we construct the source model with SMGA located including the hypocenter. The rupture within SMGA mainly propagates southwest direction from the hypocenter. The size of SMGA is 108.2 km^2. The stress drop of SMGA is estimated to be 111.8 MPa. The short-period level of acceleration source spectrum calculated from the size and stress drop of SMGA is 1.2×10^{20} Nm/s^2, which is comparable to that expected from the empirical scaling relationship for intra-slab earthquakes occurring in the Pacific plate (Arai et al., 2015). Overall, the simulated ground motion generated from the SMGA explain well the observed acceleration, velocity, and displacement waveforms, however, there is still room to improve the reproducibility of observed ground motions. The fault geometry and parameters of SMGA need to be examined objectively in more detail.

Acknowledgements: We use the strong motion data of K-NET and KiK-net operated by NIED.

Keywords: 2021 off Fukushima earthquake, Strong motion generation area, Empirical Green's function method

©2021. Japan Geoscience Union. All Right Reserved.

[J] Poster | S (Solid Earth Sciences)：S-EM Earth's Electromagnetism

Sun. Jun 6, 2021 5:15 PM - 6:30 PM JST | Sun. Jun 6, 2021 8:15 AM - 9:30 AM UTC | Ch.11_1

[S-EM13] Geomagnetism, paleomagnetism and rock magnetism

convener:Chie Kato(Faculty of Social and Cultural Studies, Kyushu University), Tetsuro Sato(Earthquake Research Institute, The University of Tokyo)

We are going to discuss the issues on the magnetic fields of the Earth and planets, paleomagnetism, rock-magnetism, and their applications. This session includes following topics: (1) observation and analysis of the magnetic fields of the Earth and other planets, (2) paleomagnetic field variations obtained from natural and archaeological materials, (3) numerical simulations on the magnetic fields of the Earth and planets, (4) measurements and theories of magnetic properties of rocks, minerals, meteorites, and other materials, (5) climate changes and surface tectonics based on the paleomagnetic measurements of rocks and sediments, (6) observations of the magnetic anomalies and the crustal magnetization models of the Earth, planets, and satellites, and (7) developments of the measurement method and data analysis. We also encourage papers stimulating an interdisciplinary collaboration relating to establishment of the SEDI-Japan community. The presentations and discussions will be made in Japanese or English in this session.

[SEM13-P01] Brunhes-Matuyama geomagnetic reversal record from Terasaki, Boso Peninsula

*Hirokuni Oda[1], Hiroomi Nakazato[2], Futoshi Nanayama[1], Yumiko Harigane[1] (1.Institute of Geology and Geoinformation, Geological Survey of Japan, AIST, 2.National Agriculture and Food Research Organization)

[SEM13-P02] Plaeomagnetic study of the Kusatsu-Shirane volcano, Gunma, Japan

*Nagisa Sawada[1], Nobuko Kametani[2], Kazuo Kawasaki[1], Yasuo Ishizaki[1], Akihiko Terada[3] (1.University of Toyama, 2.Mount Fuji Research Institute, Yamanashi Prefectural Government, 3.Tokyo Institute of Technology)

[SEM13-P03] The Laschamp and a new post-Laschamp excursions repeating directional swings from Lake Suigetsu varved sediments

*Masayuki Hyodo[1,2], Takeshi Nakagawa[3], Hayato Matsushita[2], Ikuko Kitaba[3], Keitaro Yamada[3], Shota Tanabe[2], Balazs Bradak[1,4], Danielle McLean[5], Richard A. Staff[6], Victoria C. Smith[5], Paul G. Albert[5], Akiteru Yamasaki[7], Junko Kitagawa[8,7] (1.Research Center for Inland Seas, Kobe University, 2.Department of Planetology, Kobe University, 3.Research Centre for Palaeoclimatology, Ritsumeikan University, 4.Department of Physics, University of Burgos, 5.School of Archaeology, University of Oxford, 6.Scottish Universities Environmental Research Centre (SUERC), University of Glasgow, 7.Fukui Prefectural Satoyama-Satoumi Research Institute, 8.Varve Museum)

[SEM13-P04] Rock-magnetic properties of topmost sediments in Omura Bay, Nagasaki Prefecture

*Naoto Ishikawa[1], Yoriko Yokoo[2], Kazumi Matsuoka[3] (1.Faculty of Sustainable Design, Toyama University, 2.Faculty of Scinece and Engineering, Doshisha University, 3.Institute for East China Sea Research, Nagasaki University)

[SEM13-P05] Paleomagnetic Dating on Tsunami Boulders from the Kingdom of Tonga

*Tetsuro Sato[1], Norihiro Nakamura[2], Hiroyuki Nagahama[3], Masahiko Sato[4], Kazuhisa Goto[4], Masashi Watanabe[5], Akira Ikeda[3], Kenji Satake[1], Taaniela Kula[6] (1.Earthquake Research Institute, The University of Tokyo, 2.Institute for Excellence in Higher Education, Tohoku University, 3.Department of Earth Science, Tohoku University, 4.Department of Earth and Planetary Science, The University of Tokyo, 5.Faculty of Science and Engineering, Chuo University, 6.Ministry of Lands and Natural Resources)

[SEM13-P06] Influence of biogenic magnetite on paleointensity estimations inferred from FORC-PCA of sediments from the western equatorial Pacific

Kosuke Inoue[1], *Toshitsugu Yamazaki[1], Yoichi Usui[2] (1.Atmosphere and Ocean Research Institute, The University of Tokyo, 2.Japan Agency for Marine-Earth Science and Technology)

[SEM13-P07] Solitary magnetostrophic Rossby waves

*Kumiko Hori[1,2], Steve M Tobias[2], Chris A Jones[2] (1.Graduate School of System Informatics, Kobe University, 2.Department of Applied Mathematics, University of Leeds)

[SEM13-P08] Effects of driving mode of convection on a spherical dynamo action with a small inner core

*Futoshi Takahashi[1], Hinami Taniguchi[2] (1.Faculty of Science, Kyushu University, 2.School of Science, Kyushu University)

[SEM13-P09] Rock-magnetic and mineralogical properties of the exsolved magnetite in plagioclase crystal

*Masahiko Sato[1], Masashi Ushioda[2], Ryoichi Nakada[3], Yujiro Tamura[4], Shinji Yamamoto[4] (1.The University of Tokyo, 2.Shikoku Research Institute Inc., 3.Japan Agency for Marine-Earth Science and Technology, 4.Yohohama National University)

[SEM13-P10] Rock-magnetic properties of isocubanite from submarine hydrothermal deposits in the Okinawa Trough

*Chie Kato[1], Masao Ohno[1], Yoshihiro Kuwahara[1], Tadahiro Hatakeyama[2], Yasuhiro Yamada[3], Shuhei Totsuka[4], Kazuhiko Shimada[1], Jun-ichiro Ishibashi[1], Toshiro Nagase[5] (1.Kyushu University, 2.Okayama University of Science, 3.Tokyo University of Science, 4.National Institute of Advanced Industrial Science and Technology, 5.Tohoku University)

[SEM13-P11] Contribution of equatorially antisymmetric buoyancy to polarity reversals in geodynamo models

*Takumi Kera[1], Hiroaki Matsui[3], Masaki Matsushima[2], Yuki Nishida[1], Yuto Katoh[1] (1.Department of Geophysics, Graduate School of Science, Tohoku University, 2.Tokyo Institute of Technology, 3.Dept. of Earth and Planetary Sciences, University of California, Davis)

[SEM13-P12] **Simultaneous observation of the geomagnetic field at different sites using two SQUID magnetometer systems**

*Jun Kawai[1], Miki Kawabata[1], Masakazu Miyamoto[1] (1.Applied Electronics Laboratory, Kanazawa Institute of Technology)

Brunhes-Matuyama geomagnetic reversal record from Terasaki, Boso Peninsula

*Hirokuni Oda[1], Hiroomi Nakazato[2], Futoshi Nanayama[1], Yumiko Harigane[1]

1. Institute of Geology and Geoinformation, Geological Survey of Japan, AIST, 2. National Agriculture and Food Research Organization

We report Brunhes-Matuyama geomagnetic reversal records from Terasaki, which is several km northeast of Chiba Section, Boso Peninsula. Oriented paleomagnetic drill core samples were taken from ~3.5m thickness silt layers at intervals of a few to ten centimeters. Three volcanic ash layers were identified and the middle ash layer could be recognized as Byk-E, which is assigned as a key bed for Chibanian. Paleomagnetic analyses were conducted using (1) stepwise alternating field demagnetization (AFD), (2) stepwise thermal demagnetization (ThD), (3) stepwise ThD up to 175-300˚C followed by stepwise AFD, etc. Although the third method was most successful in identifying primary magnetization, it is not always successful. In order to extract primary magnetization from most of the samples, we conducted combined analysis of remagnetization circles (McFadden&McElhinny, 1988) using a software paleomagnetism.org (Koymans et al., 2016). The calculated paleomagnetic directions (VGP latitudes) are consistent with those reported by Haneda et al. (2020). Correlation of VGP latitude in combination with rock magnetic results suggest the sedimentation rate at the studies site is about 3 times lower than that at Chiba Section. Further, we plan to discuss on the origin of magnetic minerals including magnetite and greigite, and its relation to decay/alterlation during thermal demagnetization.

Keywords: Paleomagnetism, Boso Peninsula, Geomagnetic Reversal, greigite, combined analysis of remagnetization circles

©2021. Japan Geoscience Union. All Right Reserved.

Plaeomagnetic study of the Kusatsu-Shirane volcano, Gunma, Japan

*Nagisa Sawada[1], Nobuko Kametani[2], Kazuo Kawasaki[1], Yasuo Ishizaki[1], Akihiko Terada[3]

1. University of Toyama, 2. Mount Fuji Research Institute, Yamanashi Prefectural Government, 3. Tokyo Institute of Technology

The ring of fire in Japan has 111 active volcanoes. Some have erupted frequently and caused serious loss of life and damages. The Kusatsu-Shirane volcano at Gunma prefecture, Japan is an active volcano and had a sudden phreatic eruption occurred with 12 casualties in 2018. Understandings of past volcanic eruptions are essential for minimizing future losses and therefore accurate age information of past eruptions is important. Paleomagnetic analyses were carried out on 36 volcanic ash specimens and 11 paleosoil specimens from 47 units. Rock magnetic analyses show that the major magnetic mineral in the specimens is likely pseudosingle-domain titanomagnetite. The characteristic remanent magnetization (ChRM) directions of individual specimens were isolated by alternating field demagnetization. The unit mean ChRM directions at which radius of 95% confidence circle is less than 8˚ were selected for estimating the palaeomagnetic age. The 19 unit mean ChRM directions are compared to the three different composite paleosecular variation curves from either Lake Biwa in Japan or the Tohoku-oki earthquake rupture zone, and found that the BIWA SV-3 curve from Lake Biwa is well-matched for the ChRM of the Kusatsu-Shirane sediments. The results indicate that the observed unit mean ChRM directions likely record the secular variation, giving palaeomagnetic ages for 18 units. The observed paleomagnetic ages show good agreements with radiocarbon dates and provided for previously-undated tephra layers at 11 units. Therefore, the paleomagnetic dating method for the volcaniclastic debris (volcanic ash) deposited on land at the Kusatsu-Shirane volcano is an effective method for directly dating the tephra layers to determine past volcanic eruptions.

Keywords: Paleomagnetic secular variation , Kusatsu-Shirane Volcano, Holocene, Tephra

©2021. Japan Geoscience Union. All Right Reserved.

The Laschamp and a new post-Laschamp excursions repeating directional swings from Lake Suigetsu varved sediments

*Masayuki Hyodo[1,2], Takeshi Nakagawa[3], Hayato Matsushita[2], Ikuko Kitaba[3], Keitaro Yamada[3], Shota Tanabe[2], Balazs Bradak[1,4], Danielle McLean[5], Richard A. Staff[6], Victoria C. Smith[5], Paul G. Albert[5], Akiteru Yamasaki[7], Junko Kitagawa[8,7]

1. Research Center for Inland Seas, Kobe University, 2. Department of Planetology, Kobe University, 3. Research Centre for Palaeoclimatology, Ritsumeikan University, 4. Department of Physics, University of Burgos, 5. School of Archaeology, University of Oxford, 6. Scottish Universities Environmental Research Centre (SUERC), University of Glasgow, 7. Fukui Prefectural Satoyama-Satoumi Research Institute, 8. Varve Museum

Geomagnetic excursions represent dynamic natures of the geodynamo during declined dipole-field periods. Many sedimentary records of excursions have been reported since 1970s, but none of them resolves sub-centennial scale field-changes. We report a tri-decadal resolution Laschamp Excursion record from Lake Suigetsu varved sediments that reveals many detailed features. A high resolution ^{14}C dates and varve chronology-based Bayesian age model reveals the Laschamp Excursion ranges from 42,340 to 41,410 IntCal13 (42,400 to 41,700 IntCal20) yr BP, consisting of five short (20 to 110 yr) excursional directional-swings. We found another excursion ranging from 38,580 to 38,030 IntCal13 (39,080 to 38,580 IntCal20) yr BP composed with similar swings. Both excursions coincided with the $\Delta^{14}C$ maxima in Lake Suigetsu as well as the ^{10}Be flux maxima in Greenland. We simulated how the high-frequency directional swings in the high sedimentation rate (s.r.) (72 cm/kyr) sediments are altered when recorded in sediments with lower s.r., by downsizing the data assuming response functions defined by a sample thickness and a half lock-in depth of post depositional remanent magnetization. As s.r. decreases, the short directional swings are gradually filtered-out and/or combined, which causes (1) stepwise decreases in the time duration of excursion, and (2) a drastic change of virtual geomagnetic pole (VGP)-pass from multiple linear swings between northern high-latitudes and northern mid-/southern latitudes to a large clockwise open loop with a precursory small episode. These features of the downsized Lake Suigetsu data are consistent with many previous observations in sediment with lower s.r. The excursional VGPs of Lake Suigetsu repeat swinging constrained by two longitudinal bands through the Pacific Ocean and the Indian Ocean-Africa. In addition, they make four clusters centered in the North Pacific, the South Pacific, the South Indian Ocean, and the eastern Africa in chronological order, which accounts for the apparent clockwise open loop of VGP-pass in low s.r. records. The clusters include the VGPs inferred from lava flows associated with the Laschamp Excursion from various regions of the world, which indicate dominance of non-axial dipolar fields whose sources located under the four clusters during the excursion.

Keywords: Paleomagnetism, Laschamp Excursion, dipolar field dominance, Lake Suigetsu, varved sediments, IntCal13/IntCal20 ages

©2021. Japan Geoscience Union. All Right Reserved.

Rock-magnetic properties of topmost sediments in Omura Bay, Nagasaki Prefecture

*Naoto Ishikawa[1], Yoriko Yokoo[2], Kazumi Matsuoka[3]

1. Faculty of Sustainable Design, Toyama University, 2. Faculty of Scinece and Engineering, Doshisha University, 3. Institute for East China Sea Research, Nagasaki University

We are analyzing magnetic properties of topmost sediments in Omura Bay, Nagasaki Prefecture, in order to differentiate magnetic signals from magnetic grains of different sources in the sediments. The bay is a highly enclosed bay with the water depth of 15-20m, connecting to East China Sea through two narrow channels. There is no large river loading to the bay. Sediments above 4.5 m below seafloor consists of homogenous silty clay with the medium grain size of 4 micrometer. Severe hypoxia expands every summer in bottom water (July-August). We are also examining the effect of such an anoxic condition in the bottom water on magnetic properties in the topmost sediments.
Sediment cores of about 15 cm long were sampled at the central part of the bay in July and October 2017 by a G.S. type-gravity core sampler. The cores were sliced at 1cm interval, and each slice was freeze-dried. Dry powder samples were packed into 1cc-plastic cubes. The cubes and remaining powder samples were subjected to rock magnetic experiments.
Results from thermo-magnetic analyses with magnetic balance and progressive thermal demagnetization experiments of composite isothermal remanences (IRMs) indicate the existence of magnetite, maghematized magnetite and hematite as principal magnetic minerals. Values of initial magnetic susceptibility, saturation magnetization and saturation remanent magnetization show no remarkable change through the cores. Downcore increase of the susceptibility of anhysteretic remanence and S-ratio (S_-0.1T) and downcore increase of the coercivity of remanence are detected. Results from coercivity distribution analyses of IRM acquisition and demagnetization curves suggest that the contribution of high-coercivity magnetic grain, probably hematite, to the whole of IRM increase downcore although its amount does not change. It may be implied that a downward selective dissolution of fine-grained magnetite by the effect of early diagenesis in the topmost sediments results in downward increases of magnetic grain size and contribution (relative amount) of hematite. We have not found any difference in magnetic properties and their variations mentioned above between the two cores of different month.

Keywords: rock-magnetic property, topmost marine sediment, origin of magentic minerals, eary diagenesis

©2021. Japan Geoscience Union. All Right Reserved.

Paleomagnetic Dating on Tsunami Boulders from the Kingdom of Tonga

*Tetsuro Sato[1], Norihiro Nakamura[2], Hiroyuki Nagahama[3], Masahiko Sato[4], Kazuhisa Goto[4], Masashi Watanabe[5], Akira Ikeda[3], Kenji Satake[1], Taaniela Kula[6]

1. Earthquake Research Institute, The University of Tokyo, 2. Institute for Excellence in Higher Education, Tohoku University, 3. Department of Earth Science, Tohoku University, 4. Department of Earth and Planetary Science, The University of Tokyo, 5. Faculty of Science and Engineering, Chuo University, 6. Ministry of Lands and Natural Resources

Viscous remanent magnetization partially overprints the natural remanent magnetization in reworked boulders. The magnitude of such magnetization depends on the time passed since reworking, as well as ambient temperature, for which there is a well-known theoretical time-temperature relationship of remanent magnetization. Most references used the paleomagnetic dating protocol, which is applicable to single-domain particle assemblages, while experimental data often disagree with other dating applications (e.g., radiocarbon and U-series dating). Here, we use modified time-temperature relationship based on a stretched exponential relaxation function that accounts for the complex magnetic structures. Samples of tsunami boulders from the Kingdom of Tonga have chemical-viscous remanent magnetization, and their non-exponential relaxation is well fitted by the stretched exponential relaxation function. Combining the modified time-temperature relationship of remanent magnetization, which considers the observed stretching exponent value, and sea level change data, we estimate the reworked age of the tsunami boulders.

Keywords: Tsunami boulder, Age estimation, Remanent magnetization

©2021. Japan Geoscience Union. All Right Reserved.

Influence of biogenic magnetite on paleointensity estimations inferred from FORC-PCA of sediments from the western equatorial Pacific

Kosuke Inoue[1], *Toshitsugu Yamazaki[1], Yoichi Usui[2]

1. Atmosphere and Ocean Research Institute, The University of Tokyo, 2. Japan Agency for Marine-Earth Science and Technology

Relative paleointensity (RPI) is estimated from sediments as normalized intensity: natural remanent magnetization (NRM) intensity divided by artificial magnetization intensity such as anhysteretic remanent magnetizaton (ARM). This method requires that magnetic particle composition is uniform and hence normalized intensity depends only on their abundance and geomagnetic intensity. Recent studies have shown wide occurrence of biogenic magnetite in marine sediments, which are originated from magnetotactic bacteria with magnetite chains in their cells. Difference of NRM and ARM acquisition efficiencies between biogenic and terrigenous magnetite needs to be understood for RPI estimations.

In this study, a relation between normalized intensity and magnetic mineral compositions was investigated using three sediment cores taken from the western equatorial Pacific, in which the average normalized intensities are largely different. In the western equatorial Pacific, high solar radiation makes sea surface temperature the highest in the world. The variations of precipitation in the western equatorial Pacific are related with the Inter Tropical Convergence Zone, whose southward migration causes increasing precipitation and fluvial discharge in New Guinea. Undercurrents deliver fluvial particles from New Guinea to the studied region. The ratio of biogenic to detrital magnetic particles is expected to vary with the distance from New Guinea, which helps to estimate the relation between normalized intensity and magnetic particle compositions.

First-order reversal curves (FORCs) are measured by sweeping the inside of a magnetic hysteresis loop, and magnetization (M) is given by function of a reversal field (Br) and a given field (B). FORC distribution ρ (B, Br) is defined as a mixed second derivative of M by B and Br, and plotted in the (Bc, Bu) axes to which (B, Br) is rotated -45°, called FORC diagram. Bc and Bu represent coercivity and magnetostatic interactions, respectively. In geological samples, biogenic and terrigenous magnetites are characterized by a narrow “central ridge” along the Bc axis and by a broad distribution with a significant vertical spread (background component), respectively. Bending and collapse of biogenic magnetite chains also contribute to the background component. This study conducted principal component analysis (PCA) of FORC diagrams and decomposed into the biogenic magnetite and the terrigenous input. It is revealed that the ratio of biogenic and terrigenous magnetite influences the normalized intensity. Larger contribution of biogenic magnetite causes lower relative paleointensity. Even when biogenic magnetite dominates, difference in chain bending could influence the normalized intensity. In conclusion, for estimating relative paleointensity, it is necessary to consider the effect of the variations of biogenic and terrigenous contributions and the difference in the preservation of biogenic-magnetite chain structure.

Keywords: FORC diagram, relative paleointensity, biogenic magnetite

©2021. Japan Geoscience Union. All Right Reserved.

Solitary magnetostrophic Rossby waves

*Kumiko Hori[1,2], Steve M Tobias[2], Chris A Jones[2]

1. Graduate School of System Informatics, Kobe University, 2. Department of Applied Mathematics, University of Leeds

Finite-amplitude hydromagnetic Rossby waves in the magnetostrophic regime are studied. We consider the slow mode, which travels in the opposite direction to the hydrodynamic or fast mode, in the presence of a toroidal magnetic field and zonal flow by means of quasi-geostrophic models for thick spherical shells. The weakly nonlinear long waves are derived asymptotically using a reductive perturbation method. The problem at the first order is found to obey a second-order ordinary differential equation, leading to a hypergeometric equation for a Malkus field and a confluent Heun equation for an electrical wire field, and is non-singular when the wave speed approaches the mean flow. Investigating its neutral non-singular eigensolutions for different basic states, we find the evolution is described by the Korteweg–de Vries equation. This implies that the nonlinear slow wave forms solitons and solitary waves. These may take the form of a coherent eddy, such as a single anticyclone. We speculate on the relation of the anticyclone to the asymmetric gyre seen in the Earth’ s fluid core, and in state-of-the-art dynamo direct numerical simulations.

Keywords: Magnetohydrodynamics, Waves in rotating fluids, Earth's core

©2021. Japan Geoscience Union. All Right Reserved.

Effects of driving mode of convection on a spherical dynamo action with a small inner core

*Futoshi Takahashi[1], Hinami Taniguchi[2]

1. Faculty of Science, Kyushu University, 2. School of Science, Kyushu University

Paleomagnetic studies suggest that the geodynamo has been working for ca. 4.2 billion years (Tarduno et al., 2020). During the long lifetime of the geodynamo it is often argued that the geomagnetic field is maintained without the solid inner core in the Hadean and Archean eons. Moreover, high electrical conductivity of the core material suggests a young age of the inner core (e.g., Ohta et al., 2016). Geomagnetic signature restored from paleomagnetic samples is possibly the only tool to infer the age of inner core nucleation based on observations (Biggin et al. 2016). However, we still have little knowledge how to properly interpret paleomagnetic data, which is, in part, ascribed to lack of the understanding of geodynamo behavior in an old era and the mechanisms controlling it. In order to enhance our understanding of the geodynamo, we have investigated basic features of convection and dynamos relying on numerical dynamo modeling. Also in this study, we will proceed along this line.

We focus on the buoyancy source distribution to drive convection in the Earth’s core. Light element ejection and latent heat release upon inner core growth fuels convection from the bottom, while various mechanisms such as uniformly distributed heat source, secular cooling of the core, iron-snow etc. provide negative buoyancy from the top. In fact, the geodynamo is driven by a mixture of the “bottom-up” and “top-down” buoyancy, strongly depending on the origin and evolution history of the Earth. Bearing the fact in mind, here we try to understand the effects of the individual driving mode on convection and magnetic field generation processes as a first step.

We consider a problem of an MHD dynamo in a rotating spherical shell, of which the inner to outer core radius ratio is 0.2. This geometry may suitably mimic that of the Earth’s core in the past well after inner core nucleation. The non-dimensional parameters are the Prandtl number (Pr = 1), the magnetic Prandtl number (Pm = 3), the Ekman number ($E = 10^{-4}$), and the Rayleigh number (Ra) kept close to the threshold for maintaining the dynamo, which is searched by trial and error. Note that equatorial symmetry (anti-symmetry) is assumed for the velocity (magnetic) field. The present results would be compared with the full 3-dimensional simulations to elucidate non-linear coupling between different symmetries. As a result of the runs, it is found that the minimum Rayleigh number required for a successful dynamo in terms of the critical value for the onset of convection, Ra_c, is substantially different between the two modes. Dynamo is not maintained even at 20 Ra_c for the bottom-up mode, while lower supercriticality of 4.5 Ra_c is sufficient for the top-down mode. In both cases, dipolarity is not as high as the present geomagnetic field, suggesting importance of symmetry-breaking interaction in maintaining a dipole-dominant dynamo (Takahashi et al., 2019). Analysis of kinetic energy budget reveals that the zonal flows are dominantly powered by the Reynolds stress in most of the runs. Furthermore, magnetic field morphology and characteristic force balance will be compared and discussed.

Acknowledgements: This work was supported by JSPS KAKENHI Grant Number JP18K03808.

©2021. Japan Geoscience Union. All Right Reserved.

Keywords: Dynamo, Convection, Core

©2021. Japan Geoscience Union. All Right Reserved.

Rock-magnetic and mineralogical properties of the exsolved magnetite in plagioclase crystal

*Masahiko Sato[1], Masashi Ushioda[2], Ryoichi Nakada[3], Yujiro Tamura[4], Shinji Yamamoto[4]

1. The University of Tokyo, 2. Shikoku Research Institute Inc., 3. Japan Agency for Marine-Earth Science and Technology, 4. Yohohama National University

Natural plagioclase crystals sometimes contain fine-grained magnetite inclusions, which are considered to be originated from exsolution at subsolidus condition. The exsolution process can crystalize and hold nearly pure fine-grained magnetite in deep crustal rocks, and natural remanent magnetizations (NRM) carried by the magnetite bearing plagioclase should play an important role in the source of magnetic anomaly. Therefore, to elucidate crystallization mechanism of magnetite in plagioclase crystal and to understand origin of its NRM is of prime importance in paleomagnetism and rock-magnetism, while the mechanism has been poorly understood yet. In this study, to precisely determine the chemical species of Fe in the plagioclase crystals and to better understand the crystallization mechanism of magnetite, magnetic measurements combined with microscopic observation and synchrotron radiation study were conducted for single grain plagioclase crystals. The plagioclase crystals were prepared from natural mafic-plutonic rocks. The plagioclase crystals were collected under a stereoscopic microscope and used for the measurements after a hydrochloric acid leaching. The main series of measurements for the single grain plagioclase crystals were as follows: (1) To estimate a content of magnetic mineral in the plagioclase crystals, magnetic hysteresis loop was measured using an Alternating Gradient Magnetometer. (2) To investigate the average valence state of Fe, L_{III}-edge X-ray absorption near edge structure (XANES) measurement was performed at synchrotron radiation facilities. (3) To investigate chemical compositions of the plagioclase crystals, microscopic observation was conducted using electron microprobes. The plagioclase crystals used in this study showed the Fe valence state of 2.5–2.9, and it was confirmed that there was inverse relationship between the magnetite content and average valence states of Fe. Combining the mineralogical properties with the rock-magnetic properties such as an intensity of thermal remanent magnetization, we will discuss the exsolved magnetite contribution to the crustal magnetization.

Keywords: Exsolved magnetite, Plagioclase

©2021. Japan Geoscience Union. All Right Reserved.

Rock-magnetic properties of isocubanite from submarine hydrothermal deposits in the Okinawa Trough

*Chie Kato[1], Masao Ohno[1], Yoshihiro Kuwahara[1], Tadahiro Hatakeyama[2], Yasuhiro Yamada[3], Shuhei Totsuka[4], Kazuhiko Shimada[1], Jun-ichiro Ishibashi[1], Toshiro Nagase[5]

1. Kyushu University, 2. Okayama University of Science, 3. Tokyo University of Science, 4. National Institute of Advanced Industrial Science and Technology, 5. Tohoku University

In recent years, submarine hydrothermal deposits have been attracting attention as a new mineral resource. To understand the nature of the deposits and constrain the possible area of hidden ore, it is necessary to gather information about the environment where deposits occur and grow based on investigations of mineral composition and texture of known deposits. Some of the ore minerals exhibit characteristic magnetic properties which potentially enable us a quick identification of such specific minerals. However, magnetic properties are not well documented except for a small number of minerals since they vary not only by mineral species but by chemical composition and texture.

In this study, we searched for ore minerals that can be identified by magnetic measurements from a series of samples collected at the Okinawa Trough submarine hydrothermal deposits and investigated the magnetic properties in detail. Samples were a suite of drilled subseafloor core samples and a block sample of a hydrothermal chimney collected from Noho site and Hakurei site in the Okinawa Trough under the framework of the Next-Generation Technology for Ocean Resources Exploration Project, Cross-ministerial Strategic Innovation Promotion Program (SIP) by the Japanese cabinet office.

First, low temperature magnetometry was conducted to seek for a characteristic signal which appear among different samples. In several samples we found a common feature that a magnetic transition occurs at ~100 K and below this temperature the magnetic moment is larger than at higher temperatures. On those samples or samples taken from nearby depth, we conducted XRD measurements, optical microscopic observation and EPMA analysis and found out that a Cu-Fe sulfide mineral isocubanite should be responsible for the magnetic feature. We further conducted detailed magnetic measurements and Mössbauer spectroscopy on a sample portion consisting almost exclusively of isocubanite that was separated from the chimney samples in which isocubanite appears most prominently. As a result, it was revealed that magnetic properties, Mössbauer spectrum, crystal structure, and the occurrence of intimate lamellar structure with chalcopyrite are generally consistent with ‘aged isocubanite’ which was originally collected at the Snake Pit, Mid-Atlantic Ridge, reported by Wintenberger et al. (1994). On the other hand, chemical composition and texture (with or without exsolution of chalcopyrite) varied among isocubanite samples indicating that the magnetic transition at 100 K is common to isocubanite in wide range of its solid solution, while the sharpness of the transition and the strength of the magnetic moment at low temperature seem to differ by Cu/Fe ratio.
From these results we conclude that low temperature magnetometry on ore samples may be effective to detect isocubanite and have the potential to make contribution to our understanding of the nature of submarine hydrothermal deposits.

Keywords: isocubanite, submarine hydrothermal deposits, low-temperature magnetometry

©2021. Japan Geoscience Union. All Right Reserved.

Contribution of equatorially antisymmetric buoyancy to polarity reversals in geodynamo models

*Takumi Kera[1], Hiroaki Matsui[3], Masaki Matsushima[2], Yuki Nishida[1], Yuto Katoh[1]

1. Department of Geophysics, Graduate School of Science, Tohoku University, 2. Tokyo Institute of Technology, 3. Dept. of Earth and Planetary Sciences, University of California, Davis

Paleomagnetic observations revealed that the geomagnetic field has reversed its polarity. Numerical dynamo simulations have represented dipole reversals and provided an insight into physical processes that give rise to polarity reversals. Both paleomagnetic observations and numerical dynamos have inferred that the equatorial symmetry of the magnetic and velocity fields is related to polarity reversals. The paleomagnetically inferred degree of the symmetry of the Earth's magnetic field during the past 150 Ma shows that geomagnetic field reversed polarity more frequently when the geomagnetic field was more symmetrical with respect to the equator (McFadden et al., 1991). Dynamo simulations revealed a strong inverse correlation between the stability and the equatorial symmetry of the magnetic field (Coe and Glatzmaier, 2006). Olson et al., (2004) proposed a process of magnetic polarity reversals in a dynamo model. In their model, the reversed magnetic field flux is produced locally in the convective plumes and transported from south to north by the meridional circulation. This result suggests that anti-symmetric flow with respect to the equator plays a role in reversals. However, it is an open question how to generate anti-symmetric flow under the condition of the strong rotation, in which symmetric flows with respect to the equator is dominant. In the present research, we investigate how anti-symmetric flow is growing and maintained in the dynamo in which reversals occur.

We perform three dynamo simulations using Calypso (Matsui et al., 2014) to represent dipole dominant dynamo with and without reversals and multipole dynamo, and compare the equatorial symmetry among the cases. In the present study, we set the fixed heat flux, non-slip, and connecting the potential field at the inner and outer boundaries as the boundary conditions for temperature, velocity, and magnetic field, respectively. For the dimensionless numbers, we fixed the three dimensionless numbers to $E = 6\times10^{-4}$, $Pr = 1$, and $Pm = 5$. We also set $Ra = 1500$, 2000, and 2700 for the non-reversal dipolar, dipolar with reversal, and multipolar cases, respectively. For each case, we investigate the structure of velocity and magnetic field in terms of the symmetricity with respect to the equator.

For dipolar dynamo with reversals, flow and magnetic field structure for axial components is similar to the structure of non-reversal dynamo, when the dipole magnetic field sustains stably. The symmetric component is dominant for the velocity field, while the anti-symmetric component is dominant for the magnetic field. On the other hand, during the reversal, the structure is very similar to the multipolar case. Outside the tangent cylinder, flow fields are nearly anti-symmetric and anti-symmetric component of the magnetic field is larger than the symmetric component in the entire domain. This dominance of flow energy of anti-symmetric component during reversals may be caused by buoyancy flux associated with anti-symmetric temperature field. We also give an investigation of buoyancy flux due to symmetric and anti-symmetric components with respect to the equator.

Keywords: dynamo, reversal, core, equatorial symmetry, geomagnetic field, buoyancy

©2021. Japan Geoscience Union. All Right Reserved.

Simultaneous observation of the geomagnetic field at different sites using two SQUID magnetometer systems

*Jun Kawai[1], Miki Kawabata[1], Masakazu Miyamoto[1]

1. Applied Electronics Laboratory, Kanazawa Institute of Technology

We performed simultaneous observation test of the geomagnetic field using two superconducting quantum interference devise (SQUID) magnetometer systems at different sites. The observation sites were Nishiyama (NSY : 36.16N, 136.6E) in Hakusan-city and Minazuki (MNZ : 37.36N, 136.76E) in Wajima-city. The observation period was from 2020.9.11 to 2020.11.25.

The field resolution and field sensitivity of the SQUID magnetometer system were ~ 30 fT/√Hz at 10 Hz and ~ 77 nT/V in a flux-locked loop operation, respectively. The observed data were acquired with a 27-bit data logger with a GPS function (HKS-9700, Keisokugiken Corp.), and the sampling frequency was 200 Hz.

We could observe the Ionospheric Alfvén resonator (IAR) in the night-time at both sites. The phase of IAR signals detected at both sites was almost the same, but the amplitude of IAR signals obtained at MNZ was bigger than that obtained at NSY. We speculate the difference in amplitude is because of the difference in latitude, as known according to the previous studies. From this result, we could confirm the reliability of the simultaneous geomagnetic observation using two SQUID magnetometer systems.

In this presentation, we show the summary of the observation test and discuss the data obtained at both sites.

Keywords: geomagnetic field, SQUID, ionospheric Alfvén resonator, high sensitivity

©2021. Japan Geoscience Union. All Right Reserved.

[J] Poster | S (Solid Earth Sciences)：S-MP Mineralogy & Petrology

Sun. Jun 6, 2021 5:15 PM - 6:30 PM JST | Sun. Jun 6, 2021 8:15 AM - 9:30 AM UTC | Ch.12_1

[S-MP25] Deformed rocks, Metamorphic rocks and Tectonics

convener:Yumiko Harigane(Geological Survey of Japan, National Institute of Advanced Industrial Science and Technology (AIST)), Yoshihiro Nakamura(Geological Survey of Japan, National Institute of Advanced Industrial Science and Technology)

We invite all researchers who aim to understand the dynamics of the earth's crust and mantle at the plate boundaries, to discuss the latest results from various viewpoints. The scope will include contributions through petrology and structural geology as well as various techniques including rheology and transformation of heat and mass.

[SMP25-P01] Multiple igneous activities recorded in the Nidar ophiolite complex, eastern Ladakh

*Akinori Sato[1], Takeshi Imayama[1], Dripta Dutta[2] (1.Okayama University of Science, 2.Indian Institute of Technology Bombay)

[SMP25-P02] Geology and missing tectonics in the Inashi-Hase area of the eastern part of the Ryoke belt, central Japan

*Akira Ono

[SMP25-P03] Kinematics of North Almora Thrust estimated from mylonite, India

*Hirotoshi Kotama[1], Jun-ichi Ando[1], Kaushik Das[1], Dyuti Prakash Sarkar[1] (1.Hiroshima University)

[SMP25-P04] Illite crystallization and faulting caused by hydrothermal fluid

*Jun-ichi Ando[1], Kota Kojima[1], Kaushik Das[1], Naotaka Tomioka[2], Seiichiro Uehara[3] (1.Department of Earth and Planetary Systems Science, Hiroshima University, 2.Kochi Institute for core sample research, Japan Agency for Marine-Earth Science and Technology, 3.The Kyushu university museum)

[SMP25-P05] Episodic fluid explosion in shallow and middle crust revealed by hydrothermal brecciation

*Geri Agroli[1], Atsushi Okamoto[1], Masaoki Uno[1], Noriyoshi Tsuchiya[1] (1.Tohoku University)

[SMP25-P06] Pseudotachylyte in a marble from the Takine Group (Abukuma Terrane) and its similarity to pseudotachylyte from the Higo Mertamorphic Rocks

*Tadao Nishiyama[1], Ebo Adou Douha[1] (1.Department of Earth and Environmental Sciences, School of Science, Graduate School of Science and Technology, Kumamoto University)

[SMP25-P07] Frictional melting process during formation of pseudotachylyte, Sarwar-Junia fault zone, India

*Jun-ya Okazaki[1], Jun-ichi Ando[1], Kaushik Das[1] (1.Earth and Planetary Systems Science Program, Division of Advanced Science and Engineering, Hiroshima University)

[SMP25-P08] Neoarchean magmatism and Paleoproterozoic high-pressure granulite-facies metamorphism from the southern Motloutse Complex, eastern Botswana: Implications for the western extension of the Central Zone of the Limpopo Complex

*Thembiso Otladisang Basupi[1,2], Toshiaki Tsunogae[1,3], Kazuki Takahashi[1], Yukiyasu Tsutsumi[4] (1.Graduate of Life and Environmental Sciences, University of Tsukuba, 2.Department of Earth and Environmental Sciences, Botswana International University of Science and Technology, 3.Department of Geology, University of Johannesburg, 4.Department of Geology and Paleontology, National Museum of Nature and Science)

[SMP25-P09] Petrography of a sulfide-rich garnet-sillimanite-biotite gneiss from Brattnipene, Sør Rondane Mountains, East Antarctica

*Hayato Ikeda[1], Tetsuo Kawakami[1] (1.Kyoto University)

[SMP25-P10] Microstructural characteristics of ultra-high pressure metamorphic rocks from the Dabie-Shan, eastern China

*Katsuyoshi Michibayashi[1], Kouhei Asano[1] (1.Department of Earth and Planetary Sciences, Graduate School of Environmental Studies, Nagoya University)

[SMP25-P11] Metamorphic history of the Suo metamorphic rocks inferred from two-stage garnet in pelitic schist

*Shunsuke Endo[1], Maki Ito[1] (1.Department of Earth Science, Interdisciplinary Faculty of Science and Engineering, Shimane University)

[SMP25-P12] Hidden intact coesite in deeply subducted rocks and its geological implications

*Tomoki Taguchi[1], Yui Kouketsu[2], Yohei Igami[3], Tomoyuki Kobayashi[4], Akira Miyake[3] (1.Department of Earth Sciences, Faculty of Education and Integrated Arts and Sciences, Waseda University, 2.Department of Earth and Planetary Science, Graduate School of Environmental Studies, Nagoya University, 3.Department of Geology and Mineralogy, Graduate School of Science, Kyoto University, 4.Faculty of Health and Sports, Nagoya Gakuin University)

[SMP25-P13] Metamorphic zoning and *P–T* conditions of contact metamorphic rocks in the Unai area, Yamaguchi prefecture, Japan.

*Kakeru Sakamoto[1], Toshiaki Shimura[1] (1.Graduate School of Sciences and Technology for Innovation, Yamaguchi University)

[SMP25-P14] Progressive metamorphism of the Ryoke metamorphic rocks from No-jima Island, South of Yamaguchi Prefecture

*ZEJIN LU[1] (1.Graduate School of Science and Engineering for Innovation, Yamaguchi University)

[SMP25-P15] *P–T–t* path of Ryoke metamorphic rocks in Kitsuki area, Kunisaki Peninsula, Oita prefecture, Japan.

*Kentaro Mutabaru[1], Toshiaki Shimura[1] (1.Yamaguchi University)

[SMP25-P16] *P-T* estimations of Ryoke metamorphic rocks in the Takato-Ohshika area, Nagano, Japan

*Yoshihiro Nakamura[1], Kazuhiro Miyazaki[1], Yutaka Takahashi[1] (1.Geological Survey of Japan, National Institute of Advanced Industrial Science and Technology)

[SMP25-P17] Ultrahigh-temperature HP granulite facies stage of the Early Jurassic pre-Sanbagawa metamorphism

*Kenta Yoshida[1], Sota Niki[3], Hikaru Sawada[1], Ryosuke Oyanagi[1], Takafumi Hirata[3], Kenji Asakura[2], Takao Hirajima[2] (1.Japan Agency for Marine-earth Science and Technology, 2.Kyoto University, 3.The University of Tokyo)

[SMP25-P18] **Meliorating the spatial resolution of SEM-EBSD**

*Thomas Jing Yi Yeo[1], Norio Shigematsu[1] (1.Research Institute of Earthquake and Volcano Geology, Geological Survey of Japan, National Institute of Advanced Industrial Science and Technology)

[SMP25-P19] Strain in quartz inclusion probed by Raman spectroscopy

*Yui Kouketsu[1], Yuki Tomioka[1], Tomoki Taguchi[2] (1.Department of Earth & Planetary Sciences, Graduate School of Environmental Studies, Nagoya University, 2.Department of Earth Sciences, Faculty of

Education and Integrated Arts and Sciences, Waseda University)

Multiple igneous activities recorded in the Nidar ophiolite complex, eastern Ladakh

*Akinori Sato[1], Takeshi Imayama[1], Dripta Dutta[2]

1. Okayama University of Science, 2. Indian Institute of Technology Bombay

The Nidar ophiolite complex (NOC) is exposed within the Indus suture zone (ISZ) in eastern Ladakh, India. The NOC comprises of a sequence of ultra-mafic rocks (*base to top*) gabbros, doleritic and basaltic rocks, and volcanic sedimentary assemblages. Previous studies considered that the NOC was formed by supra-subduction zone (SSZ) igneous activity in the early Cretaceous period (e.g. Ahmad et al. 2008), although multiple igneous activities from the late Jurassic to late Cretaceous periods are known in other ophiolites (e.g. Spongtang and Dras) from within the ISZ (e.g. Parsons et al., 2020). In this study, we identified the gabbro and dolerite of the NOC to be products of MORB, implying multiple igneous activities similar to that of the other ophiolites in the ISZ. In addition, metamorphic minerals are distinguished from the igneous ones based on detailed petrological work of the gabbro, dolerite, and basalt of the NOC. The gabbro mainly consists of clinopyroxene and plagioclase, and is subdivided into Type-1 and Type-2. The former is non-metamorphosed and clinopyroxene-rich, while the later is plagioclase-rich and contains epidote and chlorite. The Mg# [Mg/(Mg+Fe2+) ratio] of pyroxene in the rocks decrease down the stratigraphic level from gabbro (0.85-0.92) to dolerite (0.79), and basalt (0.66-0.77). The amphiboles in the dolerite show a compositional zoning –Mg-rich core (Mg#:0.73-0.90) surrounded by Fe-rich rim (Mg#:0.54-0.71). The Mg# of the actinolite and horblende grains in the basalt lie within 0.58-0.62. The plagioclase in the gabbro is bytownite (An: 70-90%), whereas the An content in the plagioclase grains of the dolerite varies from 5% to 89%. The euhedral plagioclase in the basalt are randomly oriented and rich in An (94-99%). In contrast, the anhedral grains are albitic (An: 0.2-2.2%). These indicate that the pyroxene and An-rich plagioclase are igneous minerals. The type-2 gabbro, dolerite and basalt experienced greenschist- to lower amphibolite-facies metamorphism to form An-poor plagioclase, Fe-rich hornblende, epidote, and chlorite. The SiO_2 content of Type-1 gabbro is 55 wt%, which is significantly higher than that of Type-2 gabbro (45 wt%). The Al_2O_3, MgO, and CaO contents decrease with increasing SiO_2, while that of the other major oxides increase. Six samples of the Type-1 gabbro yield flat REE patterns, which are consistent with those noted for SSZ-type igneous rocks (e.g. Ahmad et al. 2008). On the other hand, three samples of the Type-2 gabbro have low REE concentrations and are depleted in the LREE content, which is a characteristic of the MORB-type igneous rocks and not the SSZ rocks. Therefore, it is likely that the NOC is not a product of a single igneous event in the SSZ, but of multiple igneous activities including the formation of the MORB.

©2021. Japan Geoscience Union. All Right Reserved.

Geology and missing tectonics in the Inashi-Hase area of the eastern part of the Ryoke belt, central Japan

*Akira Ono

The Median Tectonic Line (MTL) in central Japan was formed during the opening of the Japan Sea, and large-scale tectonic movements and missing of geological bodies occurred near the MTL [1]. The eastern end of the Ryoke belt in the Ina-Valley area was strongly influenced by the missing tectonics [2, 3]. Here, we present an overview of the geology of the Hase-Ichinose area and confirm the missing tectonics.

Ryoke gneiss, Hiji tonalite and Awasawa metamorphic rocks are distributed in the Ryoke belt of the Hase-Ichinose area (Figure A). Many small meta-sediments derived from Ryoke metamorphic rocks are intercalated in the eastern margin of Hiji tonalite (the light blue region in Figure A). Regarding these xenoliths, pelitic and psammitic mylonites are distributed in Yamabuki Valley to the west of Awasawa village. On the other hand, chert and tuff-derived mylonites are common in the Magoi-Nakao area. The pelitic and psammitic mylonites near Yamabuki Valley are derived from Ryoke gneisses. This is based on the following geological facts. (1) Garnet-cordierite gneisses remain in two places (gneiss in Figure B). (2) Partialy resolved garnet porphyroclast (Figure C) is present in many rock samples, although garnet is not found in the matrix of mylonite.

For pelitic mylonites in and around Yamabuki Valley, the average grain sizes of matrix quartz and feldspar are about 20-30 μm in the upstream region and about 10-20 μm in the downstream region (Figure B). The increase of the grain sizes suggests the increase in metamorphic temperature. However, the metamorphic temperatures estimated by the feldspar geothermometer are almost the same for the two regions. That is, the Ab content of the matrix K-feldspar is almost constant for all the studied samples. Many tonalites in the upstream area are not suffered from mylonitization. For such tonalites, quartz and plagioclase of 70-100 μm in diameter are common.

Original rocks of meta-sediments in the Magoi-Nakao area are mainly mudstone, sandstone, chert, siliceous mudstone, siliceous tuff, conglomerate and mixed rock. These belong to the Hase unit of the accretionary complex [3]. Most of the pelitic mylonites derived from the Hase unit are very fine, and the grain sizes of quartz are about 5-15 μm. Moreover, fine sedimentary structure (Figure D) and radiolarian fossils (Figure E, H) were observed. It is reasonable to conclude that the meta-sediments were metamorphosed under lower temperatures than those of the garnet-cordierite zone. The main constituent minerals of the unaltered pelitic mylonites are biotite, muscovite, plagioclase and quartz. K-feldspar is rare and garnet is not recognized. However, fine garnets are present in calcite-rich pelitic mylonites. Coarse-grained andradite-rich garnets are found for a sample (Figure F).

The radiolarian fossils are not strongly deformed, and pressure shadows have not developed for many porphyroclasts (Figure G). Hence, shear deformation was not very strong as supposed before.

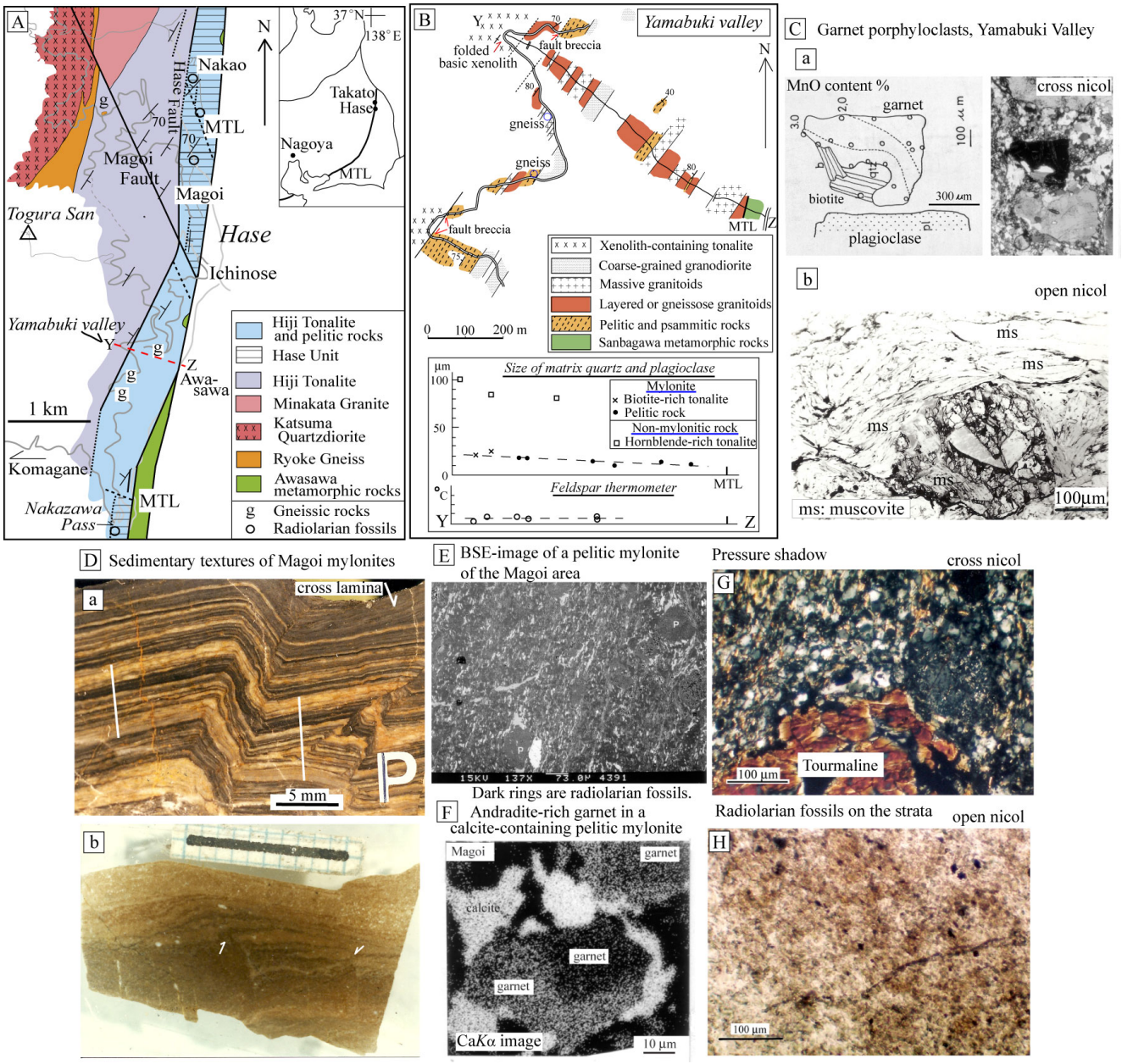
The Hase unit is distributed in the vicinity of MTL over a long distance from the Takato-Itayama area to the Hase-Awasawa area. However, the Hase unit is not confirmed in the Awasawa area, and it is presumed that the Hase unit in the Awasawa area was lost due to the Miocene tectonics. The Hase unit in the Magoi-Nakao area is narrow, and the strikes of foliations are significantly oblique to the directions of the MTL and Hase fault. The Hase unit was a large geological unit in the Paleogene, but most of it was lost by

©2021. Japan Geoscience Union. All Right Reserved.

the Miocene tectonics [1-3].

[1] Ono, 2020, JpGU-AGU Joint Meeting 2020, SGL33-P07. [2] Ono, 2016, JpGU Meeting, SGL37- P16. [3] Ono, 2018, GSJ Meeting, R15-P13.

Keywords: Ryoke belt, Inashi-Hase, Hase unit, Kashio mylonite, missing tectonics



©2021. Japan Geoscience Union. All Right Reserved.

Kinematics of North Almora Thrust estimated from mylonite, India

*Hirotoshi Kotama[1], Jun-ichi Ando[1], Kaushik Das[1], Dyuti Prakash Sarkar[1]

1. Hiroshima University

The purpose of this study is to clarify the faulting process of the North Almora Thrust (NAT) which belongs to a fault system of the Main Central Thrust, based on the characteristics of rock deformation microstructures. The study area lies in the north of Almora, Uttarakhand, India. The results obtained from the field study demonstrate that the granite and sandstone are mylonitized within ca. 7 km south of NAT. The mylonitization tends to change from "proto-mylonite" to "mylonite" closer to NAT, eventually to "ultramylonite". The strikes of these mylonite foliations are almost parallel to that of the NAT. The microstructures of mylonites are studied using an optical microscope, SEM, and SEM-EBSD. These methods combined with image analysis using ImageJ are used to measure the aspect ratio and grain size of dynamically recrystallized quartz. Similar measurements are also conducted using the orientation maps revealed by the SEM-EBSD analyses. The above microstructural observations helped us to determine 1) temperature, shear sense, three-dimensional strain field, and flow stress under which mylonitization occurred, and 2) the effect of phyllosilicate minerals on NAT faulting. In this presentation we shall report the faulting process of the NAT based on the above results.

Keywords: c-axis fabric, phyllosilicate minerals, mylonite

©2021. Japan Geoscience Union. All Right Reserved.

Illite crystallization and faulting caused by hydrothermal fluid

*Jun-ichi Ando[1], Kota Kojima[1], Kaushik Das[1], Naotaka Tomioka[2], Seiichiro Uehara[3]

1. Department of Earth and Planetary Systems Science, Hiroshima University, 2. Kochi Institute for core sample research, Japan Agency for Marine-Earth Science and Technology, 3. The Kyushu university museum

Based on the field survey and microstructural observations of massive chert block, we shall report that there is a strong possibility that illite crystallized from fluids contributed to fault formation.

The fault studied was developed in a massive chert block exposed in Watarai, Mie Prefecture, which belongs to the Southern Chichibu Belt. This massive chert block includes many stylolites and white bands, which develop parallel to the fault plane. The white band is particularly unique, and its width is about 0.5 mm to 1 cm. The massive chert is composed of trace amounts of chlorite along with quartz. On the other hand, the stylolite and white band are composed of quartz as well as trace amounts of chlorite and illite, and large amounts of illite, respectively. The white band also contains numerous voids less than a few μm in diameter, which might have caused due to pressure solution. These facts indicate that the illite was crystallized from a fluid. Furthermore, from the fact that a large amount of illite that was affected by fault slip can be seen on the fault plane, we summarize that the white band became a weak plane and acted finally as a fault plane in the massive chert block. The crystallinity of illite existing on the fault plane is better than those of stylolites and white bands. We propose that this is due to frictional heat caused by fault slip.

Keywords: Chert, Stylolite, Illite, Fluid, Fault

©2021. Japan Geoscience Union. All Right Reserved.

Episodic fluid explosion in shallow and middle crust revealed by hydrothermal brecciation

*Geri Agroli[1], Atsushi Okamoto[1], Masaoki Uno[1], Noriyoshi Tsuchiya[1]

1. Tohoku University

High energy released in the middle to shallow crust in the form of episodic fluid explosion. This phenomenon is triggered by several factors primarily an accumulation of fluid pressure from the dehydrated magmatic-hydrothermal system. The episodic fluid explosion is exemplified by intensive crustal failure through fracturing and brecciation. Further investigation of breccia elucidates the origin and characteristic of fluid and brecciation mechanism. Here we examined samples from 3 different locations to demonstrate how common fluid explosions occur in the middle to the shallow crust.

The Sør Rondane Mountains, in East Antarctica is part of the Pan-African collision zone between East and West Gondwana during Precambrian (650-500 Ma). Northeastern terrane of this mountain occupied by metamorphic sequence (granulite) and some locality of syn-metamorphic intrusion of old granite/diorite followed by younger granite which later makes up the breccia clast on this area and represents explosive activity in the middle crust. On the other hand, Breccia on porphyry deposit of Erdenet in Mongolia which occur in Mesozoic (245-235 Ma) and Cenozoic (9-7 Ma) volcanic breccia in Yuze, Japan represent brecciation processes in the shallow crust. The breccia in Sør Rondane Mountains (SRM) comprise of granulite clast cemented by carbonate rock (refer as carbonate breccia dyke) and subsequent granitic dyke which capture carbonate, granite, and gneiss as the clast. Estimated P-T conditions of this brecciation were P=200Mpa and T=580-700˚C which indicating middle crustal condition. Erdenet Porphyry (EP) comprises of 2 distinct breccia type of polymict-breccia which consist of granodiorite porphyry (with potassic alteration) cemented by biotite (phlogopite) located in the bottom part of the drilling-core and monomict-breccia which consist of quartz-porphyry (with sericite alteration) cemented by calcite, quartz, and gypsum occupied the middle and shallower part. We estimated this breccia occurs as multiple fluid processes during the evolution of ore processed. Phlogopite capture fluid temperature at ~700-750˚C with pressure <200Mpa and subsequent brecciation occur in lower temperature mark by low titanium content in quartz-matrix as well as the presence of gypsum which perhaps derived from hydration process of anhydrite indicate the ingress meteoric fluid in the system. Yuze breccia (YB) exhibit polymict breccia where volcanic and plutonic clasts cemented by aphanitic rock texture. Particle/Clast size distribution (PSD) shows that SRM clast primarily has boulder size (>5m) with an aspect ratio (Rs/Rl) of 0.4-0.5 and YB have cobble-pebble size ~50-100 mm with an aspect ratio of 0.5-0.6. As opposed to EP which represents hand specimen size breccia has a fine clast <5mm primarily with an aspect ratio of ~0.6 for all breccia types. Cumulative distribution for all breccia shows that fractal distribution with fractal dimension less or equal to two. And clast arrangement exhibit typical fluid assisted brecciation texture such as jigsaw and mosaic without significant rotation and subsequent wearing processes.

This suggests that brecciation due to overpressurized fluid commonly occurs from the middle to shallow part of the earth's crust. This overpressurized fluid follows by an episodic explosion which abruptly changes the crustal condition and enhanced permeability hence, the fluid can percolate and bring a high amount of energy or precipitate precious metal up to the shallower part of the crust.

Keywords: Fluid explosion, Breccia, Erdenet, Sør Rondane Mountains, Yuze

©2021. Japan Geoscience Union. All Right Reserved.

©2021. Japan Geoscience Union. All Right Reserved.

Pseudotachylyte in a marble from the Takine Group (Abukuma Terrane) and its similarity to pseudotachylyte from the Higo Mertamorphic Rocks

*Tadao Nishiyama[1], Ebo Adou Douha[1]

1. Department of Earth and Environmental Sciences, School of Science, Graduate School of Science and Technology, Kumamoto University

We have reported a pseudotachylyte in a marble from the Higo Metamorphic Rocks in central Kyushu (Nishiyama, et al., 2019 and 2020, JpGU Meeting). This time we investigated marbles in the Takine Group (Abukuma Terrane or Abukuma Belt), the Tohoku Region, and found pseudotachylytes which have characteristics very similar to those from the Higo Metamorphic Rocks. In this report, we present petrography of some pseudotachylytes in a marble at the Shin-Takine Mine (Asahi Koumatsu Co. Ltd.), Tamura City, Fukushima Prefecture, and discuss the possible genesis in comparison with pseudotachylytes from the Higo Metamorphic Rocks.

A large body (1×7 km^2) of marble associated with metasediments, metabasites, and metaperidotites occurs as an isolated mass (roof pendant) in a granitic pluton in Tamura City, about 20 km apart from the main body of the Abukuma Metamorphic Terrane. Ehiro et al. (1989) named them the Takine Group and gave detailed petrography for the metamorphic rocks, revealing that the Takine Group has undergone the contact metamorphism by Cretaceous granites. It is unknown whether it had undergone the regional metamorphism of the Abukuma Metamorphic Rocks prior to the contact metamorphism. It is also unknown to which geological unit the Takine Group belongs (Ehiro et al., 1989). The protolith age is not known, either.

In the Shin-Takine Mine, several metabasite dykes up to 2 meters thick occur in a massive marble. The metabasite dykes are strongly weathered and the mineral assemblage cannot be identified. The marble is a massive monomineralic rock consisting of coarse-grained calcite. However, a layered structure can be seen in part of the marble, in which grey layers several millimeters thick recurrently occur in the marble with a frequency of several centimeters. Quartz, diopside, tremolite and dolomite occur in the grey layers, but no wollastonite occurs. Apatite also occurs as an accessory mineral. These layers show intersecting relations in part, implying the origin not of original bedding but of fluid pathway (i.e., veins).

A quartz (1^{st}-stage quartz) vein develops along the contact between a metabasite dyke and a marble, and black veins 1 to 2 centimeters thick occur in this quartz vein and also in the marble, showing branching and layering. Observations with a SEM-EDS reveal following characteristics.

(a) The black vein consists mainly of dolomite, quartz (1^{st}- and 2^{nd}-stage), and kaolinite-group clay mineral (hereafter abbreviated as Al-Si clay) with a small amount of calcite. 1^{st}-stage quartz is anhedral and polycrystalline, partially dissolved by dolomite. Some quartz grains show fracturing. Quartz (2^{nd}-stage) also occurs as inclusions in dolomite, which have very irregular shape.
(b) Dolomite shows compositional heterogeneity with respect to Fe-Mg exchange. Some dolomite crystals show growth zoning.
(c) Al-Si clay rarely includes K-feldspar, indicating that the Al-Si clay is an alteration product of K-feldspar.
(d) Al-Si clay is frequently associated with quartz (2^{nd}-stage). In a rare case, an idiomorphic quartz (2^{nd}

©2021. Japan Geoscience Union. All Right Reserved.

-stage) crystal occurs within Al-Si clay.
(e) Pyrite occurs in dolomite, showing dissolution texture.
(f) Calcite occurs as inclusions with irregular shape in dolomite.

These characteristics indicate that this black vein is not a simple fault gouge. Because the country rock is a marble ($CaCO_3$), the occurrence of dolomite, Al-Si clay (originally K-feldspar) and 2nd-stage quartz implies mass transfer of Mg, Fe, Al, K, and Si from the exterior. Fracturing is only observed in 1st-stage quartz. Growth zoning in dolomite and an idiomorphic quartz (2^{nd}-stage quartz) crystal in Al-Si clay suggest crystallization of these minerals in fluid or melt. Dissolution texture of pyrite prefers reaction with dolomite melt rather than fluid. These lines of evidence indicate that this black vein represents a recrystallization product of dolomite and silicate melts formed by frictional melting associated with faulting, namely a kind of pseudotachylyte.

Reference
Ehiro, M., Kanisawa, S., and Teketani, Y. (1989) Pre-Tertiary Takine Group in the central Abukuma Massif. Bull. Fukushima Museum, No.3, 21-37.

Keywords: pseudotachylyte, marble, Abukuma Terrane, Takine Group, Higo Metamorphic Rocks

©2021. Japan Geoscience Union. All Right Reserved.

Frictional melting process during formation of pseudotachylyte, Sarwar-Junia fault zone, India

*Jun-ya Okazaki[1], Jun-ichi Ando[1], Kaushik Das[1]

1. Earth and Planetary Systems Science Program, Division of Advanced Science and Engineering, Hiroshima University

Introduction: Pseudotachylyte (Pst) is dark, aphanitic rock formed by frictional melting of host rock resulting from seismic rapid slip, and it develops along fault plane as vein and network. Therefore, Pst is a significant rock that preserves the information of the past seismic activity. Although Pst are generally formed in brittle deformation zone (or shallow crust), Pst deformed plastically and associated with mylonite are also reported (e.g., Chattopadhyay et al., 2008), and thus it suggests that seismic fault activity can occur in ductile deformation zone (or deep crust). Contributions of slip propagation from brittle deformation zone and plastic instabilities to fault generation mechanism in ductile deformation zone are suggested, but the mechanism is still not completely definite. In this study, it is the purpose that the frictional melting processes and the fault generation mechanism in ductile deformation zone are revealed by the results of microstructural observation and mineral phase identification using the two types of Pst samples within granitic gneiss from Sarwar-Junia Fault Zone, India.

Result: In the field observation, two types of Pst veins were observed in relation to the foliation of the host rock. One vein was parallel to the foliation (“P-Pst”) and another vein cut the foliation at a high angle (“C-Pst”). It is considered that “P-Pst” was formed in the same stress field as the ductile deformation of the host rock.

In the microstructural observation of the Pst veins, both veins have the black margins at both ends (chilled margin), and there were formed by the quench of the melt. The width of chilled margin of “P-Pst” is larger than the one of “C-Pst”. It is caused by the difference of the quench rates and indicates that “P-Pst” had the slower quench rate and “C-Pst” had the faster quench rate, respectively. Comparing the minerals survived as clasts within Pst veins, “P-Pst” mainly preserves quartz and sillimanite, while “C-Pst” mainly preserves quartz, sillimanite, plagioclase and K-feldspar. In addition, biotite grains, contained many in the host rock, don’t survive as clast within both veins, therefore it is considered that these grains were completely melted during Pst formation. On the other hand, especially in “P-Pst”, many acicular biotite grains are formed in the matrix, and it indicates the crystallization from the melt. The melting points of these minerals suggests that the maximum temperatures of melt were 1400-1726 ℃ for the “P-Pst” and 1200-1300 ℃ for the “C-Pst”, respectively. However, considering the non-equilibrium melting and the drop in melting point due to the dehydration of biotite, the actual temperature was probably lower than estimated. From the above, it is considered that “P-Pst” and “C-Pst” were formed in the ductile deformation zone and the brittle deformation zone, respectively, and their frictional melting processes are as follows. First, the host rock was fractured by fault activity, then the frictional melting occurred resulting from rapid slip. At this time, maximum melt temperature of “P-Pst” was higher than the temperature of “C-Pst”. Subsequently, because of slower quench rate of “P-Pst”, wider chilled margins were formed and acicular biotite grains crystallized from the melt.

In addition, it is considered that the formation of “P-Pst” in ductile deformation zone was contributed by the preferred orientation of biotite grains. However (001) plane of biotite grains in the host rock randomly directed, the preferred orientation of the (001) plane parallel to the foliation (or Pst vein) develop as approaching the Pst vein. The plane is bonded by van der Waals forces and has very low

©2021. Japan Geoscience Union. All Right Reserved.

strength. From the observation, the (001) plane of biotite grain works as weak plane, and concentration of stress and increasing of strain rate occurred on the plane, then brittle deformation (seismic fault activity) occurred in ductile deformation zone.

Keywords: Pseudotachylyte, Frictional melting, Plastic deformation, Biotite

©2021. Japan Geoscience Union. All Right Reserved.

Neoarchean magmatism and Paleoproterozoic high-pressure granulite-facies metamorphism from the southern Motloutse Complex, eastern Botswana: Implications for the western extension of the Central Zone of the Limpopo Complex

*Thembiso Otladisang Basupi[1,2], Toshiaki Tsunogae[1,3], Kazuki Takahashi[1], Yukiyasu Tsutsumi[4]

1. Graduate of Life and Environmental Sciences, University of Tsukuba, 2. Department of Earth and Environmental Sciences, Botswana International University of Science and Technology, 3. Department of Geology, University of Johannesburg, 4. Department of Geology and Paleontology, National Museum of Nature and Science

We provide the first record of the occurrence of high-pressure garnet-bearing amphibolite and mafic granulite hosted by the amphibolite of amphibolite facies –lower granulite facies from the Maope area of southern Motloutse Complex in eastern Botswana. Our results also provide for the first time Neoarchean magmatic age preserved in the mafic granulite. The mineral assemblages of the rocks are garnet + hornblende + plagioclase + ilmenite + rutile + quartz (garnet-bearing amphibolite), hornblende + orthopyroxene + clinopyroxene + plagioclase + quartz (mafic granulite), and hornblende + plagioclase + quartz + ilmenite + epidote + titanite (host amphibolite). The poikiloblastic garnet from the garnet-bearing amphibolite contains inclusions of hornblende, ilmenite, quartz, and plagioclase as prograde mineral and is mantled by hornblende + plagioclase coronae, which formed during retrograde metamorphism. In the mafic granulite, orthopyroxene is coarse-grained, and the hornblende occurs as a thin retrograde corona around the plagioclase and clinopyroxene. The geochemical signature of the mafic granulite and amphibolite, combined with the enrichment of large-ion lithophile elements and depletion of high-field strength elements (Nb and Ta), indicates subduction-related volcanic arc affinity, and the garnet-bearing amphibolite indicate subduction-related volcanic arc and within-plate basalt affinity. The peak metamorphic condition of the garnet-bearing amphibolite was obtained at 850˚C–910˚C at 10–10.5 kbar using phase equilibrium modeling in the Na_2O-CaO-FeO-MgO-Al_2O_3-SiO_2-H_2O-TiO_2-Fe_2O_3 (NCFMASHTO) system and was consistent with results from geothermobarometry. The conventional geothermobarometry results estimated from the mafic granulite and amphibolite are 745˚C–826˚C and 488˚C–736˚C at 7 kbar, respectively. The pressure-temperature (*P-T*) condition results suggest high-pressure garnet-bearing amphibolite, granulite-facies for the mafic granulite, and amphibolite-lower granulite facies for amphibolite. Zircon grains from the garnet-bearing amphibolite, with a discordance of <5% and Th/U of <2.5, recorded a metamorphic age of 2020.2 ±4.9 Ma whereas the zircon from mafic granulite with a discordance of <5% and Th/U of 0.44 to 0.86 recorded a magmatic age of 2648.8 ±9.8 Ma. The results of the *P-T* condition and the geochronology from the garnet-bearing amphibolite suggest that the southern Motloutse Complex is a high-pressure granulite terrane that underwent a single clockwise *P-T* evolution in the Paleoproterozoic Era (~2.02 Ga). Our results also suggested for a 2.6 Ga magmatic emplacement of mafic rocks recorded from the mafic granulite. The results further, suggest that the southern Motloutse Complex is nearly equivalent to the Beit Bridge Complex in the Central Zone of Limpopo Complex.

Keywords: Neoarchean, Paleoproterozoic, Motloutse Complex, High-pressure granulite, Garnet-bearing amphibolite, Mafic granulite

©2021. Japan Geoscience Union. All Right Reserved.

Petrography of a sulfide-rich garnet-sillimanite-biotite gneiss from Brattnipene, Sør Rondane Mountains, East Antarctica

*Hayato Ikeda[1], Tetsuo Kawakami[1]

1. Kyoto University

The Sør Rondane Mountains (SRM) is located in eastern Dronning Maud Land, East Antarctica, where the lower crust of the East-West Gondwana collision zone is exposed. The SRM is divided into the NE terrane and the SW terrane by the Main Tectonic Boundary (MTB) (Osanai et al., 2013). The NE terrane is characterized by clockwise pressure-temperature (*P-T)* path of granulite-facies metamorphic rocks and inherited zircons older than 1200 Ma, whereas the SW terrane is characterized by the counter-clockwise *P-T* path and inherited zircons younger than 1200 Ma. In Brattnipene, two counter-clockwise *P-T* paths have been proposed previously (Adachi et al., 2013; Baba et al.,2013). However, these studies have weakness of constructing the *P-T* path using boulder samples (Baba et al., 2013) or using samples from distant outcrops (Adachi et al., 2013). In this study, we utilized a pelitic gneiss sample from the Nakayubi-ridge, Brattnipene to constrain the retrograde *P-T* path.
The sample used in this study is a sulfide-rich garnet-sillimanite-biotite gneiss (sample TK2009120403D2) mainly composed of garnet, sillimanite, cordierite, biotite, Fe-sulfides (pyrite and pyrrhotite), plagioclase, K-feldspar, and quartz. Quartz ribbons are developed parallel to the gneissosity. Accessory minerals are rutile, apatite, zircon, monazite and graphite. Garnet (XMg ~ 0.53) includes abundant sillimanite in the core. Garnet rim (XMg ~ 0.27) is replaced by secondary cordierite (XMg ~ 0.85) + Fe-sulfide + sillimanite + quartz or cordierite (XMg ~ 0.88) + Fe-sulfide + biotite (XMg = 0.77-0.81) + quartz. The former mineral assemblage tends to appear near the garnet when both assemblages are observed. Common sulfide occurrence in the assemblage implies that infiltration of sulfur-bearing fluid/melt triggered the breakdown of garnet. The presence of sillimanite in the replacement assemblage suggests that the garnet breakdown took place under the sillimanite stability field, and the formation of cordierite probably represents decompression process. Rutile enclosed in the secondary cordierite is finer-grained and shows higher Cr, V and Al concentrations compared to matrix rutile. Therefore, inclusion rutile is likely a product formed during the garnet breakdown. Zr-in-rutile thermometry (Tomkins et al., 2007) applied to the inclusion rutile gave ~700 $^{\circ}$C for the pressure of the sillimanite stability field, and this probably represents the temperature of the garnet breakdown. Although further detailed analysis is required, the observed decompression reaction texture in the sillimanite stability field contrasts with counter-clockwise *P-T* paths previously proposed for Brattnipene, and thus timing of the garnet breakdown reaction needs to be determined in order to understand its geological meaning in the tectonic framework proposed by Osanai et al. (2013).

Keywords: metamorphic rock, continental collision

©2021. Japan Geoscience Union. All Right Reserved.

Microstructural characteristics of ultra-high pressure metamorphic rocks from the Dabie-Shan, eastern China

*Katsuyoshi Michibayashi[1], Kouhei Asano[1]

1. Department of Earth and Planetary Sciences, Graduate School of Environmental Studies, Nagoya University

Ultrahigh-pressure (UHP) metamorphic rocks with their origin of continental material, which have formerly been subducted to mantle depths more than 80 km, are located in the Dabie-Shan, China. UHP rocks often record geodynamic processes during a series of subduction and exhumation. Deformation microstructures of UHP rocks at peak metamorphic conditions provide important information about rheological behavior of deeply subducted crustal material within subduction channel. However, it is pretty rare to preserve deformation microstructures of UHP rocks at peak metamorphic conditions due to subsequent retrograde metamorphism during exhumation. Here, we present deformation microstructures and crystallographic-preferred orientations (CPOs) of UHP rocks from the Dabie-Shan in order to study rheological behavior of deeply subducted continental material at UHP conditions. We investigated three mafic-ultramafic rocks: eclogite (garnet-omphacite-quartz), garnet-clinopyroxenite (garnet-Ca-pyroxene) and garnet peridotite (olivine-garnet-Ca-pyroxene) and one felsic rock: jadeite-quartzite (quartz-jadeite-garnet). Whereas the mafic-ultramafic rocks show distinctly high-strained microstructures such as intense elongated foliations with strong grain size reduction, the felsic rock preserves relatively low-strained microstructures such as weakly foliated granular texture, indicating that the jadeite-quartzite have been less deformed than mafic-ultramafic rocks. We argue that coesite occurrence after quartz in the felsic rock at the UHP condition can explain the deformation contrast between the mafic-ultramafic and the felsic rock. The presence of coesite with higher strength than quartz may result in increasing the bulk strength of felsic rocks, leading to strain localization in mafic-ultramafic rocks. EBSD analyses of the jadeite-quartzite revealed that the intracrystalline strains have been accumulated only within quartz grains, resulting in dense but irregular grain boundary formation, in contrast to the other minerals maintaining coarse grains with serrated grain boundaries. The formation of shear zones associated with strain localization at HP/UHP conditions can induce the detachment of subducted crustal material from subducting lithosphere, which is one of the necessary processes for exhumation of UHP rocks. We propose that strain localization in mafic-ultramafic rocks may trigger the exhumation of UHP rocks. Therefore, coesite could significantly influence rheological behavior of crustal material subducted to the depths where coesite is stable at UHP condition.

Keywords: Ultrahigh pressure metamorphic rock, Deformation microstructure, Rheology

©2021. Japan Geoscience Union. All Right Reserved.

Metamorphic history of the Suo metamorphic rocks inferred from two-stage garnet in pelitic schist

*Shunsuke Endo[1], Maki Ito[1]

1. Department of Earth Science, Interdisciplinary Faculty of Science and Engineering, Shimane University

Pelitic schist is the main lithology in coherent-type high-P/T metamorphic complexes such as the Sanbagawa and Suo metamorphic belts in SW Japan, and analyses of its subduction-exhumation records are important to constrain the thermal regime of subduction channels as well as spatial-temporal changes of force balance acting on the subduction interface. Since pelitic schist is generally subjected to high-strain ductile deformation and strong recrystallization during exhumation, subduction-stage records are only preserved within rigid minerals such as garnet. Here we report detailed petrological data on garnet-bearing pelitic schist from the Nichinan area in the Chugoku Mountains, where high-grade part of the Jurassic Suo metamorphic rocks is exposed. Detailed microstructural observations reveal that two stages of garnet growth punctuated by a garnet dissolution stage are common in the Nichinan pelitic schist. Euhedral garnet grains consist of a resorbed core and an overgrown rim. The garnet core preserves growth zoning and contains inclusions of quartz, rutile, zircon, phengite and box-shaped paragonite + clinozoisite aggregates (possible pseudomorph after lawsonite). Zr-in-rutile thermometry and pseudosection modelling (with garnet isopleths) reveal that the garnet core grew in the lawsonite stability field from ~1.8 GPa, 470℃ to ~1.6 GPa, 500℃. The garnet rim formed synchronous with the growth of titanite and albite porphyroblasts at ~0.8 GPa and 500℃. These microstructures and P-T evolution are very similar to those of pelitic schist in the eclogite unit of the Sanbagawa metamorphic belt. Onset of highly oblique subduction and shear heating at crustal levels may account for the decompression heating and Barrovian-type overprint during exhumation of coherent-type high-P/T metamorphic complexes, and this process largely obliterates subduction-stage high-P/T records.

Keywords: garnet, pelitic schist, Suo metamorphic rocks

©2021. Japan Geoscience Union. All Right Reserved.

Hidden intact coesite in deeply subducted rocks and its geological implications

*Tomoki Taguchi[1], Yui Kouketsu[2], Yohei Igami[3], Tomoyuki Kobayashi[4], Akira Miyake[3]

1. Department of Earth Sciences, Faculty of Education and Integrated Arts and Sciences, Waseda University, 2. Department of Earth and Planetary Science, Graduate School of Environmental Studies, Nagoya University, 3. Department of Geology and Mineralogy, Graduate School of Science, Kyoto University, 4. Faculty of Health and Sports, Nagoya Gakuin University

Coesite, a high-pressure phase of SiO_2, is a diagnostic indicator of ultrahigh-pressure (UHP) metamorphism, oftentimes implying subduction of a rock to a minimum depth of 80 km. Deciphering the petrology of UHP rocks will improve interpretations of not only the tectono-metamorphic evolution in ancient subduction and collision zones, but also the underlying framework of plate tectonics. Tracking the spatial extent of UHP metamorphic terranes within a convergent plate margin is the first step toward understanding the fluxes of subducted crust. Previous petrological studies indicate that metamorphic coesite rarely occurs as inclusions in rigid minerals, such as zircon and garnet (Chopin, 2003 and references therein). Most coesites are often partially or completely obscured owing to the formation of polycrystalline quartz grains surrounded by radial cracks (i.e., quartz pseudomorphs), driven by an increase in the volume during the exhumation process. In contrast, recent numerical modeling and deformation experiments show that UHP conditions may reach shallower depths in the lithosphere than previously estimated, presumably via overpressure at both microscopic and macroscopic scales (e.g., Schmalholz and Podladchikov, 2013; Richter et al., 2016). This debatable conflict between petrographic observations and theoretical notions has led to intense debate regarding the pressure-to-depth conversion of metamorphic rocks. Through integrated micro-Raman analyses and modern nano-observation techniques employing a focused ion beam system and transmission electron microscopy (FIB–TEM), this study reports the occurrence of minuscule coesite (<20 μm) as abundant inclusions in garnet-rich impure quartzites from the Lago di Cignana Unit (LCU) in the Italian Western Alps.

Coesite was identified by a strong Raman band at a wavenumber (ν) of 521 cm^{-1}. Representative bands of coesite inclusions completely sealed inside garnet grains showed slight shifts to higher frequencies (ν = ~522 cm^{-1}), which is indicative of residual pressures retained by the coesite inclusion in the garnet. Raman intensity maps revealed that these SiO_2 inclusions are composed entirely of coesite, with no quartz present. The results obtained via Raman intensity mapping of the LCU samples yielded residual pressure values for coesite inclusions of up to 0.5 GPa, with heterogeneous stress observed within the crystals. Bright-field TEM images show that the interface structures form notably sharp boundaries with no crystal defects, such as dislocations, stacking faults, or microcracks observed within either coesite or garnet. The high-resolution TEM image displays the lattice fringes of coesite along the [100] direction, corresponding to the lattice spacings of the (020) plane for coesite (d values = 0.62 nm). Our TEM results show only the lattice fringes of either coesite or garnet, further indicating that no quartz crystallized at the nano-interfaces.

We suggest that common coesite-derived quartz pseudomorphs are less typical structures in UHP metamorphic rocks. The discovery of such intact coesite inclusions may fill the gaps in the predicted and observed abundance of coesite worldwide. In addition, abundant intact minuscule coesite inclusions may be hidden in many established UHP localities, and overlooked because of their size. Our findings would play an essential role in reappraisal of the extent of deeply subducted rocks and their rheology.

©2021. Japan Geoscience Union. All Right Reserved.

Keywords: Coesite, Quartz pseudomorph, Phase transition, Raman spectroscopy, Transmission electron microscopy

©2021. Japan Geoscience Union. All Right Reserved.

Metamorphic zoning and *P–T* conditions of contact metamorphic rocks in the Unai area, Yamaguchi prefecture, Japan.

*Kakeru Sakamoto[1], Toshiaki Shimura[1]

1. Graduate School of Sciences and Technology for Innovation, Yamaguchi University

The Unai area lies near the boundary between Ube city and Mine city, Yamaguchi prefecture, belongs to the Suo Belt. Kishi et al. (2007) reported that this area was intruded by the plutonic complex composed of Amago intrusive rocks, Kurogoro plutonic rocks, and Iwago-yama granite. These K–Ar ages are 97.9 ±2.2 Ma, 94.0 ±4.8 Ma, and 92.8 ±2.0 Ma, respectively. The plutonic complex is exposed over an area of 14 × 8 km and its intrusion caused contact metamorphism to the Suo metamorphic rocks in the Unai area (Seo, 1976).
This study reports the metamorphic zoning, and *P–T* conditions of the contact metamorphism.

The Unai area is underlain by metamorphic rocks and granodiorites. Metamorphic rocks are composed of contact metamorphic rocks (dominant pelitic schist, and a small amount of calc-silicate schist) and the Suo metamorphic rocks (precursor).
In this area, granodiorites are distributed in the central part. Contact metamorphic rocks are distributed around the margin of granodiorite with a width of about 500 m, and most of them are pelitic schist, but calc-silicate schist also occurs as a small lens shape.

The dominant pelitic rocks had been used for zonal mapping in this area. It can be divided into six metamorphic zones. The critical mineral paragenesis are as follows.
For pelitic rocks,
Zone Ⅰ (Crd zone): Qz + Pl + Ms + Bt + Crd + (Chl)
Zone Ⅱ (And zone): Qz + Pl + Ms + Bt + And + Crd
Zone Ⅲ (Kfs zone): Qz + Pl + Bt + Ms + Kfs + Crn + And + Crd + Ilm
Zone Ⅳ (Grt zone): Qz + Pl + Bt + Kfs + Opx + Crd + And + Spl + Alm
Zone Ⅴ (Spl zone): Qz + Pl + Bt + Kfs + Opx + Crd + And + Spl
Zone Ⅵ (Sil zone): Bt + Opx + Pl + Kfs + Crd + Qz + Spl + Sil + Ilm
For calc-silicate rocks,
Zone Ⅵ (Sil zone): Pl + Cpx + Cal + Qz + Grs.

Zone Ⅰ pelitic rocks have a strong schistosity which originated precursor Suo metamorphic rocks. It is mainly composed by muscovite and biotite. This zone is characterized by the appearance of cordierite porphyroblast. Zone Ⅱ is characterized by andalusite porphyroblast. Zone Ⅲ is characterized by the occurrence of K-feldspar and euhedral corundum (up to 0.2 mm), they are coexisting with biotite. Zone Ⅳ is characterized by the appearance of orthopyroxene, which is coexisting with cordierite, biotite, and K-feldspar. Spinel (hercynite) also appear in this zone. Zone Ⅴ is almost same mineral paragenesis with that of Zone Ⅳ, but it is characterized by the disappearance of almandine. Zone Ⅵ pelitic rocks are characterized by the appearance of sillimanite (about 0.1 mm). The sillimanite is not fibrolite but is prismatic crystals. Calc-silicate rocks of Zone Ⅵ are mainly composed of calcite, clinopyroxene, and grossular.

The mineral chemistry of pelitic schist are as follows. In this abstract, we use X_{Mg} = Mg / (Fe + Mg) and X_{Mg^*} = Mg / (Mg + Fe^{2+} + Fe^{3+}). On spinel, Fe^{3+} and Fe^{2+} were calculated by stoichiometry. Plagioclase has

©2021. Japan Geoscience Union. All Right Reserved.

An = 4.1–43.9% in composition. Biotite has X_{Mg} = 0.34–0.62. Muscovite has X_{Mg} = 0.53–0.61. Orthopyroxene has X_{Mg} = 0.42–0.43. Spinel has X_{Mg^*} = 0.29–0.33, Zn = 0.002–0.007 apfu, and Cr = 0.005–0.020 apfu. Garnet has $Alm_{55.4–58.7}Prp_{41.0–44.3}Sps_{0.2–0.5}Grs_{0.1}$ in composition.
The mineral chemistry of calc-silicate rocks are as follows. Plagioclase has *An* = 91.0–96.8% in composition. Clinopyroxene has X_{Mg} = 0.68–0.79, diopside composition. Garnet has $Alm_{10.5–16.8}Prp_{1.3–2.2}Sps_{0.4–1.3}Grs_{80.1–87.5}$ in composition.

The variations of these mineral paragenesis and the variations in mineral chemical compositions reflect the metamorphic grade. The metamorphic pressure is about 0.8 kbar, and the metamorphic temperatures are about 500 ˚C for Zone Ⅰ, 500–550 ˚C for Zone Ⅱ, and 550–600 ℃ for Zone Ⅲ, 600–750 ˚C for Zone Ⅳ and Zone Ⅴ, and about 750 ˚C or higher for Zone Ⅵ. The highest metamorphic condition reached to the pyroxene hornfels facies.

References

Kishi et al. (2007) *Jour. Geol. Soc. Japan.*, **113**, 479-491.
Seo (1976) *Professor G. Kojima Memorial Volume*, 276-285.

Keywords: Unai area, contact metamorphism, metamorphic zoning, mineral chemistry

©2021. Japan Geoscience Union. All Right Reserved.

Progressive metamorphism of the Ryoke metamorphic rocks from No-jima Island, South of Yamaguchi Prefecture

*ZEJIN LU[1]

1. Graduate School of Science and Engineering for Innovation, Yamaguchi University

No-jima Island is located in the Seto Inland Sea, Yamaguchi Prefecture. It is thought to be the region that has undergone Cretaceous low-pressure type regional metamorphism (Ryoke metamorphism). No-jima Island is underlain by crystalline schists and metabasalts. Metabasalts show the geochemical character similar to the within plate basalts, for instance the green stones in the Mino-Tamba belt. Moreover, the metamorphic grade of the schists corresponds to the biotite zone of the Yanai region of the Ryoke belt, but the petrological character of the rocks from No-jima Island has been unclear. In addition, the geological correlation with the neighboring area, Kasado-jima Island, the Oshima peninsula, and Ohtsu-jima Island has not been understood yet. Therefore, the aim of this study, based on the mineral paragenesis of the pelitic schists, is to discuss the metamorphism of the rocks from No-jima Island, and also to unravel the thermal structure of the low-pressure type metamorphism, the Ryoke belt, in this region.

The metabasalts are mainly exposed on the northeastern part of the island but occur rarely in the west coast of the island. They are included in the schists of sedimentary origin as blocks. The metamorphic rocks are composed mainly of the pelitic schist and metamorphosed chert with bedded structure (siliceous schist hereafter) with trace amounts of calc-silicate schist as thin layers or lenses. The pelitic and siliceous schists are intermittently distributed on the western and southeastern coast of the island. Fold structures such as close folds often develop in the southern part of the island. Granite dikes with 1–2 m width intrude the schists on the western coast.

The metabasalt is porous and has a prominent pillow structure and often shows the amygdaloidal texture. Phenocryst minerals of igneous origin are of clinopyoroxene and plagioclase with minor amounts of amphibole. It contains recrystallized fibrous amphiboles partially coexisting with biotite. Calcite locally fill the amygdules and occurs as veins. The pelitic and siliceous schists show the repidoblastic texture. The calc-silicate schist is composed of Bt+Cal+Qtz. The mineral assemblage of the pelitic schists changes from north to south of the island; Bt+Ms+Chl+Pl±Grt in the north and Bt+Ms+Grt+Pl+Kfs in the south. On the other hand, the mineral assemblage of siliceous schist is mainly Ms+Bt+Grt+Pl.

The garnet of pelitic schist and siliceous schist shows a normal zoning with reduced spessartine toward the rim, probably formed during prograde metamorphism. The chemical composition of biotite depends on the mineral combination. Biotite that coexists with garnet and K-feldspar, has a high XFe in pelitie schist. Plagioclase is fine-grained and the zoning is not prominent. The composition differs for each rock such as politic schist and siliceous schist.

In addition to the change in mineral combination, the grain size becomes coarser in the south. A reaction is expected from the north to the south due to the symbiotic relationship with minerals. Therefore, the island can be divided into the biotite zone in north and the garnet zone in south in terms of the mineral paragenesis of the pelitic schists.

The geothermobarometers for garnet-biotite (Ferry and Spear, 1978) and garnet-pagioclase-biotite-quartz

©2021. Japan Geoscience Union. All Right Reserved.

(Hoish, 1990) are adapted to the pelitic schist. As a result, the peak metamorphic temperature and pressure conditions are estimated to be 480–530℃ and 180–300 MPa, respectively. According to the result, the thermal structures around the Seto Inland Sea region are discussed.

The metamorphic garnet zone of No-jima Island and its cordierite zone of Kasado-jima Island, Oshima peninsula and Ohtsu-jima Island show the same metamorphic conditions. Therefore, it is considered that the cause of garnet depends on the chemical composition of pelitic rocks. As a result of comparing the chemical composition of bulk and minerals, it is considered that the crystallization of garnet is affected not only by high XFe but also by XMn values.

Keywords: Ryoke metamorphism, Low-pressure type, Garnet isograd

©2021. Japan Geoscience Union. All Right Reserved.

P–T–t path of Ryoke metamorphic rocks in Kitsuki area, Kunisaki Peninsula, Oita prefecture, Japan.

*Kentaro Mutabaru[1], Toshiaki Shimura[1]

1. Yamaguchi University

The Kitsuki area of Oita prefecture belongs to the Ryoke metamorphic belt (Moriyama et al. 1983; Brown, 1998; Ishizuka et al., 2005; Isozaki et al., 2010). The Cretaceous Ryoke metamorphic rocks are less exposed in the Kitsuki area because they are widely covered by the Miocene volcanic and pyroclastic rocks. Ishizuka et al. (2005) indicated that the metamorphic grade of the Ryoke metamorphic rocks in this area corresponds to the sillimanite–K-feldspar zone in the Yanai area, Yamaguchi prefecture. This study discusses the *P–T–t* path of Ryoke metamorphic rocks in the Kitsuki area.
The Ryoke metamorphic rocks in Kitsuki area composed of pelitic gneiss, siliceous gneiss, and a few mafic metamorphic rocks. Ms–Bt granite and Hbl–Bt granodiorite are distributed around the Ushiyashiki and Kuranari area, respectively. Hbl–Bt granodiorite has weak foliation, and encloses pelitic gneiss as a xenolith.
The dominant mineral assemblages of pelitic gneiss in this area are the following.
Assemblage-I: And + Sil + Ms + Grt + Bt + Pl + Qz
Assemblage-II: Sil + Ms + Kfs + Grt + Bt + Pl + Qz
Assemblage-III: Sil + Kfs + Grt + Bt + Pl + Qz
Assemblage-I is recognized at the western part of this area. Assemblage-II is predominant in this area, and it contains tourmaline occurs as a minor phase. Assemblage-III is distributed in the eastern part in this area. Ti content of biotite increases from assemblages-I to III. Garnet grossular component of assemblage-I is poor than that of assemblages-II and III.
In this study area, the following two metamorphic reactions must be important. These are;
(1) And = Sil and
(2) Ms + Qz = Als + Kfs + H_2O.
Reaction curve (1) has negative slope, whereas (2) has positive slope. Because these two reaction curves are crossing each other in a *P-T* space, two bathozones or bathograds can be defined (e.g. Carmichael, 1978). In this study area, two bathozones (A and B) are recognized, and these two bathozones are further subdivided into three *P-T* fields (1, 2, and 3), as follows;

Bathozone-A (lower-*P* condition, ca. $P < 2.2$ kbar)
P–T field A-1 (lower-*T* condition): mineral assemblage is And + Ms
P–T field A-2 (middle-*T* condition): mineral assemblage is And + Kfs
P–T field A-3 (higher-*T* condition): mineral assemblage is Sil + Kfs
Bathozone-B (higher-*P* condition, ca. $P > 2.2$ kbar)
P–T field B-1 (lower-*T* condition): mineral assemblage is And + Ms
P–T field B-2 (middle-*T* condition): mineral assemblage is Sil + Ms
P–T field B-3 (higher-*T* condition): mineral assemblage is Sil + Kfs

These two prograde reactions can be observed as the following order;
And →Sil in the assemblage-I,
Ms + Qz →Sil + Kfs + H_2O in the assemblage-II.
On the other hand, these two retrograde reactions can be observed
Sil →And in the assemblage-I,

©2021. Japan Geoscience Union. All Right Reserved.

Sil (and And) + Kfs + H_2O →Ms + Qz in the assemblages-I and II.
These two retrograde reactions occurred almost at the same time. This *P–T* condition is the boundary between bathozones A and B, and it is about 620 ℃ and 2.2 kbar. Assemblage-I rocks passed through this point at the retrograde stage.
Metamorphic pressure condition was higher ($P > 2.2$ kbar) at the prograde stage, whereas it was lower (ca. 2.2 kbar) at the retrograde stage. Therefore, Ryoke metamorphic rocks in this study area was experienced a clockwise *P–T–t* path.

References

Brown, M. (1998) *Jour. Metamorph. Geol.*, **16**, 3–22.
Carmichael, D. M. (1978) *Amer. Jour. Sci.,* **278**, 769-797.
Ishizuka, Y. et al. (2005) *1:50,000 Geol. Map, Bungo-kitsuki. Geol. Surv. Japan.*, 11–18.
Isozaki, Y. et al. (2010) *Jour. Tokyo Geogr. Soc.*, **199**, 999–1053.
Moriyama, Z. et al. (1983) *Fac. Educ. Oita Univ.*, 29–62.

Keywords: Kitsuki area, Ryoke metamorphic belt, metamorphic P-T-t path, bathozone

©2021. Japan Geoscience Union. All Right Reserved.

P-T estimations of Ryoke metamorphic rocks in the Takato-Ohshika area, Nagano, Japan

*Yoshihiro Nakamura[1], Kazuhiro Miyazaki[1], Yutaka Takahashi[1]

1. Geological Survey of Japan, National Institute of Advanced Industrial Science and Technology

Low–*P/T* type metamorphism is closely related to the arc magmatism and the detailed *P–T–t–D* estimations of metamorphic rocks associated with granitoids lead to be understanding of the tectonic evolution of active convergent margin. Recently, a lot of U-Pb zircon ages from Ryoke granitoids and metamorphic rocks in Yanai and Mikawa regions were reported (e.g., Skrzypek et al. 2016; Takatsuka et al. 2018). These age data imply that the reconsideration of the classical intrusive relationship between gneissose older and massive younger Ryoke granitoids closely related to the low-*P/T* type metamorphism is required. Hence, we attempted to assess the detailed *P–T–D* estimations of mylonitic metasediments along the MTL in the Takato-Oshika area. The area is located in the eastern most part of the Ryoke metamorphic belt, where is suitable for comparison with other areas previously reported.

In the study area, the gneissose Hbl–Bt tonalite (the so-called Hiji tonalite) is widely exposed along the MTL, but there have been few reports on the Ryoke metamorphic rocks before. In this study, we conducted a detailed geologic field mapping survey, during which meter- and centimeter-scale blocks of Ryoke metamorphic rocks within the Ryoke granitic mylonite were successfully sampled. The mylonitic metasediments are locally associated with *C'* -type shear bands, suggesting sinistral shearing. The representative mineral assemblage of the mylonitic metasediments comprises garnet, biotite, muscovite, cordierite pseudomorphs (muscovite aggregates), plagioclase, and quartz, with minor amounts of apatite, zircon, tourmaline, sillimanite, and platy graphite. The highest-grade metamorphic rocks in the Grt–Crd zone of the Ryoke metamorphic belt are exposed at distances of ~1800 m from the MTL. Detailed petrological analyses coupled with conventional thermobarometers and *P–T* pseudosection modeling give estimated peak *P–T* conditions of 760–790 ˚C at 4.6–5.3 kbar. Likewise, the surrounding gneissose Ryoke granitoids were emplaced at around 680–710 ˚C and 4.6–5.8 kbar by Al in hornblende barometry and Hbl–Pl thermometry.

On the other hand, peak *P–T* estimations of mylonitic metasediments have been estimated to be 560 to 710 ˚C at 2.0–5.1 kbar, suggesting the decrease in peak *P–T* conditions with approaching the MTL. Such rocks correspond to the Kfs–Sill to Bt zone of the Ryoke metamorphic belt and are structurally upper unit to the highest-grade Ryoke metamorphic rocks. However, the present Ryoke metamorphic rocks and granitoids show a monoclinal structure with a dip of about 50–70˚W and the structurally upper unit in the Bt and Kfs–Sill zones of Ryoke belts were stacked at the lower portion of the highest-grade metamorphic rocks in the Grt–Crd zone. This suggests that the primary metamorphic zonation during the low-*P/T* type metamorphism has a tight asymmetric anticline at around the MTL. In addition, we revealed that a large pressure difference of >10 km was inferred from peak *P–T* conditions between the highest-grade metamorphic rocks and mylonitic rocks in a width of only ~1500m at around the MTL. These data suggest that a considerable amount of geologic mass in the middle crust was shortened or stretched, and upper units of Ryoke metamorphic rocks in the Bt and Kfs–Sill zones were selectively dragged into the deeper crust by ductile deformation related to the MTL.

[Reference]: Skrzypek et al. (2016), Lithos, 260, 9-27; Takatsuka et al. (2018), Lithos, 308-309, 428-445.

©2021. Japan Geoscience Union. All Right Reserved.

Keywords: Ryoke metamorphic rocks, MTL, Low-P/T type metamorphism

©2021. Japan Geoscience Union. All Right Reserved.

Ultrahigh-temperature HP granulite facies stage of the Early Jurassic pre-Sanbagawa metamorphism

*Kenta Yoshida[1], Sota Niki[3], Hikaru Sawada[1], Ryosuke Oyanagi[1], Takafumi Hirata[3], Kenji Asakura[2], Takao Hirajima[2]

1. Japan Agency for Marine-earth Science and Technology, 2. Kyoto University, 3. The University of Tokyo

The Sanbagawa metamorphic terrane records at least two distinct stages of metamorphism, i.e. the early metamorphism of granulite to epidote-amphibolite facies occurred at Early Cretaceous (c. 120 Ma) and the later high-pressure metamorphism covering eclogite facies, so-called Sanbagawa metamorphism, at Late Cretaceous (c. 90 Ma) (e.g., Aoya and Endo, 2017 and references therein). The evidence of the early Sanbagawa metamorphism is preserved in some coarse-grained mafic bodies in central Shikoku, such as the Western Iratsu body (Endo et al., 2009), and their protolith ages are considered to Early Jurrasic based on the U-Pb ages of zircon (c. 200 Ma) that represent the ages of the arc magmatism (Aoki et al., 2020).

We report the first evidence of the metamorphic event preceding the above ones (pre-Sanbagawa metamorphism), whose P-T conditions correspond to ultrahigh-temperature high-pressure (UHT-HP) granulite facies with the age of Early Jurrasic.

The studied sample is a high-pressure marble collected from the Eastern Iratsu body, which is composed of calcite, garnet, diopside, quartz, and minor minerals including titanite, and zircon. The eclogite facies metamorphism has been recognized by omphacite (jadeite content up to 50%) in the matrix garnet and within garnet-diopside aggregate (GDA), suggesting that diopside had become stable before the eclogite facies stage. In-situ U-Pb dating of the garnet in the quartz-rich domain yielded 96 +/- 9 Ma which is in good agreement with the previous estimates of the eclogite-facies metamorphism (Niki, Yoshida et al., JpGU2021). The sample records a unique evidence of fluid activity during the exhumation. The occurrence of datolite [$CaBSiO_4(OH)$] in a specific part of garnet, the P-T conditions of which were well constrained, indicates the boron-rich fluid activity during the juxtaposition of the eclogite unit to the surrounding non-eclogite rocks (Yoshida et al., 2021 JMPS).

The new evidence of the pre-Sanbagawa metamorphism was discovered using titanite in the same marble. Titanite occurs in the matrix and inter-grain minerals within GDA. Titanite grains in the matrix show spindle shape while those in GDA show irregular shape. In high-contrast back-scattered electron image (BSI), most titanite are homogeneous (Ttn1), but some grains have thin rim showing dark color in BSI (Ttn2). The formation P-T conditions of Ttn1 were well constrained by means of quartz-in-titanite Raman elastic barometer (Kohn, 2014) and Zr-in-titanite thermometer (Hayden et al., 2008), yielding 900-1100 degreeC and 1.5-1.8 GPa assuming a specific range of $aTiO_2$.

LA-ICP-MS U-Pb dating was performed for titanite and zircon. Zircon and Ttn1 yielded concordant age of Early Jurassic (200-180 Ma) while Ttn2 show a clear mixing line in the Terra-Wasserburg Concordia diagram whose lower intercept age was 126 Ma. In addition, few Ttn1 grains show intermediate ages around 164 Ma. All titanite and zircon analyzed show low Th/U ratios and thus are metamorphic origin. The Early Cretaceous age of Ttn2 is comparable to that of the early Sanbagawa metamorphism although P-T conditions were not constrained. On the contrary, Ttn1 and zircon preserved an Early Jurassic metamorphism of UHT-HP granulite conditions that has never reported from the Sanbagawa metamorphic terrane.

©2021. Japan Geoscience Union. All Right Reserved.

The oldest metamorphic ages of the Sanbagawa metamorphic terrane in the previous studies were c. 120 Ma of the early Sanbagawa metamorphism while our new data provide an evidence of the older metamorphic event. The 138 Ma of Nd-Sm age reported from the Nikubuchi peridotite body within the Eastern Iratsu body (Senda et al., 2006) was interpreted as either granulite facies metamorphism or magmatic event, which indicates that the Eastern Iratsu body records a longer history than other members of the Sanbagawa metamorphic terrane. The newly-reported pre-Sanbagawa metamorphism may provide a key to decipher tectonic evolution of the subducting Izanagi plate.

Keywords: Sanbagawa metamorphic terrane, HP granulite, U-Pb dating, high pressure metamorphism, titanite

©2021. Japan Geoscience Union. All Right Reserved.

Meliorating the spatial resolution of SEM-EBSD

*Thomas Jing Yi Yeo[1], Norio Shigematsu[1]

1. Research Institute of Earthquake and Volcano Geology, Geological Survey of Japan, National Institute of Advanced Industrial Science and Technology

Electron Backscatter Diffraction (EBSD) is a commonly applied analytical practice for quantitative analysis in the scanning electron microscope (SEM). The spatial resolutions of SEM-EBSD are known to be about a few μm for the tungsten filament electron gun SEM and a few tens of nm for the Schottky field-emission electron gun SEM.

Quartz grain size provides important information regarding the flow stress during the plastic deformation of mylonite (Stipp and Tullis, 2003). Some mylonite samples contains quartz grains with size of smaller than 1 μm (Okudaira and Shigematsu, 2012). It has been described that these quartz grains developed through dynamic recrystallisation mechanism. Thus, a higher spatial resolution is required during EBSD mapping in order to fully represent the microstructures of such sub-micro scale grains and techniques to meliorate the spatial resolution is essential for this purpose.

The SEM used for this study is located in the GSJ laboratory of AIST, Japan with a Hitachi SU-3500 (W filament gun SEM) and HKL Nordlys EBSD sensor. Quartz, a common mineral on the continental crust is first chemo-mechanically polished with colloidal silica before the analysis. The investigation was preformed with the sample coated with a 0.2 nm thick Osmium coating to reduce the charging effects.

There is a trade-off between the spatial resolution and the signal intensity of the EBSD, which is control by the probe diametre and accelerating voltage. This trade-off was investigated by adjusting the objective lens movable aperture, condenser lens and accelerating voltage to obtain the most optimal condition. The spatial resolution is qualitatively and quantitatively analysed from the kikuchi bands images obtained through a line profile. We investigated the spatial resolution for both X (parallel to the tilt axis) and Y axes (perpendicular to the tilt axis) as samples used for EBSD analysis are generally tilted at 70˚, thus yielding different spatial resolutions at both X and Y directions.

The knife-edge method was also applied to measure the beam diameter at different optical conditions. In this presentation, we show the preliminary results.

Keywords: SEM-EBSD, Spatial resolution, Quantitative microanalysis

©2021. Japan Geoscience Union. All Right Reserved.

Strain in quartz inclusion probed by Raman spectroscopy

*Yui Kouketsu[1], Yuki Tomioka[1], Tomoki Taguchi[2]

1. Department of Earth & Planetary Sciences, Graduate School of Environmental Studies, Nagoya University, 2. Department of Earth Sciences, Faculty of Education and Integrated Arts and Sciences, Waseda University

The residual pressure is maintained on the host–inclusion system that reflect the metamorphic conditions when the inclusion was trapped in the host mineral due to the difference in the volume change during their exhumation. In recent years, Raman geothermobarometers have been developed to estimate the metamorphic conditions from the peak shift of Raman spectra of inclusion minerals. The conventional Raman geothermobarometers have assumed that the inclusion minerals are uniformly stressed from the surrounding mineral under the hydrostatic pressure, but in reality, the inclusion minerals are under deviatoric stress due to the anisotropy of the elastic modulus of host and inclusion minerals, and are subjected to the different strains in each axial direction. Murri et al. (2018) proposed a method to estimate the strains from the peak shifts of Raman spectrum using the Grüneisen tensor. In this study, we used a strain calculation program based on this principle (stRAinMAN; Angel et al., 2019) to estimate the strains of quartz inclusions in garnet and kyanite host minerals.

Quartz eclogite from the Gongen area of the Sanbagawa belt, SW Japan, and Lawsonite eclogite from the Motagua Fault Zone, Guatemala, were used for analysis. In addition, we also used garnetite data from the Lago di Cignana unit in the Western Alps reported by van Schrojenstein Lantman et al. (2020). For all samples, the Raman spectra of quartz inclusions in garnet were obtained and the peak shifts from the standard quartz were calculated to estimate the strain. In addition to quartz inclusions in garnet, quartz inclusions in kyanite were also analyzed in quartz eclogite samples from the Sanbagawa belt. The strains were calculated using the values of the peak shifts at 464 cm^{-1}, 205 cm^{-1}, and 128 cm^{-1} and the Grüneisen tensor of quartz (γ_1+ γ_2, γ_3) reported by Murri et al. (2018), and the strains of ε_1+ε_2 and ε_3 were obtained.

Calculations of the strain of quartz inclusions in garnet show that quartz eclogite from the Sanbagawa belt shows ε_1+ε_2 ranging from -12×10^{-3} to -24×10^{-3} and ε_3 from $+1\times10^{-3}$ to -4×10^{-3}, whereas Lawsonite eclogite from Motagua Fault Zone shows ε_1+ε_2 ranging from -19×10^{-3} to -26×10^{-3} and ε_3 from -3×10^{-3} to -8×10^{-3}. In the garnetite of the Lago di Cignana unit reported in the previous study, ε_1+ε_2 ranges from -12×10^{-3} to -24×10^{-3} and ε_3 from $+1\times10^{-3}$ to -5×10^{-3}, which is almost the same range as that of quartz eclogite in the Sanbagawa belt. On the other hand, the calculated strains of quartz inclusions in kyanite in the quartz eclogite of the Sanbagawa belt show a range of ε_1+ε_2 from -5×10^{-3} to -21×10^{-3} and ε_3 from $+4\times10^{-3}$ to -4×10^{-3}.

The strains estimated from the Raman spectra of quartz inclusions tended to be retained closer to the hydrostatic conditions for the samples with lower peak temperature conditions. Conversely, the sample of the highest temperature condition, the quartz eclogite of the Sanbagawa belt, tended to show a smaller *c*-axis strain (ε_3) than under hydrostatic conditions. This result indicates that the higher the peak metamorphic temperature, the more easily the inclusion strain is relaxed, especially in the *c*-axis direction. In addition, the ε_3 tended to be more relaxed for quartz inclusions in kyanite host. This is due to the anisotropy of the elastic modulus of kyanite, which may lead to resolve the strain, depending on the relationship of the crystal orientation of host and inclusion. Strain analysis of inclusion minerals using Raman spectroscopy is expected to provide new clues to reconstruct the metamorphic history in more

©2021. Japan Geoscience Union. All Right Reserved.

detail.

References

Angel, R. J. et. al. (2019). *Zeitschrift Für Kristallographie - Crystalline Materials*, 234(2), 129–140.
Murri, M., et. al. (2018). *American Mineralogist*, 103(11), 1869–1872.
van Schrojenstein Lantman, H. W. et. al. (2020). *Journal of Metamorphic Geology*, 1–18.

Keywords: strain, inclusion mineral, Raman spectroscopy, quartz, garnet, kyanite

©2021. Japan Geoscience Union. All Right Reserved.

[J] Poster | S (Solid Earth Sciences)：S-MP Mineralogy & Petrology

Sun. Jun 6, 2021 5:15 PM - 6:30 PM JST | Sun. Jun 6, 2021 8:15 AM - 9:30 AM UTC | Ch.12_2

[S-MP26] Physics and Chemistry of Minerals

convener:Masahiro KAYAMA(Department of General Systems Studies, Graduate School of Arts and Sciences, The University of Tokyo), Itaru Ohira(Department of Chemistry, Faculty of Science, Gakushuin University)

Minerals are important constituent materials of the Earth and planetary bodies.
New results and findings of the physics and chemistry of minerals (including crystal, amorphous and melts) obtained from various analytical approaches, experimental methods (e.g, electron microscope, X-ray diffraction, FT-IR, and Raman spectroscopy), and computer simulations) will be discussed here.

[SMP26-P01] Pressure-induced phase transitions in wülfingite (Zn(OH)2): Raman spectroscopic and First-principles study

*Masami Kanzaki[1], Longli Guan[1], Ran Wang[1] (1.Institute for Planetary Matereials, Okayama University)

[SMP26-P02] Elastic wave velocity of ε-FeOOH across the pressure-induced spin transition of iron

*Osamu Ikeda[1], Tatsuya Sakamaki[1], Hiroshi Fukui[2,3], Hiroshi Uchiyama[4], Alfred Q.E. Baron[3,4], Akio Suzuki[1] (1.Department of Earth Science, Graduate School of Science, Tohoku University, 2.Graduate School of Material Science, University of Hyogo, 3.RIKEN SPring-8 Center, 4.Japan Synchrotron Radiation Research Institute)

[SMP26-P03] Phase transition of M3+OOH-type oxyhydroxides under high pressure

*Akio Suzuki[1] (1.Department of Earth Science, Graduate School of Science, Tohoku University)

[SMP26-P04] Density measurement of silicate melt by the buoyancy test under high pressure

*Akio Suzuki[1] (1.Department of Earth Science, Graduate School of Science, Tohoku University)

[SMP26-P05] Structural study on the $Ca_2MgAl_2Si_4O_{14}$ composition melt under pressure

*Natsumi Adachi[1], Satoru Urakawa[1], Hidenori Terasaki[1] (1.OKAYAMA UNIVERSITY)

[SMP26-P06] Unique luminescence of rhodochrosite at low temperature

*Reina Masuda[1], Ayane Asano[1], Nobuhiro Kusano[1], Hirotsugu Nishido[1] (1.Biosphere-Geosphere Science, Okayama University of Science)

[SMP26-P07] Amesite and Al-serpentine accompanied with the serpentinite in Yakiyama, Iizuka, Fukuoka

*Yuki Isshiki[1], Seiichiro Uehara[2], Yuya Takeda[1] (1.Department of Earth and Planetary Sciences Faculty of Science, Kyushu University, 2.The Kyushu University Museum)

[SMP26-P08] Phase transitions and pressure calibration points

*Shigeaki Ono[1] (1.Japan Agency for Marine-Earth Science and Technology)

[SMP26-P09] The study on stability and properties of N-doped spinel Based on CGCNN and DFT

*SOK I TAM[1], CHI PUI TANG[1], Pak Kin Leong[1], Kin Tak U[1] (1.Macau University of Science and Technology)

Pressure-induced phase transitions in wülfingite (Zn(OH)2): Raman spectroscopic and First-principles study

*Masami Kanzaki[1], Longli Guan[1], Ran Wang[1]

1. Institute for Planetary Matereials, Okayama University

$Zn(OH)_2$ has several polymorphs at ambient pressure, and one of which, epsilon phase, is known as the mineral wülfingite. Wülfingite has a cristobalite-like structure, and pressure-induced phase transitions were found at 1.1 and 2.1 GPa using in-situ X-ray diffraction study by Kusaba et al.[1] Since the coordination number of Zn is 4 in most of those polymorphs known so far, which is very different from that of brucite ($Mg(OH)_2$), the hydrogen bonding behavior is expected to be different. In this study, we investigated structural changes and the associated changes in hydrogen bonding using in-situ Raman spectroscopy and first-principles calculations.

Wülfingite was synthesized as follows. Zinc sulfate 7-hydrate was dissolved in water and sodium hydroxide solution was added to it to form a white precipitate. This precipitate was ZnO. When the filtered solution of the precipitate was left at room temperature for several weeks, large, transparent crystals grew, but small white crystals adhered to the surface. The clear crystals were identified as wülfingite and the white crystals as ZnO from powder X-ray diffraction and Raman spectroscopy. Clear crystal without ZnO was selected for DAC study. The pressure medium was a methanol-ethanol mixture, and ruby fluorescence method was used for pressure measurements.

In the high-pressure in situ Raman measurements, several new peaks appeared at about 1 GPa in addition to the previous Raman peak of wülfingite. According to Kusaba et al.[2], the transition at 1 GPa is reported to be a single-crystal-to-single-crystal transition from orthorhombic wülfingite to a tetragonal structure. This single-crystal-to-single-crystal transition was also confirmed by observation using a Raman microscopy. Wülfingite shows OH stretching peaks at 3190 and 3300 cm^{-1} at ambient pressure, but after the transition, the peaks shift to around 3410 cm^{-1} (with shoulders at 3350 and 3500) and the hydrogen bonding becomes weaker. As the pressure was further increased, the sharp Raman peaks disappeared at around 2 GPa and were replaced by broad peaks, which is consistent with previous X-ray studies showing a change to a broad X-ray pattern at 2.1 GPa. The OH stretching Raman peaks are observed at 3600 and 3650 cm^{-1}. The position of the 3650 cm^{-1} peak at is close to that of $Mg(OH)_2$, suggesting that the coordination number of Zn may have changed to 6. The Raman spectrum does not show a pattern characteristic of amorphous, and the OH peak is not particularly broad, suggesting poor crystallinity of the high-pressure phase rather than amorphization.

First-principles calculations were performed using Quantum-Espresso to optimize the known structures under pressure and to see the pressure changes in volume and enthalpy. Wülfingite, the tetragonal phase found at 1~2 GPa, and the brucite phase were performed. The phase found above 2 GPa could not be calculated due to its unknown structure. The enthalpies at 0 K predict a transition from wülfingite to the tetragonal phase at 4.5 GPa and from the tetragonal phase to the brucite phase at 9 GPa. The brucite phase has been reported to be synthesized at 11~14 GPa, but requires a certain temperature (~400 ^{o}C). In the compression of wülfingite, the transition to the tetragonal phase could not be reproduced, but a transition to a different structure was observed. In this structure, the coordination number of Zn was 5, which increased to 6 at further higher pressures. During decompression of this structure, another 4-coordinated structure was obtained. However, these structures could not explain the X-ray diffraction

©2021. Japan Geoscience Union. All Right Reserved.

patterns observed above 2 GPa, and their enthalpies did not seem to indicate that they could be stable phases. The hydrogen bond distances (O-H...O) of the tetragonal phase is longer than that of wülfingite, which is in agreement with the Raman results.

Both Raman and first-principles calculations show that the hydrogen bonding tends to weaken with pressure. The relatively stronger hydrogen bonding in the 4-coordinate compared to the 6-coordinate cannot be explained by bond strength or bond valence, but is due to the stronger covalent nature of Zn-O in the 4-coordinate. Since Raman spectra of the phases appearing above 2 GPa are very broad, we are planning to obtain good crystallinity data by using an external DAC with higher temperature.

1) Kusaba, K. et al., https://doi.org/10.1088/1742-6596/215/1/012001
2) Kusaba, K. et al., https://doi.org/10.1016/j.cplett.2007.02.009

Keywords: wulfingite, Zn(OH)2, pressure-induced phase transition, Raman spectroscopy, First-principles calculation

©2021. Japan Geoscience Union. All Right Reserved.

Elastic wave velocity of ε-FeOOH across the pressure-induced spin transition of iron

*Osamu Ikeda[1], Tatsuya Sakamaki[1], Hiroshi Fukui[2,3], Hiroshi Uchiyama[4], Alfred Q.E. Baron[3,4], Akio Suzuki[1]

1. Department of Earth Science, Graduate School of Science, Tohoku University, 2. Graduate School of Material Science, University of Hyogo, 3. RIKEN SPring-8 Center, 4. Japan Synchrotron Radiation Research Institute

ε-FeOOH is a high-pressure polymorph of α-FeOOH (goethite), and has been reported to be a crucial candidate of the water carriers into deep mantle via subduction (Nishi et al., 2019; Liu et al., 2019). Despite the importance of ε-FeOOH for water transportation, its elastic property is still unclear. At pressure of ~45 GPa, the phase shows the electronic high-spin to low-spin transition of iron which leads the density to higher along compression (Gleason et al., 2013). The elasticity is expected to be significantly affected by the spin transition.

We present the effect of the spin transition on the elastic wave velocity of ε-FeOOH under pressure. The sample was polycrystalline ε-FeOOH, which was synthesized in advance from a powder of α-FeOOH at a high-pressure and high-temperature condition. A pellet of the sample was enclosed in each sample chamber of a diamond anvil cell with either NaCl or glycerol as a pressure medium. The high-pressure experiments have been conducted at BL35XU in SPring-8 (Baron et al., 2000), and the longitudinal wave velocity, V_P, and density were measured up to a pressure 56 GPa at room temperature, combining non-resonant Inelastic X-ray scattering (IXS) spectroscopy and powder X-ray diffraction (XRD) method. Incident X-ray was monochromatized to 17.794 keV and focused to 16 ×16 μm. Scattered X-ray was analyzed by 12 analyzer crystals whose scattering angles correspond to the momentum transfer Q of 4.2–8.4 nm^{-1}, and the dispersion curve of the longitudinal acoustic phonon was determined. Diffracted X-ray was captured by a flat panel detector and the unit-cell parameters of the sample were obtained. V_P, which is the gradient of the dispersion curve at $Q \rightarrow 0$, was yielded by fitting the curve with a sine function. The pressure was calculated using the equations of state of the sample (Thompson et al., 2020).

In the pressure range below 20 GPa, V_P of ε-FeOOH in this study was consistent with that of a previous study using the ultrasonic method and multi-anvil apparatus (Ikeda et al., 2019). A ~4% drop in V_P was observed at pressures 40, 41, and 42 GPa, which is ~4 GPa below the spin transition in ε-FeOOH. This drop is considered to be the results of a decrease of shear modulus, or of an unstable state of electrons at around the transition pressure. V_P in the pressure range 45–56 GPa (the low-spin state) overlapped with the extrapolated V_P from the pressure below 40 GPa.

Reference:

Baron, A.Q.R., Tanaka, Y., Goto, S., Takeshita, K., Matsushita, T. and Ishikawa, T. (2000) An X-ray scattering beamline for studying dynamics. *Journal of Physics and Chemistry of Solids*, **61**, 461–465.
Gleason, A.E., Quiroga, C.E., Suzuki, A., Pentcheva, R. and Mao, W.L. (2013) Symmetrization driven spin transition in ε-FeOOH at high pressure. *Earth and Planetary Science Letters*, **379**, 49–55.
Ikeda, O., Sakamaki, T., Ohashi, T., Goto, M., Higo, Y. and Suzuki, A. (2019) Sound velocity measurements of ε-FeOOH up to 24 GPa. *Journal of Mineralogical and Petrological Sciences*, **114**, 155–160.
Liu, X., Matsukage, K.N., Nishihara, Y., Suzuki, T. and Takahashi, E. (2019) Stability of the hydrous phases of Al-rich phase D and Al-rich phase H in deep subducted oceanic crust. *American Mineralogist*, **104**,

©2021. Japan Geoscience Union. All Right Reserved.

64–72.
Nishi, M., Tsuchiya, J., Kuwayama, Y., Arimoto, T., Tange, Y., Higo, Y., Hatakeyama, T. and Irifune, T. (2019) Solid solution and compression behavior of hydroxides in the lower mantle. *Journal of Geophysical Research: Solid Earth*, **124**, 10231–10239.
Thompson, E.C., Davis, A.H., Brauser, N.M., Liu, Z., Prakapenka, V.B. and Campbell, A.J. (2020) Phase transitions in ε-FeOOH at high pressure and ambient temperature. *American Mineralogist*, **105**, 1769–1777.

Keywords: ε-FeOOH, High pressure, Spin transition, Inelastic X-ray scattering

©2021. Japan Geoscience Union. All Right Reserved.

Phase transition of M3+OOH-type oxyhydroxides under high pressure

*Akio Suzuki[1]

1. Department of Earth Science, Graduate School of Science, Tohoku University

Water is transported by the subducting slab into the Earth’s interior by hydrous phases. Suzuki et al. (2000) synthesized a high-pressure phase of AlOOH and named it the delta-phase. The crystal structure of the delta-phase is isostructural with InOOH. The study on the stability and transition of the M3+OOH-type oxyhydroxides is very important to investigate the transportation of hydrogen in the Earth’s interior. In this study, the phase transition of InOOH was investigated under high pressures and high temperatures. In situ X-ray diffraction study was carried out using multianvil techniques and synchrotron light source at the High Energy Accelerator Research Organization (KEK) in Japan. Based on the time-resolved diffraction measurements, we observed the phase transition from the distorted rutile structure to the pyrite structure of InOOH around 10 GPa.

Keywords: hydrous phase, mantle, high pressure, water, AlOOH, InOOH

©2021. Japan Geoscience Union. All Right Reserved.

Density measurement of silicate melt by the buoyancy test under high pressure

*Akio Suzuki[1]

1. Department of Earth Science, Graduate School of Science, Tohoku University

Density of magma (silicate melt) controls its transportation in the Earth’ s interior. Therefore, it is important to determine the density of silicate melts under high pressure. We adopted the buoyancy test of the density marker crystals in the silicate melt using a multianvil apparatus installed at Tohoku University. Based on the observation of sinking and flotation of the crystals in the melts, we determined the compression curves of sodium and potassium silicate melts.

Keywords: magma, density, mantle, high pressure, sink/float method

©2021. Japan Geoscience Union. All Right Reserved.

Structural study on the $Ca_2MgAl_2Si_4O_{14}$ composition melt under pressure

*Natsumi Adachi[1], Satoru Urakawa[1], Hidenori Terasaki[1]

1. OKAYAMA UNIVERSITY

Natural magmas are predominantly aluminosilicate in composition, and therefore the studies on structural properties of aluminosilicate under pressure is important for understanding the physical properties of magma at depth. The structure of the $Di_{50}An_{50}$ composition ($Ca_2MgAl_2Si_4O_{14}$) melt was studied by X-ray diffraction analysis and molecular dynamics simulations up to 7 GPa and 2200 K. The high pressure and temperature X-ray diffraction experiments were performed by MAX80 installed at AR-NE5C of PF, KEK. X-ray diffraction profiles were measured by energy dispersive X-ray diffractions method. The MD simulations were conducted with the MXDORTO code. The simulation system was composed of 2400 atoms.

Assuming the coordination number of Si is fixed to be four, we evaluated the coordination number of Al from the experimentally determined radial distribution function. It is increases to about five by 7 GPa. Increasing trend of the coordination number of Al with pressure is consistent with the results from the MD simulations. The FSDP of the structure factor shifts toward higher-*Q* side with increasing pressure, indicating shrinkage of intermediate range order by compression. The pressure dependence of the position of the FSDP changes around 4 GPa, showing intermediate range order does not change much above 4 GPa. Shrinkage of intermediate range order is thought to be correlated to the reorganization of TO_4 networks. These structural changes in the $Ca_2MgAl_2Si_4O_{14}$ melt were considered to correspond to the physical properties, such as viscosity, of the basaltic magma under pressure.

Keywords: magma, aluminosilicate, X-ray diffraction, molecular dynamics simulation

©2021. Japan Geoscience Union. All Right Reserved.

Unique luminescence of rhodochrosite at low temperature

*Reina Masuda[1], Ayane Asano[1], Nobuhiro Kusano[1], Hirotsugu Nishido[1]

1. Biosphere-Geosphere Science, Okayama University of Science

Cathodoluminescence (CL) of carbonate minerals has been widely applied in earth science as it has become a common method in carbonate sedimentology. In most cases of calcite-type carbonate minerals, their CL involve two types of impurity centers as activator of Mn^{2+} and quencher of Fe^{2+}. If the content of Fe^{2+} is low in the carbonates, the concentration of Mn^{2+} almost controls the CL emission intensity. It has been believed that the CL activated by Mn^{2+} should be quenched above ~50,000 ppm of Mn due to concertation quenching (e.g., Machel et al., 1991). Walker et al. (1989) reported that rhodochrosite ($MnCO_3$) emits an intense luminescence below 77 K, but extinction at room temperature. However, the mechanism of CL emission in high-Mn carbonates has not yet been elucidated. In this study, we have conducted to clarify the emission mechanism in rhodochrosite by spectral analyses of CL data obtained at various temperatures.

The single crystals of fourteen rhodochrosite from various localities were employed for CL measurements. The CL spectra were obtained by using an SEM-CL system (SEM combined with a grating monochromator) ranging from 300 to 800 nm under a control of sample temperature from −192 to 25 ºC with a cryo-stage. The digitized data were totally sensitive-corrected for all optical paths including grating and photomultiplier tube.

Most samples begin to emit CL in a red region below −100 ºC and increase rapidly during cooling down to near liquid nitrogen temperature, whereas no emission was detected in all samples at room temperature. The CL data were converted into energy unit from wavelength unit for quantitative spectral analysis. Each spectrum is composed of a broad emission band at ~700 nm, which shows clearly higher than previously reported values of calcite: Mn (~620 nm) and magnesite: Mn (~650 nm). It implies that the crystal-field strength (Dq) should be quite higher than other calcite-type carbonates due to a shorter distance between metal (Mn) and ligand in rhodochrosite. A drastic reduction of the CL intensity with increasing temperature can be well explained by a temperature quenching theory known as Mott-Seitz model based on an increase in the probability of non-radiative transition with the rise of temperature (calculated activation energy of ~0.03 eV). The fact suggests that a sample temperature strongly controls the travelling range of the energy, which causes concertation quenching by transfer to the adjacent Mn ions. Consequently, a unique CL in rhodochrosite should be understood as the result of the competition between the effects of temperature quenching and concertation quenching possibly by Förster energy transfer (FRET) model.

<references>
Machel, G., Mason, R., Mariano, N. and Mucci, A. (1991) Causes and emission of luminescence in calcite and dolomite, SEPM Short Course Notes, 25, 9-25.
Walker, G., Abumere, O. and Kamaluddin, B. (1989) Luminescence spectroscopy of Mn^{2+} centers in rock-forming carbonates, Mineralogical Magazine, 53, 103-140.

Keywords: Luminescence, Rhodochrosite, Temperature quenching, Concertation quenching

©2021. Japan Geoscience Union. All Right Reserved.

Amesite and Al-serpentine accompanied with the serpentinite in Yakiyama, Iizuka, Fukuoka

*Yuki Isshiki[1], Seiichiro Uehara[2], Yuya Takeda[1]

1. Department of Earth and Planetary Sciences Faculty of Science, Kyushu University, 2. The Kyushu University Museum

1.Introduction

Serpentine has an ideal chemical composition of Mg3Si2O5(OH)4, and generally contains small amounts of Fe and Al. Amesite (Mg, Al)3(Si, Al)2O5(OH)4 is one of the mineral that has a solid solution relationship with serpentine, and the intermediate composition is called Al-serpentine. Al-serpentine (7 Å) is polymorphic with clinochlore (14 Å) and is considered to be a low-temperature phase (metastable phase), which is mineralogically important. However, the occurrence of Al-serpentine and amesite is relatively rare, and detailed mineralogical descriptions are scarce. In this study, we found amesite and Al-serpentine in rodingites associated with serpentine bodies in this area, and investigated their occurrence and mineralogical properties.

2. samples and experiments

We observed rodingites in serpentinites and examined their constituent minerals in and around Yakiyama, Iizuka City. The samples were observed by naked eye and Stereoscopic microscopes followed by X-ray diffraction analysis (Rigaku Ultima IV, Rigaku RINT RAPID II), polarized light microscopy and scanning electron microscopy (SEM-EDS: JEOL JSM-7001F). TEM (JEOL JEM-3200FSK, JEM-ARM200CF) at the Research Center for Ultramicroscopic Analysis, Kyushu University was also used to observe the microstructure of thin film and powder samples.

3. results

Eleven rodingite outcrops were identified by field observations. Rodingites are composed of Ca- and Al-rich minerals such as epidote-clinozoisite, calcite, grossular, clinochlore, thomsonite, prehnite, and titanite. Amesite was found in three rodingite outcrops (samples Rod3, 7 and 9). Amesite and Al-serpentine are found in two types: veinlets in the rodingites and scattered with calcite and thomsonite around the veins.

Sample Rod3 contains white opaque Al-serpentine with associated light brown transparent amesite. The XRD analysis of both samples is consistent with the pattern of lizardite-$6T_1$. The white opaque part had very small crystals (about 50-300 nm) and was a mixture of plate-like, hollow cylindrical with plate-like crystals inside, fibrous, and irregularly shaped. The chemical composition of each crystalline particle was three phases: amesite, lizardite, and an excess of Si or Al than amesite-lizardite. Microstructural observation showed that these were mixed together. The hollow cylindrical part shows polygonal columnar lattice fringes by TEM observation, but the shape of the sectors is irregular and the lattice fringes at the sector boundaries cannot be confirmed, which is different from polygonal serpentine reported so far. In addition, the hollow cylindrical part has an Al cation number of about 1.3 (O=7), suggesting that it may be a mineral with a kaolin-like structure in which the size of the tetrahedral and octahedral sheets is reversed from that of ordinary serpentine, and the combination of the two sheets is reversed. Inside the hollow cylindrical section, there is a plate-like section bisecting the circle and parallel to the cylinder. The plate-part have an excess of Si or Al, and TEM observation shows a mixture of 7 Åand 14 Ålayers.

The light brown transparent part is coarse-grained (200 μm), and at the boundary with the white part,

©2021. Japan Geoscience Union. All Right Reserved.

there is a 1 μm filamentous crystal extending toward the white part. The composition of the crystals is non-uniform even within a single crystal, and EDS mapping revealed two types of crystals: one with a mosaic-like non-uniform composition and the other with a clear separation of Al concentration. The former was euhedral with a clear cleavage, while the latter was semi-euhedral, and the filamentous crystals described above were derived from this crystal. The composition of each is generally consistent with a solid solution of lizardite-amecite, but the Al-rich part tends to be Al or Si-rich, and may contain OH-rich material due to the low compound total.

Keywords: serpentine, amesite, rodingite, chlorite, Al-serpentine

©2021. Japan Geoscience Union. All Right Reserved.

Phase transitions and pressure calibration points

*Shigeaki Ono[1]

1. Japan Agency for Marine-Earth Science and Technology

Some phase transitions have been used as pressure calibration in high-pressure experiments, because reliable characterization of the pressure and temperature environment is of essential importance when we apply laboratory data to the study of the Earth's interior. In order to know reliable pressure environment, we can use the synchrotron X-ray source for the high-pressure studies. The in-situ pressure measurement has been accessible by the synchrotron X-ray technique. In the case of conventional laboratory experiments, this technique cannot be used and the conventional pressure calibration is of great interest to understand the Earth's interior. We have investigated several high-pressure phase transitions used as the pressure calibration points. Precise determinations of phase boundaries of SiO_2 [1], Fe_2SiO_4 [2], $CaGeO_3$ [3], ZnS [4], ZnSe [5], GaAs [6], GaP [7], Zr [8], and Bi [9] were performed by the multi-anvil press or the diamond anvil cell apparatuses combined with the synchrotron X-ray diffraction technique. Most transition pressures determined our studies were in general agreement with those reported by previous studies. However, some significant discrepancies for the pressure values or the slopes, dP/dT, of transitions between our and previous studies were confirmed. These discrepancies are due to the significant kinetics effect at the phase transition, because an apparent hysteresis was confirmed at relatively low temperature conditions. This indicates that the phase transitions accompanied with the significant hysteresis are not suitable for the pressure calibration.

[1] S. Ono et al. (2017) In situ determination of the phase boundary between coesite and stishovite in SiO_2, Phys. Earth Planet. Inter., 264, 1-6.

[2] S. Ono et al. (2013) In situ observation of a phase transition in Fe_2SiO_4 at high pressure and high temperature, Phys. Chem. Minerals, 40, 811-816.

[3] S. Ono et al. (2011) In situ observation of a garnet-perovskite transition in $CaGeO_3$, Phys. Chem. Minerals, 38, 735-740.

[4] S. Ono, T. Kikegawa, (2018) Determination of the phase boundary of ZnS, Phase Transition, 91, 9-14.

[5] S. Ono (2020) Phase transition in ZnSe at high pressures and high temperatures, J. Phys. Chem. Solids, 141, 109409.

[6] S. Ono, T. Kikegawa (2018) Phase transformation of GaAs at high pressures and temperatures, J. Phys. Chem. Solids, 113, 1-4.

[7] S. Ono, T. Kikegawa (2017) Determination of the phase boundary of GaP using in situ high-pressure and high-temperature X-ray diffraction, High Press. Res., 37, 28-35.

[8] S. Ono, T. Kikegawa (2015) Determination of the phase boundary of the omega to beta transition in Zr using in situ high-pressure and high-temperature X-ray diffraction, J. Solid State Chem., 225, 110-113.

©2021. Japan Geoscience Union. All Right Reserved.

[9] S. Ono (2020) High-pressure phase transition of bismuth, High Press. Res., 38, 414-421.

Keywords: Phase transformation, High-pressure experiment

©2021. Japan Geoscience Union. All Right Reserved.

The study on stability and properties of N-doped spinel Based on CGCNN and DFT

*SOK I TAM[1], CHI PUI TANG[1], Pak Kin Leong[1], Kin Tak U[1]

1. Macau University of Science and Technology

Spinel (AB_2X_4) is an essential mineral in geology and an important semiconductor and ceramic material. Doping with different atoms will change the properties of spinel and give them unique properties. The crystal graph convolutional neural network (CGCNN) developed by Xie et al. They use graphs to represent the crystal structure and apply neural graph networks to material performance prediction. Taking perovskite as an example, CGCNN has excellent prediction performance.

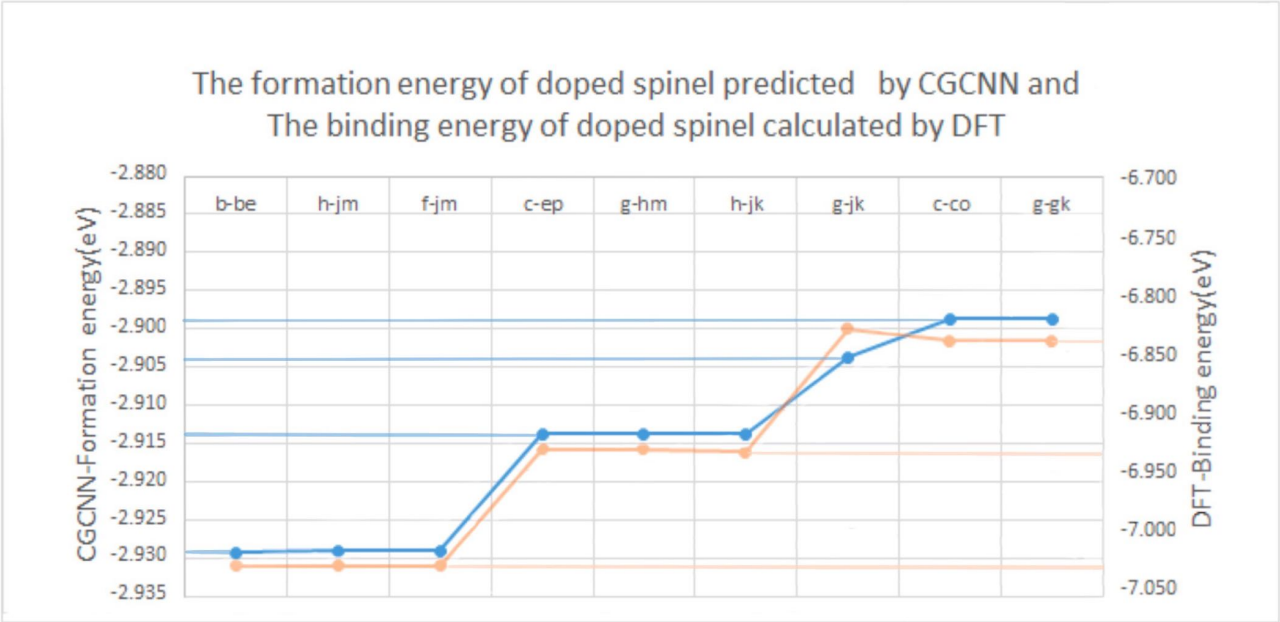
This study verified whether CGCNN is suitable for predicting the formation energy of doped spinel. The formation energy predicted by CGCNN is compared with the theoretical energy (binding energy) calculated by DFT.

From thousands of CGCNN predicted formation energies of doping Mg_2SiO_4 structure, which Mg is replaced by Si and O is replaced by N at different atomic ratios. We choose 3 data from the lowest, middle, and highest values respectively (9 data in total). And use DFT to calculate the binding energy at the corresponding structure of doping Mg_2SiO_4. The calculation results are shown that the changing trend between CGCNN and DFT is almost the same in Figure 1. It implies that CGCNN is suitable for predicting doped spinel. Through the auxiliary exploration of CGCNN. We found a possible nitrogen-doped oxygen structure of spinel ($MgAl_2O_{3.5}N_{0.5}$) in other work.

This work is supported by the Science and Technology Development Fund of Macau (File No. 0111/2020/A, 0042/2018/A2)

Keywords: CGCNN, DFT, Spinel

©2021. Japan Geoscience Union. All Right Reserved.



©2021. Japan Geoscience Union. All Right Reserved.

[J] Poster | S (Solid Earth Sciences)：S-VC Volcanology

Sun. Jun 6, 2021 5:15 PM - 6:30 PM JST | Sun. Jun 6, 2021 8:15 AM - 9:30 AM UTC | Ch.13_1

[S-VC27] Mitigation of volcanic disasters - basic and applied researches

convener:Shinji Takarada(Geological Survey of Japan, National Institute of Advanced Industrial Science and Technology), Mitsuhiro Yoshimoto(Mount Fuji Research Institute, Yamanashi Prefectural Government), Tatsuro Chiba(Asia Air Survey Co., Ltd.), Yousuke Miyagi(National Research Institute for Earth Science and Disaster Resilience)

Volcanic disasters are caused by wide range of volcanic phenomena including ash fall, pyroclastic flow, debris avalanche, lahar, and lava flow. To mitigate volcanic disasters, wide range of technologies including simulation, data processing on GIS, and communication techniques are required. Researches on volcanic hazards mapping, eruption scenarios, estimation of tephra falls, and probabilistic eruption assessments are getting important. This session invites presentations and broad reviews related to these topics. Contributions on database technology, case studies of social and school educations, the Next Generation Volcano Research, and specific examples of eruption crisis events are also encouraged.

[SVC27-P01] Disaster-stricken vehicles dug up for the first time in 30 years and characteristics of pyroclastic surge deposits in 1991 on Unzen Volcano

*Daisuke Nagai[1], Shinichi Sugimoto[2] (1.Mt.Unzen disaster memorial hall, 2.Unzen volcanic area global geopark)

[SVC27-P02] Selective pulverization of pumiceous groundmass in pumice pulverization processes in a laboratory

*Shingo Takeuchi[1] (1.Central Research Institute of Electric Power Industry, Civil Engineering Research Laboratory, Geosphere Sciences)

[SVC27-P03] A case of sediment-related disaster in a volcanic area due to an earthquake off the coast of Fukushima Prefecture on February 13, 2021

*Takayama Toko[1], Tatsuro Chiba[1], Hiromichi Moriike[1], Tatsuya Ochiai[1] (1.Asia Air Survey Co.,Ltd.)

[SVC27-P04] Accelerating Two-Dimensional Lava Flow Simulations with OpenACC

*Yasuhiro Ishimine[1] (1.Mount Fuji Research Institute, Yamanashi Prefectural Government)

[SVC27-P05] Present situation of water pollution problem caused by 2018 Iwo-Yama volcano eruption in Kirishima volcanic complex

*Yoshikazu Kikawada[1], Haruka Yamamoto[2] (1.Faculty of Science and Technology, Sophia University, 2.Graduate School of Science and Technology, Sophia University)

[SVC27-P06] Training program of the human resource development for volcanic disaster management officers in JAPAN -Preliminary report-

*Kenji Niihori[1], Akio Sato[1], Maokoto Konno[1], Mitsuhiro Yoshimoto[2] (1.Organization of Volcanic Disaster Mitigation, NPO., 2.Mount Fuji Research Institute, Yamanashi Prefectural Government)

[SVC27-P07] Experiment for understanding of climber's movement and tendency in Nasu Volcano

*Yousuke Miyagi[1], Mitsuhiro Yoshimoto[2], Yasuhiro Ishimine[2], Ryo Honda[2], Tomohiro Kubo[2] (1.National Research Institute for Earth Science and Disaster Resilience, 2.Mount Fuji Research Institute, Yamanashi Prefectural Government)

[SVC27-P08] Eruption Sequences and Precursory Activities of Large-scale Volcanic Eruptions, and Construction of Large-scale Volcanic Eruption Database

*Shinji Takarada[1], Yasuaki Kaneda[1], Fumihiko Ikegami[1], Yuki Nishino[1], Nobuo Geshi[1] (1.Geological Survey of Japan, National Institute of Advanced Industrial Science and Technology)

Disaster-stricken vehicles dug up for the first time in 30 years and characteristics of pyroclastic surge deposits in 1991 on Unzen Volcano

*Daisuke Nagai[1], Shinichi Sugimoto[2]

1. Mt.Unzen disaster memorial hall, 2. Unzen volcanic area global geopark

It has been 30 years since the eruption of Mt. Unzen Fugen killed 43 people. In the local area, the improvement plan of the disaster area is being made and the construction is being carried out. In the construction on February 8, 2021, 4 damaged cars were excavated and visited as they were 30 years ago. The vehicles will be installed on concrete foundations after volcanic ash and other soil is removed. Since the vehicle was salvaged by a heavy machine at the time of this excavation, we had an opportunity to investigate the damage of the entire vehicle which had not been investigated after the disaster, and the pyroclastic surge deposits accumulated in and around the vehicle body in 1991. The investigation was carried out in Kitakamikiba Town, Shimabara City, where many reporters called "fixed point" were present at that time, in a vehicle blown about 70 m downstream from a road by a pyroclastic flow generated on June 3, 1991. Two cars are placed close to each other at the same place, and the cars on the upstream side are placed facing the rear side with the north side facing the front, while the other cars on the downstream side are placed facing the obliquely rear side with the south side facing the front and are placed to lean against the cars on the upstream side. Judging from the testimonies at the time and the pictures and images left by the victims just before the disaster, it is assumed that the two taxis were chartered by the press. Through the excavation, license plates were dug up from cars on the mountain side, and it was discovered that the cars were "Koarashi Taxi".No license plate that could be read from the other car was found, but as a result of identifying the rest of the damaged cars, it was found that the car belonged to the "Maruzen Taxi". The body of the driver of Maruzen Taxi was found near the fixed point. On the other hand, it is probable that the driver of the Koarashi Taxi was in the taxi and suffered from the disaster because he was found somewhere between the fixed point and the excavated vehicle (About 30 m downstream from the fixed point) and communicated with his colleague's vehicle by radio until just before the excavation. In the aerial photograph taken on June 5, there was a damage on the wall surface of the gutter southeast of the location where both cars were supposed to have been, as if something had hit the wall surface, and further downstream, there was a cut mark of about 3 m in width and about 10 m in length, as if the ground had been dragged. Since there is a damaged vehicle on the extension of the cut mark, it is probable that this cut mark was made in the process in which the vehicle was transported by the impact of the pyroclastic surge. The entire engine section and the body of the vehicle were damaged so that they could be broken, and the bumpers, the bonnet, the roof, the bottom surface of the vehicle, and the entire body were found to have large dents that received an impact. It is presumed that the car body was carried rolling because there were relatively uniform dents in the whole car body and no falling marks on the ground. When the car body was dug out, an electric wire was caught around the body. It is known that there was a utility pole nearby, and it is known that the utility pole got entangled with electric wires and wound around the car body as the car moved. A pyroclastic surge deposit on June 3, 1991 around the vehicle was also found. The sediments are about 3 cm thick. The thickness diagram of the pyroclastic surge deposits including the surrounding observation sites suggests that the area was located near the major axis in the distribution basin. The excavated vehicles will be displayed on the site and will be used as a base for disaster learning by the local residents' association. It is hoped that the remains will enhance people's awareness of disaster prevention.

©2021. Japan Geoscience Union. All Right Reserved.

Keywords: pyroclastic surge, volcanic disaster, disaster prevention education



©2021. Japan Geoscience Union. All Right Reserved.

Selective pulverization of pumiceous groundmass in pumice pulverization processes in a laboratory

*Shingo Takeuchi[1]

1. Central Research Institute of Electric Power Industry, Civil Engineering Research Laboratory, Geosphere Sciences

The pulverization characteristics of volcanic rocks have recently been the subject of much experimental research from the viewpoint of volcanic ash generation during the eruption processes. The pulverization characteristics are also important for preparing artificial volcanic ash by pulverizing volcanic rocks and sieving the pulverized materials for experimental studies on the adverse effects of volcanic ash on equipment and facilities. The author has been experimentally investigating the pulverization characteristics of porous volcanic rocks for manufacturing artificial volcanic ash (Takeuchi, 2020). In this presentation, I investigate the variation in the ratio of crystal to glass at each ϕ-scale sieve class by pulverizing phenocryst-bearing pumice samples.

The Osumi pumice (Os), which is available in large quantities and is expected to produce pumiceous particles, was used as a raw material for the pulverization experiments. Lapilli with -1 ϕ (2000 μm) class were prepared as starting samples by a jaw crusher and manual sieving. The intensity of a disk mill used to pulverize the starting samples was varied by adjusting the slit width between the rotating metal discs. A Vibratory Sieve Shaker (FRITSCH A-3PRO) was used to sieve the pulverized material. The Vibratory Sieve Shaker is electro-magnetically controlled and can be loaded with vertical vibrations of 3000 times/min in the amplitude range of 0.1 to 3.0 mm, and the mass variation with the sieving time can also be confirmed to maintain objectivity in judging the end of sieving.

The difference in pulverization intensity produced a difference in the particle size distribution of the pulverized material as follows. For the wide and narrow slit widths, the median particle sizes (f_{50}) are -1.0 ϕ (2000 μm) and 1.5 ϕ (354 μm), and the mass fractions with a sieve class of less than 4 ϕ are 9% and 34%, respectively.

Based on the bulk rock composition obtained by XRF analysis and the average composition of each crystal and glass obtained by EPMA analysis, the mass fraction of crystal and glass for each class was quantified by mass balance calculation. As a result, the following characteristics of the crystal content, which changed during the pulverization and sieving processes, were clarified. Compared to crystal content (about 10%) of the raw material, the crystal content increases (up to ca. 30%) in the 1 ϕ (500 μm) to 3 ϕ (125 μm) particles. Crystal content decreases down to ca. 5% in the pulverized material of less than 4 ϕ (63 μm). Weak pulverization tended to result in a greater crystal content in sieve classes larger than 1 ϕ. The -1 ϕ (2000 μm) sieve class in the pulverized material has a lower crystal fraction than the starting sample (-1 ϕ, 2000 μm). The size distribution of the crystals (phenocryst) in the Os pumice obtained from image analysis of the elemental and electronic images of EPMA for the polished section of pumice lapilli was consistent with the crystal-rich sieve class of the pulverized material. I interpret that when the material is subjected to disk milling, the phenocryst in pumice is likely to be separated as free crystals, and the separated phenocryst is relatively difficult to be pulverized, and the pumiceous glassy matrix was selectively pulverized to a sieve class of less than 4 ϕ (63 μm). This variation in crystal content in pulverization and sieving processes of phenocryst-bearing pumices is an important note on the properties of artificial volcanic ash when using for experiments.

©2021. Japan Geoscience Union. All Right Reserved.

Keywords: pumice pulverization and sieving experiments, volcanic ash hazard, phenocryst, volcanic glass

©2021. Japan Geoscience Union. All Right Reserved.

A case of sediment-related disaster in a volcanic area due to an earthquake off the coast of Fukushima Prefecture on February 13, 2021

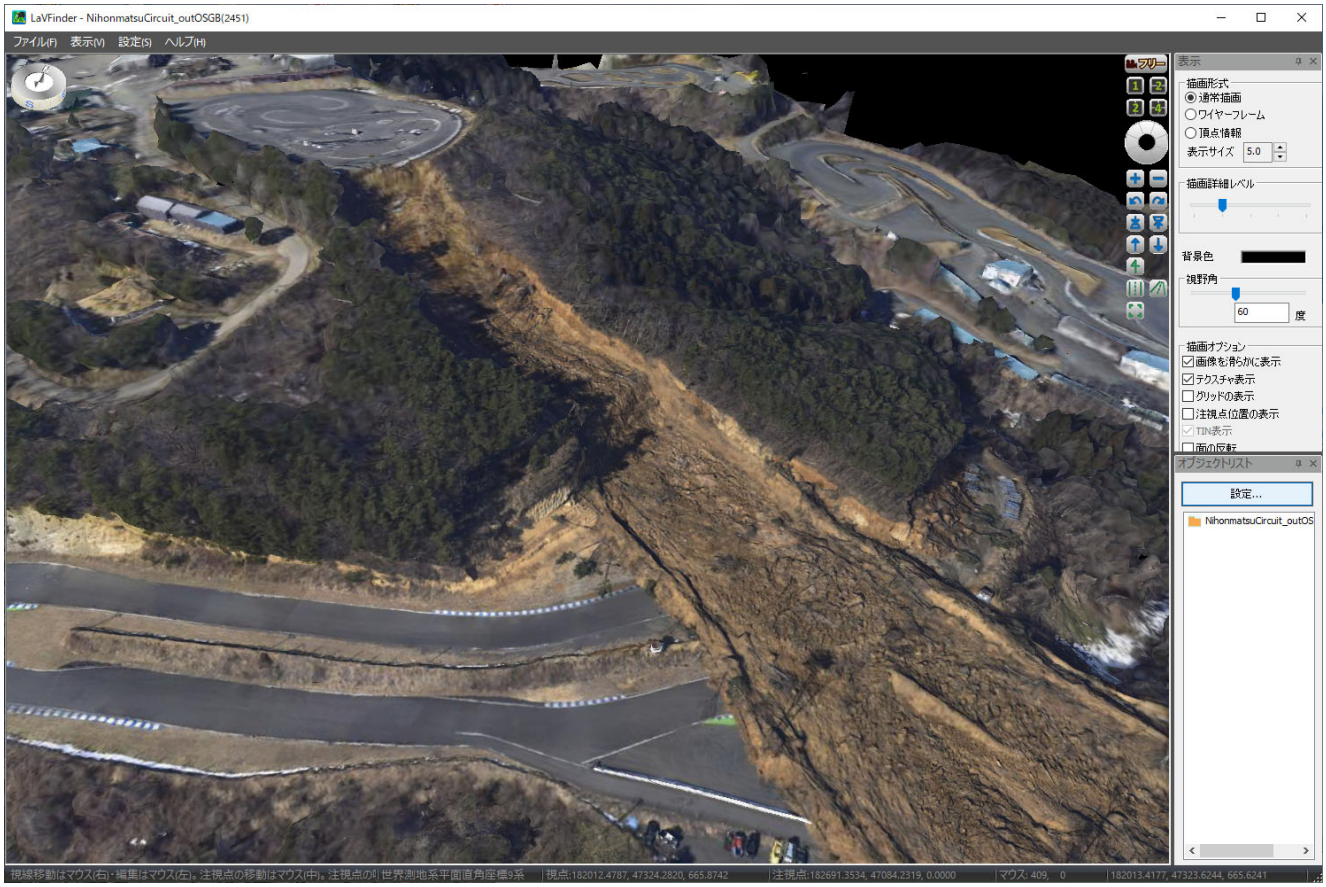
*Takayama Toko[1], Tatsuro Chiba[1], Hiromichi Moriike[1], Tatsuya Ochiai[1]

1. Asia Air Survey Co.,Ltd.

Sediment disasters were found in several places due to an earthquake that occurred off the coast of Fukushima Prefecture on February 13, 2021. In Nihonmatsu City, Fukushima Prefecture, a large-scale landslide occurred on the slope at the foot of Mt. Adatara in the volcanic area.

In order to grasp the scale of the collapse and to contribute to the mechanism analysis, aerial photogrammetry by the SfM-MVS method was carried out using the aerial oblique photograph taken on February 14, the following day of the earthquake, and generated a three-dimensional landform model. In addition, the authors created photographic map (simple orthographic image) and topographic map (Red Relief Image Map).
The authors report the results of analyzing about the landslides, such as the scale of landslide, using remote sensing data.

Keywords: Earthquake, Landslide, Tephra, Structure from Motion –Multi View Stereo, Three-dimensional terrain model



©2021. Japan Geoscience Union. All Right Reserved.

Accelerating Two-Dimensional Lava Flow Simulations with OpenACC

*Yasuhiro Ishimine[1]

1. Mount Fuji Research Institute, Yamanashi Prefectural Government

The performance of Graphics Processing Unit, or GPU, has been much grown in these few decades. While GPU has been originally developed for drawing 3D graphics for video games on computers, for example, at a high speed, GPU can be used for calculating double-precision floating-point values under certain conditions. That enhances General-Purpose Computing on GPUs, or GPGPU, in the field of high-performance computing. In particular, GPGPU research activities are rapidly expanding since the standardization of OpenACC has been initiated in 2011. Here, OpenACC is a directive-based programming model designed to provide a simple and effective approach.

Mount Fuji Research Institute has launched a research project entitled “Improvement of Numerical Simulation Techniques for Enhancing the Validity of Hazard Maps for Volcanic Eruptions” in 2020 and installed a computer with Titan V, which is a GPU developed by nVidia with a theoretical peak performance of 13.8 TFlops for single-precision floating-point calculations. We will present preliminary results of numerical simulations of lava flows that are performed with a numerical model developed by Ishihara (1990) and accelerated with OpenACC.

Keywords: Lava Flow, Numerical Simulation, GPGPU, OpenACC

©2021. Japan Geoscience Union. All Right Reserved.

Present situation of water pollution problem caused by 2018 Iwo-Yama volcano eruption in Kirishima volcanic complex

*Yoshikazu Kikawada[1], Haruka Yamamoto[2]

1. Faculty of Science and Technology, Sophia University, 2. Graduate School of Science and Technology, Sophia University

In April 2018, the first eruption in 250 years occurred at the Iwo-Yama volcano of the Kirishima volcanic complex. The newly opened vents with the phreatic eruptions gushed out the strongly acidic hydrothermal fluids containing toxic metal ions like lead and arsenic. The hydrothermal fluids were transported by a river to the Kakuto Basin at the volcano's foot and significantly impacted the agriculture and fishery in the lower reaches. The hydrothermal discharge from the volcano was prolonged, and the water pollution problem in the lower reaches finally came to an end near three years after the eruption. This study reviews the river water pollution in the Sendai River system caused by the 2018 Iwo-Yama volcano's eruption.

The new small craters opened on the south and west sides of the Iwo-Yama volcano summit area in April 2018, causing phreatic eruptions. There was one eruption at each crater, but a large amount of muddy thermal water discharged from the craters flowed into the Akago River, which originated from the area, and was carried to the Nagae River and the Sendai River. At this time, fish carcasses floated up in the river, and farmers had to give up paddy rice cultivation in the river basin. After that, the craters became thermal water pools, and a large amount of water that overflowed continued to be carried downstream, resulting in the water pollution problem in rivers for several years.

In May 2019, a demonstration experiment of a river neutralization system was started in the Akago River, and all river water, including thermal water from the craters of the Iwo-Yama volcano, began to flow down through the neutralization facility. The system works to reduce the solubility of metal ions dissolved in the river water and produces a neutralization product, resulting in a lower concentration of harmful dissolved components. The water quality of downstream rivers has improved significantly since the start of the neutralization demonstration experiment. At first glance thus, it seems that the effect of river neutralization has appeared. However, at that time, the hydrothermal activity of the Iwo-Yama volcano significantly decreased. The decreased activity resulted in lower acidity and lower concentrations of dissolved components in the crater pool. Besides, the amount of overflow from the pool also decreased at the same time. Consequently, it is unclear whether water quality improvement is due to river neutralization or decreased volcanic activity. On the other hand, referring to the data of river water quality monitoring by Miyazaki Prefecture [1], no significant fluctuations have been seen in river water quality in the downstream area since May 2019, which must be the effect of river neutralization.

As of the end of 2020, the Iwo-Yama volcano's volcanic activity is not so active, and there is little hydrothermal overflow from the thermal pool. The water quality of the Nagae River and the Sendai River in the Iwo-Yama volcano's lower reaches is stable and meets the environmental standard.

[1] Results of Water Quality Inspection of Akago River, Nagae River and Sendai River in Ebino City, https://www.pref.miyazaki.lg.jp/kankyokanri/kurashi/shizen/ebino.html (accessed 2021-02-12)

©2021. Japan Geoscience Union. All Right Reserved.

Keywords: Kirishima volcanic complex, Iwo-Yama volcano, phreatic eruption, water pollution, arsenic, thermal water pool

©2021. Japan Geoscience Union. All Right Reserved.

Training program of the human resource development for volcanic disaster management officers in JAPAN -Preliminary report-

*Kenji Niihori[1], Akio Sato[1], Maokoto Konno[1], Mitsuhiro Yoshimoto[2]

1. Organization of Volcanic Disaster Mitigation, NPO., 2. Mount Fuji Research Institute, Yamanashi Prefectural Government

There are many kinds of training program for natural disaster prevention officers in Japan. However, when it comes to volcanic disaster prevention, only few training programs exist because of the low frequent disaster. On the other hand, national and local government officers in Japan have to change their positions in a few years. Then it is very difficult for them to be specialists against volcanic hazard. In this research, we performed some types of training programs for volcanic disaster prevention officers from all over Japan, and questionnaire survey was conducted in the training programs. As a result, we could reveal the request from natural disaster prevention officers in Japan. From their request, we could re-build up a new type of training programs and method of volcanic disaster prevention.

Keywords: prevention of volcanic disaster, volcanic disaster management officers, training program

©2021. Japan Geoscience Union. All Right Reserved.

Experiment for understanding of climber’ s movement and tendency in Nasu Volcano

*Yousuke Miyagi[1], Mitsuhiro Yoshimoto[2], Yasuhiro Ishimine[2], Ryo Honda[2], Tomohiro Kubo[2]

1. National Research Institute for Earth Science and Disaster Resilience, 2. Mount Fuji Research Institute, Yamanashi Prefectural Government

Recently, many climbers are enjoying climbing in Japan, and can approach to an active vent in many volcanoes, for example Mt. Fuji or Mt. Nasu. In the tragic disaster of Ontake Volcano in 2014, it was difficult for local governments to grasp whereabouts of climbers and to conduct rescue and search for victims. The same issue was raised also in the 2019 eruption of Kusatsu-Shirane Volcano. Therefore, it is quite important to grasp whereabouts of climbers in the event of disaster for proper decision of rescue and search.

Experiments to acquire data of climbers have conducted in Mt. Nasu in 2020, named “Mt. Nasu Challenge”. In the experiment, we distribute 2,000 of beacons to climbers, and 15 of receivers which are set in mountain trails detect signals from the beacons, then we can grasp the number and location of climbers who have the beacons. And it took about two hours to grasp locations of 90% of climbers.

In this research, we are going to use the climber’ s data for disaster prevention. In the event of disaster, it is possible to reduce the time for grasping climber’ s information. In the normal time, local governments can refer the data to make evacuation plans, including establishment of shelters or evacuation routes. We evaluate exposures of climbers against volcanic hazards, including ash fall, volcanic materials, pyroclastic flow, mad flow, and lava flow, cited from Nasu volcano hazard map by using GIS software. First, we convert hazard map data that have been already published to GIS data, and make spatial analysis with the climber’ s data from the experiment. From results of the evaluation, we can make simple damage estimation of climbers.

Keywords: Nasu Volcano, experiment for understanding of climber's movement, evaluation of climber's exposures

©2021. Japan Geoscience Union. All Right Reserved.

Eruption Sequences and Precursory Activities of Large-scale Volcanic Eruptions, and Construction of Large-scale Volcanic Eruption Database

*Shinji Takarada[1], Yasuaki Kaneda[1], Fumihiko Ikegami[1], Yuki Nishino[1], Nobuo Geshi[1]

1. Geological Survey of Japan, National Institute of Advanced Industrial Science and Technology

Volcanic hazards can occur thousands of kilometers away from the volcano due to large-scale PDCs and tephra falls produced from the VEI 5-8 class large-scale eruptions. It is thus important to reveal the past eruption sequences of large-scale eruptions and their long-term and short-term precursory activities for an effective volcanic hazards mitigation measures. Many variations can be observed for the eruption sequences of large-scale eruptions and long-term and short-term precursory activities, which generally do not follow a common pattern. The Geological Survey of Japan, AIST, started a project to compile the characteristics of eruption products, eruption sequences, long-term and short-term precursory and post-caldera activities of large-scale volcanic eruptions. The contents and website of this large-scale eruption database are introduced in this presentation.

The long-term and short-term precursory activities, eruption sequences of main caldera-forming eruption, and post-caldera activities have been currently compiled for a total of 17 large-scale eruptions. These eruptions are the 946AD Chanbaishan-Tomakomai, 6.4 cal ka Ikeda caldera-forming, 7.3 cal ka Kikai-Akahoya, 7.6 cal ka Mashu Main-caldera-forming, 14.6 cal ka Nigorikawa, 15.5 cal ka Towada-Hachinohe, 30 cal ka Aira-Ito, 32 cal ka Towada-Ofudo, 40 cal ka Kutcharo I, 46 cal ka Shikotsu, 60 cal ka Daisen-Kurayoshi, 87-89 ka Aso-4, 95 ka Kikai-Nagase, 106 ka Toya, 108 ka Ata, 110-115 ka Sambe-Kisuki and 120 ka Kutchro IV eruptions. Part of descriptions of these eruptions are published in GSJ Openfile reports (no. 680 and 699; Nishino et al., 2019, Kaneda et al., 2020a).

The precursory activities of large-scale eruptions are categorized into two types: Type I, precursor activities were observed in the last 50 ka, and Type II, no precursor activities were observed. Type I precursory activities are subdivided into 3 types based on the average eruption rates until the main caldera-forming eruptions occur: increased (Type I-1), stayed constant (Type I-2) and decreased (Type I-3) (Kaneda et al., 2020b).

We have developed a Large-scale Eruption Database website, where users can browse and search the long-term and short-term precursory activities, sequences of main caldera-forming eruptions and post-caldera volcanic activities (Figure). Map of the distributions of major eruption products are displayed which could be zoomed in and zoomed out using WebGIS technology. The distributions of tephra falls and pyroclastic flows and the shape of caldera-rims are digitized and saved in GIS format and could be shown using the system. This website will be made accessible to the public within the fiscal year 2021, together with the Plinian Eruption Database, which is also currently developed.

Figure caption: Example of the website of the Large-scale Eruption Database (Aira-Tn Ash Fall descriptions during the main caldera-forming eruption).

©2021. Japan Geoscience Union. All Right Reserved.

Keywords: Large-scale, Eruption sequence, Precursor activities, Caldera, Database

姶良－入戸火砕流噴火

30 cal ka

Aira-Ito Pyroclastic Flow Eruption

総噴出量: 見かけ体積～700 km^3，700×10^{12} kg

姶良Tn火山灰

あいらてぃーえぬかざんばい

Aira Tn Volcanic Ash

年代: 30 cal ka –

Smith et al. (2013)

噴出源: 姶良カルデラ

▼ 噴火推移: プリニー式噴火→大規模火砕流発生 (カルデラ形成)

姶良－入戸火砕流噴火によって噴出し，遠方まで飛散した降下火山灰を姶良Tn火山灰 (AT)と呼ぶ．AT火山灰は姶良カルデラから約1,500 km離れた北海道や，北太平洋の海底からも報告されている．AT火山灰の見かけ体積は150 km^{3}以上と見積もられている (町田・新井，2003)．

AT火山灰は，その岩相からいくつかの降下ユニットに区分されている (Nagaoka, 1988, 河合・三宅，1999)．そのうち，基底のAT1層が大隅降下軽石の遠方相，AT2層 (Nagaoka, 1988のAT Ⅰ，町田・新井1992のA層) 妻屋火砕流の，AT3層及びf4層 (Nagaoka, 1988のAT Ⅱおよび Ⅲ，町田・新井1992のB及びC層) が入戸火砕流からのco-ignimbrite ashと考えられる (河合・三宅，1999)．

分布

日本列島全域を覆い，日本海全域・東シナ海・北太平洋の海底や朝鮮半島からも分布が報告されている (町田・新井，2003)．

噴出量

見かけの体積 > 150 km^3

構成要素体積 [km^3]

> 150

VEI

7

噴出量文献

町田・新井 (2003)

岩質

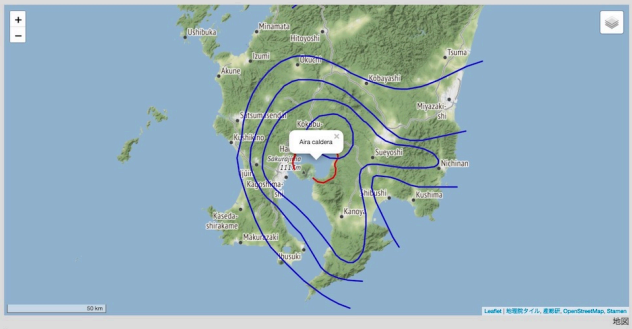
輝石流紋岩

構成物

主にバブルウォール型の火山ガラスからなるが，軽石型も含まれる．遊離結晶は主に輝石である (町田・新井，2003)．

岩相

複数の降下ユニットからなる降下火山灰層 (Nagaoka, 1988, 河合・三宅，1999)．



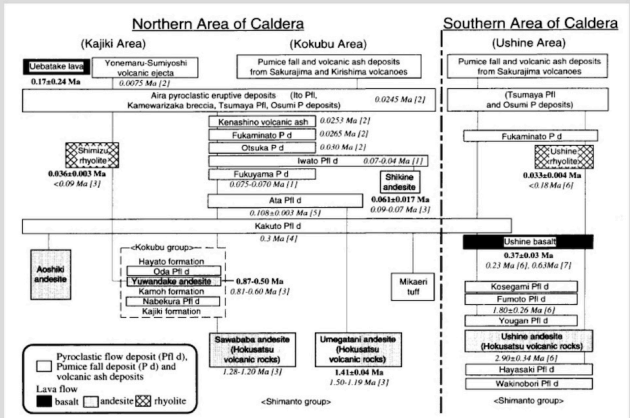


Fig. 3. Block diagrams showing the volcanic history of northern (Kajiki and Kokubu) and southern (Ushine) areas of Aira caldera summarized from Aramaki (1969), Hase *et al.* (1987), Kobayashi *et al.* (1977) Kobayashi and Iwamatsu (1980), Nagaoka *et al.* (1997), New Energy and Industrial Technology Development Organization (1987), Otsuka and Nishiinoue (1980) and Uto *et al.* (1997a). The ages obtained in this study (bold) and reported in the literatures (italic) are also indicated. The blocks whose stratigraphical relations are geologically observed each other are connected by thin lines. References: [1] Nagaoka *et al.*, 1997, [2] Okuno, 1997, [3] New Energy and Industrial Technology Development Organization, 1987, [4] Machida and Arai, 1992, [5] Matsumoto and Ui, 1997, [6] Kaneoka *et al.*, 1984, [7] Inoue, 1994 ms.

姶良カルデラ周辺の火山岩の年代 (周藤ほか，2000)

主要文献

Nagaoka (1988)

文献

Smith et al. (2013): https://www.sciencedirect.com/science/article/pii/S0277379113000413
町田・新井 (2003): http://www.utp.or.jp/book/b301896.html
Nagaoka (1988): https://ci.nii.ac.jp/naid/110008616087/
河合・三宅 (1999): https://www.jstage.jst.go.jp/article/geosoc1893/105/9/105_9_597/_article/-char/ja/

©2021. Japan Geoscience Union. All Right Reserved.

[J] Poster | S (Solid Earth Sciences)：S-VC Volcanology

Sun. Jun 6, 2021 5:15 PM - 6:30 PM JST | Sun. Jun 6, 2021 8:15 AM - 9:30 AM UTC | Ch.13_2

[S-VC29] Hydrothermal systems of volcanoes

convener:Yasuhiro Fujimitsu(Department of Earth Resources Engineering, Faculty of Engineering, Kyushu University), Wataru Kanda(Volcanic Fluid Research Center, School of Science, Tokyo Institute of Technology), Takeshi Ohba(Department of chemistry, School of Science, Tokia University)

There is a diversity of hydrothermal systems between magmas and the ground surface in various geoscientific environments. Understanding of the hydrothermal systems contributes to understanding of the earth systems, and is essential for utilization of geothermal energy and prediction of volcanic eruption. In this session, we will discuss the topics on subsurface structures and heat and fluid flows of "hydrothermal systems of volcanoes" from the perspectives of geophysics, geochemistry, geology and geothermal reservoir engineering. Any research approaches, theoretical, observational and experimental, are welcome.

[SVC29-P01] Groundwater composition around the Aso caldera: multivariate statistical analysis and its implications for independent variables and geographical variations

*Hikaru Iwamori[1], Hitomi Nakamura[2], Noritoshi Morikawa[2], Masaaki Takahashi[2], Akihiko Inamura[2], Satoru Haraguchi[1], Tatsuji Nishizawa[3], Shuhei Sakata[1] (1.Earthquake Research Institute, The University of Tokyo, 2.AIST, 3.TITECH)

[SVC29-P02] Temporal variation of chemical composition of hot spring waters at Ebinokogen Ioyama Volcano in Kirishima Volcanic Group

*Keigo Mori[1], Jun-ichiro Ishibashi[1], Takeshi Matsushima[1], Harue Masuda[2], Syogo Oshima[3], Saki Tsutsumi[3], Yasuhisa Tajima[4] (1.Graduate School of Science, Kyushu University, 2.Graduate school of Science, Osaka City University, 3.West Japan Engineering Consultants, Inc,, 4.Nippon Koei Co., Ltd,)

[SVC29-P03] Temporal variations of helium and carbon isotopic compositions of fumarolic gases from Kusatsu-Shirane volcano

*Tomoya Obase[1], Hirochika Sumino[1], Kotaro Toyama[1], Takeshi Ohba[2], Muga Yaguchi[3], Akihiko Terada[4] (1.Department of General Systems Studies, Graduate School of Arts and Sciences, University of Tokyo, 2.Department of chemistry, School of Science, Tokai University, 3.Meteorological Research Institute, Japan Meteorological Agency, 4.Volcanic Fluid Research Center, Tokyo Institute of Technology)

[SVC29-P04] Change in fluoride ion concentration in Bandaiko hot spring at east flank of Kusatsu-Shirane volcano and its relationship with volcanic activity

*Haruka Yamamoto[1], Yoshikazu Kikawada[2] (1.Graduate School of Sophia University, 2.Faculty of Science and Technology, Sophia University)

[SVC29-P05] Volcanic ash from the June 17, 1962 eruption of Yakedake volcano, and its water-soluble components

*Muga Yaguchi[1], Yasuo Hirayama[2], Takeshi Ohba[3], Nozomi Numanami[3] (1.Meteorological Research Institute, JMA, 2.Nagano Meteorological Office, JMA, 3.School of Science, Tokai University)

[SVC29-P06] Tectonic controlled and hydrothermal alterations of geothermal reservoirs in El Salvador

*JOSE ANIBAL ERAZO[1], Noriyoshi Tsuchiya[1], Masaoki Uno[1], Arturo Quezada[2], Pedro Antonio Santos[2], Ryoichi Yamada[1], Hiroyuki Yamagishi[1], Shinichi Yamasaki[1], Alvaro Josue Amaya[3] (1.Graduate school of environmental studies , 2.LaGeO _ El Salvador, 3.UES _ El Salvador)

[SVC29-P07] DAS-Seismic and temperature data acquisition using DAS and DTS measurements at the Ohnuma, geothermal field, Tohoku, Japan

*Junzo Kasahara[1,2], Yoko Hasada[1,3], Kuzume Haruyasu[1], Hitoshi Mikada[4], Yoshihiro Fujise[5] (1.ENAA, 2.Shizuoka University, 3.Daiwa Exploration and Consulting Co. Ltd., 4.Graduate School of Kyoto University, 5.WELMA)

[SVC29-P08] **Ground surface Heat balance measurements at Izu-Oshima volcano**

*Shin'ya Onizawa[1], Nobuo Matsushima[2] (1.Volcanology Research Department, Meteorological Research Institute, JMA, 2.Geological Survey of Japan, National Institute of Advanced Industrial Science and Technology)

[SVC29-P09] Behavior of magmatic hydrothermal system of Kusatsu-Shirane Volcano inferred from numerical simulations

*Yasuo Matsunaga[1], Wataru Kanda[1] (1.School of Science, Tokyo Institute of Technology)

[SVC29-P10] Comprehension of hydrothermal systems in the East African Rift System –Collaborative Research with Kenya by SATREPS–

*Yasuhiro Fujimitsu[1], Jun Nishijima[1], Takeshi Tsuji[1], Kotaro Yonezu[1], Tatsuya Wakeyama[2], Ryuichi Itoi[3] (1.Department of Earth Resources Engineering, Faculty of Engineering, Kyushu University, 2.Platform of Inter-/Transdisciplinary Energy Research, Kyushu University, 3.School of Engineering, Kyushu University)

Groundwater composition around the Aso caldera: multivariate statistical analysis and its implications for independent variables and geographical variations

*Hikaru Iwamori[1], Hitomi Nakamura[2], Noritoshi Morikawa[2], Masaaki Takahashi[2], Akihiko Inamura[2], Satoru Haraguchi[1], Tatsuji Nishizawa[3], Shuhei Sakata[1]

1. Earthquake Research Institute, The University of Tokyo, 2. AIST, 3. TITECH

The compositional variability of groundwater (including hot/mineral spring waters) reflects the origin and circulation processes of groundwater, such as fluid sources, fluid-rock reactions, flow rates and residence times; e.g., identification of fluid sources by hydrogen-oxygen isotope ratio (Matsubaya et al., 1973), reaction with bedrock by Sr isotope ratio (Notsu et al., 1991), and evaluation of residence time of deep-seated fluid based on helium isotope ratio (Morikawa et al., 2005). By integrating these analyses, it is possible to forward our understanding of the origins of fluid and the circulation processes more comprehensively. Kusuda et al. (2014) integrated the geochemical data of the Arima spring waters with the dehydration simulation of the subducting plate to infer that the Arima-type brine is originated from the subducted Philippine Sea plate. Nakamura et al. (2016) and Iwamori et al. (2020) discussed the origin of Arima-type brine in the Arima-Kii Peninsula to be rooted from the subducting plate and geochemical processes during ascent to the surface, based on multivariate statistical analysis of the spring water compositions, including rare earth elements.

In this study, the existing composition data set of groundwater (Takahashi et al., 2018) is used to identify the geochemical sources and processes recorded in the groundwater composition over the area of about 120 km east-west and 80 km north-south surrounding the Aso caldera in central Kyushu. In particular, we aim to distinguish the volcanic and deep-seated fluid components from those related to meteoric water circulation, and ultimately to understand (1) fluid processes associated with magmatic activity under the Aso caldera, and (2) active tectonics and the large-scale fluid circulation from the subducting plate to the surface, including magmatism in central Kyushu.

As a pilot study for this purpose, in this presentation, we examine whether information on independent sources and processes can be extracted from the high-dimensional composition data set (590 samples containing 12 major dissolved elements of Na, K, Mg, Ca, Li, Cl, SO_4, HCO_3, F, NO_3, Br, and total C), based on multivariate statistical analyses. The statistical methods used were "whitened-data based k-means cluster analysis (KCA)" and "independent component analysis (ICA)" (Iwamori et al., 2017). Principal component analysis (PCA), a standard multivariate analysis, can extract information for independent sources and processes only if the data show a (joint) normal distribution. For data showing a non-normal distribution, the above KCA and ICA should be used. The data set used in this study shows clear non-normality, for which KCA and ICA are suitable. Based on the eigenvalue analysis of the data, we set the number of clusters and independent components to eight and attempted to detect statistically independent features in their compositional and geographical spaces.

As a result, a concentric spatial structure (distinguished with the 8 clusters) was found both in the Aso caldera and in the wide area surrounding the Aso volcano, with a broad decrease in the concentrations of Na, Li, Cl, HCO_3, Br, total C toward the outside. Even when focusing only on the inside of caldera, four clusters were mainly distributed concentrically, and two of them were distributed so as to surround basalt

©2021. Japan Geoscience Union. All Right Reserved.

and felsic rock bodies and lava. Except for the Aso caldera, the two clusters occur characteristically in the Kuju volcano centered around Mt. Kuju, which suggests that the two clusters are of magmatic origins.

The distribution and compositional characteristics of these clusters suggest that KCA and ICA are useful for the detection and identification of independent sources and processes involved in the origin of groundwater, especially the magmatic components. In the future, we plan to characterize the individual clusters with more elements and isotopic compositions, and to apply this statistical approach to other volcanic areas. This research was partly supported by JSPS KAKENHI Grant Numbers JP18H03747, JPJSBP120204804, JP17KK0018, JPJSBP120194830, and the Nuclear Regulation Authority "Research on Knowledge Development of Giant Eruption Processes, FY 2020".

Keywords: groundwater, composition, volcano, deep-seated fluid, statistical analysis

©2021. Japan Geoscience Union. All Right Reserved.

Temporal variation of chemical composition of hot spring waters at Ebinokogen Ioyama Volcano in Kirishima Volcanic Group

*Keigo Mori[1], Jun-ichiro Ishibashi[1], Takeshi Matsushima[1], Harue Masuda[2], Syogo Oshima[3], Saki Tsutsumi[3], Yasuhisa Tajima[4]

1. Graduate School of Science, Kyushu University, 2. Graduate school of Science, Osaka City University, 3. West Japan Engineering Consultants, Inc,, 4. Nippon Koei Co., Ltd,

Vigorous emanation of hot spring waters and fumarolic gases has been observed at Ebinokogen Ioyama Volcano, since the eruption in April 2018. We have conducted periodic sampling of hot waters emanating from the craters and fumarolic vents since July, 2018, and monitored temporal variation of their chemical composition which could be related to magmatic and hydrothermal activities. We report temporal variation of major cation compositions as well as anion compositions, to discuss factors which control fluid chemistry. Water samples were collected from W4 hot spring formed at the eruption crater located about 500 meters west from the Iwoyama crater, Y2a and Y2b hot springs formed at the eruption crater 50 meters south from the Iwoyama crater, and small fumarolic vents located in the area between them (Tajima et al., 2020). During the fluid sampling, water temperature, pH, ORP (oxidation-reduction potential) and EC (electrical conductivity) were measured on site using probes. Chemical composition of major cations (Na, K, Mg, Ca) and Si of the spring waters was determined by ICP-OES (inductivity coupled plasma optical emission spectrometry) and that of major anions (Cl, SO_4) was determined by IC (ion chromatography).

Long-term variation of major cations for two and half years duration basically follows the trend observed in that of major anions (such as Cl/SO_4 ratio). The most drastic change in W4 hot spring water chemistry was recognized at the early winter at year 2020; concentrations of major cations were high till Dec. 2019, while they significantly decreased since Feb. 2020. To characterize behavior of each cation, the observed concentration in the W4 hot spring water (defined as Ci) is compared with the concentration expected from complete dissolution of andesite from Ioyama by interaction with the acidic hot spring water (defined as Di), following the model proposed in Ohba et al. (2008). For Na and Mn, Ci was extremely high compared with Di in the duration till Dec. 2019, but Ci was decreased to comparable with Di after Feb. 2020. For Ca and Si, Ci was usually low compared with Di. For K, Ci was lower than Di till Dec. 2019, but Ci was higher than Di after Feb. 2020. These temporal variations are attributed to a shift of cation sources for W4 hot spring. After Feb. 2020, the cation composition can be explained by complete dissolution of andesite interaction with the acidic water and removal of some cations by formation of secondary minerals such as alunite. Whereas, the cation composition is likely to be dominantly controlled by other source till Dec. 2019, and hydrothermal aquifer had been developed beneath the volcano is presumed as the possible source. We discuss this model in detail from data of temporal variation of minor cations (Li, Rb, Cs) composition.

Keywords: fluid rock interaction, monitoring of time series change

©2021. Japan Geoscience Union. All Right Reserved.

Temporal variations of helium and carbon isotopic compositions of fumarolic gases from Kusatsu-Shirane volcano

*Tomoya Obase[1], Hirochika Sumino[1], Kotaro Toyama[1], Takeshi Ohba[2], Muga Yaguchi[3], Akihiko Terada[4]

1. Department of General Systems Studies, Graduate School of Arts and Sciences, University of Tokyo, 2. Department of chemistry, School of Science, Tokai University, 3. Meteorological Research Institute, Japan Meteorological Agency, 4. Volcanic Fluid Research Center, Tokyo Institute of Technology

Kusatsu-Shirane is an active stratovolcano consists of three pyroclastic cones, Mt. Shirane, Mt. Ainomine, and Mt. Motoshirane. A phreatic eruption occurred on 23 January 2018 at Mt. Motoshirane. Phreatic eruptions often occur without precursor geophysical signals, but chemical and isotopic compositions of volcanic gases may reflect some precursor events such as pressure rise at a gas reservoir. Helium ($^3He/^4He$) and carbon ($\delta^{13}C = (^{13}C/^{12}C)_{gas}/(^{13}C/^{12}C)_{PDB} - 1$) isotopic ratios are potential tracers of volcanic activity as they exhibit unique values corresponding to the origins. For example, $^3He/^4He$ ratios are ~8 Ra in the mantle (1 Ra equals to the atmospheric $^3He/^4He$) and <0.1 Ra in the crust, and $\delta^{13}C$ values are -6.5±2.5‰ in the mantle and <-20‰ for organic carbon. Pre-eruptive $^3He/^4He$ rises have been reported in some volcanoes, suggesting increase in magmatic He supply preceding the eruptions [e.g., 1]. Here we report $^3He/^4He$, $\delta^{13}C\text{-}CO_2$, and $^3He/CO_2$ of volcanic gases from five fumaroles at Kusatsu-Shirane volcano sampled from 2014 to 2020.

The $^3He/^4He$ ratios (corrected for atmospheric He contamination by $^4He/^{20}Ne$) of three Kitagawa fumaroles on the northern flank of Mt. Shirane roughly synchronized each other and temporally varied in the range of 7.1 to 8.1 Ra, suggesting that magmatic He supply changed during the sampling period. The temporal variations of $\delta^{13}C\text{-}CO_2$ values (-4.9 –-1.4‰) were inversely correlated to $^3He/^4He$, indicating low $\delta^{13}C\text{-}CO_2$ during high magmatic gas supply. On the other hand, the $\delta^{13}C$ values of the Sesshogawara and Manza fumaroles (located the east and west of Kusatsu-Shirane volcano, respectively) varied in the ranges of -4.5 –-0.8‰ and -3.7 –-0.5‰, respectively, were not correlated with each $^3He/^4He$ ratio.

The $^3He/CO_2$ ratios of Kitagawa fumaroles ($(0.3 – 2.0) \times 10^{-9}$) negatively correlated with $\delta^{13}C\text{-}CO_2$, indicating high $^3He/CO_2$ ratios in the periods of high magmatic gas supply. A trend for Manza fumarole is completely different that the $^3He/CO_2$ ratios show less variation ($(0.3 – 0.5) \times 10^{-9}$) that positively correlate with $\delta^{13}C\text{-}CO_2$. The $^3He/CO_2$ ratios of Sesshogawara fumarole ($(0.3 – 0.7) \times 10^{-9}$) were slightly higher than those of Manza fumarole and do not correlate with $\delta^{13}C\text{-}CO_2$. The $^3He/CO_2$ ratios of Sesshogawara and Manza fumaroles with high $\delta^{13}C\text{-}CO_2$ values were similar to the $^3He/CO_2$ ratios of Kitagawa fumaroles in the periods of low magmatic gas supply.

These trends can be explained by a mixing of two gas components with organic CO_2. One is the magmatic gas with high $^3He/CO_2$ and low $\delta^{13}C\text{-}CO_2$ values directly degassed from the magma. The other is probably the gas separated from hydrothermal fluids with low $^3He/CO_2$ and high $\delta^{13}C\text{-}CO_2$ values produced by addition of the crustal CO_2 with a high $\delta^{13}C$ value (~1.1‰ around Kusatsu-Shirane volcano [2]) to the magmatic gas. This model suggests that both magmatic and hydrothermal gases contribute to the fumarolic gases of Kitagawa. The Manza fumarole is fed by the hydrothermal fluid only, resulting in the small temporal variation of $^3He/CO_2$ ratios. The positive correlation between the $^3He/CO_2$ and $\delta^{13}C\text{-}CO_2$ values is attributable to the addition of the organic CO_2 to various extents. The Sesshogawara fumarole is mainly fed by the hydrothermal fluid with small contributions of the magmatic gas and organic CO_2.

©2021. Japan Geoscience Union. All Right Reserved.

The presence of a hydrothermal fluid reservoir at depths of 1-3 km broadly extending from beneath Mt. Shirane to Mt. Motoshirane was suggested by magnetotelluric investigation [3]. If the reservoir supplies fluids to the Sesshogawara and Manza fumaroles, the episodic drop of $^{3}He/^{4}He$ ratios following the 2018 phreatic eruption at Mt. Motoshirane [4] might be attributable to a decrease in the supply of fluids that carry magmatic He to both fumaroles, resulting in crustal He more apparent.

References

[1] Padrón et al. (2013) Geology. [2] Sano et al. (1994) Appl. Geochem. [3] Matsunaga et al. (2020) J. Volcanol. Geotherm. Res. [4] Sumino et al. JpGU2020.

Keywords: helium isotope, carbon isotope, volcanic gas, Kusatsu-Shirane volcano, temporal variation, hydrothermal system

©2021. Japan Geoscience Union. All Right Reserved.

Change in fluoride ion concentration in Bandaiko hot spring at east flank of Kusatsu-Shirane volcano and its relationship with volcanic activity

*Haruka Yamamoto[1], Yoshikazu Kikawada[2]

1. Graduate School of Sophia University, 2. Faculty of Science and Technology, Sophia University

In a phreatic eruption, apparent seismic activity and crustal movements that can be regarded as precursors of eruption may not be observed. Therefore, for volcanoes with extensive hydrothermal activity, geochemical observations on fumaroles and hot springs are important in addition to geophysical observations. Chloride ions and fluoride ions derived from HCl and HF in volcanic gas are dissolved into active crater lakes and volcanic hot spring water. Their dissolved concentrations and concentration ratios are often used as indicators of volcanic activity. In particular, HF reacts readily with rocks mainly composed of silicates and is easily incorporated into rocks. Thus, an increase in the concentration of fluoride ions in volcanic geothermal water can be a more remarkable indicator of volcanic activity than that of chloride ions.

On the other hand, due to fluoride ions' strong complex-forming ability, direct determination by using an ion chromatography or an ion-selective electrode may give erroneous results. Therefore, in volcanic geothermal water containing a high concentration of metal ions complex with fluoride ions, it is essential to isolate fluoride ions by distillation prior to the determination of fluoride ions. For example, a trimethylsilylating distillation method is known.[1)] However, since the distillation operation is troublesome and time-consuming, the determination of fluoride ions is often omitted. In this study, we investigated a simple method that directly determines fluoride ions with an ion-selective electrode without distillation by using a specific total ionic strength adjustment buffer and confirmed its precision and accuracy. After that, we applied the simple method to the water of Yugama, the crater lake of the Kusatsu-Shirane volcano, and the water of Bandaiko hot spring located on the eastern flank of the volcano stored in our laboratory, and reconstructed the time-series data of the fluoride ion concentrations over the past decades. Subsequently, we discussed the relationship between the fluoride ion concentrations and the activity of the Kusatsu-Shirane volcano.

The Kusatsu-Shirane volcano consists of three pyroclastic cones, Mt. Shirane, Mt. Moto-Shirane, and Mt. Ainomine. In January 2018, a phreatic eruption occurred at Mt. Moto-Shirane. The fluoride ion concentration of Bandaiko located on the eastern flank of Mt. Moto-Shirane gradually increased from 2012 to 2017, then increased significantly coincidently with the eruption at Mt. Moto-Shirane. After that, fluoride ion still maintains high concentration until 2020, while a small fluctuation in the concentration has been observed. In the case of chloride ion, which is also halide ion, a gradual increase in the concentration was observed from 2012 to 2017 as same as fluoride ion concentration. However, unlike fluoride ion, no increase in the concentration coincident with the eruption of Mt. Moto-Shirane was seen, and no increase was observed after that.
On the other hand, the concentrations of both fluoride and chloride ions in Yugama, the crater lake of Mt. Shirane, increased from 2014 to 2016 and then gradually decreased. There was no significant increase in their concentrations coincident with the eruption of Mt. Moto-Shirane in January 2018, unlike Bandaiko, but the concentrations began to increase from around June 2018. After that, the concentrations have remained at a high while a small fluctuation has been observed. The F/Cl concentration ratio also

©2021. Japan Geoscience Union. All Right Reserved.

increased significantly from June to September 2018 and has remained high since then.

Seismic activity and ground inflation have been observed around Yugama intermittently after the eruption at Mt. Moto-Shirane. The fluctuation of fluoride ion concentration in Yugama and Bandaiko occur to follow those volcanic activities. However, the change in fluoride ion concentration coincident with the eruption of Mt. Moto-Shirane in January 2018 is observed in Bandaiko, but not in Yugama. Accordingly, the chemistry of Yugama reflects volcanic activity around the summit area of Mt. Shirane, while Bandaiko may reflect the activities of the entire Kusatsu-Shirane volcano or that of Mt. Moto-Shirane, which do not appear in Yugama. Since the changes in halide ion concentrations are different between Bandaiko and Yugama, we would like to keep an eye on future changes.

1)Tsuchiya *et al.* (1985) Separation of microamounts of fluoride coexisting with large amounts of aluminum and silica by improved trimethylsilylating distillation. *Analytica Chimica Acta* **176,** 151-159.

Keywords: fluoride ion, Kusatsu Shirane Volcano, hydrothermal system, geothermal fluid, hot spring, active crater lake

©2021. Japan Geoscience Union. All Right Reserved.

Volcanic ash from the June 17, 1962 eruption of Yakedake volcano, and its water-soluble components

*Muga Yaguchi[1], Yasuo Hirayama[2], Takeshi Ohba[3], Nozomi Numanami[3]

1. Meteorological Research Institute, JMA, 2. Nagano Meteorological Office, JMA, 3. School of Science, Tokai University

Mt. Yakedake is one of the active volcanoes, and several phreatic eruptions have been recorded. The most recent eruptions occurred in 1962-1963. The ash fall from the June 17 eruption, the first eruption in the series of 1962-63 eruptions, was distributed mainly on the eastern flank of this volcano [1]. The volcanic ash from this eruption has already been analyzed by Ossaka and Ozawa, and it is considered that the 1962 eruption was not caused by ascending magma but by an explosion in a mud reservoir because volcanic ash does not contain essential materials but contains montmorillonite [2]. On the other hand, for example, microscopic images of the ash particles and analytical results of water-soluble components of the ash have not been available as far as we know. In this presentation, we present the results of microscopic observation and analysis of water-soluble components of the volcanic ash from the June 17, 1962 eruption.

The ash sample we analyzed in this study was collected from the roof of a house on the morning after the eruption on June 17, 1962, which was collected before being exposed to rainfall or contaminated by soil materials. Water-soluble Cl and SO4 were analyzed by ion-chromatography after the ultrasonic extraction into pure water. The ash after extraction was rinsed and dried for microscopic observation.

Under microscopic observation, most of the ash before ultrasonic extraction was less than 500 μm in size, covered with fine particles, and gray in color. On the other hand, the washed volcanic ash is dominated by particles smaller than 100-200 μm. Most of these particles are transparent to white, accompanied by altered rock and crystal fragments that appear to be pyrite. No particle that was clearly derived from fresh magma was found. On the other hand, as a result of the analysis of water-soluble components, 1,250 mg of Cl and 10,800 mg of SO4 were detected per 1 kg of ash sample. These amounts of water-soluble components are clearly higher than those of volcanic ashes discharged from typical magmatic eruptions (e.g., the 1707 Hoei eruption of Mt. Fuji and the 2017 eruption of Nishinoshima) and are consistent with the characteristics of volcanic ashes discharged from phreatic eruptions (e.g., the 1982-83 eruption of Kusatsu-Shirane volcano and the 2015 eruption of Hakone volcano). These results suggest that the June 17, 1962 eruption was not caused by fresh magma ascending but by a phreatic explosion in the hydrothermal alteration zone, and this suggestion is consistent with previous studies. In this presentation, we also show another analytical result, such as powder XRD analysis, and the geochemical characteristics of this ash will be discussed.

[1] Murai I. (1962) Bull. Earthq. Res. Inst., 40, 805-814. [2] Ossaka J. and Ozawa T. (1966) Bull. Volcanol. Soc. Japan, 11, 17-29.

Keywords: Yakedake volcano, the June 17, 1962 eruption, phreatic eruption, volcanic ash, water-soluble components

©2021. Japan Geoscience Union. All Right Reserved.

Tectonic controlled and hydrothermal alterations of geothermal reservoirs in El Salvador

*JOSE ANIBAL ERAZO[1], Noriyoshi Tsuchiya[1], Masaoki Uno[1], Arturo Quezada[2], Pedro Antonio Santos[2], Ryoichi Yamada[1], Hiroyuki Yamagishi[1], Shinichi Yamasaki[1], Alvaro Josue Amaya[3]

1. Graduate school of environmental studies , 2. LaGeO _ El Salvador, 3. UES _ El Salvador

A comparative study of magma-hydrothermal activities of main geothermal fields (Ahuachapán, Berlín, San Vicente, and Chinameca) was carried out in El Salvador/ Central America, where significant relationships were identified between volcanism and geothermal activities.

All geothermal fields are located north and/or northwest flank of the volcanic complex inside ESFZ (El Salvador Fault Zone). Geothermal reservoirs are controlled by fault system, which direction is mainly N-S, NE-SW, NW-SE, and E-W. The reservoirs are developed in the intersected area of those faults.

Most of the reservoir are developed in the San Salvador Cuscatlán and Bálsamo formation of Pliocene-Holocene in age.

The top depths of geothermal reservoirs are ranging from 600 to 2000 m. Ahuachapán is relatively shallow (below 600 to 1500 m, thickness around 800 to 1200 m), and Berlín (below 1500 m, thickness around 600 to 1000 m). Geothermal reservoirs of San Vicente and Chinameca were estimated around 1100 to 1400 m in depth. The temperatures of the reservoirs in the different geothermal fields range from 200 to 300˚C.

The mineral alteration facies in the four fields have a very similar distribution (Fig. 1), and Propylitic, Phyllitic-Propylitic, Phyllitic zones correspond to the geothermal reservoir. In the different facies, key minerals are Argillitic: Low-temperature clays like Smectites (Montmorillonite, Saponite); Argillitic-Phyllitic: Chloritic clays (mixed-layer clay minerals) like Corrensite; Phyllitic: Chlorite; Phyllitic-Propylitic: Incipient epidote or in very low percentages. Propylitic: key mineral: epidote. Other minerals are also present in each facie. In the shallow zone, the Argillic alteration is dominant and is in the range of temperatures of 50°C-120°C, the Argillic-Phyllitic mineral alteration is found in the temperature range of 100°C-180°C, Phyllitic-Propylitic mineral alteration type is found in the temperature range of 200°C-260°C and in the deepest zone, the Propylitic type mineral alteration is dominant, found it at temperatures ranging from 250°C to temperatures around 300°C.

The chemical composition of trace elements of volcanic rocks in El Salvador shows a subduction setting through Miocene to the present. The Miocene-Pliocene volcanoes located northward of ESFZ were similar to the back-arc setting. A wide range of mineral assemblages of volcanic rocks was observed (Mainly from the series calc-alkaline from basalts to rhyolites), however, it is rare to contain quartz.

In the case of Quaternary volcanoes distributed inside ESFZ (and parallel to the Middle America Trench), the magma chamber was presumed to be slightly shallower, and variation of geochemical behaviors may show that El Salvador is located as a transition zone of the subduction system of the Cocos Plate between Guatemala and Nicaragua

©2021. Japan Geoscience Union. All Right Reserved.

Keywords: hydrothermal, mineral alteration, geothermal reservoirs , magma

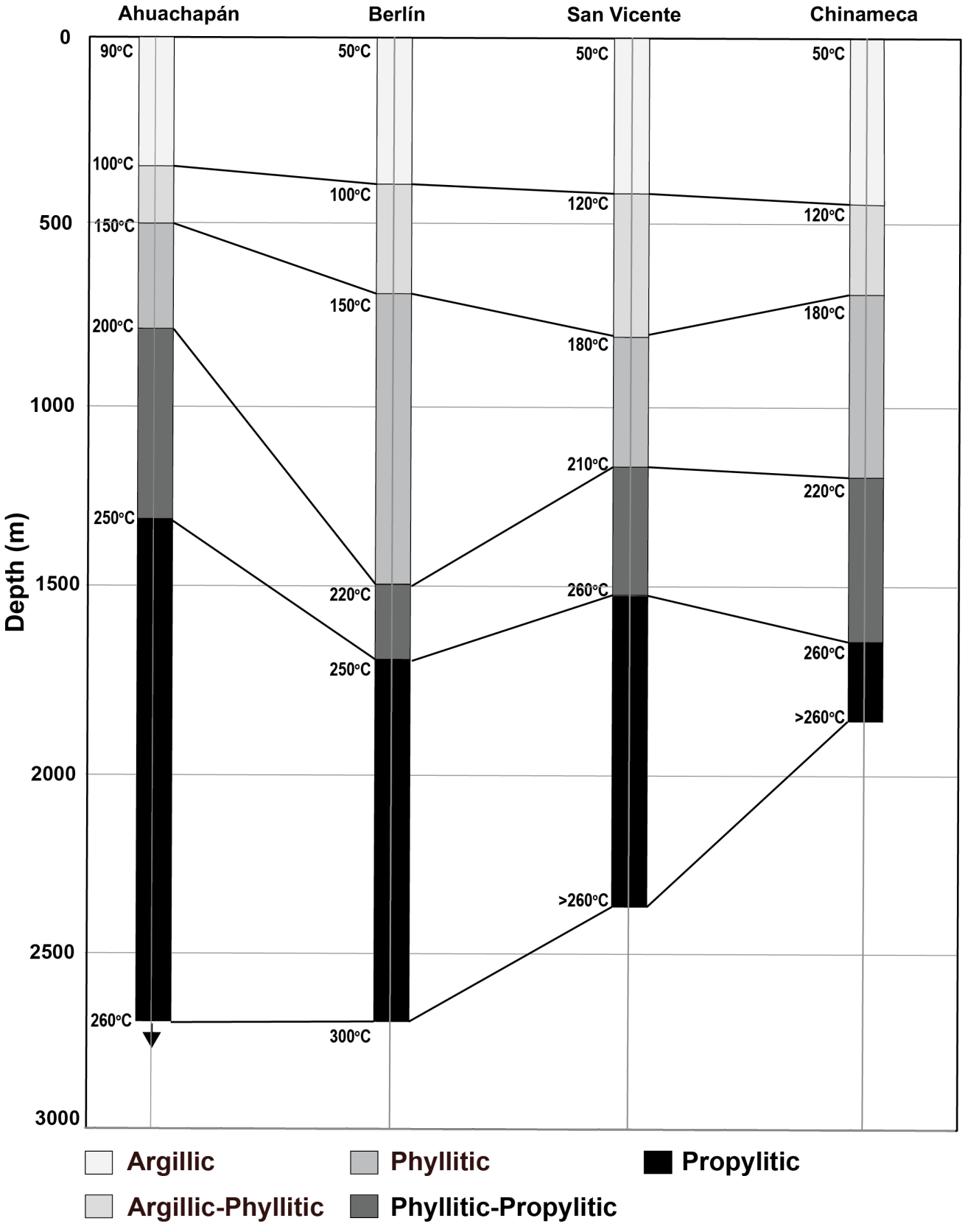


Fig. 1 Depth of mineral alteration facies in different geothermal fields in El Salvador.

©2021. Japan Geoscience Union. All Right Reserved.

DAS-Seismic and temperature data acquisition using DAS and DTS measurements at the Ohnuma, geothermal field, Tohoku, Japan

*Junzo Kasahara[1,2], Yoko Hasada[1,3], Kuzume Haruyasu[1], Hitoshi Mikada[4], Yoshihiro Fujise[5]

1. ENAA, 2. Shizuoka University, 3. Daiwa Exploration and Consulting Co. Ltd., 4. Graduate School of Kyoto University, 5. WELMA

The New Energy and Industrial Technology Development Organization (NEDO) in Japan has promoted the use of supercritical water for geothermal power generation under a project called “Research and Development of Supercritical Geothermal Resources. In September, 2020, we carried out a seismic survey as a part of this NEDO project using distributed acoustic sensor (DAS) method by an optical fiber system. We deployed an optical fiber system in the O-13R borehole at the Ohnuma geothermal power plant owned by Mitsubishi Materials Corporation. The Ohnuma geothermal power station, the third commercial geothermal power plant in Japan, was completed in 1974; its installed capacity is 9.5 MW. The optical fiber reached to the depth of 1,973 m. The temperature was measured as 235 ˚C at around 1,130 m depth using the DTS mode. We operated a medium size seismic source at nine locations. We repeated the frequency sweep of 10–75 Hz 480 times a day for nine days. To enhance the signal to noise ratio (S/N), we stacked the DAS data and correlated the seismic records with the source signature. By stacking for a long duration, we obtained excellent DAS records down to the bottom of the boreholes. Using the migration of observed and synthetic DAS seismic records, we recognized intense seismic reflections from 2.8–3.0 km depth, suggesting the possibility of geothermal reservoirs in or above basement rock and/or igneous intrusions (Fig. 1).

Acknowledgements

This study was supported by the New Energy and Industrial Technology Development Organization (NEDO). We greatly appreciate Mitsubishi Materials Corporation for their kind permission for fieldwork in their power plant. Mr. Kimura provided us with Schlumberger hDVS measurements. YK Engineering Co. and Fujitsu Research Institute Co. provided DAS data. WELMA Co. provided us with a borehole fiber-optic system and measured the temperatures in the borehole. The staff of the Kawasaki Geological Engineering Co. and Daiwa Exploration and Consulting Co. assisted our surface seismological measurements during the field study. The IVI EnviroVibe operation was performed by JGI Inc.

References

Kasahara, J., Hasada, Y., Kuzume, H., Mikada, H., and Fujise, Y. [2020a] The second seismic study at the geothermal field in southern Kyushu, Japan using an optical fiber system and surface geophones, 44th Workshop on Geothermal Reservoir Engineering, Stanford University, Stanford, CA.

Kasahara, J., Hasada, Y., and Kuzume, H. [2020b] Possibility of high Vp/Vs zone in the geothermal filed suggested by the P-to-S conversion, 44th Workshop on Geothermal Reservoir Engineering, Stanford University, Stanford, CA.

Kubota, Y. [1985] Conceptional model of the north Hachmantai-Yakeyama geothermal area, Journal of Geothermal Society of Japan, **7**(3), 231-245.

©2021. Japan Geoscience Union. All Right Reserved.

Kubota, Y., Hatakeyama, K., Banba, M., Kato, H. [1989] Chemical changes of Ohnuma geothermal fluid since operation and related reservoir management, Journal of JGEA (Japan Geothermal Energy Association), **26**(1), 1-20.

Yora, M., Wakita, K., and Honda, S. [1973] Exploration of Onuma geothermal field, northern Japan, Journal of JGEA (Japan Geothermal Energy Association), **10**(4), 27-44.

Yora, M, [1976] Drilling of Onuma geothermal wells, specially O-3Rb, Journal of JAPT (Japanese Association of Petroleum Technology), **41**(5), 13-19.

Yora, M., Watanabe, K., Ito, J., Wakita, K., Kubota, Y. [1977] On the geothermal system of the northern Hachimantai, Mining Geology, **27**, 233-244.

Keywords: Geothermal exploration, supercritical water, DAS, seismic reflection, migration imaging, geothermal reservoir

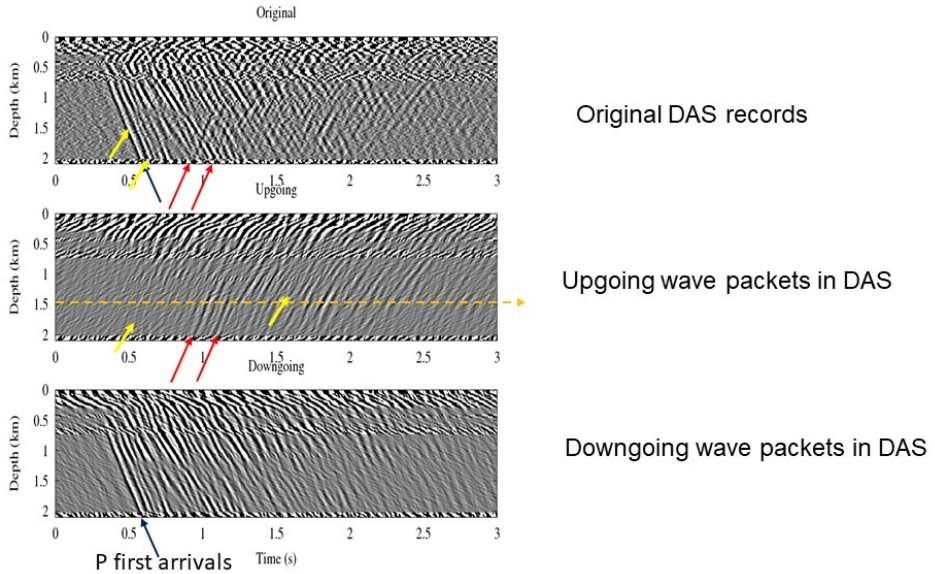


Fig. 1: Using original DAS records at the C8 seismic source, we calculated upgoing phases (reflection phases) and upgoing phases(direct waves). The Red and the yellow arrows indicate reflections. The yellow broken line is a possible layer boundary and fracture zone.

©2021. Japan Geoscience Union. All Right Reserved.

Ground surface Heat balance measurements at Izu-Oshima volcano

*Shin'ya Onizawa[1], Nobuo Matsushima[2]

1. Volcanology Research Department, Meteorological Research Institute, JMA, 2. Geological Survey of Japan, National Institute of Advanced Industrial Science and Technology

1. Introduction

During the 1986 eruption of Izu-Oshima volcano, phenomena suggesting the development of the underground hydrothermal system were observed. Thus, thermal observation is important for grasping such the transitions of volcanic activities. In order to understand the thermal activity, underground and surface temperature measurements are often performed. However, the temperature near the ground surface strongly affected by external factors such as radiation from the sun and atmosphere and meteorological factors. Therefore, in order to detect and quantify thermal signs associated with volcanic activity, it is necessary to understand the effect of these external factors. For the purpose of clarifying these factors, heat balance observation devices were installed at two locations in caldera area of the Izu-Oshima volcano.

2. Measurement System

The system consists of sensors that measure not only the surface and underground temperatures, but also the radiations from the sun and the atmosphere and meteorological factors that can affect them. Further, as auxiliary information, the soil moisture and the thermal conductivity in the ground are measured.

Sensors

T-type thermocouple thermometers (CHINO SCHS1-5) are installed at 5 depths (10, 30, 50, 70 and 100 cm) for the underground temperatures. For ground surface temperature, infrared radiation thermometer (Apogee SI-431) is installed. The meteorological parameters (wind speed and direction, atmospheric pressure, temperature, relative humidity, precipitation, and hail) are measured by the weather transmitter Vaisala WXT536. The albedometer (Hukseflux SRA01) is used to measure short-wave radiations (solar radiation and its reflection from the ground surface), and the long-wave radiometer (Hukseflux IR02) is used to measure atmospheric radiation (infrared radiation). The sensors of the soil moisture meter (Sentek EnviroSMART) were installed at the same depth of 5 as the underground temperature. In addition, the thermal properties sensor (Huluseflux TP01) is installed at a depth of about 20 to 30 cm in order to estimate the effective thermal conductivity of the medium.

Data Record and Transmission

Measurements were performed at a minimum interval of 10 seconds, and these were recorded with a data logger (Campbell Scientific CR-1000X). In addition, data is transmitted to the Meteorological Research Institute using a mobile phone line.

3. Observation

This device was installed at two locations inside the caldera of Izu-Oshima volcano. One is in a fumarolic area and the other is in a non-fumarolic area. Both were set up in March 2020.

HB01 (Eastern Crater Floor of Mt. Mihara)

It was installed in a steaming ground distributed along a crack in the eastern crater floor of Mt. Mihara. It is near a fixed point where the Japan Meteorological Agency has been continuously measuring fumarolic temperature since 1991. According to this, what was about 80 ˚C in 1991 has decreased over time, and has been around 45 to 50 ˚C in recent years.

HB02 (Southeastern Caldera Floor)

©2021. Japan Geoscience Union. All Right Reserved.

While HB01 was installed in a the fumarolic area, this site was selected from areas where thermal signs associated with volcanic activity were not observed, because the purpose was to understand the heat balance due to external factors such as radiation and meteorological conditions. It was installed in the bare land in the southeastern caldera floor. The ground surface is covered with scoriaceous silt, sand and lapilli.

4. Characteristics of Observed Data

Characteristics of changes in the surface and underground temperatures are totally different between two sites. At the HB02 in non-fumarolic area, diurnal and seasonal (that are considered to be annual) changes are clearly observed. In particular, it is strongly affected by solar radiation, and the amplitude of temperature changes attenuate and the phase is delayed as it gets deeper. On the other hand, at HB01 in the fumarolic area, such the changes are not prominent in the underground temperatures, although diurnal changes in temperature are observed on the ground surface. The underground temperatures are almost constant at about 45 to 48 ˚C at depths from 10 cm to 100 cm during the seasons. However, when the average wind speed for 10 minutes exceeds approximately 5 m/s, the temperature decreases from the surface to the deeper often occur, suggesting that sensible heat transport or latent heat transport is promoted.

In this presentation, we show the outlines of the measurements and characteristics of observed data.

Keywords: Izu-Oshima volcano, heat balance measurement

©2021. Japan Geoscience Union. All Right Reserved.

Behavior of magmatic hydrothermal system of Kusatsu-Shirane Volcano inferred from numerical simulations

*Yasuo Matsunaga[1], Wataru Kanda[1]

1. School of Science, Tokyo Institute of Technology

Kusatsu-Shirane Volcano (KSV) is an active volcano known for its significant hydrothermal activity and phreatic eruptions in recent years. According to geological studies, frequent magmatic eruptions were estimated at Mt. Motoshirane, which constitutes the southern part of KSV, until 1500 years ago. Therefore, it is expected that the magma produced at that time has not yet cooled and solidified.

To infer the extent of the magmatic-hydrothermal system of KSV, broadband magnetotelluric observations covering the entire region of KSV were conducted from 2015 to2020. The study found a remarkable conductive zone extending from a depth of ~1.5 km below the summit area to a depth of ~10 km northwest of the KSV. The lower part (5–10 km deep) of this conductor showed moderately low resistivities (~50 Ωm) and the upper part (1.5–5 km deep) showed extremely low resistivities (< ~1 Ω m)(Matsunaga et al., 2020). The lower half of the conductor can be explained as a zone containing hydrous silicate melt, because it exhibited low resistivities on the order of 10 Ωm (Pommier et al., 2011). Based on previous geochemical studies and the seismicity, we interpreted the upper half of this conductor as a fluid-rich zone strongly affected by magmatic volatiles.

Since the hypocenters of volcanic earthquakes are distributed from the top of this conductor to the summit area, it is likely that these conductive zones are involved in the various volcanic activities observed in KSV. Therefore, it is crucial to consult the behavior of hydrothermal fluids to understand the magmatic hydrothermal system of KSV. However, it is still difficult to estimate the exact position and volume of molten rocks because the MT data collected has low resolution and sensitivity, particularly in the lower part. Since the geothermal and geochemical processes observed near the surface are strongly influenced by the behavior of shallow hydrothermal systems, it is also difficult to infer the deep processes of volcanoes which have well-developed hydrothermal systems like KSV.

One possible way to estimate the thermal state and process inside a conductor is to numerically simulate the movement of geothermal fluids using the observed data and the inferred subsurface structure as constraints. To construct a hydrothermal fluid circulation model of KSV, we use a multi-phase and multi-component TOUGH3 model (Jung et al., 2017). In the presentation, we will show some of the simulation results.

Keywords: Kusatsu-Shirane, hydrothermal system, resistivity structure, numerical simulation

©2021. Japan Geoscience Union. All Right Reserved.

Comprehension of hydrothermal systems in the East African Rift System –Collaborative Research with Kenya by SATREPS–

*Yasuhiro Fujimitsu[1], Jun Nishijima[1], Takeshi Tsuji[1], Kotaro Yonezu[1], Tatsuya Wakeyama[2], Ryuichi Itoi[3]

1. Department of Earth Resources Engineering, Faculty of Engineering, Kyushu University, 2. Platform of Inter-/Transdisciplinary Energy Research, Kyushu University, 3. School of Engineering, Kyushu University

SATREPS is an acronym standing for Science and Technology Research Partnership for Sustainable Development, and is a joint research program for 3 to 5 years between Japan and developing countries that aims to find solutions to issues of a global scale. Japan Science and Technology Agency (JST) and Japan International Cooperation Agency (JICA) are responsible for the areas of Environment/Energy (Global-scale Environmental Issues, and Low Carbon Society/Energy), Bioresources and Disaster Prevention and Mitigation. The research topic “Comprehensive Solutions for Optimum Development of Geothermal Systems in East Africa Rift Valley” proposed by Kyushu University (Principal Investigator: Yasuhiro Fujimitsu; Research Period: FY2020 to FY2024; Partner Country: Kenya) was adopted in FY2019.

The participants Kyushu University (Faculty of Engineering, Faculty of Science, and Platform of Inter-/Transdisciplinary Energy Research) and West Japan Engineering Consultants, Inc. in Japan and Jomo Kenyatta University of Agriculture and Technology, The University of Nairobi, Kenya Electricity Generating Company and Geothermal Development Company in Kenya. It was scheduled that the project started from FY2020 with a preparation period in FY2019. However, the actual commencement becomes FY2021 caused by a worldwide pandemic of COVID-19. In order to obtain 4 outputs of this research topic (I: Development of high resolution geothermal reservoir models, II: Understanding of silica scale formation mechanism in highly alkaline hot water and examination of countermeasures, III: Proposal of a scenario for enhancement of social acceptance by the expansion of cascade use of geothermal energy, IV: Cultivation of human resources in geothermal development and research capability of the counterpart institutions), we conduct collaborative research of Olkaria and Menengai geothermal areas with the Kenyan institutions.

Keywords: East African Rift System, hydrothermal system, SATREPS

©2021. Japan Geoscience Union. All Right Reserved.

[J] Poster | S (Solid Earth Sciences)：S-CG Complex & General

Sun. Jun 6, 2021 5:15 PM - 6:30 PM JST | Sun. Jun 6, 2021 8:15 AM - 9:30 AM UTC | Ch.15_3

[S-CG44] Petrology, Mineralogy & Resource Geology

convener:Koichi Momma(National Museum of Nature and Science), Yu Nishihara(Geodynamics Research Center Ehime University), Tatsuo Nozaki(Submarine Resources Research Center, Research Institute for Marine Resources Utilization, Japan Agency for Marine-Earth Science and Technology), Nobutaka Tsuchiya(Department of Geology, Faculty of Education, Iwate University)

We widely invite presentations in the fields of petrology, mineralogy and resource geology. Especially description of minerals and rocks, investigation of their origin and evolution by field investigation and/or laboratory experiments, and development of new methods are accepted.

[SCG44-P01] Intrusive and emplacement process of the Tono plutonic complex: Constraints from dating and isotopic analysis of zircons

*Yasuhiro Ogita[1], Kazusa Sando[2], Kozue Ishibashi[3], Shuhei Sakata[4], Takeshi Ohno[5], Satoshi Suzuki[3], Tatsunori Yokoyama[1], Saya Kagami[1], Mitsuhiro Nagata[1], Takashi Yuguchi[2] (1.Tono Geoscience Center, Japan Atomic Energy Agency, 2.Faculty of Science, Yamagata University, 3.Graduate school of Science and Engineering, Yamagata University, 4.Earthquake Research Institute, University of Tokyo, 5.Faculty of Science, Gakushuin University)

[SCG44-P02] Whole-rock chemical composition of the Nojima granodiorite in northern part of Awaji Island, southwestern Japan

*Akihiro Ishihara[1], Motohiro Tsuboi[1] (1.Kwansei Gakuin University)

[SCG44-P03] Influence of inclusions on hydrogen generated during low temperature serpentinization

*Asuka Sugawara[1], Ryohei Kawakita[1], Tsubasa Otake[2], Tsutomu Sato[2] (1.Graduate school of Engineering, Hokkaido University, 2.Faculty of Engineering, Hokkaido University)

[SCG44-P04] **Detailed characteristics of Raman spectra of carbonaceous materials in fault rocks nearby the Median Tectonic Line**

*Hiroshi Mori[1], Yuki Nobe[1], Ken Yamaoka[2], Yosuke Tomooka[1], Yui Kouketsu[3], Tetsuya Tokiwa[1] (1.Shinshu University, 2.The University of Tokyo, 3.Nagoya University)

[SCG44-P05] Trace element composition of chromian spinel in the Sanbagawa ultramafic rocks

*Yuki Aoshima[1], Yuji Ichiyama[1], Jung-Woo Park[2] (1.Chiba University, 2.Seoul National University)

[SCG44-P06] The trace element composition of sapphire in the xenolith of garnet-bearing andesitic tuff of the Donzurubo Formation, the Nijo Group, Japan.

*Mayuko Fukuyama[1], Masatsugu Ogasawara[2] (1.Graduate School of Engineering Science, Akita University, 2.Geological Survey of Japan, National Institute of Advanced Industrial Science and Technology)

[SCG44-P07] **Microstructures of spherical pyrite in the Kuroko deposits: possible mechanism of pyrite growth on bubble**

*Atsushi Okamoto[1], Yoeri van de Ridder[2], Oliver Plumper[2], Markus Ohl[2], Ryoichi Yamada[1] (1.Tohoku University, 2.Utrecht University)

[SCG44-P08] **The mineral occurrence of kaolinitic saprolite beneath the sedimentary kaolin deposit at Seto district**

*Haruna Asai[1], Kikuchi Ryosuke[1], Tsubasa Otake[1], Tsutomu Sato[1] (1.Hokkaido University)

[SCG44-P09] Borate concentration processes in modern evaporitic and hydrothermal environments: Constraints on the formation of a boron-rich environment on prebiotic earth

*Sara Rinka Christensen [1], Akizumi Ishida[1], Takeshi Kakegawa[1] (1.Department of Earth Science, Graduate School of Science, Tohoku University)

[SCG44-P10] Experimental study on propagation of elastic wave in supercritical geothermal reservoirs

*Katsuya Mizuno[1], Noriyoshi Tsuchiya[1], Nobuo Hirano[1] (1.Tohoku university)

Intrusive and emplacement process of the Tono plutonic complex: Constraints from dating and isotopic analysis of zircons

*Yasuhiro Ogita[1], Kazusa Sando[2], Kozue Ishibashi[3], Shuhei Sakata[4], Takeshi Ohno[5], Satoshi Suzuki[3], Tatsunori Yokoyama[1], Saya Kagami[1], Mitsuhiro Nagata[1], Takashi Yuguchi[2]

1. Tono Geoscience Center, Japan Atomic Energy Agency, 2. Faculty of Science, Yamagata University, 3. Graduate school of Science and Engineering, Yamagata University, 4. Earthquake Research Institute, University of Tokyo, 5. Faculty of Science, Gakushuin University

Introduction

Tono plutonic complex (TPC), northeast Japan, consists of adakitic rocks (central facies) and calk-alkaline rocks (main facies and marginal facies) surrounding the central facies [1,2]. Some previous studies have reported TPC zircon U-Pb ages; 117.5 ±2.4 Ma in the central facies; 118.9 ±2.6 Ma and 118.0 ±1.2 Ma in the main facies [3,4]. These ages are related to last stage of igneous activity in the Kitakami Mountains. Revealing the formation process of zonal granitic pluton such as TPC can constrain for the history of the Cretaceous igneous activities in the Kitakami Mountains. Although intrusive relations among the facies are estimated from field observations [5] and whole rock Nd and Sr isotopic compositions [6], there is no discussion regarding to zircon U-Pb ages associated with solidification temperature and origin of magma. Zircon collected from a granitic pluton provides its crystallization age and crystallization temperature [7] from zircon U-Pb dating and titanium (Ti) concentration analysis, respectively. The pairs of data enable to reveal the sequential formation process from intrusion through emplacement to crystallization/solidification of plutonic body [8]. Hafnium isotopic compositions of zircon provide us the information of their source of magma [4]. In this study, we estimated crystallization age and temperature of TPC zircons deduced from U-Pb isotopic analysis and quantitative analysis of Ti, respectively. Moreover, Hf isotopic analysis of TPC zircons are carried out to discuss their source magma.

Samples and methods

Zircons were separated from each rock samples of TPC three lithofacies, and observed through cathodoluminescence images using scanning electron microscope at Yamagata University to clarify the internal structures related to crystal growths. On the basis of the observation, we performed simultaneous determination of U-Pb age and Ti concentration by using laser ablation-inductively coupled plasma-mass spectrometry (LA-ICP-MS) [9] at Gakushuin University. Hf isotopic analysis are carried out at Tono Geoscience Center, Japan Atomic Energy Agency by using LA-ICP-MS.

Results and discussion

As the result of U-Pb isotopic analysis of zircons, age ranges of TPC three lithofacies overlap (**Table 1**). There are no significant age differences between core and rim of each zircon grain. Weighted means of U-Pb age are listed (**Table 1**). The zircon U-Pb age of central facies is older than reference age [3], whereas that of main facies is consistent with results of previous studies [3,4].

Ti concentrations have ranges between 1.96 ±0.28 ppm and 4.74 ±0.44 ppm for the central facies (9 grains, 23 spots), 4.07 ±0.42 ppm and 13.61 ±0.96 ppm for the main facies (12 grains, 32 spots), and 6.65 ±0.59 ppm and 8.81 ±0.71 ppm for the marginal facies (1 grain, 10 spots) (**Table 1**). Crystallization

©2021. Japan Geoscience Union. All Right Reserved.

temperature estimated by Ti-in-zircon geothermometer (assuming both SiO_2 activity and TiO_2 activity were 1.0.) [10] range 613 ±38 ℃ to 680 ±39 ℃ for the central facies, 668 ±39 ℃ to 775 ±43 ℃ for the main facies, and 709 ±40 ℃ to 734 ±41 ℃ for the marginal facies. Since these temperature conditions are close to solidus of granitic magma, zircon U-Pb age and crystallization temperature reflect the emplacement age and thermal condition in magma chamber, respectively. In future works, to make further consideration on intrusive and emplacement process of each TPC lithofacies, additional analysis and new perspective such as Hf isotope are required.

Acknowledgments

This study was carried out under a contract with the Ministry of Economy, Trade and Industry (METI), Japan, as part of its R&D supporting program titled “Establishment of Advanced Technology for Evaluating the Long-term Geosphere Stability (2020 Fy)”.

References

[1] Tsuchiya and Kanisawa, 1994, J. Geophysical Research, **99**, 205 –220. [2] Mikoshiba and Kanisawa, 2008, Earth Sci. (Chikyu Kagaku), **62**, 183 –201. (in Japanese with English abstract) [3] Tsuchiya et al., 2015, Japanese Magazine of Mineralogical and Petrological Sci., **44**, 69 –90. (in Japanese with English abstract) [4] Osozawa et al., 2019, J. Asian Earth Sci., **184**, e103968. [5] Nishimura et al., 1999, The Memoirs of the Geological Society of Japan, **53**, 177 –188. (in Japanese with English abstract) [6] Tsuchiya et al., 2007, J. Volcanology and Geothermal Reseach, **167**, 134 –159. [7] Watson et al., 2006, Contribution to Mineralogy and Petrology, **151**, 413 - 433. [8] Yuguchi et al., 2016, J. Mineralogical and Petrological Sci., **111**, 9 –34. [9] Yuguchi et al., 2020, Lithos, **372 –373**, e105682. [10] Ferry and Watson, 2007, Contribution to Mineralogy and Petrology, **154**, 429 –437.

Keywords: zircon, U-Pb age, Ti concentration, Hf isotope, Tono plutonic complex

©2021. Japan Geoscience Union. All Right Reserved.

Table 1. Zircon U-Pb age and titanium concentration in Tono plutonic complex.

lithology			Cetral fafies	Main facies	Marginal facies
U-Pb age			9 grains, 23 spots	12 grains, 32 spots	1 grain, 10 spots
		range	108.7 ± 9.0 Ma - 153.9 ± 12.2 Ma	96.1 ± 10.7 Ma - 135.0 ± 12.1 Ma	121.6 ± 7.6 Ma - 147.5 ± 10.3 Ma
		weighted mean	125.6 ± 2.0 Ma	116.8 ± 2.1 Ma	133.8 ± 2.7 Ma
	core		7 grains, 9 spots	8 grains, 12 spots	1 grain, 3 spots
		range	108.8 ± 9.0 Ma - 153.9 ± 12.2 Ma	100.2 ± 9.7 Ma - 134.2 ± 13.0 Ma	121.6 ± 7.6 Ma - 147.5 ± 10.3 Ma
		weighted mean	125.3 ± 3.4 Ma	112.17 ± 3.2 Ma	134.2 ± 5.0 Ma
	rim		9 grains, 14 spots	9 grains, 20 spots	1 grain, 7 spots
		range	114.6 ± 7.5 Ma - 146.4 ± 12.3 Ma	96.1 ± 10.7 Ma - 135.0 ± 12.1 Ma	130.8 ± 7.2 Ma - 140.2 ± 12.2 Ma
		weighted mean	125.8 ± 2.5 Ma	120.1 ± 2.7 Ma	133.6 ± 3.2 Ma
Ti concentration			9 grains, 23 spots	12 grains, 32 spots	1 grain, 10 spots
		range	1.96 ± 0.28 ppm - 4.74 ± 0.44 ppm	4.07 ± 0.42 ppm - 13.61 ± 0.96 ppm	6.65 ± 0.59 ppm - 8.81 ± 0.71 ppm
		weighted mean	2.86 ± 0.07 ppm	7.73 ± 0.11 ppm	7.65 ± 0.20 ppm
	core		7 grains, 9 spots	8 grains, 12 spots	1 grain, 3 spots
		range	1.96 ± 0.28 ppm - 4.74 ± 1.96 ppm	5.19 ± 0.50 ppm - 13.61 ± 0.96 ppm	7.63 ± 0.65 ppm - 8.81 ± 0.71 ppm
		weighted mean	3.00 ± 0.11 ppm	7.38 ± 0.18 ppm	7.98 ± 0.39 ppm
	rim		9 grains, 14 spots	9 grains, 20 spots	1 grain, 7 spots
		range	2.19 ± 0.27 ppm - 4.09 ± 0.40 ppm	4.07 ± 0.42 ppm - 12.19 ± 0.90 ppm	6.65 ± 0.59 ppm - 8.57 ± 0.68 ppm
		weighted mean	2.78 ± 0.08 ppm	7.96 ± 0.15 ppm	7.52 ± 0.24 ppm

©2021. Japan Geoscience Union. All Right Reserved.

Whole-rock chemical composition of the Nojima granodiorite in northern part of Awaji Island, southwestern Japan

*Akihiro Ishihara[1], Motohiro Tsuboi[1]

1. Kwansei Gakuin University

The Late Cretaceous to Paleogene granitic rocks in the inner belt of southwestern Japan is divided into three zones from north to south: the Sanin belt, the Sanyo belt, and the Ryoke belt (1). Granitic rocks in Awaji Island in Hyogo Prefecture belongs to the Ryoke or Sanyo belt. The granitoids of Awaji Island are divided into three groups (granitoids I, II, and III) and eleven rock types according to the intrusion sequences (2). The Nojima granodiorite is a medium-grained hornblende biotite granodiorite to granite that is classified as granitoids Ⅱ. The chemical compositions of whole-rocks and minerals of the granitoids of Awaji Island have been reported (3), however, the chemical compositions of rare earth elements are rarely reported. In this study, chemical composition of the Nojima granodiorite including rare earth elements were analyzed and the formation process and petrogenesis were investigated. Major and trace elements were measured by using wavelength-dispersive X-ray fluorescence spectrometer (XRF). Rare earth elements were determined by inductively coupled plasma mass spectrometer (ICP-MS). SiO_2 content is in the range of 58.7-72.8 wt%. Fe_2O_3, MnO, TiO_2, CaO, P_2O_5 and MgO decreases and K_2O increases with increasing SiO_2. Al_2O_3 and Na_2O shows almost constant. Alumina saturation index (Al_2O_3 /(CaO+Na_2O+K_2O)) ranges from 0.87 to 1.10. Alumina saturation index increases with increasing SiO_2. On the Chondrite normalized REE pattern diagram, the light rare earth elements (La, Ce, Pr, Nd, Sm, Eu) are more abundant than the heavy rare earth elements (Gd, Tb, Dy, Ho, Er, Tm, Yb, Lu). This may be due to the relationships between ionic radii of REE and differentiation process of parental magma. It shows negative Eu anomalies for three samples and positive Eu anomalies for two samples among six samples. Two samples show negative Ce anomalies among six samples.

(1)Ishihara, S. (1971) Modal and chemical compositions of the granitic rocks related to the major molybdenum and tungsten deposits in the Inner Zone of Southwest Japan. Jour. Geol. Soc. Japan, 77, 441-452.

(2)Takahashi, Y. and Hattori H. (1992) Granitic rocks in Awaji Island-with an emphasis on the foliated granites-. Bull. Geol. Surv. Japan, 43, 335-357.

(3)Takahashi, Y. (1995) Major element geochemistry and mineral chemistry of granitic rocks in Awaji Island-Implications for the zonal distribution of Cretaceous granitic rocks, Inner Zone of Southwest Japan-. Bull. Geol. Surv. Japan, 46, 23-40.

Keywords: granodiorite, X-ray fluorescence, inductively coupled plasma mass spectrometer, rare earth elements, Awaji Island

©2021. Japan Geoscience Union. All Right Reserved.

Influence of inclusions on hydrogen generated during low temperature serpentinization

*Asuka Sugawara[1], Ryohei Kawakita[1], Tsubasa Otake[2], Tsutomu Sato[2]

1. Graduate school of Engineering, Hokkaido University, 2. Faculty of Engineering, Hokkaido University

Low temperature serpentinization, a hydration reaction of ultramafic rocks occurring at < 100℃, may generate hydrogen near Earth’ s surface environment. Fluids containing abundant hydrogen and methane formed by low temperature serpentinization (e.g., Lost City at the Mid-Atlantic Ridge) may have played key roles in abiotic synthesis of organic materials and therefore the origin of life in the Earth. However, the detail mechanism of the hydrogen generation during the reaction is poorly understood. Previous experimental studies have demonstrated that fresh peridotites produced more hydrogen than serpentinites suggesting that dissolution of olivine and pyroxene generates hydrogen. On the other hand, Klein et al. (2019) suggests that olivine-hosted fluid inclusions in which serpentinization progresses during cooling from magmatic temperatures are the important reservoir of hydrogen and abiotic methane released during low temperature serpentinization in the Earth’ s surface environments.
The objective of this study is to evaluate olivine-hosted inclusions as a potential source for hydrogen released during low temperature serpentinization experiments using different ultramafic rocks from the previous studies.

Harzburgites from Konde Hill (Soroako), Sulawesi, Indonesia and Horoman, Hokkaido were used in this study since they are the two samples that generated the greatest amount of hydrogen by low temperature serpentinization experiments. Although, both samples are relatively fresh harzburgites (< 0.7 wt% of water content), the generated amount of hydrogen was higher in Konde Hill (322 μmol/kg) than Horoman (146 μmol/kg). We observed the occurrence of olivine-hosted inclusions in the thin section samples using petrographic microscope under transmitted light and analyzed their mineralogical and gaseous compositions by confocal Raman spectroscopy.
Raman spectroscopy indicated that olivine-hosted inclusions are predominantly composed of some secondary minerals (i.e., serpentine, brucite) as well as methane in both samples. None of the samples show inclusions containing water molecules. These results suggest that serpentinization had occurred in the fluid inclusions with exhausting water. Whereas 33% of the gas inclusions contain hydrogen in the Konde Hill sample, none of the gas inclusions contain hydrogen in the Horoman sample. Based on the Raman spectroscopic analysis, we estimated the possible contribution of hydrogen in the gas inclusions to hydrogen generated during low temperature serpentinization experiments, which account for 230 μmol/kg. This amount of hydrogen may actually explain the difference between the two samples in the generated amounts of hydrogen during the experiments which can cover all of the differences measured in the previous study.

Therefore, this study suggests that olivine-hosted inclusions are an important source for the hydrogen generated during low temperature serpentinization. However, since the Horoman sample does not have any inclusion containing hydrogen, a significant amount of hydrogen was also likely produced by dissolution of olivine at the low temperature.

Reference

Klein, F., Grozeva, N. G., & Seewald, J. S. (2019). Proc. Natl. Acad, Sci. U.S.A., 116, 17666–17672.

©2021. Japan Geoscience Union. All Right Reserved.

Keywords: low temperature serpentinization, hydrogen, inclusion

©2021. Japan Geoscience Union. All Right Reserved.

Detailed characteristics of Raman spectra of carbonaceous materials in fault rocks nearby the Median Tectonic Line

*Hiroshi Mori[1], Yuki Nobe[1], Ken Yamaoka[2], Yosuke Tomooka[1], Yui Kouketsu[3], Tetsuya Tokiwa[1]

1. Shinshu University, 2. The University of Tokyo, 3. Nagoya University

Based on sensitivity of Raman spectra of carbonaceous material (CM) to the degree of graphitization of CM and the close relationship between the graphitization and metamorphic temperature, the Raman CM geothermometry has been developed and well used to estimate the maximum attained temperature in sedimentary and metamorphic rocks. In contrast, some studies pointed out that the degree of graphitization of CM is modified by brittle shearing. Therefore, to obtain the reliable maximum temperatures from fault rocks by this method, it is important to clarify the effects of brittle shearing on the Raman spectra of CM and here we conducted the Raman spectral analyses of CM in pelitic fault rocks nearby the Median Tectonic Line (MTL)—which is the largest on-land fault in Japan—in the Mizoguchi outcrop, Nagano Prefecture, central Japan.

In the Mizoguchi outcrop, the MTL is well exposed and recognized as the geological boundary separating the high-P/T Sanbagawa and low-P/T Ryoke belts. Five pelitic samples within 13 m from the MTL in the Sanbagawa side and three pelitic samples within 3.5 m in the Ryoke side were collected. As microstructural characteristics, brittle deformation structures are well developed in all samples and CM are contained in highly sheared matrix parts and also as inclusions in rock fragments or in porphyroblasts. In addition, the intensity of brittle shearing increases towards the MTL. To compare these structural characteristics, we respectively analyzed CM of matrix parts (matrix-CM) and of inclusion parts (inclusion-CM) and estimated temperature for each Raman spectrum by using the Raman CM geothermometry to use this value as an index of the degree of graphitization.

The average temperatures of inclusion-CM are ~370–430 ºC in the Sanbagawa belt and ~400–520 ºC in the Ryoke belt while those of matrix-CM are ~360–380 ºC in the Sanbagawa belt and ~370–410 ºC in the Ryoke belt. Comparison the data between inclusion- and matrix-CM in same samples implies lower average temperatures and smaller heterogeneities of matrix samples than those of inclusion-CM. In addition, as the special trends of the average temperatures, inclusion-CM show decreasing of temperature towards the MTL on both sides of the MTL while those of matrix-CM show no clear change. Based on a characteristic that temperature estimated by the Raman CM geothermometry increases as increasing the degree of graphitization of CM and the observed close relationship between microstructural characteristic and estimated temperature, effects of secondary brittle shearing result in the lower values of matrix-CM, while inclusion-CM preserve metamorphic conditions recorded before brittle shearing although some parts of the inclusion-CM (especially in samples within ~1m from the MTL) suffered brittle shearing. These suggest not only that the Raman spectral analysis of CM in fault rock is a useful tool to extract the metamorphic temperature recorded before faulting also that importance of careful selection of CM based on comparing microstructures of the brittle deformation.

Keywords: Raman spectral analysis, carbonaceous material, Median Tectonic Line, Sanbagawa belt, Ryoke belt, fault rock

©2021. Japan Geoscience Union. All Right Reserved.

©2021. Japan Geoscience Union. All Right Reserved.

Trace element composition of chromian spinel in the Sanbagawa ultramafic rocks

*Yuki Aoshima[1], Yuji Ichiyama[1], Jung-Woo Park[2]

1. Chiba University, 2. Seoul National University

The Sanbagawa belt, which is distributed from the Kanto Mountains to the eastern part of Kyushu Island, is a Cretaceous high-pressure-type metamorphic terrane and records Cretaceous subduction zone tectonics. In the Higashi-Akaishi area, the central part of Shikoku Island, a large ultramafic body is exposed associated with metamorphic rocks (mafic gneiss, metagabbro, etc.), which experienced eclogite-facies metamorphism (e.g., Kugimiya and Takasu, 2002). Also, there are exotic rocks of ultramafic volcanic rocks in an ophiolitic belt (Mikabu belt) in the south of the Sanbagawa belt and serpentinite blocks in low-grade pelitic schist, as seen in the Fujiwara body. In this study, major- and trace-element analyses of chromian spinel for the Sanbagawa ultramafic rocks were performed to reveal the origin of various ultramafic rocks in the Sanbagawa belt. Chromian spinel in the Higashi-Akaishi dunites and chromitite show high Cr# (= Cr / [Cr + Al]; >0.6) and low TiO2 (<0.3 wt.%) content and are poor in Ga, Ti, and Ni in normalized elemental patterns. No positive anomaly in Ru is present in platinum-group element patterns. These results suggest that the Higashi-Akaishi dunites and chromitite formed as cumulates crystallized from the same parental magma, which is derived from the highly depleted mantle like boninite in an island arc setting. On the other hand, chromian spinel in the serpentinite in the Fujiwara body and picrite in the Mikabu belt show intermediate Cr# (0.4-0.6) and TiO2 (0.4-1.7 wt.%) content relative to those of the Higashi-Akaishi body rocks. The trace element patterns show enrichment in Ga, Ti, and Ni and the platinum-group element patterns are characterized by a significant positive anomaly in Ru. These results suggest that the Fujiwara serpentinite and Mikabu picrite are derived from the intraplate magma produced by the upwelling of a large mantle plume, as proposed by the previous studies (Ichiyama, 2014). The metamorphic rocks associated with the Higashi-Akaishi body were formed in an oceanic island arc in the Early Jurassic (Aoki et al., 2019; 2020). The Higashi-Akaishi ultramafic rocks would have been parts of the lower crust of an Early Jurassic oceanic island arc on the Izanagi plate, whereas the Fujiwara serpentinite and Mikabu picrite are probably fragments of a Late Jurassic oceanic plateau. These results imply that all ultramafic rocks in the Sanbagawa metamorphic belt were brought through the subduction process of the Izanagi plate.

Keywords: Sanbagawa belt, ultramafic rocks, chromian spinel, platinum group elements

©2021. Japan Geoscience Union. All Right Reserved.

The trace element composition of sapphire in the xenolith of garnet-bearing andesitic tuff of the Donzurubo Formation, the Nijo Group, Japan.

*Mayuko Fukuyama[1], Masatsugu Ogasawara[2]

1. Graduate School of Engineering Science, Akita University, 2. Geological Survey of Japan, National Institute of Advanced Industrial Science and Technology

The Donzurubo Formation is a member of the Middle Miocene Nijo Group in the Mt. Nijo, Japan. The Donzurubo Formation consists of three sub-formations, the Lower Donzurubo Formation: garnet-biotite rhyolitic welded tuff, the Middle Donzurubo Formation: garnet-biotite andesite (Ishikiriba Volcanics), garnet-biotite andesitic clastic rocks, garnet-hornblend-orthopyroxene andesite (Hata Volcanics), and the Upper Donzurubo Formation: garnet-biotite rhyolite (Medake Volcanics), garnet-biotite rhyolitic clastic rocks. The volcanic rocks in the Nijo Group are a typical Setouchi Volcanic Rocks which are characterized by the occurrence of high-Mg andesite in Miocene. The volcanic rocks in Nijo Group contains abundant garnets. The occurrence of corundum as a xenolith of garnet-bearing andesite were reported in previous studies (e.g. Omori, 1942, Morimoto, 1949). On the other hand, the euhedral sapphires and garnets are found in Takeda river which is downstream from Mt. Nijo.
In this study, we present the occurrence of corundum-bearing xenolith which is found in garnet-biotite andesitic tuff in the Lower Donzurubo Formation. The euhedral pastel blue sapphire grains are also collected from river sands in Takeda river. The mineral assemblage of corundum-bearing xenolith is corundum, orthopyroxene, plagioclase, sillimanite, garnet, spinel, zircon, monazite, and ilmenite. The corundum is replaced by sillimanite, spinel and plagioclase. The sillimanite and spinel are a product of metamorphic reaction as; 5 corundum + garnet = 3 sillimanite + 3 spinel. This reaction takes place at high temperature condition (> 750 ^{o}C).
The corundum in xenolith are Fe-poor (1178-1707 μg/g), Ga-poor (43-63 μg/g), Cr-poor (81-159 μg/g), Ti-rich (273-975 μg/g), and Mg-rich (114-240 μg/g). Some of sapphires from Takeda river shows similar trace element composition to the corundum in xenolith, but some of them shows the different compositions which may indicate the different origin of sapphires. Trace elements in corundum are often used for origin determination. In the case of blue sapphire, the discrimination diagram of sapphire is difficult to identify their origin (Groat et al., 2019) but trace element compositions of corundum and sapphires in this study clearly shows the metamorphic origin.
The basement rocks of the Nijo Group consist of granitoids and high-temperature metamorphic rocks of the Ryoke belt. The mineral assemblage of xenolith and trace elements of corundum indicate that the origin of xenolith could be lateritic metamorphic rock at high-T condition which might be the Ryoke metamorphic rocks.

Acknowledgement
We appreciate the Hikia Group for obtaining samples.

References
Groat at al. (2019) Gems & Gemology, 55, 512-535.
Morimoto (1949) The Journal of the Geological Society of Japan, 55, 38-43.
Omori (1942) The Journal of the Japanese Association of Mineralogists, Petrologists and Economic Geologists, 27, 27-58.

©2021. Japan Geoscience Union. All Right Reserved.

Keywords: sapphire, corundum, trace element, LA-ICP-MS, Mt. Nijo

©2021. Japan Geoscience Union. All Right Reserved.

Microstructures of spherical pyrite in the Kuroko deposits: possible mechanism of pyrite growth on bubble

*Atsushi Okamoto[1], Yoeri van de Ridder[2], Oliver Plumper[2], Markus Ohl[2], Ryoichi Yamada[1]

1. Tohoku University, 2. Utrecht University

The submarine hydrothermal vents are one of the most active sites of mineralization in the Earth. The Kuroko deposits provide the significant insights on the mineralization processes at the active submarine hydrothermal systems. It is known that various forms of pyrite exist within the Kuroko deposits, but the formation mechanism and controlling factor have not been fully understood. In this study, we show the microstructural features of the spherical pyrite of the Kuroko deposits by using the EBSD, EDX and micro X-ray CT analyses, and discuss the formation processes within the hydrothermal vent. The sample was a part of chimney collected from the Kannondo deposit in the Hanaoka mine, NE Japan. The sample show the banded structure mainly composed of pyrite, barite, sphalerite with lessor amount of chalcopyrite and aluminosilicate. The pyrite particles show a spherical shape with 10-100 micrometer in diameter. The spherical pyrite grains often have hollow at the center, and some of them are filled by later minerals (barite and Cu-rich phase). The detailed microstructural analyses revealed that the spherical pyrite is composed of needle-like pyrite crystals, all of which are oriented with <100> direction. The needles are wider outward, suggesting the growth from the center to the margin. These features suggest the growth of pyrite crystals on bubble template as follows. Pyrite nano particles were initially formed in fluids, and they were attracted to a bubble surface by electrostatic double-layer forces and hydrophobic forces in response to specific pH, pS and pFe conditions. The preferential faces were attached on the bubble, and developed their face to grow in <100> direction. Such particle with hollow could have advantages on transport with low particle density.

Keywords: spherical pyrite, Kuroko, bubble surface

©2021. Japan Geoscience Union. All Right Reserved.

The mineral occurrence of kaolinitic saprolite beneath the sedimentary kaolin deposit at Seto district

*Haruna Asai[1], Kikuchi Ryosuke[1], Tsubasa Otake[1], Tsutomu Sato[1]

1. Hokkaido University

Kaolin is the common clay minerals in the Earth’ s surface, and important non-metallic mineral commodity used for ceramics, refractories and paper filler. The cluster of sedimentary kaolin deposits distributed in the Seto-Tono district is the largest kaolin field in Japan. Kibushi clay (ligneous clayey sediment) and Gerome clay (unsorted sediment consisting of coarse-grained quartz and fine-grained kaolin) in this district resulted from granitic clastics and have been mined for many years owing to its high plasticity, refractoriness and whiteness after baking. Recently, however, it is concerned that remained resource is being exhausted, and thus, utilization of kaolinitic saprolite which is the weathered crust of the basement granite underlying the kaolin deposit has been considered. Moreover, the close relationship between this kaolinitic saprolite and kaolin deposit is expected as a window to elucidate the formation condition for high quality kaolin deposit[1]. In this study, we investigated mineralogical characteristics of kaolinitic saprolite and chemical forms of iron which is undesirable impurity for industrial uses.

The samples used were obtained from the active mining area in the northern Seto-city, Aichi prefecture, where the kaolin deposits are embedded in the lower Tokai Group, Seto porcelain clay formation (Late Miocene to Pliocene). Several samples were collected from Kibushi, Gaerome clays and kaolinitic saprolite (hereafter “Green saprolite”, named after its greenish grey color). Bulk and the elutriated clay fraction of 0.2 –2 μm size were analyzed by XRF, powder XRD and SEM-EDS to clarify the chemical and mineralogical compositions. All of three types of clays (Kibushi, Gaerome and Green saprolite) consist of quartz, feldspar and kaolinite, but SEM found the difference in kaolinite morphology: The kaolinite in Kibushi and Gaerome clays were fine particles, whereas Green saprolite contained both larger (~ several hundreds of μm), highly crystalline kaolinite grains and fine particles. Further analysis indicated that the fine kaolinite particles were derived from feldspar and the larger crystalline grains were formed by alteration of biotite. Dithionite-citrate-bicarbonate (DCB)[2] extractable Fe was measured to distinguish the free Fe from the structural Fe in the total Fe in both bulk and clay fraction of Green saprolite. More than the half of Fe in the clay fraction was extractable by the DCB method, while only ~ 25% of Fe in the bulk was extracted. This indicate that Fe in the clay fraction was distributed both in the structure of kaolinite and low crystalline, ferric iron hydroxides/oxides, and the bulk sample including the larger kaolinite grains contained structural Fe in the remnants of altered biotite. Further analysis using Mö ssbauer spectroscopy indicated that Fe valence ratio (Fe^{2+}/Fe^{3+}) in the fine kaolinite particles of the green saprolite was 7/5, and this Fe^{2+} is the possible cause of its greenish color. Our analysis suggests that the Green saprolite layer can be improved as a resource of kaolin commodity by separating clay fractions and removing free iron in hydroxides/oxides.

References

[1] Takagi, T., Shin, K. C., Jige, M., Hoshino, M., & Tsukimura, K. (2021). Microbial nitrification and acidification of lacustrine sediments deduced from the nature of a sedimentary kaolin deposit in central Japan. *Scientific Reports*, 1–17.

©2021. Japan Geoscience Union. All Right Reserved.

[2] Mehra, O. P., & Jackson, M. L. (1958). Iron oxide removal from soils and clays by a dithionite-citrate system buffered with sodium bicarbonate. *Clays and Clay Minerals*, *7*(1), 317–327.

Keywords: kaolinite, Green saprolite, SEM-EDS, DCB method

©2021. Japan Geoscience Union. All Right Reserved.

Borate concentration processes in modern evaporitic and hydrothermal environments: Constraints on the formation of a boron-rich environment on prebiotic earth

*Sara Rinka Christensen [1], Akizumi Ishida[1], Takeshi Kakegawa[1]

1. Department of Earth Science, Graduate School of Science, Tohoku University

Boron-rich environments are favored places for the evolution of prebiotic nucleotides. Modern evaporitic borate basins are often considered as modern analogs of ancient boron-rich environments. Despite this, the (1) source of highly concentrated boron, (2) factors in accumulation of boron, and (3) post-deposition modification of initial boron-bearing minerals in modern evaporitic borate basins are not yet decided.

In order to approach the above problems, the borate mine in Boron, California (= ‘Boron mine’, hereafter), and boron-enriched (up to 980 ppm) hot spring waters of Shin-appi hot spring, Iwate prefecture were studied. The Boron mine in California is one of the biggest boron-ore mines in the world. A huge borax occurs together with Miocene lake sediments. At Shin-appi hot spring in Iwate prefecture, which has the highest boron concentration in the region, aragonite and calcite precipitates rapidly around the discharging areas. Geochemical and mineralogical studies were performed on samples from Boron mine and Shin-appi hot spring which include mineral precipitate and water samples.

Shin-appi hot spring was abnormally enriched in bicarbonate, sodium, LILEs, REEs and radioactive elements. Measured $d^{13}C$ values of dissolved inorganic carbon ranged from -5 to -3 per mil. Such geochemical characteristics suggest that the source of boron-rich waters at Ninohe are deep magmatic brines evolved from felsic plutons. No boron-containing minerals were found in the precipitates, although the chemistry of the water seemingly allows for the formation of tourmalines and other boro-silicates. Instead, borax was found precipitating from an actively evaporating area with minor halite. This suggests the difficulty to precipitate boron-bearing minerals in aquatic environments, even with the high availability of boron.

Chemical analyses of borax and kernite samples from the Boron mine indicated that both were enriched in water-mobile heavy elements. These heavy metals were likely supplied by hydrothermal activity through the constraining faults of the mine. Magmatic brines formed by ancient felsic magma were considered as a source of boron-rich hydrothermal fluids at Boron mine, the same as in Shin-appi hot spring. Ancient boron-rich hydrothermal fluids were discharged into the evaporitic sedimentary basin at the Boron mine, where boron minerals initially precipitated with other chemical and clastic components. The texture of borax and kernite indicate that initial boron minerals were dissolved and reprecipitate as borax and kernite during later diagenesis, by separating other chemical and clastic components. Such later processes could further concentrate boron in a specific environment.

From the above, we found that evaporitic borate deposits may require (1) brine evolved from felsic plutons, (2) rapid separation of components other than borate, and (3) reprecipitation by diagenesis. This environment may have occurred on the surface of the proto-arc on the early Earth, which was likely ideal for the evolution of prebiotic nucleotides.

©2021. Japan Geoscience Union. All Right Reserved.

©2021. Japan Geoscience Union. All Right Reserved.

Experimental study on propagation of elastic wave in supercritical geothermal reservoirs

*Katsuya Mizuno[1], Noriyoshi Tsuchiya[1], Nobuo Hirano[1]

1. Tohoku university

Elastic wave velocity of rocks have been applied to the exploration of geothermal resources in geothermal development or the understanding of underground structures. Many laboratory scale studies have been conducted on elastic wave velocity measurements of rocks used to interpret seismic data measured in the field, but most of them were conducted under room temperature and pressure. However, Since the physical properties of rocks has changed by temperature and pressure, it is important to measure the elastic wave velocity of rocks under the in situ high temperature and pressure conditions of underground in order to achieve more accurate geothermal resource exploration. J.W. Spencer Jr & A.M. Nur, (1976), H.B. Morta & F. Wuttke, (2016) has measured elastic wave velocity in supercritical conditions of granite and amphibolite, respectively. In order to develop geothermal energy in more deep-seated regions in the future, elastic wave velocity measurements for other rocks will be necessary. The purpose of this study is to provide a new interpretation of seismic data through the measurement of elastic wave velocity of rocks under supercritical water conditions.

In this study, we started by measuring the elastic wave velocity of water as a function of temperature in order to prove that the elastic wave measurement data obtained from the experimental system for in situ measurements is correct. Then we measured the elastic wave velocity for gabbro, which is universally present in the lower crust, and compare it with the data for granite measured under the same conditions.

References

James W. Spencer Jr., Amos M. Nur, The effects of pressure, temperature, and pore water on velocities in westerly granite, JGR Vol.81, Issue5, 10 February 1976, 899-904

H.B. Morta & F. Wuttke, Temperature dependence of elastic P- and S-wave properties of rocks: Applications to geothermal reservoir evaluation, Energy Geotechnics (2016), 311-316

Keywords: Supercritical fluid, Supercritical geothermal reservoirs, Elastic wave

©2021. Japan Geoscience Union. All Right Reserved.

[J] Poster | S (Solid Earth Sciences)：S-CG Complex & General

Sun. Jun 6, 2021 5:15 PM - 6:30 PM JST | Sun. Jun 6, 2021 8:15 AM - 9:30 AM UTC | Ch.16_1

[S-CG53] Reducing risks from earthquakes, tsunamis & volcanoes: new applications of realtime geophysical data

convener:Masashi Ogiso(Meteorological Research Institute, Japan Meteorological Agency), Masumi Yamada(Disaster Prevention Research Institute, Kyoto University), Yusaku Ohta(Research Center for Prediction of Earthquakes and Volcanic Eruptions, Graduate School of Science, Tohoku University), YAMAMOTO Naotaka CHIKASADA(National Research Institute for Earth Science and Disaster Resilience)

As the number of population centers grows in regions with earthquake, tsunami and volcano hazards, the importance of improving methods for rapid, realtime estimates of activity increases. Realtime monitoring, analysis, and prediction of seismic ground motion, crustal movement and tsunami will be powerful tools to contribute to earthquake and tsunami disaster preparedness/mitigation. Tsunami and Earthquake Early Warning systems exist today in many locations around the world. Now JMA has started to promptly provide Eruption Notices to inform people of impending and beginning volcanic eruptions. Large events like the 2011 Tohoku Earthquake (Mw9.0) have demonstrated some of the shortcomings of existing techniques. In this session, we invite presentations on new ideas, methods and applications of (near) realtime analysis of seismic, geodetic and tsunami data, to the problem of realtime prediction aimed at improving disaster preparedness/mitigation in the fields of earthquake, tsunami and volcano observation. Presentation is encouraged to bring together scientists, engineers, and practitioners from a broad range of backgrounds from around the world, and to promote collaborative communication at the leading edge of the science and technologies.

[SCG53-P01] High precision of Realtime tsunami prediction based on the amplification

*Narumi Takahashi[1], Kentaro Imai[2] (1.National Research Institute for Earth Science and Disaster Resilience, 2.Japan Agency for Marine-Earth Science and Technology)

[SCG53-P02] Generation Requirements of PL Waves for Shallow Earthquakes around Japan-Possibility of Immediate Tsunami Prediction

*Keishi Osuga[1], Takashi Furumura[1] (1.Department of Earth and Planetary Science, School of Science, The University of Tokyo)

[SCG53-P03] Evaluation of simple source time function in rapid source parameter determination system (AQUA)

*Hisanori Kimura[1], Youichi Asano[1] (1.National Research Institute for Earth Science and Disaster Resilience (NIED))

High precision of Realtime tsunami prediction based on the amplification

*Narumi Takahashi[1], Kentaro Imai[2]

1. National Research Institute for Earth Science and Disaster Resilience, 2. Japan Agency for Marine-Earth Science and Technology

We have developed a realtime tsunami prediction system based on the tsunami amplification. The system predicts tsunami arrival times, the heights, inundation area and inundation depth for each target points in turn, in proportion to observed pressure values on observatories of the oceanfloor network like Dense Oceanfloor Network system for Earthquakes and Tsunamis (DONET). The prediction information is extracted from a database of the system for the observatories, which composed of calculated waveforms using many fault models changing the magnitude, depth, dip angle and strike. The merits are simplified system using only one PC playing a roles data transmission, making prediction information and visualization, easy revise even though coastline changes, and robustness of the prediction under the local anomalies of tsunami by landslides on the seafloor. We implemented it on local government of Wakayama and Mie prefectures and an electric power company using DONET. Recently, it was implemented on Chiba prefecture using Seafloor observation network for earthquakes and tsunamis along the Japan trench (S-net).

The error of the prediction is brought by following items, which are noises on observatories of the oceanfloor network, complicated tsunami propagation for the local topography, and contamination of the crustal displacement on the observatories. S-net data sometimes includes large offset for the strong motion due to rotation and unstable posture of the sensor. Sometimes observatories subside by liquefaction on seafloor. We resolved this noise issue statistically by comparison of the observed data among the triggered sensor and dismissal of abnormal data. Second issue of dispersion of the tsunami height due to complicated tsunami propagation are resolved by specification of fault models using detected direction of the source. For the last issue of contamination of the composition of crustal displacement, we introduce distribution of the observed crustal displacement on the oceanfloor network and omit fault models with large difference of the composition of crustal displacement. In particular, The crustal displacement around the prediction target point brings large dispersion on the inundation areas. We realized the high precision of the tsunami prediction by devise on settings and extraction of the fault models.

Keywords: Oceanfloor network system, pressure data

©2021. Japan Geoscience Union. All Right Reserved.

Generation Requirements of PL Waves for Shallow Earthquakes around Japan-Possibility of Immediate Tsunami Prediction

*Keishi Osuga[1], Takashi Furumura[1]

1. Department of Earth and Planetary Science, School of Science, The University of Tokyo

PL is a long period phase with a period of several seconds to several tens of seconds, which is observed between P wave and S wave. P-waves emitted from shallow epicenters interfere with each other as they propagate through the crust by multiple wide-angle reflections, forming long-period wave groups. Sommville (1930) named this wave PL, meaning P-long wave, which was later interpreted by Oliver and Major (1960) as the leaking mode of Rayleigh waves. A longer-period (100-1000 s) phase generated by a similar mechanism in the upper mantle was named W-phase by Kanamori (1993) and is widely used for CMT analysis of large earthquakes and immediate tsunami prediction. Recently, W-phase analysis has also been applied to wave groups with periods of tens of seconds or less (i.e., PL waves) in near-field strong-motion records (e.g., Duputel et al., 2012; Hayes et al., 2009; Usui and Yamauchi, 2013). In this study, in order to utilize the PL waves in the near-field wavefield as an indicator to immediately determine the possibility of tsunami generation, the characteristics of PL waves in large trench earthquakes and their generation and propagation requirements were investigated based on seismic wave propagation simulations.

As an example of PL waves observation, Figure 1a shows the vertical motion velocity record of K-NET during the foreshock of the 2009/3/9 off the Pacific coast of the Eastern Japan Earthquake (M7.3, 8 km depth). At the AOM014 (K-NET Nenokuchi) station, located at the epicentral distance of 310 km, a wave group of PL waves with a period of about 20 s is clearly observed between the P and S phases of the Radial (R) and Vertical (Z) components. It is possible to evaluate the size and depth of the earthquake, namely the possibility of tsunami generation, from the seismic amplitude of PL waves in the near-field strong-motion records.

In order to confirm the generation and propagation characteristics of PL waves caused by shallow, large trench earthquakes, we performed seismic wave propagation simulations using the two-dimensional finite difference method. We selected a cross-sectional area from off Miyagi to northeast Japan (Fig. 2a), set up sedimentary layers, crust and mantle structures using the JIVSM (Koketsu et al., 2012) model, and calculated seismic wave propagation. The epicenter was set as a point source for simplicity, and seismic waves were radiated using a triangular source-time function with a period of 20 seconds based on the GCMT analysis results of the 2009/3/9 earthquake. The record section of the Z-component velocity waveform is shown in Figure 2b. The record section of the Z-component velocity waveform is shown in Figure 2b, and the waveforms at the epicenter distance of 310 km for different source depths of 1, 2, 4, 8, 16, 32, and 64 km are compared in Figure 2c. As a result, it is confirmed that PL waves with the same amplitude as S waves or Rayleigh waves are generated in earthquakes shallower than 8 km depth, and the amplitude weakens with depth.

©2021. Japan Geoscience Union. All Right Reserved.

Observations of PL waves with periods of about 20 s in large (>M7) and shallow (< 40 km) epicentral earthquakes occurring in the ocean may provide a simple assessment of tsunami generation potential prior to CMT inversion analysis of W-phase (PL waves) using far- and near-field waveform records. Earthquakes that occurred inland and propagated overland are dominated by short-period PL waves with periods around 7 s (Furumura and Kennett, 2018), which can be distinguished from earthquakes that occurred in the ocean. In this study, we focused on the Miyagi-oki earthquake. However, the propagation characteristics and prevailing period of PL waves are considered to be affected by deep structures such as the thickness of the crust, as shown by the difference in PL waves between land and sea propagation paths. It is necessary to confirm the regional characteristics of PL wave propagation by analyzing observed waveforms and simulating seismic wave propagation in other regions, such as along the Nankai Trough and the eastern margin of the Japan Sea.

Keywords: PL Waves, Seismic Wave Propagation, Difference Method, Immediate Tsunami Prediction

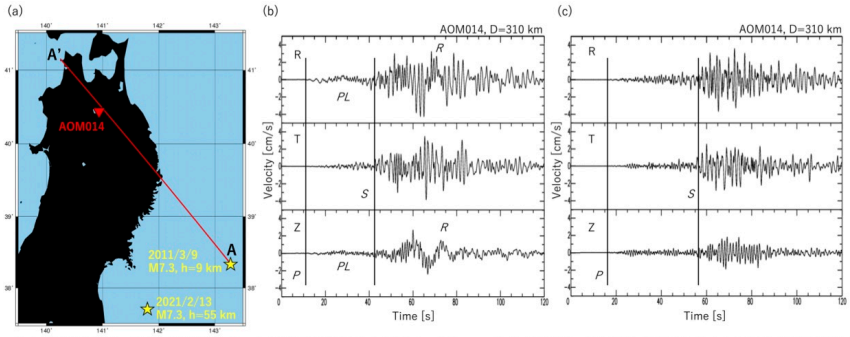


図１ 海溝型地震に見られるPL波の例。(a)震源と観測点およびスナップショットの水平位置。(b)2011/3/9東北地方太平洋沖地震の前震（M7.3、深さ8 km）の３成分速度波形と、Radial/Vertical成分のＰ～Sの間に見られる卓越周期20秒のPL波。(c) 2021/2/13福島県沖の地震（M7.3, 深さ55 km）。

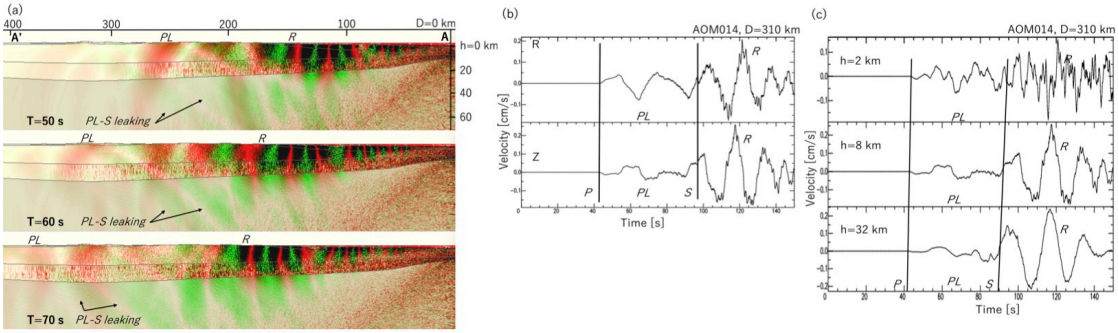


図２　２次元差分法による地震波伝播シミュレーション結果。(a) 地震波伝播のスナップショット（赤がP波、緑はS波を表す）。地震発生から、50、60、70秒後。
(b) AOM014観測点（震源距離310 km）におけるRadial/Vertical成分速度波形、(c)　震源の深さを2、8、32kmとした場合の、同観測点における上下動速度波形とPL波の波形変化。

©2021. Japan Geoscience Union. All Right Reserved.

Evaluation of simple source time function in rapid source parameter determination system (AQUA)

*Hisanori Kimura[1], Youichi Asano[1]

1. National Research Institute for Earth Science and Disaster Resilience (NIED)

In the rapid source parameter determination system called Accurate and QUick Analysis System for Source Parameters (AQUA), source parameters including location, size, and moment tensor (MT) are automatically determined with good accuracy. By incorporating the velocity type strong motion seismometer in the NIED full-range seismograph network (F-net) and changing the processing flow, it became possible to analyze the 2011 off the Pacific coast of Tohoku earthquake (M9.0)(Kimura et al., 2020). However, its size was underestimated as Mw8.6. Since appropriate estimation of the earthquake size is important for disaster mitigation including tsunami warning and initial damage assessment, the simple source time function (STF) in AQUA was evaluated, as suggested by Asano and Kimura (2012).

The isosceles triangle type STF is incorporated into the current processing flow after determining the MT solution with fixed horizontal location (called as ´AQUA-MT´) and its source duration is estimated by a grid search. Here, the centroid time and depth are fixed to those of AQUA-MT to shorten the processing time. When the variance reduction (VR) decreases, the source duration with the highest VR is used hereafter, including the horizontal location estimation (called as ´AQUA-CMT´). Based on this flow, we reanalyzed the 2011 Off Tohoku earthquake and its major aftershocks and earthquakes with Mw6.8 or greater. In addition, the 2003 Tokachi-oki Earthquake (Mjma8.0) and the 2004 Kii Peninsula and Tokaido-oki earthquake (Mjma7.4) were reanalyzed as past major earthquakes. For these two earthquakes, waveform data recorded by the F-net broadband seismometer with epicentral distance of 400 km or more is used.

In the 2011 Off Tohoku earthquake, selecting a 70 sec source duration increased VR from 67.0% to 81.4% and Mw from 8.6 to 8.8. The centroid time, depth, and the focal mechanism are almost the same. The additional processing time was estimated to be about 1 sec. The source duration of major aftershocks of the 2011 Off Tohoku earthquake (15:08 and 15:15, 11 March 2011 (JST); Mjma7.4 and 7.6; note that the latter is the largest aftershock) and two past major earthquakes were estimated as 50, 30, 40, and 40 sec, respectively. Mw increased from 7.4 to 7.6, 7.8 to 7.9, 7.8 to 8.0, and 7.4 to 7.5, respectively.

The incorporation of the STF reduced the underestimation of Mw for the 2011 Off Tohoku earthquake while its size is still underestimated. The source duration of 70 sec is comparable with analysis of rupture process (e.g., Suzuki et al., 2012) and can be considered to represent a major part of the slip history. This duration is not negligible compared to the bandwidth of the analysis (50-200 sec). Hence, we can consider that the incorporation of the STF improved size underestimation. Mw of GlobalCMT for the aftershock on 15:15 and the 2003 and 2004 earthquakes are 7.9, 8.3, and 7.4, respectively. Incorporation of the STF reduced difference from GlobalCMT in most cases.

A grid search of the source duration with a fixed centroid time and depth suppresses a significant increase in processing time. Since STF is introduced only when VR increases after determination of AQUA-MT, the determination ratio would be maintained. By incorporating STF, we can expect to be able to better estimate earthquake size while maintaining process speed and determination ratio.

©2021. Japan Geoscience Union. All Right Reserved.

Keywords: the 2011 off the Pacific coast of Tohoku earthquake, rapid source parameter determination system, Centroid moment tensor

©2021. Japan Geoscience Union. All Right Reserved.

[J] Poster | S (Solid Earth Sciences)：S-CG Complex & General

Sun. Jun 6, 2021 5:15 PM - 6:30 PM JST | Sun. Jun 6, 2021 8:15 AM - 9:30 AM UTC | Ch.16_2

[S-CG54] Ten years from the 2011 Tohoku Earthquake: A milestone of Solid Earth Science

convener:Ryota Hino(Graduate School of Science, Tohoku University), Shuichi Kodaira(Research Institute of Marine Geodynamics, Japan Agency for Marine-Earth Science and Technology), Toru Matsuzawa(Research Center for Prediction of Earthquakes and Volcanic Eruptions, Graduate School of Science, Tohoku University), Takeshi Iinuma(National Research and Development Agency Japan Agency for Marine-Earth Science and Technology)

In the 2011 JpGU Meeting held immediately after the 2011 Tohoku-Oki Earthquake, an emergency session related to this earthquake was set up and 188 research results were reported. Not only was there a preliminary report of research and observations regarding this giant earthquake and tsunami, but also various important ideas indicating directions of subsequent solid-earth science researches were presented: the mechanism of earthquake generation including possible processes leading its large-scaled seismic rupture, the impact of the Tohoku-Oki earthquake on the inland crust, and limitations and effectiveness of early warning regarding earthquakes and tsunamis. Ten years after the 2011 JpGU, which was held just two months after the quake, how far has our understanding of these research themes progressed? In addition to the accumulation of 10 years of researches, our understanding of giant earthquakes and tsunamis has dramatically increased through the observations of post-Tohoku Earthquake phenomena of various kinds that have been progressing over a long period of time and through the newly developed observation networks in the offshore area. In this session, not only the researches on the Tohoku-Oki earthquake and tsunami itself, but also the research results in various solid-earth science fields that have clarified after this earthquake and tsunami will be brought together, to discuss the direction of research that should be aimed at in the future.

[SCG54-P01] Ground motion waveforms in the epicentral area of the 2011 Tohoku-Oki earthquake with large displacements, retrieved from ocean-bottom dynamic pressure change data

*Tatsuya Kubota[1], Tatsuhiko Saito[1], Hiroaki Tsushima[2], Ryota Hino[3], Yusaku Ohta[3], Syuichi Suzuki[3], Daisuke Inazu[4] (1.National Research Institute for Earth Science and Disaster Resilience, 2.Meteorological Research Institute, Japan Meteorological Agency, 3.Tohoku University, 4.Tokyo University of Marine Science and Technology)

[SCG54-P02] Detectability of short-term seafloor deformation by S-net pressure observation

*Ryota Hino[1], Tatsuya Kubota[2], Naotaka YAMAMOTO CHIKASADA[2], Yusaku Ohta[1], Hideto Otsuka[1] (1.Graduate School of Science, Tohoku University, 2.National Research Institute for Earth Science and Disaster Resilience)

[SCG54-P03] Vertical seafloor movement after the 2011 Tohoku earthquake and remarkable uplift near the trench axis off Sanriku

*Chie Honsho[1], Motoyuki Kido[2], Fumiaki Tomita[3], Ryota Hino[1] (1.Research Center for Prediction of Earthquakes and Volcanic Eruptions, Graduate School of Science, Tohoku University, 2.International Research Institute of Disaster Science, Tohoku University, 3.Japan Agency for Marine-Earth Science and Technology)

[SCG54-P04] Improvement of spatial resolution and evaluation of uncertainty for the coseismic slip distribution of the 2011 Tohoku-oki Earthquake

*Fumiaki Tomita[1], Takeshi Iinuma[1], Motoyuki Kido[2], Ryota Hino[3], Yusaku Ohta[3], Ryoichiro Agata[1], Takane Hori[1], Naoki Uchida[3] (1.Japan Agency for Marine-Earth Science and Technology, 2.International Research Institute of Disaster Science, Tohoku University, 3.Graduate School of Science, Tohoku University)

[SCG54-P05] Resolving 3D rheology of northeastern Japan using postseismic deformation following the 2011 Tohoku-oki earthquake

*Jun Muto[1], Dhar Sambuddha[1], James Daniel Paul Moore[2], Satoshi Miura[3], Yusaku Ohta[3], Takeshi Iinuma[4] (1.Department of Earth Sciences, Tohoku University, 2.Earth Observatory of Singapore, Nanyang Technological University, Singapore, 3.Department of Geophysics, Tohoku University, 4.Japan Agency for Marine-Earth Science and Technology)

[SCG54-P06] Numerical simulation of earthquake generation cycles along the Japan Trench

*Ryoko Nakata[1], Takane Hori[2], Seiichi Miura[2], Ryota Hino[1] (1.Graduate School of Science, Tohoku University, 2.Research Institute for Marine Geodynamics, Japan Agency for Marine-Earth Science and Technology)

[SCG54-P07] Seismicity near the trench axis and in the outer rise region of southern Japan Trench: Results from ocean bottom seismograph observations

*Koichiro Obana[1], Gou Fujie[1], Yojiro Yamamoto[1], Yuka Kaiho[1], Yasuyuki Nakamura[1], Seiichi Miura[1], Shuichi Kodaira[1] (1.Research Institute for Marine Geodynamics, Japan Agency for Marine-Earth Science and Technology)

[SCG54-P08] Microseismicity prior to the 2011 Tohoku-Oki earthquake around the mainshock hypocenter

*Hirofumi Goto[1], Ryota Hino[1] (1.Graduate School of Science, Tohoku University)

[SCG54-P09] Characteristics of tectonic tremor activity along the Japan Trench before the 2011 Tohoku Oki earthquake

*Hidenobu Takahashi[1,2], Ryota Hino[1], Naoki Uchida[1], Ryosuke Azuma[1], Susumu Kawakubo[1], Kazuaki Ohta[3], Masanao Shinohara[4] (1.Graduate school of Science Tohoku University , 2.Central Research Institute of Electric Power Industry, 3.National Research Institute for Earth Science and Disaster Resilience, 4.Earthquake Research Institute, The university of Tokyo)

[SCG54-P10] Application of ensemble learning noise classifier to automatically determined earthquake catalog after the 2011 Tohoku Earthquake

*Koji Tamaribuchi[1] (1.Meteorological Research Institute)

[SCG54-P11] **Core-Mantle boundaries state estimation applying the strain analysis on frequency domain**

seiji matsumura[2], *Makoto OKUBO[1] (1.Natural Science Cluster, Kochi University, 2.Faculty of Science and Technology)

[SCG54-P12] Tomography and megathrust earthquakes in the Tohoku forearc

*Dapeng Zhao[1] (1.Department of Geophysics, Tohoku University)

[SCG54-P13] Trench fill and graben fill sediments on the incoming plate around the Japan trench

*Yasuyuki Nakamura[1], Shuichi Kodaira[1], Gou Fujie[1], Seiichi Miura[1], Koichiro Obana[1], Mikiya Yamashita[2] (1.Japan Agency for Marine Earth Science and Technology, 2.National Institute of Advanced Industrial Science and Technology)

Ground motion waveforms in the epicentral area of the 2011 Tohoku-Oki earthquake with large displacements, retrieved from ocean-bottom dynamic pressure change data

*Tatsuya Kubota[1], Tatsuhiko Saito[1], Hiroaki Tsushima[2], Ryota Hino[3], Yusaku Ohta[3], Syuichi Suzuki[3], Daisuke Inazu[4]

1. National Research Institute for Earth Science and Disaster Resilience, 2. Meteorological Research Institute, Japan Meteorological Agency, 3. Tohoku University, 4. Tokyo University of Marine Science and Technology

Introduction

Recent studies have shown that ocean-bottom pressure gauges (OBPs) can record seismic waves in addition to tsunamis and seafloor permanent displacements. Recently the method to numerically simulate more realistic OBP signals inside the focal area based on the theory of tsunami generation (Saito, 2013; 2019) has been established (e.g., Lotto et al., 2015; Saito et al., 2019; Maeda et al., 2020), although the method to appropriately decompose the OBP signal to the seismic and tsunami signals has not been established well (Saito & Tsushima, 2016). If the seismic waveforms inside the focal area are obtained, our understandings for the source process of earthquakes will be deepened, as well as the seismic wave propagation process inside the focal area. In this study, we develop a method to decompose the in-situ OBP records into the tsunami and seismic motion components based on the theory of tsunami generation and apply the method to the OBP data during the 2011 Tohoku-Oki earthquake.

How to extract ground motions from OBP data

When we focus on the low frequency band ($f < \sim 10^{-1}$ Hz) where the elasticity of the seawater can be ignored and we can suppose the seawater is incompressible, the ocean bottom pressure change $p(t)$ can be expressed as a sum of the hydrostatic pressure change $p(t) = \rho_0 g_0[\eta(t) - u(t)]$ (ρ_0: seawater density, g_0 : gravity acceleration, $\eta(t)$: sea surface height change, $u(t)$: seafloor vertical displacement) and the dynamic pressure change $p(t) = \rho_0 h_0 \partial^2 u / \partial t^2$ (h_0: seawater depth) (e.g., Saito, 2013). The seafloor pressure change inside the focal area at nth OBP $p_n(t)$ can be expressed as a superposition of the contributions by the Green's functions for the hydrostatic pressure ($G_{i,n}^{\text{hydrostatic}}(t)$) and dynamic pressure ($G_{i,n}^{\text{dynamic}}(t)$), generated by the seafloor vertical ground motion at ith element: $p_n(t) = \sum_i [m_i\{G_{i,n}^{\text{hydrostatic}}(t) + G_{i,n}^{\text{dynamic}}(t)\}]$. By estimating the amplitude of each unit source, m_i, based on this equation, we can obtain the time series of vertical ground motion.

Application to the 2011 Tohoku-Oki earthquake

We apply this method to the in-situ OBP records during the Tohoku-Oki earthquake, installed by Tohoku University and the University of Tokyo (Maeda et al. 2011; Hino et al. 2014). After removing the tidal component, we apply a low-pass filter with a cutoff of 0.05 Hz to remove the high-frequency acoustic component. The vertical displacement waveforms obtained by the analysis show large displacement offsets at stations GJT3, P08, and P09, located in the area where the seafloor displacement was extremely large (e.g., Saito et al. 2011). The final displacement offsets of these stations were in good agreement with the permanent displacements detected by the hydrostatic pressure offset change, indicating the validity of our proposed method. The velocity waveforms at stations P08 and P09 just above the epicenter showed two peaks, which suggests that the two moment releases near the epicenter during the rupture (e.g., Ide et al., 2011). In addition, the waveforms recorded by the nearest coastal seismographs from each station were similar, except for the arrival time delay.

©2021. Japan Geoscience Union. All Right Reserved.

High-sensitivity ocean bottom seismographs, commonly used for the offshore seismic observation, cannot record seismic waveforms correctly because of waveform saturation. Because of the broadband and broad dynamic range observations by the OBPs (Kubota et al., 2020), OBPs can observe high frequency seismic components without saturation. In addition to the tsunami early warning (e.g., Tsushima et al., 2012), the OBP installed inside the focal area is expected to make the important contribution as an instrument to record nearfield strong ground motion.

Keywords: Ocean bottom pressure gauge, Tsunami, Dynamic pressure change, The 2011 Tohoku-Oki earthquake, Seafloor ground motion

©2021. Japan Geoscience Union. All Right Reserved.

Detectability of short-term seafloor deformation by S-net pressure observation

*Ryota Hino[1], Tatsuya Kubota[2], Naotaka YAMAMOTO CHIKASADA[2], Yusaku Ohta[1], Hideto Otsuka[1]

1. Graduate School of Science, Tohoku University, 2. National Research Institute for Earth Science and Disaster Resilience

Long-term continuous observation of seafloor pressure is effective for detecting unsteady seafloor vertical deformations associated with transient tectonic phenomena such as slow slip event. A series of crustal vertical movements that occurred before and after the 2011 Tohoku-Oki Earthquake were captured by seafloor pressure observations and played significant roles in constraining the distributions of coseismic slip and aseismic slip preceded the mainshock, and the contribution of viscoelastic relaxation in the postseismic crustal deformation. Recently, number of new discoveries have been made in the slow earthquake activities along the Japan Trench. The continuous seismic records over a wide offshore area obtained by Seafloor observation network for earthquakes and tsunamis along the Japan Trench (S-net) showed that low-frequency tectonic tremors occurred repeatedly. It is expected that a slow slip event (SSE) occurs in the background of the tremor activity. If the crustal deformation caused by SSEs can be detected, it will greatly contribute to a comprehensive understanding of interplate coupling in the area. In this paper, we report quality of seafloor pressure data obtained by S-net in the geodetic frequency band, as the first step to capture the seafloor vertical motions associated with SSEs.
The characteristics of continuous records at all of the 150 stations from August 2016 to January 2020 were examined based on the RMS amplitudes of the pressure time series after the tidal components were removed. To remove the tidal components, a “tide killer filter”, a low-pass filter that effectively removes each tidal tide component. The filter output is composed of pressure variations with periods of two-days or more. Looking at the time series for about 3.5 years, it turned out that many records contain remarkable slow fluctuations with a time constant of several months or more. There are irregular variations of unknown cause that cannot be interpreted as fluctuations due to pressure sensor drift or transient fluctuations during the settlement of instruments on the seabed after the deployment. Since we can expect that the duration of SSE is about 1 to 2 weeks, which is the duration of low-frequency tremor activity episodes, the accompanying crustal movements may be detected even if long-period noise levels are high and we inspected the RMS amplitudes in a time window of 100 days. Only ~40 out of 150 stations provide pressure data with noise levels less than 10 hPa (10 cm in terms of vertical displacement), which is a guideline for detecting transient crustal movements, whereas about a half of the S-net stations show noise level more than 20 hPa. The noise level of the S-net pressure data is considerably higher than the data obtained by the pop-up type ocean bottom pressure gauge (OBP) used in many previous studies. It is thought that the difference in performance is related to the difference in the sensor installation method on the seafloor and also in the structure of the instruments. The longer path of pressure transmission to the sensor and the larger amount of self-heating of the device can raise noise level of pressure data. However, the noise level of the pressure data by DONET, another submarine cabled observation system, is not inferior to the data obtained by OBPs. We will inspect characteristics of the noises in S-net pressure data more in detail to identify the causes and also to find a way to reduce the noise so that the S-net pressure records can be used to monitor the SSEs along the Japan Trench.

Keywords: Seafloor pressure measurement, Slow Slip Event, noise characteristics

©2021. Japan Geoscience Union. All Right Reserved.

©2021. Japan Geoscience Union. All Right Reserved.

Vertical seafloor movement after the 2011 Tohoku earthquake and remarkable uplift near the trench axis off Sanriku

*Chie Honsho[1], Motoyuki Kido[2], Fumiaki Tomita[3], Ryota Hino[1]

1. Research Center for Prediction of Earthquakes and Volcanic Eruptions, Graduate School of Science, Tohoku University, 2. International Research Institute of Disaster Science, Tohoku University, 3. Japan Agency for Marine-Earth Science and Technology

We have continuously conducted GNSS-Acoustic observation since September 2012 at the 20 benchmarks distributed off Aomori to Ibaraki. Tomita et al. (2017) first revealed the broad distribution of horizontal seafloor movement and thereby discussed viscoelastic relaxation and afterslip of the 2011 Tohoku earthquake. The horizontal movement has been improving through revision of analysis method (Honsho and Kido, 2017; Honsho et al., 2019) and continued observation. Recently, by the application of a revised method for the traveltime determination in acoustic ranging (Honsho et al., 2021), the distribution of vertical movement has been revealed. Overall, it shows uplift to the east of a trench-parallel boundary ~20–30 km landward from the trench axis, along which little vertical movement occurs, and subsidence to the west; the uplift or subsidence becomes larger as it goes away from the boundary. Except for Site G06 off Sanriku, to be described later, the fastest uplift 3.2 cm/year was observed at Site G01, located on the Pacific plate and ~70 km away from the trench axis. The fastest subsidence was 3.5 cm/year at Site G14 located ~100 km landward from the trench axis.

The observed movement was compared with a model of postseismic deformation of the 2011 Tohoku earthquake by Agata et al. (2019). The model incorporates power-law viscoelastic flow, and the plate interface is considered as a frictional interface on which afterslip or backslip (fault locking) occurs according to frictional conditions. The calculation period of the model is 2.8 year after the earthquake and thus much shorter than the period of our observations (1.5–9.3 year after the earthquake). Nevertheless, the model surface movements become rather steady 2 years after the earthquake, and therefore, the model displacements during the period of 2.0–2.8 year were used to calculate the displacement rate to be compared with our observation. The overall pattern of resulting vertical movement was in excellent agreement with the observed one; uplift in the seaward and subsidence in the landward across a trench-parallel zero line located a little landward of the trench axis. However, the model magnitude of uplift or subsidence was generally two to three times as large as the observed one. Because the vertical movement is mainly caused by viscoelastic relaxation, the result would suggest that the model viscoelastic structure leave room for further adjustment.

Remarkable uplift was observed at the three adjacent sites off Sanriku: Site G04 (located at 39˚34'N, 2.6 cm/year), Site G06 (39˚18'N, 3.4 cm/year), and Site G07 (38˚57'N, 1.9 cm/year). Such significant uplift in this area cannot be explained by viscoelastic relaxation. The local uplift seems to exactly occur in the mid-slope terrace, a flat area ~4,500–5,000 m deep elongated parallel to the trench axis. Active slow earthquakes have been observed in the downdip of these sites (e.g., Nishikawa et al., 2019), and a slow slip event occurred in the early 2015 (Uchida et al., 2018; Honsho et al., 2019). Uplift of the seafloor can be qualitatively explained by fault slip only in the downdip side of these sites, or backslip only in the updip side, or both. Our observations are not frequent enough to determine whether the uplift is episodic or steady movement. However, our result suggests that fault slip in the downdip side, including the slow slip event in 2015, does not reach the trench axis but stops around these sites located ~20–30 km from the trench axis.

©2021. Japan Geoscience Union. All Right Reserved.

Keywords: GNSS-Acoustic, The 2011 Tohoku earthquake, Postseismic deformation

©2021. Japan Geoscience Union. All Right Reserved.

Improvement of spatial resolution and evaluation of uncertainty for the coseismic slip distribution of the 2011 Tohoku-oki Earthquake

*Fumiaki Tomita[1], Takeshi Iinuma[1], Motoyuki Kido[2], Ryota Hino[3], Yusaku Ohta[3], Ryoichiro Agata[1], Takane Hori[1], Naoki Uchida[3]

1. Japan Agency for Marine-Earth Science and Technology, 2. International Research Institute of Disaster Science, Tohoku University, 3. Graduate School of Science, Tohoku University

Due to the 2011Tohoku-oki earthquake, a large coseismic deformation was detected not only by the onland geodetic observational network but also by the seafloor geodetic observations (GNSS-Acoustic observations, ocean bottom pressure observations and differential bathymetry observations). These observations revealed that large coseismic slip reached to the Japan trench off Miyagi [e.g., Iinuma et al., 2012, JGR; Sun et al., 2016, Nat. Comm.]. However, southern and northern extent of the large coseismic slip along the trench was not well constrained due to low spatial resolution in the northern and southern areas because the seafloor geodetic observation sites mainly located in the central part (off-Miyagi region). Meanwhile, it is essential to evaluate uncertainties of the slip parameters to discuss the extent of the large coseismic slip. Although the linear slip inversion methods generally assume Gaussian distribution for the unknown parameters, this assumption was not necessarily right. Here, we examined the following two approaches: 1) Constraining the coseismic slip distribution by postseismic geodetic observational data via a viscoelastic inversion [Tomita et al., 2020, EPS], 2) Evaluating the uncertainties of the slip parameters by introducing a MCMC technique.

Introduction of the viscoelastic inversion: Viscoelastic relaxation, which is a transient deformation after the large earthquake, is caused by stress changes due to coseismic slips. Thus, postseismic geodetic observational data have information of the coseismic slip via the viscoelastic relaxation. Then, we tried to constrain the coseismic slip distribution from the postseismic geodetic observational data by simultaneously estimating the co- and post-seismic slip distribution via viscoelastic Green functions. We calculated the viscoelastic Green functions assuming a simple horizontally stratified viscoelastic structure [Fukahata & Matsu’ura, 2005; 2006, GJI]. As a result, the spatial resolution of the coseismic slip distribution can be improved using the seafloor geodetic observational data in the postseismic period (Tomita et al., 2017, Sci. Adv.). The conventional elastic inversion method showed that large coseismic rupture area was concentrated in the narrow region where the spatial resolution was high. By contrast, in the viscoelastic inversion method, the high spatial resolution region was relatively wide along the trench, and the large coseismic slip area was also extended. The northern and southern limits of the large coseismic slip (over 20 m) area were estimated as ~39.2°N and ~37.0°N, respectively.

Introduction of the MCMC technique: Using the MCMC technique, posterior probability density function (PDF) following a non-Gaussian distribution can be estimated by sampling unknown parameters. In this study, we divided the fault space using Voronoi cells and estimated number of the unknown parameters (number of the Voronoi cells) by a reversible-jump MCMC (rj-MCMC) technique to perform the slip inversion without using any spatial smoothing constraints. Note that we conducted the rj-MCMC analysis only using the coseismic geodetic data and investigated the performance of the rj-MCMC method. As a result, we successfully obtained the posterior PDFs following the non-Gaussian distributions for the slip parameters and found the region where large coseismic slip might occur in a low probability.

Through above two approaches, we successfully improved the inversion methods of the coseismic slip

©2021. Japan Geoscience Union. All Right Reserved.

distribution of the 2011 Tohoku-oki earthquake in terms of the spatial resolution and evaluation of uncertainties. We plan to perform the viscoelastic inversion assuming a realistic viscoelastic structure and to apply the rj-MCMC technique to the viscoelastic inversion method in the future.

Keywords: The 2011 Tohoku Earthquake, Viscoelastic relaxation, Reversible-jump MCMC technique, Seafloor geodesy

©2021. Japan Geoscience Union. All Right Reserved.

Resolving 3D rheology of northeastern Japan using postseismic deformation following the 2011 Tohoku-oki earthquake

*Jun Muto[1], Dhar Sambuddha[1], James Daniel Paul Moore[2], Satoshi Miura[3], Yusaku Ohta[3], Takeshi Iinuma[4]

1. Department of Earth Sciences, Tohoku University, 2. Earth Observatory of Singapore, Nanyang Technological University, Singapore, 3. Department of Geophysics, Tohoku University, 4. Japan Agency for Marine-Earth Science and Technology

In the ten years since the 2011 Tohoku-oki earthquake geodetic observations of the postseismic deformation, recorded both onshore and offshore, have revealed a highly complex rheological structure in the subsurface of Japan. In addition to the nation-wide geodetic network (GEONET), Tohoku University deployed dense networks of GNSS stations in the Miyagi-Yamagata and Fukushima-Niigata regions. Observations from these networks illustrate a pronounced heterogeneity in the surface deformation across northeastern (NE) Japan. In particular, the Miyagi-Yamagata region closer to the main rupture area exhibits intense forearc uplift with localized subsidence around the volcanic front (Muto et al., 2019, Sci. Adv.), whereas uplift has been observed throughout the volcanic front and forearc of the Fukushima-Niigata region.

Over the past decade, a number of studies have gleaned new insight from the postseismic deformation of NE Japan, shedding light on the subsurface rheology and the role of coupled interactions between viscoelastic flow in the mantle and stress-driven afterslip on the plate interface (e.g., Agata et al., 2019, Nat. Commun; Freed et al., 2017, EPSL; Hu et al., 2016, JGR; Muto et al., 2019, Sci.Adv.). Recent studies have not only highlighted the presence of small-scale low viscosity bodies beneath a number of Quaternary volcanoes (Muto et al., 2016, GRL), but also the stagnancy and ubiquity of the forearc mantle (Uchida et al., 2020, Nat. Commun). Furthermore, a strong contrast has been observed in the frictional behavior of the megathrust between central areas near Miyagi and southern areas near Fukushima (Nishikawa et al., 2019, Science).

We have taken advantage of newly acquired observations along the Fukushima-Niigata area and utilized these observations to explore three-dimensional rheological heterogeneities in the mantle wedge mechanically coupled to afterslip on the megathrust interface with variable frictional properties. We developed a numerical model using laboratory-derived constitutive laws to reproduce the geodetic observations (Ozawa et al., 2012, JGR; Tomita et al., 2015, Sci. Adv.; Watanabe et al., 2014, GRL). Our results suggest that the rapid uplift in the Miyagi forearc was caused by deep afterslip underlying a narrow cold nose in the mantle wedge, in contrast to a wider cold nose beneath the Fukushima forearc without significant deeper afterslip. The model resolves along-arc rheological heterogeneity in good agreement to the cumulative observations across ten years in both magnitude and azimuth, as well as their time-series over the 5 years. Our results illuminate the forearc mantle rheology highlighting the variability of cold nose geometry and frictional properties on the subduction zone plate boundary along the arc. Therefore, the dense geodetic network, as well as the numerical model based on the laboratory constrained flow laws of rocks contribute to resolve 3D rheological heterogeneity of the NE Japan imaged through the postseismic deformation of the 2011 Tohoku-oki earthquake.

Keywords: 2011 Tohoku-oki Earthquake, Postseismic deformation, Rheology, Viscoelastic relaxation, Afterslip

©2021. Japan Geoscience Union. All Right Reserved.

©2021. Japan Geoscience Union. All Right Reserved.

Numerical simulation of earthquake generation cycles along the Japan Trench

*Ryoko Nakata[1], Takane Hori[2], Seiichi Miura[2], Ryota Hino[1]

1. Graduate School of Science, Tohoku University, 2. Research Institute for Marine Geodynamics, Japan Agency for Marine-Earth Science and Technology

Seismic, geodetic and paleoseismological studies have demonstrated that the large coseismic slip in the shallow area which caused the 2011 Tohoku-Oki earthquake was limited to the middle segment of the Japan Trench [e.g., Iinuma et al., 2012; Ikehara et al., 2016]. In contrast, in the shallow area off the coast of Fukushima Prefecture, i.e. the southern segment of the trench, postseismic slips were predominant [Iinuma et al., 2016; Tomita et al., 2017]. The observed negative residual gravity anomaly area [Bassett et al., 2016] in the southern segment corresponds to the postseismic slip area. At the southern segment, slow earthquakes include low-frequency earthquakes, tectonic tremors, and very-low-frequency earthquakes, which are distributed complementary to the coseismic slip and overlapping the postseismic slip area of the Tohoku-Oki earthquake [Matsuzawa et al. 2015; Nishikawa et al., 2019; Ohta et al., 2019]. In the northern segment, slow-slips [Uchida et al., 2016] and tsunami earthquakes [Tanioka & Satake, 1996; Satake et al., 2017] occurred. We conducted numerical simulation of earthquake generation cycles along the Japan Trench. In the southern segment, we assumed evident frictional heterogeneity caused by a thick low-velocity channel layer in the shallow part of the off Fukushima [Tsuru et al, 2002; Miura et al., 2003; 2005]. Then, we efficiently reproduced M9 earthquakes recurring only in the middle, followed by evident postseismic slips in the south. In the northern segment, we are conducting the simulations to reproduce a situation in which the 2011 M~9 earthquake and the 1896 M~8 Meiji-Sanriku earthquake have occurred independently even though their source areas are adjacent to each other. In our presentation, we will discuss the factors that control these complementary spatial distributions of slips along the Japan Trench.

©2021. Japan Geoscience Union. All Right Reserved.

Seismicity near the trench axis and in the outer rise region of southern Japan Trench: Results from ocean bottom seismograph observations

*Koichiro Obana[1], Gou Fujie[1], Yojiro Yamamoto[1], Yuka Kaiho[1], Yasuyuki Nakamura[1], Seiichi Miura[1], Shuichi Kodaira[1]

1. Research Institute for Marine Geodynamics, Japan Agency for Marine-Earth Science and Technology

The 2011 Mw 9.0 Tohoku-oki earthquake ruptured the subduction mega-thrust fault in the central Japan Trench. The 2011 Tohoku-oki earthquake is characterized by large coseismic slip along the plate boundary fault reaching the trench axis. Based on the seismic and geodetic observations, main rupture area with the coseismic slip over 50 m occurred on the shallow subduction plate interface in the central Japan Trench. The post-seismic deformation following the 2011 earthquake shows along-trench variations. Westward post-seismic deformations were observed by seafloor geodetic measurements in the central Japan Trench, which can be explained by the viscoelastic relaxation. On the other hand, eastward post-seismic deformations were observed in the southern Japan Trench, south of the main rupture area. The eastward deformations suggest the afterslip on the shallow subduction zone near the trench. In contrast, normal-faulting earthquakes in the trench-outer rise region occurred in both central and southern Japan Trench. We investigate the aftershock activity in the southern Japan Trench to the south of the main rupture area by using ocean bottom seismographs deployed both landward and seaward of the trench. In the trench-outer rise region seaward of the trench axis, several ~100 km long linear earthquake trends both parallel and oblique to the southern Japan Trench have been identified. The trench-strike changes from N-S to NNE-SSW to the south of the main rupture area of the 2011 Tohoku-oki earthquake. The earthquake trend oblique to the southern Japan Trench is a southern extension of the trench-parallel linear earthquake trend in central to northern Japan Trench. This suggests that faults of large outer-trench normal-faulting earthquakes can extend linearly beyond the bend of the trench. The trench-oblique faults should be considered as a substantial part of the outer-rise earthquakes and related tsunamis. In the trench landward slope, we found regular earthquakes along the shallow plate interface near the trench of the southern Japan Trench, where the afterslip of the 2011 Tohoku-oki earthquake is expected from the eastward post-seismic deformations. The near-trench shallow earthquakes locate seaward of the episodic tremor activities reported by Ohta et al. (2019). Temporal correlations between the near-trench earthquakes and the tremor activities suggest that the slow-slip on the shallow subduction plate interface extends close to the trench axis. As indicated by the proximity of the regular earthquakes and slow slips, the diverse slip behavior in the shallow subduction zone is a distinct feature of the southern Japan Trench. The diverse slip behavior in the shallow subduction zone of the southern Japan Trench could be related to smaller scale structure heterogeneity, such as the thickness variation in the low-velocity interplate sedimentary unit imaged by seismic reflection surveys (Tsuru et al. 2002).

Keywords: Japan Trench, Outer rise, Tohoku-oki Earthquake

©2021. Japan Geoscience Union. All Right Reserved.

Microseismicity prior to the 2011 Tohoku-Oki earthquake around the mainshock hypocenter

*Hirofumi Goto[1], Ryota Hino[1]

1. Graduate School of Science, Tohoku University

It has been pointed out that slow earthquakes driving intense foreshock activities cause stress concentration on the epicenters of eventual large earthquakes and trigger mainshocks (e.g. Obara and Kato, 2016). In the 2011 Tohoku-oki Earthquake, foreshock activity thought to be accompanied by a slow earthquake was observed from about one month before the mainshock on March 11 (Kato et al., 2012). At that time, ocean bottom seismometers (OBSs) were installed in this area. In the seismic waveform records obtained by this observation, many events that seemed to be small earthquakes that were not the subject of the previous research were observed. By inspecting such numerous micro earthquakes, it is expected that we will be able to deepen our understanding of the spatiotemporal distribution of foreshock activity and clarify new features of processes preceding large earthquakes. Here, we detected foreshocks and estimated their hypocenter distribution prior to the Tohoku-oki earthquake including tiny events, to discuss the characteristics of the spatiotemporal development of the foreshock activity.

In this study, the waveforms obtained from the OBSs installed around the epicenter of the Tohoku-oki earthquake were used to detect the earthquake and estimate the epicenter by the envelope correlation method (Obara, 2002). As a result, 1963 events were detected during the three days of the analysis period, from March 9 to March 11, and about 70% of them were located with epicenter errors within 10 km. Using this result, the spatial distribution of foreshock activity was investigated in detail. It was found that microearthquakes were concentrated into two regions, separated by the coseismic rupture area of the largest foreshock (M 7.3, March 9 11:45 JST), on the northeastern and southwestern sides, respectively. This is in good agreement with the general picture pointed out for aftershock distributions of many large earthquakes, in which aftershock activities become low in the main coseismic slip area of mainshocks.

The onset timing of seismicity is different between these two active areas. On the northeastern side, activity began immediately after the occurrence of the largest foreshock, showing temporal expansion from the epicenter of the largest foreshock. On the southwest side, activity began about 9 hours after the occurrence of the largest foreshock. This activity expanded from the west side (down-dip side), and the second largest foreshock (M 6.8, March 10 06:24 JST) occurred on the east side (up-dip side).

The number of earthquakes in each active area showed a temporal variation; several increases associating large earthquakes (M> 6) occurrences. However, a sudden increase of the seismicity without any large earthquakes was observed in the northeastern active area. With this activation, the activity of the small repeating earthquakes (Kato et al., 2012) seem to have reactivated. It is suggested that there is a temporal fluctuation in the aseismic process behind the foreshock activity.

Keywords: 2011 Tohoku-Oki earthquake, foreshock activity

©2021. Japan Geoscience Union. All Right Reserved.

Characteristics of tectonic tremor activity along the Japan Trench before the 2011 Tohoku Oki earthquake

*Hidenobu Takahashi[1,2], Ryota Hino[1], Naoki Uchida[1], Ryosuke Azuma[1], Susumu Kawakubo[1], Kazuaki Ohta[3], Masanao Shinohara[4]

1. Graduate school of Science Tohoku University , 2. Central Research Institute of Electric Power Industry, 3. National Research Institute for Earth Science and Disaster Resilience, 4. Earthquake Research Institute, The university of Tokyo

Recently, slow earthquakes have been discovered in Tohoku-oki by using the Seafloor Observation Network for Earthquakes and Tsunamis along the Japan Trench (S-net) (Nishikawa et al., 2019). The characteristics of the slow earthquakes in Tohoku-oki differ from those in the Nankai Trough (Obara and Kato, 2016). Along the Nankai Trough, sources of slow earthquakes are continuously distributed along the deeper and shallower sides of the seismogenic zone, whereas those show complex spatial distribution along the Japan Trench (Nishikawa et al., 2019). In Tokachi-Oki, Tanaka et al. (2019) observed tremors within several kilometers from moderate-sized interplate earthquakes, suggesting small-scaled frictional heterogeneities on the plate interface in the area. Mixed distribution of regular earthquakes and tremors, as well as high regular earthquake activity, make the Japan trench ideal place to study the relationships between tremors and regular earthquakes.

Takahashi et al. (2020, AGU) detected tremors based on the ocean bottom observations from October 2007 to October 2008 along the Japan trench. As a result, tremors occurred before the 2011 Tohoku-Oki earthquake in Iwate-Oki (39.3–40.2˚N), Miyagi-Oki (38.7˚N–39.2˚N), Fukushima-Oki (36.5–37.0˚N), and Ibaraki-Oki (35.5–36.5˚N). In this study, we compare spatio-temporal relationships between tremors and regular earthquakes based on the same data set with those used in our previous study. We focused on if spatial complementarity of tremors and regular earthquakes distributions, and synchronicity of tremors and nearby regular earthquakes activation.
In the depth range between 10–20 km, where tremors are active, most of the regular earthquakes were concentrated in several clusters, like tremors, and these regular earthquake clusters were clearly separated from the tremor clusters. However, tremor and regular earthquake clusters are close to each other, and in many cases, both are adjacent to each other at a distance of a few kilometers or less.

The most active cluster of regular earthquakes during our observation period in Iwate–Oki is located in between two isolated tremor clusters. These regular earthquakes were concentrated in time and its timing is immediately after the nearby tremor episodes. The location of the regular earthquake cluster was located near the end of the tremor cluster where the tremor migration terminated. A similar pattern was observed in Ibaraki–Oki. The cluster of regular earthquakes was observed adjacent to the tremor sources, and this cluster also activated after the cessation of the tremor episode with source migration and was located near the terminal of the migrating. However, not all the tremor activities are accompanied by regular earthquake activity. In the case of tremor activity followed by the regular earthquake activity, tremor distribution tends to be broaden toward the regular earthquake cluster, suggesting variety of interaction between tremor and regular earthquake.

The spatial complementarity of tremors and regular earthquakes suggests that these occur in different conditions on the plate boundary, like other subduction zones, but their spatial closeness indicates that the frictional heterogeneity has a scale of several kilometers on the plate interface in the Japan Trench subduction zone. The observed synchronicity of tremor and regular earthquake activities can be

©2021. Japan Geoscience Union. All Right Reserved.

explained by a common phenomenon, SSEs. The variety of the association between tremors and regular earthquakes can be attributed to the fluctuation in the generation of SSEs: only when the SSEs, initiated from tremor sources, expanded to a nearby seismogenic area, the slip activates regular earthquakes.

Keywords: The Tohoku Oki earthquake, Slow earthquake

©2021. Japan Geoscience Union. All Right Reserved.

Application of ensemble learning noise classifier to automatically determined earthquake catalog after the 2011 Tohoku Earthquake

*Koji Tamaribuchi[1]

1. Meteorological Research Institute

A microseismic catalog is one of the big data that is important for earthquake research and disaster prevention. However, because the 2011 Mw 9.0 Tohoku earthquake caused an enormous number of aftershocks and induced earthquakes, it was impossible to process all the detectable earthquakes. Thus, the microseismic activity remains hidden. Tamaribuchi and Nakagawa [2020] applied the automatic hypocenter determination method to the continuous seismic waveform data for March 2011. The automatically determined earthquake catalog was more than twice in the JMA unified catalog.

On the other hand, it is necessary to remove the noise efficiently because the automatically determined catalog contains several percent of false detections due to noise. Therefore, Tamaribuchi et al. [2020, SSJ Fall Meeting] applied ensemble learning, a kind of supervised machine learning, to the automatically determined catalog and confirmed that we could remove about 80% of false detections. In this study, we apply the supervised ensemble learning to the aftershocks of the 2011 Tohoku earthquake and create a denoised earthquake catalog.

Tamaribuchi et al. [2020, SSJ Fall Meeting] created a training dataset of earthquakes and noise by visual inspection based on the data recorded in the automatically determined catalog from January to February 2020. We then created a noise classifier based on the supervised ensemble learning (Adaboost). The classifier uses hypocenter information such as magnitude, location, and the number of P- and S-phases at 20 stations near the epicenter for learning. In this study, we applied the classifier trained on the data from January to February 2020 to the March 2011 data. There were no living stations near the epicenter due to the lack of an observation network in some cases. Therefore, we used only alive stations when selecting the 20 stations near the epicenter.

For March 2011, the automatic process determined 122353 events all over Japan. As a result of applying the classifier, 119037 (97.3% of the total) and 3316 (2.7%) were classified as earthquakes and noises, respectively. The time taken for classification was 31 minutes (0.02 seconds per event). Most of the noises were in the aftershock areas and Ryukyu islands, and we can classify the noise appropriately in a realistic processing time. On the other hand, compared with the JMA unified catalog, 124 misclassified cases are in aftershock areas. We will consider improving the generalization performance, such as including data from 2011 in the training data.

Keywords: Earthquake catalog, Automatic hypocenter determination, The 2011 Tohoku Earthquake, Machine learning

©2021. Japan Geoscience Union. All Right Reserved.

Core-Mantle boundaries state estimation applying the strain analysis on frequency domain

seiji matsumura[2], *Makoto OKUBO[1]

1. Natural Science Cluster, Kochi University, 2. Faculty of Science and Technology

It is well known that seismic waves, especially surface waves, of a huge earthquake can go around on surface of the earth many times. Surface waves trace on a spherical earth surface many times and become a standing wave, deform the earth, such as to expand and contract or to twist, periodically. These periodical deformations of the earth are so called 'earth free oscillation.' Observing the amplitude and period of these oscillation mode of the earth, we can understand a condition of inner structure of the earth.

In this study, we applied strain analysis on the frequency domain (so called FSA; *c.f.* Okubo, 2007) to the dynamic strain records, which observed at the 2011 off the coast of Tohoku Earthquake. Originally, applying strain analysis, we can determine the principal strain magnitude and its direction from time series changes of the independent three horizontal components. on the other hands, FSA is able to estimate the principal strain azimuth for each frequency. Dynamic strain records we used (UWA1 belonging AIST) contain independent four horizontal components, thus the four principal strain directions can be determined independently, and can be evaluated the mean value, and determination accuracy from the deviations. We determined the natural frequencies of earth free oscillations, and Q values representing the attenuation of the amplitude corresponding to the state of Core-Mantle boundaries (CMB).
We first applied a Fourier analysis to each of the four horizontal components with a data length of 37 hours (133200 s) from 00:00 on March 11, 2011, and obtained amplitude-phase spectra. Next, we estimate averaged the principal strain azimuths and deviations from four spectra applying with Okubo (2009) procedure. Since the earth free oscillation phenomenon is a periodic global vibration, deviations of the determination should be small. Therefore, we set a threshold 5 degrees for deviation, and surveyed nearby frequencies predicted by PREM (Dziewonski and Anderson, 1980). As a result, three frequencies of 0.315 mHz, 0.382 mHz, and 0.818 mHz were obtained, corresponding to ${}_0S_2$, ${}_0T_2$ and ${}_0S_0$, respectively. These frequencies are almost same as the frequencies predicted by PREM. Furthermore, performing the same procedure with the start time shifted a hour, we determined the temporal changes in amplitude for the three frequencies. We finally estimated the Q^{-1} value corresponding to each frequency mode, fitting with the damped oscillation equation.

As a result, we obtained 378.5, 31.3, and 235.7, corresponding to ${}_0S_2$, ${}_0T_2$ and ${}_0S_0$, respectively. In PREM, these values were mentioned 509.6, 250.4, and 5327.6, our results seems to smaller than PREM.

Keywords: Q, Dynamic Strain, Earth Free Oscillation

©2021. Japan Geoscience Union. All Right Reserved.

Tomography and megathrust earthquakes in the Tohoku forearc

*Dapeng Zhao[1]

1. Department of Geophysics, Tohoku University

Tomographic studies have been made continuously for the Tohoku forearc region in the past two decades. Using P-wave arrival-time data recorded at land-based seismic stations of suboceanic earthquakes relocated with sP depth phases (Umino et al., 1995), Zhao et al. (2002) and Mishra et al. (2003) determined the first 3-D P-wave velocity (Vp) images of the Tohoku forearc from the Japan trench to the Pacific coast and found a correlation between the Vp variations of the megathrust zone and the hypocentral distribution of large megathrust earthquakes (M> 6.0). Later studies of both Vp and Vs tomography of the region have confirmed the first findings (Mishra & Zhao, 2004; Wang & Zhao, 2005; Zhao et al., 2007, 2009; Huang et al., 2011). Since the occurrence of the great 2011 Tohoku-oki earthquake (Mw 9.0), more tomographic studies have been made using P and S wave data of the aftershocks relocated with sP depth phases (Zhao et al., 2011; Huang & Zhao, 2013a,b; Liu et al., 2014; Zhao, 2015; Liu & Zhao, 2018). Zhao et al. (2011) relocated the Tohoku mainshock, 339 foreshocks and 5609 aftershocks during 9–27 March 2011 using a 3-D velocity model and local P and S wave arrival times, and suggested that the rupture nucleation of the largest events in the Tohoku-oki sequence, including the mainshock, was controlled by structural heterogeneities in the megathrust zone. Liu & Zhao (2018) constrained the structure of the Tohoku forearc using seismic tomography, residual topography, and gravity data, which reveal a close relationship between structural heterogeneities in and around the megathrust zone and rupture processes of the 2011 Tohoku-oki earthquake. They suggested that the structural heterogeneities in and around the megathrust zone originate from both the overriding Okhotsk plate and the subducting Pacific plate, which controlled the nucleation and rupture processes of the Tohoku-oki earthquake. Recently, P and S wave arrival-time data of suboceanic events recorded by the permanent ocean-bottom seismic network (S-net) have been used to improve the tomographic images of the Tohoku forearc, in particular, near the Japan trench (Hua et al., 2020; Yu & Zhao, 2020; Katayama et al., 2021). All these results indicate structural control on the generation of megathrust earthquakes in the Tohoku forearc.

References

Hua, Y., D. Zhao, G. Toyokuni, Y. Xu (2020). *Nature Communications 11*, 1163.
Huang, Z., D. Zhao, L. Wang (2011). *Geophys. J. Int.* 184, 1428-1444.
Huang, Z., D. Zhao (2013a). *Tectonophysics* 586, 35-45.
Huang, Z., D. Zhao (2013b). *J. Asian Earth Sci.* 70, 160-168.
Katayama, Y., D. Zhao, G. Toyokuni (2021). Joint Symposium of Sciences and Lift Science, Tohoku University on February 19, 2021.
Liu, X., D. Zhao, S. Li (2014). *J. Geophys. Res.* 119, 1094-1118.
Liu, X., D. Zhao (2018). *Science Advances* 4, eaat4396.
Mishra, O.P., D. Zhao et al. (2003). *Geophys. Res. Lett.* 30, GL017736.
Mishra, O.P., D. Zhao (2004). *Geophys. Res. Lett.* 31, L09610.
Umino, N., A. Hasegawa, T. Matzuzawa (1995). *Geophys. J. Int.* 120, 356–366.
Wang, Z., D. Zhao (2005). *Phys. Earth Planet. Inter.* 152, 144-162.
Yu, Z., D. Zhao (2020). *J. Geophys. Res.* 125, e2019JB018600.
Zhao, D., O.P. Mishra, R. Sanda (2002). *Phys. Earth Planet. Inter.* 132, 249-267.
Zhao, D. et al. (2007). *Bull. Seismol. Soc. Am.* 97, 1121-1132.
Zhao, D. et al. (2009). *Tectonophysics* 467, 89-106.

©2021. Japan Geoscience Union. All Right Reserved.

Zhao, D. et al. (2011). *Geophys. Res. Lett.* 38, L17308.
Zhao, D. (2015). *J. Asian Earth Sci.* 98, 26-49.

Keywords: Tohoku forearc, great earthquake, seismic tomography

©2021. Japan Geoscience Union. All Right Reserved.

Trench fill and graben fill sediments on the incoming plate around the Japan trench

*Yasuyuki Nakamura[1], Shuichi Kodaira[1], Gou Fujie[1], Seiichi Miura[1], Koichiro Obana[1], Mikiya Yamashita[2]

1. Japan Agency for Marine Earth Science and Technology, 2. National Institute of Advanced Industrial Science and Technology

The input material to the subduction trench is one of the key elements to the subduction zone processes like megathrust earthquakes and tsunamis. In the Japan Trench where the 2011 Tohoku earthquake occurred, the variation of the incoming sediment thickness correlates with the extent of the large shallow coseismic slip during the 2011 Tohoku earthquake (Fujie et al. 2020). We present the complete map of the incoming sediments in the Japan Trench and discuss characteristics of the seismic structure focusing on the trench and graben fill sediments.

Since the 2011 Tohoku earthquake, extensive seismic surveys have been conducted in the Japan Trench. More than 100 reflection seismic profiles were obtained in the vicinity of the trench axis off Ibaraki to the south and off Aomori to the north with 4-8 km survey line separation. The incoming sediments show generally weak semicontinuous reflections which parallel to the strong basement reflections. The seafloor reflection also generally parallels that of the basement, gently inclined landward. However, we also observe sediments which cover or onlap the inclined “original” sediments on the Pacific plate. These sediments are mostly distributed at the trench axis and trench-ward end of the grabens. Two types of seismic characters are observed on these fill sediments; one is chaotic, the other is horizontally stratified. The graben fills mostly show the stratified characters, but chaotic graben fills are also observed in some locations. These chaotic graben fills seem to be brought from the failure of the sediments on the horst edge located east of the graben. The trench fill sediments show chaotic character in many cases, which should be related to the failure of the slope immediately landward of the trench. In some locations, the stratified units are interbedded in the chaotic units in the trench fills. These trench fills and graben fills are identified in the southern and northern part of the Japan Trench, but not dominant in the central part where the shallow slip occurred during the 2011 Tohoku earthquake. The fill sediments increase the thickness of the input sediments to the subduction zone and could increase the water content of the input materials, which could be related to the plate boundary slip behavior.

Keywords: Japan Trench, input sediments, fill sediments

©2021. Japan Geoscience Union. All Right Reserved.

[J] Poster | S (Solid Earth Sciences)：S-CG Complex & General

Sun. Jun 6, 2021 5:15 PM - 6:30 PM JST | Sun. Jun 6, 2021 8:15 AM - 9:30 AM UTC | Ch.16_3

[S-CG55] Oceanic plate as inputs to subduction zone: from oceanic spreading ridge to subduction trench

convener:Gou Fujie(Japan Agency for Marine-Earth Science and Technology), Makoto Yamano(Earthquake Research Institute, the University of Tokyo), Tomoaki Morishita(School of Geoscience and Civil Engineering, College of Science and Technology, Kanazawa University), Takanori Kagoshima(University of Toyama)

As the inputs to subduction zone, the nature of the incoming oceanic plate, such as surface relief, thermal state, lithology, and the water content, affects various processes occurring in the subduction zone, including arc magmatism and interplate and intraplate seismic activities. The oceanic plate is formed in the oceanic spreading ridge and moves through the ocean basin for a long time and subducts from the oceanic trench. The nature of the incoming oceanic plate is determined by all the processes occurring from the spreading ridge to the subduction trench; e.g., hydrothermal circulation, sedimentation and diagenesis for more than millions years at the oceanic basin, and plate bending-related faulting near the subduction trench. Therefore, for studying the nature of the subduction inputs, it is essential to reveal the various evolution processes of the oceanic plate between the spreading ridge and the subduction trench.

We welcome contributions from a broad range of earth science (geophysics, geology, petrology, drilling science, and so on) discussing topics related to the inputs to subduction zones, such as tectonic process associated with the plate bending prior to subduction, post-spreading volcanic activities including large seamount formation and petit-spot volcanoes, and the nature of the "normal" or "typical" oceanic plate.

This session is supported by the focus group of hard rock drilling science.

[SCG55-P01] Compilation of bathymetry and seismic reflection data to characterize outer rise faults in the Kuril Trench

*Shuichi Kodaira[1], Tetsuo No[1], Yasuyuki Nakamura[1], Gou Fujie[1], Koichiro Obana[1], Seiichi Miura[1] (1.Research Institute for Marine Geodynamics, Japan Agency for Marine-Earth Science and Technology)

[SCG55-P02] Characteristics of the oceanic plate near the Nosappu fracture zone revealed by the extensive seismic structure studies

*Gou Fujie[1], Koichiro Obana[1], Shuichi Kodaira[1], Katsuyoshi Michibayashi[2] (1.Japan Agency for Marine-Earth Science and Technology, 2.Nagoya University)

[SCG55-P03] Hydrothermal experiments in olivine-orthopyroxene-H2O system at 200-400C: implications for hydrogen generation at high temperatures

*Shuhei Tanaka[1], Atsushi Okamoto[2], OTGONBAYAR DANDAR[2], Masaoki Uno[2], Masakazu Fujii[3] (1.Tohoku University, 2.Graduate school of environmental studies, Tohoku University, 3.National institute of Polar research and SOKENDAI)

[SCG55-P04] Hydration processes of a forearc mantle wedge inferred from the Takadomari serpentinite body in the Kamuikotan Belt, central Hokkaido, Japan

*Shun Takamizawa[1], Yuji Ichiyama[1], Shusaku Yamazaki[2], Akihiro Tamura[3], Tomoaki Morishita[3] (1.Chiba University , 2.Civil Engineering Research Institute for Cold Region, 3.School of Geoscience and Civil Engineering, College of Science and Technology, Kanazawa University)

[SCG55-P05] Petrological features and formation processes of lower crustal cumulate xenoliths from Oki-Dogo Island: A possibility of mantle plume origin

*Rio Higuchi[1], Yuji Ichiyama[1], Akihiro Tamura[2], Tomoaki Morishita[2] (1.Chiba University, 2.Faculty of Geosciences and Civil Engineering, Kanazawa University)

Compilation of bathymetry and seismic reflection data to characterize outer rise faults in the Kuril Trench

*Shuichi Kodaira[1], Tetsuo No[1], Yasuyuki Nakamura[1], Gou Fujie[1], Koichiro Obana[1], Seiichi Miura[1]

1. Research Institute for Marine Geodynamics, Japan Agency for Marine-Earth Science and Technology

It has been reported that stress changes in the oceanic plate associated with an interplate megathrust earthquakes cause to activate seismic activity in the oceanic plate before subduction, which is sometimes accompanied with a large normal fault earthquake. For example, along the Kuril Trench, an extensional earthquake (Mw=8.1) occurred within the oceanic plate in 2007, following a shallow megathrust event (Mw=8.3) at the plate boundary in 2006. In the Japan Trench region, normal fault earthquakes in the outer-rise have been activated immediately after the 2011 Tohoku-oki earthquake. Based on results of our previous earthquake observations and seismic imaging, it has been concluded that, i) the outer rise normal fault earthquakes dominantly occur along the horst-and-graben structure formed by plate bending, ii) the horst-and-graben structure is mainly developed oblique to the fabric of the oceanic plate, and iii) dip of the normal fault is as high as 70˚ at the depth of the crust and uppermost mantle. On the other hand, in the Kuril Trench, the trench axis and oceanic fabric run almost parallel, and the development of bend-related faults along the oceanic fabric can be confirmed from bathymetry data. In order to clarify the differences in a formation process of outer-rise faults and fault geometry between the Japan Trench, where new bend-related faults are dominantly formed, and the Kuril Trench, where bend-related faults develop along the oceanic fabric, this study compiles high resolution seismic reflection data, conventional seismic reflection data, and detailed bathymetry data, which have been acquired in the Kuril Trench by JAMSTEC since 2016. The results indicate that the half-graben fault structure formed by seaward trending high-angle normal faults is dominant in the Kuril Trench, unlike the Japan Trench where horst-and-graben faults dominantly develop. The conventional seismic reflection data also shows oceanic Moho, but the current processing of the data does not allow us to identify if there is an offset of the Moho associated with normal faulting. Reflection events indicating normal faults in the oceanic crust are not imaged, but it is still unknow whether this is due to structure or processing. Further data processing focusing on fault images in the oceanic crust and Moho offsets is necessary. We will use these data to describe the fault geometry and discuss the formation process of the outer rise fault. As a final goal of the project, we will also create a fault map of the offshore Kuril Trench to contribute mitigation of tsunami hazards.

Keywords: Kuril Trench, Outer rise earthquake, Bend-related fault

©2021. Japan Geoscience Union. All Right Reserved.

Characteristics of the oceanic plate near the Nosappu fracture zone revealed by the extensive seismic structure studies

*Gou Fujie[1], Koichiro Obana[1], Shuichi Kodaira[1], Katsuyoshi Michibayashi[2]

1. Japan Agency for Marine-Earth Science and Technology, 2. Nagoya University

The global compilation studies on the seismic structure of the oceanic crust, such as Christeson et al. (2019) and Grevemeyer et al. (2018), indicate that the fast spreading oceanic crust, in comparison with the slow spreading oceanic crust, is laterally uniform in thickness and seismic velocities, and has relatively higher seismic velocities within both the oceanic layer 2 and layer 3. The northwestern part of the oceanic Pacific plate off northeast Japan arc was formed at a fast spreading ridge more than 100 million years ago. We JAMSTEC have conducted extensive controlled-source seismic surveys in this region and confirmed that the oceanic crust is quite simple and laterally uniform in most areas. The typical thickness of the oceanic crust is approximately 7 km and the seismic velocities at the top of the oceanic layer 3 is 6.5 km/sec in most areas. These features are well consistent with the global compilation studies.

However, our data show that the oceanic crust become thinner when it approaches to the Nosappu fracture zone. As the crust become thinner, seismic velocities within the oceanic crust become lower and the boundary between the layer 2 and layer 3, which is estimated by the changes in the vertical velocity gradient, becomes unclear. These characteristics are not consistent with those of the fast spreading oceanic crust but somewhat similar to those of the slow spreading oceanic crust. In addition to the oceanic crust, we found that the oceanic mantle shows strange characteristics toward the Nosappu fracture zone. Generally, the topmost oceanic mantle formed at the fast spreading center shows strong seismic anisotropy, which can be explain by the alignments of the olivin crystal due to the fast mantle flow at the spreading center. Since the mantle flow is expected to be perpendicular to the ridge axis, the fast axis of the seismic anisotropy is perpendicular to the ancient ridge axis which is represented by the magnetic anomaly lineation. In the northwestern part of the oceanic Pacific plate, the topmost oceanic mantle shows a strong anisotropy, more than 8 percent, and the fast axis is perpendicular to the magnetic anomaly lineation in most areas (Kodaira et al., 2014). However, when it approaches to the Nosappu fracture zone, the direction of the fast axis seems to rotate by more than 45 degrees although the strength of the seismic anisotropy suggested by the shear wave splitting is roughly the same (about 8 percent). If the strong anisotropy is caused by the mantle flow at the spreading center, our observation implies that the mantle flow near the Nosappu fracture zone was oblique to the ridge axis when the oceanic plate was formed. The oblique mantle flow might be explained by the existence of the transform fault (the current Nosappu fracture zone) near the spreading center and might be responsible for the slow-spreading-like oceanic crust there.

In this presentation, we will show the existing seismic data and seismic structures that support our hypothesis. In addition, we would like to propose an integrated marine geophysical observation, including seismic, electromagnetic, and gravity, to test our hypothesis.

Keywords: oceanic plate, Fracture zone, seismic survey, mantle anisotropy

©2021. Japan Geoscience Union. All Right Reserved.

Hydrothermal experiments in olivine-orthopyroxene-H2O system at 200-400C: implications for hydrogen generation at high temperatures

*Shuhei Tanaka[1], Atsushi Okamoto[2], OTGONBAYAR DANDAR[2], Masaoki Uno[2], Masakazu Fujii[3]

1. Tohoku University, 2. Graduate school of environmental studies, Tohoku University, 3. National institute of Polar research and SOKENDAI

Hydrogen and hydrocarbon production during serpentinization provide significant impacts on microbial activities within the oceanic lithosphere. At the slow- to ultraslow spreading ridges, the alkaline hydrothermal vents with a special ecosystem has been discovered such as Lost City in Mid Atlantic Ridge. These hydrothermal vents are relatively low-temperatures, compared to the those in the fast-spreading ridges. Recently, it is suggested that serpentinization proceeds by seawater penetrating to the deep high-temperature fracture zones, and the bending faults, which potentially higher extent of hydration and hydrogen production. However, there has been few studies on serpentinization and hydrogen generation at temperature exceeding 300C.

In this study, we conducted hydrothermal experiments on serpentinization, focusing on (1) temperature, (2) silica (orthopyroxene) and (3) mass transport (batch vs. flow-through). The experiments were conducted in Ol-H_2O system and Ol-Opx-H_2O system. Batch type experiments were conducted for 576 hours at 200, 250, 280, 300, 350C at the vapor-saturated pressure and 400℃ at 30 MPa. Flow-through type experiments were conducted at 35 MPa and flow rate of 0.1 ml/min at 300C and 350C for the Ol-H_2O system and 300C and 380C for the Ol-Opx-H_2O system for 207-284 hours. After each run, the water content and magnetic susceptibility were measured, and microstructures were observed by using SEM.

In the Ol-H2O system, the extent of the serpentinization is highest at 300, and serpentinization did not proceed at 400C. In contrast, in the Ol-Opx-H_2O system, the rate of the serpentinization was 1.5 times larger at 300C and >10 times larger at 400C than in the Ol-H_2O system. In the flow-through type experiments, the reaction progress was 10 times larger than in the batch type experiments for both systems. These results indicates that the serpentinization proceeded after orthopyroxene faster in particular at high temperatures, and leaching of SiO_2 by flow-through systems. The EDS analyses suggest that serpentinine minerals do not contain Fe3+ in any conditions. In contrast, magnetite linearly increased with the progress of serpentinization in the Ol-H2O system, whereas it does not increase in the Ol-Opx-H2O system. This can be understood in the activity diagram of silica activity and oxygen fugacity that iron is included in serpentine minerals in high silica activity. Our results suggest that serpentinization proceeds in harzburgite even at high temperature of >350, but the iron contents in orthopyroxene does not contribute to the hydrogen production. The production of hydrogen energy occurs at olivine-rich rocks at relatively low temperature.

Keywords: serpentinization, hydrogen

©2021. Japan Geoscience Union. All Right Reserved.

Hydration processes of a forearc mantle wedge inferred from the Takadomari serpentinite body in the Kamuikotan Belt, central Hokkaido, Japan

*Shun Takamizawa[1], Yuji Ichiyama[1], Shusaku Yamazaki[2], Akihiro Tamura[3], Tomoaki Morishita[3]

1. Chiba University , 2. Civil Engineering Research Institute for Cold Region, 3. School of Geoscience and Civil Engineering, College of Science and Technology, Kanazawa University

Subduction zones are the place where the recycling of Earth's surface materials has been taking place. In particular, the water cycle, which is caused by the subduction of the hydrated oceanic crust, is thought to be related to hydration of mantle wedges and consequent igneous and hydrothermal activities in subduction zones, but the details of hydration processes have been unclear. The Kamuikotan Belt in central Hokkaido consists mainly of Cretaceous high-pressure metamorphic rocks and ultramafic rocks. Because the high-pressure metamorphic rocks are interpreted to be derived from ancient subducted slabs, the ultramafic rocks associated with them can be regarded as mantle wedge materials beneath a subduction zone. The Takadomari serpentinite body in the Kamuikotan Belt. Consist of highly depleted serpentinized peridotite, which is interpreted as the residual mantle after the release of high-Mg andesitic magma, such as boninite, beneath an oceanic island arc (Tamura et al., 1999). The Takadomari serpentinite body contact with the high-pressure metamorphic rocks by faults, and the degrees of antigoritization increase towards the boundary with the metamorphic rocks (e.g., Igarashi, 1985). The presence of amphibolite tectonic blocks with blueschist-facies overprints (e.g., Ishizuka and Imaizumi, 1980) suggests that high-pressure metamorphism also affected the Takadomari serpentinite body. In this study, field survey, petrographic observations, and major and trace element analyses of minerals for the Takadomari serpentinite body in the Kamuikotan Belt, were performed to understand the spatial and temporal hydration processes of a mantle wedge. In the Takadomari serpentinite body, highly depleted harzburgite and dunite (Spinel Cr# = 0.6-0.9) are highly serpentinized. In particular, antigoritization tends to be strong in the southern part of the body near the high-pressure metamorphic rocks. This trend is consistent with the observation of Igarashi (1985), but highly antigoriteized serpentinites are also broadly distributed the Takadomari serpentinite body. Antigoritization is more pronounced in dunite than harzburgite. The Takadomari serpentinites usually have talc and Ca amphibole with tremolite to magnesio-hornblende compositions, as replacements of pyroxene. The Ca amphibole in the Takadomari serpentinites can be divided into two types, based on the Na_2O content. Estimated temperatures and pressures using thermobarometries for the Na-rich Ca amphibole (ca. 830 ℃ and 1.2 GPa) are higher than those of the Na-poor Ca amphibole (ca. 780 ℃ and 0.5 GPa). The occurrence of the Na-rich Ca amphibole is restricted to the northern part of the Takadomari serpentinite body, and rare phlogopite-bearing serpentinite is also present. After the formation of Ca amphibole, subsequent cooling resulted in talc. Further cooling formed richterite, Fe-rich metamorphic olivine, and clinopyroxene in association with antigorite in serpentinites near the boundary with high-pressure schist. In these serpentinites, olivine with stripe structure or parting is also present. These mineral paragenesis indicate that the serpentinites experienced prograde and retrograde events at around 500-600 ℃. In contrast, Mg-rich metamorphic olivine associated with antigorite and magnetite, was formed by prograde events at lower temperatures (around 400 ℃). The petrological characteristics of the Takadomari serpentinites are closely similar to those of the Mariana forearc serpentinites, indicating that the Takadomari serpentinite body was part of a forearc mantle wedge. The trace element patterns of Ca amphibole and richterite are significantly enriched in fluid mobile elements, such as Cs, Rb, and Pb. Similar trends are also observed in

©2021. Japan Geoscience Union. All Right Reserved.

the Mariana forearc serpentinite (Ichiyama et al., 2021), implying that the metasomatic agent for the Takadomari serpentinites body would have been fluids derived from subducted slabs. The slab-derived fluids at high temperatures were probably K-rich, as implied by the presence of phlogopite, but those at low temperatures were Na-rich due to the formation of richterite. The Takadomari serpentinite body, was finally emplaced on land together with the high-pressure Kamuikotan metamorphic rocks as an ancient forearc mantle wedge and an underlying slab.

Keywords: Subduction zone, Mantle wedge, Slab-derived Fluid, Metasomatism, Kamuikotan Belt

©2021. Japan Geoscience Union. All Right Reserved.

Petrological features and formation processes of lower crustal cumulate xenoliths from Oki-Dogo Island: A possibility of mantle plume origin

*Rio Higuchi[1], Yuji Ichiyama[1], Akihiro Tamura[2], Tomoaki Morishita[2]

1. Chiba University, 2. Faculty of Geosciences and Civil Engineering, Kanazawa University

In Oki-Dogo Island, the northern part of Shimane Prefecture, Pliocene alkali basalts often include ultramafic and mafic xenoliths (e.g., Aoki, 1977; Takahashi, 1976). Takahashi(1976) reconstructed a petrologic structure from crust to upper mantle beneath Oki-Dogo Island, based on the lithofacies of the xenoliths. Abe et al. (2003) investigated lherzolitic mantle peridotite xenoliths from Oki-Dogo Island and revealed that they are characterized by Fe- and rare-earth element (REE)-enrichment and the presence of aluminous spinel. They also proposed that the Oki-Dogo peridotite xenoliths are involved with the Middle Miocene backarc spreading of the Japan Sea. In contrast to attention to the mantle peridotite xenoliths, mafic and ultramafic xenoliths derived from the lower crust have not yet been studied. In this study, the petrographic observation and major- and trace-element analyses for the lower crustal cumulate xenoliths, olivine-gabbro, orthopyroxene-gabbro, granulite, clinopyroxenite, and wehrlite were performed to examine the petrological features and formation processes and to reveal their source mantle composition and tectonic implications for the circum-Japan Sea region. The lower crustal xenoliths exhibit the cumulate texture of poikilitic plagioclase with olivine and clinopyroxene oikocrysts, and the estimated equilibrium temperatures (>700℃) indicate that they formed in the lower crust. Olivine Mg# [=Mg/(Mg+Fe)] in the cumulates is lower than those of MORB (0.7–0.8), at a given NiO content, and spinel Cr# [=Cr/(Cr+Al)] is significantly low (<0.1). The REE patterns of clinopyroxene show light REE-enrichment. These petrological characteristics indicate that the lower crust cumulates were crystallized from the magma that was produced by low degrees of partial melting of the source mantle. The estimated REE patterns of the parental magma of the cumulates are different from those of basalts formed during the Japan Sea backarc-spreading in the Middle Miocene but resemble those of the Late Miocene-Pliocene alkali basalts, formed by mantle plumes in the post-backarc-spreading magmatism. The lherzolite xenoliths can be the source mantle for the estimated parental magma of lower crustal cumulates. The Oki-Dogo spinel- lherzolite xenoliths are possibly enriched mantle material derived from the Late Miocene-Pliocene mantle plumes.

Keywords: Backarc-spreading, Backarc-spreading of the Japan Sea, Xenolith, Mantle plume, Lower crust, Southwest Japan

©2021. Japan Geoscience Union. All Right Reserved.

[J] Poster | B (Biogeosciences)：B-PT Paleontology

Sun. Jun 6, 2021 5:15 PM - 6:30 PM JST | Sun. Jun 6, 2021 8:15 AM - 9:30 AM UTC | Ch.17_2

[B-PT02] Biotic History

convener:Isao Motoyama(Faculty of Science, Yamagata University), Takao Ubukata(Division of Geology & Mineralogy, Department of Earth & Planetary Sciences, Kyoto University), Kazuyoshi Moriya(Department of Earth Sciences, Faculty of Education and Integrated Arts and Sciences, Waseda University)

The Biotic History session covers all aspects of ancient life and the history of biosphere through the geologic time. The study of ancient life is essential for unveiling mysteries of our planet earth. It also provides evidence for evolution of oceans, continents and island arcs. Modern progress in this field has been enhanced by interdisciplinary collaboration with allied sciences, such as paleoceanography and evolutionary biology. Our session intends to be a hub of communication amongst all earth scientists studying the biosphere; we welcome biological and biogeochemical approaches toward the understanding of the history of life.

[BPT02-P01] Preliminary reports on the ecology of Cretaceous pantrionychian turtles based on the carapace bone histology

*Haruka Fukasawa[1], Kohei Tanaka[1], Yasuhisa Nakajima[2] (1.University of Tsukuba, 2.Tokyo City University)

[BPT02-P02] Asexual reproduction of planktonic foraminifera: Discovery and its significance

*Haruka TAKAGI[1], Atsushi KURASAWA[2], Katsunori KIMOTO[3] (1.Chiba University, 2.Marine Works Japan Ltd., 3.JAMSTEC)

[BPT02-P03] Oceanic anoxic event 2 observed in Southwestern Newfoundland Ridge

*Kazuyoshi Moriya[1], Yasuko Miyakura[2], Takashi Hasegawa[3], Akiko S. Goto[4] (1.Department of Earth Sciences, Faculty of Education and Integrated Arts and Sciences, Waseda University, 2.Major in Earth Sciences, Resources and Environmental Engineering, Graduate School of Creative Science and Engineering, 3.Faculty of Earth Science and Civil Engineering, Institute of Science and Engineering, Kanazawa University, 4.Center for Ecological Research, Kyoto University)

[BPT02-P04] Radiolarians from the upper Neogene Tatsunokuchi Formation, Miyagi Prefecture: An attempt to research depth-related distribution of extinct species.

*Isao Motoyama[1], Mizuho Aizawa[1] (1.Faculty of Science, Yamagata University)

Preliminary reports on the ecology of Cretaceous pantrionychian turtles based on the carapace bone histology

*Haruka Fukasawa[1], Kohei Tanaka[1], Yasuhisa Nakajima[2]

1. University of Tsukuba, 2. Tokyo City University

Pantrionychia is a group of non-marine, cryptodiran turtles that includes Nanhsiungchelyidae, Adocidae, and extant superfamily Trionychia (Trionychidae and Carettochelyidae). Pantrionychia originated in the Early Cretaceous of Asia and dispersed to North America during Cenomanian and Santonian. The Late Cretaceous turtle fauna in North America was thus likely influenced by the migration of Pantrionychia. Nevertheless of the importance, however, little is known about the ecology of Cretaceous Pantrionychia. Previous studies on bone/carapace morphology and/or taphonomic evidence suggest that extinct Adocidae was aquatic, whereas Nanhsiungchelyidae is still in debate between aquatic and fully terrestrial. Consequently, it is uncertain whether the clade Pantrionychia evolved from an aquatic or terrestrial form. The aim of this study therefore is to estimate their mode of lifestyles (i.e., terrestrial, freshwater, or marine) and discuss their evolutionally history.

The mode of lifestyle in tetrapods can be inferred based on bone histology. As a general trend, bone compactness is higher in freshwater animals than in terrestrial ones. Marine animals can acquire very high bone compactness (e.g., manatees) or very low (e.g., extant whales) according to animal’s swimming ecology. Such trends are also found in extant turtle limb bones, suggesting that the bone histology method can be applied for fossil Pantrionychia. Turtle limb bones, however, are relatively rare in the fossil record, comparing with abundant discoveries of carapace fragments. Thus, if the carapace histology reflects lifestyles, it can be an easy and powerful tool to infer the ecology of turtles.

In order to test whether the carapace bone histology can be used to infer the mode of lifestyles in turtles, we examined diverse extant taxa, including terrestrial, freshwater, and marine forms, before we applied the method to fossil taxa. Our results revealed that the carapace bone compactness is not necessarily correlated to their lifestyles, differing from previous speculations. However, we found that the size (cross-sectional area) of each intertrabecular space is correlated to the mode of lifestyles, at least between terrestrial and aquatic forms: the cross sectional area is significantly higher in terrestrial species than in aquatic species. The size of each intertrabecular space therefore can be an indicator of the lifestyles in turtles.

Based on the method above, we examined three fossil pantrionychian taxa discovered from the Late Cretaceous (Campanian) deposits in Alberta, Canada (Oldman and/or Dinosaur Park formations): *Basilemys* sp. (Nanhsiungchelyidae), *Adocus* sp. (Adocidae), and *Aspideletoides* sp. (Trionychidae). Our preliminary results revealed that *Basilemys* possesses a relatively large cross-sectional area of intertrabecular space, suggesting a terrestrial lifestyle. In contrast, *Adocus* and *Aspideletoides* show a relatively small cross-sectional area, suggesting an aquatic lifestyle. These results suggest that Pantrionychia changed their lifestyles though their evolutional history, which may be related to their radiation pattern.

Keywords: Pantrionychia, bone histology, ecology, Late Cretaceous, carapace, turtle

©2021. Japan Geoscience Union. All Right Reserved.

Asexual reproduction of planktonic foraminifera: Discovery and its significance

*Haruka TAKAGI[1], Atsushi KURASAWA[2], Katsunori KIMOTO[3]

1. Chiba University, 2. Marine Works Japan Ltd., 3. JAMSTEC

Marine protists have developed diverse modes of reproduction such as binary fission, multiple fission, and budding as means of asexual reproduction, and gametogamy and gamontogamy as means of sexual reproduction. Foraminifera, a group of protists in the Rhizaria, comprise mainly benthic species that generally reproduce both sexually and asexually alternately in their life cycles. However, for planktonic species, gamete release alone has been frequently observed in laboratory cultures. It has been taken as evidence that these organisms produce new generations exclusively by sexual reproduction. We report here the first observation of asexual reproduction in *Globigerinita uvula*, based on the evidence of the vertical transmission of their endosymbionts.
The foraminiferal sample was collected during Cruise MR13-04 of the R/V Mirai in the western North Pacific, July 2013. Four days after isolation, we found a matured individual releasing numerous two-chambered tests from its aperture. The juvenile specimens were immediately separated and utilized for either (1) DNA analysis, (2) culturing and observation, or (3) active fluorometric measurement to investigate photosymbionts. Based on the 18S rDNA analysis, the juveniles were identified to be *G. uvula*. Based on the morphological features, the reproduced matured individual was identified to be *G. uvula* as well, which convinced us that it is the parent of the juveniles. Chlorophyll active fluorescence was detected from the offspring through the culture period, and the intracellular algae were identified to be a pelagophyte alga phylogenetically closest to *Pelagomonas calceolata*. The presence of symbionts in the newborn, two-chambered offspring indicates that the symbionts were probably transferred vertically from the parent. The vertical transmission of symbionts cannot occur via sexual reproduction since the gametes are too small to hold symbionts. Therefore, our observation strongly suggests that the offspring were asexually reproduced by multiple fissions together with the symbionts.
The trigger for asexual reproduction and its ecological or evolutionary roles remain unknown. Considering that *G. uvula* is known to dominate opportunistically at times of high phytoplankton production, their ability of asexual reproduction may support their rapid population growth under changing environment.

Keywords: Planktonic foraminifera, Asexual reproduction, Symbiont transmission, Life cycle

©2021. Japan Geoscience Union. All Right Reserved.

Oceanic anoxic event 2 observed in Southwestern Newfoundland Ridge

*Kazuyoshi Moriya[1], Yasuko Miyakura[2], Takashi Hasegawa[3], Akiko S. Goto[4]

1. Department of Earth Sciences, Faculty of Education and Integrated Arts and Sciences, Waseda University, 2. Major in Earth Sciences, Resources and Environmental Engineering, Graduate School of Creative Science and Engineering, 3. Faculty of Earth Science and Civil Engineering, Institute of Science and Engineering, Kanazawa University, 4. Center for Ecological Research, Kyoto University

We have re-examined Oceanic Anoxic Event 2 (OAE2) at Southwestern Newfoundland Ridge. Mid-Cretaceous sequences including a major black shale approximately 40 cm thick and a few minor black shale layers were recovered by Integrated Ocean Drilling Program Expedition 342 at Site U1407. Shipboard and shore-based biostratigraphy indicates that the sections including these black shales are correlated to the Cenomanian through Turonian. Here, we report total organic carbon content (TOC), organic carbon/total nitrogen ratio (C/N ratio), and organic stable carbon isotope ratio ($\delta^{13}C_{org}$). Maximum TOC observed becomes more than 20 wt% at the major black shale, while background TOC is less than 1 wt%. $\delta^{13}C_{org}$ stratigraphy suggests well-known isotope signature at OAE2, namely, first build-up (FB), trough interval (TI), second build-up (SB), plateau (PT), and recovery (RV), is preserved at this site. At the PT interval, $\delta^{13}C_{org}$ shows an approximately 5‰ positive excursion from the pre-excursion background. The magnitude of this positive excursion is comparable to that observed in Oceanic Drilling Program Site 1276 at Newfoundland Basin. On the other hand, stratigraphic distribution of Black shales in Site U1407 is different from those in Site 1276. In Site 1276, the deposition of black shales started at the base of FB and continued up to PT. However, the major black shale in Site U1407 observed only at SB and PT. Estimated paleodepth at the mid-Cretaceous is deeper than 2000 m for both sites, indicating depths may not regulate the timing of the black shale deposition. Considering bathymetry of western north Atlantic and position of Grand Banks, we hypothesize that these two sites were under the different bottom water current system at the Cenomanian through Turonian.

©2021. Japan Geoscience Union. All Right Reserved.

Radiolarians from the upper Neogene Tatsunokuchi Formation, Miyagi Prefecture: An attempt to research depth-related distribution of extinct species.

*Isao Motoyama[1], Mizuho Aizawa[1]

1. Faculty of Science, Yamagata University

Radiolarians are marine micro-zooplanktons today living in a wide environmental range from tropic to polar regions as well as from shallow to great depths in the world ocean. Therefore, their fossil siliceous remains in sediments are stratigraphically and ecologically useful material to reconstruct the history of the Earth’ s life and surface environments. Going back in deep time, however, living species that are proxies of oceanographic environments become less and less frequent in geological records. Paleobiogeography of extinct species can be a key to understand oceanic biofacies and ecological realms but it is rather difficult to research depth-related distribution in the water column of extinct species.

The Tatsunokuchi Formation is dominated by marine fine-grained sediments deposited in a paleo-bay in northeastern Japan during the latest Miocene to the early Pliocene. This formation yields the Tatsunokuchi Fauna characterized by abundant, diversified fossils including mollusks, crabs, sharks, whales and seals, which indicate cool water condition and water depths shallower than 50 m. This formation provides an opportunity to study ancient planktonic fauna of shallow water environments.

We collected samples from the Tatsunokuchi Formation from the southernmost part of Miyagi Prefecture to the northern border. Most of the samples yielded radiolarian fossils. Some of these samples contain well-preserved extinct species including *Stichocorys peregrina*, *Stichocorys delmontensis*, *Didymoyrtis penultima* and *Cycladophora sphaeris*. *S. peregrina* is the commonest component among the samples and the others occurred in rare abundance from one or two samples. The occurred specimens of *S. peregrina* and *D. penultima* have well-developed siliceous skeletons. *S. peregrina* and *C. sphaeris* are known to be abundant in age-equivalent deep-sea sediments in offshore drilled sites (e.g., DSDP/ODP Sites 438, 1150, 1151). *D. penultima* is a zonal marker species of the *D. penultima* Zone. *Didymocyrtis tetrathalamus*, a modern descendant of the *Didymocyrtis* lineage, is known to be a surface water dweller.
Our results suggest that *S. peregrina* and *D. penultima* lived in surface waters shallower than 50 m. It is likely that both were shallow water taxa, although it cannot be excluded that they had wide depth ranges from the surface to deeper layers. It is not certain that *S. delmontensis* and *C. sphaeris* dwelt in abundance in the paleo-Tatsunokuchi bay because of their rare, sporadic occurrence.

Keywords: radiolarians, paleo-ecology, Tatsunokuchi Formation

©2021. Japan Geoscience Union. All Right Reserved.

[J] Poster | G (General)：General

Sun. Jun 6, 2021 5:15 PM - 6:30 PM JST | Sun. Jun 6, 2021 8:15 AM - 9:30 AM UTC | Ch.03_1

[G-01] Disaster prevention education

convener:Hitoshi Nakai(Kobuchisawa Research Institute for Nature and Education), Jiro Komori(Teikyo Heisei University), Shintaro Hayashi(Akita University Graduate School of Education), Tetsuhiko Asano(Senshu University Matsudo Junior High School High School)

This session, slated for the 2021 convention, will mark the 10th time the meeting has been convened since the first public session was held a year after the Great East Japan Earthquake. We have consistently focused on how to provide disaster prevention education that is universally and continuously applicable. Almost every year since the first session has been marked by earthquakes and meteorological disasters, and each time we discovered defects in our preparatory measures to mitigate the effects of disasters. The accumulation of such bitter experiences must lead to the creation of new disaster prevention measures. For this purpose, it is necessary to share the experiences of regions right across the country. In particular, people involved in disaster prevention education must extract, from what has been learned in individual regions, those lessons that are universally applicable to any region, and pass them on to future generations. The year 2021 will mark the 10th anniversary of the Great East Japan Earthquake, which resulted in the death or loss of more than 18,000 people, and many more injuries, within the space of just a few hours. The last 10 years has revealed a number of issues to be addressed in disaster prevention education. We would like to review and discuss these issues.

[G01-P01] Considering limits of hazard map: A case of a debris flow disaster that struck a village at the southern foot of Yatsugatake in September 1898.

*Hitoshi Nakai[1] (1.Kobuchisawa Research Institute for Nature and Education)

[G01-P02] **A Quantitative Analysis of Nationwide Municipalities' Disaster Prevention Portals**

*Haruka Matsuoka[1], Ami Mori[1], Kei Takashima[1], Tsukasa Sano[1], Asako Sano[2], Seiji Hori[1], Minako Noda[1] (1.Department of Business and Informatics, Tsukuba Gakuin University, 2.Faculty of Home Economics, Otsuma Women's University)

Considering limits of hazard map: A case of a debris flow disaster that struck a village at the southern foot of Yatsugatake in September 1898.

*Hitoshi Nakai[1]

1. Kobuchisawa Research Institute for Nature and Education

Hazard maps that describe sediment disaster warning areas and inundation areas are extremely important sources of safety information for residents. For sediment-related disasters, the warning area (and the special warning area) due to collapse of steep slopes and those for debris flow are designated. The steep slopes mentioned here refer to slopes with an inclination of 30 degrees or more, but flat areas within 10 m from the upper end of each slope and flat areas within 50 m from the lower end of each slope are also included in the warning area (Sediment Disaster Prevention Law Enforcement Regulations). However, the designation is made for "the area of land where it is recognized that there is a risk of harm to the lives or bodies of residents, etc. in the event of a collapse of a steep slope" (Sediment Disaster Prevention Law). Therefore, steep slopes in the mountains are not generally designated as a warning area. However, if a slope collapse occurs when heavy rain continues for a long time in a mountainous area, the debris flow may extend with a plenty of water to a region that is not expected as a sediment disaster warning area. It may consequently occur a significant disaster. Since such a case of the slope collapse under continuing heavy rain is not assumed in the current hazard map, inhabitants have to know about past catastrophes occurred in their area in detail.

In this presentation, we will discuss one of the debris flow disasters that once occurred at the southern foot of Yatsugatake as an example. Around 1:30 am on September 7, 1898, heavy rain brought about by a typhoon caused a debris flow in the Yato Area of Oizumi Village (Hokuto-city Yamanashi) at the southern foot of Yatsugatake. Consequently, 57 were killed, and 51 were injured. The author identified the locations of the damaged houses based on the "Storm Damage Investigation Report" compiled in the Meiji era and archived in the Imperial Household Agency, and the records of the land register stored in the Legal Affairs Bureau. It was found that most of the damaged houses had been located along an agricultural canal that flowed through the village. The author also compared the distribution of damaged houses in the disaster area with the results of debris flow simulations, which was made using the Hyper KANAKO system, and found that the local topographic features were the primary cause of the concentration of victims in a specific group of houses.

Based on the investigation of this historic disaster, it is pointed out that the debris flow may extend beyond the warning area designated on the hazard map, and that a minimal topography of the residential area could cause enormous damage. Farther, these findings suggest that general commentaries on the hazard map is not only insufficient as the disaster prevention education, but it may instill a dangerous sense of security in the inhabitants.

Keywords: hazard map, sediment disaster, historical documents of disaster

©2021. Japan Geoscience Union. All Right Reserved.

A Quantitative Analysis of Nationwide Municipalities' Disaster Prevention Portals

*Haruka Matsuoka[1], Ami Mori[1], Kei Takashima[1], Tsukasa Sano[1], Asako Sano[2], Seiji Hori[1], Minako Noda[1]

1. Department of Business and Informatics, Tsukuba Gakuin University, 2. Faculty of Home Economics, Otsuma Women's University

Japan is a country of frequent natural disasters, with casualties tallied every year. Disaster prevention information and education are therefore very important to mitigate the human and material damages resulting from natural disasters.

One of the familiar disaster educational materials for people is the disaster prevention portal site in the prefecture where they reside. All prefectures in Japan have their own disaster prevention portal sites, which contains various information and educational contents pertaining to natural disaster prevention.

In this study, the disaster prevention portal sites from forty six prefectures were investigated. The results suggest that there is disparity concerning variety contents and structure, which makes it difficult to analyze comparatively or statistically. The twenty eight categories were therefore defined for the information and/or the functions that each portal contains. The value 0 or 1 were then applied to indicate the absence or presence of them. Using these numerical values, correlation analyses were conducted to evaluate the strength of the relationship between the variety among categories and some values or indexes associated with a natural disaster. Additionally, Quantification Method III was also used for multi-dimensional scaling to quantify the characteristics of the portal sites.

The variety of disaster prevention information and education seems to have almost no-correlation with both the index of susceptibility for disasters and the number of victims from disasters over the past five years. The characteristics of the portals possibly are indicated by two components involved in the information it containes, these being the degree of emergency and of concreteness for evacuation actions.

Keywords: Disaster Prevention, Disaster Education, Quantification Method of the Third Type

©2021. Japan Geoscience Union. All Right Reserved.

[J] Poster | G (General)：General

Sun. Jun 6, 2021 5:15 PM - 6:30 PM JST | Sun. Jun 6, 2021 8:15 AM - 9:30 AM UTC | Ch.03_2

[G-02] Outreach and geoscience education

convener:Jiro Komori(Teikyo Heisei University), Naoko HASEGAWA(Ochanomizu University), Ken Tsukada(Hiratsuka City Museum), Satoko Oki(Faculty of Environment and information Studies)

The aims of Outreach and geoscience education are to encourage developments that raise public awareness of geosciences through schools and/or public outreach by not only educators but also researchers. Therefore, any presentation related with these aims will be welcomed to this session. Depending on schedule and venue,some presentation will be changed to Poster presentations.

[G02-P01] Astronomy outreach with multiple perspectives by music, painting, and tourism

★Invited Papers

*Uenoyama Sachiyo[1], Akihiko Tomita[1], Masami Okyuudo[1] (1.Wakayama University)

[G02-P02] Astronomical environment in which outreach targets are interested and outreach methods utilizing it

*Miyuki Tsuchiya, Mie Enomoto

Astronomy outreach with multiple perspectives by music, painting, and tourism

*Uenoyama Sachiyo[1], Akihiko Tomita[1], Masami Okyuudo[1]

1. Wakayama University

As stated in the Strategic Plan 2020-2030 of the International Astronomical Union, astronomy is deeply related to and has a significant impact on the fields of “culture and society” in addition to “science and research” and “technology and skills.” Although the discussion here stands from a point of view of astronomy, the same point of view can be applied to any discipline and field in the broad field of earth and planetary sciences. In the area of “culture and society,” we would like to focus on the inspiration and the raising of awareness of the need to create communities for sustainable development that come from a sense of awe in contact with great nature. Music, painting, and tourism have a high affinity with astronomy, and many of such outreach activities have been conducted to acquire the above-mentioned power in the “culture and society” area. On the other hand, many researchers have been struggling with the methodology of how to measure and evaluate these powers.

The outreach that will be examined here is the practice at Deti, a facility for Japanese students to study English in Negros Island, Philippines. It is a residential school that aims to help students acquire English through encounters with local people, culture, and values. The schedule was 12 days, from August 5 to August 16, 2019. Participants included parents and their children studying abroad from Japan (5 adults and 7 children), Filipino English teachers (about 20), Japanese tourists (several), Japanese staff and their families (6), and Japanese interns of students and adults (7).

The practices included, (1) “Star storytelling and star-watching party” was held almost every day, (2) “Storytelling about constellations and the arpa” while playing the arpa (a South American harp), concerts at night pools while looking at the stars, self-help and healing music, “Obon” music ceremonies, etc, (3) Psychological counseling sessions to look at the way of life, (4) Mural painting on the wall of the child house in the Deti campus, (5) Projecting illustrations of picture books and reading them, and reading anti-war picture books with background music by a local harp player. The participants’ comments and actions during the practice were recorded in writing, and from the records, we found cases that led people to have a broader perspective and to think about their way of life and community, and examined the conditions of the environment in which the cases happened. This is the material and method we have adopted for the measurement and evaluation.

Twenty-four episodes were identified as examples to focus on. For example, they noticed that the night sky was different due to the difference in latitude, and became aware of the planet Earth. They also learned about each other’s thoughts and way of life, and at the same time, began to talk about the changes in each person’s behavior and mental attitude. For each case, we wrote down the timing of the case, the participants’ actions, and the educator’s impression and evaluation. The four physical environments needed for the cases are: (1) the good atmosphere and climate of the region, (2) the good physical settings (building, educational discipline), (3) the appropriate timing (period and time of year), and (4) a simple and highly functional astronomical software. The three human environments needed for the cases are: (1) the collaborative and ambitious mind of the staff (mediators and collaborators), (2) the high level of awareness of the participants, and (3) the educator’s wide range of skills and knowledge.

©2021. Japan Geoscience Union. All Right Reserved.

Keywords: astronomy outreach, astro-turism

©2021. Japan Geoscience Union. All Right Reserved.

Astronomical environment in which outreach targets are interested and outreach methods utilizing it

*Miyuki Tsuchiya, Mie Enomoto

This paper considers Tokyo Disney Sea as an astronomical environment in which outreach targets are of daily interest, and considers the specific astronomical environment by adding new knowledge, taking into consideration previous research. Next, we will take up Shuichiro Yoshioka's "The Relationship between Astrology and Astronomy, its History"(1943,The Heavens) and consider how astrologyshould be viewed. As an outreach method that takes advantage of the astronomical environment of interest, we propose to hold summits by organizations and organizations with the symbol "Foucault pendulum" currently installed in 59 locations nationwide, including TDS.@Points to keep in mind when using the astronomical environment at TDS for outreach.TDS is a daily source of interest to outreach targets, with an average of about 30 million visitors a year. Previous research by Hiroaki Ying, Reiji Hibara, and Sayaka Nabeshima "Utilizing Artificial Materials in Earth Science Education : A Utilizing Example of Earth Science Materials at TDS" (Education of earth science 61(4)," 133-139, 2008-07-25), Chii Shimomura, Noritsugu Takahashi, "Utilization of Geological Education Materials in TDS" (Research on Space Education, (1), 85-89, 2020-07-07)TDS already has 11 astronomical objects in its main case alone, and it is already well unders been unders been grasped in detail that it is a rich astronomical environment. However, only the fact is pointed out though one of the points pointed out there is a point where not only the earth movement theory but also the astronomical object according to the heavenly movement theory is installed. When using TDS as an outreach method, we propose to actively view it as a material to explain the history of astronomy from the theory of heaven to the earth movement theory. It should also be pointed out accurately to the outreach target that the stoned position of the ground indicating the age of the moon is reversed, even if the reason is not clear. @Shuichiro Yoshioka" The Relationship between Astrology and Astronomy, ItsHistory" (1943, Heaven), astrology as the history of astronomy.Shuichiro Yoshioka is a "relationship between astrology and astronomy, its history" (1943, Tenkai 23(268), In 305-310, 1943-10-25, and 23(269), 344-347, 1943-12-28), astrology born in Babylonia is one with astronomy, and what is born there is also utilized in the system of units and other fundamentals of modern life. Astrology, so to speak, is a living witness to astronomy and embodies the history of astronomy. And in light of modern standards, even if it is unscientific, it is certain that it has been passed down to modern society as a culture related to astronomical texts. In that respect, it is thought that it is near the religion, and it should be calmly caught as the same kind as the annual event of daily such as the new year's visit. @Proposal for holding the " Foucault pendulum " Summit as an Outreach Method As examined in @1 a huge " Foucault pendulum " is installed in TDS along with other astronomical objects. Looking at the number of " Foucault pendulum " currently installed nationwide, there are a total of 59 locations. Therefore, various organizations and organizations that have established this " Foucault pendulum " will set up a network and hold a summit with the symbol " Foucault pendulum ", and propose that it be an opportunity to widely interest in astronomical texts. The content of the summit is not only knowledge of the astronomical text itself, but also the participation of researchers in fields and fields that deal with astronomical events in various forms. Specifically, it assumes areas such as literature, painting, film, architecture, urban planning, calendar, annual events, naming, astrology, religion, politics, etc.

Keywords: Outreach, Foucault pendulum, Tokyo Disney Sea, Astrology

©2021. Japan Geoscience Union. All Right Reserved.

[J] Poster | G (General)：General

Sun. Jun 6, 2021 5:15 PM - 6:30 PM JST | Sun. Jun 6, 2021 8:15 AM - 9:30 AM UTC | Ch.03_3

[G-03] G03Geoscience education from elementary school to university students

We will provide and discuss various educational practices (teachings and procedures)
for elementary, junior high school, high school, and university students. We also welcome ONLINE education, fieldwork reports, and outreach reports for all grades.
Besides, especially for liberal arts level geoscience education of undergraduate,
we will consider the problems, such as online education, contents, and prospects of our current geoscience situation.
Furthermore, we will also think about fundamental teaching material development and the sharing of teaching material data.

[G03-P01] Practice of Inquiry Activities based on the Field of Earth Science in High School

*Kazuya Kawakatsu[1] (1.Hyogo Prefectural Himeji Higashi senior high school)

Practice of Inquiry Activities based on the Field of Earth Science in High School

*Kazuya Kawakatsu[1]

1. Hyogo Prefectural Himeji Higashi senior high school

1 Introduction
In order to revitalize the inquiry activities, in the first year (2019) when I was invited to the incumbent school, I was introduced the Themed Research to all 280 students in the first grade. Due to this achievement and expectations for new educational goals, it was designated as a Super Science High School (SSH) by the Ministry of Education, Culture, Sports, Science and Technology in 2020 (Received designation for 5 years). From now on, we will carry out research and development on the educational themes listed, and disseminate the results nationwide.

2 Goals of inquiry activities
The specific goals of our school's SSH agenda are the following.

(1) Challenge to international activities based on earth science and foster science girls who can work internationally
(A) In order to inherit the lessons learned from the Great Hanshin-Awaji Earthquake, it is necessary to learn both disaster prevention education and natural science understanding. But in the current high school education, education to understand disasters as a whole is not effectively conducted. Therefore, based on the field of earth science, we will educate the four fields of science in a cross-disciplinary manner ("Natural Science Inquiry Basics").
(B) All first-grade students conduct themed research and acquire the power of inquiry ("Basics of Inquiry in Science and Mathematics"). All subject teachers are in charge of themed research, and provide guidance and advice. In addition to scheduling and ensuring safety, the teacher will draw out new ideas from students by participating in discussions, and giving advice.
(C) The excellent students found in this process will proceed to the science course after 2021, and will spend two years doing full-scale themed research. Students who wish to conduct a field survey in southeastern Australia with the cooperation of the University of Sydney will present the results obtained at the international conference.
(D) Support the activities of female students who aspire to science. Next year, we will hold "Girl's Expo with Science Ethics" centered on female researchers and female students.

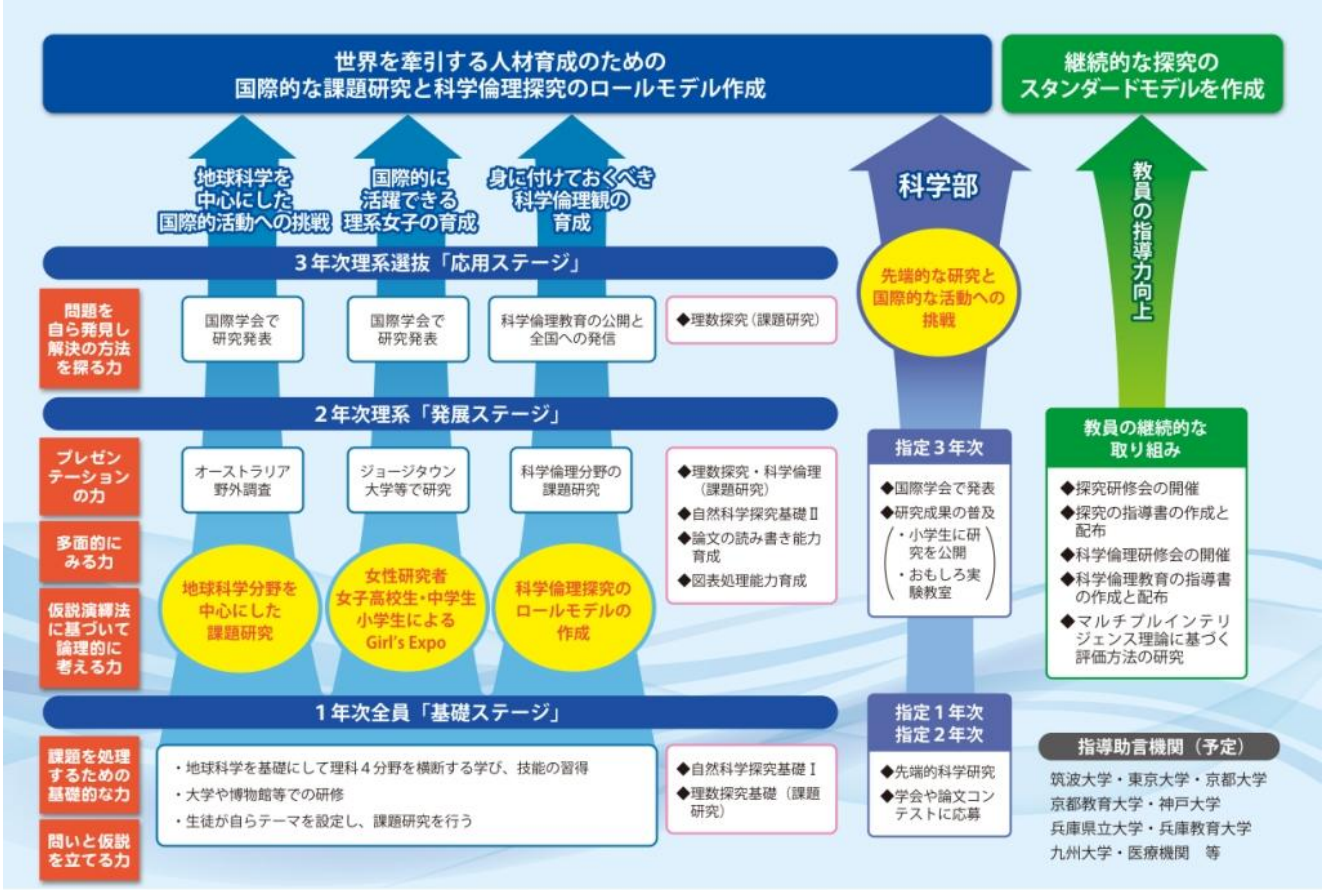
(2) Fostering science ethics that should be acquired for scientific research
(A) In order to learn the responsible behavior of scientists toward society and the science ethics that should be acquired as a member of society, we will conduct research on science ethics issues related to the research on natural science conducted by students. We will present it at the "Girl's Expo with Science Ethics".
(B) Through this activity, we will create a program for fostering science ethics and disseminate it nationwide. Students who are motivated to challenge the international arena will challenge research and presentation at international conferences at domestic and overseas universities such as Georgetown University.

(3) Support for cutting-edge research and challenges for international activities conducted by the Science

©2021. Japan Geoscience Union. All Right Reserved.

Club
(A) Rather than simply relying on advanced analytical equipment, we will conduct research with flexible ideas and ingenuity that are typical of high school students, and achieve excellent results that will lead the themed research of our students.
(B) Actively carry out dissemination activities in the region.

Keywords: Super Science High School, Inquiry Activities, Themed Research, Science Ethics



兵庫県立姫路東高等学校　SSH概要図

©2021. Japan Geoscience Union. All Right Reserved.

[J] Poster | M (Multidisciplinary and Interdisciplinary)：M-IS Intersection

Sun. Jun 6, 2021 5:15 PM - 6:30 PM JST | Sun. Jun 6, 2021 8:15 AM - 9:30 AM UTC | Ch.19_2

[M-IS13] Dynamics of eruption cloud and cumulonimbus; modelling and observation

convener:Eiichi Sato(Meteorological Research Institute), Fukashi Maeno(Earthquake Research Institute, University of Tokyo), Takeshi Maesaka(National Research Institute for Earth Science and Disaster Resilience)

Volcanic eruption clouds (eruption column, pyroclastic flow, and umbrella cloud) and cumulonimbus are similar phenomena in the atmosphere. Models that can precisely reproduce the physical processes in such phenomena, and accurate observations have been required. Recently, the development of remote sensing techniques such as weather radar and weather satellite are remarkable, and they are being adopted for volcanic eruption monitoring. However, it is indispensable to verify the results of modeling and remote sensing using in-situ observations. In this session, we will discuss the modelling and the observations of eruption clouds and cumulonimbus from the viewpoint of meteorology, volcanology, geology, and other related fields. The related phenomena such as ashfall, rainfall, snowfall, hail and volcanic block will also be discussed.

[MIS13-P01] Estimation of ash refractive index and improvement of Himawari-8 volcanic ash algorithm

★Invited Papers

*Hiroshi Ishimoto[1], Masahiro Hayashi[1], Yuzo Mano[1], Rei Kudo[1] (1.Meteorological Research Institute)

[MIS13-P02] Multi-sensor observation of cloud evolution from cumulus to cumulonimbus in Tokyo metropolitan area

*Takeshi Maesaka[1], Tadayasu Ohigashi[1], Koyuru Iwanami[1], Shin-ichi Suzuki[1], Namiko Sakurai[1], Yukari Shusse[1], Kaori Kieda[1], Shingo Shimizu[1], Yasushi Uji[1], Nobuhiro Takahashi[2], Hiroshi Hanado[3], Katsuhiro Nakagawa[3], Tomoo Ushio[4] (1.National Research Institute for Earth Science and Disaster Resilience, 2.Nagoya University, 3.National Institute of Information and Communications Technology, 4.Osaka University)

[MIS13-P03] Application to the volcanic ash obserbation of the X-band solid state marine radar

*Takaaki NISHI[1], Masayuki MAKI[1], Takehiko KOBORI[1], Kanji ENDO[2], Kazuhiko KAIGA[2], Masato IGUCHI[3] (1.Kagoshima Univ., 2.Koden Electronics Co., Ltd, 3.Kyoto Univ.)

[MIS13-P04] Modification of probabilistic estimation method for eruption plume height using weather radars

*Eiichi Sato[1] (1.Meteorological Research Institute)

[MIS13-P05] Ash fall observation using 2D-Video Disdrometer (2)

*Eiichi Sato[1], Kosei Takishita[2], Masato Iguchi[3] (1.Meteorological Research Institute, 2.Division of Earth and Planetary Sciences, Graduate School of Science, Kyoto University, 3.Sakurajima Volcano Research Center, Disaster Prevention Research Institute, Kyoto University)

[MIS13-P06] Sedimentary process of ash deposits from long-term activity of repeated vulcanian eruptions at Sakurajima volcano, Japan

*Takahiro Miwa[1], Futoshi Nanayama[2] (1.National research institute for earth science and disaster resilience, 2.Geological Survey of Japan, AIST)

Estimation of ash refractive index and improvement of Himawari-8 volcanic ash algorithm

*Hiroshi Ishimoto[1], Masahiro Hayashi[1], Yuzo Mano[1], Rei Kudo[1]

1. Meteorological Research Institute

For continuous near-real time monitoring of volcanic ash clouds (VAC) in both day and night, satellite observations by using infrared sensors are particularly useful. Because volcanic silicate has a characteristic absorption band around 10μm wavelength, VAC of fine ash particles can be easily detected and distinguished from water/ice clouds by measurements of brightness temperature difference between two channels in this absorption band. Applying further constraints for microphysical properties of the ash particles, such as particle size distribution, and for atmospheric profile, retrieval of physical properties for VAC (cloud height, particle effective radius, optical depth, and the associated ash mass loading) has been realized by adding the measurements of other infrared channels of high-resolution satellite imagers. These retrieval analyses are based on the results of numerical simulations for the measured infrared brightness temperature by radiative transfer calculations for VAC under the assumption of atmospheric profiles and surface condition, and therefore, optical properties of the ash particles are essential. In particular, the complex refractive index (RI) is one of the important and upstream parameters in estimation of the ash optical properties and their wavelength dependences.
From the data of satellite infrared sounder measurements for VAC and radiative transfer calculations, we estimate optimal refractive index models of the volcanic ash material to simulate the measured brightness temperature spectrum. In addition, we have developed an algorithm of 1DVAR analysis (OVAA) that estimates the physical properties of VAC from the data of multi-wavelength satellite imager such as Himawari-8. By using the optimal RI model estimated by the infrared sounder and using OVAA, high accuracy Himawari-8 analysis for the physical parameters of VAC is expected.

Keywords: volcanic ash clouds , refractive index, Himawari-8

©2021. Japan Geoscience Union. All Right Reserved.

Multi-sensor observation of cloud evolution from cumulus to cumulonimbus in Tokyo metropolitan area

*Takeshi Maesaka[1], Tadayasu Ohigashi[1], Koyuru Iwanami[1], Shin-ichi Suzuki[1], Namiko Sakurai[1], Yukari Shusse[1], Kaori Kieda[1], Shingo Shimizu[1], Yasushi Uji[1], Nobuhiro Takahashi[2], Hiroshi Hanado[3], Katsuhiro Nakagawa[3], Tomoo Ushio[4]

1. National Research Institute for Earth Science and Disaster Resilience, 2. Nagoya University, 3. National Institute of Information and Communications Technology, 4. Osaka University

Recently, weather radar network which consists of X- and C-band polarimetric radars has matured in Japan. This nationwide network enables Quantitative Precipitation Estimation (QPE) with high resolutions (1 minute and 250 m), and is used for a monitoring of localized heavy rain. So now a social request is shifting from the monitoring to the forecast of the heavy rain. This kind of forecast needs a seed of cumulonimbus development as an initial condition. The weather radar is a suitable instrument to find the seed. But when the ordinary weather radar finds it, the rainfall has already started. To make the lead time of the forecast longer, we should monitor the pre-stages of cumulonimbus, such as horizontal convergence and cumulus clouds. For this purpose, we installed microwave radiometers, Doppler lidars, Ka-band cloud radars around Tokyo metropolitan area. Furthermore, X-band Multi-Parameter Phased Array Weather Radar (MP-PAWR) also covers the area, and is a powerful instrument to capture the three-dimensional structure of precipitation system. In this presentation, an evolution from cumulus to cumulonimbus is analyzed by using multi-sensor data.

We analyzed the cloud activities on 3 August 2018. Many cumulus clouds appeared and dissipated, before the precipitation started, cloud size and its reflectivity gradually became larger with time. Finding the clouds in transition stage (reflectivity of about -5 dBZ, and echo size of about 5 km^2) is important for monitoring the evolution from cumulous to cumulonimbus. Cumulus activity moistened mid-troposphere, and this moistening may help the cumulonimbus development.

Keywords: Cumulus, Cumulonimbus, Cloud radar, MP-PAWR

©2021. Japan Geoscience Union. All Right Reserved.

Application to the volcanic ash obserbation of the X-band solid state marine radar

*Takaaki NISHI[1], Masayuki MAKI[1], Takehiko KOBORI[1], Kanji ENDO[2], Kazuhiko KAIGA[2], Masato IGUCHI[3]

1. Kagoshima Univ., 2. Koden Electronics Co., Ltd, 3. Kyoto Univ.

Volcanic ash Sakurazima and Kirishima has been observed by Ku band radar(Ku-RAD) of Kagoshima University. In addition, marine radar had shorter search time than Ku-RAD was able to observe volcanic ash. On the other hand, marine radar produced a transmission signal in magnetron which was necessary to change magnetron in a fixed period. This time, we borrowed solid state marine radar which was no necessary to change solidified transmission device and can observe volcanic ash. At first solid satate marine radar was installed on the Kagoshima University Shimoarata campus roof and measured the Sakurajima area in PPI and RHI. Furthrtmore, to move, and to observe eruption of Sakurajima, the marine solid state radar was installed in the boat, the volcanic ash of Sakurajima was observed under navigation. These observation methods were effective for volcanic ashes observation.

Keywords: X-band SSR, volcanic ash, PPI, RHI

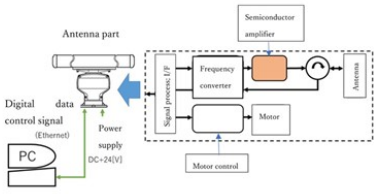
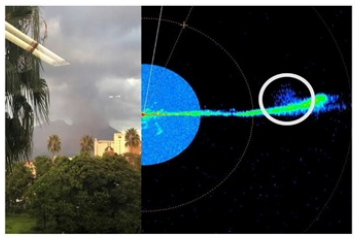
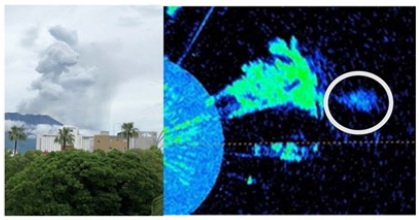


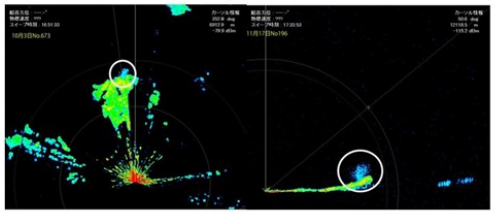
図1 船舶用固体化レーダ(SSR : solid-state marine radar) 基本構成



(a) 18:00 (b) 17:58 1400m
図3 9月17日2019年桜島噴煙の写真(a)とSSRによって観測された噴煙(b)



(a) 10:54 (b) 10:44 3200m
図2 7月4日2019年桜島噴煙の写真(a)とSSRによって観測された噴煙(b)



(a)10月 3 日16:51 1700m (b) 11月17日 17:33
図 4 2020年 SSRによって観測された桜島噴煙のPPI映像(a)とRHI映像(b)

©2021. Japan Geoscience Union. All Right Reserved.

Modification of probabilistic estimation method for eruption plume height using weather radars

*Eiichi Sato[1]

1. Meteorological Research Institute

Sato et al. (2018) developed a probabilistic estimation method for eruption plume height and applied it to the 2016 Mt. Aso eruption case.In this presentation, we will show the result of applying the improved probabilistic estimation method (MPE method) to the 2018 Kusatsu-Shirane (Motoshirane) eruption case.

The main improvements of the method are that the refractive index of the atmosphere was calculated from the GPV of the initial value of the Mesoscale Model (MSM) of the Japan Meteorological Agency, and that the effect of the earth ellipsoid was included. In addition, the correction of geoid altitude is also included.

As a result of applying the MPE method to the 2018 eruption of Mt. Kusatsu-Shirane (Mt. Motoshirane), the eruption plume height is estimated to be 5,580 m ±506 m (1 σ).

Based on this result, the author also tried to estimate the amount of ejecta by applying four methods for estimating the mass eruption rate from the eruption altitude.

The author also discusses the adequacy of applying these techniques to phreatic eruptions.

Keywords: weather radar, eruption plume height, probabilistic estimation method, refractivity, earth ellipsoid

©2021. Japan Geoscience Union. All Right Reserved.

Ash fall observation using 2D-Video Disdrometer (2)

*Eiichi Sato[1], Kosei Takishita[2], Masato Iguchi[3]

1. Meteorological Research Institute, 2. Division of Earth and Planetary Sciences, Graduate School of Science, Kyoto University, 3. Sakurajima Volcano Research Center, Disaster Prevention Research Institute, Kyoto University

Meteorological Research Institute (MRI) is conducting ash fall observations at Sakurajima Volcano using two-dimensional video disdrometers (2DVDs). 2DVD is originally a ground-based instrument that observes precipitation particles, and it is possible to obtain the three-dimensional shape and falling velocity of each target particle. This instrument is used in meteorology to verify polarimetric (dual-polarization) radar and to observe precipitation particles on the ground, but in volcanology there are few observations. MRI is developing a technology for estimating the amount of volcanic ash inside the eruption plume using a polarimetric radar. In addition, 2DVD observations are being conducted to obtain the “ground truth” data.
Here, we describe the main previous researches and current issues. Suh et al. (2019) conducted an indoor ash fall experiment to discuss the characteristics of volcanic ash particle shape, falling velocity, and canting angle, however, it is necessary to investigate the characteristics of the actual ash fall. Kozono et al. (2019) is an example of ash fall observation by a disdrometer in the natural environment. However, since the disdrometer used in this paper cannot recognize the shape of particles, it is not suitable for verification of dual-pol radar data.
In this presentation, we will report the outline of the quality control method of ash fall observation data by 2DVD and the verification method of the amount of volcanic ash retrieved using a polarimetric radar.

Keywords: 2D-Video Disdrometer, Sakurajima volcano, ash fall, dual-polarization/polarimetric radar

©2021. Japan Geoscience Union. All Right Reserved.

Sedimentary process of ash deposits from long-term activity of repeated vulcanian eruptions at Sakurajima volcano, Japan

*Takahiro Miwa[1], Futoshi Nanayama[2]

1. National research institute for earth science and disaster resilience, 2. Geological Survey of Japan, AIST

Ash deposit from a long-term activity of repeated vulcanian eruptions are important for understanding the development of a volcanic edifice. In this study we discussed the sedimentary system of ash deposits produced by long-term vulcanian activity from Showa crater of Sakurajima volcano, Japan, based on the grain size distributions of falling ash from individual eruptions. We sampled falling ash particles from 21 individual vulcanian eruptions between March 3–11, 2010. The grain size distributions of the ash samples were unimodal, bimodal, and trimodal characteristics. The median particle size of the main subpopulation decreases with distance from the Showa crater. The low standard deviation of the grain size of the main subpopulation implies deposition from transient volcanic plumes (Walker, 1971). For the finest subpopulation in the polymodal samples, the median particle size is very fine ash (<30 μm) which is difficult to fall as individual particles due to low terminal velocity, indicating that this subpopulation was originated from ash aggregates. Overall, the sedimentary process of the repeated vulcanian eruptions at Sakurajima volcano is explained by accumulation of ash particles from transient plumes and ash aggregation, and the latter controlled the behavior of the very fine ash. We consider the model proposed in this study reflects the long-term activity of repeated vulcanian eruptions, based on the following: (1) The vulcanian eruptions considered in this study were typical of Sakurajima volcano; (2) the Md–distance relationship of main subpopulation from this study are similar to those for the March 26 2016 vulcanian eruption (Miwa et al. 2020) and the July 28–August 3 2013 vulcanian eruptions at Sakurajima volcano (Gabellini et al. 2020). Deposition of ash particles during long-term vulcanian activity generates a close-concentric spatial distribution of ash grain size and thickness around the crater (Imura, 1995), and builds the volcanic edifice, along with the eruptive products from large-scale eruptions. Year-long monitoring of ash accumulation should be suggested for future research.

Keywords: Volcanic ash, Deposit, Vulcanian eruption, Sakurajima volcano

©2021. Japan Geoscience Union. All Right Reserved.

[J] Poster | M (Multidisciplinary and Interdisciplinary)：M-IS Intersection

Sun. Jun 6, 2021 5:15 PM - 6:30 PM JST | Sun. Jun 6, 2021 8:15 AM - 9:30 AM UTC | Ch.19_3

[M-IS15] Tsunami deposit: research progress after the 2011 Tohoku-oki earthquake and prospects

convener:Masaki Yamada(Department of Geology, Faculty of Science, Shinshu University), Takashi Ishizawa(International Research Institute of Disaster Science, Tohoku University), Masashi Watanabe(Chuo University), Koichiro Tanigawa(Geological Survey of Japan, National Institute of Advanced Industrial Science and Technology)

The 2011 off the Pacific coast of Tohoku Earthquake and associated tsunami have an influence on the development of tsunami deposit research. After the tsunami, a lot of findings have been reported in various research fields. However, it has been still uncertain how to use the tsunami deposit to estimate its size and source and the risk assessment. As it commemorates the 10th anniversary of the 2011 off the Pacific coast of Tohoku Earthquake, we would like to review research progress over the past decade and share in the vision of future researches. In this session, we welcome research from all aspects of sedimentary records of modern and paleo tsunamis and numerical and experimental modeling studies for risk assessment. We also include research on other event deposits, such as river floodings and storm surges, that they are considered important for identification of tsunami deposits in geological strata.

[MIS15-P01] A study for correlation of mega-tsunami in the Kuril Trench based on the tsunami deposits in the Erimo area, Hokkaido

*RYO NAKANISHI[1], Juichiro Ashi[1,2], Yosuke Miyairi[1], Yusuke Yokoyama[1,3] (1.Atmosphere and Ocean Research Institute, The University of Tokyo, 2.Graduate School of Frontier Science, The University of Tokyo, 3.Department of Earth and Planetary Sciences, Graduate School of Science, The University of Tokyo)

[MIS15-P02] Characteristics of event deposits and their distributions based on a drilling survey in Sekine-hama, the northern part of the Shimokita Peninsula, Aomori Prefecture

*Daisuke Ishimura[1], Masaki Yamada[2], Takashi Ishizawa[3], Kaori Aoki[4], Kai Sato[2] (1.Department of Geography, Tokyo Metropolitan University, 2.Department of Geology, Faculty of Science, Shinshu University, 3.International Research Institute of Disaster Science, Tohoku University, 4. Research Center for Volcanic Hazards and Their Mitigation, Tokyo Metropolitan University)

[MIS15-P03] Tsunami source estimation of paleotsunami deposits formed in the 17th century at Sekinehama, northern Shimokita Peninsula, Aomori Prefecture

*Kai Sato[1], Masaki Yamada[1], Daisuke Ishimura[2], Takashi Ishizawa[3], Toshitaka Baba[4] (1.Depatment of Geology, Faculty of Science, Shiushu University, 2.Department of Geography, Tokyo Metropolitan University , 3.International Research Institute of Disaster Science, Tohoku University, 4.Graduate School of Science and Technology, Tokushima University)

[MIS15-P04] Revised paleotsunami history at Kirikiri, Northeast Japan

*Takashi Ishizawa[1], Yusuke Yokoyama[2], Yosuke Miyairi[2] (1.International Research Institute of Disaster Science, Tohoku University, 2.Atmosphere and Ocean Research Institute, the University of Tokyo)

[MIS15-P05] Distribution and characteristics of the 1983 Nihonkai-chubu earthquake tsunami deposit along the Akita coastal area, Japan

*Takashi Chiba[1], Yuichi Nishimura[2] (1.Faculty of Bioresource Sciences, Akita Prefectural University, 2.Institute of Seismology and Volcanology (ISV), Faculty of Science, Hokkaido University)

[MIS15-P06] Event deposits in a coastal lake at Minami-ise Town, Mie Prefecture during the last 3000 years

*Yumi Shimada[1], Yuki Sawai[1], DAN MATSUMOTO[1], Koichiro Tanigawa[1], Yuichi Namegaya[1], Masanobu Shishikura[1], Kazumi Ito[1], Toru Tamura[1], Shigehiro Fujino[2] (1.Geological Survey of Japan, AIST, 2.Faculty of Life and Environmental Sciences, University of Tsukuba)

[MIS15-P07] Distributions and occurrences of sandy tsunami deposits in caves located along the East Coast of Ishigaki Island, Okinawa Prefecture

*Yoshiro Ishihara[1], Miyu Kitahara[1], Yuuka Okita[1], Ayano Shimabukuro[2], Hajime Naruse[3], Chiaki Katagiri[4], Rintaro Ono[5], Kazuhisa Yoshimura[6] (1. Fukuoka Univ., 2.Yaeyama Museum, 3.Kyoto Univ., 4.Okinawa Prefectural Archaeological Center, 5.National Museum of Ethnology, 6.Kyushu Univ.)

[MIS15-P08] Examining grain-size changes in sediment transport modeling of the 2011 Tohoku-oki tsunami in the Sendai Plain

*Wataru Nakamura[1], Daisuke Sugawara[1] (1.Tohoku University)

[MIS15-P09] Comparison of Observations and Numerical Simulations of Sediment Transport Using the 1707 CE Hoei Tsunami Source Model: Application to Kanigaike Pond in Kochi Prefecture, Japan

*Satoshi Kusumoto[1], Kentaro Imai[1], Narumi Takahashi[2,1], Takane Hori[1], Daisuke Sugawara[3] (1.JAMSTEC, 2.NIED, 3.Tohoku University)

[MIS15-P10] Uncertainty of geological information used in identification of tsunami deposit - Preliminary assessment –

*Takumi Yoshii[1], Takaomi Hamada[1], Yuki Ito[1], Shiro Tanaka[1], Masafumi Matsuyama[1] (1.Central Research Institute of Electric Power Industry)

A study for correlation of mega-tsunami in the Kuril Trench based on the tsunami deposits in the Erimo area, Hokkaido

*RYO NAKANISHI[1], Juichiro Ashi[1,2], Yosuke Miyairi[1], Yusuke Yokoyama[1,3]

1. Atmosphere and Ocean Research Institute, The University of Tokyo, 2. Graduate School of Frontier Science, The University of Tokyo, 3. Department of Earth and Planetary Sciences, Graduate School of Science, The University of Tokyo

In order to clarify the spatial diversity of the rupture mode of giant earthquakes with recurrence intervals of hundreds to thousands of years, it is necessary to obtain information from a geological record such a tsunami deposit, because observational data alone are insufficient. In the southern part of the Kuril Trench, the geological studies reveal the existence of giant earthquakes that cannot be explained by the earthquakes observed (Sawai, 2020). These giant earthquakes have intervals of several hundred years, and the last one is said to have occurred in the 17th century. However, there have been few cases of comparing the ages of sand layers at different sites, and the spatio-temporal distribution of fracture areas over long-time scales has not been clarified. In this study, we focused on the east coast of Erimo, which has not been investigated, and examined the magnitude of the 17th century tsunami and the possibility of contrasting older events. In the Erimo town, 8-10 sand layers were found during the past 4000 years, which were judged to be tsunami deposits based on their supply from the beach sand and anomalous distribution. Numerical simulations showed that the 17th-century tsunami can be explained by the same rupture zone as the 17th-century tsunami widely observed in eastern Hokkaido (Ioki and Tanioka, 2016). The ^{14}C dating results show that the depositional ages of the sand layers in this area are similar to those of the sites facing the Tokachi-oki segment, while some sand layers do not have candidates comparable to those of the sites facing the Nemuro-oki segment. The age of the sand layers in the area west of Erimo Cape also correlated with the age of the sand layers in the southern part of Hidaka, suggesting that the sand layers in the southern part of Hidaka are likely to have originated from the giant earthquake in the Kuril Trench.

Keywords: Tsunami deposits, Kuril Trench, Radiocarbon dating, Hokkaido, Numerical simulation

©2021. Japan Geoscience Union. All Right Reserved.

Characteristics of event deposits and their distributions based on a drilling survey in Sekine-hama, the northern part of the Shimokita Peninsula, Aomori Prefecture

*Daisuke Ishimura[1], Masaki Yamada[2], Takashi Ishizawa[3], Kaori Aoki[4], Kai Sato[2]

1. Department of Geography, Tokyo Metropolitan University, 2. Department of Geology, Faculty of Science, Shinshu University, 3. International Research Institute of Disaster Science, Tohoku University, 4. Research Center for Volcanic Hazards and Their Mitigation, Tokyo Metropolitan University

This study reports the event deposits found at Sekinehama, Aomori Prefecture, which is the northernmost part of the Shimokita Peninsula. Tsunamis associated with earthquakes along the Japan and Kuril trenches and volcanic activities in the 17th-18th century possibly could reach this site. Therefore, tsunami deposit research at this site provides information for the assessment of tsunami hazards in this area and understanding of the mechanism of earthquakes and tsunamis along the subduction zone.

Our study site, Sekinehama, is located between Omazaki and Shiriyazaki, and the late Pleistocene marine terraces and sand dunes were distributed behind the coast. In the 2011 Tohoku-oki earthquake, tsunami runup height of 2 to 6 m was reported (The 2011 Tohoku Earthquake Tsunami Joint Survey (TTJS) Group (http://www.coastal.jp/ttjt/)). The outcrops are exposed along the coastline and its height is ca. 5 m. In 2020, we conducted the coring survey with the Handy-Geoslicer (GS) and obtained nine cores at the lowland in the incised valley of the late Pleistocene marine terrace. In this study, we conducted core descriptions, X-ray CT imaging, grain size analysis, tephra analysis, and radiocarbon dating.

At the outcrops, we found more than 10 sandy event deposits interbedded within the soil and marsh sediments. Additionally, we identified two tephras; one is the Baegdusan-Tomakomai (B-Tm) tephra (AD946; Oppenheimer et al., 2017), another is the Towada-Chuseri (To-Cu) tephra (ca. 6 ka; Mclean et al., 2018; Ishimura and Hiramine, 2020). We identified four event deposits above the B-Tm tephra. One of them after 530-490 calBP (1420-1460 calAD) showed an erosional feature at the base, indicating a large flow speed. Below the B-Tm tephra, we also identified some event deposits with grading and erosive contact at the base.

In the preliminary research, we found one sandy event deposit after 530-490 calBP (1420-1460 calAD) at the lowland in the incised valley of the late Pleistocene marine terrace. From the grain analysis, this sandy deposit has a similar grain size distribution with the modern beach sediments. In the GS cores, drilled at 200-400 m distance from the coast, we traced this sandy layer up to 400 m from the coast. From this drilled survey, we confirmed that this sandy layer was only one event deposit above the B-Tm tephra. The sandy layers above the B-Tm tephra show multiple units in the seaside cores and its thickness decreases toward inland. These characteristics indicate that the sand layer is related to paleo-tsunami events after the 15th century. On the other hand, several event deposits were also identified below the B-Tm tephra and radiocarbon dates revealed that the GS cores cover the recent six thousand years. We will show the grain size analysis and additional radiocarbon dates in the presentation.

This work was supported by the Sasakawa Scientific Research Grant from The Japan Science Society. This study was partially performed under the cooperative research program of the Center for Advanced Marine Core Research, Kochi University (Accept No. 20B052).

©2021. Japan Geoscience Union. All Right Reserved.

Keywords: tsunami deposits, Shimokita Peninsula, B-Tm tephra

©2021. Japan Geoscience Union. All Right Reserved.

Tsunami source estimation of paleotsunami deposits formed in the 17th century at Sekinehama, northern Shimokita Peninsula, Aomori Prefecture

*Kai Sato[1], Masaki Yamada[1], Daisuke Ishimura[2], Takashi Ishizawa[3], Toshitaka Baba[4]

1. Depatment of Geology, Faculty of Science, Shiushu University, 2. Department of Geography, Tokyo Metropolitan University , 3. International Research Institute of Disaster Science, Tohoku University, 4. Graduate School of Science and Technology, Tokushima University

This study reports the source estimation based on tsunami deposits at Sekinehama, Aomori Prefecture, northern Japan. In the 17th century, it is known that two huge tsunamis, 1611 CE Keicho tsunami and 17th century earthquake tsunami, have occurred along Japan and Kuril trenches, but their source areas, especially 1611 CE Keicho tsunami, are not well constrained yet. Besides, it is also uncertain whether two tsunamis were generated by discrete earthquakes or identical one. Their tsunami deposits have been identified along Sanriku coast and Sendai Plain and Tokachi to Nemuro coast along the Pacific coast of Hokkaido, respectively. Since our study area, Sekinehma, northern Shimokita Peninsula, is located between Kuril and Japan trenches, geological surveys in such location will give a significant information to solve the relationship of two huge tsunamis. Previous investigations revealed that there are widely-distributed a sand layer that are probable tsuami deposit showing the depositional age of the 17th century at Sekinehama. In this study, we conducted numerical simulations on tsunamis occurred in the 17th century in order to clarify tsunami source of the paleotsunami deposits at Sekinehama.

We used existing ten fault models which reconstruct the 1611 CE Keicho tsunami occurred along Japan Trench, 1677 CE Enpo-Sanriku and 17th century tsunamis occurred along Kuril Trench, and the tsunami caused by uplift of offshore active fault located on northern Shimokita Peninsula. To examine tsunami influence on Sekinehama, the ratio of computed tsunami inundation to the coastal lowland (<300 m from shoreline) was roughly evaluated near the place where probable tsunami deposits were found. In this study, calculations were performed using JAGRUS with an assumption that the topography in the 17th century is not much different from the present at Sekinehama. It is interpretated from the computed inundation rate at Sekinehama that large influences at the study area were given by three models which have >25 m slip amount along the south part of the Kuril Trench (>Mw 8.8; Ioki and Tanioka, 2016; Okamura and Namegaya, 2011; The Hokkaido Disaster Prevention Council, 2012) and one model which has 80 m slip amount along the north part of the Japan Trench (1611 CE Keicho tsunami model with Mw 9.0; Fukuhara and Tanioka, 2017). This suggests the possibility that the study area is inundated by a tsunami when its source is placed off the Pacific coast of Hokkaido rather than off Sanriku coast.
We then compared the calculated inundation rate for tsunami deposits distributed at coastal lowlands along Iburi coast in Hokkaido and east coast of Aomori Prefecture. These tsunami deposits are thought to be deposited in the 17th century, but their sources are still unknown. According to the computation results, the Kuril–Japan trench interlocking model can only explain the distribution of these tsunami deposits as well as that at Sekinehama. In addition, 1640 CE tsunami caused by Mt. Komagatake collapse should be also taken into consideration as a tsunami source at Sekinehama. However, there is no model restored a detailed process from mountain collapse to tsunami. As the result of preliminary simulation used a simple model by Nakanishi and Okamura (2019), 90% inundation rate and 4.6 m maximum height were calculated at Sekinehama, suggesting that the 1640 CE tsunami is one of the possible sources for the tsunami deposits at Sekinehama.

©2021. Japan Geoscience Union. All Right Reserved.

We inferred the Interlocking earthquake model and 1640 CE tsunami model caused by Mt. Komagatake eruption as the source of tsunami deposits at Sekinehama. For future, we plan to create highly accurate source models by changing fault parameters of mainly these two models to recover tsunami deposit distribution at study area.

This work was partly supported by the Sasakawa Scientific Research Grant from The Japan Science Society.

©2021. Japan Geoscience Union. All Right Reserved.

Revised paleotsunami history at Kirikiri, Northeast Japan

*Takashi Ishizawa[1], Yusuke Yokoyama[2], Yosuke Miyairi[2]

1. International Research Institute of Disaster Science, Tohoku University, 2. Atmosphere and Ocean Research Institute, the University of Tokyo

Tsunami deposits are defined as reworked sediment which is transported by a tsunami. The distribution area of tsunami deposits is often related to the inundation area of the tsunami and thus is useful for the reconstruction of paleotsunami. In general, age correlations of tsunami deposits were performed to identify tsunami deposits that were formed by the same tsunami. However, several problems (e.g., erosion and re-sedimentation by a tsunami, sample selection for ^{14}C dating) make it difficult to accurately estimate the age of tsunami deposit. Herein, we conducted dating of tsunami deposits at Kirikiri, Iwate prefecture where paleotsunami history was not established well. ^{14}C dating was performed by a few sample types at the same stratigraphic horizon. Our results indicated that wood samples showed younger age than the age of overlying sediments. Moreover, sediment from the same stratigraphic horizon with the wood also showed younger age than the age of overlying sediments. The reversion of age might be due to penetration of younger wood and surrounded sediment of the wood might also be affected by the wood. From the results, we revised the ages of paleotsunami deposits and our results were well consistent with the paleotsunami history of the surrounded area. Such detailed re-examination of paleotsunami ages was crucially important for the correlation of widely distributed tsunami deposits.

Keywords: Tsunami deposit, Radiocarbon dating

©2021. Japan Geoscience Union. All Right Reserved.

Distribution and characteristics of the 1983 Nihonkai-chubu earthquake tsunami deposit along the Akita coastal area, Japan

*Takashi Chiba[1], Yuichi Nishimura[2]

1. Faculty of Bioresource Sciences, Akita Prefectural University, 2. Institute of Seismology and Volcanology (ISV), Faculty of Science, Hokkaido University

The Nihonkai-chubu earthquake occurred off the western coast of Noshiro City in Akita Prefecture, northeastern Japan on 26th May 1983. The tsunami due to the earthquake caused widespread damage to the west coastal area of the northeastern Japan, including Akita coastal region, depositing sand and mud transported by the tsunami. We conducted geological surveys from December 2019 to January 2020 within the pine-based coastal protecting forests planted along the coastal region of Akita Prefecture in the period of 1948 to 1970. Sand layers that exhibit inland thinning were observed in the soil at a depth of <10 cm at Happo Town, Noshiro City and Mitane Town, Akita Prefecture. As this sand layer contains well preserved brackish-marine diatoms such as *Fallacia* sp. and *Thalassiosira nanolineata*, it is highly probable that it was transported inland from the coast; a continuity distribution was confirmed from the coast to ~300 m inland only within the coastal protecting forest. According to historical records, we postulate that this sand layer is the result of deposition by the 1983 tsunami, as the area could not have been reached by any means other than the tsunami produced by the Nihonkai-chubu Earthquake. There are few reports of tsunami deposits with specific ages in Japan, so they are an important historical record of past disasters. It has been noted that tsunami deposits lose their sedimentary structures and constituents over time due to changes in weather conditions; therefore, the samples of these deposits can also be used to study the weathering processes of tsunamis deposits.

On the other hand, we also recognized another thin sand layer upper the tsunami deposits. There is a high probability that this sand layer was formed by the strong wind of the Typhoon 9119 reached in 28th September 1991, because no major floods or tsunamis caused damage to our study area have occurred after the 1983 tsunami event.

In this presentation, we report the distribution and characteristics of deposits from the tsunami generated by the 1983 Nihonkai-chubu earthquake and the eolian sand formed by the Typhoon 9119 recognized in coastal protecting forests planted along the Happo Town, Noshiro City and Mitane Town.

Keywords: 1983 Nihonkai-chubu earthquake, Tsunami deposit, Microfossils

©2021. Japan Geoscience Union. All Right Reserved.

Event deposits in a coastal lake at Minami-ise Town, Mie Prefecture during the last 3000 years

*Yumi Shimada[1], Yuki Sawai[1], DAN MATSUMOTO[1], Koichiro Tanigawa[1], Yuichi Namegaya[1], Masanobu Shishikura[1], Kazumi Ito[1], Toru Tamura[1], Shigehiro Fujino[2]

1. Geological Survey of Japan, AIST, 2. Faculty of Life and Environmental Sciences, University of Tsukuba

Sediment cores taken at Kogare-ike, a coastal lake in Minami-ise town facing the Nankai Trough, contain the sixteen event deposits likely representing tsunamis or storm surges. Nine of the event deposits were invisible but identified by computed tomography (CT) images. Depositional ages of the event deposits were estimated by combination of ^{137}Cs concentration and radiocarbon ages from pollens and plant macrofossils. An age-depth model was then established from these radiometric analyses was constructed using Bchron (Haslett & Parnell, 2008). This model revealed that the event deposits in the study site had settled during the last 3000 years. In order to detect environmental changes during the period, fossil diatom assemblages from the core taken at the center of the lake were identified and counted. Until the deposition of the youngest event deposit (E1), diatom assemblages were dominated by freshwater species such as *Tabellaria fenestrata* and *Staurosira* spp. After the deposition of the E1, however, assemblages were dominated by brackish species such as *Amphora coffeiformis*, *Bacillaria paxillifer*, *Navicula gregaria*.

There are some causes of event deposits in coastal lakes: tsunamis, storm surges and floods. However, the event deposits are likely to represent seawater inundation associated with tsunamis and/or storm surges, not river floods, because Kogare-ike has no significant fluvial input. The youngest event deposit (E1) exists above the lowest horizon occurrence of ^{137}Cs. Because the first occurrence of the cesium shows a timeline of 1940's, E1is likely to be correlated by the recent documents with the 1959 Isewan typhoon. The change in diatom assemblages before and after the E1 suggested breaching of the barrier generated with the storm surge that enabled more seawater to flow into the study site. As for the other event deposits at Kogare-ike, some of them may represent tsunami because there are the written documents and the tsunami monuments at Minami-ise town inferring the repetitive inundation by tsunamis associated with the earthquakes along the Nankai Trough (e.g. Nakata, 1991; Namegaya & Tsuji, 2005).

Keywords: event deposits, tsunami, storm, lacustrine sediments, fossil diatom assemblages, Nankai Trough

©2021. Japan Geoscience Union. All Right Reserved.

Distributions and occurrences of sandy tsunami deposits in caves located along the East Coast of Ishigaki Island, Okinawa Prefecture

*Yoshiro Ishihara[1], Miyu Kitahara[1], Yuuka Okita[1], Ayano Shimabukuro[2], Hajime Naruse[3], Chiaki Katagiri[4], Rintaro Ono[5], Kazuhisa Yoshimura[6]

1. Fukuoka Univ., 2. Yaeyama Museum, 3. Kyoto Univ., 4. Okinawa Prefectural Archaeological Center, 5. National Museum of Ethnology, 6. Kyushu Univ.

Many "tsunami-ishi" boulders are distributed along the east coast and coastal lowlands of Ishigaki Island, Yaeyama Islands, Okinawa Prefecture. Detailed investigations have revealed that the boulders were moved and settled by several tsunami events of different ages. The trench excavated near the coast also revealed several sandy tsunami deposits containing marine fossils. These boulders and deposits suggest that tsunamis originating from the Ryukyu Trench repeatedly struck the east coast of Ishigaki Island.
Along the coasts of the Yaeyama Islands, many limestone caves are located in marine terraces composed of limestone of the Ryukyu Group. These limestone caves are isolated from weathering of the surface environment and maintain a stable environment, which results in good preservation of sediments and fossils. As a result, these caves often include artifact remains and human bones and are sometimes recognized as archaeological sites. The speleothems found in the caves may also contain records of events such as tsunamis. In the cave deposits of the Shirahosaonetabaru Cave Site, a historic site located within the New Ishigaki Airport, a few tens of centimeters thick sandy gravel bed containing many corals and other marine fossils is presumed to be tsunami-derived deposits. This sandy graved bed was deposited about 1,800 years ago, and the cave entrance that in-flowed this sediment is estimated to have existed at an elevation of about 40 m. Therefore, it is considered evidence of a large-scale tsunami, comparable to the "Okinawa Sakishima Tsunami".
We investigate the cave sediments along the east coast of Ishigaki Island for artifacts and fossils, and tsunami event deposits in the cave sediments. In this presentation, we will show the distribution of the tsunami deposits in the caves. This work was supported by JSPS KAKENHI Grant Number JP20K04138.

Keywords: Ishigaki Island, Tsunami deposit, Cave, Archaeological site, speleothem

©2021. Japan Geoscience Union. All Right Reserved.

Examining grain-size changes in sediment transport modeling of the 2011 Tohoku-oki tsunami in the Sendai Plain

*Wataru Nakamura[1], Daisuke Sugawara[1]

1. Tohoku University

Information of past tsunami events inferred from tsunami deposits is useful in preparing for future tsunami disasters. Existing tsunami sediment transport modeling is intended to correlate characteristics of tsunami deposits with tsunami source from wave heights and source parameters. In such simulations, either single or multiple grain size class is assumed for particle composition. Although some studies conducted sediment transport modeling considering multiple grain-size classes, majorities have been performed with the single grain-size assumption. However, the single grain-size simulations cannot resolve lateral and horizontal variations of grain-size composition. Major sedimentological features of sandy tsunami deposits, such as landward and upward fining, cannot be used for comparison of field data and numerical simulations. In this study, we examined and compared the sediment transport simulations of the 2011 off the Pacific coast of Tohoku Earthquake Tsunami, considering single and multiple grain-size compositions. The study area is located in the neighborhood of the right bank of the Nanakita River in the Sendai Plain. A detailed field survey for the tsunami deposit was carried out previously (Abe et al., 2012) along a shore-normal transect (transect B). The Delft3D, which has been developed by Deltales, was used for the modeling. It includes cross-sectional simulations along transect B (1-D model) and two-dimensional horizontal simulations (2-D model) covering transect B. The fault parameters proposed by Imamura et al. (2012) was used to generate the initial water level of the 2-D tsunami simulations. Time series of the water level at 2 km offshore of transect B, generated by the 2-D simulation, was used for the input of the 1-D simulations. We assumed an initial thickness of 5 m for movable bed, which corresponds to the entire seafloor and the land areas from shoreline to the Teizan canal; meanwhile the areas further inland were assumed to be fixed bed (initial sediment thickness of zero). Four grain-size classes (sediment 1 to 4) were used to synthesize the grain-size distribution of the movable bed, based on the grain size data of the tsunami deposits (e.g., Szczuciński et al., 2012). The Manning’ s roughness coefficient map constructed by Sugawara et al. (2014) was used for the computation of the tsunami-induced flow.
Modeling results showed that inundation distance, flow depth and distribution of the tsunami deposit were generally consistent with those measured by Abe et al. (2012), although there were some discrepancy in the flow depth near the shoreline. The simulations with single grain size class (mode diameter) and the multiple grain-size classes were almost similar. This is probably because of the assumption of the normal distribution for the grain-size composition and higher percentage of the mode diameter. Comparison of the 2-D and 1-D simulations showed a slight difference, due to effects from topography that cannot be considered in the 1-D simulations.

Keywords: tsunami numerical simulation, multiple grain size, the 2011 Tohoku-oki tsunami

©2021. Japan Geoscience Union. All Right Reserved.

Comparison of Observations and Numerical Simulations of Sediment Transport Using the 1707 CE Hoei Tsunami Source Model: Application to Kanigaike Pond in Kochi Prefecture, Japan

*Satoshi Kusumoto[1], Kentaro Imai[1], Narumi Takahashi[2,1], Takane Hori[1], Daisuke Sugawara[3]

1. JAMSTEC, 2. NIED, 3. Tohoku University

The Nankai Trough subduction zone have repeatedly produced large earthquakes with tsunamis (e.g., Ando, 1975; Ishibashi, 2004). The 1707 CE Hoei Nankai earthquake and tsunami caused serious damages to the southwestern coast of Japan. Its damages have been described many historical documents and its tsunami deposits have been found from the coastal lowlands from Kyusyu to Tokai (e.g., Cabinet Office, 2011; Kitamura and Kobayashi, 2014). Therefore, it is considered that the 1707 CE Hoei earthquake was a M9-class event on the Nankai Trough subduction zone. The source models have been proposed based on its tsunami heights and its tsunami deposits (e.g., Furumura et al., 2011; Sugawara et al., 2019). However, they are still not enough. In this study, we examine the sedimentary process of the tsunami deposits from the comparison of observation and numerical simulation of tsunami sediment transport using the revised 1707 CE Hoei tsunami source model (Furumura et al., 2011).
Study site is a coastal pond (Kanigaike pond) in Kochi Prefecture, Japan. The sand movements were computed using a coupled numerical model of tsunami inundation and sediment transport developed by Takahashi et al. (1999). The saturation concentration of suspended sediments.was also adopted (e.g., Sugawara et al., 2014; Yamashita et al., 2016). The mean grain size of the sand was set to be 0.267 mm and grain-size dependent parameters (i.e., the coefficients of bedload rate and exchange rate, settling velocity, and critical shear stress) were provided by Takahashi et al. (2011).
Our results showed a sand deposition of ~1 m near the shoreline. However, few sand deposition took place in the pond. According to the tsunami deposit survey performed by Kochi University and Okamura and Matsuura (2012), the 1707 CE Hoei tsunami deposits were ~50 cm in thickness. Our results did not match the observations, suggesting the need of reevaluation with different slip amount and width of the subfaults.
We concluded that the 1707 CE Hoei tsunami source model should be reexamined based on geological evidences, although there are several uncertainties in tsunami sediment transport modeling (Jaffe et al., 2016; i.e., incompleteness of the theory, topographic and bathymetric changes, parameter setting). Further studies would lead to further understanding of the Nankai Trough megathrust earthquakes.

Keywords: 1707 CE Hoei earthquake, Tsunami deposit, Tsunami sediment transport simulation

©2021. Japan Geoscience Union. All Right Reserved.

Uncertainty of geological information used in identification of tsunami deposit - Preliminary assessment –

*Takumi Yoshii[1], Takaomi Hamada[1], Yuki Ito[1], Shiro Tanaka[1], Masafumi Matsuyama[1]

1. Central Research Institute of Electric Power Industry

Tsunami deposit can provide important information about the local history of tsunamis. The geological record of tsunamis has been used to improve hazard maps in coastal cities and to develop the countermeasures against tsunamis in important facilities, such as nuclear power plants. However, the identification of tsunami deposit has uncertainties inherent in geological analysis. To consider the uncertainties in the identification, the authors presented probabilistic identification method for deposit made by natural hazards including tsunami [1]. In this method, deposit with little geological information on its formation is attributed to potential several natural hazards. To utilize this identification method, we must assess the uncertainties of geological information obtained from deposit.

In this study, we assessed the uncertainties of the information obtained from diatom analysis, which is widely used to identify tsunami deposit. We analyzed tsunami deposits formed by the 2011 Tohoku-oki earthquake tsunami [2]. The result showed that the 31% of the tsunami deposit has no marine diatom and more than half of tsunami deposit has marine to brackish diatom (>10% in the total diatom assemblage). The only 8% of the tsunami deposit has no marine to brackish diatom. These results indicate that the fraction of marine to blackish diatom can be the useful proxy to infer the source of deposit. Although choice of better proxy helps reducing uncertainties in geological information inferred from the deposit, we still must take account of the persisting uncertainty on geological information.

[1] Yoshii, T., Tanaka, S., Ito, Y., Hamada, T., Matsuyama, M., Identification method of event deposits caused by natural hazards, JpGU meeting 2019, 2019.
[2] Yoshii, T., Hamada, T., Sasaki, T., Matsuyama, M., Tanaka, S., Ito, Y., Watanabe, M., Okuzawa, K., Sedimentological features of tsunami deposit caused by the 2011 Tohoku-oki earthquake tsunami, JpGU meeting 2014, 2014.

Keywords: Tsunami deposit, Identification method, Probabilistic assessment

©2021. Japan Geoscience Union. All Right Reserved.

[J] Poster | M (Multidisciplinary and Interdisciplinary)：M-IS Intersection

Sun. Jun 6, 2021 5:15 PM - 6:30 PM JST | Sun. Jun 6, 2021 8:15 AM - 9:30 AM UTC | Ch.22_2

[M-IS22] Geopark

convener:Takayuki Arima(Yokohama City University), Keiichi Tadokoro(Research Center for Seismology, Volcanology and Earthquake and Volcano Research Center, Nagoya University), Marekazu OHNO(Unzen Volcanic Area Geopark Promotion Office), Takayuki Ogata(Graduate School of Engineering and Science, University of the Ryukyus)

This session targets interdisciplinary and multidisciplinary discussion on geopark, involving geoheritage, geodiversity, geoconservation, geotourism, sustainable development, governance, risk management, science communication and geoscientific education. These topics contribute to scientific and attractive activities in geoparks.

[MIS22-P01] Scientific Roles of the JpGU Session "Geopark"

*Takayuki Ogata[1] (1.Graduate School of Engineering and Science, University of the Ryukyus)

[MIS22-P02] Discussion

Scientific Roles of the JpGU Session "Geopark"

*Takayuki Ogata[1]

1. Graduate School of Engineering and Science, University of the Ryukyus

The session of "Geopark" has been held in JpGU meeting for 10 years. The author reviews 185 presentations from 2012 to 2020, and discusses scientific roles of this session and its future. The co-sponsored session with several society members of JpGU has provided as a collaborative session which targets interdisciplinary and multidisciplinary discussion on geopark, involving geoheritage, geodiversity, geoconservation, geotourism, sustainable development, governance, risk management, science communication and geoscientific education. Studies presented in this session seem to be classified into methodology on education, cases of outreach and geotourism, and geoscientific studies in geosites. The author especially expects field observation on regional geography and historical geology in many geoparks.

Keywords: geopark, geoscience, field observation

©2021. Japan Geoscience Union. All Right Reserved.

[J] Poster | M (Multidisciplinary and Interdisciplinary) | M-IS Intersection

[M-IS22] Geopark

convener:Takayuki Arima(Yokohama City University), Keiichi Tadokoro(Research Center for Seismology, Volcanology and Earthquake and Volcano Research Center, Nagoya University), Marekazu OHNO(Unzen Volcanic Area Geopark Promotion Office), Takayuki Ogata(Graduate School of Engineering and Science, University of the Ryukyus)

Sun. Jun 6, 2021 5:15 PM - 6:30 PM Ch.22

This session targets interdisciplinary and multidisciplinary discussion on geopark, involving geoheritage, geodiversity, geoconservation, geotourism, sustainable development, governance, risk management, science communication and geoscientific education. These topics contribute to scientific and attractive activities in geoparks.

5:15 PM - 6:30 PM

[MIS22-P02]Discussion

©Japan Geoscience Union

[J] Poster | M (Multidisciplinary and Interdisciplinary)：M-IS Intersection

Sun. Jun 6, 2021 5:15 PM - 6:30 PM JST | Sun. Jun 6, 2021 8:15 AM - 9:30 AM UTC | Ch.18_2

[M-IS24] Geophysical fluid dynamics-Transfield approach to geoscience

convener:Keita Iga(Atmosphere and Ocean Research Institute, The University of Tokyo), Shigeo Yoshida(Department of Earth and Planetary Sciences, Faculty of Sciences, Kyushu University), Takatoshi Yanagisawa(Research Institute for Marine Geodynamics, Japan Agency for Marine-Earth Science and Technology), Hidenori AIKI(Nagoya University)

This session on geophysical fluid dynamics is open to discussions and researches on fluid phenomena in whatever fields of earth and planetary sciences, e.g., motions in the earth and planetary interior, oceans, atmospheres, volcanoes, and the ionosphere, conducted with whatever methods. Talks intending to stimulate exchange of ideas among multiple fields of researches or those identifying concepts that are commonly applicable to wide range of geophysical fluids are especially welcome.

[MIS24-P01] Two-dimensional ideal MHD waves and the continuous Alfvén spectrum on a rotating sphere with a background toroidal magnetic field

*Ryosuke Nakashima[1], Shigeo Yoshida[2] (1.Faculty of Science, Kyushu University, 2.Department of Earth and Planetary Sciences, Faculty of Science, Kyushu University)

[MIS24-P02] Development of sea surface wave breaking observation system using industrial millimeter radar and optical particle size counter

*Hidenori AIKI[1], Fumiyoshi Kondo[2], Haruya Minda[1] (1.Nagoya University, 2.Japan Coast Guard Academy)

[MIS24-P03] Axisymmetric flows and non-axisymmetric phenomena in a cylindrical tank with a rotating bottom

*Keita Iga[1] (1.Atmosphere and Ocean Research Institute, The University of Tokyo)

[MIS24-P04] We examined **Origin of Great Red Spot of Jupiter, Deep Ocean Floor, Pacific Rim Arcuate Archipelago, Origin of Gomagnetic Reversal, and Origin of Asteroid Belt.**

*Akira Taneko[1] (1.SEED SCIENCE Lab.)

Two-dimensional ideal MHD waves and the continuous Alfvén spectrum on a rotating sphere with a background toroidal magnetic field

*Ryosuke Nakashima[1], Shigeo Yoshida[2]

1. Faculty of Science, Kyushu University, 2. Department of Earth and Planetary Sciences, Faculty of Science, Kyushu University

Two-dimensional magnetohydrodynamic (MHD) linear waves on a rotating sphere are investigated for perfectly conducting fluids permeated by an azimuthal magnetic field whose magnitude may depend on the colatitude θ. If the toroidal background field is expressed as $B_{0\Phi} = B_0 \sin\theta$, where B_0 is constant and Φ is the azimuth, two types of waves exist: westward-propagating fast magnetic Rossby waves and eastward-propagating slow counterparts. Except for this profile of the imposed field, the wave equation of this system can possess regular singular points at which the zonal phase velocity of an eigenmode is equal to a local Alfvén wave velocity devided by $\sin\theta$. Since the positions of critical latitudes depend on the azimuthal phase speed of a chosen eigenmode, this means that continuous spectra appear due to Alfvén resonance in spite of the closed region such as a sphere surface. Similar situations include the linear problem in the inviscid parallel shear flow, which can yield critical layers where the phase velocity coincides with a local mean flow velocity (e.g. Case, 1960).

We solved the eigenvalue problem for $B_{0\Phi} = B_0 \sin\theta\cos\theta$ numerically and confirmed the existence of the Alfvén continuum. Since the eigenfrequencies of continuous modes areally spread on the dispersion diagram, there is a possibility that the branches of discrete eigenmodes are buried under the continuous spectrum. We therefore scanned the buried branches by calculating the energy partition of each eigenmodes. Remarkably, discrete branches of slow magnetic Rossby waves were not found in the case of this main field configuration. Thus, the choice of the background field profile might have an influence of the appearance of these slow waves in the ideal MHD case.

Numerical study gives the structure of continuous eigenmodes and shows that these conform to the superposition of the two linearly independent solutions resulted from the Frobenius technique around a critical latitude and to their theoretical connection conditions. When the magnitude of the applied field is small, these eigenfunctions tend to be evanescent on the north side of the critical latitude in the north hemisphere for westward-propagating continuous modes and on the south side of the critical latitude in the north hemisphere for eastward-propagating continuous modes, although there is an exception. This feature is consistent with the WKBJ approximation in slowly varying magnetic shear (Acheson, 1972; Eltayeb & McKenzie, 1977), which suggests the critical level absorption of MHD waves with high wavenumber in rotating fluids. Although Acheson (1972) proposed the "valve" effect, which means that MHD waves can penetrate through the critical layer in limited circumstances, our problem is out of range of its condition, that is, horizontal angular velocity Ω_θ vanishes.

Keywords: MHD waves, critical latitude, magnetic shear, continuous Alfvén spectrum, rotating fluid

©2021. Japan Geoscience Union. All Right Reserved.

Development of sea surface wave breaking observation system using industrial millimeter radar and optical particle size counter

*Hidenori AIKI[1], Fumiyoshi Kondo[2], Haruya Minda[1]

1. Nagoya University, 2. Japan Coast Guard Academy

When a typhoon passes over the sea surface, strong winds cause waves to develop and countless whitecap waves are generated. Large and small droplets are simultaneously generated in the atmospheric boundary layer by the whitecap breaking waves. Large droplets play an important role in the transport of momentum, heat, and CO2 between the atmosphere and the ocean due to their large mass. The small droplets become oceanic aerosols that form cloud condensation nuclei a few kilometers above the surface and contribute to the radiation budget of the atmosphere. Conventional observation of whitecap breaking waves using a CCD camera was affected by fog and sunlight and was not suitable for continuous observation during stormy weather or day and night. In this study, we develop a system to measure the spatio-temporal structure of whitecap breaking waves at sea using millimeter-wave radar electronic circuit boards for automobile parts. Since the resolution of millimeter-wave radar is a few millimeters to a few centimeters, it is ideal for capturing the dynamics of individual whitecap waves and sea spray layer. Since the temporal variation of the particle size distribution is also important information, the optical particle size counter for marine observation developed by the authors is used in combination with the radar.

©2021. Japan Geoscience Union. All Right Reserved.

Axisymmetric flows and non-axisymmetric phenomena in a cylindrical tank with a rotating bottom

*Keita Iga[1]

1. Atmosphere and Ocean Research Institute, The University of Tokyo

In the terrestrial and planetary atmospheres, even under axisymmetric enviroenments, the symmetry is often broken to cause various non-axisymmetric phenomena. Such non-axisymmetric phenomena can be realized in a simple laboratory experiment in a cylindrical tank which is filled with water and whose bottom rotates rapidly.
These phenomena have been investigated by many researchers, mainly by laboratory experiments and by theoretical analyses. On the other hand, the same problem has been investigated using numerical calculations. However, due to the restirictions of the computational resources, the parameter range of the calculated situation has been apart from those used in the laboratory experiments, where the boundary layers play important roles in the interesting phenomena.
Recently, the numerical calculations with closer parameters are performed, and in some cases, we can discuss the boundary layers formed in the numerical calculations. We compare the structures of the numerical results and those obtaied in labotaroty experiments and theoretically.

Keywords: rotating flow, laboratory experiments, axisymmetry breaking, boundary layers

©2021. Japan Geoscience Union. All Right Reserved.

We examined Origin of Great Red Spot of Jupiter, Deep Ocean Floor, Pacific Rim Arcuate Archipelago, Origin of Gomagnetic Reversal, and Origin of Asteroid Belt.

*Akira Taneko[1]

1. SEED SCIENCE Lab.

Hypothesis can be tested by Abduction using Results (Features) of Evolution. More Results (Characteristics) of multiple Evolutions can be explained consistently with One Hypothesis, More True it becomes. First was a hypothesis explaining Origin of Moon. It also explains Origin of Earth's Plate Tectonics and Driving Forces in other Sessions.
In this time, we explained each the detailed reasons for Origin of Jupiter's Great Red Spot, Origin of Deep Ocean Floor, and Origin of Asteroid Belt using the multi-impact hypothesis. I believe that if we can explain Everything with Cosmic Law (Universal Gravitational Force) of Geophysical Fluid Dynamics and explain Three Themes of Origin of planets, Earth, and Solar System with One Hypothesis, we can attract Audience of SCIENTIST beyond Interdisciplinary.

1.Origin of **Jupiter's Great Red Spot**
From circumstantial evidence, the Shoemaker-Ninth Comet Jupiter collision occurred in 1993. Collision traces formed multiple small white spots and disappeared over time. In Previous Encounter, it collided with Comet Train in a Row in Same Orbit. A Collision Flash was also observed after being Photographed. In Malti-Impact hypothesis, assuming a Martian-sized Protoplanet CERRA at Ceres Position, CERRA Orbit was flattened into an Elliptical Orbit by Perturbation of Giant Mass Jupiter, which accumulated behind Outer Orbit.

In Multi-Impact Hypothesis, assuming a Mars-sized protoplanet CERRA at Ceres Position, CERRA Orbit flattened into an Elliptical Orbit due to Perturbation of Giant Mass Jupiter that accumulated behind Outer Orbit. At Point where Gravitational pulls of Sun and Jupiter are balanced, CERRA ruptures Tide and Orbits in a Row as Train Mantle rupture Fragments.
At Position where it intersects Earth's Orbit, it collides intermittently at Each Meeting Period. Inevitable Collision Mechanism of Mantle Impactor is completed. If it does not rupture, it is an Inevitable Collision of Giant Impact Mars. Here, Collision Velocity and Angle can be calculated from Theory, and their values are Same. **V=12.43km /s** and **36.45 ˚**.
At Time of this CERRA Rupture, Mantle Rupture that collided with Jupiter is a Fragment Larger than a Comet, pierces Liquid Core and Solid Core of Jupiter, and rotates with Jupiter Core. Naturally, **Birth of** Great Red Spot **Soliton**. If Material is different from that of Jupiter Core and Thermal Conductivity is low, Debris will become an Enlarged Vortex and will have a Long Life if it is not buried.

2.Origin of **Earth's Deep Ocean Floor**
Rupture of CERRA in Malti-Impact Hypothesis caused Intermittent Collisions of Train Mantle Fragments with Earth, resulting in Multiple Earth Mantle Ejections and Detachments. Largest of these is Lunar Ejection, a Defect in Pacific Ocean, Indian Ocean, Antarctic Ocean, and Arctic Ocean.

Theory that Crust Breaks due to thermal stress is Nonsense. There are No Planets in Solar System that are broken like Turtle Shell. There is No Mechanism to heat it even though it has Cooled Down. Pacific Ocean

©2021. Japan Geoscience Union. All Right Reserved.

is in more than Double Collision. Crust does not crack under Internal Forces such as Mantle Convection. Even with Pressure, it just spouts from One Point and does not last.

Earth's Mantle Cracks due to Impact Force from Outside and Melts when Pressure drops. Mantle is classified into Lithosphere (Plate), Asthenosphere (Rock Basin), partially melted and flowing, and Mesosphere (Lower Mantle Solid). In other words, when Crust is cracked and divided, a Layer called a Plate Easily moves on Fluidized Bed called Asthenosphere. Crustal Defects are balanced and interconnected at an Average Depth of 4 km by Isostasy, occupying **70%** of Earth's Surface.

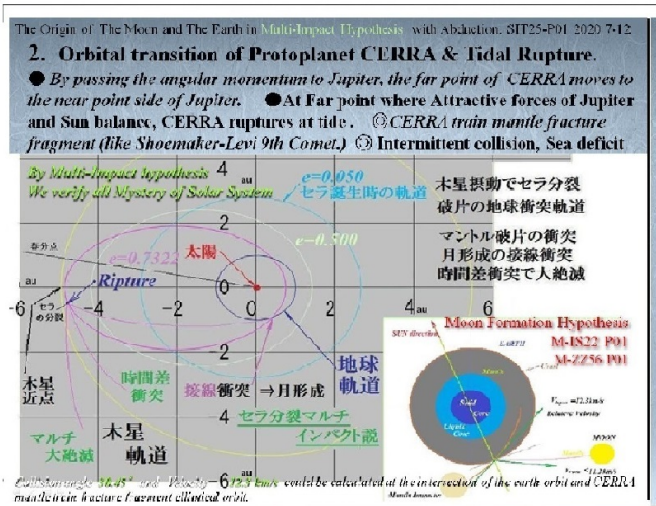
3.**Pacific Rim Arc Archipelago and Geomagnetic Reversal**
CERRA Fragment caused Lunar Ejection and Pacific mantle defect due to Earth's Collision. Isostasy uplifted Seafloor. Surrounding Mantle is dented to form an Ocean Basin, forming Pacific Rim Arcuate Archipelago. Liquid core was also Eccentric, and Van Allen Belt was also Eccentric. Rotation of Solid Core and Mantle deviated, Direction of Flow of Liquid Core was reversed, and Magnetic Poles were replaced.

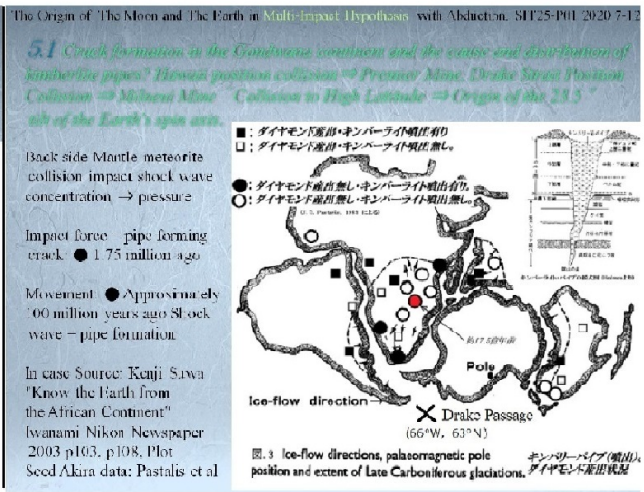
4.Origin of **Asteroid Belt**
Due to Rupture of CERRA in Malti-Impact Hypothesis, Mantle fragments scattered in all directions other than Train Mantle shards formed an Asteroid Belt and orbited Sun. Objects that collided and accumulated with each other became **Mantle-only Asteroids** (Itokawa and Ryugu) that differentiated as **Love Pile Objects**. **Most of Core + Mantle Fragments** became **Mercury (Core rich)** due to Decrease in Peripheral Speed due to Law of Energy Equipartition.

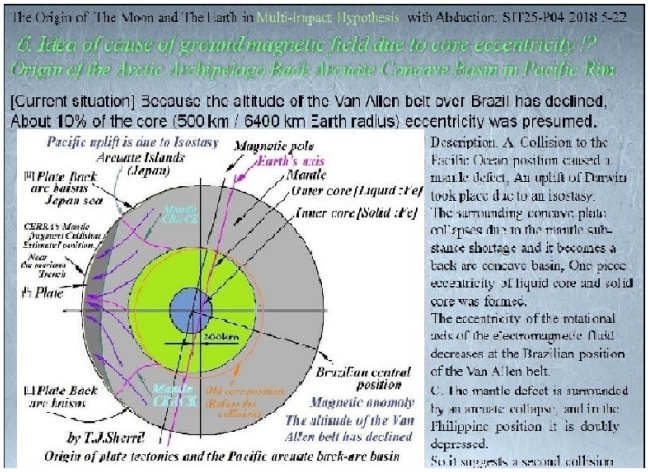
Evolution include fluid to gas, solid to collisional melting, tidal bursting, melt scattering and accumulation, etc.

Keywords: Multi-impact hypothesis, Abduction using Evolutionary Results , Origin of Jupiter's Great Red Spot , Origin of Earth's Deep Ocean Floor, Origin of Asteroid Belt, Origin of Asteroid, Origin of Mercury (Core Rich) , Titius-Bode's Law, Feeding Zone

©2021. Japan Geoscience Union. All Right Reserved.









©2021. Japan Geoscience Union. All Right Reserved.

[J] Poster | M (Multidisciplinary and Interdisciplinary)：M-IS Intersection

Sun. Jun 6, 2021 5:15 PM - 6:30 PM JST | Sun. Jun 6, 2021 8:15 AM - 9:30 AM UTC | Ch.18_3

[M-IS25] Atmospheric electricity: Electrical phenomena associated with extreme weather

convener:Yasuhide Hobara(Graduate School of Information and Engineering Department of Communication Engineering and Informatics, The University of Electro-Communications), Daohong Wang(Gifu University)

In recent years, extreme weather events have occurred frequently not only in Japan but also in other countries around the world. In particular, last year's typhoons 15 and 19 caused tremendous damage in Japan. This year's Atmospheric Electricity session will focus on observational and theoretical studies of atmospheric electrical phenomena associated with extreme weather.
This session will consist of invited presentations introducing above-mentioned fields by leading experts, and contributed presentations on the latest observational and theoretical research results in these fields. For example, we welcome lightning activity associated with many of extreme weather events such as typhoons, heavy rains, wind gusts, and their effects on the upper atmosphere/ionosphere. Besides, we certainly welcome papers regarding all topics on atmospheric electricity including lightning physics, lightning observation technology, electrical effects of thunderstorms, mesospheric transient luminous events (TLEs), lightning-related high-energy phenomena, global electric circuit, atmospheric ion, aerosol, fair-weather electricity, lightning protection, terrestrial electromagnetic noise environment (e.g. wave propagation in the magnetosphere and ionosphere).

[MIS25-P01] X-band radar and disdrometer observations of winter thunderclouds emitting gamma rays

*Yuuki Wada[1], Teruaki Enoto[1], Mamoru Kubo[2], Kazuhiro Nakazawa[3], Taro Shinoda[3], Daisuke Yonetoku[2], Tatsuya Sawano[2], Takayuki Yuasa, Tomoo Ushio[4], Yousuke Sato[5], Gabriel Sousa Diniz[1], Harufumi Tsuchiya[6] (1.RIKEN, 2.Kanazawa University, 3.Nagoya University, 4.Osaka University, 5.Hokkaido University, 6.JAEA)

[MIS25-P02] Observation of thundercloud gamma-rays in FY2020 with the GOOSE detector aiming at altitude measurements

*Yuuna Tsuji[1], Kazuhiro Nakazawa[1], Shohei Hisadomi[1], Yusaku Ikami[1], Daiki Odani[1], Teruaki Enoto[2], Yuuki Wada[2], Takayuki Yuasa, Harufumi Tsuchiya[3], Taro Shinoda[4], Keigo Ookuma[1], Gabriel Diniz[2] (1.Nagoya University, 2.RIKEN, 3.JAEA, 4.ISEE. Nagoya Univ.)

[MIS25-P03] Hydrometeor distribution in a thundercloud related to a gamma-ray emission event

*Takemoto Kiyomichi[1], Taro Shinoda[1], Masaya Kato[1], Shohei Hisadomi[2], Yuuna Tsuji[2], Kazuhiro Nakazawa[2], Yuuki Wada[3], Teruaki Enoto[3] (1.Institute for Space-Earth Environmental Research, Nagoya University, 2.Department of Physics, Nagoya University, 3.Institute of Physical and Chemical Research)

[MIS25-P04] A Study of 3D Precipitation Core Tracking Method Using Multi-Parameter Phased Array Weather Radar

*Keitaro Asai[1], Hiroshi Kikuchi[1], Yasuhide Hobara[1], Tomoo Ushio[2] (1.The University of Electro Communications, 2.Osaka University)

[MIS25-P05] Special negative lightning strokes in winter with extremely short preceding discharges

*Ting Wu[1], Daohong Wang [1], Nobuyuki Takagi[1] (1.Gifu University)

[MIS25-P06] Simultaneous Observations of a Winter Lightning Flash in Japan

*Haitao Huang[1], Daohong Wang[1], Ting Wu[1], Nobuyuki Takagi[1] (1.Gifu University)

[MIS25-P07] Spatio-temporal characteristics of lightning energy in Southeast Asia deduced from ELF observations

*Shunsuke Akama[1], Shu Hirai[1], Yasuhide Hobara[1], Hiroshi Kikuchi[1], Amir Izzani Mohamed[2], Chandima Gomes[3], Kazuo Shiokawa[4], Michael Stock[5] (1.The University of Electro-Communications, 2.University of Malaysia, Pahang, 3.University of the Witwatersrand, Johannesburg, 4.Institute for Space–Earth Environmental Research, 5.Earth Networks)

[MIS25-P08] Sprites observed from the summit of Mt. Fuji and their parent thunderstorm

*Suzuki Tomoyuki[1], Masashi Kamogawa[1], Syugo Hayashi[2] (1.University of Shizuoka, 2.Meteorological Research Institute)

[MIS25-P09] Coupling process of large-scale atmospheric disturbances to the ionosphere through typhoon

*Shu Hirai[1], Yasuhide Hobara[1], Hiroshi Kikuchi[1], Michael Stock[2] (1.The University of Electro-Communications, 2.Earth Networks)

X-band radar and disdrometer observations of winter thunderclouds emitting gamma rays

*Yuuki Wada[1], Teruaki Enoto[1], Mamoru Kubo[2], Kazuhiro Nakazawa[3], Taro Shinoda[3], Daisuke Yonetoku[2], Tatsuya Sawano[2], Takayuki Yuasa, Tomoo Ushio[4], Yousuke Sato[5], Gabriel Sousa Diniz[1], Harufumi Tsuchiya[6]

1. RIKEN, 2. Kanazawa University, 3. Nagoya University, 4. Osaka University, 5. Hokkaido University, 6. JAEA

Strong electric fields in thunderclouds accelerate electrons to relativistic energy even in a dense atmosphere, and bremsstrahlung gamma rays are observed as gamma-ray glows by radiation monitors on aircraft and on the ground. Since gamma rays are absorbed by the atmosphere, it is difficult to observe gamma rays emitted from summer thunderclouds at sea-level, but gamma-ray glows during winter thunderstorms in the Hokuriku region can be observed on the ground because they develop at low altitudes. We are conducting the GROWTH experiments in Ishikawa and Niigata prefectures to observe high-energy atmospheric phenomena such as gamma-ray glows. During the three seasons from 2016 to 2018, a radiation monitor installed at Kanazawa University registered a total of 11 gamma-ray glows. In each case, it was confirmed by the X-band radar operated by the Ministry of Land, Infrastructure, Transport and Tourism that a thundercloud with strong echoes exceeding 35 dBZ developed at an altitude of 2 km or more (-10 degrees or less) passed over the detector. Also a disdrometer installed at the site detected graupel precipitation during the gamma-ray glows. Therefore, it is considered that the developed thundercloud accompanied by hail contributes to the occurrence of gamma-ray glows.

Keywords: gamma rays, winter thunderstorm, high energy atmospheric physics

©2021. Japan Geoscience Union. All Right Reserved.

Observation of thundercloud gamma-rays in FY2020 with the GOOSE detector aiming at altitude measurements

*Yuuna Tsuji[1], Kazuhiro Nakazawa[1], Shohei Hisadomi[1], Yusaku Ikami[1], Daiki Odani[1], Teruaki Enoto[2], Yuuki Wada[2], Takayuki Yuasa, Harufumi Tsuchiya[3], Taro Shinoda[4], Keigo Ookuma[1], Gabriel Diniz[2]

1. Nagoya University, 2. RIKEN, 3. JAEA, 4. ISEE. Nagoya Univ.

Lightning activity emitting gamma-rays has been observed on the coast of the Sea of Japan in winter season. Those gamma rays are due to bremsstrahlung from electrons accelerated by the electrostatic field in thundercloud, and their energy reaches 30 MeV. Specifically, the gamma-ray emission events observed in an instant of less than 1 ms are called gamma-ray flash, and those observed from the thundercloud itself for a few minutes are called gamma-ray glows. We have been observing thundercloud gamma rays in the coast of the Sea of Japan in winter since 2006. The project is named GROWTH (Gamma-ray Observation of Winter Thunderclouds). In this talk, I will report on the observations in FY2020, aiming to measure the altitude of the accelerator.
For the FY2020 observations, detectors were set up at two locations in Kanazawa City, each ~2 km away from each other. Kanazawa City is an area where lightning frequently occurs, and there have been many gamma-ray observations in the past. We deployed the detector called GOOSE (Gamma-ray Orientation Observing System with Electron-monitor), which consists of collimated detectors and an electron detector. The former consist of four detectors, three of which have lead plates limiting the field of view and also inclined; directly upward, 30° eastward, and 30° westward, respectively. When the size of the accelerator is smaller than the altitude, it can be approximated as a point source. The altitude of the accelerator can be estimated using the time difference in the count rates of the three collimator detectors as they are swept by the wind. When the altitude is less than 100 m, 30 MeV electrons can be detected directly on the ground because their range in the atmosphere is longer.
Observations for FY2020 began at the end of October, and gamma-ray glows were observed at around 18:00 on January 8, 2021, and at around 6:00 on January 9, 2021. It was snowing on both days, and there was a west-southwest wind of 16.6 m/s on the 8th and a west wind of 10 m/s on the 9th events. In the collimator detectors, the count rate observed in the detectors facing upwards was 1.5-2.5 times higher than that in the detectors tilted to the east and west. This is a clear evidence for the beaming effect of bremsstrahlung. In both events, the time difference between westward and eastward included detectors was generally less than 10 seconds, and the altitude was less than ~150 m in the point source approximation. The electron detector also detected an excess of charged particles synchronized with the gamma-ray glow. The origin of this excess is still under analysis.

Keywords: gamma rays from thunderstorms, altitude measurement of the electron accelerator, electron detector

©2021. Japan Geoscience Union. All Right Reserved.

Hydrometeor distribution in a thundercloud related to a gamma-ray emission event

*Takemoto Kiyomichi[1], Taro Shinoda[1], Masaya Kato[1], Shohei Hisadomi[2], Yuuna Tsuji[2], Kazuhiro Nakazawa[2], Yuuki Wada[3], Teruaki Enoto[3]

1. Institute for Space-Earth Environmental Research, Nagoya University, 2. Department of Physics, Nagoya University, 3. Institute of Physical and Chemical Research

Lightning events are frequently bought about by a shallow convective cloud in Hokuriku region during the cold-air outbreak in winter. Gamma-ray emission events have been simultaneously observed from thunderclouds in the region. The Gamma-ray Observation of Winter Thunderclouds (GROWTH) field campaign has been conducted to investigate gamma-ray events from thunderclouds by multiple sensors around Kanazawa City, Japan (Enoto et al. 2017, Wada et al. 2019).
The gamma-ray glow, which is a kind of gamma-ray emission, is lasting a few seconds to several minutes. The gamma-ray glow is considered that phenomena originate from relativistic runaway electron avalanches (RREAs) in strong electric fields due to positively charged particles in the lower part of the cloud and negatively charged ones in the upper part of it (Wada et al., 2019). Although several gamma-ray glow events have been observed in recent years by the GROWTH field campaign, microphysical properties in a thundercloud brought about gamma-ray emission events have not been clarified. Hisadomni et al. (2020) reported double gamma-ray glows in Kanawaza at 0203 and 0206 JST on 13 January 2020. This study shows 3-dimensional hydrometeor distributions in the thunderclouds brought about the gamma-ray emission event using a hydrometeor classification algorithm (Kouketsu et al. 2015). Polarimetric parameters, i.e., reflectivity, differential reflectivity, specific differential phase, correlation coefficient between horizontal and vertical polarizations, which are obtained by XRAIN radar at the Noumi site.
High reflectivity area that exceeds 40 dBZ is observed above the gamma-ray observation sites at least 5 minutes before the gamma-ray glow. At that time, the echo-top height reaches at a height of 6 km that is relatively higher than typical one of snow clouds. Wet graupel (0.5 ~ 2 km) and dry graupel (2 ~ 5.5 km) are detected with the high reflectivity area that should correspond to the convective core. The surface temperature is 6.6 degrees Celsius at Kanazawa Meteorological Observatory at 02:00 JST. Thus, graupel particles in the lower part of the thundercloud should be positively charged by the riming electrification (Takahashi, 1978).

Keywords: Hokuriku winter thundercloud, lightning discharge, gamma-ray glow

©2021. Japan Geoscience Union. All Right Reserved.

A Study of 3D Precipitation Core Tracking Method Using Multi-Parameter Phased Array Weather Radar

*Keitaro Asai[1], Hiroshi Kikuchi[1], Yasuhide Hobara[1], Tomoo Ushio[2]

1. The University of Electro Communications, 2. Osaka University

In Japan, a weather radar network, known as the extended radar information network (XRAIN), is operated to provide regular observations of rainfall and wind distribution. The network is comprised of 16 C-band radars and 39 X-band multi-parameter (X-MP) radars that are capable of conducting dual-polarization observations. X-MP radars have parabolic-type antennas, and they require about 5 min to complete a volume scan because both the azimuth and elevation angles are scanned mechanically. Only ten elevation angles (approximately) are scanned, and areas covered at high elevation angles are limited. The Multi-Parameter Phased Array Weather Radar (MP-PAWR) has been developed as the next generation dual-polarized weather radar to address the limitations of X-MP radars. When conducting a volume scan, the MP-PAWR uses electronic and mechanical scanning in the elevation and azimuth angles, respectively, to achieve 3D observation within a radius of 60 km and an altitude of about 15 km in 30 sec.

In order to discuss the distribution and temporal change of 3D precipitation data obtained by MP-PAWR, it is necessary to develop a method to classify and track precipitation cores. In this study, a density-based clustering method, DBSCAN (Density-based spatial clustering of applications with noise), was used for clustering and tracking of 3D precipitation cores.

In this presentation, we will introduce the developed clustering and tracking method for 3D precipitation cores. The distribution and temporal characteristics of convective and stratiform precipitation analyzed by the developed method are also discussed.

Keywords: Phased Array Weather Radar, Dual-polarization Observation, Precipitation Observation

©2021. Japan Geoscience Union. All Right Reserved.

Special negative lightning strokes in winter with extremely short preceding discharges

*Ting Wu[1], Daohong Wang [1], Nobuyuki Takagi[1]

1. Gifu University

The return stroke (RS) is the most well-studied process in lightning. The first RS in a negative cloud-to-ground (-CG) flash is usually preceded by the preliminary breakdown (also called initial breakdown) and the stepped leader, and the typical time difference between the start of a -CG flash and the first RS is from several to a few tens of ms. In winter, however, thunderclouds are much shallower and the time difference can be much shorter. -CG flashes with the time difference between the first RS and the start of the flash shorter than 1 ms have been reported. In this study, we will analyze negative strokes in winter with the duration of preceding discharges shorter than 1 ms based on the observation of FALMA (Fast Antenna Lightning Mapping Array). Particularlly, we will focus on strokes with the duration of preceding discharges shorter than 200 us, and we will demonstrate that these strokes are systematically different from those with longer durations of preceding discharges. These special strokes with extremely short preceding discharges frequently occur at high mountain areas. It is estimated that their channel lengths are only hundreds of meters, an order of magnitude shorter than those of normal negative RSs.

Keywords: Return stroke, Winter lightning, Negative cloud-to-ground lightning

©2021. Japan Geoscience Union. All Right Reserved.

Simultaneous Observations of a Winter Lightning Flash in Japan

*Haitao Huang[1], Daohong Wang[1], Ting Wu[1], Nobuyuki Takagi[1]

1. Gifu University

A winter lightning flash in Japan was simultaneously recorded with multiple instruments, including a high-speed video camera, an optical imaging system LAPOS (Lightning Attachment Process Observation System), a lightning mapping system FALMA (Fast Antenna Lightning Mapping Array), and a current measuring system. This flash lasted for about 0.34 seconds with a large horizontal extent of about 40 ×40 km. It started with a multiple-stroke positive cloud-to-ground flash that consists of two positive return strokes (RSs). The first RS was located about 3.2 km from the lightning initial location. The second RS was located about 13.2 km from the first RS with an interval of 55 ms. About 1.5 ms after the second RS, an upward positive leader (UPL) was triggered from the tip of a lightning protection tower. The UPL extended straight upward without clear branches. During the initial stage, the UPL propagated in stepped mode with an average speed of about 0.8×10^5 m/s. As it propagated to the higher altitude, the UPL became more continuous with a faster velocity of about 3.6×10^5 m/s. After the UPL propagated into the thunder cloud, a nearby leader connected to the UPL channel at about 620 m above the tower tip and initiated a strong discharge process. Further analysis indicates that this connection process is similar to the lightning large bipolar event (LBE), a special type of return stroke in winter thunderstorms. About 0.22 s after the initiation of the UPL, four negative RSs struck the same termination 5.2 km from the tower with an average interval of about 5.4 ms. The negative RS lightning channel was much curved from the view of the high-speed video camera. It seems that the occurrence of the first negative RS has little connection with the UPL but is associated with discharge processes near the lightning initiation area.

Keywords: winter lightning, multiple-stroke lightning flash, upward lightning, large bipolar event (LBE)

©2021. Japan Geoscience Union. All Right Reserved.

Spatio-temporal characteristics of lightning energy in Southeast Asia deduced from ELF observations

*Shunsuke Akama[1], Shu Hirai[1], Yasuhide Hobara[1], Hiroshi Kikuchi[1], Amir Izzani Mohamed[2], Chandima Gomes[3], Kazuo Shiokawa[4], Michael Stock[5]

1. The University of Electro-Communications, 2. University of Malaysia, Pahang, 3. University of the Witwatersrand, Johannesburg, 4. Institute for Space–Earth Environmental Research, 5. Earth Networks

In the Southeast Asian region, cloud-to-ground discharges cause several million dollars of damage per year. Detailed information on electrical characteristics and spatio-temporal distributions including lightning stroke energy in the relevant region is essential for lightning disaster mitigation. In this study, we investigate the spatio-temporal characteristics of cloud-to-ground discharges in the Southeast Asian region, including the charge moment change, by using the lightning locating system in combination with the ELF magnetic field observation installed at the University of Pahang, Malaysia. Specifically, we identify the sferic waveforms in ELF band corresponding to the lightning strokes ddetected by EarthNetworks's total lightning detection network. Then we calcurate the lightning charge moment Qds, lightning peak current, and polarity for each stroke. In this presentation, initial results on spatio-temporal characteristics including Qds for lightning strikes around Malay peninsula for different seasons will be presented.

Keywords: Lightning strike, ELF magnetic field, Charge moment of lightning strikes, Transient luminous event, Atmospheric electricity, Southeast Asia

©2021. Japan Geoscience Union. All Right Reserved.

Sprites observed from the summit of Mt. Fuji and their parent thunderstorm

*Suzuki Tomoyuki[1], Masashi Kamogawa[1], Syugo Hayashi[2]

1. University of Shizuoka, 2. Meteorological Research Institute

Transient Luminous Events (TLEs) are the flash phenomena observed from the top of and above thunderstorms accompanied with active strikes. To detect the family of TLEs (e.g. sprites, jets, ELVEs), since 2012, we have installed and operated high-sensitivity charge coupled device (CCD) camera at the summit of Mt Fuji in summer season. We have succeeded in observing various TLEs from the first operation. It was found that some sprites were associated with the positive cloud-to-ground strikes (+CGSs) in the stratiform region of mesoscale convective system (MCS) but one sprite was associated with the +CGS in the leading convective line of MCS. Both region of MCS were analyzed using C-band weather radar operated by Japan meteorological agency. In this study, we present the samples of TLEs family observed from the summit of Mt Fuji, radar echo structures of stratiform and convective region, the differences of relative displacement and duration time between sprites, sprite-producing +CGSs and their optical cloud flash, which was detected by CCD camera, in the convective and stratiform region.

Keywords: Transient Luminous Events , Sprites, Thunderstorm, Mesoscale convective system, Positive cloud to ground strikes, Mt. Fuji

©2021. Japan Geoscience Union. All Right Reserved.

Coupling process of large-scale atmospheric disturbances to the ionosphere through typhoon

*Shu Hirai[1], Yasuhide Hobara[1], Hiroshi Kikuchi[1], Michael Stock[2]

1. The University of Electro-Communications, 2. Earth Networks

In recent years, tropical cyclones (TCs) have caused serious damage in the world. However, few studies have comprehensively taken into account the TC effects on the ionosphere in addition to meteorological conditions and lightning discharge characteristics of thunderstorms from TCs in the atmosphere. In this study, we investigated the coupling process of meteorological disturbances to the ionosphere from simultaneous observations of thunderstorms and ionosphere during the entire period of Typhoon 15 and Typhoon 19 in 2019. The spatial and temporal characteristics of lightning activity, meteorological characteristics (visible and infrared observations by the geostationary satellite), and lower ionospheric response (VLF/LF transmitter electric amplitude) associated with these typhoons were analyzed in detail. Distinctive features were found between parameters such as the frequency of lightning strikes, discharge polarity, development of thunderclouds, and ionospheric disturbances in different typhoon stages.

Keywords: Typhoon, Ionosphere, Atmospheric electricity, Extreme weather, Thunderstorm, meteorological disturbances

©2021. Japan Geoscience Union. All Right Reserved.

[J] Poster | M (Multidisciplinary and Interdisciplinary)：M-IS Intersection

Sun. Jun 6, 2021 5:15 PM - 6:30 PM JST | Sun. Jun 6, 2021 8:15 AM - 9:30 AM UTC | Ch.21_1

[M-IS26] Gas hydrates in environmental-resource sciences

convener:Hitoshi Tomaru(Department of Earth Sciences, Chiba University), Akihiro Hachikubo(Kitami Institute of Technology), Atsushi Tani(Department of Human Environmental Science, Graduate School of Human Development and Environment, Kobe University), Shusaku Goto(Institute for Geo-Resources and Environment National Institute of Advanced Industrial Science and Technology)

An increasing number of researches focusing on natural gas hydrates has recently been conducted from the environmental, material, and resource scientific viewpoints. This session aims to share and discuss the latest research results associated with natural/experimental gas hydrates to understand and examine the nature and potential of gas hydrates in the past-present-future of the Earth and the development/application for our life. Because the researches on gas hydrates are interdisciplinary, broad topics from field and experimental researches, modeling, etc. will be presented in this session.

[MIS26-P01] Geochemical characteristics of headspace gas and pore water in shallow sediment from the Tatar Trough

*Musashi Yokoyama[1], Ryo Murata[1], Hitoshi Tomaru[1], Ryo Matsumoto[2], A.V. Yatsuk[3], D.A. Shvalov[3] (1.Chiba University, 2.Meiji University, 3.V.I.Ilichev Pacific Oceanological Institute)

[MIS26-P02] Gas hydrate survey at the gas seepage area off Abashiri, the Sea of Okhotsk

*Yuki Moriya[1], Hiromi Kimura[1], Akihiro Hachikubo[1], Satoshi Yamashita[1], Hirotoshi Sakagami[1], Masaaki Konishi[1], Hirotsugu Minami[1], Yasuhito Uchida[2], Hiroshi Yamaguchi[3] (1.Kitami Institute of Technology, 2. Research Institute of Energy, Environment and Geology, Hokkaido Research Organization, 3.Kushiro Fisheries Research Institute, Hokkaido Research Organization)

[MIS26-P03] Total organic carbon and its carbon isotope ratio in subsurface sediments off Hokkaido area

*Daisuke Yahagi[1], Akihiro Hachikubo[1], Masaaki Konishi[1], Hirotoshi Sakagami[1], Hirotsugu Minami[1], Satoshi Yamashita[1], Yasuhito Uchida[2], Hiroshi Yamaguchi[3] (1.Kitami Institute of Technology, 2.Research Institute of Energy, Environment and Geology, Hokkaido Research Organization, 3.Kushiro Fisheries Research Institute, Hokkaido Research Organization)

[MIS26-P04] Characteristics of gas hydrate crystals and their hydrate-bound gases retrieved at the seepage field off Tokachi (the Pacific Ocean)

*Hiromi Kimura[1], Ryoya Kamata[1], Daisuke Yahagi[1], Yuki Moriya[1], Akihiro Hachikubo[1], Masaaki Konishi[1], Hirotoshi Sakagami[1], Hirotsugu Minami[1], Satoshi Yamashita[1] (1.Kitami Institute of Technology)

[MIS26-P05] Gas hydrate survey at the gas seepage area off Hidaka, the Pacific Ocean

*Ryoya Kamata[1], Hiromi Kimura[1], Akihiro Hachikubo[1], Hirotoshi Sakagami[1], Satoshi Yamashita[1], Masaaki Konishi[1], Hirotsugu Minami[1] (1.Kitami Institute Of Technology)

[MIS26-P06] Emission of hydrated gas from seafloor to water column in the western Oki Trough

*Hitoshi Tomaru[1], Tianyou Ze[1], Sonoka Ikemoto[1], Minori Chikada[1] (1.Department of Earth Sciences, Chiba University)

[MIS26-P07] Isotope fractionation between hydrate-bound and ambient gases - case study in Lake Baikal gas hydrates -

*Hiromi Kimura[1], Akihiro Hachikubo[1], Oleg Khlystov[2], Gennadiy Kalmychkov[3], Marc De Batist[4], Hirotoshi Sakagami[1], Hirotsugu Minami[1], Satoshi Yamashita[1] (1.Kitami Institute of Technology, 2.Limnological Institute, SB RAS, 3.Vinogradov Institute of Geochemistry, SB RAS, 4.Ghent University)

[MIS26-P08] Carbon isotope fractionation of carbon monoxide hydrate between gas and hydrate phases

*Hiromi Kimura[1], Akihiro Hachikubo[1], Satoshi Takeya[2] (1.Kitami Institute of Technology, 2.National Institute of Advanced Industrial Science and Technology (AIST))

[MIS26-P09] Hydrogen isotopic fractionation of methane at the formation of synthetic structure I and II gas hydrates

*Ryoya Kamata[1], Akihiro Hachikubo[1], Satoshi Takeya[2] (1.Kitami Institute Of Technology, 2.National Institute of Advanced Industrial Science and Technology (AIST))

[MIS26-P10] Experimental study of CO2 hydrate phase equilibrium in sediments

*Tatsuki Iwamoto[1], Hitoshi Tomaru[1] (1.Chiba University)

[MIS26-P11] Effect of temperature and pressure on hydration number of methane hydrate

*Akihiro Hachikubo[1], Ryoya Kamata[1], Hiromi Kimura[1], Yuta Komagata[1], Go Fuseya[1], Satoshi Takeya[2] (1.Kitami Institute of Technology, 2.National Institute of Advanced Industrial Science and Technology (AIST))

Geochemical characteristics of headspace gas and pore water in shallow sediment from the Tatar Trough

*Musashi Yokoyama[1], Ryo Murata[1], Hitoshi Tomaru[1], Ryo Matsumoto[2], A.V. Yatsuk[3], D.A. Shvalov[3]

1. Chiba University, 2. Meiji University, 3. V.I.Ilichev Pacific Oceanological Institute

The Tatar Trough is characterized by a number of mound with gas chimney and in particular gas flare with gas hydrate accumulation in shallow sediment, reflecting active gas generation at depth and migration to the surface environment. Because the trough is located in geologically active and important region for organic matter input and seawater circulation in the northern Japan Sea, origin and migration process could be constrained by the formation and development of the marginal sea. In this study, we characterized the geochemistry of headspace gas and pore water samples collected from northern to southern Tatar Trough and and examined biogeochemical processes associated with generation, migration, oxidation, and fixation of methane in the Tatar Trough.

All the methane concentrations and C1/C2 ratios in headspace gases increase with depth due to the active upward methane flux although the methane is oxidized at the sulfate-methane interface (SMI). These values in the northern area are higher than those in the middle and southern areas. The stable carbon isotopic ratio of methane in the northern area is relatively high (δ^{13}C=-55~-30‰). This value suggests that methane was generated by thermal decomposition of organic matter at depth. The depths of SMI significantly tended to be shallower to the north; average depth of SMI in the northern area is 2.9 mbsf, middle area is 5.9 mbsf, and southern area is 12 mbsf. This indicates that the organic matter responsible for methane generation was derived from the north probably by the oxygen-depleted water and was deposited in relatively anaerobic condition, which is strongly associated with a large-scaled environmental change.

Keywords: methane, gaschimney, AOM

©2021. Japan Geoscience Union. All Right Reserved.

Gas hydrate survey at the gas seepage area off Abashiri, the Sea of Okhotsk

*Yuki Moriya[1], Hiromi Kimura[1], Akihiro Hachikubo[1], Satoshi Yamashita[1], Hirotoshi Sakagami[1], Masaaki Konishi[1], Hirotsugu Minami[1], Yasuhito Uchida[2], Hiroshi Yamaguchi[3]

1. Kitami Institute of Technology, 2. Research Institute of Energy, Environment and Geology, Hokkaido Research Organization, 3. Kushiro Fisheries Research Institute, Hokkaido Research Organization

In the framework of collaboration between Kitami Institute of Technology and Hokkaido Research Organization, we have conducted research cruises off Abashiri (the Sea of Okhotsk) to investigate near-surface gas hydrates at the sea floor where active gas seepage exists. HKS16, HKS17, HKS18, HKS19, and HKS20 cruses were conducted using RV Hokushin-Maru (255t) of the Kushiro Fisheries Research Institute. We successfully retrieved gas hydrate crystals in the HKS18 cruise (September, 2018) at the new place. Although we could not get sediment cores because of bad weather condition at the HKS19 cruise (September, 2019), we got gas-rich sediment cores at the HKS20 cruise (September 2020). In the HKS20 cruise, two study sites located about 5 km east (site A) and 8 km southeast (site B) from the gas hydrate site of HKS18, respectively.

Because the tidal current speed reached 4 km h^{-1} and made the coring operation difficult, we used a hydrostatic corer optimally tuned for a small vessel and a transponder to understand exact position of the corer in the HKS20 cruise. We obtained nine sediment cores, including two gas-rich cores. Sediment gas samples were obtained by a headspace gas method. Molecular and isotopic compositions of gas samples were measured using a gas chromatograph and an isotope ratio mass spectrometer, respectively.

The depths of sulfate-methane interface (SMI) in HC2006 (site A) and HC2010 (site B) cores were around 10 cm and 50 cm, respectively, indicating high gas flux. C_1 / (C_2 + C_3) of headspace gases in the above two cores distributed between 6,100 and 37,000 below these SMI depths, and those of other sediment cores were less than 1,000, suggesting that the size of gas seepage was small and they are in the oxidation layer above the SMI depth. Concentration of C_2 in the HC2010 core was one order larger than that of HC2006 core, although both study sites located on the same ridge. C_1 $\delta^{13}C$ and δD of these cores concentrated -70‰ and -185‰, respectively. These molecular and isotopic compositions of sediment gases suggested microbial origin via CO_2 reduction. CO_2 $\delta^{13}C$ of these cores were small (around -40‰), indicating that CO_2 is also oxidized from CH_4 simultaneously by microbial processes.

Keywords: gas hydrate, the Sea of Okhotsk, gas origin

©2021. Japan Geoscience Union. All Right Reserved.

Total organic carbon and its carbon isotope ratio in subsurface sediments off Hokkaido area

*Daisuke Yahagi[1], Akihiro Hachikubo[1], Masaaki Konishi[1], Hirotoshi Sakagami[1], Hirotsugu Minami[1], Satoshi Yamashita[1], Yasuhito Uchida[2], Hiroshi Yamaguchi[3]

1. Kitami Institute of Technology, 2. Research Institute of Energy, Environment and Geology, Hokkaido Research Organization, 3. Kushiro Fisheries Research Institute, Hokkaido Research Organization

For five years we collected hydrate-bearing and gas-rich sediments at gas plume sites off Hokkaido to understand the formation process of natural gas hydrates. The research target of this study is an organic matter deposited on the sea floor, because it is an ultimate origin of hydrate-bound hydrocarbon and its total organic carbon relates to formation of natural gas hydrates. Carbon isotopes of the organic matter provides information of their origin. Here, we report total organic carbon and its $\delta^{13}C$ in subsurface sediment retrieved off Hokkaido area (the Sea of Okhotsk, Japan Sea, and the Pacific Ocean).
Sediment samples were obtained off Abashiri (C032, 1KY17, HKS17, HKS18, and HKS20), off Monbetsu (GA18 and GA19), off Esashi (HKY17), off Rebun Is. (HKY19), off Hidaka (K2-2020), and off Tokachi (C046, C061, C080, and C095). In total 446 sediment samples were dried, homogenized, and about 5 mg of samples were put into silver foil capsules. They were decarbonized with 12N hydrochloric acid for 24 h, and then dried and wrapped in tin capsules. These samples were analyzed their TOC with a Flash 2000 Elemental Analyzer connected to a Delta V isotope ratio mass spectrometer. The system was calibrated using a standard of JCAC-01 (L-alanine, -23.43‰ in V-PDB).
The median values of TOC and its $\delta^{13}C$ for all data were 0.9% and -24.2‰, respectively. Sediment cores collected at the gas seepage sites were mainly gas-rich; however, several normal cores with little gas were also included in these data. The TOC and its $\delta^{13}C$ values show distinct regional characteristics. In particular, certain areas off Tokachi and Hidaka had higher TOC (1.5% to 2.0%) and larger $\delta^{13}C$ values (-21‰). As for hydrate-bearing sediment cores, TOC-rich (from 1% to 2%) cores had $\delta^{13}C$ around -25‰, which was similar to other sediment cores without gas hydrates. On the other hand, in the C095-2002 core retrieved off Tokachi, TOC was small (0.6-0.8%) and its $\delta^{13}C$ was extremely small (from -46‰ to -30‰). Hydrate-bearing cores of 1KY17 obtained by ROV survey off Abashiri showed such small values in TOC $\delta^{13}C$ (below -30‰). The $\delta^{13}C$ of TOC was also relatively small in the case that sediments attached to gas hydrate crystals. These results suggest that the organic matter in the sediments close to gas hydrates may be affected by oxidized methane. Although little is known about the formation age of gas hydrate and the exchange processes of gas hydrate crystals with the surrounding gas (dissolved and gas bubble), some exchange of carbon between seepage gas, gas hydrate crystals, and organic matter might occur in the subsurface sediments.

Keywords: TOC, gas hydrate, methane

©2021. Japan Geoscience Union. All Right Reserved.

Characteristics of gas hydrate crystals and their hydrate-bound gases retrieved at the seepage field off Tokachi (the Pacific Ocean)

*Hiromi Kimura[1], Ryoya Kamata[1], Daisuke Yahagi[1], Yuki Moriya[1], Akihiro Hachikubo[1], Masaaki Konishi[1], Hirotoshi Sakagami[1], Hirotsugu Minami[1], Satoshi Yamashita[1]

1. Kitami Institute of Technology

We report the first recovery of natural gas hydrate off Tokachi, the Pacific Ocean. In the framework of practical education of Kitami Institute of Technology, we conducted research cruises off Tokachi since 2014, to investigate gas hydrate fields around Hokkaido. There are many gas seeps ascend from the sea floor and their height exceeded 700 m at the study area off Tokachi.
Using TS Oshoro-maru of Hokkaido University, 17 sediment cores were retrieved by gravity and hydrostatic corers during five cruises. The last C095 cruise was conducted on November 2020, and we obtained massive gas hydrate crystals. In this report we focus on the results of crystallographic properties of gas hydrate and their gas characteristics.
In the cruise of C095, we obtained six sediment cores, including a hydrate-bound core. Gas hydrate crystals were preserved at the temperature of liquid nitrogen, and sediment gases were obtained by a headspace gas method. Raman spectroscopic analysis was conducted to know crystallographic structure, hydration number and cage occupancies. Molecular and isotopic compositions of hydrate-bound and sediment gas samples were measured using a gas chromatograph (GC2014, Shimadzu) and an CF-IRMS (Delta V, Thermo Fisher Scientific), respectively.
Crystallographic structure of gas hydrate samples belonged to the structure I, and hydration number was estimated as 6.07±0.04 from the Raman peaks of hydrate-bound methane. Hydrate-bound H_2S and N_2 molecules were also detected in the Raman spectra, however, that of CO_2 was not detected.
Hydrate-bound gas was mainly methane, and C_1 / (C_2 + C_3) distributed between 3,300 and 6,800. $\delta^{13}C$ and δD of methane were -66‰ and -188‰. These molecular and isotopic compositions of hydrate-bound hydrocarbons suggested microbial origin, and methane was derived by CO_2 reduction. $\delta^{13}C$ of ethane was -52‰, therefore such light ethane seemed to be also microbial.
The depth of sulfate-methane interface (SMI) in C095-GC2002 (hydrate-bound core) was 45 cm, and those in other C095 sediment cores were less less than 1 m, indicating high methane flux from deep layer. Concentrations of H_2S in the headspace gas samples were in the same order (around 1 mM), suggesting that the process of anaerobic oxidation of methane was active. C_1 / (C_2 + C_3) of headspace gases in the hydrate-bound and gas-rich cores distributed between 970 and 2,090 below their SMI depths.
Hydrate-bound and gas-rich sediment cores contained carbonates; their $\delta^{13}C$ ranged from -43‰ to -39‰. Since $\delta^{13}C$ of CO_2 in headspace gases in these cores ranged from -58‰ to -34‰, the site of gas hydrate is characterized as depletion in ^{13}C of carbon dioxide and light carbon dioxide was derived from oxidation of light methane.

Keywords: gas hydrate, methane, the Pacific Ocean

©2021. Japan Geoscience Union. All Right Reserved.

Gas hydrate survey at the gas seepage area off Hidaka, the Pacific Ocean

*Ryoya Kamata[1], Hiromi Kimura[1], Akihiro Hachikubo[1], Hirotoshi Sakagami[1], Satoshi Yamashita[1], Masaaki Konishi[1], Hirotsugu Minami[1]

1. Kitami Institute Of Technology

Existence of gas chimneys have been reported off Hidaka (Hokkaido) in the sub-bottom profiler data of GH06 cruise (AIST 3.5kHz SBP database, https://gbank.gsj.jp/sbp_db/pages/cover.html). To investigate near-surface gas hydrates at the sea floor, we performed K2-2020 cruise using Kaiyo-Maru No. 2 belonging to Kaiyo Engineering Co. Ltd. on September 2020. Our research fields are two areas (sites 1 and 2 locate 60 km east and 60 km southeast from Cape Erimo, respectively). At the site 1, gas plumes were discovered by a multibeam survey. The largest gas plume was about 500 m high and was accompanied by some plumes (200-300 m high). Many mounds with specific heights ranging from several meters to more than ten meters were found. On the contrary, the site 2 had no gas plume but many mounds with specific heights of 10 to 20 meters. In this cruise, we used a hydrostatic corer and gravity corer to take sub-bottom sediment cores. We obtained 16 sediment cores, including some gas-rich cores. Sediment gas samples were obtained by a headspace gas method. Molecular and isotopic compositions of gas samples were measured using a gas chromatograph and an isotope ratio mass spectrometer, respectively.
Sediment gas analysis revealed that concentrations of CH_4 and H_2S at the gas plume site of the site 1 were relatively high (more than 1 mM), and C_1 / (C_2 + C_3) ranged 2,000-5,000 because of high methane concentration. C_1 $\delta^{13}C$ and δD were about -70‰ and around -185 to -170‰, respectively, suggesting microbial methane produced via CO_2 reduction. C_2 $\delta^{13}C$ ranged from -59‰ to 43‰ and became smaller with depth, indicating that microbial ethane is also generated in the sediment. CO_2 $\delta^{13}C$ was also small as well as methane, close to -60‰. Some sediment cores at the plume site had shallow SMI depths of 0.4 to 1.2 m, suggesting an active gas supply and existence of gas hydrates below the sea floor.
On the other hand, the concentration of methane was generally in the order of 0.01 mM at the mounds in site 2. Compared to normal sediment cores (methane concentrations ranged from 0.0001 to 0.001 mM), which show no signs of methane migration, the results showed ascending methane in these mounds. However, C_1 / (C_2 + C_3) was less than 1,000, suggesting that these SMI depths were lower than the core bottoms. The values of C_1 $\delta^{13}C$ and CO_2 $\delta^{13}C$ were around -80‰ and -20‰, respectively, and their profiles were uniform along with depth.

Keywords: gas hydrate, the Pacific Ocean, gas origin

©2021. Japan Geoscience Union. All Right Reserved.

Emission of hydrated gas from seafloor to water column in the western Oki Trough

*Hitoshi Tomaru[1], Tianyou Ze[1], Sonoka Ikemoto[1], Minori Chikada[1]

1. Department of Earth Sciences, Chiba University

Gas chimneys, characterized by a chaotic-columnar structure in acoustic image, are developed well on the western slope of the Oki Trough off Tottori. A significant amount of hydrocarbon, mostly methane, is liberated from the marine sediment to overlying water column in this area, the dynamics of hydrocarbon emission in gas-rich environment is a key to understand carbon/methane migration among atmosphere-seawater-sediment. The concentrations of methane dissolved in the seawater over the gas chimney were seasonally determined, which showed significant increases at the water depth of 200~300 m. This observation strongly suggests that the methane hydrates formed at the surface of emitted methane bubble just above the seafloor and ascended, and the hydrates dissolved at the upper boundary of its stability, so that methane was released efficiently to shallow seawater. In addition, the concentrations of methane near the seafloor were relatively low but seemed to vary in response to the tidal pressure change, indicating that the pressure increase enhanced methane emission from gas pocket in shallow sediment. The behavior of gas emission is constrained by the change of physical/chemical environment between seawater and sediment, and the formation/dissolution of hydrate-coated bubble plays a key role in the migration and distribution of methane in methane-rich water column.

Keywords: gas plume, gas chimney, Oki Trough

©2021. Japan Geoscience Union. All Right Reserved.

Isotope fractionation between hydrate-bound and ambient gases - case study in Lake Baikal gas hydrates -

*Hiromi Kimura[1], Akihiro Hachikubo[1], Oleg Khlystov[2], Gennadiy Kalmychkov[3], Marc De Batist[4], Hirotoshi Sakagami[1], Hirotsugu Minami[1], Satoshi Yamashita[1]

1. Kitami Institute of Technology, 2. Limnological Institute, SB RAS, 3. Vinogradov Institute of Geochemistry, SB RAS, 4. Ghent University

Isotope fractionation of methane occurs between gas and hydrate phases (Hachikubo *et al.*, 2007). However, such fractionation is not applied to understand the formation process of natural gas hydrates in the sublacustrine sediments of Lake Baikal. In this study, we compiled data on stable isotope ratios of hydrocarbons in hydrate-bound and sediment gases, which have been collected in the framework of collaboration between Limnological Institute (Russia), Ghent University (Belgium), and Kitami Institute of Technology (Japan) for 15 years.
Hydrate-bearing sediment cores were collected by R/V *G. Yu. Vereshchagin* using a gravity corer. Hydrate-bound gas was collected in vials by a water displacement method on board, and sediment gas was obtained using the headspace gas method by collecting sediment at 40 cm intervals from the sediment core sections. The gas composition and stable isotope ratios of volatile hydrocarbons were measured for these samples by gas chromatograph (GC2014, Shimadzu) and CF-IRMS (Delta V, Thermo Fisher Scientific), respectively. Comparison of stable isotope ratios of hydrate-bound and sediment gases at the same core and depth was performed.
The methane carbon isotope ratio of the hydrate-bound gas was 0 to +3‰ smaller than the sediment gas. These isotopic difference in carbon was slightly positive overall, indicating a concentration of lighter methane ($^{12}CH_4$) in the hydrate-bound gas than in the sediment gas. The difference in hydrogen between hydrate-bound and sediment gases distributed from -3‰ to +11‰ and is also positive overall as well. The average difference in δD was 5.4‰, which agreed fairly well with the previous report that approximately 5‰ light methane in δD is preferentially enclathrated at the formation of synthetic methane hydrate (Hachikubo *et al.*, 2007). Although the positive difference in δ^{13}C cannot be explained yet, these results can be explained generally by the isotopic fractionation of methane. In contrast, some sediment cores retrieved at the Kedr mud volcano showed small or reversed differences in methane carbon isotope ratios, as well as small differences in methane hydrogen isotope ratios, suggesting that dissociation of gas hydrate is occurring at that point.

References

Hachikubo A, Kosaka T, Kida M, Krylov A, Sakagami H, Minami H, Takahashi N, Shoji H (2007) Isotopic fractionation of methane and ethane hydrates between gas and hydrate phases. *Geophys Res Lett* **34**: L21502. doi:10.1029/2007GL030557

Keywords: gas hydrate, isotope fractionation, methane

©2021. Japan Geoscience Union. All Right Reserved.

Carbon isotope fractionation of carbon monoxide hydrate between gas and hydrate phases

*Hiromi Kimura[1], Akihiro Hachikubo[1], Satoshi Takeya[2]

1. Kitami Institute of Technology, 2. National Institute of Advanced Industrial Science and Technology (AIST)

It is possible that carbon monoxide hydrates exist in the icy bodies of outer planets of the solar system (Zhu *et al.*, 2014). Isotope signatures of carbon monoxide hydrates may provide useful information to understand formation processes of gas hydrate. Kimura *et al.* (2019) reported at the past JpGU conference that the carbon isotopic difference between hydrate-bound and residual gases distributed between between 1.2‰ and 1.5‰ in the case of carbon dioxide hydrate, suggesting that the hydrate rather concentrates light molecules ($^{12}CO_2$). Besides, the equilibrium pressure of $^{13}CO_2$ hydrate is slightly higher than that of $^{12}CO_2$ hydrate (Kimura *et al.*, 2020) and agreed with the result of carbon isotopic fractionation. On the contrary, there no information about carbon monoxide hydrate. In this study, we measured carbon isotopic difference between hydrate-bound and residual gases at the formation of carbon monoxide hydrate.
Samples of carbon monoxide hydrate were synthesized in a pressure cell (volume: 42 mL). Fine ice powder was put in a pressure cell and introduced the guest gas. The temperature was controlled by a liquid bath (253-273 K) and cold rooms (223-243 K) to form hydrate crystals from gas and ice powder. After their formation, isotopic compositions of both hydrate-bound and residual gases were measured by an isotope ratio mass spectrometer (CF-IRMS, DeltaV, Thermo Fisher Scientific).
The results of PXRD pattern showed that the crystallographic structure of carbon monoxide hydrate was the cubic structure I. The carbon isotopic differences between hydrate-bound and residual gas was 0.6 ± 0.1‰ at 223-273 K. In contrast to the result of carbon dioxide hydrate, the hydrate of carbon monoxide concentrated heavier molecules (^{13}CO), indicating that the equilibrium pressure of ^{13}CO hydrate is lower than ^{12}CO hydrate.

References

Kimura H, Matsuda J, Kikuchi Y, Hachikubo A, Takeya S (2019) Carbon isotope fractionation of CO_2 during the formation of clathrate hydrate. *Japan Geoscience Union Meeting 2019*, MIS21-P07
Kimura H, Hachikubo A, Takeya S (2020) Equilibrium pressure of gas hydrate enclathrated carbon dioxide isotopologues. *JpGU-AGU Joint Meeting 2020*, MIS32-11
Zhu J, Du S, Yu X, Zhang J, Xu H, Vogel SC, Germann TC, Francisco JS, Izumi F, Momma K, Kawamura Y, Jin C, Zhao Y (2014) Encapsulation kinetics and dynamics of carbon monoxide in clathrate hydrate. *Nat Commun* **5**, 4128, doi: 10.1038/ncomms5128

Keywords: gas hydrate, stable isotope, carbon monoxide, isotopic fractionation

©2021. Japan Geoscience Union. All Right Reserved.

Hydrogen isotopic fractionation of methane at the formation of synthetic structure I and II gas hydrates

*Ryoya Kamata[1], Akihiro Hachikubo[1], Satoshi Takeya[2]

1. Kitami Institute Of Technology, 2. National Institute of Advanced Industrial Science and Technology (AIST)

Hydrogen isotopic fractionation of volatile hydrocarbons occurs during the formation of gas hydrates. For example, the hydrogen isotope ratios of the hydrate-bound methane, ethane, and propane are lower than those of the ambient gases (Hachikubo *et al.*, 2007; Nikaido *et al.*, 2018). These results are supported by the difference in equilibrium pressures of hydrates encaged guest isotopologues (Ozeki *et al.*, 2018). The crystal structure of gas hydrate depends on the size of guest gas. Methane and ethane hydrates form the structure I, composed of large ($5^{12}6^2$) and small (5^{12}) cages, whereas propane hydrate forms the structure II, composed of the different size large ($5^{12}6^4$) and small (5^{12}) cages. Ethane and propane can be encaged only in their large cages due to the large guest size. Since natural gas hydrates are mixed-gas hydrates, these guest molecules share the cages of different size. In the case of methane + ethane and methane + propane systems, methane is selectively occupied in the small cages. On the contrary, methane can be rather encaged into large cages in the system of methane + argon, because argon is smaller than methane. Therefore, we can check the effect of cage size on the hydrogen isotopic difference in methane. In this study, we investigated the hydrogen isotope fractionation of methane in the mixed-gas system of methane + ethane, methane + propane, and methane + argon systems.

A pressure cell (volume: 40 mL) was filled with 0.7 g of fine ice powder in a cold room. After vacuuming the air in the cell at the temperature of liquid nitrogen, the guest gases (methane, ethane, propane, and argon) were introduced in the cell and formed the mixed-gas hydrates. In the formation processes, the partial pressure of ethane and propane was also controlled below the liquefaction pressure of propane. After the formation of mixed-gas hydrate, residual gas that was not encaged in the hydrate phase was collected. Hydrate crystals were sampled at the temperature of liquid nitrogen. The composition of the hydrate-bound and residual gases were determined by a gas chromatograph (GC-2014, Shimadzu). The hydrogen isotope ratio of methane was determined by a stable isotope ratio mass spectrometer (CF-IRMS, DeltaV, Thermo Fisher Scientific). Stable isotope compositions are reported as δ values (‰), and δD is given with reference to the V-SMOW standards.

The difference in hydrogen isotope ratios of methane (δD of residual gas – δD of hydrate-bound gas) is defined as $\Delta\delta$D. The $\Delta\delta$D values in the system of methane + ethane and methane + propane was smaller than that of pure methane reported by the previous works (Hachikubo *et al.*, 2007). Therefore, $\Delta\delta$D became small in the case that methane was encaged into small cages. On the contrary, the $\Delta\delta$D values in the system of methane + argon was not changed with their gas composition. The crystallographic structure depended on the gas composition and methane was rather encaged into large cages. We confirmed that $\Delta\delta$D values in large cages was larger than those in small cages.

References

Hachikubo A, Kosaka T, Kida M, Krylov A, Sakagami H, Minami H, Takahashi N, Shoji H (2007) Isotopic fractionation of methane and ethane hydrates between gas and hydrate phases. *Geophys Res Lett* **34**: L21502. doi:10.1029/2007GL030557

Nikaido T, Matsuda J, Hachikubo A, Takeya S (2018) Hydrogen isotope fractionation of propane and isobutane hydrates between gas and hydrate phases. *JSSI & JSSE Joint Conference –2018 in Sapporo*, doi:10.14851/jcsir.2018.0_158

Ozeki T, Kikuchi Y, Takeya S, Hachikubo A (2018) Phase equilibrium of isotopologue methane hydrates

©2021. Japan Geoscience Union. All Right Reserved.

enclathrated CH_3D and CD_4. *J Chem Eng Data* **63**(6): 2266-2270, doi: 0.1021/acs.jced.8b00203

Keywords: gas hydrate, methane, ethane, propane, hydrogen isotope ratio

©2021. Japan Geoscience Union. All Right Reserved.

Experimental study of CO2 hydrate phase equilibrium in sediments

*Tatsuki Iwamoto[1], Hitoshi Tomaru[1]

1. Chiba University

Gas hydrate is ubiquitously formed under the seafloor where the gas (methane) concentration exceeds its solubility within the equilibrated pressure-temperature condition. The equilibrium condition, however, readily changes to reflect the surrounding environments such as compositions of water, gas, and sediment. In this study, we experimentally determined the phase equilibrium pressure-temperature condition using carbon dioxide with natural sediments to examine the physical/chemical effects of sediment particles on the CO2 hydrate stability, of which physical properties are similar to those of methane hydrate. The phase equilibrium of CO2 hydrate with 10 wt% sediment changed to lower temperature (high pressure) region compared to the pure water system. This is because the clay minerals such as kaolinite absorb efficiently water molecules and form a structure similar to the hydrate lattice, preventing the formation of hydrate. In addition, ion dissolution from clay minerals may result in the depression of freezing point of hydrate, which also reduces the hydrate stability. The properties of host sediment as well as gas and water chemistry are important factor for assessing the distribution and amount of gas hydrate in natural environment.

©2021. Japan Geoscience Union. All Right Reserved.

Effect of temperature and pressure on hydration number of methane hydrate

*Akihiro Hachikubo[1], Ryoya Kamata[1], Hiromi Kimura[1], Yuta Komagata[1], Go Fuseya[1], Satoshi Takeya[2]

1. Kitami Institute of Technology, 2. National Institute of Advanced Industrial Science and Technology (AIST)

Gas hydrates are considered to be a potential resource of energy and a gas storage medium. Hydration number of methane hydrate decides the amount of gas in crystal lattice of gas hydrate. In the case of ideal full-occupation of hydrate cages, hydration number is 5.75. However, researchers have reported that the hydration number is around 6, because small amount of empty cages decrease the free energy and stabilize the crystal. Hydration number depends on temperature and pressure at the formation process (Cady, 1981; 1983) as van der Waals & Platteeuw model predicts. It has not been investigated how the hydration number changes over a wide temperature range. In this study, we investigated the effect of temperature and pressure on the hydration number of methane hydrate.
Small amount of fine ice powder (0.1 g) was placed in a pressure cell at 253 K, and methane was introduced and pressurized under the temperatures of 245 K, 255 K, and 273 K to form hydrate samples. The samples were retrieved under the temperature of liquid nitrogen. The Raman spectra of the C-H symmetric stretching vibrational mode of the methane molecules encapsulated in the large and small cages of the structure I were observed using a Raman spectrometer. The area ratios of the Raman peaks derived from the methane molecules in the large and small cages were determined by a peak fitting using the Voigt function, and the hydration number was estimated using a statistical thermodynamic calculation.
Generally, the hydration number of methane hydrate decreased with increasing formation pressure. This trend is consistent with the results obtained for hydrates of other guests such as xenon, hydrogen sulfide, and sulfur dioxide (Kamata *et al.*, 2020; Cady, 1981; 1983). Besides, it increased slightly with temperature. However, the change of hydration number of methane hydrate was relatively small, ranged from 5.92 to 6.11 under the pressure of 2 MPa to 21 MPa.

References

Cady GH (1981) Composition of clathrate gas hydrates of $CHClF_2$, CCl_3F, Cl_2, ClO_3F, H_2S, and SF_6. *J Phys Chem* **85**: 3225-3230
Cady GH (1983) Composition of Clathrate Gas Hydrates of H_2S, Xe, SO_2, Cl_2, CH_3Cl, CH_3Br, $CHClF_2$, CCl_2F_2, and C_3H_8. *J Phys Chem* **87**: 4437-4441
Kamata R, Kimura H, Sugimori E, Hachikubo A, Takeya S (2020) Direct measurement of hydration number of gas hydrates. *JpGU-AGU Joint Meeting 2020*, MIS32-P12

Keywords: gas hydrate, hydration number, methane

©2021. Japan Geoscience Union. All Right Reserved.

[J] Poster | M (Multidisciplinary and Interdisciplinary)：M-IS Intersection

Sun. Jun 6, 2021 5:15 PM - 6:30 PM JST | Sun. Jun 6, 2021 8:15 AM - 9:30 AM UTC | Ch.22_3

[M-IS27] History X Earth and Planetary Science

convener:Yasuyuki Kano(Earthquake Research Institute, The University of Tokyo), Hiroaki Isobe(Faculty of Fine Arts, Kyoto City University of Arts), Kei Yoshimura(Institute of Industrial Science, The University of Tokyo), kiyomi iwahashi(National Institute of Japanese Literature)

The history of modern observation in earth and planetary sciences is often far shorter compared with the timescales of their interests. Investigation of the long-term variations and occurrences of extremely rare events requires effective use of information derived from historical documents observed and recorded by pre-modern people. Thus, historical documents have been referred in various fields of earth and planetary sciences such as seismology, climatology, meteorology and astronomy. Sharing their records, methods and experiences will be beneficial for each field and bring new insights. It is also essential to involve experienced historians because one needs to carefully investigate the reliability and the context of each document in order to use it as scientific data. On the other hand, analyzing the record in the historical documents with the eyes of modern science may also bring new insights to the historians. Cooperative work between historians and earth scientists will provide better knowledge on disaster mitigation, and science, technology and society through understanding of human reaction to historical disasters.

In this session we overview the studies using the historical documents in various fields of the earth and planetary sciences as well as the recent advances in related topics such as historical-data assimilation and digital humanities, such as AI character recognition. The aim is to promote the communication and dialogues among the researchers in various background, and thus foster the new ideas and collaborations in the study of "History X EPS."

[MIS27-P01] An attempt to convert historical seismic data into GIS data and its challenges

*Junzo Ohmura[1,4], Miki Hamano[2], Yuta Hashimoto[3], Yasuyuki Kano[1,4] (1.Earthquake Research Institute,The University of Tokyo, 2.Graduate School of Letters, Ritsumeikan University, 3.National Museum of Japanese History, 4. Collaborative Research Organization for HistoricalMaterials on Earthquakes and Volcanoes, UTokyo)

[MIS27-P02] Historical materials of unlisted destructive earthquakes at Izu-Bonin Islands in the Meiji period: the 1873 Toshima earthquake and so on

*Kentaro Hattori[1] (1.Kyoto Univ.)

[MIS27-P03] Investigation of the stone monuments related to the hail and frost damage in the southern part of Gunma Prefecture

*Masafumi Aoyama[1] (1.Gunma University)

An attempt to convert historical seismic data into GIS data and its challenges

*Junzo Ohmura[1,4], Miki Hamano[2], Yuta Hashimoto[3], Yasuyuki Kano[1,4]

1. Earthquake Research Institute,The University of Tokyo, 2. Graduate School of Letters, Ritsumeikan University, 3. National Museum of Japanese History, 4. Collaborative Research Organization for HistoricalMaterials on Earthquakes and Volcanoes, UTokyo

Historical data on earthquakes have been collected since the Meiji era (1868-1912), and collections of historical data have been published. The collection is now being converted to electronic text. There is a plan to add location information to place names in the future.

Regarding the conversion of historical seismic data into GIS data, ohmura (2015) describes the advantages of this method. Spatial analysis is essential for the analysis of seismic phenomena. However, the identification of place names in historical documents is time-consuming and requires knowledge of history. This is one of the factors that prevent researchers outside the field from entering the field.

The Ministry of Land, Infrastructure, Transport and Tourism (MLIT) has released a number of GIS data. If the historical records of earthquakes are converted into GIS data, it will be possible to analyze them using GIS. In addition, the data can be used not only in seismology but also in other related fields.

In this study, we attempted to convert historical materials into GIS data for the 1596 Keicho-Fushimi Earthquake, for which electronic texts have already been made available.

Using GIS, we examined the relationship between the earthquake fault and the distribution of historical materials. As a result, we found that the historical materials are unevenly distributed, and it is highly possible that the epicenter cannot be estimated accurately. In analyzing historical earthquakes, it is necessary to consider the spatial bias of historical materials and to understand their limitations.

On the other hand, the tendency of the distribution of the records is different depending on the nature of the historical materials. By converting historical documents into GIS data, it is possible to examine historical documents from a spatial perspective.We plan to publish the created GIS data on the web.

In the process of converting place names into GIS data, we faced the problem of having a mixture of place names with various characteristics in the historical records. The specific problems are as follows.
1. In urban areas, there are many detailed place names, so old maps with large scales are not useful for reference.
2. There are many examples of the same place name being written differently.
3. There are place names that have disappeared in modern times.
4. We need to find out where the temples and shrines existed at the time.
5. In some cases, it is not possible to determine the location without reading before and after the historical documents.
6. Conceptual and vague place names exist.
7. There are place names that should be represented by lines and Polygon.
8. There are cases where a location is expressed as a distance from a specific point.

©2021. Japan Geoscience Union. All Right Reserved.

Keywords: historical earthquake, GIS, historical place name

©2021. Japan Geoscience Union. All Right Reserved.

Historical materials of unlisted destructive earthquakes at Izu-Bonin Islands in the Meiji period: the 1873 Toshima earthquake and so on

*Kentaro Hattori[1]

1. Kyoto Univ.

Destructive earthquakes that have occurred in the vicinity of Japan from ancient times are summarized in catalogs such as "Chronological table of earthquakes" in “Chronological scientific tables” (National Astronomical Observatory of Japan, 2020), and “Materials for a comprehensive list of Japanese destructive earthquakes 599-2012” (Usami et al., 2013). Usami et al. (2013) include earthquakes that have caused damage or changes to houses, artificial structures, or the ground. I investigate records of earthquakes that caused damage to the Izu-Bonin Islands in the Meiji period (1868 -1912) and are not listed in Usami et al. (2013).

In this study, I focus on an earthquake that occurred in 1873 (Meiji 6) and caused damage to Toshima Island (Present Toshima Village, Tokyo) in the northern Izu Islands. The earthquake caused damage to temples and shrines in Toshima Island [Toshima Village (1996a)] and caused landslides [Toshima Village (1996b)]. As for the date of the earthquake, the records in Toshima Island say "Meiji 6, 6th month, 8th day " [Toshima Village (1996a)]. These records exceptionally used the Japanese calendar system, although 1873 was the year when the Japanese calendar (lunar calendar) was switched to the Western calendar in Japan. "Meiji 6, 6th month, 8th day" on the Japanese calendar is 1873 July 2 on the Western calendar. In the study, I survey other historical records about the earthquake.

In addition, I examine the earthquake in the Izu Islands on 1885 (Meiji 18) October 26, and the earthquake in the Bonin Islands on 1885 (Meiji 18) November 4. In the former earthquake, several coastal cliffs of Niijima Island and Shikinejima Island (Present Niijima-mura, Tokyo) in the northern Izu Islands collapsed, and the channel of the water source in Shikinejima Island was blocked. In the latter earthquake, landslides occurred in the Bonin Islands such as Chichijima Island (Present Ogasawara Village, Tokyo). Neither earthquake is not listed in Utsu (1979), which compiled M6.0 or greater earthquakes and smaller destructive earthquakes in and around Japan from 1885 to 1925.

Keywords: historical earthquake, the Izu-Bonin Islands, the 1873 Toshima Island earthquake, the 1885 Niijima Island and Shikinejima Island earthquake, the 1885 Bonin Islands earthquake

©2021. Japan Geoscience Union. All Right Reserved.

Investigation of the stone monuments related to the hail and frost damage in the southern part of Gunma Prefecture

*Masafumi Aoyama[1]

1. Gunma University

We are conducting research on historical disasters in the southern part of Gunma prefecture, using disaster-related monuments. In addition to the stone monuments related to the volcanic mudflow due to the eruption of the Mt. Asama in 1783, there are many stone monuments in this area that show descriptions related to floods, debris flow and landslide disasters that occurred in 1910, 1935, and 1947. In addition to floods and landslides, there are stone monuments related to hail and frost damage, and earthquake damage. In particular, there are many stone monuments related to hail and frost damage in this area. Since this area was once a thriving area for sericulture, if mulberry leaves die due to hail and frost damage, it becomes impossible to raise silkworms that feed on mulberry leaves, causing great economic loss to sericulture farmers. When many silkworms die due to hail and frost damage, the dead bodies have buried, and created mounds on the ground, built stone monuments, and worshiped the spirits of the silkworms. The sericulture industry in this area began to flourish from the end of the Edo period and declined in the Showa period, and many stone monuments related to hail and frost damage and sericulture erected during this period are distributed. In particular, there are stone monuments with detailed descriptions of hail damage in 1887 and frost damage in 1893. These monuments are valuable records of local meteorological phenomena and meteorological disasters during the Meiji era, when meteorological observations were still vulnerable, the impact of hail and frost damage on the local community at that time, and the importance of sericulture in the local community.
Some of the stone monuments that are said to have been erected for the memorial service of silkworms caused by hail and frost damage have detailed descriptions of frost damage, but some have only the monument name and the year of construction. In this area, sericulture worship became popular with the development of sericulture, and many are said to have erected monuments in the hope of abundant cocoons. In addition, in the silkworm industry, which is the victim of silkworms, many monuments have been erected for the purpose of memorializing the silkworms that were sacrificed in the silk reeling process. These stone monuments related to sericulture have monument names such as Kokage Okami, Kokageyama Okami, and Kinugasa Myojin, but the purpose for which the monuments were erected is diverse. In this presentation, I would like to show the results of a study on the situation of hail and frost damage inferred from the inscriptions of these monuments and historical materials, which is said to be a memorial monument for silkworms caused by hail and frost damage, and the circumstance of construction of those monuments.

Keywords: hail and frost damage, silkworm industry, disaster stone monuments, historical disaster

©2021. Japan Geoscience Union. All Right Reserved.

[J] Poster | M (Multidisciplinary and Interdisciplinary)：M-AG Applied Geosciences

Sun. Jun 6, 2021 5:15 PM - 6:30 PM JST | Sun. Jun 6, 2021 8:15 AM - 9:30 AM UTC | Ch.21_3

[M-AG38] Ten years after the Fukushima Dai-ichi NPP Accident : Dynamics of radionuclides in the environment

convener:Daisuke Tsumune(Central Research Institute of Electric Power Industry), Yuichi Onda(Center for Research on Isotopes and Environmental Dynamics, University of Tsukuba), Kazuyuki Kita(Faculty of Science, Ibaraki University), Yoshio Takahashi(Department of Earth and Planetary Science, Graduate School of Science, The University of Tokyo)

Ten years have passed since the accident at the Tokyo Electric Power Company (TEPCO) Fukushima Daiichi Nuclear Power Station (NPP), which was triggered by the Great East Japan Earthquake and tsunami. Huge amount of radionuclides were emitted to the environment by the accident. They have been transported and diffused by atmospheric motion, depositing them to soil and vegetation. Deposited radionuclides are dynamically shifted in the earth environment; atmosphere, soil, inland water, ocean, and ecosystem. To understand this dynamic shift in the environment and for the long-term prediction of the disaster by the radionuclides, investigation and discussion based on not only the earth sciences including ecology but also on the radiochemistry and other related sciences. This session focus on various efforts to understand the dynamic behavior of radionuclides emitted from FDNPP accident in the earth system as well as to predict their influences on the environment, furthermore, to develop as global migration studies by generalization. It is expected that this session will offer a good opportunity to summarize the research activities of the past ten years and deepen the discussion on cross-disciplinary research issues for the next ten years.

[MAG38-P01] Effects of preferential flow on the spatial heterogeneity and chemical form of Cs-137 in a forest soil

*Junko Takahashi[1], Tetsuya Ono[1], Takuya Sasaki[1], Yuichi Onda[1] (1.Center for Research in Isotopes and Environmental Dynamics, University of Tsukuba)

[MAG38-P02] Contribution of fungal hyphal elongation to radiocesium transfer in deciduous broad-leaved litter

*Yoshito Sasaki[1], Tadafumi Niizato[1], Hiroki Amamiya[2], Kaori Yoshida[1] (1.Japan Atomic Energy Agency, 2.QJ science)

[MAG38-P03] The ^{137}Cs dynamics in a pond of urban area after decontamination

*Honoka Kurosawa[1], Misaki Usuki[1], Shota Moritaka[1], Kenji Nanba[2], Toshihiro Wada[2], Yoshifumi Wakiyama[2] (1.Graduate School of Symbiotic Systems Science and Technology, Fukushima University, 2.Institute of Environmental Radioactivity, Fukushima University)

[MAG38-P04] Variations in riverine ^{137}Cs concentration and its exportation to the ocean during high-flow events at three rivers in Hamadori area

Takuya Niida[1], *Yoshifumi Wakiyama[2], Hyoe Takata[2], Kazuki Fujita[3], Keisuke Taniguchi[4], Alexei Konoplev[2] (1.Graduate School of Symbiotic System and Technology, Fukushima Universiy, 2.Institute of Environmental Radioactivity, Fukushima Universiy, 3.Fukushima Prefectural Centre for Environmental Creation, 4.Center for Research in Isotope and Environmental Dynamics, University of Tsukuba)

[MAG38-P05] Comparison of cesium-bearing microparticles from marine and terrestrial sources

*Hikaru Miura[1], Atsushi Kubo[2], Takashi Ishimaru[3], Yukari Ito[3], Jota Kanda[3], Daisuke Tsumune[1], Yoshio Takahashi[4] (1.Central Research Institute of Electric Power Industry, 2.Shizuoka University, 3.Tokyo University of Marine Science and Technology, 4.The University of Tokyo)

Effects of preferential flow on the spatial heterogeneity and chemical form of Cs-137 in a forest soil

*Junko Takahashi[1], Tetsuya Ono[1], Takuya Sasaki[1], Yuichi Onda[1]

1. Center for Research in Isotopes and Environmental Dynamics, University of Tsukuba

1. Introduction

Rainfall infiltration is one of the most important mechanisms of downward migration of Cs-137 in forest soils. It has been pointed out that rainwater infiltration in soil can be divided into two types, which are relatively uniform matrix flow and non-uniform preferential flow through coarse pores and root surfaces. This preferential flow would contribute the downward migration of various substances, therefore it is possible that this preferential flow is a factor in the spatial heterogeneity of the vertical distribution of Cs-137 in soil. However, there have been few studies that have quantitatively evaluated the effects of preferential flow on the vertical distribution of Cs-137. In the presnt study, we conducted an artificial rainfall experiment using dyes in a forest and collected soil samples from dyed and un-dyed areas at different depths in order to quantify the spatial heterogeneity and chemical form of Cs-137.

2. Material and methods

The study site was a cedar forest located in Akougi district, Namie-town, Fukushima Prefecture. The estimated deposition amount by airborne monitoring was about 4700 kBq/m^2. One plot with 1 m x 1 m was set up in the forest, and 10 L of distilled water containing 2 g/L of Rhodamine B was sprayed by a simple sprinkler system as a dye, corresponding to a rainfall amount of 10 mm and the rainfall intensity of about 120 mm/h. Two days after sprinkling, a scraper plate was placed under the litter layer, and the visually dyed soil were collected little by little using a spoon, and then the un-dyed soil were collected. The sampling depths were 0-2 cm, 2-4 cm, 4-6 cm, and 6-10 cm. Although the soil was classified as a non-allophanic Andosol, these surface soil samples did not have andic properties. After air-drying and sieving, the soil samples were sequentially extracted (F1: water-soluble form, F2: exchangeable form, F3: Fe-Mn oxides form, F4: organic matter-bound form, F5: acid-soluble form, F6: residue). The concentrations of Cs-137 and several main elements in each solution were measured using a Ge semiconductor detector and atomic absorption spectrometer. In addition, several chemical properties of soil samples were determined.

3. Results

The dyed soil samples in all layers had higher root and fresh organic matter contents per unit soil weight, higher soil organic matter content, higher CEC, and higher water-soluble and exchangeable cation contents than those in the un-dyed soil samples. The ratios of Cs-137 concentrations in the dyed and un-dyed samples at the same depth were 0.98, 1.48, 1.51, and 2.64 for 0-2, 2-4, 4-6, and 6-10 cm, respectively. This suggests that the preferential flow played an important factor in the spatial heterogeneity of Cs-137 vertical distribution and the pathway of the preferential flow was relatively stable even after nearly 10 years from the accident. As a result of sequential extraction, the average percentages of Cs-137 at each depth in dyed and un-dyed samples were 0.031% and 0.022% in the F1 fraction, 1.10% and 0.97% in the F2 fraction, 0.57% and 0.50% in the F3 fraction, 3.64% and 3.12% in the F4 fraction, and 43.2% and 40.7% in the F5 fraction, showing that the dyed samples tended to be slightly higher in all fractions except the residue. This result suggested that plant-available Cs-137, especially

©2021. Japan Geoscience Union. All Right Reserved.

water soluble and exchangeable form, may be accumulated in areas where preferential flow frequently permeate, such as around the roots. Therefore, it is considered that the effects of preferential flow are important not only for the downward migration but also for the evaluation of root absorption.

Keywords: preferential flow, dye tracer, downward migration

©2021. Japan Geoscience Union. All Right Reserved.

Contribution of fungal hyphal elongation to radiocesium transfer in deciduous broad-leaved litter

*Yoshito Sasaki[1], Tadafumi Niizato[1], Hiroki Amamiya[2], Kaori Yoshida[1]

1. Japan Atomic Energy Agency, 2. QJ science

Radiocesium deposited in the forest released by the accident at the Fukushima Daiichi Nuclear Power Station would remain in the forest and part of it would circulate due to the small amount of outflow from the forest. One possible source of dissolved radiocesium that is easily taken up by organisms is the litter layer. To clarify the contribution of fungal mycelial elongation in the transfer of radiocesium in the litter layer, we investigated the effect of the presence of fungi on the transfer of radiocesium from litter Cs (H) with high radiocesium concentration to litter Cs (L) with low radiocesium concentration. Fungal growth was observed in the test plots where the fungi were present. Regardless of with or without fungi, the Cs-137 concentration of Cs (L) reached about 50 Bq / kg on the 50th day, and then gradually increased to about 100 Bq / kg on the 150th day. This result suggested that the radiocesium was transfered by a physical force other than the hyphal elongation of the fungus in the litter layer.

Keywords: radiocesium, deciduous broad-leaved tree, litter layer, Fukushima Dai-ichi Nuclear Power Plant accident

©2021. Japan Geoscience Union. All Right Reserved.

The ^{137}Cs dynamics in a pond of urban area after decontamination

*Honoka Kurosawa[1], Misaki Usuki[1], Shota Moritaka[1], Kenji Nanba[2], Toshihiro Wada[2], Yoshifumi Wakiyama[2]

1. Graduate School of Symbiotic Systems Science and Technology, Fukushima University, 2. Institute of Environmental Radioactivity, Fukushima University

More than 4,000 irrigation ponds in Fukushima Prefecture have been contaminated by radiocaesium released from the Fukushima Dai-ichi Nuclear Power Plant accident. The contaminated pond would cause problems such as increase of air dose rates around the pond by water drawdown and prevention of the restart/reconstruction of farming and agricultural activities. As a countermeasure, the decontamination has been conducted for ponds with more than 8,000 Bq/kgDW of radiocaesium (^{134}Cs+^{137}Cs) concentration in its bottom sediment. This study aims to evaluate the effect of decontamination and presents investigations on ^{137}Cs concentration in bottom sediment, pond water, inflow water, and outflow water at a decontaminated pond locate in urban area.
Study site is the Sakabuta pond located in urban area of Koriyama city. The decontamination was carried out in 2017. Bottom sediment was collected in 2015, 2018 and 2020. Bottom sediment was basically collected at 2 points around cage for commercial aquaculture of carp and additionally at 5 points in the whole pond once a year. The depth of 0-20 cm, 20-30 cm, and 30 cm or more was cut for 1 cm, 2 cm, 5 cm interval, respectively. Pond water was collected in 2015, 2018, and 2020, simultaneous to bottom sediment sampling. Inflow and outflow water was collected in 2020. The ^{137}Cs concentration in bottom sediment, pond, inflow, and outflow water were measured with the Ge semiconductor detector.
The ^{137}Cs concentrations in bottom sediment and pond water were compared between before and after decontamination. The ^{137}Cs concentrations in the top layer of bottom sediment at 2 points around cage were decreased from 36,100 and 25,500 Bq/kgDW to 15,800 and 15,300 Bq/kgDW. The ^{137}Cs concentration in pond water was decreased from 1.40 Bq/L to 0.950 Bq/L. It was said that the decontamination was effective because the ^{137}Cs concentrations in the top layer of the bottom sediment and pond water were significantly decreased by decontamination. However, the ^{137}Cs concentration in the top layer of bottom sediment was 8,000 Bq/kgDW or more even after decontamination. The ^{137}Cs concentrations in the top layer of bottom sediment at 5 points in the whole pond were 16,700-44,300 Bq/kgDW in 2015, 3,630-12,200 Bq/kgDW in 2018, and 6,800-13,500 Bq/kgDW in 2019.The layer of more than 8,000 Bq/kgDW of radiocesium concentration in the bottom sediment of 2019 was thicker than that of 2018. In 2019, Hagibis passed through about a month before the bottom sediment collection and increase of ^{137}Cs in 2019 was attributed to suspended solid input due to the typhoon. The sedimentary environments were compared between the points with more and less than 8,000 Bq/kgDW of raciocesium concentration. At the point with less than 8,000 Bq/kgDW of radiocesium concentration, it was suggested that new particle was not deposited after decontamination. However, at the point with more than 8,000 Bq/kgDW of radiocesium concentration, it was suggested that new particle was deposited after decontamination. The ^{137}Cs concentration in suspended solids of pond water was more than 8,000 Bq/kgDW even after the decontamination. Furthermore, the ^{137}Cs concentration in suspended solids of inflow water sometimes exceeded 8,000 Bq/kgDW. These results suggested that a large amount of soil particle would flow into the pond during the rainfall events, resulting in high concentration of ^{137}Cs in the top layer of bottom sediment.

Keywords: Fukushima Dai-ichi Nuclear Power Plant accident, Cs-137, Pond, decontamination

©2021. Japan Geoscience Union. All Right Reserved.

©2021. Japan Geoscience Union. All Right Reserved.

Variations in riverine ^{137}Cs concentration and its exportation to the ocean during high-flow events at three rivers in Hamadori area

Takuya Niida[1], *Yoshifumi Wakiyama[2], Hyoe Takata[2], Kazuki Fujita[3], Keisuke Taniguchi[4], Alexei Konoplev[2]

1. Graduate School of Symbiotic System and Technology, Fukushima Universiy, 2. Institute of Environmental Radioactivity, Fukushima Universiy, 3. Fukushima Prefectural Centre for Environmental Creation, 4. Center for Research in Isotope and Environmental Dynamics, University of Tsukuba

A considerable amount of ^{137}Cs deposited on terrestrial is exported to the ocean during high-flow events. Recent studies have reported increases of dissolved ^{137}Cs concentration in near-shore water after high-flow events assumedly due to desorption of ^{137}Cs from suspended solids. Existing literature on riverine ^{137}Cs dynamics during high-flow events have focused on upstream area, but little attention has been paid to downstream area. It remains uncertainties in transfer process of terrestrial ^{137}Cs to the ocean. This study aims to elucidate riverine ^{137}Cs dynamics and its influence on the ocean environment and presents analyses of river water samples taken at three rivers in the Hamadori area during high-flow events. River water samples were taken at 5 times at Haramachi site (206 km^2, 853 kBq m^{-2}) in the Niida river catchment, 3 times at Kiyobashi site (147 km^2, 2360 kBq m^{-2}) in the Ukedo river catchment, and 3 times at Takase site (262 km^2, 701 kBq m^{-2}) in the Takase river catchment during high-flow events occurred in the period of 2016-2020. Five to eight samples were taken per event and particulate and dissolved ^{137}Cs concentrations were measured. When sufficient amount of suspended solid was obtained, ^{137}Cs speciation and ^{137}Cs desorption by seawater were further analyzed. Mean ^{137}Cs concentration in suspended solid in the Niida, Ukedo, Takase rivers were 5100 Bq kg^{-1} (n = 32, CV = 40%), 23000 Bq kg^{-1} (n = 20, CV = 97%), and 4600 Bq kg^{-1} (n = 20, CV=46%), respectively. Mean dissolved ^{137}Cs concentration at the Niida, Ukedo, Takase rivers were 16 mBq L^{-1} (n = 32, CV = 53%), 73 mBq L^{-1} (n = 20, CV = 55%), and 15 mBq L^{-1} (n =20, CV = 40%), respectively. Concentration of ^{137}Cs in suspended solid was positively correlated with specific water discharge rate for three rivers. Dissolved ^{137}Cs concentration also showed positive correlation with specific water discharge rate, except for Takase river. Exportation of ^{137}Cs increased with increase of total rainfall amount and ranged from 6.6 to 60 GBq from the Niida river catchment, from 1.9 to 8.8 GBq from the Ukedo river catchment, and from 2.8 to 13 GBq from the Takase river catchment. The Ukedo river catchment showed low ratio of ^{137}Cs exportation to the total ^{137}Cs deposition in the catchment and low ratio of particulate ^{137}Cs exportation to the total ^{137}Cs exportation. They infered influences of the Ogaki dam located at midstream in the catchment. Ratio of ^{137}Cs desorbed by seawater to ^{137}Cs in suspended solid ranged from 2.8 to 6.6% and tended to be high for suspended solid with high exchangeable ^{137}Cs ratio. By assuming the ratio of desorption, potential release of ^{137}Cs from suspended solid to the ocean was estimated. The estimates for corresponded events ranged from 0.19 to 2.8 GBq. These values were 0.8-15 times higher than dissolved ^{137}Cs exportation. These results suggest that secondary release of ^{137}Cs from terrestrial suspended solid can be one of factor determining dissolved ^{137}Cs concentrations in the near-shore sea.

Keywords: River, Radiocesium, Suspended solid

©2021. Japan Geoscience Union. All Right Reserved.

Comparison of cesium-bearing microparticles from marine and terrestrial sources

*Hikaru Miura[1], Atsushi Kubo[2], Takashi Ishimaru[3], Yukari Ito[3], Jota Kanda[3], Daisuke Tsumune[1], Yoshio Takahashi[4]

1. Central Research Institute of Electric Power Industry, 2. Shizuoka University, 3. Tokyo University of Marine Science and Technology, 4. The University of Tokyo

Radionuclides including radioactive Cs were released into the environment due to the Fukushima Daiichi Nuclear Power Plant accident in 2011. Two years after the accident, glassy water-resistant particles incorporating radioactive Cs were first reported. Such glassy particles are called cesium-bearing microparticles (CsMPs). CsMPs have been studied because (i) they have information on the condition in the reactor at the time of the accident, and (ii) there is concern about the exposure to the humans and the other organisms.

Several types of CsMPs have been reported, which is assumed to reflect the difference in the accidental progress of each unit. It is also known that CsMPs were transported in the atmospheric plume at the time of emission and therefore have different deposition regions. Type-A CsMPs, are presumed to originate from Unit 2, deposited over a wide area including the Kanto region due to their small size (~0.1–10 μm). Type-B CsMPs, are presumed to originate from Unit 1, deposited in a limited area in the north direction because of their large size (50–400 μm). Matrix of Types-A and -B CsMPs is SiO_2 but Type-A CsMPs have higher concentration of volatile elements including Cs than Type-B CsMPs due to the difference in forming process. Type-A CsMPs were formed through gas condensation, whereas Type-B CsMPs were formed through melt solidification.

The presence of CsMPs emitted from Unit 3 in the ocean was confirmed by our research. The plume at the time of the emission of radionuclides from Unit 3 was in the ocean direction, which suggests that many CsMPs from Unit 3 deposited directly into the ocean. We will report the comparison of CsMPs from marine and terrestrial sources. In addition, we reported Type-A CsMPs from suspended particles in rivers and marine samples, such as plankton net and suspended particle samples. This fact suggests that Type-A CsMPs deposited on land and transported to the ocean through rivers. The presence of CsMPs may be the cause of the overestimation of solid–water distribution coefficient for marine sediments and particulate matters and apparent high concentration factor of marine biota of radioactive Cs.

Keywords: radiocesium-bearing microparticle, Fukushima Daiichi Nuclear Power Plant accident, Radioactive cesium

©2021. Japan Geoscience Union. All Right Reserved.

[J] Poster | M (Multidisciplinary and Interdisciplinary)：M-TT Technology & Techniques

Sun. Jun 6, 2021 5:15 PM - 6:30 PM JST | Sun. Jun 6, 2021 8:15 AM - 9:30 AM UTC | Ch.20_2

[M-TT43] Brand-new scope of coupling geophysics being established by infrasound and associated waves

convener:Masa-yuki Yamamoto(Department of systems engineering, Kochi University of Technology), Takayuki Otsu(Japan Weather Association), Mie Ichihara(Earthquake Research Institute, University of Tokyo), Nobuo Arai(Disaster Mitigation Research Center, Nagoya University)

Infrasound and associated wave studies are recently focused on coupling waves with long-distant and vertical propagation characteristics. Such kinds of waves, having with coupling process between the atmosphere and the surface of ground and ocean, are linked with elastic waves in lithosphere and oceanic sphere, as well as to atmospheric regions up to the upper atmosphere, playing a role of generating many kinds of wavelike turbulence in thermosphere. Moreover, whole on the globe, these waves excited depending on the latitude regions, as well as on the environmental regions, such as snow ice, desert, rainforest, mountain, ocean, etc., have their own characteristics. These waves can be excited by large-scale geophysical events like volcanic eruptions, tsunami, thunderstorms, etc. as well as artificial explosions, propagating with long distance. In this session, we would like to discuss such "coupling geophysics" by using many new or well-known investigated data and simulations of infrasound and associated low frequency waves. It can combine multiple spheres in geophysics and bring a brand-new scope of geophysics. Your contributions from many regions are welcome!

[MTT43-P01] Infrasound detection of mining blasts from eastwards and westwards

*Mami Nogami[1], Takayuki Otsu[1], Makiko Iwakuni[1] (1.Japan Weather Association)

[MTT43-P02] The Infrasound signals excited by a bolide on 29th November 2020

*Makiko Iwakuni[1], Masa-yuki Yamamoto[2], Hiroaki Saito[3], Islam HAMAMA[2], Nobuo Arai[4], Takayuki Otsu[1], Mami Nogami[1], Takahiko Murayama[1] (1.Japan Weather Association, 2.Department of systems engineering, Kochi University of Technology, 3.Cosmosciences, Hokkaido University, 4.Disaster Mitigation Research Center, Nagoya University)

[MTT43-P03] Atmospheric wave energy of the 2020 August 4 explosion in Beirut, Lebanon, from ionospheric disturbances

*Ai Matsushita[1], Bhaskar Kundu[2], Batakrushna Senapati[2], Kosuke Heki[1] (1.Hokkaido University Graduate School of Science, 2.National Institute of Technology, Rourkela)

[MTT43-P04] Infrasound and seismic multiple-site observation of shock waves induced by hypersonic reentry of HAYABUSA-2 sample return capsule on Dec. 6, 2020

*Masa-yuki Yamamoto[1], Yoshihiro Hiramatsu[2], Shinsuke Abe[3], Yoshihiro Kakinami[4], Norihisa Segawa[5], Hiroshi Katao[6], Yoshiaki Ishihara[7], Taichi Kawamura[8], Satoshi Nozawa[9], Muneyoshi Furumoto[10], Phil Bland[11], Eleanor Sansom[11], Hadrien Devillepoix[11], Martin Towner[11], Yuichiro Inoue[1], Islam H. Hamama[1], Masato Yazawa[12], Kazuhisa Fujita[7], Makoto Yoshikawa[7] (1.Kochi University of Technology, 2.kanazawa University, 3.Nihon University, 4.Hokkaido Information University, 5.Kyoto Sangyo University, 6.Kyoto University, 7.JAXA, 8.Institut de Physique du Globe de Paris, 9.Ibaraki University, 10.Tono Research Institute of Earthquake Science, 11.Curtin University, 12.Mathematical Assist Design Laboratory)

Infrasound detection of mining blasts from eastwards and westwards

*Mami Nogami[1], Takayuki Otsu[1], Makiko Iwakuni[1]

1. Japan Weather Association

There are several large mines in Southwestern Siberia, Russia, blasting using explosives is carried out for the topsoiling and mining of minerals. When blasting, shock waves are generated according to the power of the explosive, including expansion of high-temperature and high-pressure gases. Even if the explosives are installed in the ground, when crushed materials and pressure waves erupt into the atmosphere with the explosion, they can be observed as infrasound. In the case of known mines, the distance to the station is known, so it is possible to estimate the propagation time depending on weather conditions. Furthermore, when seismic waves propagated through the ground are observed at several seismic stations, the seismic origin position and origin time are determined, and it is also possible to determine the location of the sound source based on the azimuth analyzed from the infrasound data and the observation time.

CTBT Infrasound station of I46RU is consisted of 4 sites installed infrasound sensor (MB2000), is also deployed at Zalesovo, Russia. Within 1,000 km of the I46RU, there are several mines in operation, and infrasound by blasting can be observed from eastward, and westward during the same time. As a feature of the signals, they have a dominant frequency between 1 Hz and 4 Hz, the duration is about 10 seconds. Since the time of mining is concentrated in the day, trace velocity of many signals are analyzed that propagate roughly straight near the ground surface due to the effect of forming a reverse fault between several height and the ground surface, after that, signals of the trace velocity which seems to have been propagated by guiding between the tropopause, or the stratopause and the ground surface can be observed.

In the poster, we would like to consider the characteristics of signals when propagated from eastward and/or westward sound sources based on the differences in seasonal atmospheric conditions.

Keywords: Infrasound, Mining blast, CTBT

©2021. Japan Geoscience Union. All Right Reserved.

The Infrasound signals excited by a bolide on 29th November 2020

*Makiko Iwakuni[1], Masa-yuki Yamamoto[2], Hiroaki Saito[3], Islam HAMAMA[2], Nobuo Arai[4], Takayuki Otsu[1], Mami Nogami[1], Takahiko Murayama[1]

1. Japan Weather Association, 2. Department of systems engineering, Kochi University of Technology, 3. Cosmosciences, Hokkaido University, 4. Disaster Mitigation Research Center, Nagoya University

An infrasound observation system has been installed in Shima region, Mie prefecture since 2015 by Japan Weather Association (JWA). Kochi University of Technology (KUT) started the operation of an infrasound sensor in 2016. Currently, many infrasound sensors are deployed over the Japanese islands (widely from Kyusyu region to Hokkaido region. JWA and KUT collect these infrasound data in real time to monitor natural disasters such as tsunami and volcanic eruption. The collection of infrasound observation system of KUT is named KISONS (Kochi university of technology InfraSound Observation data Network System).

Infrasound sensors of JWA and KUT observed infrasound signals excited by a bolide which flew over off Kii channel around 01:34 on 29th of November 2020 (JST). Many people witnessed this bolide, and optical observation data gave the information that the flying route of it. At the infrasound station closest to the bolide trajectory, Toyo town in northeastern part of Kochi prefecture, the infrasound sensor detected some signals around 01:39. Other two infrasound sensors at Cape Muroto in Kochi prefecture detected signals after 01:39. On Kii peninsula, sensors of KUT in Kumano city and Owase city and sensors of JWA in Shima also detected signals. The direct distance between the height of the vanishing point of the bolide trajectory and each infrasound station, was 86 km at the nearest Toyo town and 196 km at the farthest Shima site (Shima high school). As far as we know, this is rare case to detect signals excited by a bolide at multiple infrasound stations in Japan as close as approximately 100 km distance from the bolide trajectory. It will be a valuable case to study the changes in the signals due to propagation from the bolide trajectory.

We thank SonotaCo Network members. In this group they optically observe bolides, meteors and so on, discuss the orbit. SonotaCo Network URL: http://sonotaco.jp/

Keywords: Infrasound, Meteor, Multiple infrasound stations at short distances (100km), Microbarograph

©2021. Japan Geoscience Union. All Right Reserved.

Atmospheric wave energy of the 2020 August 4 explosion in Beirut, Lebanon, from ionospheric disturbances

*Ai Matsushita[1], Bhaskar Kundu[2], Batakrushna Senapati[2], Kosuke Heki[1]

1. Hokkaido University Graduate School of Science, 2. National Institute of Technology, Rourkela

The electron distribution in the ionosphere is often disturbed by various phenomena in the atmosphere. They are observed as changes in TEC (Total Electron Content) along line-of-sight connecting GNSS (Global Navigation Satellite System) satellites and receivers. For example, large meteorites entering the Earth’ s atmosphere often explode and are recognized as fireballs. Sound waves and internal gravity waves excited by them propagate through the atmosphere, reach the ionospheric F region, and disturb TEC. A fireball appeared near Chelyabinsk, Russia, on February 15, 2013, one of the largest fireball events in the observation history, made significant disturbance signals in TEC observed with multiple GPS satellites and ground receivers.

Here I report ionospheric disturbances following the chemical explosion that occurred in Beirut, Lebanon, on August 4, 2020 using nearby continuous GNSS stations. The scale of this explosion is 1-1.5 kt (TNT), which is about 1/100 of the fireball over the Bering Sea. Despite its small scale, N-shaped TEC changes were observed thanks to the existence of a dense continuous GNSS station network to the south of Beirut. The signals were found only at southern stations with distances >200 km from the explosion site, which is due mainly to the interaction of ionospheric electrons with the magnetic field.

Currently, we also perform a numerical simulation study of the propagation of disturbances excited by the explosion. In the simulation, we assumed the sound velocity structure in the atmosphere (US Standard Atmosphere 1976), the Chapman-type altitude dependence of electron density, and the influence of the magnetic field, and simulated the upward propagation of N-shaped sound waves. As a result, N-shaped TEC changes that match the observed waveforms could be reproduced. In the future, we plan to sort out following problems in this numerical simulation, (1) the waveform cannot be reproduced for line-of-sight penetrating the region just above the explosion, (2) propagation in the east-west direction is not sufficiently considered, and (3) objective determination of the optimum period of the disturbance.

©2021. Japan Geoscience Union. All Right Reserved.

Infrasound and seismic multiple-site observation of shock waves induced by hypersonic reentry of HAYABUSA-2 sample return capsule on Dec. 6, 2020

*Masa-yuki Yamamoto[1], Yoshihiro Hiramatsu[2], Shinsuke Abe[3], Yoshihiro Kakinami[4], Norihisa Segawa[5], Hiroshi Katao[6], Yoshiaki Ishihara[7], Taichi Kawamura[8], Satoshi Nozawa[9], Muneyoshi Furumoto[10], Phil Bland[11], Eleanor Sansom[11], Hadrien Devillepoix[11], Martin Towner[11], Yuichiro Inoue[1], Islam H. Hamama[1], Masato Yazawa[12], Kazuhisa Fujita[7], Makoto Yoshikawa[7]

1. Kochi University of Technology, 2. kanazawa University, 3. Nihon University, 4. Hokkaido Information University, 5. Kyoto Sangyo University, 6. Kyoto University, 7. JAXA, 8. Institut de Physique du Globe de Paris, 9. Ibaraki University, 10. Tono Research Institute of Earthquake Science, 11. Curtin University, 12. Mathematical Assist Design Laboratory

On Dec. 6, 2020, the JAXA HAYABUSA2 spacecraft returned to the Earth and its sample return capsule (SRC) was successfully landed on the desert area of Woomera, South Australia. At the time of hypersonic reentry of SRC in the upper and middle atmosphere, shock waves can be generated from the Mach cone along the shallow angle trajectory of SRC directly injected from the outer space. In 2010, the HAYABUSA SRC also successfully landed on the ground in the same desert area. At that time, we tried to detect the shock waves coming from the Mach cone of SRC, but little bit different condition that the mother spacecraft also reentered because of the lack of its capability to escape from the Earth's gravity due to the partial malfunction, therefore, multiple shock waves were observed at 5 sensors at that time. Over 20 seismometers simultaneously detected N-type signals with an air-to-ground coupling process at that time, as well (e.g. Yamamoto et al., 2011). After the event, we have been developed new infrasound sensors of INF01 and INF04 with data loggers by ourselves collaborating with some manufacturing companies, thus this time, we can deploy 30 sensors in a 100 km scale target area. Besides, 6 low-cost seismometers were also deployed at 4 sites.

For detecting precise trajectory and yield energy from the dataset of over-pressure amplitude at each site, we deployed 30 sensors on ground in the Woomera Prohibited Area (WPA). As for the INF04 sensors, we used 7 sites using 4 sensors per each, getting N-type waveform at every 27 sensors, except for 1 possible malfunctioned sensor. The waveform was almost the same as the HAYABUSA SRC reentry but without any complex features of the followed period just after the N type signal. The air-to-ground coupling process is also roughly investigated in comparison with previous result in 2010. By using these datasets, we will show the prompt report of the whole of the observation about the infrasound and seismic observation for HAYABUSA2 reentry. The possibility of the yield energy estimation and precise trajectory determination will be discussed in this talk.

Reference:
Yamamoto, M.-Y., Ishihara, Y., Hiramatsu, Y., Kitamura, K., Ueda, M., Shiba, Y., Furumoto, M., Fujita, K., Detection of Acoustic/Infrasonic/Seismic Waves Generated by Hypersonic Re-Entry of the HAYABUSA Capsule and Fragmented Parts of the Spacecraft, Publ. Astron. Soc. Japan, 63, 971-978, 2011.

Keywords: Infrasound, Shock wave, Multiple-site array observation, Reentry, HAYABUSA2

©2021. Japan Geoscience Union. All Right Reserved.

[J] Poster | M (Multidisciplinary and Interdisciplinary)：M-ZZ Others

Sun. Jun 6, 2021 5:15 PM - 6:30 PM JST | Sun. Jun 6, 2021 8:15 AM - 9:30 AM UTC | Ch.22_4

[M-ZZ44] Studies of Geoscience : historical, philosophical and STS studies

convener:Michiko Yajima(Tokyo Metropolitan University), Shigeyuki Aoki(Faculty of Letters, Chuo University), Toshihiro Yamada(Taisho University), Akira Yamamoto

Topics on history, philosophy and STS (science, technology and society)studies of geoscience will be discussed. Any related subject is welcome, such as history of mining, historical studies of geohazards, methodology of geoscience, sociology of natural hazards, politics of environmental issues, and risk theory.

[MZZ44-P01] The begining of lady earth scientists in Japan

*Michiko Yajima[1] (1.Tokyo Metropolitan University)

[MZZ44-P02] Finding Geoscientific Evidence in Nuclear Disaster Trials 2: Is Not "responsibility of the government" Scientific?

*Mamoru Hayashi[1] (1.University of TOYAMA)

[MZZ44-P03] Wilkins’s lunar world

*Shigeyuki Aoki[1] (1.Faculty of Letters, Chuo University)

[MZZ44-P04] The Popularization of Science and the Geo-power: Cosmic Evolution, China, and Buddhism in 1920s Shinjo Shinzo

*Toshihiro Yamada[1] (1.Taisho University)

[MZZ44-P05] Japan's first female meteorologist

*Akira Yamamoto

The begining of lady earth scientists in Japan

*Michiko Yajima[1]

1. Tokyo Metropolitan University

I continue to make research on lady earth scientists in Japan. Before the war, Marie Stopes (1880-1958) and Kono Yasui (1880-1971) studied the fossils from Japan coal field. Yasui got doctoral degree in 1927 from the University of Tokyo. This is the first doctoral degree of science that Japanese lady got.
In 1943 three ladies, Takayo Fujiwara, Tami Inoue, and Mitsu Inoue, attended the annual meeting of the Geological Society of Japan. Only Fujiwara continued the science carria. She got doctoral degree from Hokkaido University in 1961 and award from JGS in 1968.
The first lady earth scientist who got doctoral degree was Fumiko Shido. She got in 1958 from the University of Tokyo.

Keywords: lady earth scientist, Fumiko Shido, Takayo Fujiwara, Tami Inoue, Kono Yasui, Marie Stopes

©2021. Japan Geoscience Union. All Right Reserved.

Finding Geoscientific Evidence in Nuclear Disaster Trials 2: Is Not "responsibility of the government" Scientific?

*Mamoru Hayashi[1]

1. University of TOYAMA

This paper examines the way of examining geoscientific evidence in the civil trial for compensation for nuclear power plant and the criminal trial of TEPCO.

It can be said that the TEPCO criminal trial judgment (Tokyo District Court, September 19, 2019) found that the management had recognized the possibility of a tsunami (foresight). However, the Tokyo District Court acquitted the management of the case, saying that the long-term evaluation by the Earthquake Headquarters was based on weak grounds and unreliable. From the scientific point of view, "reliability" covered by the long-term evaluation of the Headquarters for Earthquake Research Promotion is not the concept of the property which can deny the probability of tsunami earthquake. From the viewpoint of the standard of IAEA which the Japanese government also joins, and from the viewpoint of the standard of severe accident prevention which makes it to be under 10,000 times or under 100,000 times/year = scientific and technological principle, it could not be "unexpected". It seems that the "reliability" came out by the logic which denies the countermeasure, closing the eye for the high probability.

In comparison with the judgment of civil suit for compensation for nuclear power plant, this paper examines the discussion on "reliability" and the judgment of existence of "responsibility of the state" which accepts the judgment which deviates from the scientific and technological principle of TEPCO from the geoscientific viewpoint.

Keywords: Tokyo Electric Power Company nuclear power plant criminal trial, civil suit for compensation for nuclear power plant, tsunami predictability, probability, Criticism of the transscience theory

©2021. Japan Geoscience Union. All Right Reserved.

東電福島原発震災裁判にかかわって

- 2019年9月19日の東電刑事裁判判決は，津波予見性を必ずしも否定していないが，刑事罰を認めるには信頼性が低いとした。
- 判決が依拠したのは，判決要旨には名前がでていない東北大学松澤暢教授（地震学）の主張（北緯38.1度より南には付加体がないので福島沖では津波地震(地震動の大きさに比べ大きな津波をもたらす地震)は生じない）らしい。
- しかし，その松澤氏も民事裁判証言意見書で，南北で差があるとは思うが，南側でも北側よりは可能性が低くとも津波地震がおこりうる，北緯38.1度より南での津波地震発生の蓋然性に関しては否定でなく，五分五分の蓋然性を考えていたと示しているが，証言を依頼された被告東電を擁護（利益相反の影響の可能性）。

原発賠償訴訟松澤意見書（被告側2016年9月28日付）から

「平成21年2月に，土木学会原子力土木委員会内の津波評価部会は，私などの地震の専門家らに対して，確率論的津波評価の重み付けアンケートを実施しました。

私はよく覚えていませんでしたが，以前，東京地検の検事から，私のアンケートの回答を見せてもらったと記憶しています。

その中に，日本海溝沿い福島沖と津波地震の発生に関する項目があり，日本海溝沿い福島沖で津波地震は発生しないという選択肢，領域を南北に分けて差異を設ける選択肢，領域を1つとして1896年明治三陸津波地震と同様のものがどこでも起きるという選択肢の3つがあり，これらの可能性に0～1の数字を振って合計が1になるように重み付けをするというものでしたが，私は，順に，0.2，0.6，0.2と付けました。」

- 日本海溝沿い福島沖で津波地震は発生しない：0.2
- 領域を南北に分けて差異を設ける選択肢：0.6
- 領域を1つとして1896年明治三陸津波地震と同様のものがどこでも起きる：0.2

- つまり，南北で差があるとは思うが，南側でも北側よりは可能性が低くとも津波地震がおこりうる，そう重みづけしていたのだから，北緯38.1度より南での津波地震発生の蓋然性に関して，松澤氏は否定でなく，五分五分に近く考えていたのだとわかる。そのような大きな蓋然性を切り捨てる判断に信頼性はあるか？

蓋然性を無効化する画策（翻訳例）「他の要因に隠れてしまうほど小さい」？

- (f) In general, increases in the incidence of health effects in populations cannot be attributed reliably to chronic exposure to radiation at levels that are typical of the global average background levels of radiation. This is because of the uncertainties associated with the assessment of risks at low doses, the current absence of radiation-specific biomarkers for health effects and the insufficient statistical power of epidemiological studies. UNSCEAR（2012）報告書
  統計的有意性で検出するには統計的パワーが足りないといった議論がされているが，バックグラウンドに付け加わる要因が「隠れて」「しまう」「小さい」というニュアンスは，ここからは読み取れない。
- 「国際的な合意では，放射線による発がんのリスクは，100mSv以下の被ばく線量では，他の要因による発がんの影響によって隠れてしまうほど小さいため，放射線による発がんリスクの明らかな増加を証明することは難しいとされる。疫学調査以外の科学的手法でも，同様に発がんリスクの解明が試みられているが，現時点では人のリスクを明らかにするには至っていない」（2011年12月22日低線量被ばくのリスク管理に関するワーキンググループ報告書）→これも「ジャパン・スタンダード」。
  ＃ここでの「しまう」は，その状態の完成を表わすor不本意？。

科学論争の裏に読み取り可能な目的意識

国土を汚染した被告が避難者に罪をなすりつけられるのか

自主的避難等対象区域からの避難者について，特別の事情を留保することなく，平成２４年１月以降について避難継続の相当性を肯定し，損害の発生を認めることは，自主的避難等対象区域での居住を継続した大多数の住民の存在という事実に照らして不当である上に，自主的避難等対象区域は，本件事故後の年間積算線量が２０ミリシーベルトを超えない区域であり，前記第２のとおり，そのような低線量被ばくは放射線による健康被害が懸念されるレベルのものではないにもかかわらず，平成２４年１月以降の時期において居住に適さない危険な区域であるというに等しく，自主的避難等対象区域に居住する住民の心情を害し，ひいては我が国の国土に対する不当な評価となるものであって，容認できない。

原発賠償群馬訴訟控訴審被告第8準備書面（2019年9月11日）から

「口頭弁論で原告側弁護人が「本当に謙虚すぎるのか」と質問し，国側は「謙虚すぎる」と答えた。原告側は敗訴に対し「避難者と残った人の分断をあおり，原発事故での国の責任を棚上げしている」と指摘した。」

上毛新聞2019年9月18日付

広島・長崎の被爆者による原爆症認定訴訟において裁判所の判断の多くは，被曝によって促進される病気であれば被爆者援護法の目的に沿って，原爆症と認定すべきだとしている。すなわち，「高度の蓋然性をもって証明を厳格に要求することは，真に救済されるべき被爆者が救済されないという事態を招きかねない」などとする（H27年行政（コ）421号原爆症認定申請却下処分取消請求控訴事件資料から）。

いっぽう，政府側は，以下のように主張する。「…放射線に起因して発症したことが証明された場合に限り，他の戦争被害者には認められない高額の特別手当を支給するものであり，…被爆者手帳の支給を受けたものであれば誰でも疾病罹患のみを要件として上記のような高額の給付を受けられるということになれば，もはや被爆者援護法の趣旨を超えるものといわざるをえない。このような事態は，大なり小なり受けた戦争の犠牲を等しく甘受することで成り立ってきた社会的コンセンサスを揺るがすことになりかねず，国民の理解を得られるものではない」。

人権のための科学なのか，それとも加害者・権威者の特権のための科学なのか？

2021年2月19日 原発賠償千葉訴訟東京高裁判決要旨　から

イ　規制権限不行使の違法性

(ｱ)　**科学的知見としての長期評価**

①　長期評価と津波評価技術

平成１４年２月に土木学会により策定，公表された**津波評価技術**は，原子力発電所の設計津波の設定について，その時点で確立しており実用として使用するのに疑点がないものを取りまとめたものである。原子力規制機関は，原子炉の設置許可処分に先立つ審査にも，津波評価技術と同様の考え方を用いて津波に対する安全性を確認していた。

平成１４年７月３１日に地震調査研究推進本部により公表された**「三陸沖から房総沖にかけての地震活動の長期評価について」（長期評価）**は，「福島沖を含む日本海溝沿いの三陸沖北部から房総沖までの海溝寄りの領域」に関しては，過去４００年にマグニチュード８クラスのプレート間大地震が３回発生しているとして，この領域全体では約１３３年に１回の割合で，このような大地震が発生すると推定されるとし，明治三陸地震（１８９６年）と同様の地震は，この領域内のどこでも発生する可能性があるとする。

津波評価技術においては，想定津波の波源設定のための基準断層モデルの領域区分に福島県沖の領域が設定されていないのに対し，長期評価においては，日本海溝沿いの三陸沖北部から房総沖までの海溝寄りの領域を一体の領域としている点で異なっている。

津波評価技術と長期評価は，いずれも，過去の地震について調査結果やそれまでの知見から整理し大地震発生に関する見解を形成しているが，用いられた調査結果や知見はほぼ同様である。上記のような相違は，これらの知見が多様であり，地震や津波発生のメカニズムが十分に解明されておらず，いずれの知見もある程度は仮説の域を出ないものであることに由来するとみることができる。

津波評価技術では，津波の波源の領域区分の設定に「地震地体構造論」の知見

5

が用いられているのに対し，長期評価はこれを取り入れたことを明示していないが，この知見にも仮説の域を出ていない部分があり，これを明示的に見解形成の基礎として用いていないことによって長期評価に示された見解の科学的信頼性が大きく減殺されるとは言い難い。

長期評価について，平成１５年３月２４日に地震本部により公表された信頼度の評価では，「発生領域の評価」「発生確率の評価」の信頼度が「やや低い（C）」とされているが，これは過去の地震データが少ないことによるものであり，長期評価の基礎となっている科学的知見の信頼性が低いことを理由とするものではない。

そして，津波評価技術と長期評価のいずれもが，専門家を含む構成員が議論を重ね，議論の結果として得られた見解を一方は学術的権威のある学会が，他方は国の機関が公表したものであり，策定に関与した専門家や議論の過程，公表した主体のいずれにおいても，科学的信頼性の観点からみて，一方が他方に比して優位であるということはできない。

これらを総合すると，**長期評価に示された見解については，相応の科学的信頼性のある知見であると評価することができ，津波評価技術と比較しても，その科学的信頼性において，優位とはいえないまでも，同等であるというべきである。**

②　**長期評価を技術基準適合性の判断の基礎としなかったことの合理性と技術基準適合性の判断について**

規制機関である経済産業大臣は，津波評価技術の知見に依拠して規制権限行使の要件具備の判断をしていたのであり，少なくともこれと同等の科学的信頼性を有する長期評価に示された見解について，これを判断の基礎としないことは，著しく合理性を欠くというべきである。

科学的知見の採否は規制機関の専門的判断に委ねられているが，原子炉施設についての規制権限の目的が，ひとたび事故等により放射性物質の大量放出という事態が発生すれば，極めて深刻な被害を広範囲かつ長期間にわたってもたらす危険性がある原子炉施設について，万全の安全対策を確保することにあることに鑑みれば，規制機関がある科学的知見を基礎として規制権限の行使の要件について判断してきたが，新たな知見が示された場合において，その新たな知見にそれまで判断の基礎としてきた知見と少なくとも同程度の科学的信頼性があると評価することができるようなときは，規制機関が，当該新たな知見を判断の基礎としないとすることは著しく合理性を欠くことになるというべきである。

6

©2021. Japan Geoscience Union. All Right Reserved.

Wilkins’ s lunar world

*Shigeyuki Aoki[1]

1. Faculty of Letters, Chuo University

The shift from the geocentric world-view to the heliocentric one, during the 16th and 17th century in the midst of the Scientific Revolution, transformed the ancient plurality worlds doctrine to more concrete theses on specific satellites and planets. This presentation deals with John Wilkins, who first argued in England that the moon is probably a habitable world.

Keywords: plurality of worlds, the Scientific Revolution in England, history of planetary science, habitable zone

©2021. Japan Geoscience Union. All Right Reserved.

The Popularization of Science and the Geo-power: Cosmic Evolution, China, and Buddhism in 1920s Shinjo Shinzo

*Toshihiro Yamada[1]

1. Taisho University

This paper presents a three-fold emergency by the cosmo-geoscientist Shinjo Shinzo (1873-1938) in his 1920s:
1) The establishment of the institute for physical astronomy at the Imperial Kyoto University;
2) The activities to popularize science, especially cosmic evolution related to Buddhist terminology;
3) The historical study of ancient Chinese astronomy with the collaboration of Orientalists in the university.
We will discuss the geocosmic consciousness cultivated in these processes as well as the international relationship in the term of geo-power.

Keywords: Shinjo Shinzo, Popularization of science, Geo-power, Chinese geoscience, Buddhist terminology

©2021. Japan Geoscience Union. All Right Reserved.

Japan's first female meteorologist

*Akira Yamamoto

Kiyoko Matsuo (1918: estimated-1997) who is considered to be Japan's first female meteorologist is described.

Keywords: history of Meteorology, female scientist, gender

©2021. Japan Geoscience Union. All Right Reserved.

[J] Poster | M (Multidisciplinary and Interdisciplinary)：M-ZZ Others

Sun. Jun 6, 2021 5:15 PM - 6:30 PM JST | Sun. Jun 6, 2021 8:15 AM - 9:30 AM UTC | Ch.22_5

[M-ZZ48] Geology and culture

convener:Hisashi Suzuki(Otani University), Tohru Sakiyama(Institute of Geo History, Japan Geochronology Network), Naoki Takahashi(Natural History Museum and Institute, Chiba)

The session "geology and culture" deals with an interdisciplinary field that discusses the relationship between human and geology. We invite following research themes on the session. (1) geology as a raw material, (2) geochemical analyses of archaeological remains, (3) relationship between geology and regional cultures, (4) geoeducation with museum and geopark, (5) letters and music with geology, and (6) geology and religion. We invite presentations of research results on all geological themes concerning human being.

[MZZ48-P01] Rock species of the cornerstone of the earthen wall in the northeastern part of Ninomaru earthworks of Yamagata Castle

*Ohtomo Yukiko[1], Saito Hitoshi[2] (1.Yamagata University, 2.Yamagata City Board of Education)

Rock species of the cornerstone of the earthen wall in the northeastern part of Ninomaru earthworks of Yamagata Castle

*Ohtomo Yukiko[1], Saito Hitoshi[2]

1. Yamagata University, 2. Yamagata City Board of Education

The northeastern part of Ninomaru earthworks at Yamagata Castle encompasses the area from Higashi Otemon (Eastern Gate) to the North Gate. During an archaeological excavation conducted by the Yamagata City Board of Education from 2016 to 2018, stone walls of Ushitora Yagura and Sakanamachimukai Yagura were detected. The cornerstone of the earthen wall was successfully excavated in almost the entire area, and a geological survey was conducted on the stone walls(Ohtomo, 2020). Two periods of old and new were assigned to the cornerstone of the earthworks. It was judged that the old earthworks were updated with new construction inside because the earthworks are tilted owing to unequal subsidence(Yamagata City Board of Education, 2020). The stone materials surveyed during this project are of the new period.

Most of the cornerstones of the earthen wall are composed of andesite. In particular, 1270 of the 1383 cornerstones are andesite, accounting for 92.03%. Other major materials include dacite, granite, and rhyolite in 47, 40, and 18 cornerstones, amounting to 3.40%, 2.89%, and 1.30%, respectively . In addition, five are composed of basalt, and three are composed of tuff breccia, green tuff, and green andesite. Most occur as subcircular gravel derived from riverbeds. Most of the dacite and some of the rhyolite and granite occur as angular rock masses.

Most of the andesite is gray to black; of these, 30.39% are inclusion rocks presumed to be basalt, and 4.7% contain conspicuous volcanic gas voids. In addition, 1.89% is reddish-purple in color owing to oxidation at high temperatures.

Of the dacites, 33.33% are characterized by thin, black stripes; 31.11% have no such stripes; and 35.56% some did not distinguish between them. Both lithologies are found in the dacite bodies distributed around the Mount Sakazukiyama, although the striped lithology is limited in distribution(Ohtomo, 2016). Most of the dacite is in the form of angular rock masses having the same lithology as the rock found in the stone walls of Sakanamachimukai Yagura and Ushitora Yagura. It is believed that the dacites remaining from the stone wall construction were used in the cornerstone foundation of the earthen wall.

The granites are gravels composed of 65.00% coarse-grained biotite granite, 32.50% medium-grained biotite granite, and 2.50%, fine-grained granite originating from the granite body distributed upstream of the Mamigasakigawa River(Ohtomo et al., 2019).

The gravels assumed to be composed of basalt contain large plagioclase phenocrysts approximately l cm in diameter and numerous phenocrysts. Because this lithology is characteristic of Ryuzan basalt, the gravels of this lithology were classified as basalt.

The tuff breccia and green tuff are from the Miocene Narisawa Formation, and the green andesite is from the Houzawa Formation. The tuff breccia contains granite fragments, and the voids of the green andesite are filled with agate.

The proportion of each of these rock species is almost constant throughout the northeastern earthworks of Ninomaru; no large bias was found among the districts. In District 7, which is adjacent to Ushitora Yagura, 11 dacites having the same lithologies as those present in the stone wall are distributed.

References

Yamagata City Board of Education, 2020, Survey report on buried cultural properties in Yamagata City, Yamagata Prefecture, 39, 14-110. *

Ohtomo Y., 2016, 123rd Annu. Meet. Geol. Soc. Japan, Abstr., 190.

©2021. Japan Geoscience Union. All Right Reserved.

Ohtomo Y., 2020, IV Survey results of stone walls and cobblestone of Sumiyagura in Ninomaru. 39, 111-115. *
Ohtomo Y., et al., 2019, Applied geol. Yamagata, no.39, 89-93.
*English translation from the original written in Japanese

Keywords: cornerstone of earthen wall, rock species, Ninomaru earthworks, Yamagata Castle



©2021. Japan Geoscience Union. All Right Reserved.